ISSUED

DOE/WIPP-19-3610
Volume 1

Waste Isolation Pilot Plant

Geotechnical Analysis Report for July 2017 – June 2018

U.S. Department of Energy

October 2019

This document has been submitted as required to:

U.S. Department of Energy
Office of Scientific and Technical Information
PO Box 62
Oak Ridge, TN 37831
(865) 576-8401

Additional information about this document may be obtained by calling 1-800-336-9477

Unlimited, publicly available full-text scientific and technical reports produced since 1991 are available online at Information Bridge (www.osti.gov/bridge).

U.S Department of Energy and its contractors may obtain full-text reports produced prior to 1991 in paper form for a processing fee from:

U.S. Department of Energy
Office of Scientific and Technical Information
P.O. Box 62
Oak Ridge, TN 37831-0062
Telephone: (865) 576-8401
Facsimile: (865) 576-5728
E-mail: reports@osti.gov

Available for sale to the public from:

U.S. Department of Commerce
National Technical Information Service
5301 Shawnee Rd
Alexandria, VA 22312
Phone: (800) 553-6847 or (703) 605-6000
Fax: (703) 605-6900
Email: info@ntis.gov

Waste Isolation Pilot Plant

Geotechnical Analysis Report for July 2017 – June 2018

U.S. Department of Energy

October 2019

Approved by: //signature on file// 10/25/19
Michael R. Brown Date
Director, Office of Environmental Protection
Carlsbad Field Office

This page was intentionally left blank.

FOREWORD AND ACKNOWLEDGMENTS

This report contains an assessment of the geotechnical status of the Waste Isolation Pilot Plant (WIPP). During the excavation of the WIPP principal underground access and experimental areas, the status was reported quarterly. Since 1987, when the initial construction phase was completed, reports have been published annually. This report presents and analyzes data collected from July 1, 2017, to June 30, 2018.

This Geotechnical Analysis Report (GAR) was written to meet the needs of several audiences. It satisfies requirements contained in the WIPP Hazardous Waste Facility Permit[1] and the Certification of Compliance[2] with Subparts B and C, Title 40 *Code of Federal Regulations* (CFR) Part 191, "Environmental Radiation Protection Standards for Management and Disposal of Spent Nuclear Fuel, High-Level and Transuranic Radioactive Wastes." This report focuses on the geotechnical performance of the various components of the WIPP underground facility, including shaft stations, access drifts, and waste disposal areas. The results of investigations of excavation effects and other geotechnical studies are also included.

This report compares the geotechnical performance of the repository to the design criteria. It describes the techniques that were used to acquire the data. The depth and breadth of the evaluation of the different components of the underground facility vary according to the types and quantities of data available and the complexity of the recorded geotechnical responses. Graphic documentation of data and tabular documentation of instrument history can be provided upon request.

This GAR was prepared by Nuclear Waste Partnership LLC for the U.S. Department of Energy (DOE), Carlsbad Field Office, in Carlsbad, New Mexico. Work was supported by the DOE under Contract No. DE-EM0001971.

[1] New Mexico Environment Department (NMED), 2016, Waste Isolation Pilot Plant Hazardous Waste Facility Permit, NM4890139088-TSDF, Santa Fe, NM

[2] U.S. Environmental Protection Agency, 1998, "Criteria for the Certification and Recertification of the Waste Isolation Pilot Plant's Compliance with the Disposal Regulations: Certification Decision," *Federal Register*, Vol. 63, No. 95, pp. 27354, May 18, 1998, Washington, DC

This page was intentionally left blank.

CHANGE HISTORY SUMMARY

Revision Number	Date Issued	Description of Changes
0	10/25/19	• Initial issue.

This page was intentionally left blank.

TABLE OF CONTENTS

ACRONYMS AND ABBREVIATIONS 6

1.0 INTRODUCTION 7
1.1 Location and Description 7
1.2 Mission 10
1.3 Development Status 10
1.4 Purpose and Scope of Geomechanical Monitoring Program 11
1.4.1 Instrumentation 12
1.4.2 Data Acquisition 13
1.4.3 Data Evaluation 14
1.4.4 Data Errors 15

2.0 GEOLOGY 15
2.1 Regional Stratigraphy 15
2.1.1 Permian 16
2.1.2 Triassic 17
2.1.3 Quaternary 18
2.2 Underground Facility Stratigraphy 20
2.2.1 Disposal Horizon Stratigraphy of Panels 1, 2, 7, and 8 20
2.2.2 Disposal Horizon Stratigraphy of Panels 3, 4, 5, and 6 23
2.2.3 Northeast Area Stratigraphy 23

3.0 PERFORMANCE OF SHAFTS AND KEYS 25
3.1 Salt Shaft 25
3.1.1 Shaft Observations 27
3.1.2 Instrumentation 27
3.2 Waste Shaft 30
3.2.1 Shaft Observations 32
3.2.2 Instrumentation 32
3.3 Exhaust Shaft 35
3.3.1 Quarterly Shaft Inspection 35
3.3.2 Instrumentation 42
3.4 Air Intake Shaft 45
3.4.1 Shaft Performance 45

4.0 PERFORMANCE OF SHAFT STATIONS 47
4.1 Salt Shaft Station 47
4.1.1 Modifications to Excavation and Ground Control Activities 47
4.1.2 Instrumentation 47
4.2 Waste Shaft Station 50
4.2.1 Modifications to Excavation and Ground Control Activities 50
4.3 Air Intake Shaft Station 53
4.3.1 Modifications to Excavation and Ground Control Activities 53
4.3.2 Instrumentation 53

5.0 PERFORMANCE OF ACCESS DRIFTS 53
5.1 Modifications to Excavation and Ground Control Activities 53
5.2 Instrumentation 53
5.2.1 Extensometers 53
5.2.2 Convergence Points 55
5.3 Analysis of Convergence Point and Extensometer Data 55
5.4 Excavation Performance 57

6.0 PERFORMANCE OF THE WASTE DISPOSAL AREA 59
6.1 History 59
6.2 Modifications to Excavations and Ground Control Activities 60
6.3 Instrumentation 61
6.4 Excavation Performance 61
6.5 Analysis of Extensometer and Convergence Point Data 61

7.0 PERFORMANCE OF THE SALT DISPOSAL INVESTIGATIONS AND SALT DEFENSE DISPOSAL INVESTIGATIONS 63
7.1 Ground Control Program 63
7.2 Instrumentation 63
7.3 Analysis of Convergence Point Data 63
7.4 Excavation Performance 63

8.0 GEOSCIENCE PROGRAM 64
8.1 Observation Hole Inspections 64
8.2 Fracture Mapping 67
8.3 Stratigraphic Mapping 67
8.4 Drilling and Geologic Core Descriptions 67

9.0 SUMMARY 68

10.0 REFERENCES 70

LIST OF TABLES

Table 1-1. Geomechanical Instrumentation System 13
Table 4-1. Closure Rates in the Salt Shaft Station 50
Table 5-1. Summary of Modifications and Ground Control Activities in the Access Drifts: July 1, 2017 to June 30, 2018 54
Table 5-2. Vertical Closure Rate Changes in Excess of Twenty Percent in the Access Drifts 56
Table 9-1. Comparison of Excavation Performance to System Design Requirements. 69

LIST OF FIGURES

Figure 1-1. WIPP Location 8
Figure 1-2. Underground Mining and Waste Disposal Configuration as of June 30, 2018 9
Figure 2-1. Regional Geology 19
Figure 2-2. Repository Level Stratigraphy of Panels 1, 2, 7, and 8 22
Figure 2-3. Repository Level Stratigraphy of Panels 3, 4, 5, and 6 24
Figure 3-1. Salt Shaft Stratigraphy 26
Figure 3-2. Salt Shaft Instrumentation 28
Figure 3-3. Salt Shaft Key Instrumentation 29
Figure 3-4. Waste Shaft Stratigraphy 31
Figure 3-5. Waste Shaft Instrumentation 33
Figure 3-6. Waste Shaft Key Instrumentation 34
Figure 3-7. Exhaust Shaft Stratigraphy 37
Figure 3-8. Sample Intake of Exhaust Shaft Air Monitoring System 38
Figure 3-9. Diagram of Exhaust Shaft Fixtures and Seepage Zones (Upper 200 ft) .. 39
Figure 3-10. Location of Interception Wells and Storage Containers 40
Figure 3-11. Water Removed from the Exhaust Shaft Catch Basin and the Interception Well System 41
Figure 3-12. Exhaust Shaft Instrumentation 43
Figure 3-13. Exhaust Shaft Key Instrumentation 44
Figure 3-14. Air Intake Shaft Stratigraphy 46
Figure 4-1. Salt Shaft Station Stratigraphy 48
Figure 4-2. Salt Shaft Station Instrumentation After Roof Beam Excavation 49
Figure 4-3. Waste Shaft Station Stratigraphy 51
Figure 4-4. Waste Shaft Station Instrumentation After Roof Beam Excavation 52
Figure 5-1. Typical Convergence Point Array Configurations Showing Anchor Designations 58
Figure 6-1. Location of Geomechanical Instruments in Panels 6 and 7 62
Figure 8-1. Example of Observation Hole Layout at Lower Horizon 65
Figure 8-2. Typical Fracture Pattern at Lower Horizon 66
Figure 8-3. Example Observation Hole Layout at Upper Horizon 66
Figure 8-4. Typical Fracture Patterns at Upper Horizon 67

ACRONYMS AND ABBREVIATIONS

ASTM	American Society for Testing and Materials
bp	before present
bsc	below shaft collar
CFR	Code of Federal Regulations
CH	contact-handled
cm	centimeter(s)
DOE	U.S. Department of Energy
EPA	U.S. Environmental Protection Agency
ft	foot (feet)
GAR	Geotechnical Analysis Report
GIS	geomechanical instrumentation system
in	inch(es)
km	kilometer(s)
kVA	kilovolt ampere(s)
lb(s)	pound(s)
m	meter(s)
Ma	million years
MB	marker bed
NMED	New Mexico Environment Department
OMB	orange marker bed
psi	pound(s) per square inch
RH	remote-handled
SDI	Salt Disposal Investigation
SDDI	Salt Defense Disposal Investigation
SPDV	Site and Preliminary Design Validation
TRU	transuranic
WIPP	Waste Isolation Pilot Plant

1.0 INTRODUCTION

This Geotechnical Analysis Report (GAR) presents and interprets geotechnical data from the underground excavations at the Waste Isolation Pilot Plant (WIPP). The data, which are obtained as part of a regular monitoring program, are used to characterize conditions, to compare actual performance to the design criteria, and to evaluate and forecast the performance of the underground excavations.

WIPP GARs have been available to the public since 1983. During operation of the Site and Preliminary Design Validation (SPDV) Program, the architect/engineer for the project produced these reports quarterly to document the geomechanical performance during and immediately after early excavations of the underground facility. Since completion of the construction phase of the project in 1987, the management and operating contractor for the facility has prepared these reports annually. This report describes the performance and condition of selected areas of the WIPP for the period July 1, 2017, to June 30, 2018.

This report is divided into 10 sections. Section 1 provides background information on the WIPP, its mission, and the purpose and scope of the geomechanical monitoring program. Section 2 describes the local and regional geology of the WIPP site. Sections 3 and 4 describe the geomechanical instrumentation in the shafts and shaft stations, present the data collected by that instrumentation, and provide interpretation of these data. Sections 5 and 6 present the results of geomechanical monitoring in the two main portions of the WIPP underground (the access drifts and the waste disposal area). Section 7 introduces the Salt Disposal Investigation (SDI) and Salt Defense Disposal Investigation (SDDI) areas. Section 8 discusses the results of the Geoscience Program, which include fracture mapping and observation borehole information. Section 9 summarizes the results of geomechanical monitoring and compares the current excavation performance to the design requirements. Section 10 lists references.

1.1 Location and Description

The WIPP facility is located in southeastern New Mexico, 26 miles (42 kilometers [km]) east of Carlsbad (Figure 1-1). The surface facilities were built on flat to gently rolling terrain that is characteristic of the Los Medaños area. The underground facility is being excavated approximately 2,150 feet (ft) beneath the surface in the Salado Formation. Figure 1-2 shows a plan view of the underground configuration of the WIPP as of June 30, 2018.

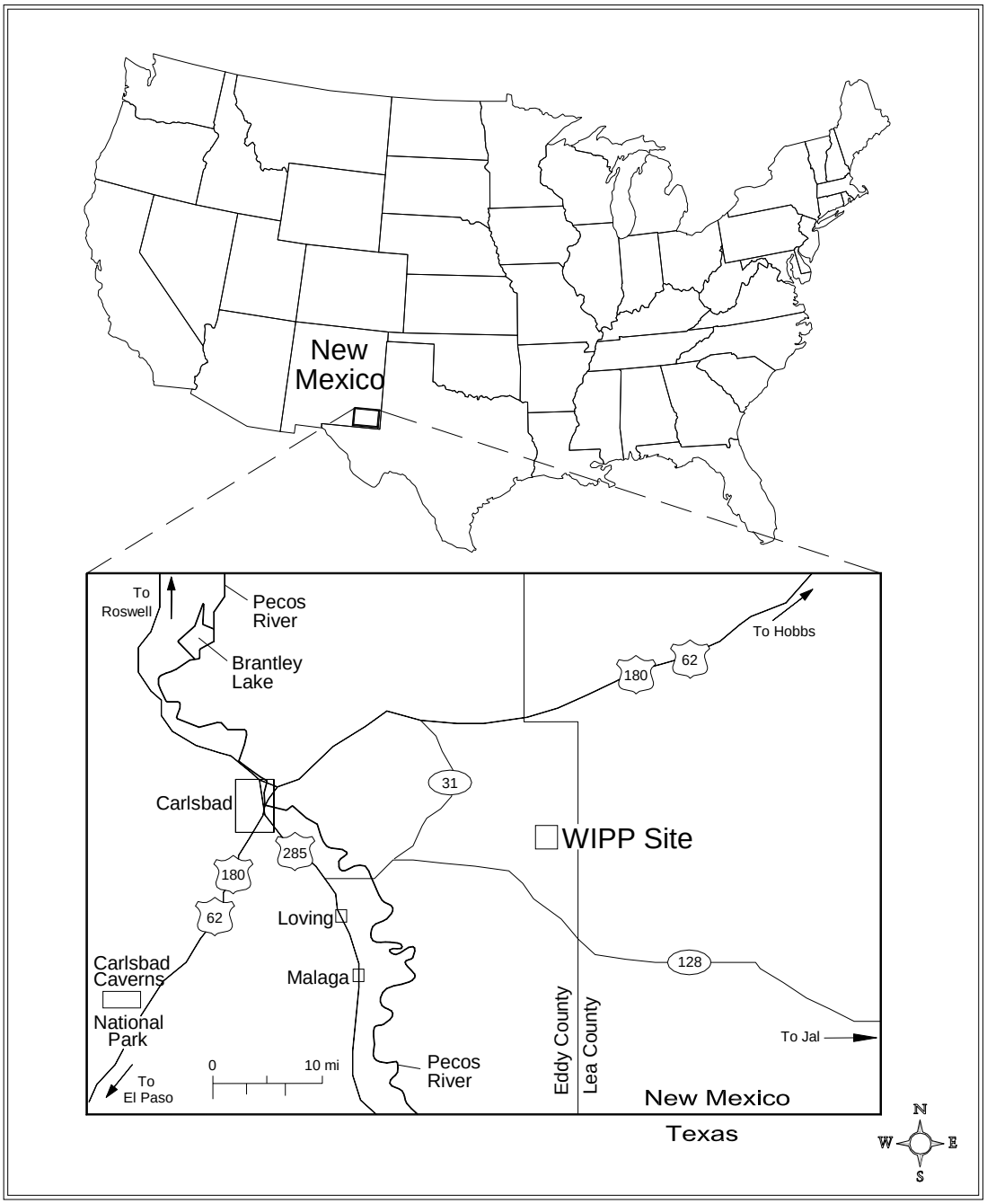

Figure 1-1. WIPP Location

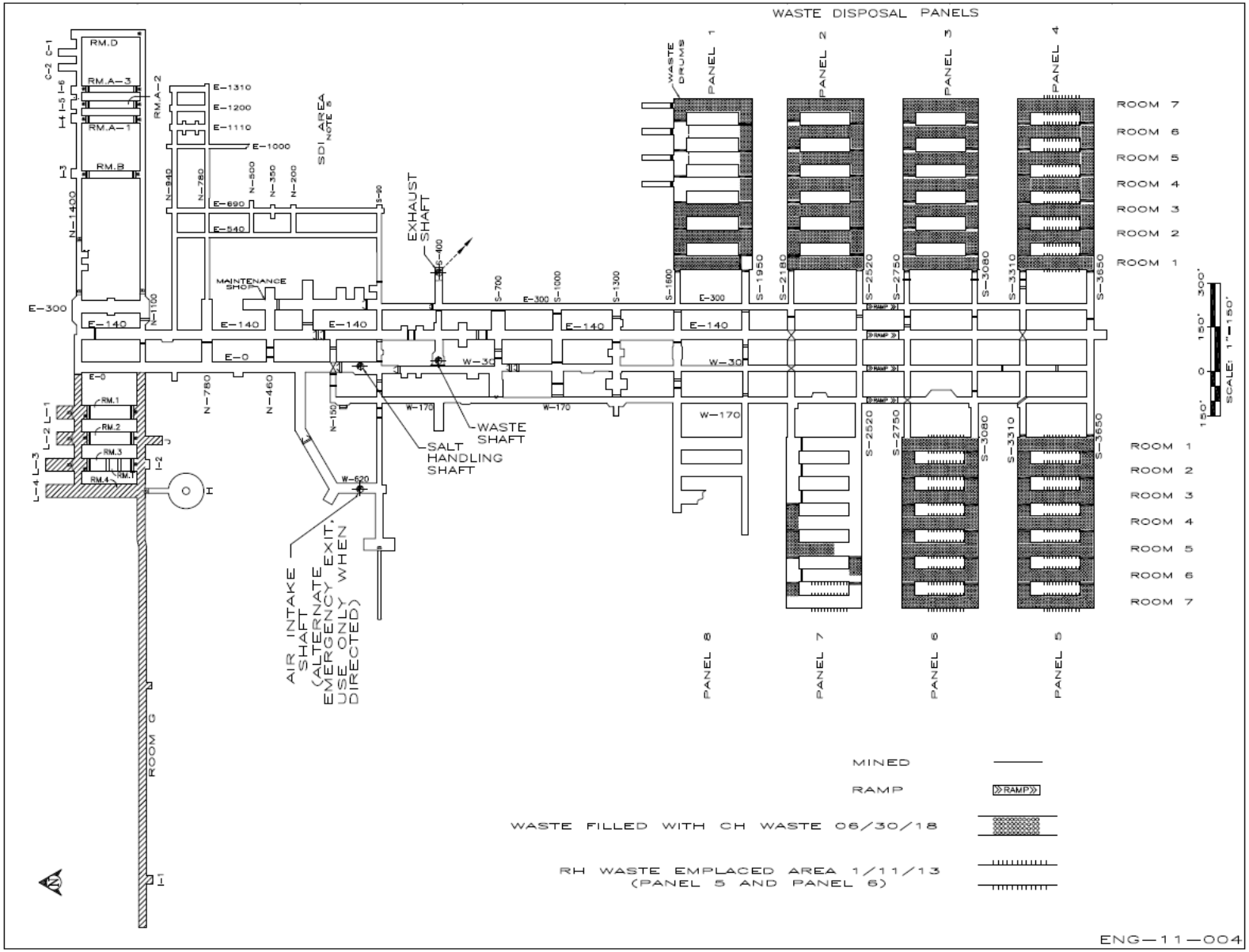

Figure 1-2. Underground Mining and Waste Disposal Configuration as of June 30, 2018

1.2 Mission

In 1979 Congress authorized the WIPP (Public Law 96-164, Department of Energy National Security and Military Applications of Nuclear Energy Authorization Act of 1980) to provide ". . . a research and development facility to demonstrate the safe disposal of radioactive wastes resulting from the defense activities and programs of the United States exempted from regulation by the Nuclear Regulatory Commission." To fulfill this mission, the U. S. Department of Energy (DOE) constructed a full-scale facility to demonstrate both technical and operational principles of the permanent disposal of transuranic (TRU) and TRU mixed wastes. Technical aspects are those concerned with the design, construction, and performance of the subsurface excavations. Operational aspects refer to the receiving, handling, and emplacement of TRU wastes in the facility. The facility was first used for *in situ* studies and experiments without the use of radioactive waste. The WIPP now receives, handles, and permanently disposes of TRU waste and TRU mixed waste.

1.3 Development Status

To fulfill its mission, the DOE developed the WIPP in a phased manner. The goal of the SPDV phase, begun in 1980, was to characterize the site and obtain *in situ* geotechnical data from underground excavations to determine whether site characteristics and *in situ* conditions were suitable for permanent waste disposal. During this phase, the Salt Shaft, a ventilation shaft, a drift to the southernmost extent of the proposed waste disposal area, a four-room experimental panel, and access drifts were excavated. Surface-based geological and hydrological investigations were also conducted. The data obtained from the SPDV investigations were reported in the Summary of the Results of the Evaluation of the WIPP Site and Preliminary Design Validation Program (DOE, 1983).

Based upon the favorable results of the SPDV investigations, additional activities were initiated in 1983. These included the construction of surface structures, conversion of the ventilation shaft for use as the Waste Shaft, excavation of the Exhaust Shaft, development of additional access drifts to the waste disposal area, excavation of the Air Intake Shaft, and excavation of additional experimental rooms to support research and development. Geotechnical data acquired during this phase were used to evaluate the performance of the excavations in the context of established design criteria (DOE, 1984). Results of these evaluations were reported in geotechnical field data reports (DOE, 1985; DOE, 1986a), and were summarized in the *WIPP Design Validation Final Report* (DOE, 1986b).

The *WIPP Design Validation Final Report* concluded that the facility, including waste disposal areas, could be developed and operated to fulfill the long-term mission of the WIPP (DOE, 1986b). All available information validated the design of underground openings to safely accommodate the permanent disposal of waste under routine operating conditions.

Panel 1 mining began in 1986 and was completed in 1988. Panel 1 was intended to receive waste for an initial operations demonstration and pilot plant phase that was scheduled to start in October 1988; however, the demonstration and pilot plant phase was not put into effect because waste could not be emplaced until permits were acquired.

In October 1996, the DOE submitted to the U.S. Environmental Protection Agency (EPA) a compliance certification application in accordance with Title 40 *Code of Federal Regulations* (CFR) Parts 191 and 194, which addressed the long-term (10,000-year) performance criteria for the disposal system. On May 18, 1998, the EPA published the final certification that allowed for the receipt of TRU waste at the WIPP. Immediately before this certification, the DOE Carlsbad Area Office completed an Operational Readiness Review, which is required by the DOE before the start-up or a process change of any nuclear facility. As a result of the review, the DOE Carlsbad Area Office notified the Energy Secretary on April 1, 1998, that the WIPP was operationally ready to receive waste. On March 26, 1999, the first shipment of TRU waste was received from Los Alamos National Laboratory. By the end of June 2013, many additional waste generator sites had shipped waste to the WIPP. The cleanup of several small-quantity waste generator sites, as well as one large-quantity site (Rocky Flats Environmental Technology Site), is now complete.

Waste disposal in Panels 1, 2, 3, 4, 5, and 6 is complete. Panels 1, 2, and 3 contain only contact-handled (CH) waste. The first remote-handled (RH) waste shipment arrived January 24, 2007. Panel 4 was the first to receive both CH and RH waste. CH and RH waste emplacement had commenced in Panel 7, but was halted initially by a truck fire in the underground. CH waste emplacement resumed in January 2017, and RH waste emplacement was resumed using shielded containers only, no additional borehole emplacement is planned for this period.

1.4 Purpose and Scope of Geomechanical Monitoring Program

As specified in the WIPP Hazardous Waste Facility Permit (New Mexico Environment Department [NMED], 2016), the purpose of the geomechanical monitoring program is to obtain *in situ* data to support the continuous assessment of the design for underground facilities.

Specifically, the program provides for:

- Early detection of conditions that could affect operational safety.
- Evaluation of disposal room closure that ensures adequate access.
- Guidance for design modifications and remedial actions.
- Data for interpreting the behavior of underground openings, in comparison with the established design criteria.

Data taken by or input into the geomechanical instrumentation system (GIS) are evaluated and reported in this GAR. This annual report fulfills the requirements set forth in Part 4.6.1.2., Attachment A2, Section A2-5b (2) of the WIPP Hazardous Waste Facility Permit (NMED, 2016), and 40 CFR §191.14, "Assurance Requirements," implemented through the certification criteria, 40 CFR Part 194.

The Geomechanical Monitoring Program generates the data for four of the compliance monitoring parameters:

- Creep closure and stresses
- Extent of deformation
- Initiation of brittle deformation
- Displacement of deformation features

The instrumentation system for geomechanical monitoring provides data for routine evaluations of safety, stability, and performance of underground openings. *In situ* data are also used to model long-term disposal system performance. Changes resulting from excavations are monitored by routine inspections of selected observation hole arrays and fracture mapping to detect and quantify occurrences of discontinuities such as fractures and bed separations. Analysis of data indicating areas of potential instability allows timely corrective action before the areas become unsafe. Other geoscience activities include geologic mapping and sampling, and seismic monitoring.

The GIS provides data that are collected, processed, and stored for analysis. The following subsections briefly describe the major components of the GIS.

1.4.1 Instrumentation

Instrumentation installed for measuring the geomechanical response of the shafts, drifts, and other underground openings includes convergence points, convergence meters, extensometers, rock bolt load cells, pressure cells, strain gauges, piezometers, and joint meters. Table 1-1 lists a summary of the specifications for geomechanical instrumentation.

Table 1-1. Geomechanical Instrumentation System

Instrument Type	Measures	Range[1]	Resolution[1]
Sonic probe extensometer	Cumulative deformation	0–2 in	0.001 in
Convergence point (tape extensometer)	Cumulative deformation	2–50 ft	0.001 in
Wire convergence meter	Cumulative deformation	0–40 in	0.001 in
Embedded strain gauge	Cumulative strain	0–3000 μin/in	1 μin/in
Spot-welded strain gauge	Cumulative strain	0–2500 μin/in	1 μin/in
Rock bolt load cell	Load	0–50 tons	40 lb
Earth pressure cell	Pressure	0–1000 psi	1 psi
Piezometer	Fluid pressure	0–500 psi	0.5 psi
Joint meter	Cumulative deformation	0–4 in	0.001 in
Vibrating wire extensometer	Cumulative deformation	0–4 in	0.001 in
Wire extensometer	Cumulative deformation	0–20 in	0.001 in

[1] Manual readout boxes for the instruments were manufactured to render measurements in U.S. customary units. Range and resolution measurement units have not been converted to metric units. Measurements from these instruments have been converted for presentation elsewhere in this report.

1.4.2 Data Acquisition

Geomechanical instruments are read either manually, using portable devices, or remotely, by electronically polling the stations from the surface, in accordance with approved operating procedures. Remotely read instruments are connected to one of the underground data loggers, and readings are collected by initiating the appropriate polling routine. Upon completion of a verification process, data are transferred to a computer database. Manual readout devices are taken to instrument locations in the underground. Data are recorded on data sheets and later entered into an electronic database.

The underground data acquisition system consists of instruments, polling devices, and a communications network. Instruments are connected to polling devices that are installed in electrical enclosures near the instrument locations. Polling devices are connected by a data link to a surface computer.

Whether acquired manually or remotely, geomechanical data are entered into the database files of the GIS data processing system. The data processing system consists of computer programs that are used to enter, reduce, and transfer the data to permanent storage files. Additional routines allow access to the permanent storage files

for numerical analysis, tabular reporting, and graphical plotting. Copies of the instrumentation database and data plots are available upon request.[3]

1.4.3 Data Evaluation

Rounding and significant digits are used in the data tables of this document. The reference document is American Society for Testing and Materials (ASTM) document ASTM D 6026-06, "Standard Practice for Using Significant Digits in Geotechnical Data."

Closure measurements are acquired manually from convergence point anchors and remotely from convergence meters. Data are presented in plots of closure versus time. Closure rate data are calculated and presented as part of the data analysis. Extensometers provide displacement data from instrumented rods or wires anchored at various depths. Plots show displacement versus time for individual anchors.

Displacement rate data from the hole (collar) to the deepest anchor are presented in the data analysis.

The annual closure rate is calculated as follows:

$$Rate\left(\frac{inches}{year}\right) = \left[\frac{reading2 - reading1}{date2 - date1}\right] * 365.25\frac{days}{year}$$

reading = the change from the initial reading (inches)

reading1 = reading closest to the beginning of the reporting period

reading2 = reading closest to the end of the reporting period

Comparisons between closure rates of the previous and current reporting periods are presented as percent changes in rate and are calculated as follows:

$$percent\ change\ in\ rate = (Rate_{Current\ Period} - Rate_{Previous\ Period}) / (Rate_{Previous\ Period}) \times 100\%$$

Rock bolt load cells are used to determine bolt support performance. Plots show load versus time for each instrumented bolt.

Earth pressure cells and strain gauges are used to determine the stresses and deformation in and around the shaft liners. Data are depicted in time-based plots.

[3] Instrumentation data and data plots are presented in "Geotechnical Analysis Report for July 2017 - June 2018 Supporting Data" (DOE/WIPP-19-3610 Volume 2). The document is available upon request from the National Technical Information Service. See page ii for details and addresses.

Piezometers are used to measure the gauge pressure of groundwater and are installed in the shafts at varying elevations to monitor the hydraulic head acting on the shaft liners. Data are plotted as pressure versus time.

Joint meters, installed perpendicular to a crack, monitor the dilation of the crack with time. Data are presented as displacement versus time.

1.4.4 Data Errors

GIS data are processed through a comprehensive database management system. Whether acquired manually or remotely, GIS data are processed and permanently stored according to approved procedures. On occasion, erroneous readings can occur. There are several possible explanations for erroneous readings, including the following:

- The measuring device was misread.
- The reading was recorded incorrectly.
- The measuring device was not functioning within specifications.

When a reading is believed to be erroneous, the suspect reading is evaluated, and, if necessary, a second reading is collected. If the second reading falls in line with the instrument trend, the first reading is discarded and the second reading is entered in the database. If the second reading and subsequent readings remain out of the instrument trend, the ground conditions in the vicinity of the instrument are assessed to determine the reason for the discrepancy. In addition, the reading frequency may be increased.

2.0 GEOLOGY

This section provides a summary of the stratigraphy of the WIPP region and the site. Readers desiring further geologic information may consult the *Geological Characterization Report, WIPP Site, Southeastern New Mexico* (Powers et al., 1978). This report was developed as a source document on the geology of the WIPP site for individuals, groups, or agencies seeking basic information on geologic history, hydrology, and geochemistry, or detailed information, such as physical and chemical properties of repository rocks. A more recent survey of WIPP stratigraphy is included in the *Geologic Mapping of the Air Intake Shaft at the Waste Isolation Pilot Plant* (Holt and Powers, 1990).

2.1 Regional Stratigraphy

The stratigraphy in the vicinity of the WIPP site includes rocks of Permian (295 to 250 million years [Ma] before present [bp]), Triassic (250 to 203 Ma), and Quaternary (1.75 Ma to present) ages. The descriptions of formations provided in this section are given in order of deposition (oldest to youngest), beginning with the Castile Formation (Figure 2-1).

2.1.1 Permian

The Permian system in southwestern North America is divided into four series. The last of these, the Ochoan Series, contains the host rock in which the WIPP repository is located.

The Ochoan Series is of mostly marine origin and consists of four formations: three evaporite formations (the Castile, the Salado, and the Rustler) and one redbeds formation (the Dewey Lake). The Ochoan evaporites overlie marine limestones and sandstones of the Guadalupian Series (Delaware Mountain Group). The younger redbeds represent a transition from the lower evaporite deposition to fluvial deposition on a broad, low-relief, fluvial plain. The Permian rocks are overlain by fluvial deposits of the Triassic and Quaternary periods.

2.1.1.1 Castile Formation

The Castile Formation, lowermost of the four Ochoan formations, is approximately 1,250 ft (380 meters [m]) thick in the WIPP vicinity. Lithologically, the Castile is the least complex of the evaporite formations and is composed chiefly of interbedded anhydrite and halite, with limestone present in minor amounts.

2.1.1.2 Salado Formation

The Salado Formation comprises nearly 2,000 ft of evaporites, primarily halite. The formation is subdivided into three informal members: the unnamed lower member, the McNutt potash zone, and the unnamed upper member. Each member contains similar amounts of halite, anhydrite, and polyhalite, and is differentiated on the basis of soluble potassium- and magnesium-bearing minerals. The WIPP disposal horizon is located within the unnamed lower member, 2,150 ft below the surface.

2.1.1.3 Rustler Formation

The Rustler Formation is subdivided into five members, starting from its base: the Los Medaños Member, the Culebra Dolomite Member, the Tamarisk Member, the Magenta Dolomite Member, and the Forty-niner Member.

In the vicinity of the WIPP site, the Rustler is approximately 310 ft thick and thickens to the east. The lower portion (Los Medaños Member) contains primarily fine sandstone to mudstone with lesser amounts of anhydrite, polyhalite, and halite. Bedded and burrowed siliciclastic sedimentary rocks with cross-bedding and fossil remains signify the transition from the strongly evaporitic environments of the Salado to the brackish lagoonal environments of the Rustler (Holt and Powers, 1990).

The upper portion of the Rustler contains interbeds of anhydrite, dolomite, and mudstone. The Culebra Dolomite Member is generally brown, finely crystalline, and locally argillaceous. The Culebra contains rare to abundant vugs with variable gypsum

and anhydrite filling, and is the most transmissive hydrologic unit within the Rustler. The Tamarisk Member consists of lower and upper sulfate units separated by a unit that varies laterally from mudstone to mainly halite. The Magenta Dolomite Member is a gypsiferous dolomite with abundant primary sedimentary structures and well-developed algal features. The Forty-niner Member consists of lower and upper sulfate units separated by a mudstone that displays sedimentary features and bedding. East of the site area, halite correlates with the mudstone. The Culebra and Magenta Dolomite members are persistent and serve as important marker units.

2.1.1.4 Dewey Lake Redbeds

The Dewey Lake Redbeds is the uppermost of the Ochoan Series formations. Within the series, the Dewey Lake represents a transition from the lower marine evaporite deposition to fluvial deposition on a broad, low-relief, fluvial plain. The redbeds, approximately 475 ft thick, consist of predominantly reddish-brown interbedded fine-grained sandstone, siltstone, and claystone. This formation is differentiated from others by its lithology and distinctive color (both of which are remarkably uniform), and by sedimentary structures, including horizontal- and cross-laminae and ripple marks. The redbeds also contain locally abundant greenish-gray reduction spots and gypsum filled fractures. The formation thickens from west to east due to eastward dips and erosion to the west.

2.1.2 Triassic

The only Triassic rocks present in the WIPP region belong to the Dockum Group.

2.1.2.1 Dockum Group

The Dockum Group consists of fine-grained floodplain sediments and coarse alluvial debris of Triassic age. From a pinch-out near the center of the WIPP site it thickens eastward, forming an erosional wedge. Local subdivisions of the Dockum Group are the Santa Rosa Sandstone and the Chinle Formation; however, only the Santa Rosa occurs in the vicinity of the site. It consists primarily of poorly sorted sandstone with conglomerate lenses and thin mudstone partings, and contains impressions and remnants of fossils. These rocks have more variegated hues than the underlying uniformly colored Dewey Lake.

2.1.3 Quaternary

Quaternary Period deposits include the Gatuña Formation, Mescalero Caliche, and surficial sediments.

2.1.3.1 Gatuña Formation, Mescalero Caliche, and Surficial Sediments

The Gatuña Formation (ranging in age from approximately 1.3 million to 600,000 years bp) (Powers and Holt, 1993) is a stream-laid deposit overlying the Dockum Group in the WIPP vicinity. At the site center, the formation consists of poorly consolidated sand, gravel, and silty clay at a thickness of approximately 13 ft. The Gatuña Formation is light red and mottled with dark stains. The unit contains abundant calcium carbonate, but is poorly cemented. Sedimentary structures are abundant (Powers and Holt, 1993, 1995).

The Mescalero Caliche (approximately 500,000 years bp) is approximately 4 ft thick in the WIPP vicinity. The Mescalero is a hard, resistant soil horizon that lies beneath a cover of wind-blown sand. The horizon is petrocalcic (i.e., very strongly cemented with calcium carbonate). Petrocalcic horizons form slowly beneath a stable landscape at the average depth of infiltration of soil moisture, and indicate stability and integrity of the land surface. Many of the surface buildings at the WIPP are founded on top of the Mescalero Caliche.

Surficial sediments include sandy soils developed from eolian material and active dune areas. The Berino Series (a soil type) covers about 50 percent of the site and consists of deep sandy soils that developed from wind-worked material of mixed origin. Based on sample analyses, the Berino soil from the WIPP site formed 330,000 ± 75,000 years bp.

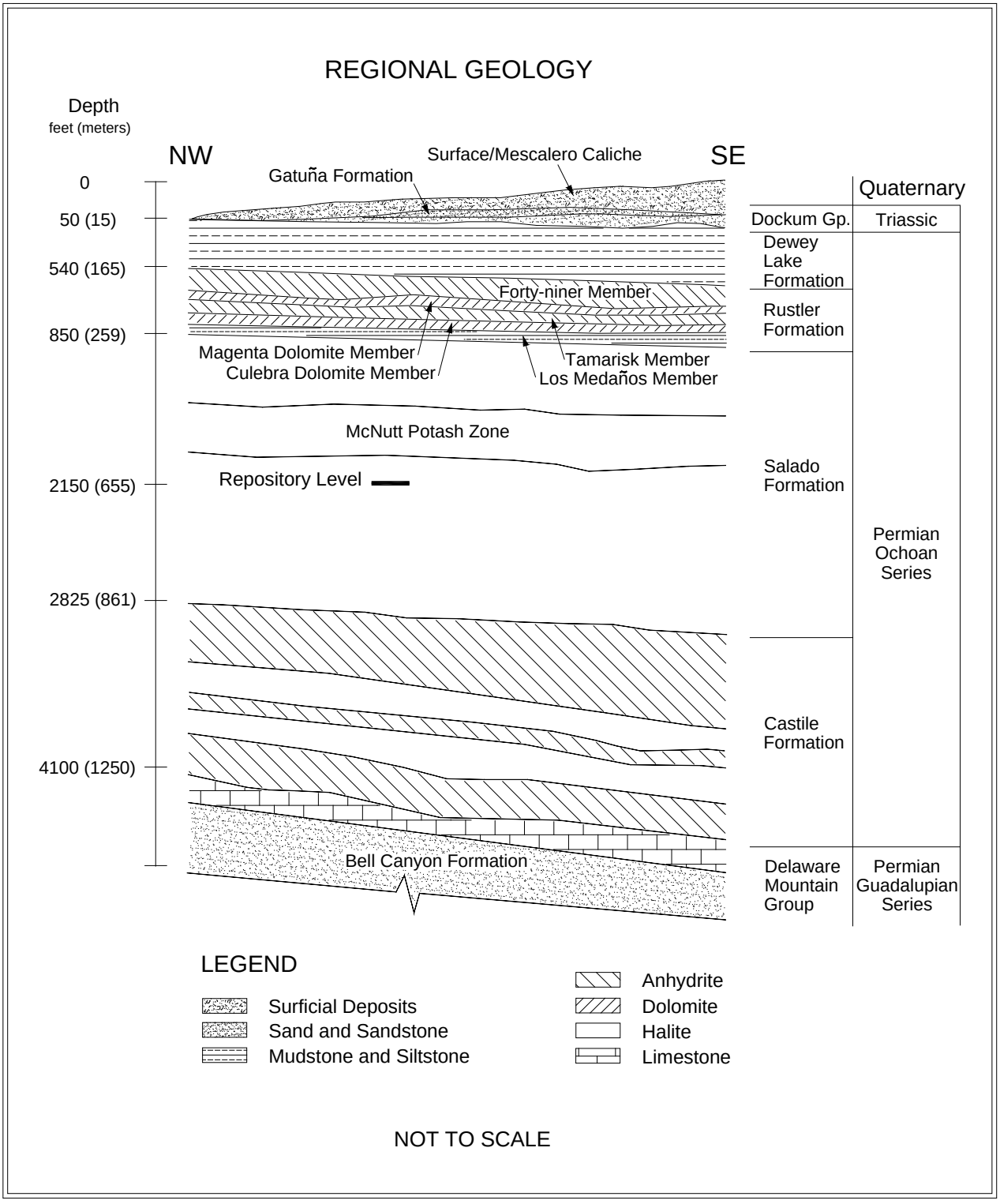

Figure 2-1. Regional Geology

2.2 Underground Facility Stratigraphy

The WIPP disposal horizon lies near the midpoint of the Salado Formation. The Salado was deposited in a shallow saline lagoon environment, which progressed through numerous inundation and desiccation cycles that are reflected in the formation. An "ideal" cycle progresses upward as follows: a basal layer consisting predominantly of claystone, followed by a layer of sulfate, which is in turn followed by a layer of halite. The entire sequence is capped by a bed of argillaceous (clay-rich) halite accumulated during a period of mainly subaerial exposure.

A regional system used for numbering the more significant sulfate beds within the Salado designates these beds as marker beds (MBs), counted from MB100 near the top of the formation to MB144 near the base. The repository is located between MB138 and MB139 within a sequence of laterally continuous depositional cycles as described above. Within this sequence, layers of clay and anhydrite that are locally designated (as shown) can have a significant impact on the geomechanical performance of the excavations. Clay layers provide surfaces along which slip and separation can occur, whereas anhydrites form brittle layers that do not deform plastically.

In the vicinity of the WIPP, the stratigraphy is fairly continuous and uniform. Beds generally dip toward the south-southeast at a slope of approximately 3 percent.

2.2.1 Disposal Horizon Stratigraphy of Panels 1, 2, 7, and 8

This disposal horizon contains Panels 1, 2, 7, and 8, all the shaft areas, the shop areas, the SPDV areas (which are now closed), and all the access drifts north of S-2620. Farther south, the four main entries rise in a ramp that starts at S-2620 and ends at S-2740. Panel 7 excavation was completed in January 2013. Panel 8 mining restarted in February 2018, and 13,300 tons of salt cumulatively has been mined.
Most underground excavations are located within this disposal horizon (Figure 2-2). In it, the Orange Marker Bed (OMB) lies near the middle of the rib (i.e., the excavation wall). The OMB is a laterally consistent unit of moderate to light reddish-orange translucent halite, about 6 inches (in) (15 centimeters [cm]) thick, that is used as a point of reference during excavation.

MB139 lies approximately 11.5 ft (3.5 m) below the OMB. MB139 is a 20- to 32-in (50- to 80-cm)-thick layer of polyhalitic anhydrite. The top of the anhydrite undulates up to 15 in (38 cm), while the bottom is sub-horizontal and is underlain by Clay E.

Above MB139, a unit of halite terminates at the base of the OMB. Within this unit, polyhalite is locally abundant and decreases upward, while argillaceous material increases upward.

Above the OMB, a thin band of argillaceous halite gives way to a thick sequence of clear halite that becomes increasingly argillaceous upward and is capped by Clay F. This constitutes a thin layer occasionally interrupted by partings and breaks and is

readily visible in the upper ribs. Above Clay F, another sequence of halite begins that, as in lower sequences, becomes increasingly argillaceous upward. This sequence terminates at the Clay G/Anhydrite "b" interface, approximately 6.5 ft (2 m) above the roof of most disposal horizon excavations, forming a roof beam that typically acts as a structural unit.

The roof of some disposal horizon excavations (e.g., the E-140 drift between S-1000 and S-1950) has been excavated to the upper contact of Anhydrite "b." In this case, a roof beam is formed by the next depositional sequence beginning with Anhydrite "b" and progressing upward to the Clay H/Anhydrite "a" interface, approximately 6.5 ft (2 m) above the upper contact of Anhydrite "b."

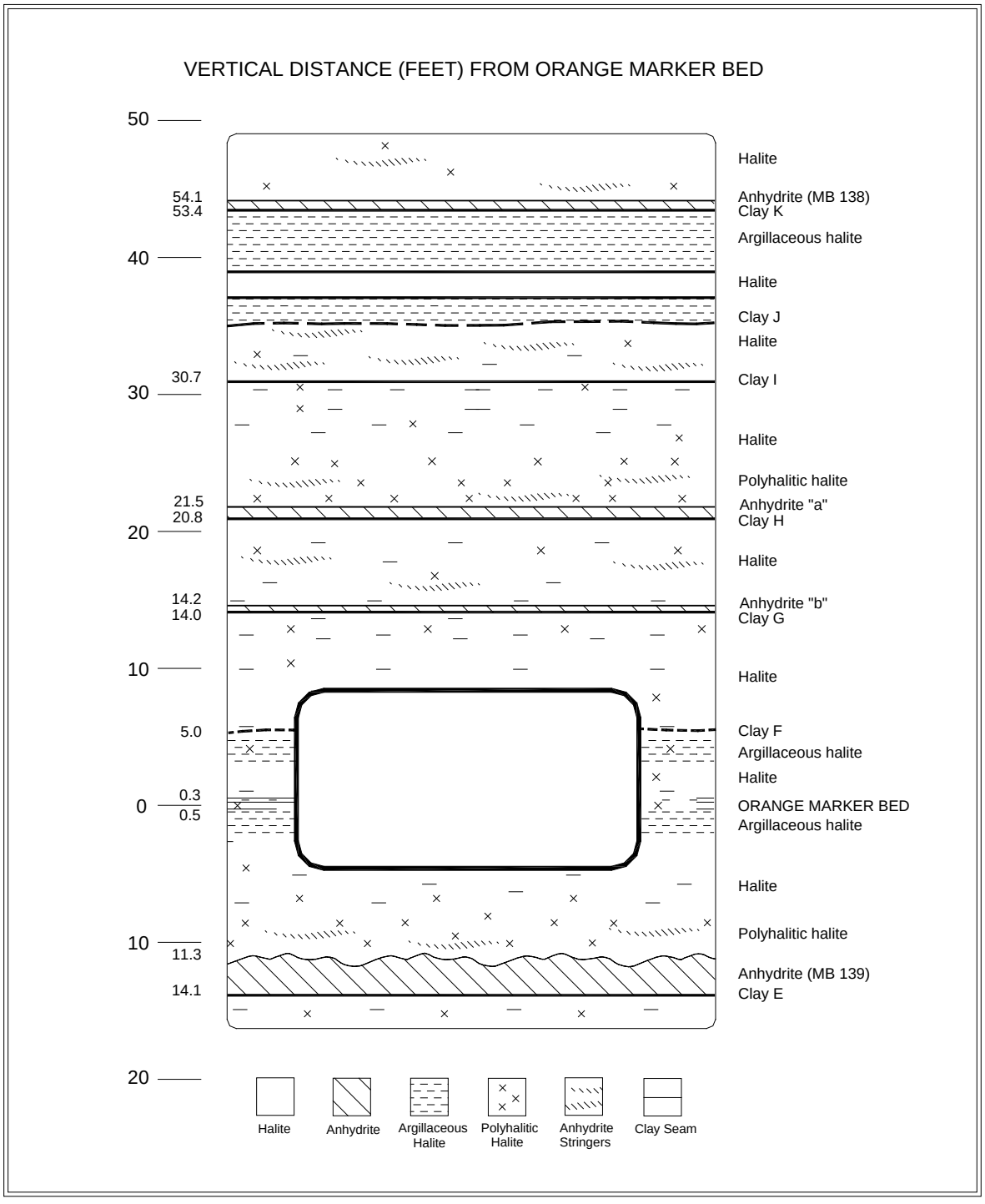

Figure 2-2. Repository Level Stratigraphy of Panels 1, 2, 7, and 8

2.2.2 Disposal Horizon Stratigraphy of Panels 3, 4, 5, and 6

Field observations and computer modeling indicated that moving the disposal horizon stratigraphically upward (so that the roof was located at Clay G) would improve long-term ground conditions and provide a more stable roof configuration without significantly impacting repository performance. In 2000, the decision was made to implement this change by moving the mining horizon up approximately 6 ft. Subsequently, in 2000 and 2001, ramps were mined in the W-170, W-30, E-140, and E-300 drifts between S-2520 and S-2750 (Figure 1-2). As a result, the disposal horizon for Panels 3, 4, 5, and 6, and the associated connecting drifts, lies above the horizon for the other panels (Figure 2-3).

In this horizon, the OMB lies at or below the floor. MB139 lies about 12 ft (3.7 m) below the floor. The roof lies at or slightly above Anhydrite "b." Clay G/Anhydrite "b" is used as the mining reference during excavation of this disposal horizon. Locally continuous anhydrite stringers are found within this horizon that extend to Clay H at Anhydrite “a,” generally concentrated in the lower portion toward Anhydrite "b." These effectively divide the roof beam itself into a series of thinner, independent beams, thereby weakening the overall beam strength.

2.2.3 Northeast Area Stratigraphy

The Northeast Area, formerly an experimental area, is now deactivated and closed for access. These excavations lie at a higher stratigraphic level than the disposal excavations. Floors are at Anhydrite "b." As in the lower units, the halite intervals between the clay seams/anhydrite beds contain relatively pure halite that becomes increasingly argillaceous upward. Above Clay I, two more halite intervals complete the underground facility stratigraphy. Clay J, at the top of the first of these intervals, may consist of a distinct seam or merely an argillaceous zone. Clay K tops the second interval and is overlain by MB138.

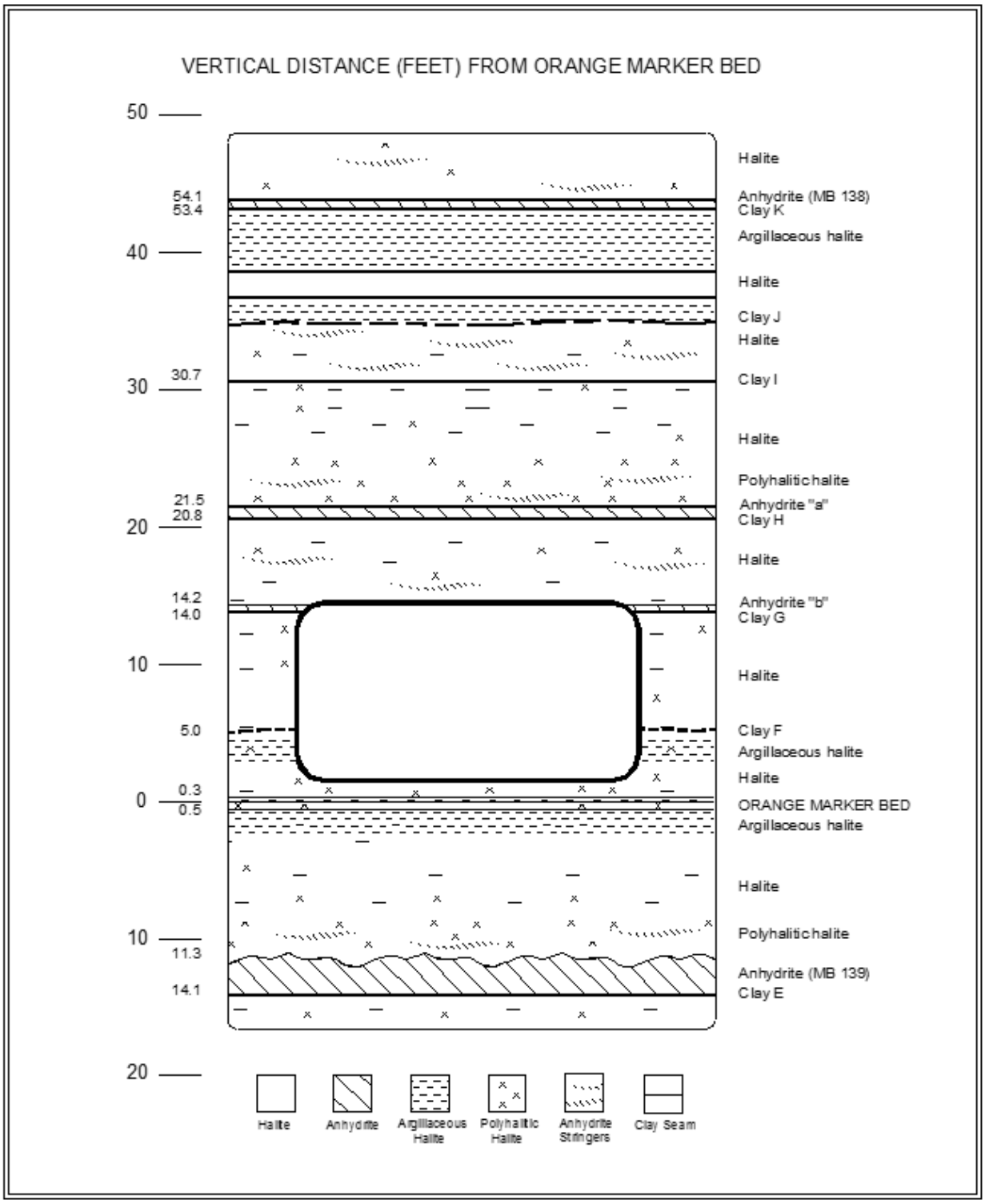

Figure 2-3. Repository Level Stratigraphy of Panels 3, 4, 5, and 6

3.0 PERFORMANCE OF SHAFTS AND KEYS

Four shafts connect the surface with the underground at the WIPP. They are the Salt Shaft, which is used primarily for removing excavated salt from the underground and for transporting personnel and materials; the Waste Shaft, which is used primarily for transporting TRU waste to the underground and for transporting personnel and materials; the Exhaust Shaft, which is used to exhaust the ventilation air from the underground; and the Air Intake Shaft, which is the primary source of fresh air ventilation to the underground. This section describes the geomechanical performance of these shafts.

Although much of the instrumentation installed in the shafts has failed through the years, there are no plans to replace it. The project has a good understanding of the expected movements in the shafts. Monitoring results up to the point of instrument failure did not indicate unusual shaft movements or displacements. Continued periodic visual inspections confirm the expected shaft performance and provide necessary observations to evaluate shaft performance. Replacement of failed instrumentation will not provide significant additional information.

3.1 Salt Shaft

The first construction activity undertaken by the SPDV Program was the excavation of the Exploratory Shaft. This shaft was subsequently referred to as the Construction and Salt Shaft, and is currently designated the Salt Shaft (see Figure 1-2). The shaft was drilled from July 4 to October 24, 1981, and geologically mapped in the spring of 1982 (DOE, 1983). Figure 3-1 presents the stratigraphy in the shaft.

The Salt Shaft is lined from the surface to 846 ft (258 m) with steel casing having an inside diameter of 10 ft (3 m). The thickness of the steel liner (including external stiffener rings) increases from 0.62 in (1.6 cm) at the top to 1.5 in (3.8 cm) at the key. Cement grout was placed between the liner and the rock face. The 10-ft (3-m)-diameter steel liner extends through the concrete shaft key to 880 ft (268 m). The shaft key is a 37.5-ft (11.4-m)-long, reinforced concrete structure that begins 3.5 ft (1.07 m) above the bottom of the steel liner. From the key to the bottom at 2,298 ft (700 m), the shaft has a nominal diameter of 12 ft (4 m).

Wire mesh anchored by rock bolts is installed in sections of the lower shaft as a safety screen to contain rock fragments that may become detached. The shaft extends approximately 140 ft (43 m) below the repository horizon in order to accommodate the skip loading equipment and a sump.

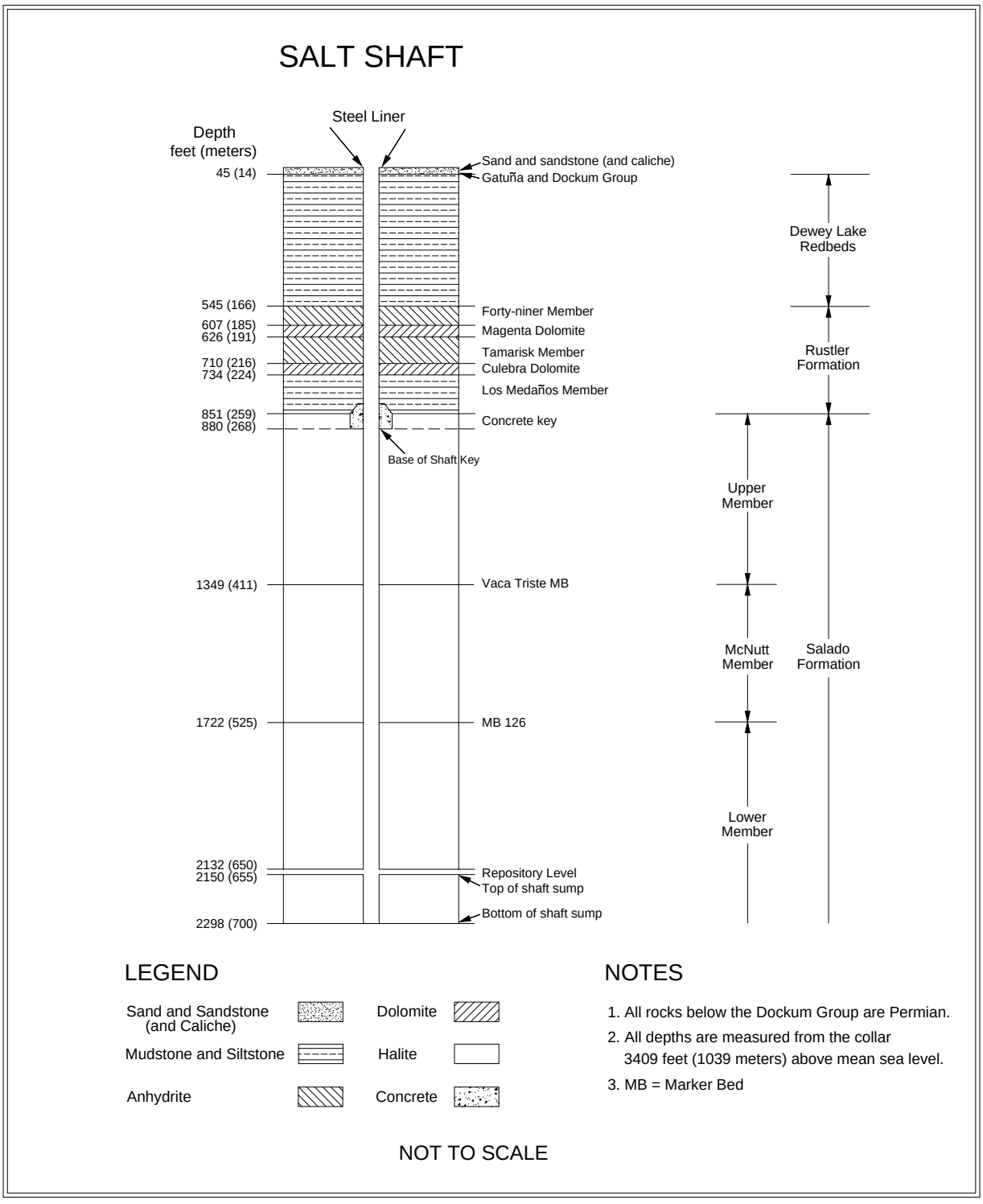

Figure 3-1. Salt Shaft Stratigraphy

3.1.1 Shaft Observations

Underground operations personnel conduct weekly visual inspections. These inspections are performed principally to assess the condition of the hoisting and mechanical systems, but they also include examining the shaft walls for water seepage, loose rock, or sloughing. Visual inspections during this reporting period found that the shaft remains in satisfactory condition. Only routine ground control activities were required.

3.1.2 Instrumentation

Geomechanical instruments (radial convergence points, extensometers, and piezometers) were installed at various levels in the shaft from April through July 1982 (Figures 3-2 and 3-3). Instruments in the shaft key included strain gauges, pressure cells, and piezometers. Radial convergence points were installed prior to outfitting. Upon completion of shaft outfitting, no more readings were taken.

Nine piezometers continue to provide data. The fluid pressures recorded at the end of this reporting period range from approximately 8 pounds per square inch (psi) at the 802-ft (259-m) level (upper section of the shaft key) to 195 psi at the 691-ft (211-m) level in the Tamarisk Member. The recorded pressures for this reporting period are generally consistent with the readings from the previous reporting period. The fluid pressure on the shaft liner will continue to be monitored on a regular basis.

Four earth pressure cells were installed in the key section during concrete emplacement at the 860-ft (262-m) level. These instruments measure the normal stress between the concrete key and the Salado Formation as salt creep loads up the key structure. Two of the earth pressure cells continue to provide data. These instruments have indicated essentially no contact pressure since their installation (readings resemble instrument drift at a zero pressure).

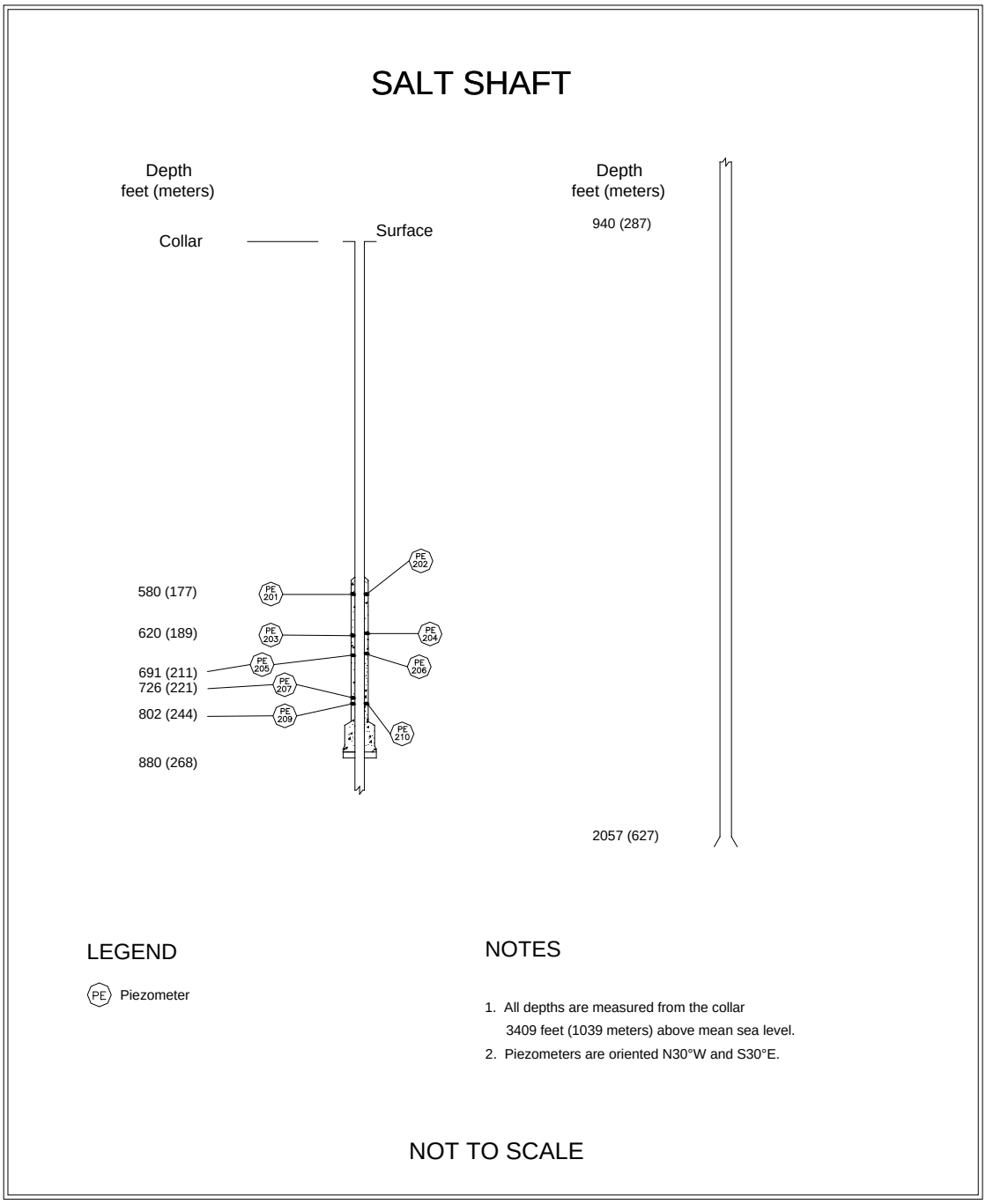

Figure 3-2. Salt Shaft Instrumentation

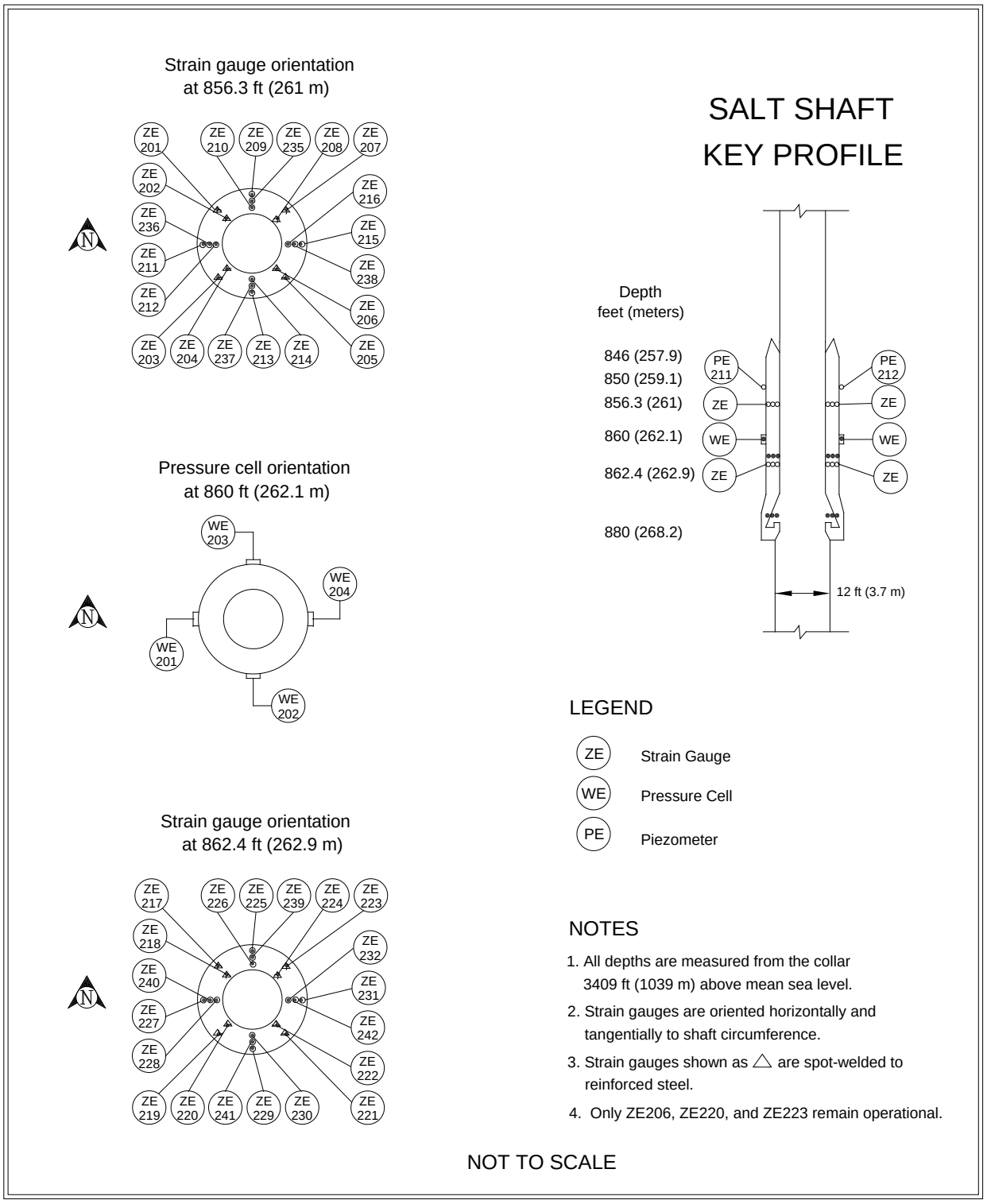

Figure 3-3. Salt Shaft Key Instrumentation

Sixteen spot-welded and 24 embedment strain gauges were installed on and in the shaft key concrete at both the 856.3-ft (261-m) level and at the 862.4-ft (263-m) level. One spot-welded strain gauge is still functioning at the 856.3-ft (261-m) level. Strains at the 856.3-ft (261-m) level recorded a maximum strain of 677 microstrain and a minimum of 443 microstrain.

Eighteen embedment strain gauges are still functioning. The strains at the 856.3-ft (261-m) level ranged from -970 to 1021 microstrain. The strains from the 6 embedment strain gauges at the 862.4-ft (263-m) level were 78 to 961 microstrain. The strain recorded by the spot-welded strain gauge and the embedment strain gauges during this reporting period are similar to the strains recorded by these instruments at the end of the previous reporting period.

3.2 Waste Shaft

As part of the SPDV Program, a 6-ft (2-m)-diameter ventilation shaft, now referred to as the Waste Shaft, was excavated from December 1981 through February 1982 (see Figure 1-2). This shaft and the Salt Shaft created a two-shaft underground air circulation system. From October 11, 1983, to June 11, 1984, the shaft was enlarged to a diameter of 20 to 23 ft (6 to 7 m) and lined above the key. Stratigraphic mapping (Figure 3-4) was conducted during shaft enlargement from December 9, 1983, to June 5, 1984 (Holt and Powers, 1984).

The Waste Shaft is lined with non-reinforced concrete having a 19-ft (6-m) inside diameter from the surface to the top of the key at 837 ft (255 m). Liner thickness increases from 10 in (25 cm) at the surface to 20 in (51 cm) at the key. The key is 63 ft (19 m) long and 4.25 ft (1.3 m) thick, and is constructed of reinforced concrete. The bottom of the key is 900 ft (274 m) below the surface. The diameter of the shaft is 20 ft (6 m) at the bottom of the key and increases to 23 ft (7 m) just above the shaft station. The shaft below the key is lined with wire mesh anchored by rock bolts. The diameter of 23 ft (7 m) extends to a depth of approximately 2,286 ft (697 m), with the shaft sump comprising the lower 119 ft (36 m) of that interval.

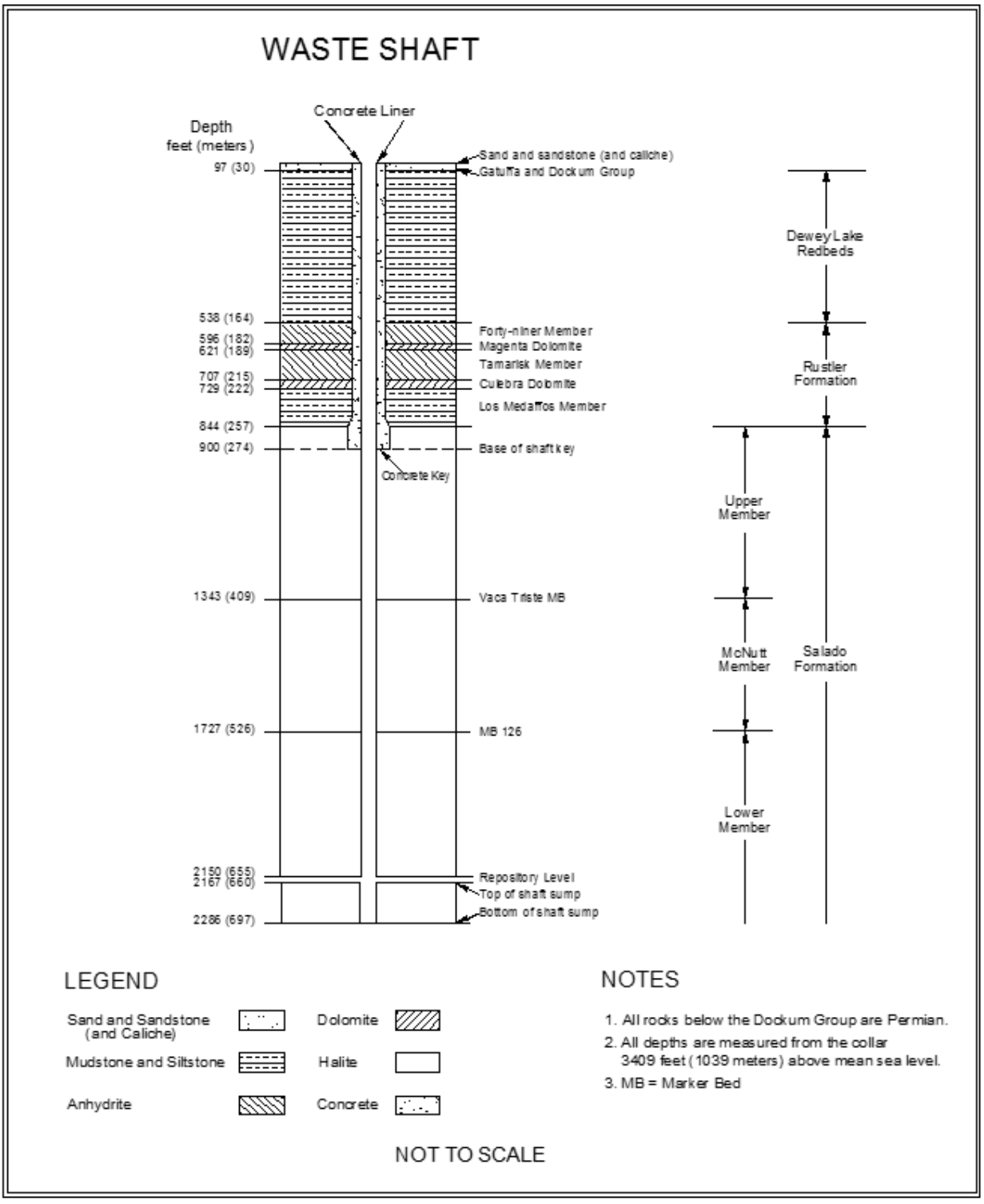

Figure 3-4. Waste Shaft Stratigraphy

3.2.1 Shaft Observations

Underground operations personnel conduct weekly visual inspections, principally to assess the condition of the hoisting and mechanical systems, but also to examine the shaft walls for water seepage, loose rock, or sloughing. The visual inspections found that the shaft was in satisfactory condition. No ground control activities other than routine maintenance were required.

3.2.2 Instrumentation

Radial convergence points, extensometers, piezometers, and earth pressure cells were installed in the Waste Shaft between August 27 and September 10, 1984. Radial convergence points were installed prior to the outfitting. Upon completion of shaft outfitting, no more radial convergence readings were taken. Figure 3-5 and Figure 3-6 show the instrument locations.

Nine multi-position extensometers were installed in arrays 1,071 ft (326 m), 1,566 ft (477 m), and 2,059 ft (628 m) below the surface, as shown in Figure 3-5. Each array consists of three extensometers. No extensometer data have been collected in recent years due to the malfunction of the data acquisition equipment. Since the extensometer type installed in the shaft over 30 years ago is no longer manufactured, remote data acquisition equipment for these extensometers is also unavailable.

Twelve piezometers were installed in the lined section of the Waste Shaft on September 7 and 8, 1984, to monitor fluid pressure behind the shaft liner and the key section. As of this reporting period, data is no longer being received from any of the piezometers.

Four earth pressure cells were installed in the key section of the Waste Shaft during concrete emplacement, which occurred between March 23 and April 3, 1984. Earth pressure cells measure the normal stress between the concrete key and the Salado Formation as salt creep loads the key structure. As of this reporting period, data is no longer being received from any of the earth pressure cells.

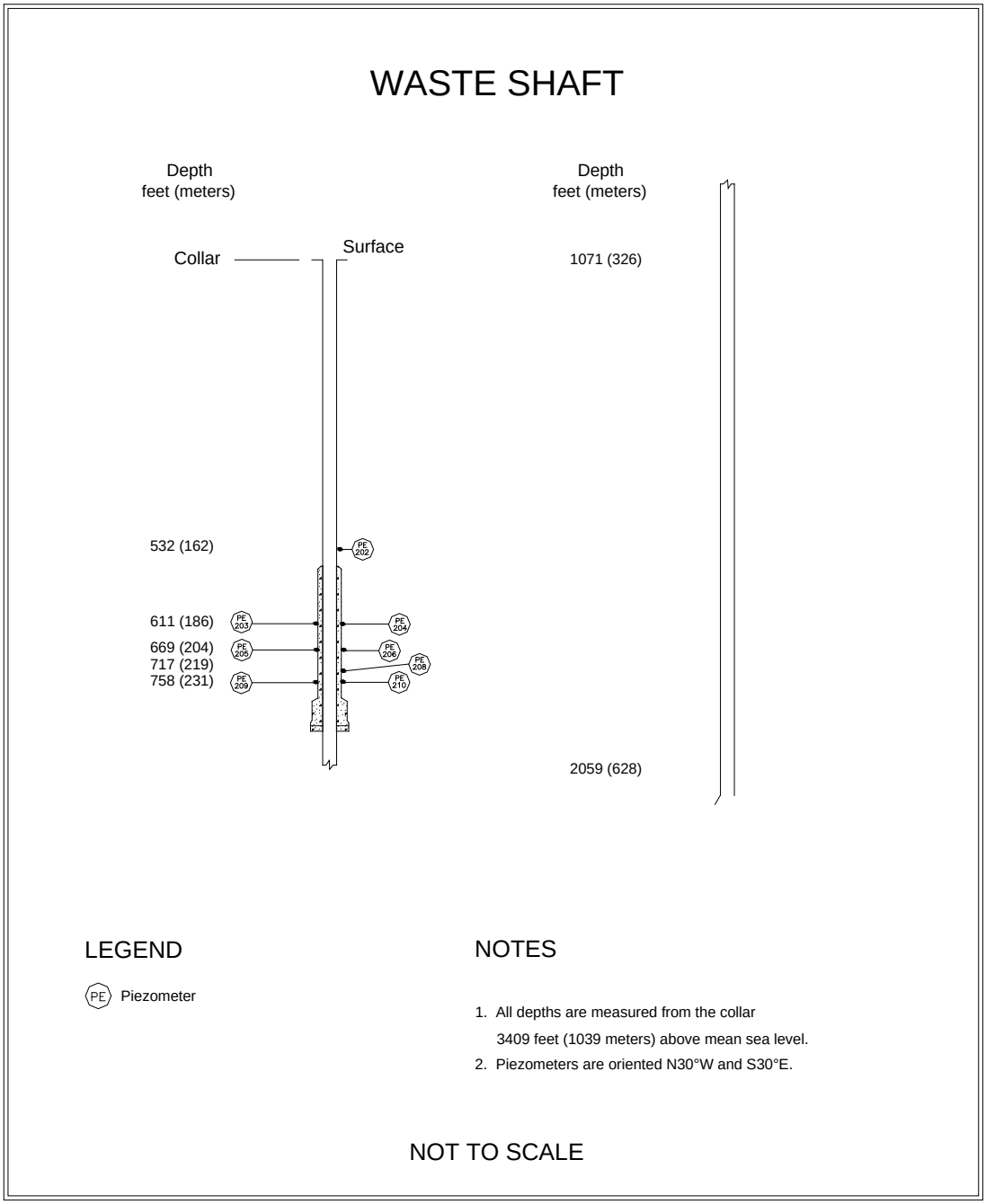

Figure 3-5. Waste Shaft Instrumentation

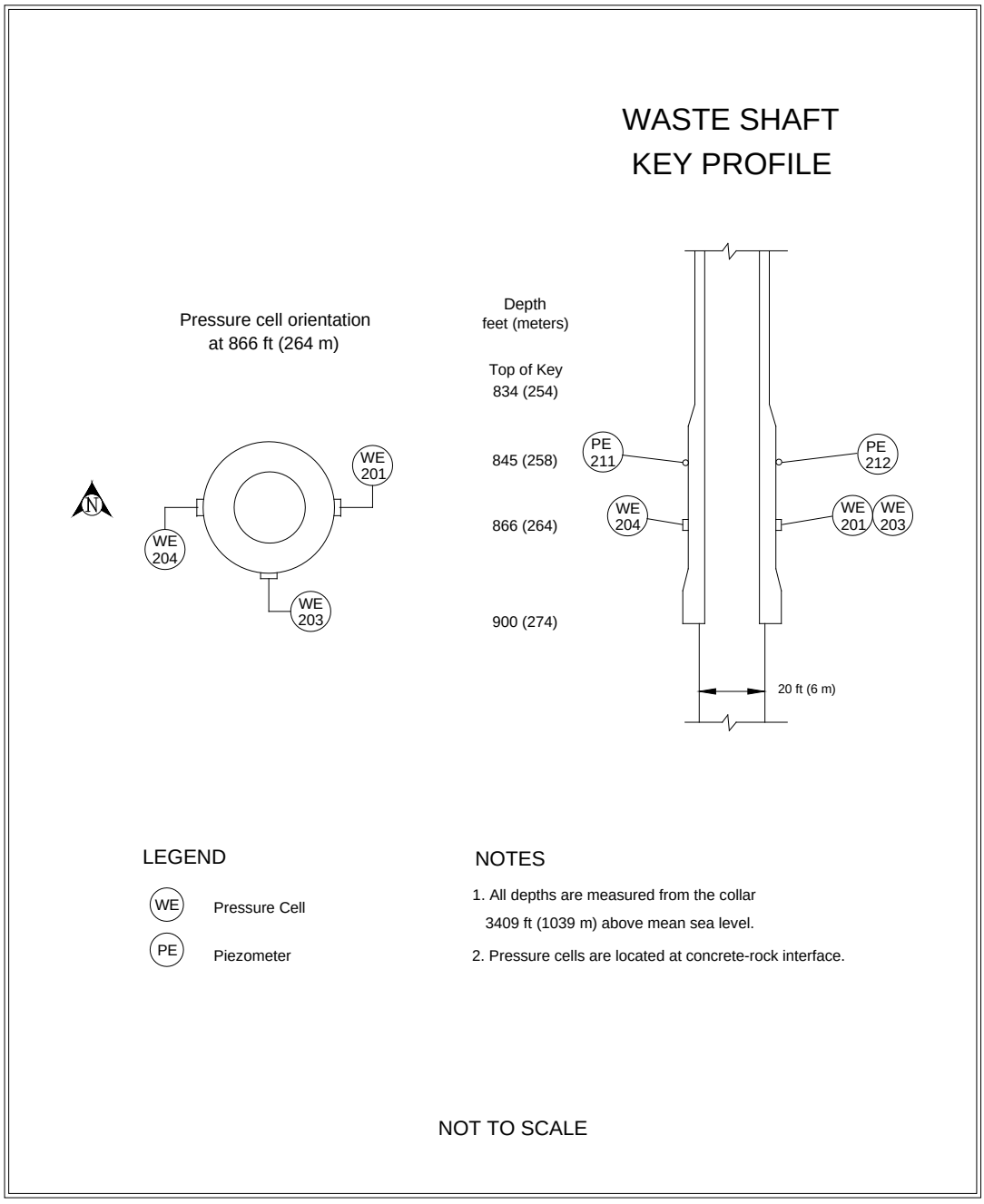

Figure 3-6. Waste Shaft Key Instrumentation

3.3 Exhaust Shaft

The Exhaust Shaft was drilled from September 22, 1983, to November 29, 1984, to establish a route from the underground to the surface for exhaust air (Figure 1-2). Stratigraphic mapping was conducted from July 16, 1984, to January 18, 1985 (DOE, 1986). Figure 3-7 illustrates the shaft stratigraphy.

The Exhaust Shaft is lined with non-reinforced concrete from the surface to the top of the shaft key at 844 ft (257 m). The liner thickness increases from 10 to 16 in (25 to 41 cm) over that interval. The key is 63 ft (19 m) long and 3.5 ft (1 m) thick. The shaft diameter below the key is 15 ft (5 m), and the interval below the key is lined with wire mesh anchored by rock bolts. The shaft terminates at the facility horizon, approximately 2,150 ft (655 m) deep. This shaft has no sump.

3.3.1 Quarterly Shaft Inspection

Quarterly video inspections of the Exhaust Shaft are conducted according to approved WIPP procedures. Inspections are performed to evaluate the condition and to verify the integrity of the shaft. The shaft is examined for cracks, corrosion, salt buildup, seeps, and debris. In addition, inspections examine the condition of anchors, brackets, and down-hole equipment. Quarterly shaft inspections were performed this reporting period, in September and November of 2017 and March and June of 2018.

3.3.1.1 Video Camera

Video inspections use a custom-designed, vertical-drop color camera in an aerodynamic housing, with pan, tilt, and zoom capability. The camera is suspended by a dual-armored cable. The cable contains five copper conductors and two multi-mode optical fibers. It is reeled out by a winch mounted in a control trailer. Inspections are recorded electronically.

3.3.1.2 Shaft Inspection Observations

Quarterly video inspection observations concentrate on four major areas: air-monitoring components, shaft liner, shaft walls, and equipment support and cabling. The air-monitoring components consist of one tube that provides a conduit for air-velocity measurements and three tubes for monitoring possible radionuclides within the exhaust air stream, as shown in Figure 3-8. The video inspection includes examination of each device, including the transport assembly, guide tubes, the sample intake, and the support brackets that extend from Station "A" above the shaft to the shaft collar. Air-monitoring components extend from the collar 21 ft into the shaft. Video inspections indicate that the air-sampling components can accumulate salt buildup of up to several inches thick.

The Exhaust Shaft liner is examined for cracks, seepage, and general shaft stability. Currently, there are three principal zones of seepage in the shaft. The first is about 50 to 55 ft below the shaft collar (bsc), the second is about 60 to 65 ft bsc, and the third is about 80 to 85 ft bsc, as shown in Figure 3-9. Monitoring of seepage horizons started before 1995. Water entering the shaft through these cracks is believed to originate from a perched-shallow-water-bearing horizon at the base of the Santa Rosa Formation. The fluid level in the Santa Rosa near the shaft is about 48 to 49 ft below the surface. Based on examination of inspection videos, the flow rate into the shaft during this reporting period is estimated at about 1 to 1½ gallons per minute. Seepage cracks are confined primarily to the eastern side of the shaft wall.

When fluid was detected seeping into the shaft, a catch basin was designed and installed at the base of the Exhaust Shaft to intercept water and prevent it from draining into the Waste Shaft sump. Fluid was removed from the catch basin from March 1996 through October 2005 as needed. The catch basin was damaged in 2004 by fallen debris, either salt or instrumentation cables or both. A new catch basin was fabricated and installed in December 2004. This basin was damaged in August 2005, most likely the result of fallen debris. An interception well system was installed between November 2005 and March 2006 to replace the catch basin. Interception wells were drilled down gradient in S-400 between E-140 and E-300 (Figure 3-10). The interception well system initially consisted of four 30-ft-deep 9-7/8-in-diameter fluid collection holes with a submersible pump and pressure transducer in each. Fluid is pumped from each hole to a series of storage containers in S-550. A data-acquisition system monitors the fluid level in each hole, turning the pump on and off between set limits as needed.

Between February 2 and 6, 2008, two additional fluid collection holes, OH631 and OH632, were drilled in S-400 to improve the total volume of fluid recovered by the interception well system. They replaced OH613 and OH614, which generated little fluid. As with the previous four holes, the additional holes were drilled at 9-7/8-in diameter to a total depth of 30 ft. Pumps were pulled from OH613 and OH614 and installed in OH631 and OH632. Figure 3-10 shows the location of the interception well system and the 500-gallon storage containers.

It was noted during the Exhaust Shaft video inspections performed in July 2017 and June 2018 that shaft conditions were generally good. There were no significant changes in the thickness of the salt in the shaft plenum, ranging from zero to several feet thick. The principle cracks and seepage horizons in the shaft liner were located at about 63-65 ft and 82-84 ft bsc. Based on examination of the fluid flow from the shaft liner and evaluation of previous shaft inspections, the estimated average flow rate of fluid seeping through the shaft liner into the shaft was 1.1 gallons per minute. The thickness of the salt has significantly decreased in the upper portion of the shaft between the shaft collar and 600 ft below ground surface. At the same time, there appears to be an increase in the buildup of salt along the shaft walls in the form of stalactites in the lower portion of the shaft.

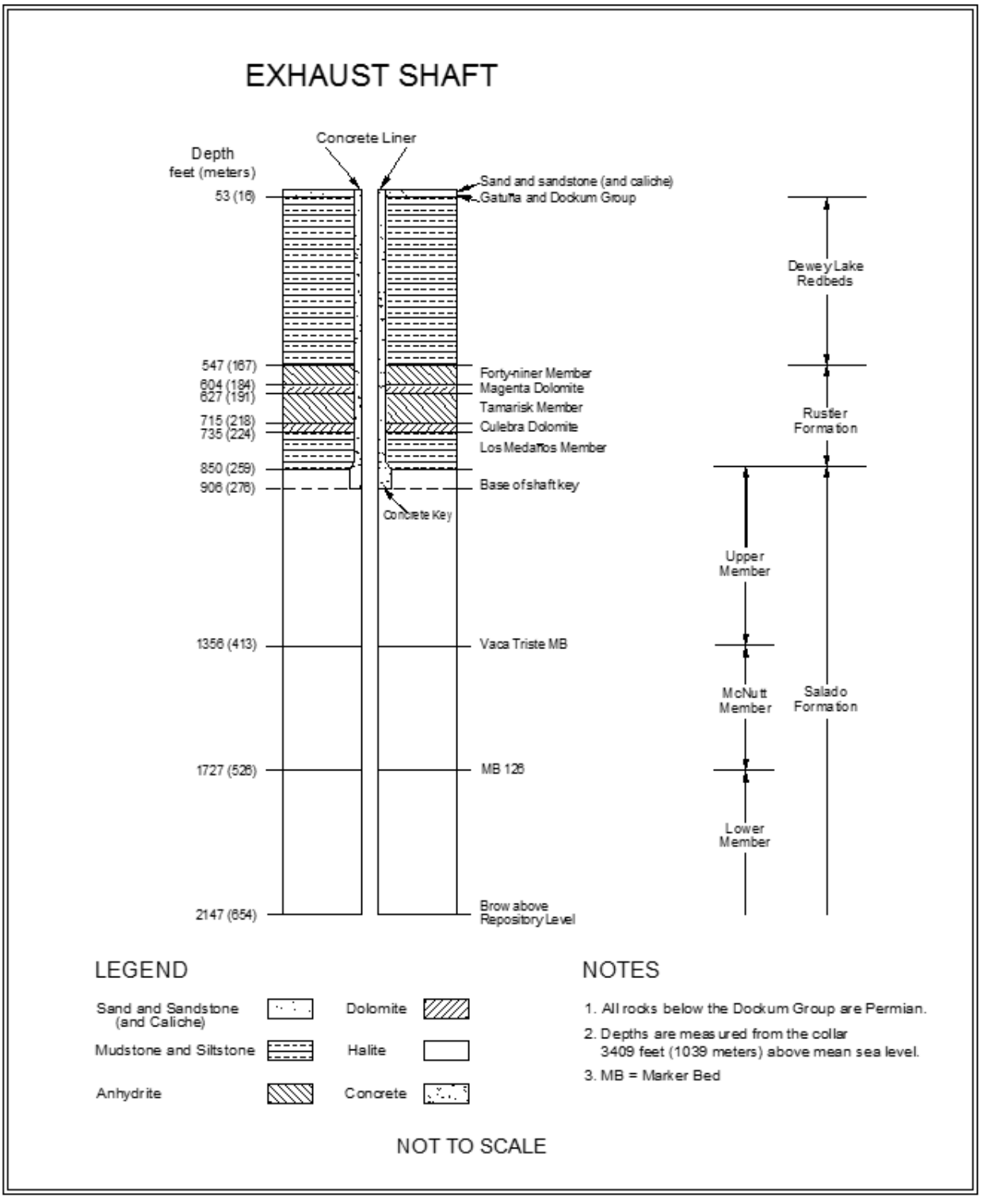

Figure 3-7. Exhaust Shaft Stratigraphy

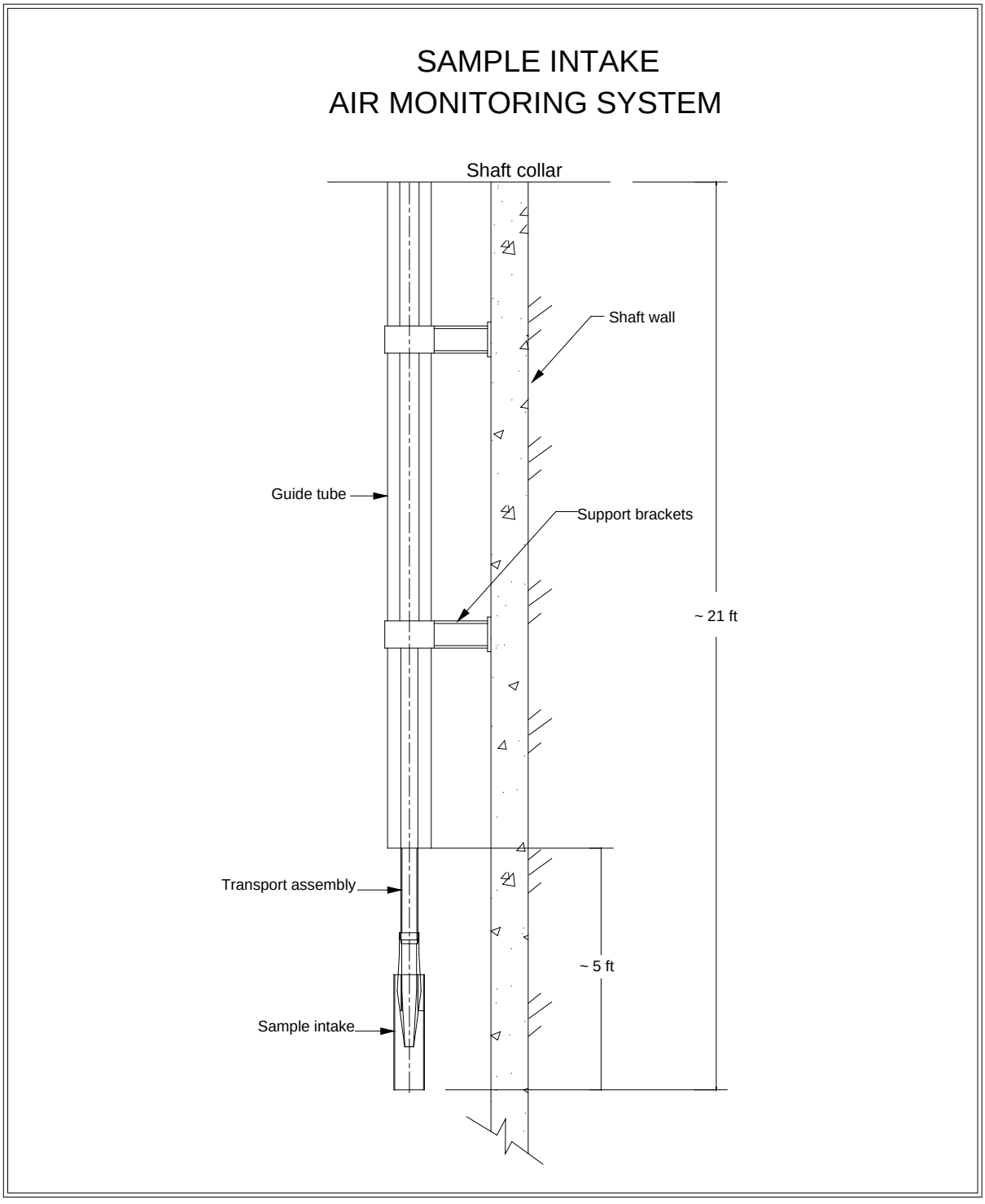

Figure 3-8. Sample Intake of Exhaust Shaft Air Monitoring System

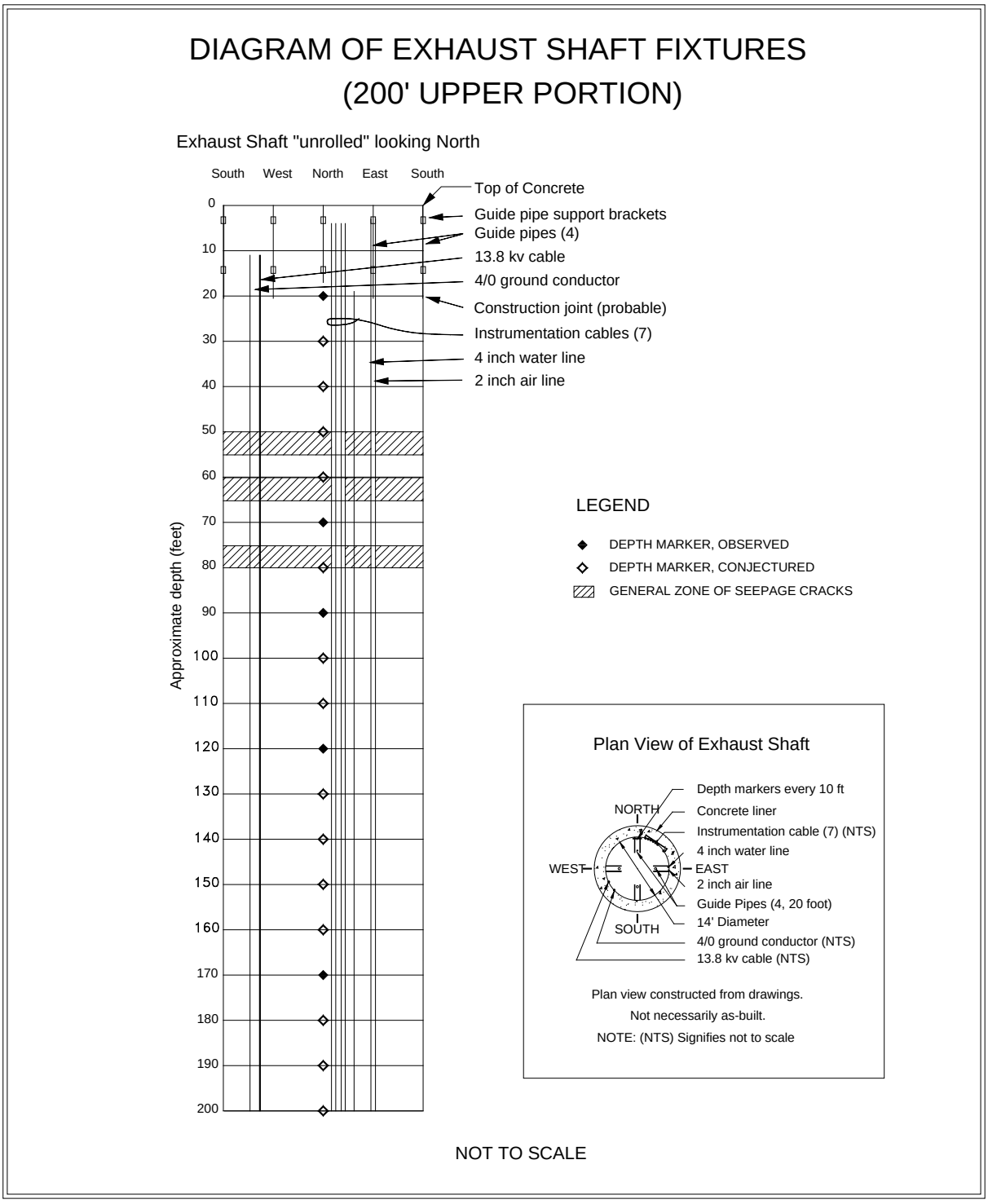

Figure 3-9. Diagram of Exhaust Shaft Fixtures and Seepage Zones (Upper 200 ft)

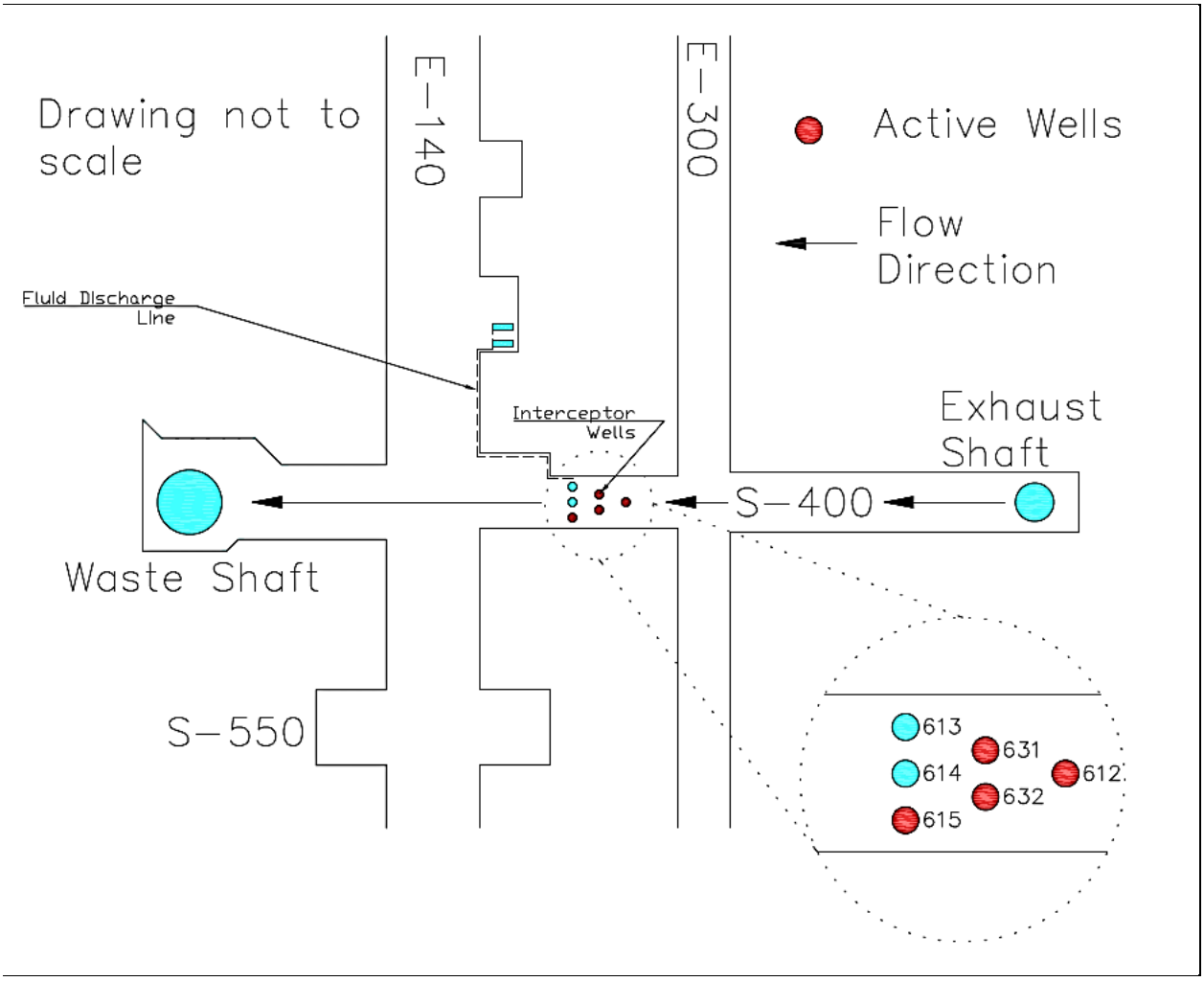

Figure 3-10. Location of Interception Wells and Storage Containers

Figure 3-11 presents the volume of fluid removed from the catch basin from July 1997 through June 2006, and by the interception well system from July 2006 through June 2018. The largest reported volumes are typically associated with periods of reduced ventilation and increased humidity. No fluid was collected by the system during this reporting period due to the relocation of the components from S-550 to S-300. The system is expected to be operational before the end of the second quarter of 2019. For a discussion of the factors affecting the quantity of fluid produced in the Exhaust Shaft, refer to DOE/WIPP-00-2000, *Brine Generation Study* (DOE, 2000).

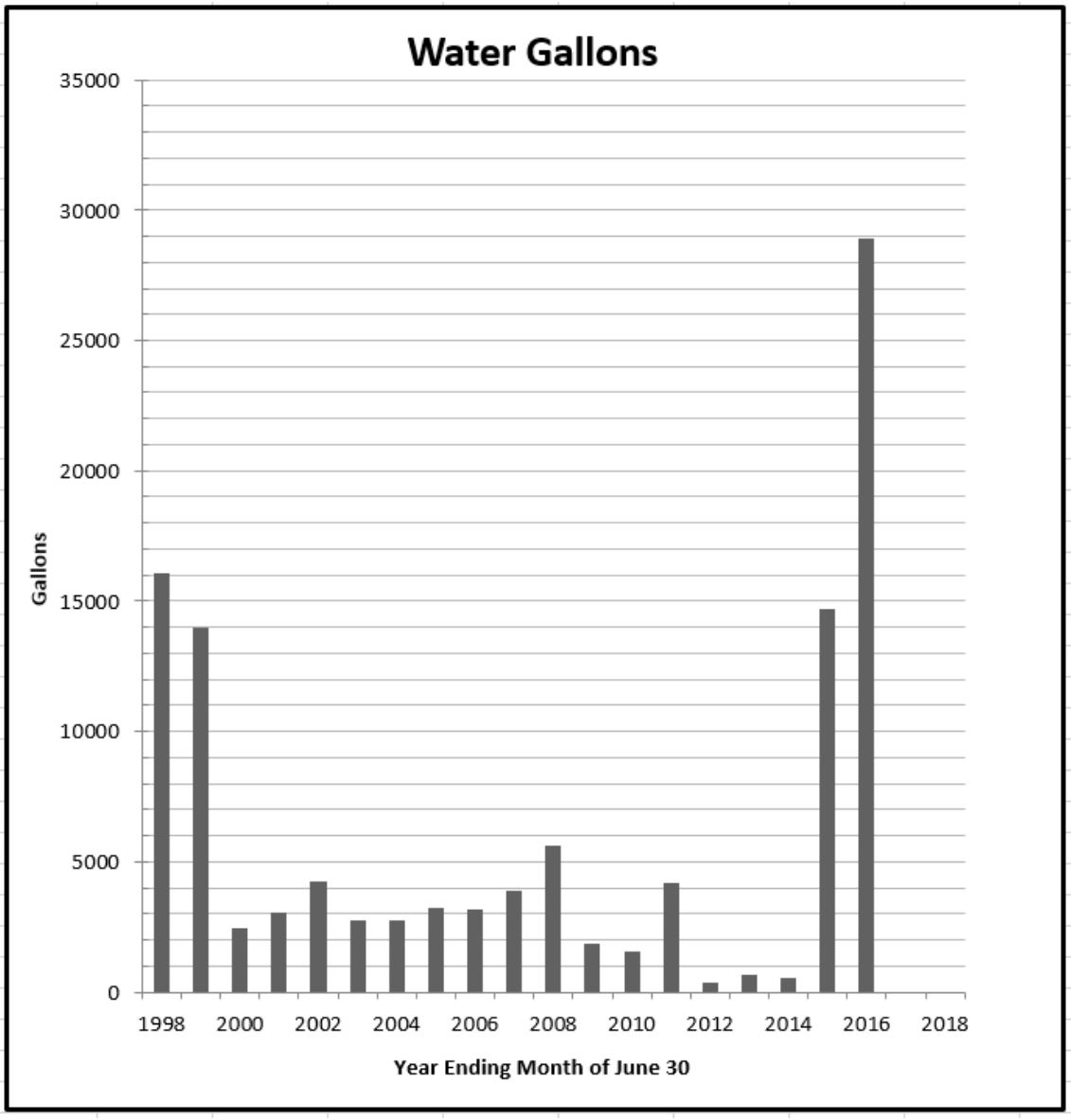

Figure 3-11. Water Removed from the Exhaust Shaft Catch Basin and the Interception Well System

The shaft walls were examined for salt buildup, cracks, moisture, and encrustations, with particular attention paid to power cables, instrument cables, air and water lines, and the three water rings occurring at the base of the Magenta and Culebra members of the Rustler Formation and at the bottom of the shaft key. The condition of the shaft wall varies depending on airflow, humidity, temperature, and underground mining activities. The principal areas in the shaft with significant salt buildup were the three water rings at the Magenta, the Culebra, and the key, and along upper portions of the shaft generally associated with power cables, support brackets, instrument cables, and the air and water lines.

Though the Magenta and Culebra water rings are encrusted with salt buildup, no water appears to originate from the shaft liner or water rings. Most of the seepage was observed along the east face of the shaft wall near the instrumentation cables and the air and water lines in the upper section of the shaft. Though the presence of water is an inconvenience, requiring periodic disposal, at this time it does not appear to have created any hazard or affected the structural integrity of the shaft. However, brine increases the probability of corrosion and deterioration of utility hangers and brackets. There are no visible signs of dissolution of the salt below the key.

Sporadic salt buildup continues on remaining cables in the shaft. The long-term implication of salt buildup is increased loading on cables and cable hangers, accompanied by intermittent falls of debris. The 4-in compressed air line and the 2-in water line extend from the surface to the bottom of the shaft. At present, neither line is being used. The integrity of the brackets holding the air and water lines was difficult to assess because of salt buildup. Many instrumentation cables and most of the 138kVA power cables have broken off and fallen to the base of the shaft.

3.3.2 Instrumentation

The Exhaust Shaft was equipped with geomechanical instrumentation in two stages. Earth pressure cells were installed behind the liner key in November 1984. Piezometers and nine multi-position extensometers were installed during November and December 1985. Figure 3-12 and Figure 3-13 show the instrument locations. None of these instruments continues to provide data.

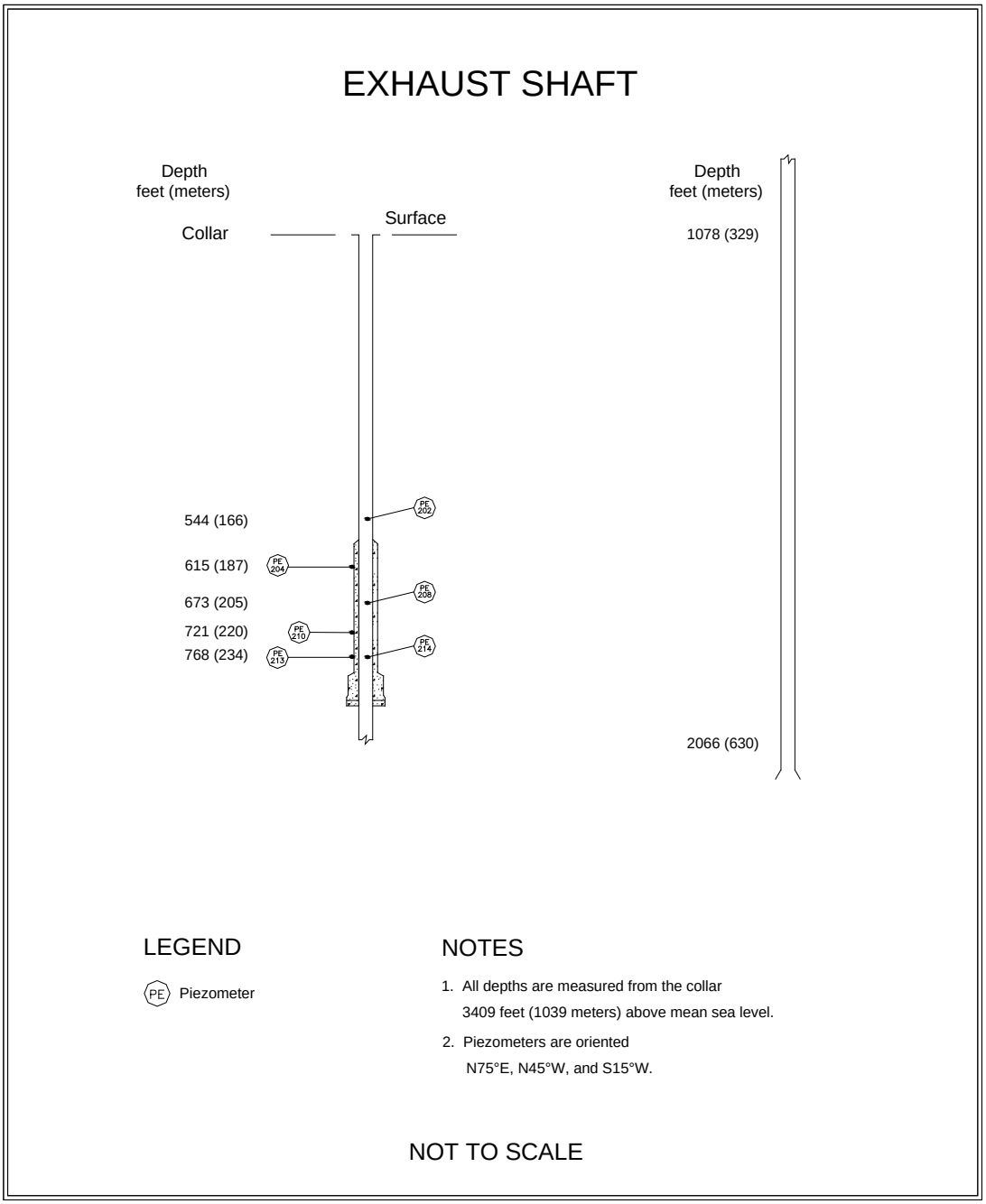

Figure 3-12. Exhaust Shaft Instrumentation

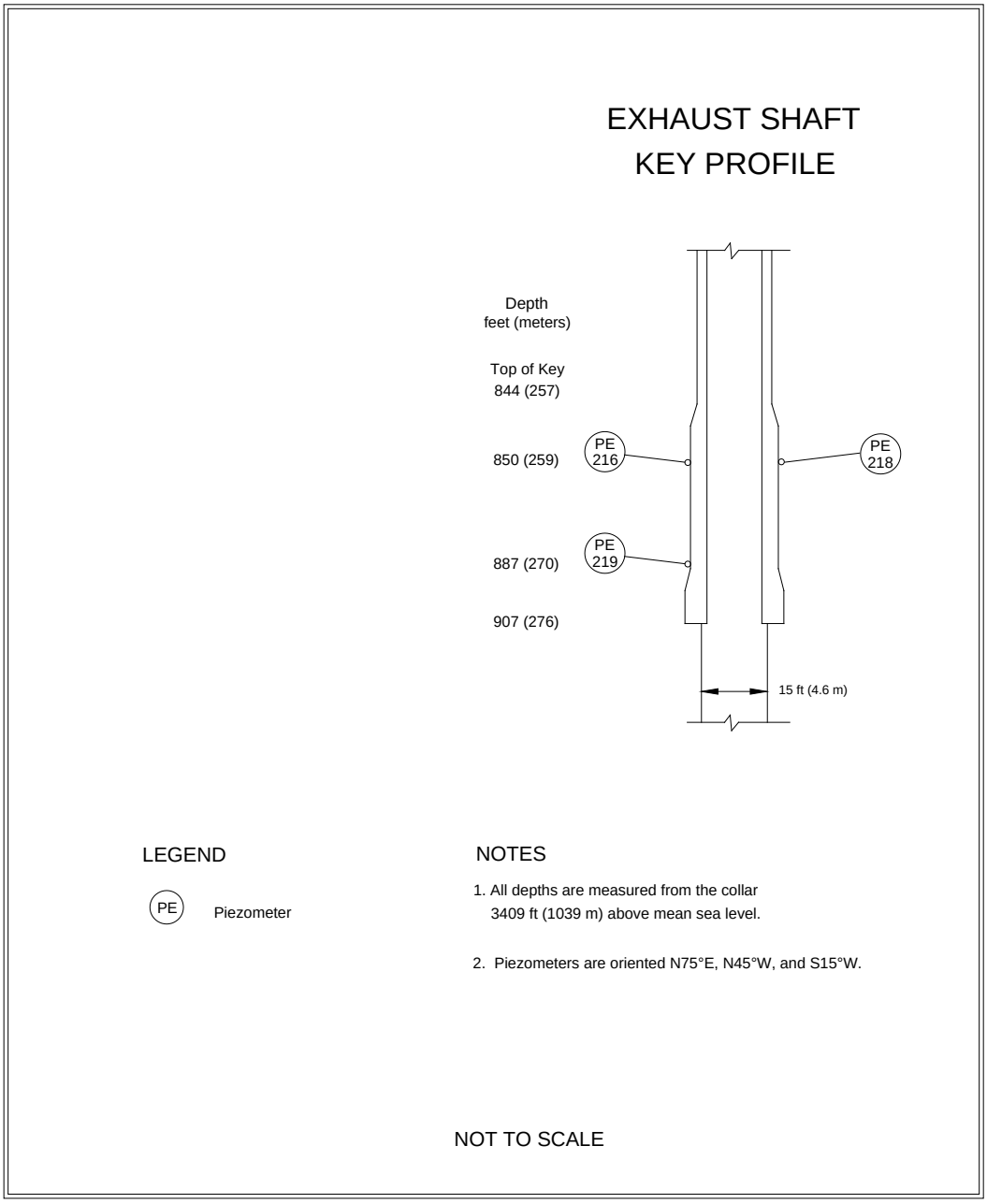

Figure 3-13. Exhaust Shaft Key Instrumentation

3.4 Air Intake Shaft

The Air Intake Shaft was drilled from December 4, 1987, to August 31, 1988, to establish a primary route for surface air to enter the repository (see Figure 1-2). The stratigraphy was mapped from September 14, 1988, to November 14, 1989 (Holt and Powers, 1990). Figure 3-14 summarizes the shaft stratigraphy.

The Air Intake Shaft is lined with non-reinforced concrete from the surface to the bottom of the shaft key at 903 ft (275 m). The key is 81 ft (25 m) long with an inside diameter of 16 ft (5 m). The shaft diameter below the key is 20 ft (6 m), and the shaft below the key is unlined to the facility horizon at 2,150 ft (655 m). The shaft walls are bolted and meshed from just below the key all the way down to the shaft station. This shaft has no sump.

3.4.1 Shaft Performance

Weekly visual inspections were performed on the Air Intake Shaft during this reporting period, and the shaft was found to be in satisfactory condition. No ground control activities other than routine maintenance were required during this reporting period.

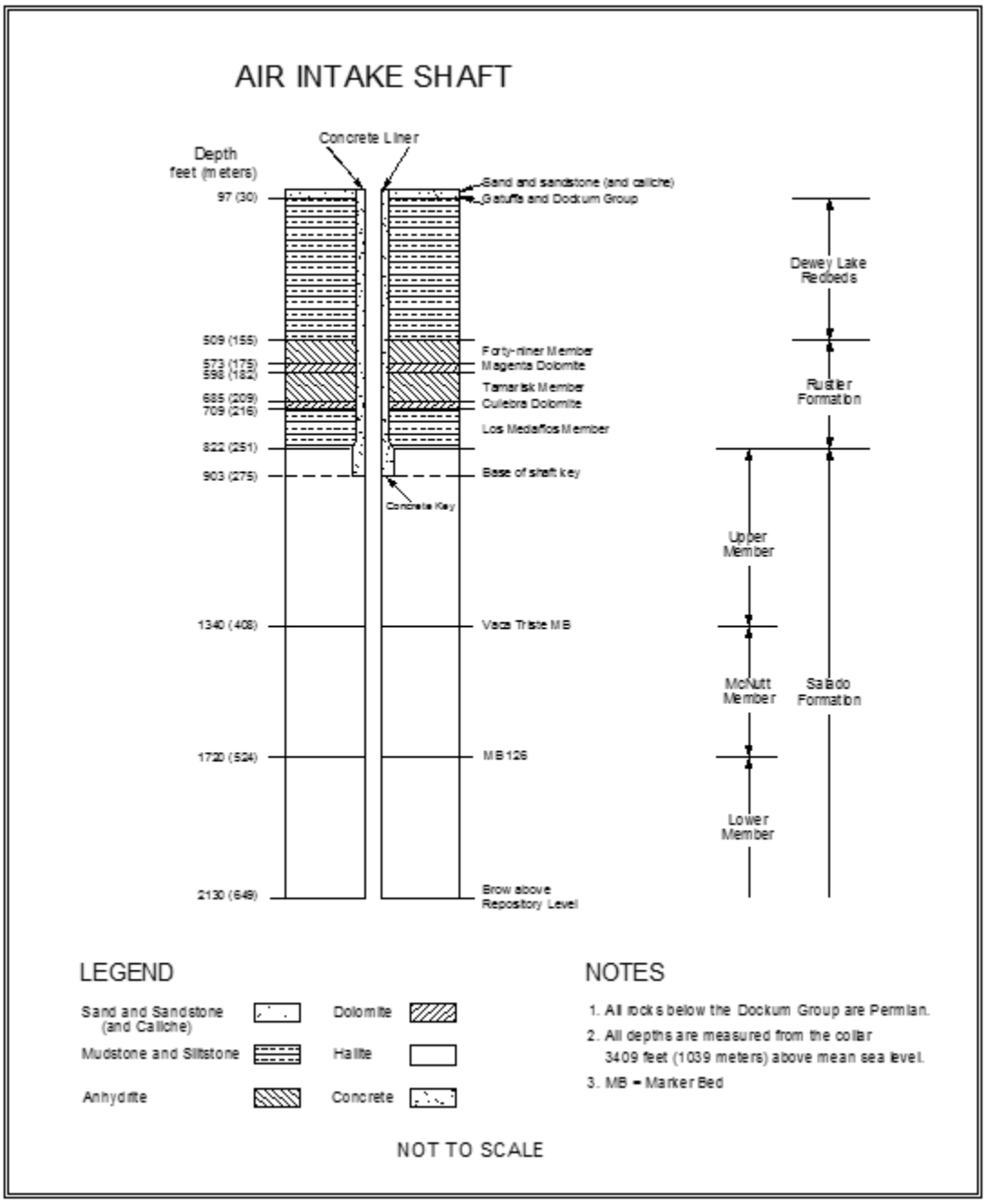

Figure 3-14. Air Intake Shaft Stratigraphy

4.0 PERFORMANCE OF SHAFT STATIONS

This section describes the instrumentation and geomechanical performance of the shaft stations at the base of the Salt Shaft, the Waste Shaft, and the Air Intake Shaft. The Exhaust Shaft does not have an enlarged shaft station; therefore, it is not included in this section.

4.1 Salt Shaft Station

The Salt Shaft Station was excavated by drilling and blasting between May 2 and June 3, 1982. In 1987, the station was enlarged by removing the roof beam up to Anhydrite "b" between S-90 and N-20 using a mechanical scaler. In 1995, the remaining roof beam at the north end of the station was also removed up to Anhydrite "b." The station area south of the shaft is 90 ft (27.5 m) long and 32 to 38 ft (10 to 12 m) wide. The height of the station south of the shaft is 18 ft (5.5 m). The station dimensions north of the shaft are approximately 30 ft (9 m) long, 32 to 35 ft (10 to 11 m) wide, and 18 ft (5.5 m) high. The shaft extends approximately 140 ft (43 m) below the facility horizon to accommodate the skip loading equipment and a sump. Figure 4-1 shows a cross section of the station.

4.1.1 Modifications to Excavation and Ground Control Activities

The Salt Shaft Station was not modified during this reporting period. Ground control activities were limited to routine maintenance.

4.1.2 Instrumentation

Geomechanical instrumentation was installed in the Salt Shaft Station between June 1982 and February 1983, with subsequent re-installation of extensometers and convergence points as necessary. Figure 4-2 shows the instrument locations after the roof beam was taken down.

Five vertical convergence points are currently monitored. Table 4-1 summarizes the vertical closure rates in the Salt Shaft Station from July 2017 through June 2018. Salt Shaft Station vertical closure rates indicate that the rates are lower than during the previous reporting period.

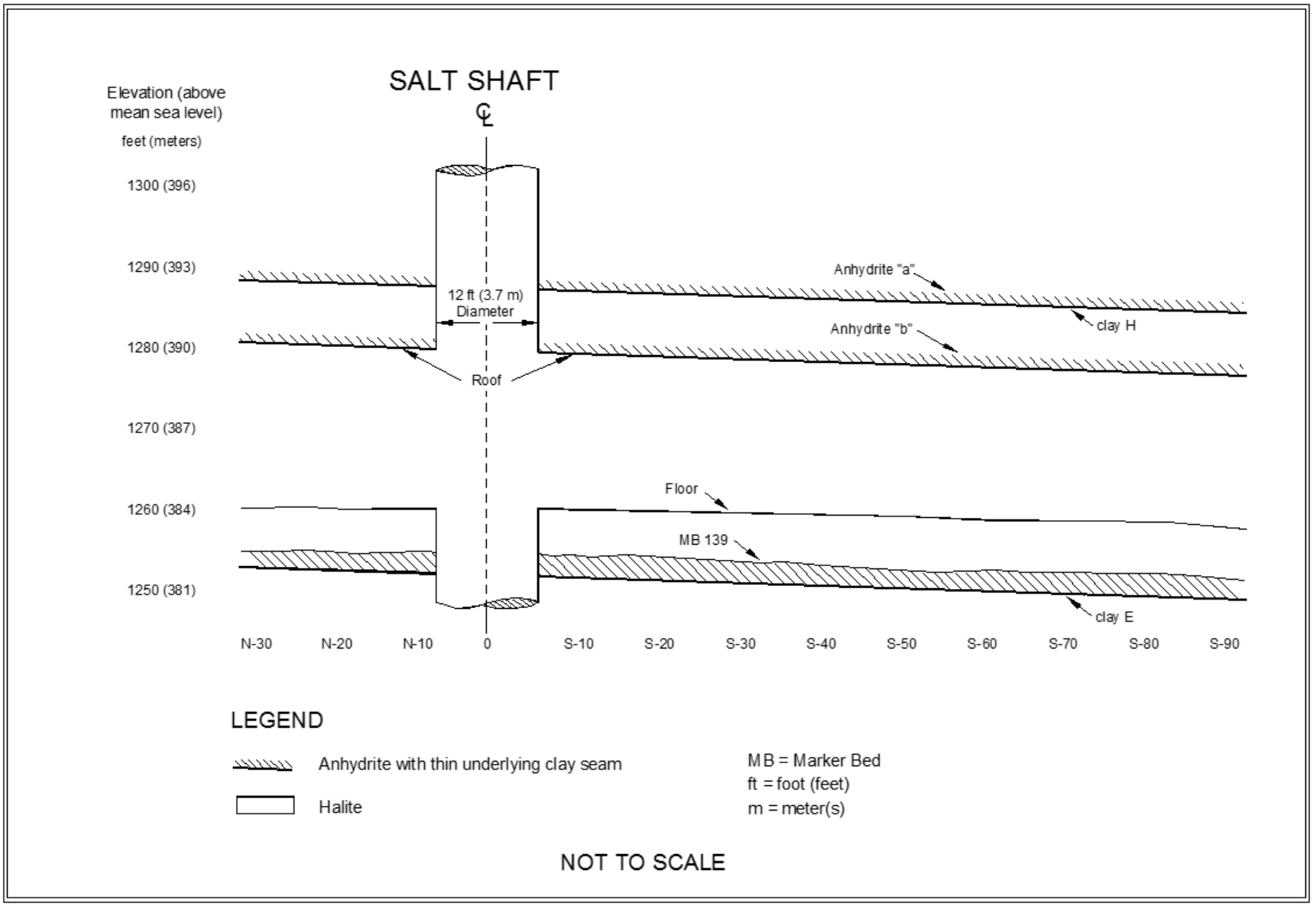

Figure 4-1. Salt Shaft Station Stratigraphy

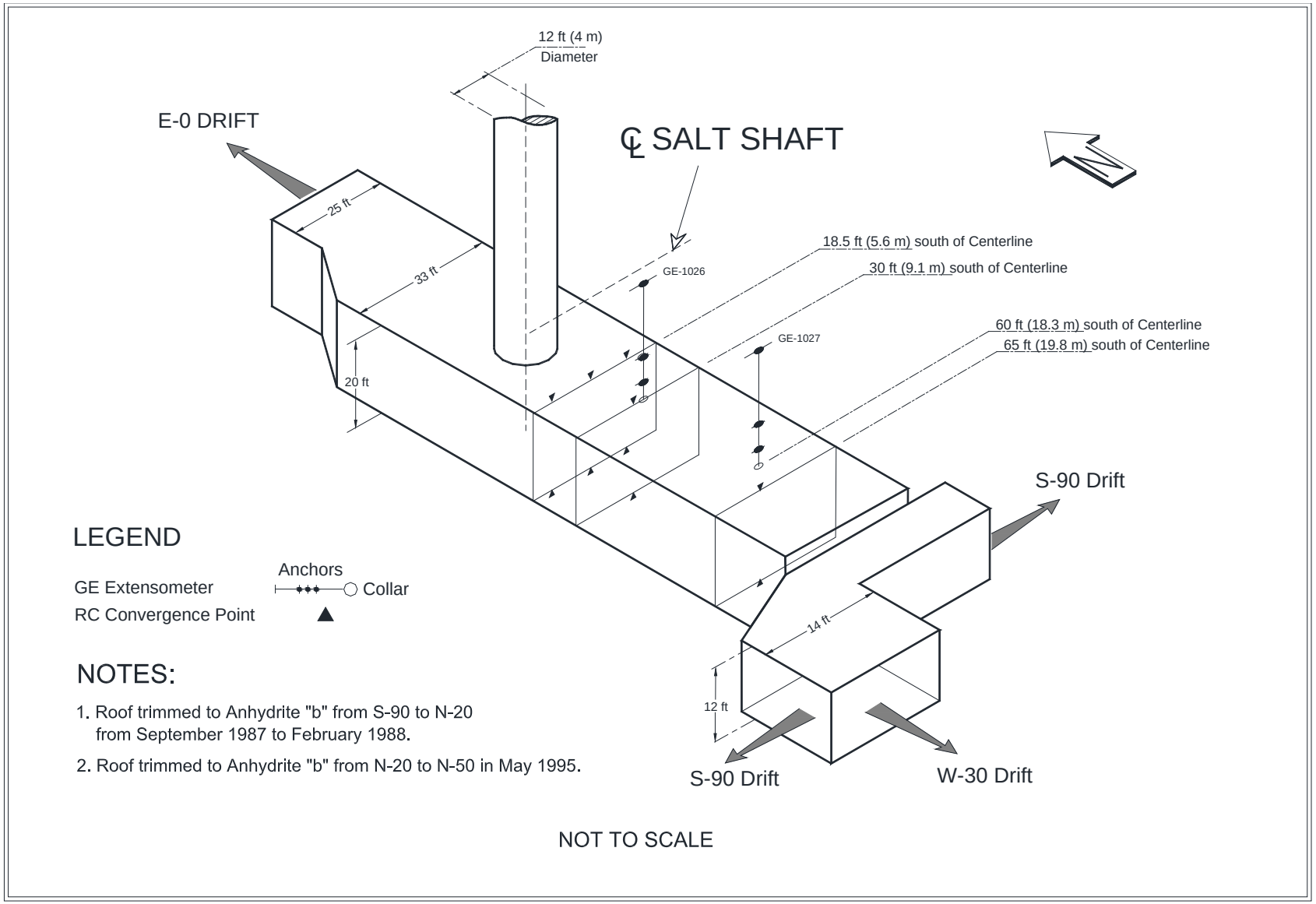

Figure 4-2. Salt Shaft Station Instrumentation After Roof Beam Excavation

Table 4-1. Closure Rates in the Salt Shaft Station

Location	Chord[1]	Last Reading	Total Cumulative Displacement (in)	Closure Rate 2017-2018 (in/yr)	Closure Rate 2016-2017 (in/yr)	Rate Change (%)
E0-S18	A-E	06/15/18	32.1	1.8	0.9	100
E0-S18	B-D	01/18/18	34.6	2.0	1.1	82
E0-S18	H-F	06/15/18	21.3	1.1	0.8	38
E0-S30	A-C	06/15/18	33.0	1.8	1.7	6
E0-S65	A-C	06/15/18	22.8	1.2	1.1	9

[1] Chord is defined in Section 5.2.2

4.2 Waste Shaft Station

The Waste Shaft Station was initially excavated with a continuous miner in November 1982 to serve as a ventilation connection to a 6-ft (2-m)-diameter exhaust shaft. In 1984, the station was enlarged to a height of 15 to 20 ft (4.5 to 6 m) and a width of 20 to 30 ft (6 to 9 m). The station is approximately 150 ft (46 m) long. In 1988, the station walls were trimmed, and concrete was placed on the floor. Since 1988, the Waste Shaft Station has undergone five major floor renovations. A 53-ft (16-m)-long section of the reinforced concrete was removed in February 1991. In 1995, an additional 30-ft (9-m) section of concrete was removed. In 2000, floor maintenance included trimming of the floor and reinstallation of the rails supported by segmented concrete panels on a crushed rock backfill. The roof of the Waste Shaft Station was mined up to Clay G in December 2008 to assure adequate operational clearance. Chain link fencing and 12-ft resin-anchored roof bolts were installed for ground support. Figure 4-3 shows a cross section of the Waste Shaft Station stratigraphy.

4.2.1 Modifications to Excavation and Ground Control Activities

No modifications to the Waste Shaft Station were made during this reporting period. Ground control activities were limited to routine maintenance.

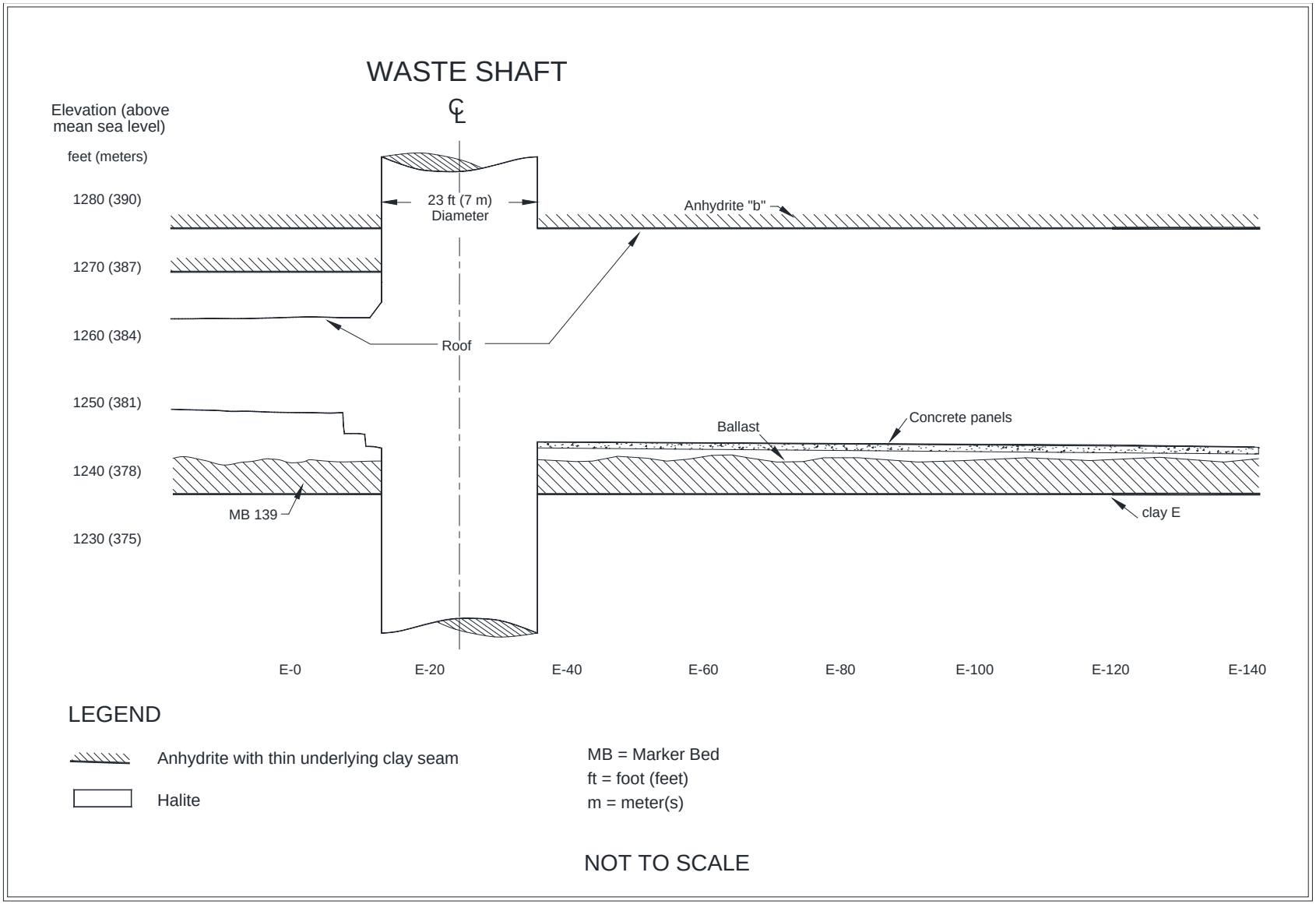

Figure 4-3. Waste Shaft Station Stratigraphy

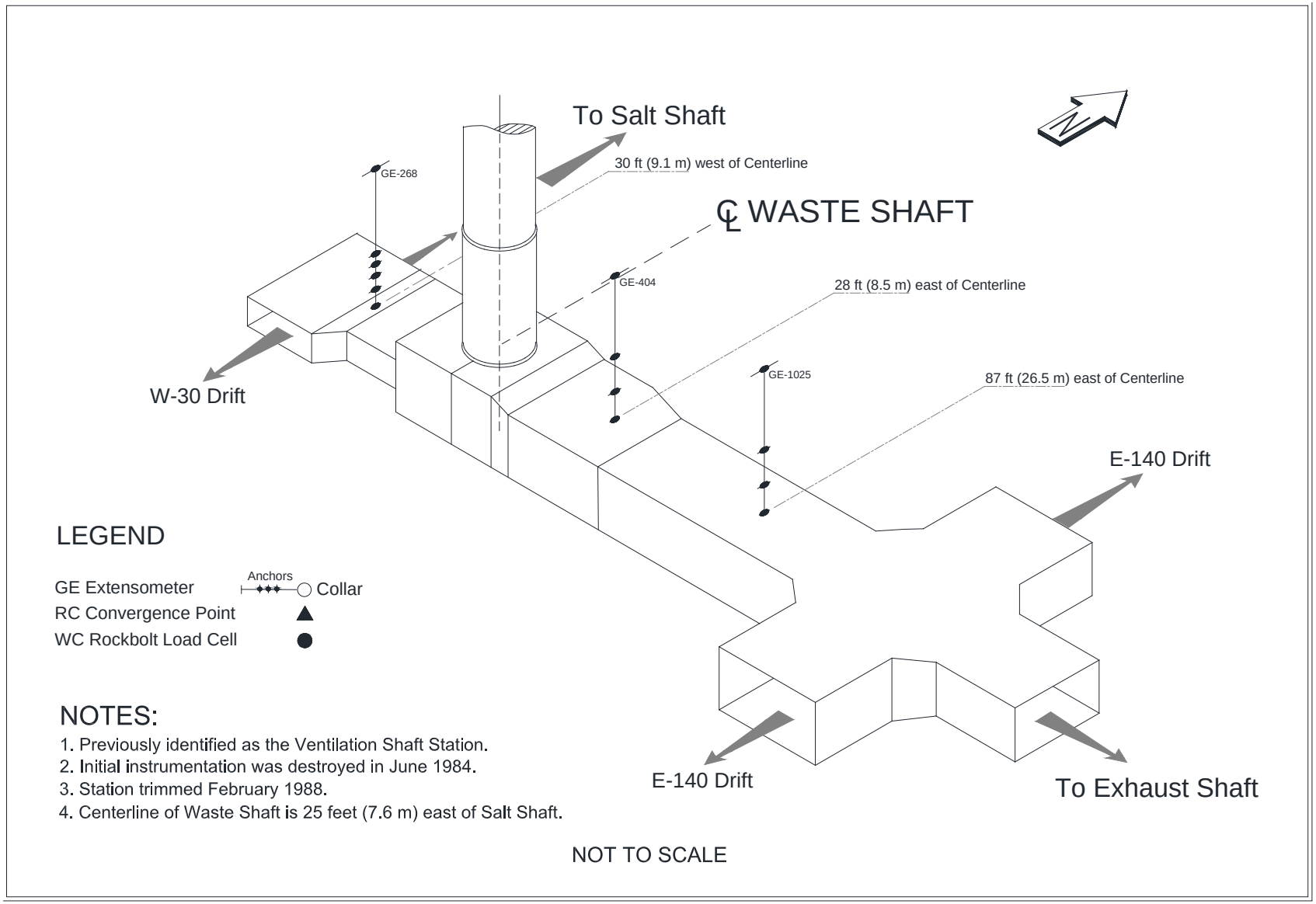

Figure 4-4. Waste Shaft Station Instrumentation After Roof Beam Excavation

4.3 Air Intake Shaft Station

The Air Intake Shaft Station was excavated in late 1987 and early 1988, using a continuous miner. The Air Intake Shaft is furnished with a work platform and a small cage that can be raised and lowered to perform routine ground maintenance. The principal purpose of that equipment is to provide emergency access.

4.3.1 Modifications to Excavation and Ground Control Activities

The Air Intake Shaft Station was not modified during this reporting period. Ground control activities were limited to routine maintenance.

4.3.2 Instrumentation

Radial convergence point and extensometer instrumentation data near the Air Intake Shaft Station are presented in Section 5.0 as part of the discussion on the performance of the access drifts. Twenty rock bolt load cells are installed in the Air Intake Shaft Station.

5.0 PERFORMANCE OF ACCESS DRIFTS

This section describes the geomechanical performance of the underground access drifts. The Waste Disposal Area is discussed in Section 6.0 and the Salt Disposal Investigation areas are discussed in Section 7.0. Four major north-south drifts in the WIPP underground are intersected by shorter east-west cross-drifts. Drift dimensions range from 13 ft (4 m) to 21 ft (6.4 m) high and from 14 ft (4.3 m) to 33 ft (9.2 m) wide.

5.1 Modifications to Excavation and Ground Control Activities

Floor trimming and rock bolting were performed during this reporting period. Table 5-1 summarizes these activities.

5.2 Instrumentation

This section discusses instrumentation details in the access drifts.

5.2.1 Extensometers

Eighteen extensometers continue to be monitored at various locations in the access drifts. Where displacement data were available, annual displacement rates were calculated (see Section 1.4.3) for each active installation and compared to the annual displacement rates from the previous reporting period.

Table 5-1. Summary of Modifications and Ground Control Activities in the Access Drifts: July 1, 2017 to June 30, 2018

Location	Work Activity
E300 S2180-S2520	Replacement of 14-ft Dywidag roof bolts
E0 N150-N780	Bolted and meshed rib
E0 N150-N1400	Replacement of 14-ft Dywidag roof bolts
E0 N1100-N1400	Bolted and meshed rib lines
E0 Salt Shaft Station	Installed 14-ft Dywidag roof bolt pattern
E140 S90-N300	Replacement of 14-ft Dywidag roof bolts
E140 S1000-S1950	Bolted up loose mesh
E140 S700-S2520	Replacement of 14-ft Dywidag roof bolts
E140, E0, W30, W170	Hand Scaled the Ribs
E140 N620-N1400	Bolted and meshed rib lines
W30 S90-S700	Installed 14-ft Dywidag roof bolt pattern
W30-S1300	Replacement of 14-ft Dywidag roof bolts
W30-S1750	Bolted loose rib
W30 S1950-S2520	Replacement of 14-ft Dywidag roof bolts
W170-S1300	Replaced broken 10-ft Mechanical bolts in brow
W170 S1900-S1950	Replacement of 14-ft Dywidag roof bolts
W170-S2520	Bolted and meshed miters
S90 W170-W30	Bolt and mesh ribs
S700 W30-W170	Installed 14-ft Dywidag roof bolt pattern
S1600-E140	Bolting entry to Wash Bay with 12-ft Dywidag
S2180 E300-E140	Installed 14-ft Dywidag roof bolt pattern
S2180 W30-W170	Replacement of 14-ft Dywidag roof bolts
Maintenance Shop	Replacement of 14-ft Dywidag roof bolts
AIS (N215 & N300)	Replacement of 14-ft Dywidag roof bolts
Panel 7	Replacement of broken 14-ft Dywidag roof bolts
Panel 7-S2180	Bolted and meshed miters
Panel 7-S2520	Bolted and meshed miters
Mine Wide	Drilled 20-ft Observation Holes

Extensometer data are obtained by measuring the displacement from the reference head anchor (collar) to each fixed anchor of the extensometer. These measurements are scheduled to be made at least monthly throughout the WIPP underground.

Many of the E-140 extensometers indicate movement in the roof beam that may be attributed to shallow fracturing and the effects of anhydrite stringer separations in the roof. Lateral deformation in the roof beam may influence the extensometer readings, causing an increase in the measured displacement. Although the extensometer data indicate continued deformation and breakup of the lower beam, the roof bolt anchorage zone remains competent.

5.2.2 Convergence Points

Convergence point data are obtained by measuring the change in distance between fixed points anchored into the rock across an opening, either from rib to rib or from roof to floor. The measurement end-points constitute a "chord." Figure 5-1 shows typical convergence point array configurations along with typical chord designations.

Normally within this section a listing of the newly installed or reinstalled convergence points is available in Table 5-2. No installation or reinstallation of convergence points occurred during this reporting period, due in part to no substantial floor trimming or new mining activities in the access drifts.

Where possible, annual closure rates were calculated from convergence point array data gathered in the access drifts. Approximately 245 active convergence points are located in the access drifts, and 59 convergence points are located in the SDI area. A complete tabulation of the convergence point data and calculated closure rates is presented in the supporting data document for this report.

Locations with increases in annual vertical closure rates of greater than 20 percent are shown in Table 5-2, Vertical Closure Rate Changes in Excess of Twenty Percent in the Access Drifts.

5.3 Analysis of Convergence Point and Extensometer Data

Vertical loading on mine pillars results in lateral stresses on the roof and floor beams. The composition of those beams, in part, determines how these structures will react to the horizontal stresses. In particular, horizontally continuous anhydrite stringers (see Section 2.2.2) divide the beam itself into a series of smaller independent beams.

Lateral strain on the beam imposed by vertical loading on the pillars is accommodated by vertical displacement over the mined opening. This requires that the horizontally oriented beam separate along the most favorable, or weakest, planes.

Where anhydrite stringers interpose the beam, they constitute a plane of weakness, and delamination occurs. The material is confined in the plane above, so that the roof accommodates the lateral strain by bending convex into the mined opening.

Two distinct results develop from this action. First, voids form within the beam as the portions closer to the opening move away from those deeper within the beam. Second, the convex portion of the bended plane is subjected to tensile loading perpendicular to the axis of the drift and superficial tears known as "tensile fractures" develop generally parallel to the axis of the drift.

Table 5-2. Vertical Closure Rate Changes in Excess of Twenty Percent in the Access Drifts

Location	Chord[1]	Last Reading Date	Closure Rate 2017 to 2018 (in/yr.)	Closure Rate 2016 to 2017 (in/yr.)	Rate Change (%)
S90-W120	B-D	05/24/18	0.7	0.5	40
W170-S232	A-C	05/22/18	0.7	0.5	40
W30-S400	A-C	05/22/18	1.1	0.8	38
E140-S1600	A-C	05/16/18	3.6	2.7	33
S1000-E120	A-C	05/16/18	1.2	0.9	33
E0-N626	A-C	06/15/18	3.3	2.5	32
S1000-E58	B-D	03/09/18	1.3	1.0	30
W30-S250	A-C	05/22/18	1.3	1.0	30
S1000-E160	A-C	05/16/18	0.9	0.7	29
W170-S560	A-C	05/22/18	0.9	0.7	29
W170-S90	A-C	05/22/18	0.9	0.7	29
E140-S1075	B-D	05/16/18	1.4	1.1	27
E140-S1225	A-E	05/16/18	3.9	3.1	26
E140-S700	B-C	05/16/18	2.0	1.6	25
S90-W590	B-D	05/22/18	0.5	0.4	25
S90-W620	A-C	05/22/18	1.0	0.8	25
E140-S1150	B-F	05/16/18	2.1	1.7	24
W30-S2067	A-C	09/13/17	3.7	3.0	23
W170-S850	C-G	05/22/18	1.1	0.9	22
W30-S700	A-C	05/22/18	2.2	1.8	22
W30-S1300	A-C	05/22/18	2.3	1.9	21

[1] Chord is defined in Section 5.2.2.

Where anhydrite stringers are small and discontinuous or absent within the beam, horizontal loading is accommodated along shear planes. These develop at angles of approximately 35 degrees with respect to the horizontal. In some cases, a plane develops preferentially on one side of the drift, and the bulk of material is pushed into the mined opening on that side. This may be thought of as a cantilevered beam.

Whatever mechanism used, vertical displacement into the mined opening is measured by convergence monitoring. Convergence points consider the displacement between two opposing surfaces: either the roof and floor or the two ribs. Extensometers consider the displacement between one surface (usually the back) and one or more points within the beam. Where a convergence point and an extensometer are adjacent to one another, it is possible to determine the individual displacements of both floor and roof beams.

This data is used to analyze the stability and mechanics of the beam, and to determine what actions may be taken to ensure the safety of personnel and equipment consistent with the safe operation of the facility.

5.4 Excavation Performance

Approximately 270 readings are collected and assessed regularly from convergence point arrays throughout the WIPP underground. Due to the effect rock temperature has on salt creep, convergence rates vary seasonally, typically increasing during the warmer summer months and decreasing during the cooler and drier winter months. These temperature effects are more pronounced nearer the fresh air intake.

The performance of the access drift excavations during this reporting period was within acceptable criteria. "Acceptable criteria" means that a drift remains accessible, and the ground can be controlled by routine maintenance. Standard remedial ground control in some areas was required to maintain the performance of the excavations. The accessible drifts remain stable and controlled. Most of the annualized rates remain steady, indicating stability. Of the 185 convergence locations measured in the access drifts, only 21 locations (11 percent) had annual closure rates in excess of 20 percent from the previous year’s value. Of those 21 locations, the average closure rate was 1.7 in/year and the average change in rate between consecutive years was 0.4 in/year.

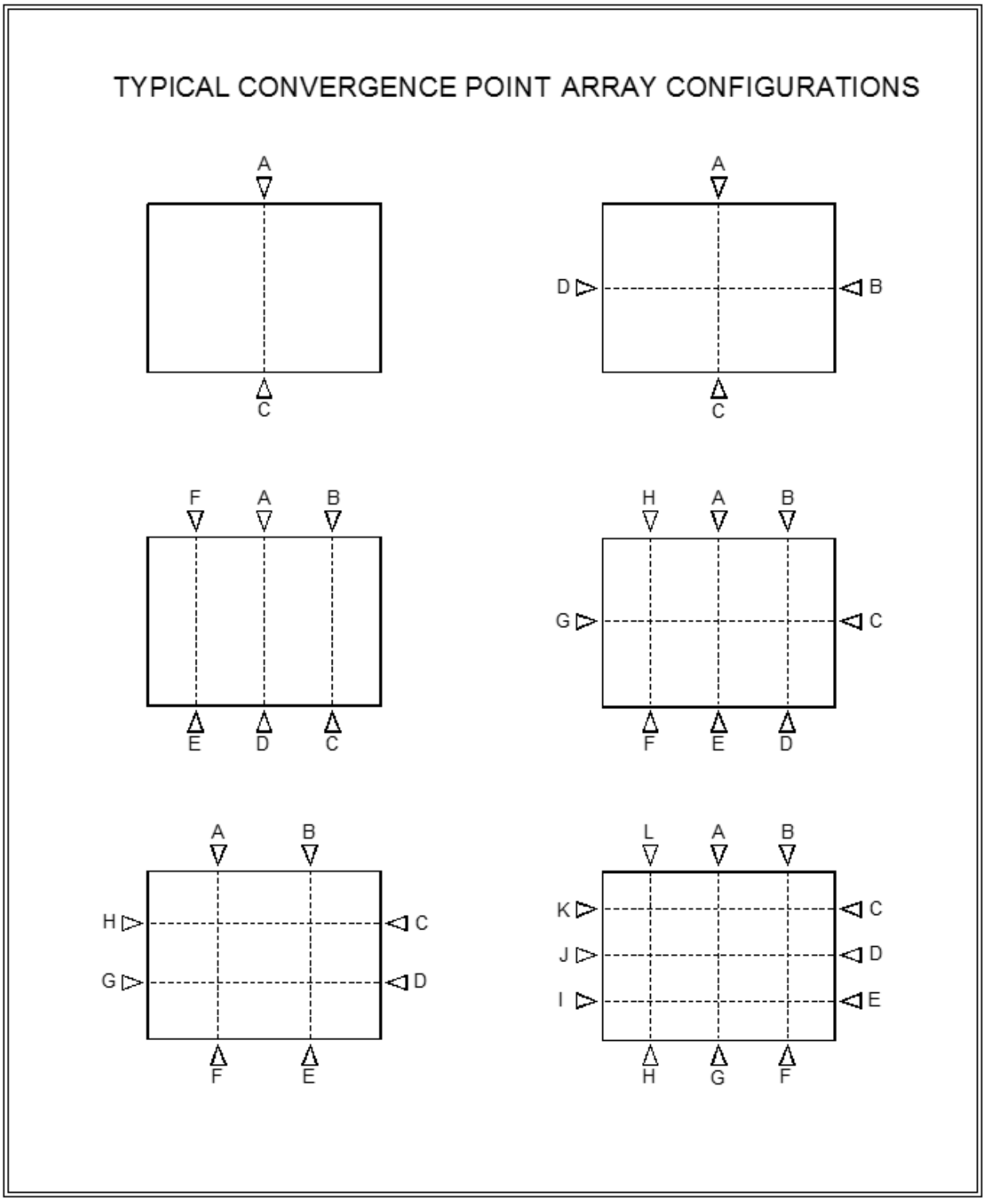

Figure 5-1. Typical Convergence Point Array Configurations Showing Anchor Designations

6.0 PERFORMANCE OF THE WASTE DISPOSAL AREA

The Waste Disposal Area as of June 30, 2018, consisted of Panels 1, 2, 3, 4, 5, 6, 7, and a partially mined Panel 8. Panels 1, 2, 3, 4, 5, and 6 were closed during previous reporting periods.

6.1 History

Excavation of Panel 1 began in May 1986 with the mining of the access entries. Initially, the disposal rooms and drifts were developed as pilot drifts that were later excavated to nominal operational dimensions of 13 ft (4 m) high, 33 ft (10 m) wide, and 300 ft (91 m) long. Room 1 was completed to these dimensions in August 1986, and pilot drifts for Rooms 2 and 3 were excavated in January and February 1987. Rooms 2 and 3 were completed in February and March 1988, and Rooms 4 through 7 were completed in May 1988. Four short access drifts designed to lead to smaller test alcoves were excavated north off the S-1600 drift and Rooms 4-7 in June 1989. Only the access drifts to the alcoves were completed; the alcoves themselves were not excavated. Panel 1 waste emplacement (in Rooms 1, 2, 3, 7, adjacent areas of S-1600, and all of S-1950) was completed during a prior reporting period, and the panel is closed to all access. The Panel 1 access entries, S-1600 and S-1950, which extend from the E-300 drift to the isolation walls, remain open, and the instrumentation in this area continues to be maintained and monitored.

Excavation of Panel 2 began in September 1999 with the mining of access entries. Initially, the disposal rooms and drifts were developed as pilot drifts that were trimmed to finished dimensions. Room 1 was completed in January 2000, and pilot drifts for Rooms 2 and 3 were excavated in February 2000. Pilot drifts were completed for Rooms 4 through 6 in April 2000. The pilot drift for Room 7 was excavated in May 2000. All the rooms were excavated to final dimensions by August 2000. Waste emplacement in Panel 2 was completed during a prior reporting period, and the panel is closed to all access. The Panel 2 access entries, S-2150 and S-2520, which extend from the E-300 drift to the isolation walls, remain open, and the instrumentation in this area continues to be maintained and monitored.

Excavation of Panel 3 began in May 2002 with the mining of access entries. As with Panel 2, the disposal rooms and drifts were initially developed as pilot drifts that were trimmed to finished dimensions. All the rooms were excavated to final dimensions by the end of March 2004. Waste emplacement in Panel 3 was completed in February 2007. Substantial barriers and bulkheads were installed in the exhaust and intake drifts of Panel 3 to prevent access into the panel and to isolate it from the ventilation circuit.

Panel 4 access drift mining began in January 2005. The disposal rooms were initially developed as pilot drifts and were later trimmed to final dimensions. Mining was completed by June 2006. Waste emplacement in Panel 4 was completed in March 2009. Substantial barriers and bulkheads were installed in the exhaust and intake drifts of Panel 4 to prevent access into the panel and to isolate it from the ventilation circuit.

Panel 5 excavation activities began in June 2006. The panel was initially mined to less-than-final dimensions and later trimmed to specification. Mining was complete by February 2008. Waste emplacement was conducted from March 2009 through July 2011. Isolation walls were completed in November 2011. Instrumentation and regular observations will continue in the accessible area up to the isolation walls.

Panel 6 mining began in April 2008. The panel was initially mined to less-than-final dimensions and later trimmed to specification. Mining was complete by April 2010. Waste emplacement began in March 2011 and was completed in January 2014.

Panel 7 mining began in April 2010 and was completed in August 2011.
Initial mining placed the floor within 2 ft of a polyhalitic halite bed (designated PH-4), which sits atop a thick anhydrite bed designated MB-139. Horizontal stresses caused significant uplift and the floor was then mined down through MB-139 and backfilled with run of mine salt. The remediation of the floor was completed in January 2013. Subsequent geomechanical monitoring indicates stable vertical convergence. RH waste emplacement began in Panel 7 in September 2013 and CH waste emplacement began in January 2014.

Panel 8 mining resumed in February 2018. The back has been mined to Clay G in the panel access drifts of Room 1 and a quarter of Room 2. The panel was originally planned to be mined on the lower horizon, but due to the interruption in mining – which resulted in significant low angle shear and separation in the immediate back – it is now being mined at the upper horizon.

6.2 Modifications to Excavations and Ground Control Activities

Ground control activities were severely restricted during this reporting period primarily due to the consequences of the radioactive release event. One limitation was the additional personal protective equipment that is required to be worn in a contaminated area. Another limitation is the reduced ventilation due to the requirement to filter the exhaust air leaving the mine. The reduced ventilation limited the amount of diesel-powered equipment that could be operated simultaneously. The ability to perform ground remediation and install ground control within 115 ft (reduced from 200 ft in 2018) of the waste face was severely impacted by the restrictions imposed by the WIPP Documented Safety Analysis and associated Technical Safety Requirements. A 7-bolt--wide roof bolt pattern was completed in Rooms 1 and 5. A roof bolt pattern will not be installed in Rooms 4, 6 (prohibited access), and 7 (partial waste emplacement and room closure). Bolting and meshing of select rib/back junctions in Rooms 2, 3, and 5 was also performed.

Geotechnical instrumentation indicates that a roof fall will likely occur in Room 6. Room 6 is not pattern bolted and will likely experience a roof fall similar in size and nature to the roof fall that occurred in Room 4 (November 3, 2016). Access to Room 6 is prohibited and is not being maintained. There are no indications of instability in the remaining accessible areas of Panel 7, as indicated by either the geomechanical data or physical observations conducted by the geotechnical group.

6.3 Instrumentation

Panel 7 instrumentation consists of the following:

- Forty-nine vertical convergence points, distributed as 14 in each of the intake and exhaust drifts and 3 in each of the rooms; and
- Eleven wire extensometers, distributed as 2 in each of the intake and exhaust drifts and 1 in each of the rooms.

A schematic of the geomechanical instrumentation layout found in Panel 7 is shown in Figure 6-1.

6.4 Excavation Performance

Waste handling activities in Panels 1 through 6 have been completed, and geomechanical monitoring inside these panels has been discontinued.

Vertical convergence rates, calculated at the center of each of the rooms in Panel 7, were compared between this and the previous reporting period. Depending on the location in Panel 7, convergence rates were either 1) remaining constant, or 2) decreasing due to recent bolting, or 3) generally increasing while bolting was pending.

6.5 Analysis of Extensometer and Convergence Point Data

Geomechanical instrumentations are installed in each disposal room and at select locations in the panel access drifts.

Panel 7 is experiencing age-appropriate roof beam deformation. Extensometer data in Panel 7, Room 5 indicate consistently slow acceleration at 1 in per year. Convergence rate in Room 3 indicates a reasonable rate for the age, at approximately 4 in per year, and extensometer readings indicate a beam dilation of about 1 in per year in Room 3.

Extensometer readings from Room 2 show a beam dilation of approximately 3½ in per year. Similarly, convergence rate in Room 2 indicates 3½ in per year. Room 1 indicates a convergence rate of 4 in per year. The intersection of Room 3 and the S-2520 drift is slightly over 5 in per year, largely due to floor heave. Closure rates in S-2180 indicate a steady rate of 3 in per year, with no acceleration.

Convergence monitoring in Panel 8, Room 1 indicate a closure rate of 5 in per year with a very slow acceleration. Room 2 data shows a steady rate of 3½ in per year. The S-1600 access drift shows an average rate of 4 in per year. Access was prohibited in the S-1950 drift of Panel 8 during this reporting period; hence, no data are available.

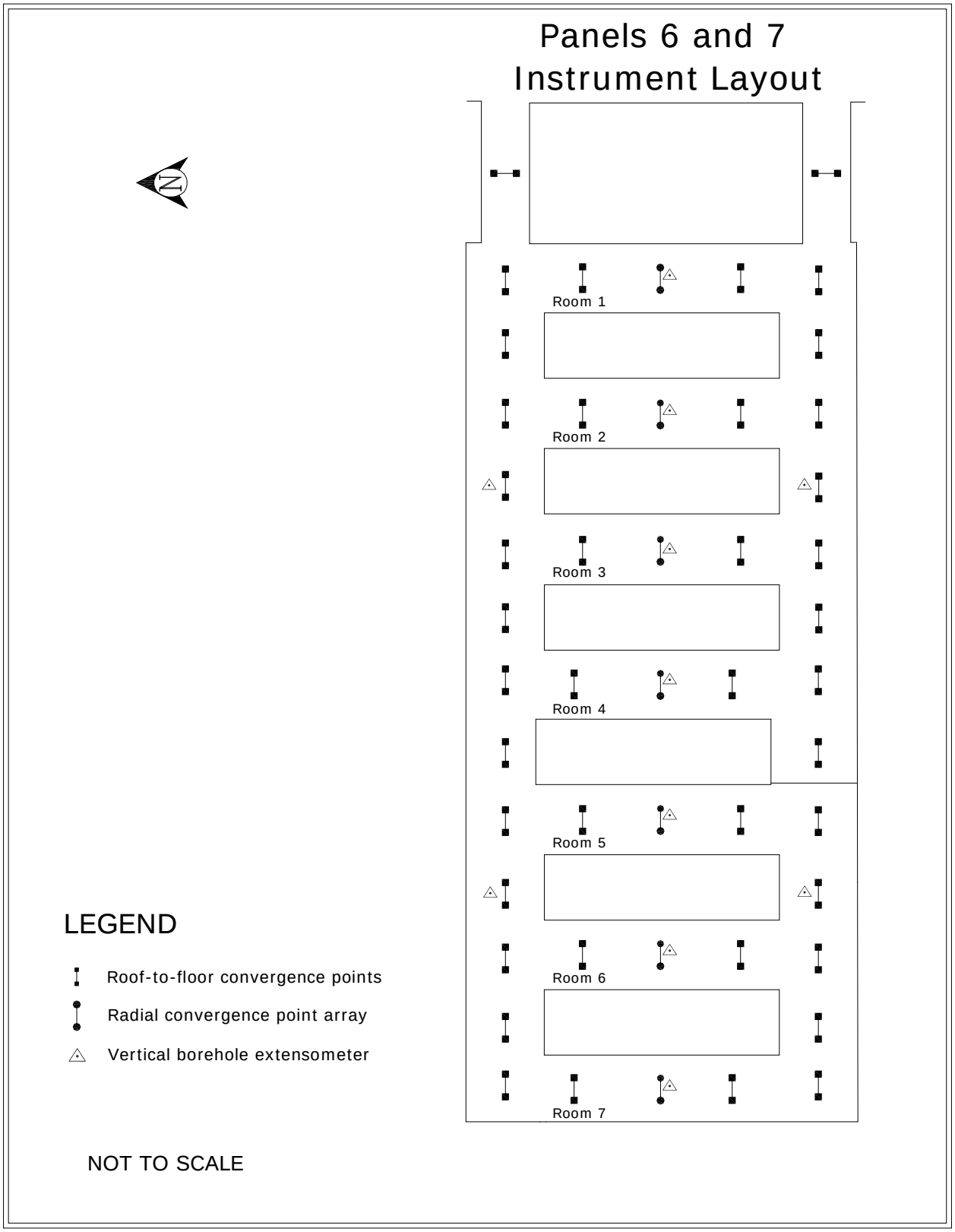

Figure 6-1. Location of Geomechanical Instruments in Panels 6 and 7

7.0 PERFORMANCE OF THE SALT DISPOSAL INVESTIGATIONS AND SALT DEFENSE DISPOSAL INVESTIGATIONS

This chapter describes the geomechanical performance of the SDI and SDDI areas (hereafter referred to as SDI). Development of the area began in January 2012. When completed, most of the area will have nominal dimensions of 13 ft high and 16 ft wide.

7.1 Ground Control Program

Due to the relatively narrow drifts (nominally 16 ft across) and favorable mining horizon, ground control plans in the SDI area are confined to routine maintenance, such as spot-bolting where localized drummy surface features develop. More substantial engineered ground control systems may be applied in the event that ongoing geomechanical monitoring and analysis of the area identify a need.

7.2 Instrumentation

Fifty-eight convergence arrays have been installed in the SDI area. The arrays are read on a periodic basis.

7.3 Analysis of Convergence Point Data

As a rule, the area behaves as expected, with relatively high initial rates rapidly decreasing as the stresses redistribute to load the surrounding salt pillars.

7.4 Excavation Performance

A combination of ground control and ventilation challenges led the Operations Department to prohibit access to the SDI area during this reporting period so the resources could be channeled to address more significant ground control remediation in other areas.

A comparison between the rates of closure between the two previous reporting periods had shown that every measured location in the SDI area, with the exception one, in SDI had a reduction in the rate of roof to floor closure. The single exception had a very insignificant increase of 0.1 inches per year. This was expected as the reduction in the higher initial strain following excavation was continuing to dampen as the excavations approach the steady state phase of salt creep. It is fully expected that had measurements been taken this reporting period the convergence rates would be either be still reducing or would have reached a steady state (near constant value).

8.0 GEOSCIENCE PROGRAM

The activities of the geoscience program were not performed during the July 1, 2017 through June 30, 2018 reporting period, primarily due to logistical problems associated with the radiological release event e.g., reduced ventilation minimized diesel equipment operation, unavailability of non-diesel equipment in Panel 7. A description of the various aspects of the geoscience program is presented in the remainder of Section 8.0.

The geoscience program confirms the suitability of the site through the collection of various geologic data and excavation characteristics from the underground. These include the inspection of open observation holes for fractures (separations) and offsets (lateral displacements) in roof beams, and the mapping of fracture development on roof surfaces. Data collected through these activities support the design and evaluation of ground support systems.

Normally, the following activities are performed:

- Observation hole inspections
- Fracture mapping
- Stratigraphic mapping
- Drilling and Geologic Core Descriptions

Fracture development in the roof is primarily caused by the concentration of compressive stresses in the roof beam and is influenced by the size and shape of the excavation and the stratigraphy in the immediate vicinity of the opening. In a thick roof beam, pillar deformations induce lateral compressive stresses into the immediate roof and floor. With time, the buildup of stress causes differential movement along stratigraphic boundaries. This differential movement is identified as offsets in observation holes and by the bends in failed rock bolts. Large strains associated with lateral movements can induce fracturing in the roof, which is frequently seen near the ribs. However, this process may take years to develop.

At the upper repository horizon, clay or anhydrite stringers exert significant influence over the effective thickness of the roof beam. The presence of these stringers causes the roof beam to behave as a series of thin independent beams. Little or no tensile support is provided across the stringer interface. As horizontal end-loading continues, each beam can deflect downward causing a tensile fracture to develop along the bottom of the beam. These tensile fractures can develop in relatively new excavations soon after separation occurs along the stringer interface.

8.1 Observation Hole Inspections

Geotechnical observation holes are drilled at various locations throughout the underground facility. A location may contain one or more holes arranged in an array. These holes are drilled to depths that allow the monitoring of fracture development and offsetting and are inspected for the development of those features. Roof observation holes usually extend up past Clays G and H (Figure 8-1 and Figure 8-2).

The clay seams nearest the excavation surfaces define the immediate roof beam. The roof beam is bounded by Clay G in most of the access drifts and Panels 1, 2, 7, and 8. Some areas, such as the Salt Shaft Station, portions of the E-0 and E-140 drifts, the south mains south of S-2620, and Panels 3, 4, 5, and 6, are excavated to Clay G and have roof beams bounded by Clay H.

The offset in an observation hole is determined by visually estimating the degree of occlusion. The direction of offset along clay seams is observed as the movement of the strata nearer to the observer relative to the strata farther away. Typically, the nearer strata move toward the center of the excavation (Figure 8-3 and Figure 8-4). Based on previous observations in the underground, the magnitude of offset is usually greater in holes located near ribs than in those located along excavation centerlines. Offsetting along the clay layers is observable until total offset is reached or visibility is obstructed by intervening offsets at other clay seams or fractures.

Observation holes are inspected for fractures using an aluminum rod with a flattened steel wire probe attached to one end perpendicular to the rod (referred to as a "scratch rod"). Fractures and clay seams are located by moving the probe along the inside of the hole until it is snagged in one of these features. Depth to each feature is recorded, as is the magnitude of separations encountered. A fiber scope camera is available for use in addition to the scratch rod to visually document features of interest in a hole.

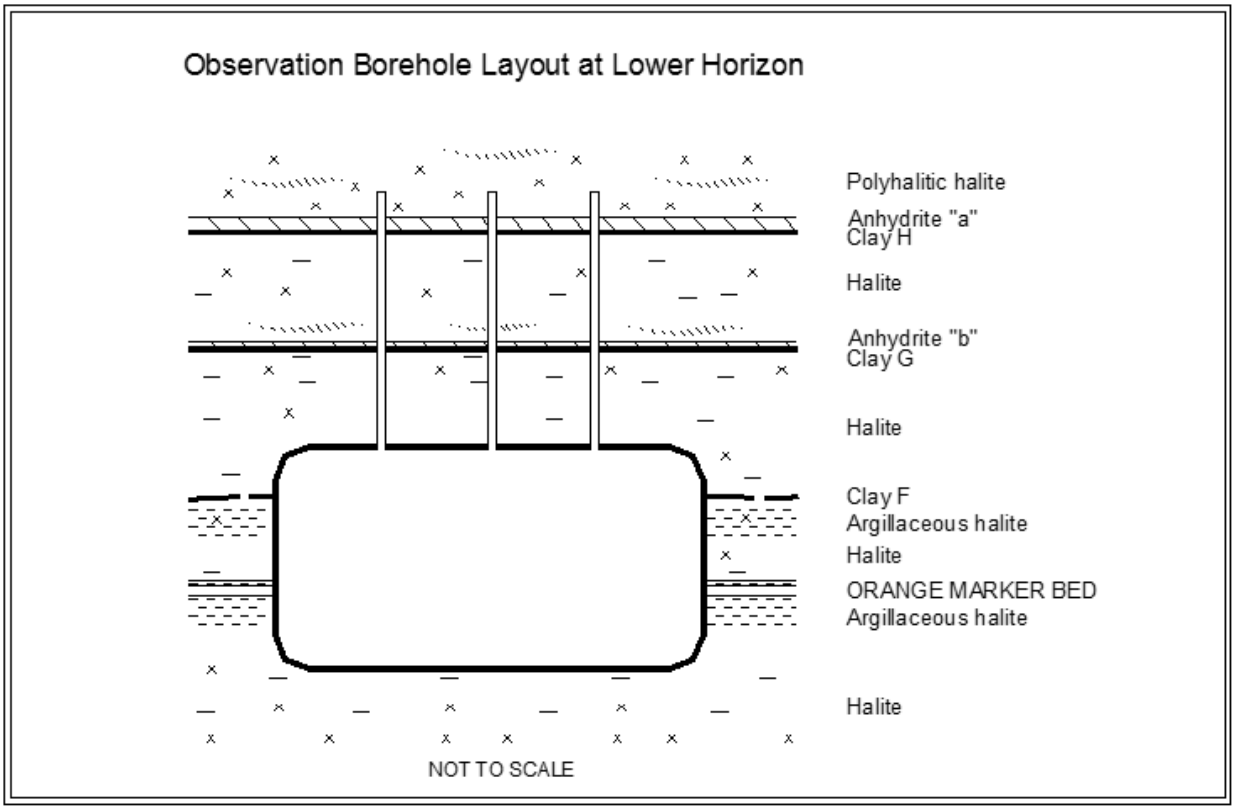

Figure 8-1. Example of Observation Hole Layout at Lower Horizon

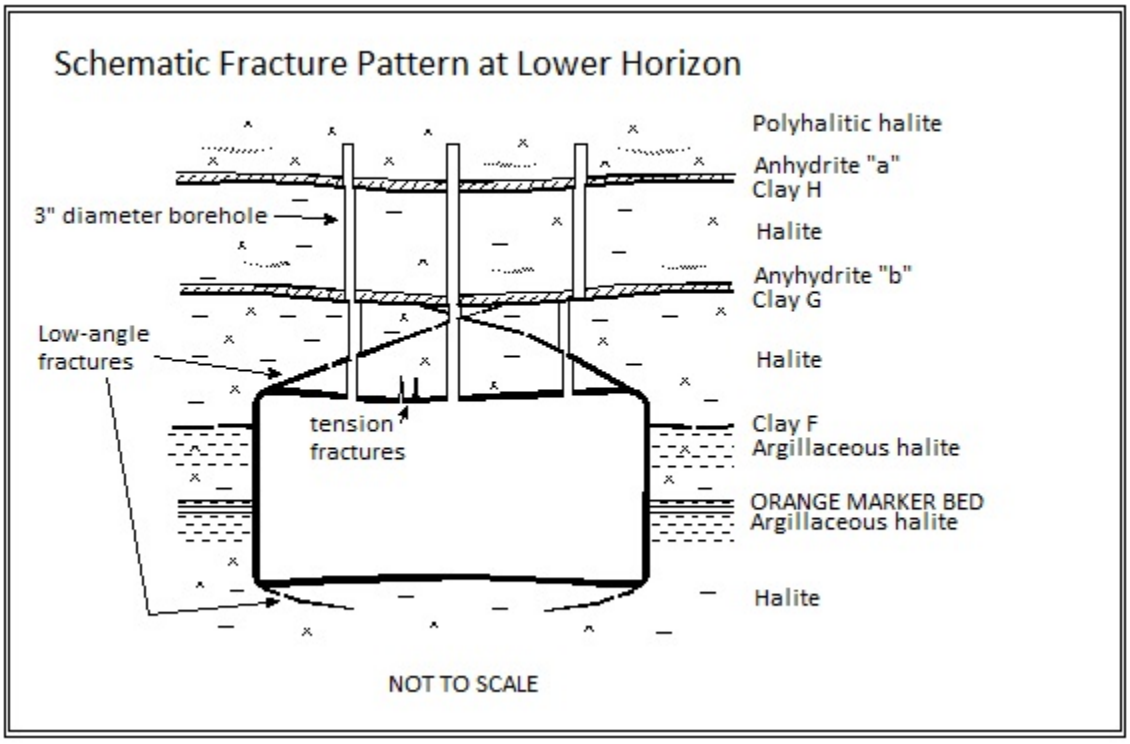

Figure 8-2. Typical Fracture Pattern at Lower Horizon

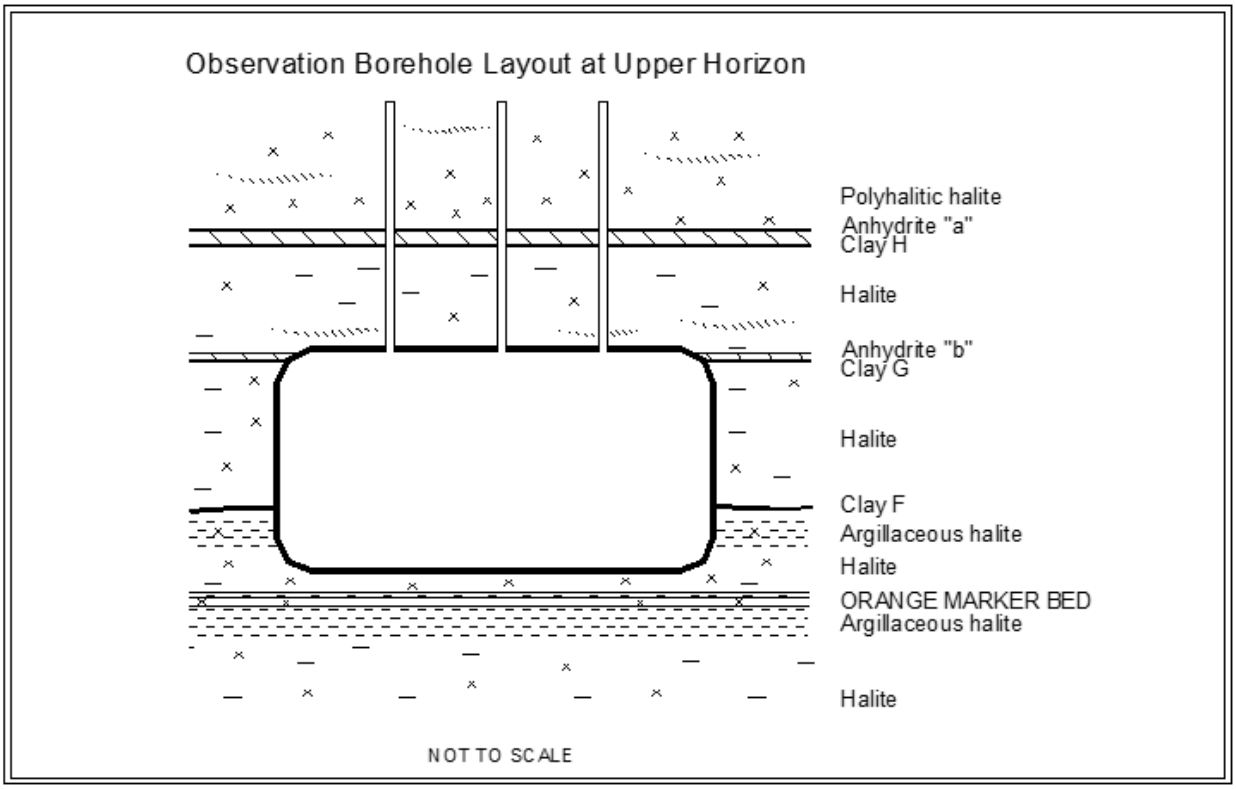

Figure 8-3. Example Observation Hole Layout at Upper Horizon

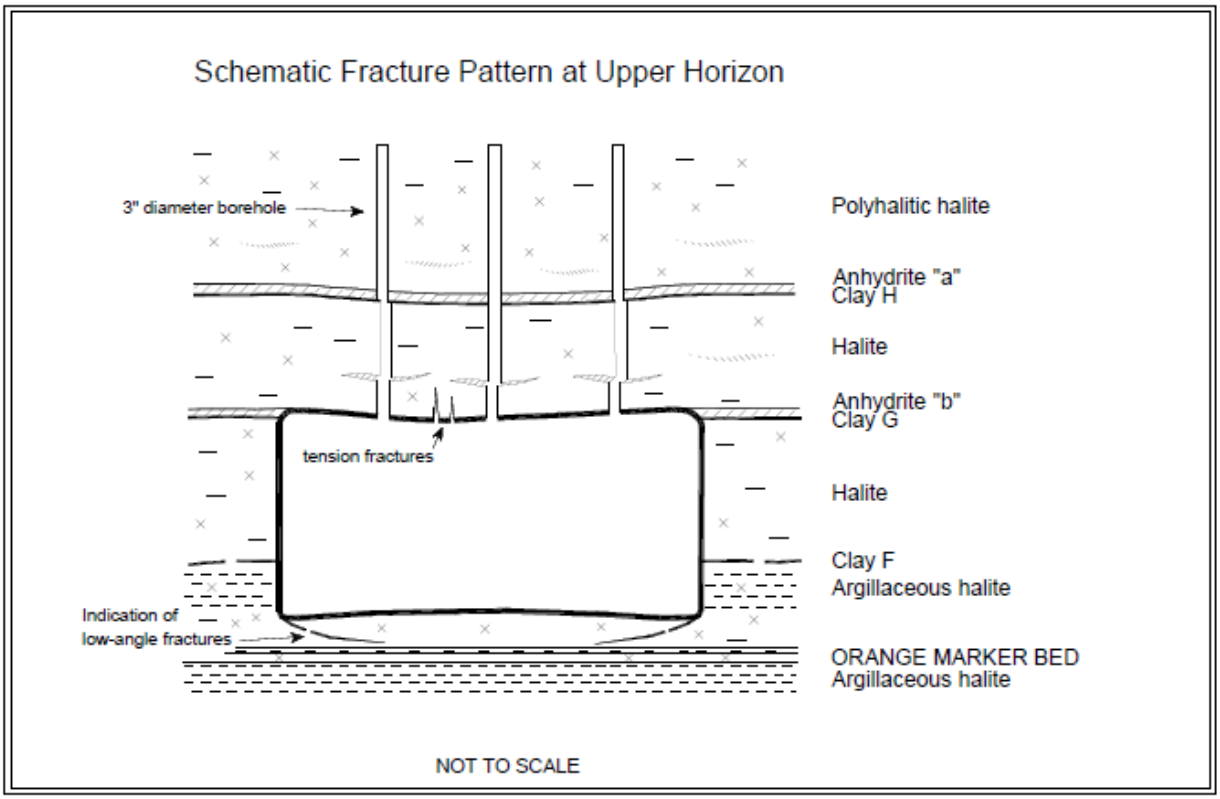

Figure 8-4. Typical Fracture Patterns at Upper Horizon

8.2 Fracture Mapping

Routine mapping documents the progression of fractures in the roof exposed on the excavation surfaces of the drifts and rooms in the underground repository. The fracture surveys are generally performed on an annual basis, and the fracture maps are updated. The fracture maps facilitate the analysis of strain in the immediate roof-beam because they document the development and propagation of fractures through time.

8.3 Stratigraphic Mapping

Stratigraphic mapping is the identification and partitioning of the sequence of rock strata based on their form, distribution, and lithologic composition. It is used to verify that there are no nonconformities in the geology within the waste disposal horizon at the WIPP.

8.4 Drilling and Geologic Core Descriptions

As new panels and new experimental areas are excavated, holes are typically drilled and cored vertically into the back and into the floor to depths of 50 ft to identify and describe the stratigraphic units present.

9.0 SUMMARY

At the inception of the WIPP, criteria were developed that address the design requirements (DOE, 1984). They pertained to all aspects of the mined facility and its operation as a pilot plant for the demonstration of technical and operational methods for permanent disposal of CH and RH TRU waste. In 1994, as the WIPP focus moved toward the permanent disposal of TRU waste, these design requirements were reassessed and replaced by a new set of requirements called system design descriptions. Table 9-1 shows the comparison of these design requirements with conditions actually observed in the underground from July 2017 through June 2018.

Replacement of failed rock bolts was performed at various locations during this reporting period. The pace of bolt replacement maintained before the radiological release event could not be met due to an increase in personal protection equipment requirement and the reduction in ventilation. This resulted in some areas being placed under restricted access or prohibited access until ground maintenance could be performed. Access to the W-170 drift from S-2180 to S-2520 was prohibited. A roof fall is thought to have occurred in Panel 7, Room 6 (a prohibited area) around January 1, 2019 – outside the current reporting period. The potential for a fall to occur was predicted by increasing room closure rates. Communication with the room closure instrumentation could not be established on January 2, 2019, inferring a roof fall had occurred.

The *in situ* performances of the accessible and bolted excavations generally continue to satisfy the appropriate design criteria. Although improvements to ground control maintenance activities in accessible areas in the underground have been made, additional efforts are still needed. Future changes to the planned life of some of the openings may require a change to the geometry of the access drifts, thus by removing unstable roof beam or rib spalls, milling the floor for added clearance, and installing roof bolts with mesh or straps.

In addition to underground instrumentation, qualitative assessments of fracture development are documented through mapping the underground repository and inspecting the observation holes. Although, as indicated in Section 8.0, no significant geoscience activities occurred during the current reporting period, the accumulation of many years of collected information acquired from these programs contributes to the understanding of the dynamic geomechanical processes in the WIPP underground. This aids in the design of effective ground control and support systems.

Table 9-1. Comparison of Excavation Performance to System Design Requirements

Requirement	Comments
"The lining shall be designed for a hydrostatic pressure. . . ."	Water pressure observed on piezometers located behind the shaft liners remains below design levels.
"The key shall be designed to resist the lateral pressure generated by salt creep."	Visual inspections of all shaft keys do not indicate any deterioration due to creep loading.
"The key shall be designed to retain the rock formation and will be provided with chemical seal rings and a water collection ring with drains to prevent water from flowing down the unlined shaft from the lining above."	Shaft inspection observations show no indication of instability due to salt dissolution. No water has been observed flowing along the rock-liner interface.
"The underground waste disposal facilities shall be designed to provide space and adequate access for the underground equipment and temporary storage space to support underground operations."	Geomechanical instrument data and visual observations indicate that the current design provides adequate access and storage and disposal space. Ground control maintenance is performed as necessary to maintain access. If ground control activities cannot be performed in a timely manner and the geomechanical data suggest potential instability, access to the drift is to be restricted or even prohibited until ground remediation can occur.
"Entries and subentries to the underground disposal area and the experimental areas shall be provided and sized for personnel safety, adequate air flow, and space for equipment."	Deformation of excavation remains within the required limits. Normal periodic maintenance consisting of rock bolting, wire meshing, trimming, and scaling continue throughout accessible areas of the repository. Areas such as the waste transport route undergo periodic floor trims in order to maintain adequate operating height.
"Geomechanical instrumentation shall be provided to measure the cumulative deformation of the rock mass surrounding mined drifts. . . ."	Geomechanical instrumentation is operated and maintained to meet this requirement. This annual report provides a summary and analysis of the geomechanical data.

10.0 REFERENCES

ASTM, 2006, D6026-06, *Standard Practice for Using Significant Digits in Geotechnical Data*.

Public Law 96-164, *Department of Energy National Security and Military Applications of Nuclear Energy Authorization Act of 1980*.

Title 40 CFR Part 191, *Environmental Radiation Protection Standards for Management and Disposal of Spent Nuclear Fuel, High-Level and Transuranic Radioactive Wastes.*

Title 40 CFR Part 194, *Criteria for the Certification and Re-certification of the Waste Isolation Pilot Plant's Compliance with the 40 CFR Part 191 Disposal Regulations.*

Holt, R. M., and D. W. Powers, 1990, *Geologic Mapping of the Air Intake Shaft at the Waste Isolation Pilot Plant*, DOE/WIPP 90-051, Waste Isolation Pilot Plant, Carlsbad, New Mexico.

Holt, R. M., and D. W. Powers, 1984, *Geotechnical Activities in the Waste Handling Shaft, Waste Isolation Pilot Plant (WIPP) Project, Southeastern New Mexico*, WTSD TME 038, Waste Isolation Pilot Plant, Carlsbad, New Mexico.

New Mexico Environment Department (NMED), 2016, Waste Isolation Pilot Plant Hazardous Waste Facility Permit, NM4890139088-TSDF, Santa Fe, New Mexico.

Powers, D. W., and R. M. Holt, 1993, *The Upper Cenozoic Gatuña Formation of Southeastern New Mexico, New Mexico Geological Society Guidebook*, 44th Field Conference, Carlsbad Region, New Mexico and West Texas, D. W. Love et al., Eds., pp 271-282.

Powers, D. W., and R. M. Holt, 1995, *Gatuña Formation (Miocene to Pleistocene) Geology and Paleohydrology*, prepared for Westinghouse Waste Isolation Division by International Technology Corporation, Albuquerque, New Mexico.

Powers, D. W., S. J. Lambert, S. E. Shaffer, L. R. Hill, and W. D. Weart, Eds.,1978, *Geological Characterization Report, Waste Isolation Pilot Plant (WIPP) Site, Southeastern New Mexico, Vols. I and II*, SAND 78 1596; Sandia National Laboratories, Albuquerque, New Mexico.

U.S. Department of Energy (DOE), 2000, *Brine Generation Study,* DOE/WIPP 00-2000, Waste Isolation Pilot Plant, Carlsbad, New Mexico.

U.S. Department of Energy (DOE), 1986a, *Interim Geotechnical Field Data Report,* DOE/WIPP 86-012, Waste Isolation Pilot Plant, Carlsbad, New Mexico.

U.S. Department of Energy (DOE), 1986b, *Waste Isolation Pilot Plant Design Validation Final Report*, DOE/WIPP 86-010; Prepared by Bechtel National, Inc., for the U.S. Department of Energy, San Francisco, California.

U.S. Department of Energy (DOE), 1985, *Quarterly Geotechnical Field Data Report*, DOE/WIPP-221, Waste Isolation Pilot Plant, Carlsbad, New Mexico.

U.S. Department of Energy (DOE), 1984, *Design Criteria, Waste Isolation Pilot Plant (WIPP) Revised Mission Concept-IIA*, DOE/WIPP-071; Waste Isolation Pilot Plant, Carlsbad, New Mexico.

U.S. Department of Energy (DOE), 1983, *Summary of the Results of the Evaluation of the WIPP Site and Preliminary Design Validation Program*, DOE/WIPP-161; Waste Isolation Pilot Plant, Carlsbad, New Mexico.

U.S. Environmental Protection Agency, 1998, "Criteria for the Certification and Recertification of the Waste Isolation Pilot Plant's Compliance with the Disposal Regulations: Certification Decision," *Federal Register*, Vol. 63, No. 95, pp. 27354, May 18, 1998, Washington, DC.

This page was intentionally left blank.

ISSUED

DOE/WIPP-19-3610
Volume 2

Waste Isolation Pilot Plant

Geotechnical Analysis Report For July 2017 – June 2018

Supporting Data

U.S. Department of Energy

October 2019

This page was intentionally left blank.

Waste Isolation Pilot Plant

Geotechnical Analysis Report For July 2017 – June 2018

Supporting Data

U.S. Department of Energy

UNITED STATES DEPARTMENT OF ENERGY

Approved by: \\Signature on File\\ Date: 10/25/19

Michael Brown
Director, Office of Environmental Protection
Carlsbad Field Office

This page was intentionally left blank.

This document has been submitted as required to:

U.S. Department of Energy
Office of Scientific and Technical Information
PO Box 62
Oak Ridge, TN 37831
(865) 576-8401

Additional information about this document may be obtained by calling 1-800-336-9477

Unlimited, publicly available full-text scientific and technical reports produced since 1991 are available online at Information Bridge (www.osti.gov/bridge).

U.S Department of Energy and its contractors may obtain full-text reports produced prior to 1991 in paper form for a processing fee from:

U.S. Department of Energy
Office of Scientific and Technical Information
P.O. Box 62
Oak Ridge, TN 37831-0062
Telephone: (865) 576-8401
Facsimile: (865) 576-5728
E-mail: reports@osti.gov

Available for sale to the public from:

U.S. Department of Commerce
National Technical Information Service
5301 Shawnee Rd
Alexandria, VA 22312
Phone: (800) 553-6847 or (703) 605-6000
Fax: (703) 605-6900
Email: info@ntis.gov

This page was intentionally left blank.

FOREWORD AND ACKNOWLEDGMENTS

This report contains an assessment of the geotechnical status of the Waste Isolation Pilot Plant (WIPP). During the excavation of the WIPP principal underground access and experimental areas, the status was reported quarterly. Since 1987, when the initial construction phase was completed, reports have been published annually. This report presents and analyzes data collected from July 1, 2017, to June 30, 2018.

This Geotechnical Analysis Report (GAR) was written to meet the needs of several audiences. It satisfies requirements contained in the WIPP Hazardous Waste Facility Permit[1] (HWFP) and the Certification of Compliance[2] with Subparts B and C, Title 40 *Code of Federal Regulations* (CFR) Part 191, "Environmental Radiation Protection Standards for Management and Disposal of Spent Nuclear Fuel, High-Level and Transuranic Radioactive Wastes." This report focuses on the geotechnical performance of the various components of the WIPP underground facility, including the shafts, shaft stations, access drifts, and waste disposal areas. The results of investigations of excavation effects and other geotechnical studies are also included.

The report compares the geotechnical performance of the repository to the design criteria. It describes the techniques that were used to acquire the data. The depth and breadth of the evaluation of the different components of the underground facility vary according to the types and quantities of data available and the complexity of the recorded geotechnical responses. Graphic documentation of data and tabular documentation of instrument history can be provided upon request.

This GAR was prepared by Nuclear Waste Partnership LLC for the U.S. Department of Energy (DOE), Carlsbad Field Office in Carlsbad, New Mexico. Work was supported by the DOE under Contract No. DE-EM0001971.

[1] New Mexico Environment Department (NMED), 2017, Waste Isolation Pilot Plant Hazardous Waste Facility Permit, NM4890139088-TSDF, Santa Fe, NM

[2] U.S. Environmental Protection Agency (EPA), 1998, "Criteria for the Certification and Recertification of the Waste Isolation Pilot Plant's Compliance with the Disposal Regulations: Certification Decision," Federal Register, Vol. 63, No. 95, pp. 27354, May 18, 1998, Washington, DC

This page was intentionally left blank.

TABLE OF CONTENTS

1.0 Introduction 17
1.1 Instrumentation 17
1.2 Data Plot Explanation 18
1.3 Report Organization 18
2.0 Instrumentation Summary for Shafts 18
3.0 Instrumentation Summary for Shaft Stations 27
4.0 Instrumentation Summary for the Access Drifts 39
5.0 Instrumentation Summary for the Waste Disposal Area 141
6.0 Instrumentation Summary for the SDI Area 157
7.0 Geoscience Summary for the Waste Disposal Area 159

LIST OF TABLES

Table 2-1 Salt Handling Shaft Data Analysis 19
Table 3-1 Salt Handling Shaft Station Data Analysis 28
Table 3-2 Waste Shaft Station Data Analysis 31
Table 3-3 Air Intake Shaft Station Data Analysis 33
Table 4-1 Access Drifts Data Analysis 40
Table 5-1 Panel 7 Access Drifts Data Analysis 142

LIST OF FIGURES

Salt Handling Shaft and Key

Figure 2-1 Piezometers Salt Handling Shaft – Level 580 at the Forty-niner Member 21
Figure 2-2 Piezometer Salt Handling Shaft – Level 620 at the Magenta Dolomite Member 21
Figure 2-3 Piezometers Salt Handling Shaft – Level 691 at the Tamarisk Member .. 22
Figure 2-4 Piezometer Salt Handling Shaft – Level 802 at the Los Medaños Member 22
Figure 2-5 Piezometer Salt Handling Shaft – Level 850 at the Rustler-Salado Contact 23
Figure 2-6 Earth Pressure Cells – Salt Handling Shaft Key – Level 860 23
Figure 2-7 Spot Welded Strain Gauge – Salt Handling Shaft Key – Level 856.3 24
Figure 2-8 Embedment Strain Gauge – Salt Handling Shaft Key – Level 856.3 24
Figure 2-9 Embedment Strain Gauge – Salt Handling Shaft Key – Level 862.4 25
Figure 2-10 Embedment Strain Gauge – Salt Handling Shaft Key – Level 856.3 25
Figure 2-11 Embedment Strain Gauge – Salt Handling Shaft Key – Level 862.4 26
Figure 3-1 Convergence Point Array – Salt Handling Shaft Station at S18 – Centerline – Roof to Floor 29
Figure 3-2 Convergence Point Array – Salt Handling Shaft Station at S18 – Quarter Point – Roof to Floor 29
Figure 3-3 Convergence Point Array – Salt Handling Shaft Station at S30 – Roof to Floor 30
Figure 3-4 Convergence Point Array – Salt Handling Shaft Station at S65 – Roof to Floor 30
Figure 3-5 Extensometer 51-GE-00404-2 Waste Shaft Station at E35 – Roof 32
Figure 3-6 Extensometer 41X-GE-00122 – Air Intake Shaft Station at W620 S65 – Roof 34
Figure 3-7 Extensometer 41X-GE-00123 – Air Intake Shaft Station at W620 N93 – Roof 34
Figure 3-8 Extensometer 51X-GE-00440 Air Intake Shaft at North Brow Station 35
Figure 3-9 Extensometer 51X-GE-00441 Air Intake Shaft South Brow Station 35
Figure 3-10 Extensometer 51X-GE-00401 Air Intake Shaft Station at W620 N20 – Roof 36
Figure 3-11 Rock Bolt Load Cells – Air Intake Shaft Station – South Brow Support – Bolts (1-5) 36
Figure 3-12 Rock Bolt Load Cells – Air Intake Shaft Station – South Brow Support – Bolts (6-10) 37
Figure 3-13 Rock Bolt Load Cells – Air Intake Shaft Station – North Brow Support – Bolts (1-5) 37
Figure 3-14 Rock Bolt Load Cells – Air Intake Shaft Station – North Brow Support – Bolts (6-10) 38
Figure 4-1 Wire Convergence Meter 51X-CW-01037 – E140 S2750 – Roof to Floor 49
Figure 4-2 Wire Convergence Meter 51X-CW-01039 – W170 S2735 – Roof to Floor 49
Figure 4-3 Wire Convergence Meter 51X-CW-01038 – W30 S2750 – Roof 50

Figure 4-4 Wire Convergence Meter 51X-GE-00442 – E300 S2750 – Roof 50
Figure 4-5 Extensometer 51X-GE-00355 – E0 N300 – Roof 51
Figure 4-6 Extensometer 51X-GE-00353 – E0 N626 – Roof 51
Figure 4-7 Extensometer 51X-GE-00352 – E0 N940 – Roof 52
Figure 4-8 Extensometer 51X-GE-00364 – E140 N1266 – Roof 52
Figure 4-9 Extensometer 51X-GE-00428-2 – E140 S1150 – Roof 53
Figure 4-10 Extensometer 51X-GE-00429 – E140 S1450 – Roof 53
Figure 4-11 Extensometer 51X-GE-00431 – E140 S1775 – Roof 54
Figure 4-12 Extensometer 51X-GE-00432 – E140 S1850 – Roof 54
Figure 4-13 Extensometer 51X-GE-00433-2 – E140 S2065 – Roof 55
Figure 4-14 Extensometer 51X-GE-00434 – E140 S2265 – Roof 55
Figure 4-15 Extensometer 51X-GE-00374 – E300 N1186 – Roof 56
Figure 4-16 Extensometer 51X-GE-00388 – E300 N1266 – Roof 56
Figure 4-17 Extensometer 51X-GE-00373 – E300 N1341 – Roof 57
Figure 4-18 Core Storage Library – Roof to Floor – Centerline 57
Figure 4-19 Convergence Point Array – E0 N75 – All Chords 58
Figure 4-20 Convergence Point Array – E0 N225 – Roof to Floor – Centerline 58
Figure 4-21 Convergence Point Array – E0 N300 – Roof to Floor – Centerline 59
Figure 4-22 Convergence Point Array – E0 N460 – Roof to Floor – Centerline 59
Figure 4-23 Convergence Point Array – E0 N562 – All Chords 60
Figure 4-24 Convergence Point Array – E0 N626 – Roof to Floor – Centerline 60
Figure 4-25 Convergence Point Array – E0 N686 – Roof to Floor – Centerline 61
Figure 4-26 Convergence Point Array – E0 N780 – Roof to Floor – Centerline 61
Figure 4-27 Convergence Point Array – E0 N940 – All Chords 62
Figure 4-28 Convergence Point Array – E0 N1100 – Roof to Floor – Centerline 62
Figure 4-29 Convergence Point Array – E0 N1266 – All Chords 63
Figure 4-30 Convergence Point Array – E0 N1420 – All Chords 63
Figure 4-31 Convergence Point Array – N140 E90 – All Chords 64
Figure 4-32 Convergence Point Array – E140 N5 – All Chords 64
Figure 4-33 Convergence Point Array – E140 N150 – Roof to Floor – Centerline 65
Figure 4-34 Convergence Point Array – E140 N220 – Roof to Floor – Centerline 65
Figure 4-35 Convergence Point Array – E140 N355 – All Chords 66
Figure 4-36 Convergence Point Array – E140 N460 – Roof to Floor – Centerline 66
Figure 4-37 Convergence Point Array – E140 N562 – All Chords 67
Figure 4-38 Convergence Point Array – E140 N626 – All Chords 67
Figure 4-39 Convergence Point Array – E140 N686 – All Chords 68
Figure 4-40 Convergence Point Array – E140 N780 – Roof to Floor – Centerline 68
Figure 4-41 Convergence Point Array – E140 N940 – All Chords 69
Figure 4-42 Convergence Point Array – E140 N1100 – Roof to Floor – Centerline 69
Figure 4-43 Convergence Point Array – E140 N1266 – Roof to Floor – Centerline 70
Figure 4-44 Convergence Point Array – E140 N1420 – Roof to Floor – Centerline 70
Figure 4-45 Convergence Point Array – E140 S90 – Roof to Floor – Centerline 71
Figure 4-46 Convergence Point Array – E140 S262 – All Chords 71
Figure 4-47 Convergence Point Array – E140 S460 – All Chords 72
Figure 4-48 Convergence Point Array – E140 S550 – All Chords 72
Figure 4-49 Convergence Point Array – E140 S700 – Roof to Floor – Centerline 73

Figure 4-50 Convergence Point Array – E140 S700 – Roof to Floor – East Quarter Point..... 73
Figure 4-51 Convergence Point Array – E140 S700 – Roof to Floor – West Quarter Point..... 74
Figure 4-52 Convergence Point Array – E140 S850 – Roof to Floor – Centerline 74
Figure 4-53 Convergence Point Array – E140 S1000 – Roof to Floor – Centerline 75
Figure 4-54 Convergence Point Array – E140 S1025 – Roof to Floor – Centerline 75
Figure 4-55 Convergence Point Array – E140 S1075 – Roof to Floor – Centerline 76
Figure 4-56 Convergence Point Array – E140 S1075 – Roof to Floor – East Quarter Point..... 76
Figure 4-57 Convergence Point Array – E140 S1075 – Roof to Floor – West Quarter Point..... 77
Figure 4-58 Convergence Point Array – E140 S1150 – Roof to Floor – Centerline 77
Figure 4-59 Convergence Point Array – E140 S1150 – Roof to Floor – East Quarter Point..... 78
Figure 4-60 Convergence Point Array – E140 S1150 – Rib to Rib 78
Figure 4-61 Convergence Point Array – E140 S1150 – Roof to Floor – West Quarter Point..... 79
Figure 4-62 Convergence Point Array – E140 S1225 – Roof to Floor – Centerline 79
Figure 4-63 Convergence Point Array – E140 S1225 – Roof to Floor – Quarter Points 80
Figure 4-64 Convergence Point Array – E140 S1300 – Roof to Floor – Centerline 80
Figure 4-65 Convergence Point Array – E140 S1378 – Roof to Floor – Centerline 81
Figure 4-66 Convergence Point Array – E140 S1378 – Roof to Floor – East Quarter Point..... 81
Figure 4-67 Convergence Point Array – E140 S1378 – Roof to Floor – West Quarter Point..... 82
Figure 4-68 Convergence Point Array – E140 S1450 – Roof to Floor – Centerline 82
Figure 4-69 Convergence Point Array – E140 S1450 – Roof to Floor – East Quarter Point..... 83
Figure 4-70 Convergence Point Array – E140 S1450 – Rib to Rib 83
Figure 4-71 Convergence Point Array – E140 S1450 – Roof to Floor – West Quarter Point..... 84
Figure 4-72 Convergence Point Array – E140 S1534 – All Chords..... 84
Figure 4-73 Convergence Point Array – E140 S1534 – Roof to Floor – East Quarter Point..... 85
Figure 4-74 Convergence Point Array – E140 S1534 – Roof to Floor – West Quarter Point..... 85
Figure 4-75 Convergence Point Array – E140 S1600 – Roof to Floor – Centerline 86
Figure 4-76 Convergence Point Array – E140 S1687 – Roof to Floor – Quarter Point 86
Figure 4-77 Convergence Point Array – E140 S1775 – Roof to Floor – Centerline 87
Figure 4-78 Convergence Point Array – E140 S1775 – Roof to Floor – East and West Quarter Points..... 87
Figure 4-79 Convergence Point Array – E140 S1775 – Rib to Rib 88
Figure 4-80 Convergence Point Array – E140 S1862 – Roof to Floor – Centerline 88

Figure 4-81 Convergence Point Array – E140 S1862 – Roof to Floor – East and West Quarter Points 89
Figure 4-82 Convergence Point Array – E140 S1950 – Roof to Floor – Centerline 89
Figure 4-83 Convergence Point Array – E140 S2007 – Roof to Floor – Centerline 90
Figure 4-84 Convergence Point Array – E140 S2065 – Roof to Floor – Centerline 90
Figure 4-85 Convergence Point Array – E140 S2122 – Roof to Floor – Centerline 91
Figure 4-86 Convergence Point Array – E140 S2275 – Roof to Floor – Centerline 91
Figure 4-87 Convergence Point Array – E140 S2350 – Roof to Floor – Centerline 92
Figure 4-88 Convergence Point Array – E140 S2425 – All Chords 92
Figure 4-89 Convergence Point Array – E140 S2520 – Roof to Floor – Centerline 93
Figure 4-90 Convergence Point Array – E140 S2634 – All Chords 93
Figure 4-91 Convergence Point Array – E300 N45 – Roof to Floor – Centerline and West Quarter Points 94
Figure 4-92 Convergence Point Array – E300 N170 – Roof to Floor – Centerline and West Quarter Points 94
Figure 4-93 Convergence Point Array – E300 N280 – Roof to Floor – Centerline 95
Figure 4-94 Convergence Point Array – E300 N300 – Roof to Floor – Centerline 95
Figure 4-95 Convergence Point Array – E300 N440 – Roof to Floor – Centerline 96
Figure 4-96 Convergence Point Array – E300 N500 – Roof to Floor – Centerline 96
Figure 4-97 Convergence Point Array – E300 N1100 – Roof to Floor – Centerline 97
Figure 4-98 Convergence Point Array – E300 N1262 – All Chords 97
Figure 4-99 Convergence Point Array – E300 N1341 – All Chords 98
Figure 4-100 Convergence Point Array – E300 N1420 – Roof to Floor – Centerline 98
Figure 4-101 Convergence Point Array – E300 S45 – Roof to Floor – All Chords 99
Figure 4-102 Convergence Point Array – E300 S90 – Roof to Floor – Centerline 99
Figure 4-103 Convergence Point Array – E300 S250 – All Chords 100
Figure 4-104 Convergence Point Array – E300 S700 – Roof to Floor – Centerline 100
Figure 4-105 Convergence Point Array – E300 S2275 – Roof to Floor – Centerline 101
Figure 4-106 Convergence Point Array – E300 S2350 – Roof to Floor – Centerline 101
Figure 4-107 Convergence Point Array – E300 S2634 – All Chords 102
Figure 4-108 Convergence Point Array – N215 W500 – All Chords 102
Figure 4-109 Convergence Point Array – N215 W620 – Roof to Floor – Centerline 103
Figure 4-110 Convergence Point Array – N250 E220 – Roof to Floor – Centerline 103
Figure 4-111 Convergence Point Array – N250 E220 – Roof to Floor – Quarter Points 104
Figure 4-112 Convergence Point Array – N250 E220 – Roof to Floor – West Quarter Point 104
Figure 4-113 Convergence Point Array – E300 N170 – Roof to Floor – Centerline 105
Figure 4-114 Convergence Point Array – E300 N170 – Roof to Floor - Centerline 105
Figure 4-115 Convergence Point Array –N460 E70 – All Chords 106
Figure 4-116 Convergence Point Array – N780 E70 – Roof to Floor – Centerline 106
Figure 4-117 Convergence Point Array – N1420 E212 – All Chords 107
Figure 4-118 Convergence Point Array – N1420 E79 – Roof to Floor – Centerline 107
Figure 4-119 Convergence Point Array – S1000 E120 – Roof to Floor – Centerline 108
Figure 4-120 Convergence Point Array – S1000 E160 – Roof to Floor – Centerline 108
Figure 4-121 Convergence Point Array – S1000 E58 – All Chords 109
Figure 4-122 Convergence Point Array – S1000 W98 – All Chords 109

Figure 4-123 Convergence Point Array – S1300 E120 – Roof to Floor – Centerline .. 110
Figure 4-124 Convergence Point Array – S1300 E160 – Roof to Floor – Centerline .. 110
Figure 4-125 Convergence Point Array – S1300 E24 – Roof to Floor – Centerline 111
Figure 4-126 Convergence Point Array – S1300 W100 – Roof to Floor – Centerline . 111
Figure 4-127 Convergence Point Array – S1600 E110 – Roof to Floor – Centerline .. 112
Figure 4-128 Convergence Point Array – S1600 E170 – Roof to Floor – Centerline .. 112
Figure 4-129 Convergence Point Array – S1950 E113 – Roof to Floor – Centerline .. 113
Figure 4-130 Convergence Point Array – S1950 E160 – Roof to Floor – Centerline .. 113
Figure 4-131 Convergence Point Array – S1950 E226 – Roof to Floor – Centerline .. 114
Figure 4-132 Convergence Point Array – S1950 W100 – Roof to Floor – Centerline . 114
Figure 4-133 Convergence Point Array – S2180 E220 – All Chords..... 115
Figure 4-134 Convergence Point Array – S2520 E220 – All Chords..... 115
Figure 4-135 Convergence Point Array – S2520 W100 – All Chords..... 116
Figure 4-136 Convergence Point Array – S700 E180 – All Chords..... 116
Figure 4-137 Convergence Point Array – S700 E205 – All Chords..... 117
Figure 4-138 Convergence Point Array – S700 W98 – Roof to Floor – Centerline 117
Figure 4-139 Convergence Point Array – S90 W120 – All Chords..... 118
Figure 4-140 Convergence Point Array – S90 W400 – All Chords..... 118
Figure 4-141 Convergence Point Array – S90 W590 – All Chords..... 119
Figure 4-142 Convergence Point Array – S90 W620 – Roof to Floor – Centerline 119
Figure 4-143 Convergence Point Array – W170 N150 – Roof to Floor – Centerline ... 120
Figure 4-144 Convergence Point Array – W170 S5 – All Chords..... 120
Figure 4-145 Convergence Point Array – W170 S90 – Roof to Floor – Centerline 121
Figure 4-146 Convergence Point Array – W170 S232 – All Chords..... 121
Figure 4-147 Convergence Point Array – W170 S400 – Roof to Floor – Centerline ... 122
Figure 4-148 Convergence Point Array – W170 S560 – All Chords..... 122
Figure 4-149 Convergence Point Array – W170 S700 – Roof to Floor – Centerline ... 123
Figure 4-150 Convergence Point Array – W170 S850 – Roof to Floor – Centerline ... 123
Figure 4-151 Convergence Point Array – W170 S850 – Rib to Rib 124
Figure 4-152 Convergence Point Array – W170 S1000 – Roof to Floor – Centerline . 124
Figure 4-153 Convergence Point Array – W170 S1150 – Roof to Floor – Centerline . 125
Figure 4-154 Convergence Point Array – W170 S1150 – Rib to Rib 125
Figure 4-155 Convergence Point Array –W170 S1300 – Roof to Floor – Centerline .. 126
Figure 4-156 Convergence Point Array – W170 S1445 – All Chords..... 126
Figure 4-157 Convergence Point Array – W170 S1600 – Roof to Floor – Centerline . 127
Figure 4-158 Convergence Point Array – W170 S1779 – All Chords..... 127
Figure 4-159 Convergence Point Array – W170 S1950 – Roof to Floor – Centerline . 128
Figure 4-160 Convergence Point Array – W170 S2060 – Roof to Floor – Centerline . 128
Figure 4-161 Convergence Point Array – W170 S2180 – Roof to Floor – Centerline . 129
Figure 4-162 Convergence Point Array – W170 S2520 – Roof to Floor – Centerline . 129
Figure 4-163 Convergence Point Array – W30 S90 – Roof to Floor – Centerline 130
Figure 4-164 Convergence Point Array – W30 S120 – Roof to Floor – Centerline 130
Figure 4-165 Convergence Point Array – W30 S250 – All Chords..... 131
Figure 4-166 Convergence Point Array – W30 S400 – Roof to Floor – Centerline 131
Figure 4-167 Convergence Point Array – W30 S500 – All Chords..... 132
Figure 4-168 Convergence Point Array – W30 S700 – Roof to Floor – Centerline 132
Figure 4-169 Convergence Point Array – W30 S850 – Roof to Floor – Centerline 133

Figure 4-170 Convergence Point Array – W30 S850 – Quarter Points 133
Figure 4-171 Convergence Point Array – W30 S1000 – Roof to Floor – Centerline ... 134
Figure 4-172 Convergence Point Array – W30 S1150 – Roof to Floor – Centerline ... 134
Figure 4-173 Convergence Point Array – W30 S1300 – Roof to Floor – Centerline ... 135
Figure 4-174 Convergence Point Array – W30 S1453 – All Chords..... 135
Figure 4-175 Convergence Point Array – W30 S1600 – Roof to Floor – Centerline ... 136
Figure 4-176 Convergence Point Array – W30 S1775 – All Chords..... 136
Figure 4-177 Convergence Point Array – W30 S1950 – Roof to Floor – Centerline ... 137
Figure 4-178 Convergence Point Array – W30 S2067 – All Chords..... 137
Figure 4-179 Convergence Point Array – W30 S2520 – Roof to Floor – Centerline ... 138
Figure 4-180 Convergence Point Array – W30 S2635 – All Chords..... 138
Figure 4-181 Joint Meter – S1950 E300 Overcast 139
Figure 4-182 Joint Meter – E140 S1529 139
Figure 4-183 Joint Meter – E140 S1545 140
Figure 4-184 Joint Meter – E140 S1795 140
Figure 5-1 Convergence Point Array – S2180 W285 – Roof to Floor..... 143
Figure 5-2 Convergence Point Array – S2180 W585 – Roof to Floor..... 143
Figure 5-3 Convergence Point Array – S2180 W660 – Roof to Floor..... 144
Figure 5-4 Convergence Point Array – S2180 W790 – Roof to Floor..... 144
Figure 5-5 Convergence Point Array – S2180 W855 – Roof to Floor..... 145
Figure 5-6 Convergence Point Array – S2180 W920 – Roof to Floor..... 145
Figure 5-7 Convergence Point Array – S2180 W985 – Roof to Floor..... 146
Figure 5-8 Convergence Point Array – S2180 W1050 – Roof to Floor..... 146
Figure 5-9 Convergence Point Array – W390 S2275 – Roof to Floor..... 147
Figure 5-10 Convergence Point Array – W390 S2350 – Roof to Floor..... 147
Figure 5-11 Convergence Point Array – W390 S2425 – Roof to Floor..... 148
Figure 5-12 Convergence Point Array – W520 S2275 – Roof to Floor..... 148
Figure 5-13 Convergence Point Array – W520 S2350 – Roof to Floor..... 149
Figure 5-14 Convergence Point Array – W520 S2425 – Roof to Floor..... 149
Figure 5-15 Convergence Point Array – W660 S2275 – Roof to Floor..... 150
Figure 5-16 Convergence Point Array – W660 S2350 – Roof to Floor..... 150
Figure 5-17 Convergence Point Array – W660 S2425 – Roof to Floor..... 151
Figure 5-18 Convergence Point Array – W920 S2350 – Roof to Floor..... 151
Figure 5-19 Convergence Point Array – W920 S2425 – Roof to Floor..... 152
Figure 5-20 Convergence Point Array – S2520 W285 – Roof to Floor..... 152
Figure 5-21 Convergence Point Array – S2520 W390 – Roof to Floor..... 153
Figure 5-22 Convergence Point Array – S2520 W455 – Roof to Floor..... 153
Figure 5-23 Convergence Point Array – S2520 W520 – Roof to Floor..... 154
Figure 5-24 Convergence Point Array – S2520 W585 – Roof to Floor..... 154
Figure 5-25 Convergence Point Array – S2520 W660 – Roof to Floor..... 155
Figure 5-26 Convergence Point Array – S2520 W725 – Roof to Floor..... 155
Figure 5-27 Convergence Point Array – S2520 W790 – Roof to Floor..... 156
Figure 5-28 Convergence Point Array – S2520 W855 – Roof to Floor..... 156
Figure 5-29 Convergence Point Array – S2520 W920 – Roof to Floor..... 157
Figure 6-1 Ground Control Map - July 2017..... 158

1.0 INTRODUCTION

This report is a compilation of geotechnical data presented as plots for each active instrument installed in the underground at the Waste Isolation Pilot Plant (WIPP) through June 30, 2018. A summary of the geotechnical analyses that were performed using the compiled data is provided in Volume 1 of the Geotechnical Analysis Report (GAR).

1.1 Instrumentation

Geomechanical instrument data included in this report reflect the measurements of the geomechanical response of the underground within the mine. The instruments consist of convergence points, borehole extensometers, rock bolt load cells, pressure cells, strain gauges, piezometers, and joint meters.

Closure measurements are taken at convergence points. Rock displacement is calculated by measuring the distance between two opposing points. Displacement is monitored over time and is plotted as closure versus time. Annual rates of closure are calculated for the convergence data and are compared with annual closure rates from previous reporting periods.

Borehole extensometers are used to determine the absolute movements of the ground around the openings within the mine. With these instruments, stainless steel cables are installed into a hole and anchored at various depths. The displacement at the extensometer head (located near the excavation face) is measured relative to each of the fixed anchors. These data are used in the extensometer *displacement* plots presented in this report. Annual rates of displacement are calculated for each extensometer and are compared with the annual displacement rate reported during the previous reporting period.

Rock bolt load cells are used to measure the load exerted by the overburden and the effectiveness of rock bolts. Plots for each instrumented rock bolt are presented as load versus time.

Earth pressure cells and strain gauges are used in and around the shaft liners to determine their loads. These are also depicted in time-based plots. Monitoring of these instruments indicate whether there are stress buildup in the shaft lining systems.

Piezometers are used to measure the gauge pressure of groundwater. They have been installed in the shafts at varying elevations to monitor the hydraulic head acting on the shaft liners. Plots from piezometers are presented as pressure versus time.

Joint meters are installed perpendicular to a crack and monitor changes in separation of the crack which may occur over time.

1.2 Data Plot Explanation

Data are presented in graphical form for ease of interpretation. Time-based plots are used in this report. Each plot generally displays a legend in the upper right-hand corner that gives the array name and specific location of the instrument or point evaluated. The legend ties the graphical cross-sectional representation of the drift or shaft typically presented in the lower right-hand corner to the symbols on the curve in the graph. For extensometers, each anchor is designated with an alpha character "A" closest to the collar and "B," "C," "D," or "E" for the furthest point from the collar (the deepest anchor). For convergence points, the horizontal and vertical sections of the drift are referred to as chords. Breaks in the graph for convergence data and a numeric designator added to the legend typically indicate that the convergence point was lost due to normal mine maintenance activities and later reinstalled.

1.3 Report Organization

Chapter 1.0 provides an introduction to this Supporting Data volume of the GAR. Chapter 2.0 provides instrument data analysis for the Salt Shaft, followed by data plots for the piezometers, earth pressure cells, spot welded strain gauges, and embedment strain gauges installed in the Salt Shaft. Chapter 3.0 provides instrument data analysis for the Salt Shaft Station and Waste Shaft Station and an instrument data summary only for the area immediately surrounding the Air Intake Shaft, and data plots for extensometers, convergence points, and rock bolt load cells for all three locations. Chapter 4.0 provides instrument data analysis for the access drifts followed by data plots for the extensometers, convergence points, joint meters and rock bolt load cells. Chapter 5.0 provides instrument data analysis for the Waste Disposal Area followed by data plots for the extensometers and convergence points. Chapter 6.0 provides convergence point instrument data analysis for the Salt Disposal Investigations (SDI) area. Chapter 7.0 provides geologic data collected through the mapping of fractures, stratigraphic mapping and the observed displacements in vertical boreholes.

2.0 INSTRUMENTATION SUMMARY FOR SHAFTS

Originally, the Salt, Waste, and Exhaust Shafts were instrumented with Geomechanical instrumentation. The instrument readings from the Waste and Exhaust Shafts are no longer available due to failed instruments, broken cabling, and/or inoperable/obsolete data acquisition equipment. Table 2-1 presents data and analysis of the Salt Shaft instrumentation. Plots of the instrument data are presented as Figures 2-1 through 2-11.

Table 2-1 Salt Handling Shaft Data Analysis

Piezometers

Field Tag	Level feet	Figure Number	Date of 2017-2018 Max. Reading	2017-2018 Maximum Pressure Readings (psi)	Date of 2016-2017 Max. Reading	2016-2017 Maximum Pressure Readings (psi)	Change in Maximum Pressure From Previous Year (psi)	Comments
37X-PE-00201	580	2-1	02/19/18	85	03/06/17	75	10	
37X-PE-00202	580	2-1	05/29/18	110	06/12/17	112	-2	
37X-PE-00203	620	2-2	03/26/18	171	03/06/17	174	-3	
37X-PE-00204	620	2-2	03/19/18	150	06/12/17	192	-42	
37X-PE-00205	691	2-3	05/29/18	195	06/20/17	189	6	
37X-PE-00206	691	2-3	05/29/18	190	06/20/17	183	7	
37X-PE-00210	802	2-4	04/24/18	8	05/22/17	-1	9	
37X-PE-00211	850	2-5	10/10/17	34	01/30/17	33	1	
37X-PE-00212	850	2-5	07/11/17	77	06/20/17	91	-14	

Earth Pressure Cells

Field Tag	Level feet	Figure Number	Date of 2017-2018 Max. Reading	2017-2018 Maximum Pressure Readings (psi)	Date of 2016-2017 Max. Reading	2016-2017 Maximum Pressure Readings (psi)	Change in Maximum Pressure From Previous Year (psi)	Comments
37X-WE-00201	862.4	2-6	09/18/17	-11	06/20/17	-13	2	
37X-WE-00202	862.4	2-6	06/26/18	-27	06/12/17	-27	0	

Spot-Welded Strain Gauges

Field Tag	Level feet	Figure Number	Date of 2017-2018 Max. Reading	2017-2018 Maximum Strain Readings (με)	Date of 2016-2017 Max. Reading	2016-2017 Maximum Strain Readings (με)	Change in Maximum Strain From Previous Year (με)	Comments
37X-ZE-00206	856.3	2-7	07/11/17	677	06/20/17	674	3	

Table 2-1 Salt Handling Shaft Data Analysis (continued)

Embedment Strain Gauges								
Field Tag	Level feet	Figure Number	Date of 2017-2018 Max. Reading	2017-2018 Maximum Strain Readings (με)	Date of 2016-2017 Max. Reading	2016-2017 Maximum Strain Readings (με)	Change in Maximum Strain From Previous Year (με)	Comments
37X-ZE-00209	856.3	2-8	01/08/18	-549	01/30/17	-541	-8	
37X-ZE-00210	856.3	2-8	07/11/17	1021	06/20/17	1018	3	
37X-ZE-00211	856.3	2-8	08/01/17	356	06/26/17	351	5	
37X-ZE-00212	856.3	2-8	01/02/18	-970	01/30/17	-805	-165	
37X-ZE-00213	856.3	2-8	08/01/17	434	06/26/17	431	3	
37X-ZE-00214	856.3	2-8	07/11/17	171	06/20/17	168	3	
37X-ZE-00215	856.3	2-8	08/01/17	161	06/26/17	157	4	
37X-ZE-00216	856.3	2-8	06/26/18	699	06/20/17	697	2	
37X-ZE-00225	862.4	2-9	08/01/17	340	06/26/17	332	8	
37X-ZE-00226	862.4	2-9	08/01/17	78	06/26/17	68	10	
37X-ZE-00229	862.4	2-9	08/01/17	961	06/26/17	946	15	
37X-ZE-00230	862.4	2-9	05/29/18	736	06/06/17	723	13	
37X-ZE-00235	856.3	2-10	01/08/18	-401	01/30/17	-402	1	
37X-ZE-00236	856.3	2-10	06/26/18	208	06/20/17	194	14	
37X-ZE-00237	856.3	2-10	07/11/17	146	06/20/17	147	-1	
37X-ZE-00238	856.3	2-10	08/01/17	581	06/20/17	576	5	
37X-ZE-00239	862.4	2-11	08/01/17	443	06/26/17	435	8	
37X-ZE-00242	862.4	2-11	08/01/17	161	03/06/17	-163	324	

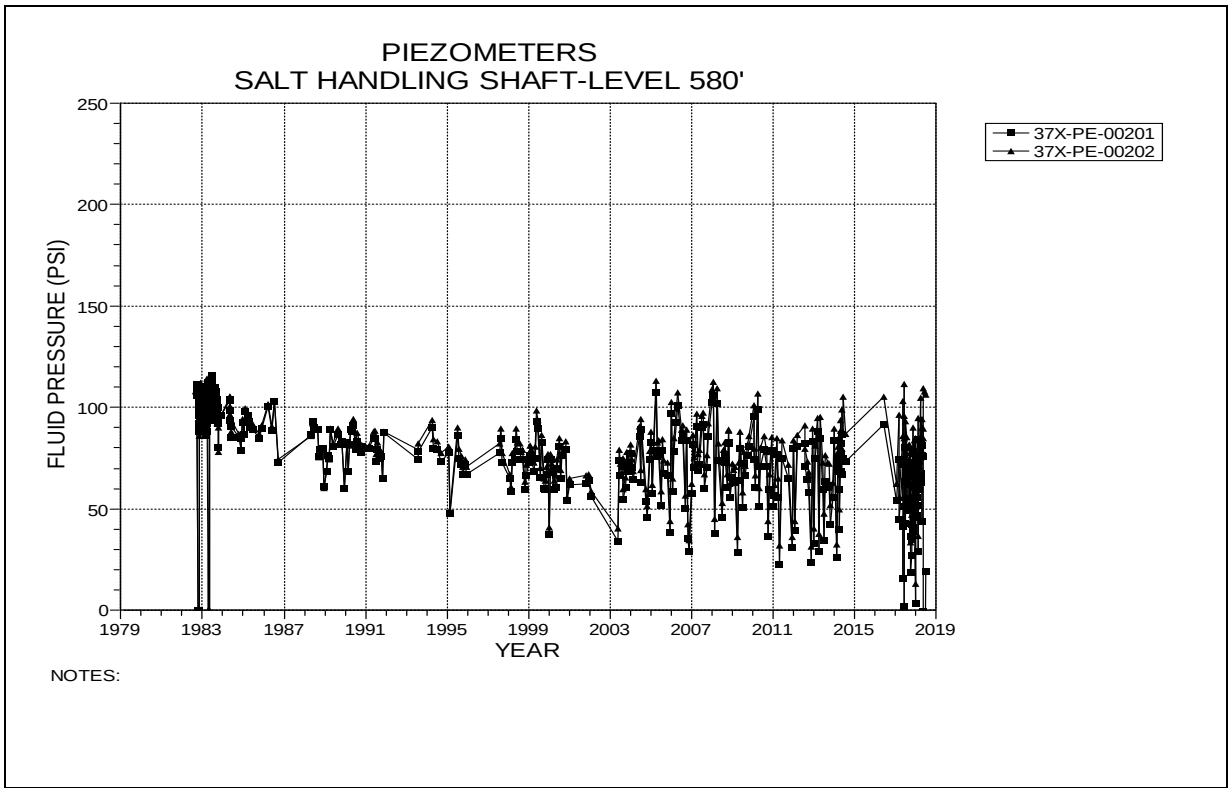

Figure 2-1 Piezometers Salt Handling Shaft – Level 580 at the Forty-niner Member

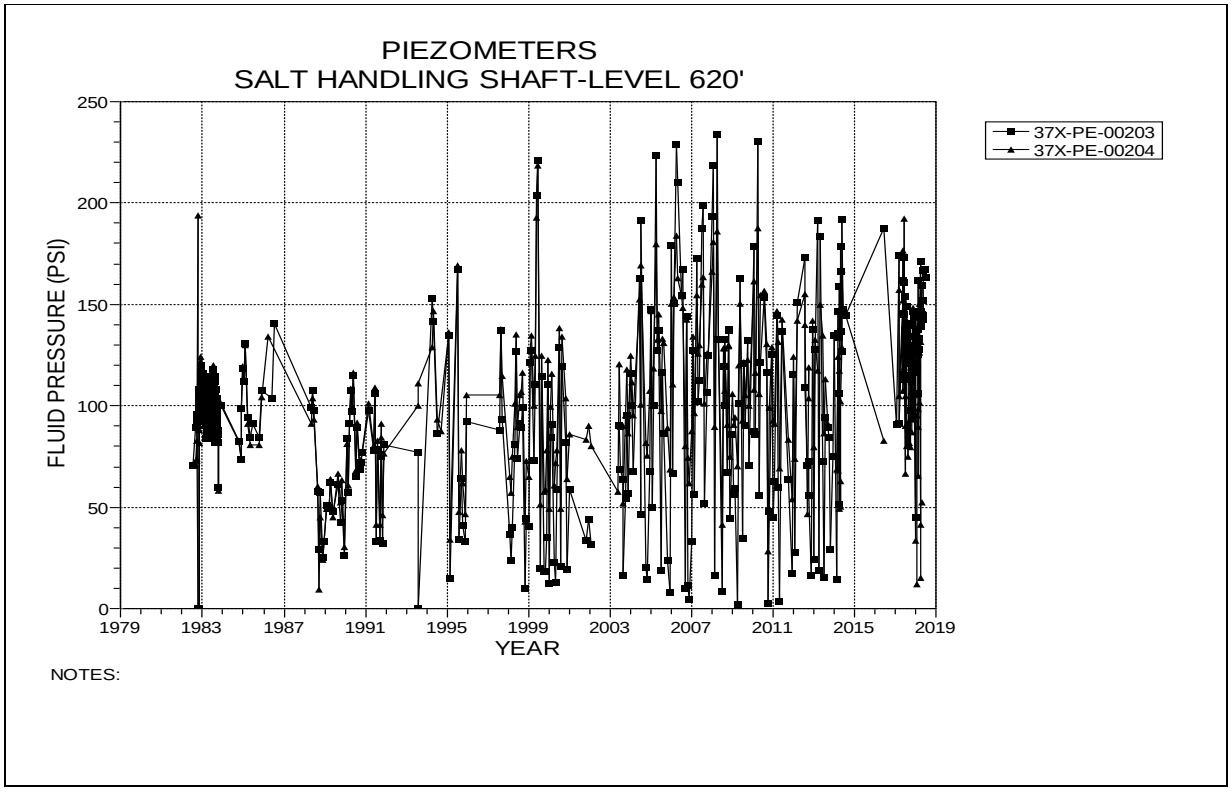

Figure 2-2 Piezometer Salt Handling Shaft – Level 620 at the Magenta Dolomite Member

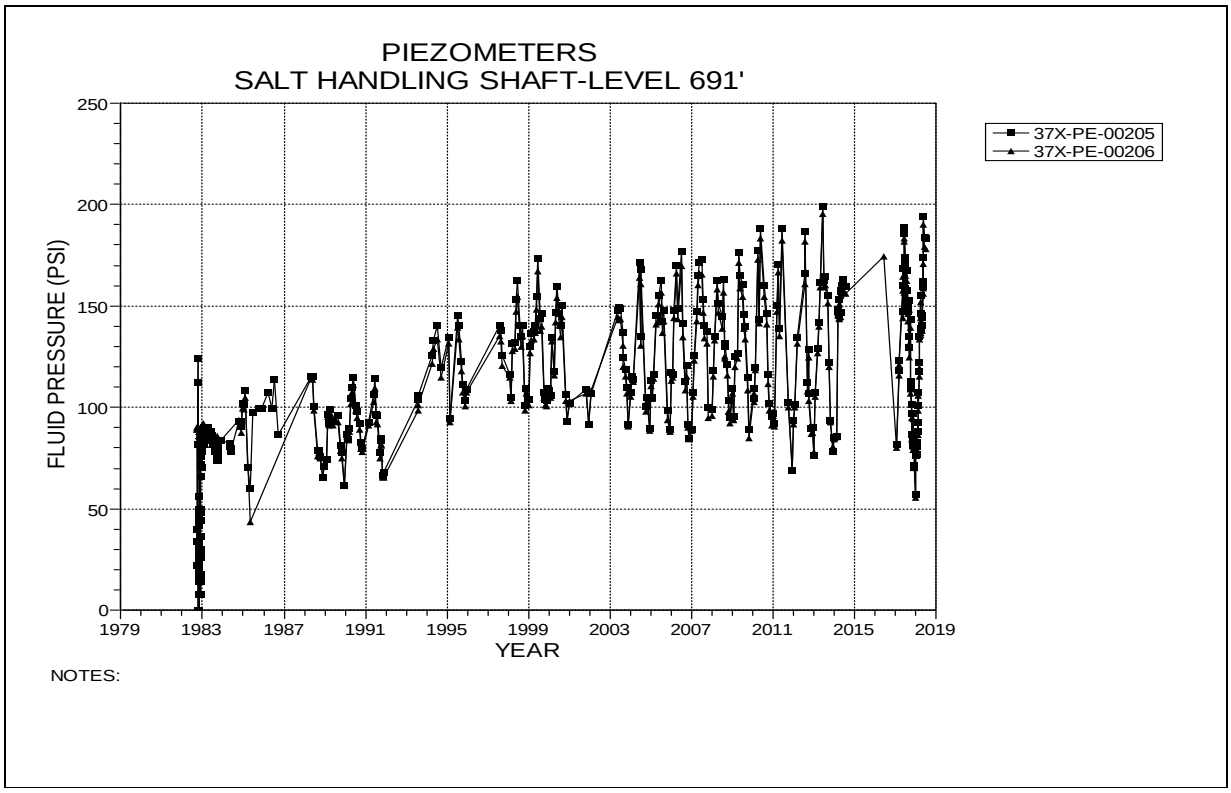

Figure 2-3 Piezometers Salt Handling Shaft – Level 691 at the Tamarisk Member

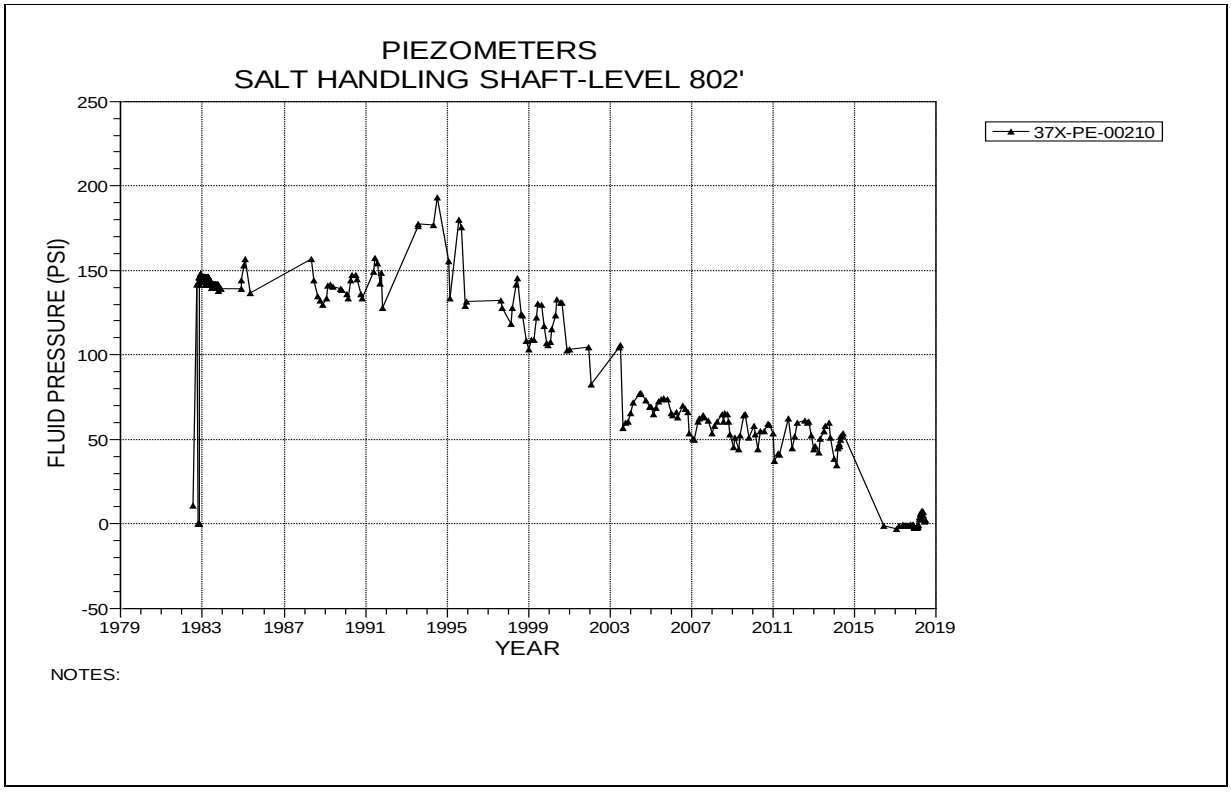

Figure 2-4 Piezometer Salt Handling Shaft – Level 802 at the Los Medaños Member

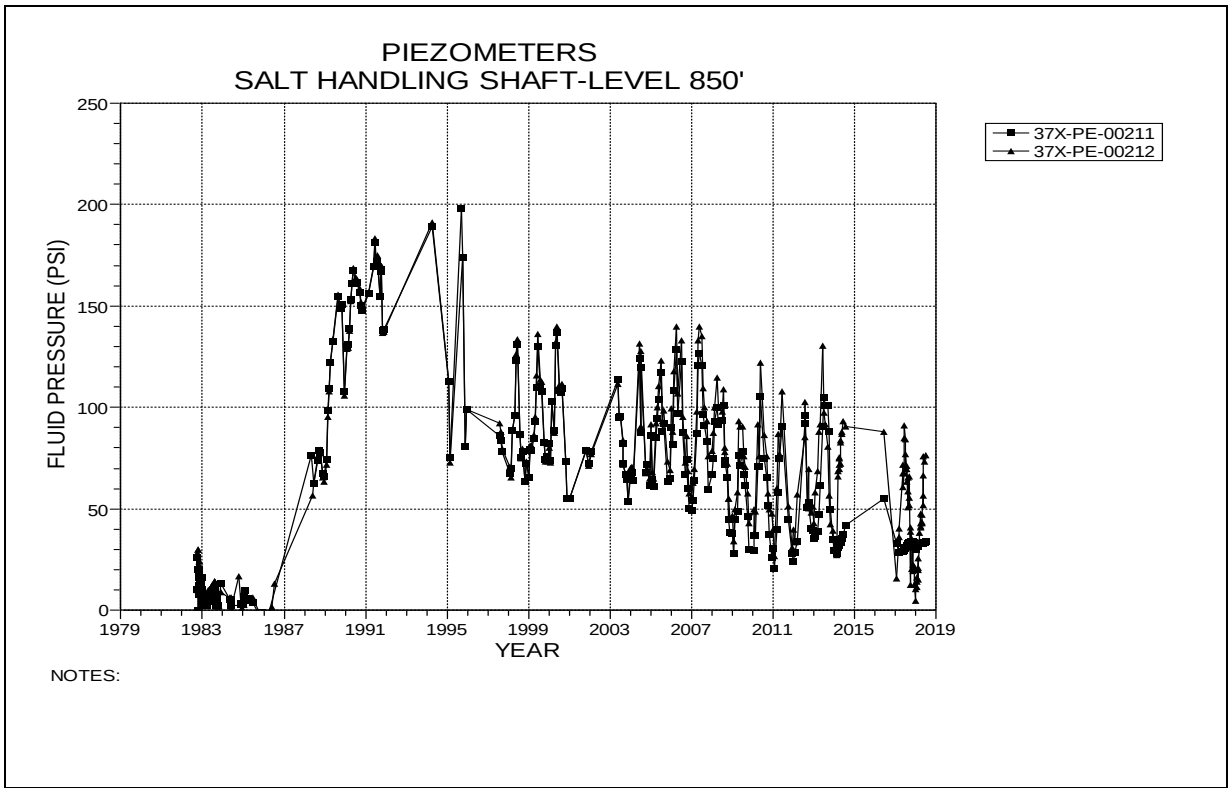

Figure 2-5 Piezometer Salt Handling Shaft – Level 850 at the Rustler-Salado Contact

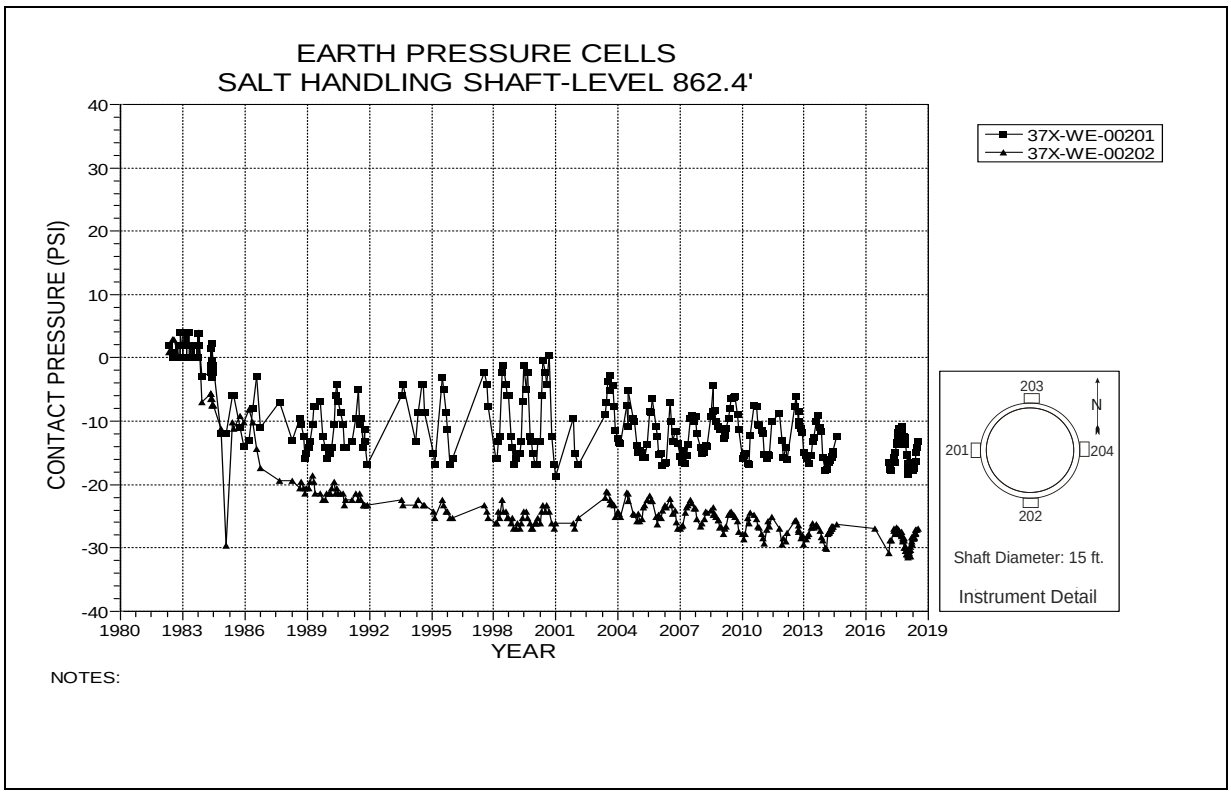

Figure 2-6 Earth Pressure Cells – Salt Handling Shaft Key – Level 860

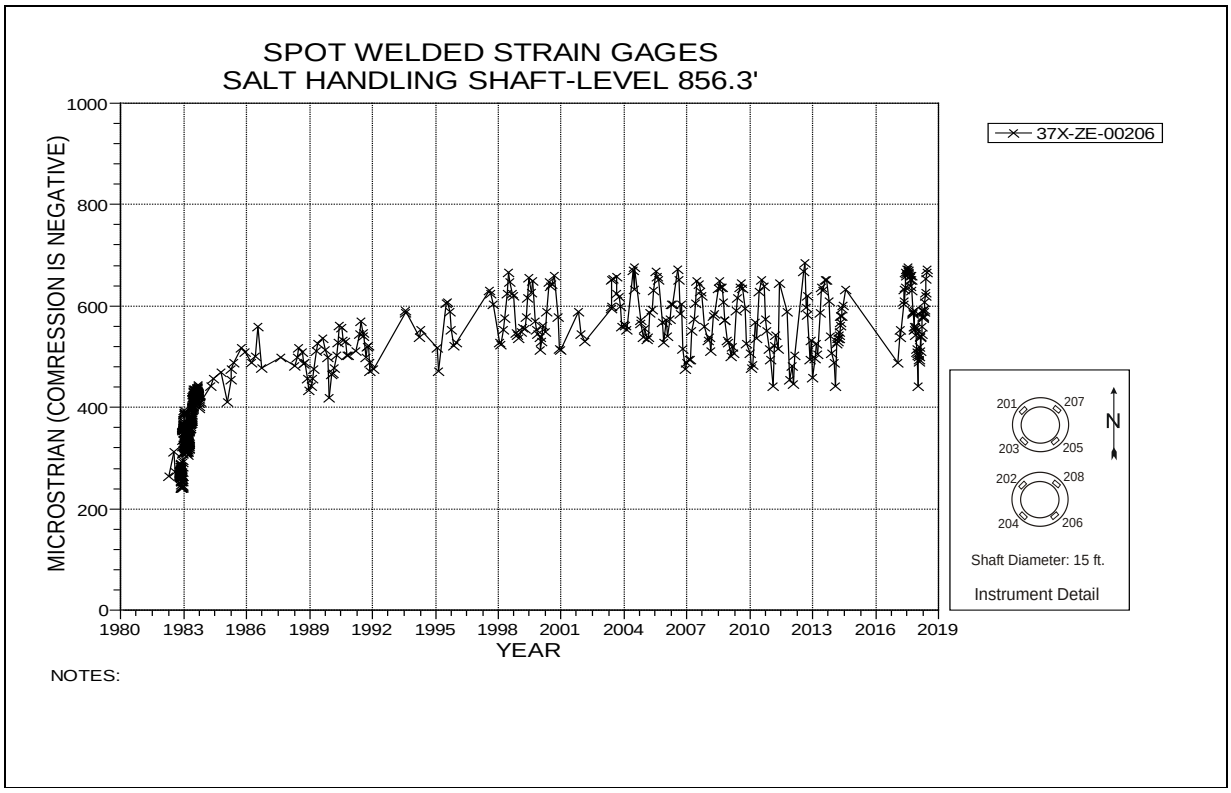

Figure 2-7 Spot Welded Strain Gauge – Salt Handling Shaft Key – Level 856.3

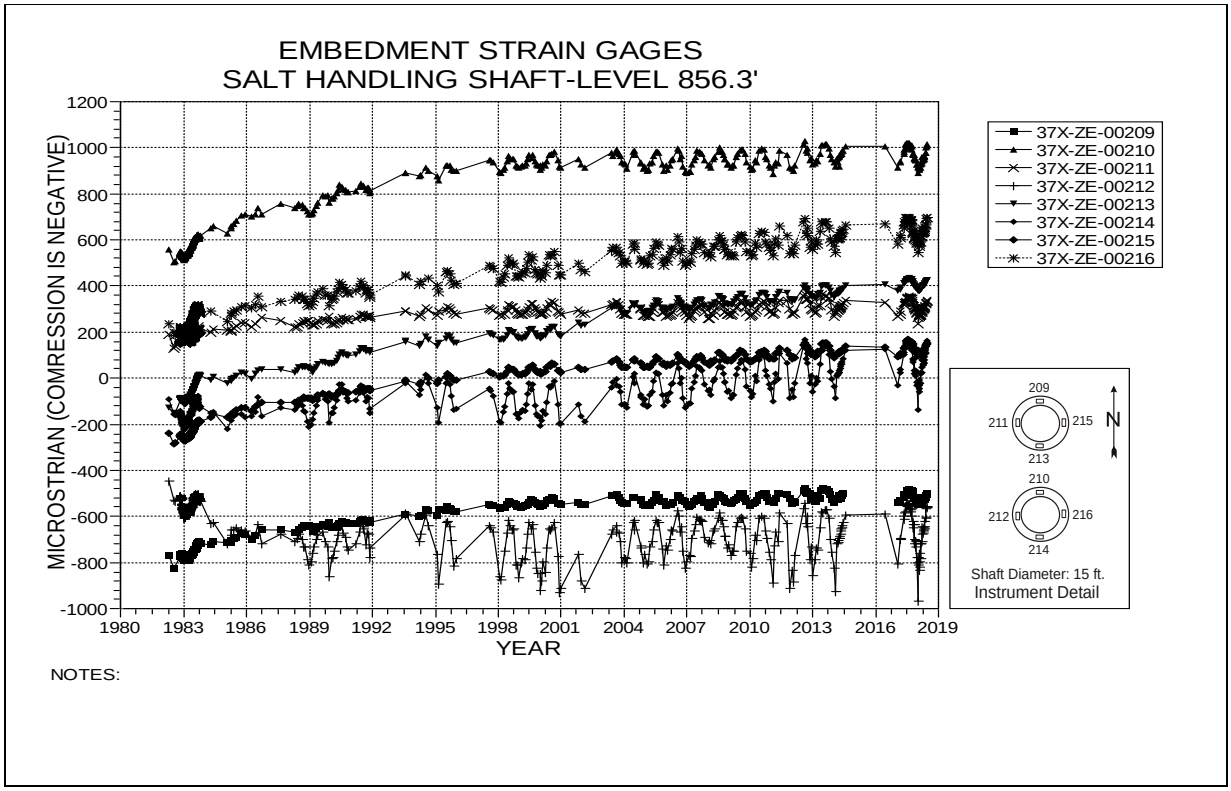

Figure 2-8 Embedment Strain Gauge – Salt Handling Shaft Key – Level 856.3

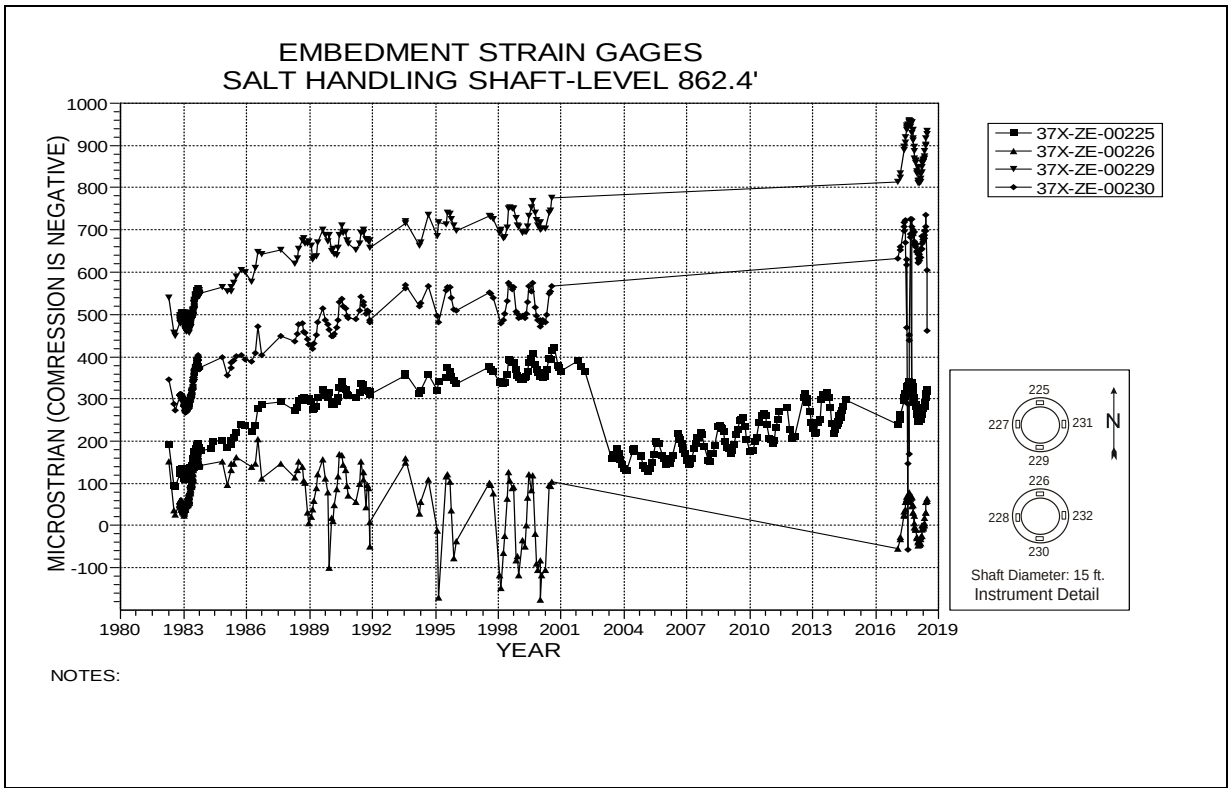

Figure 2-9 Embedment Strain Gauge – Salt Handling Shaft Key – Level 862.4

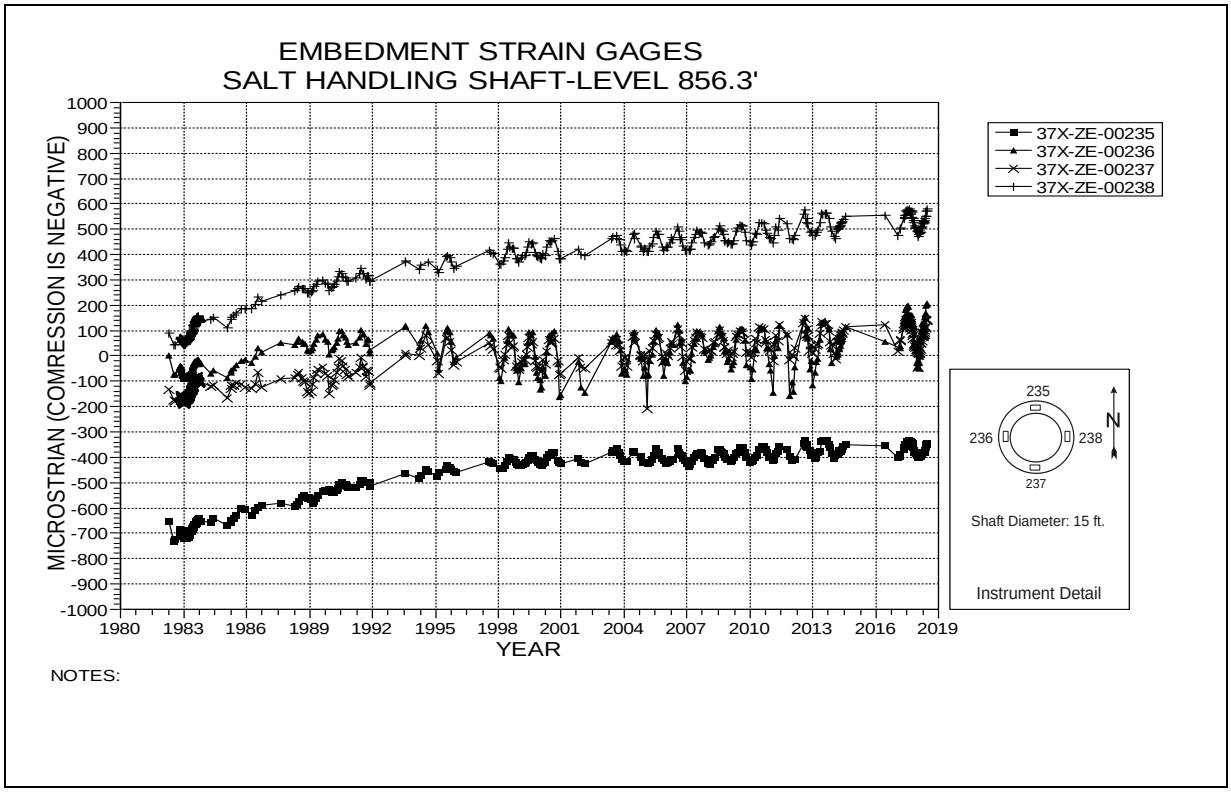

Figure 2-10 Embedment Strain Gauge – Salt Handling Shaft Key – Level 856.3

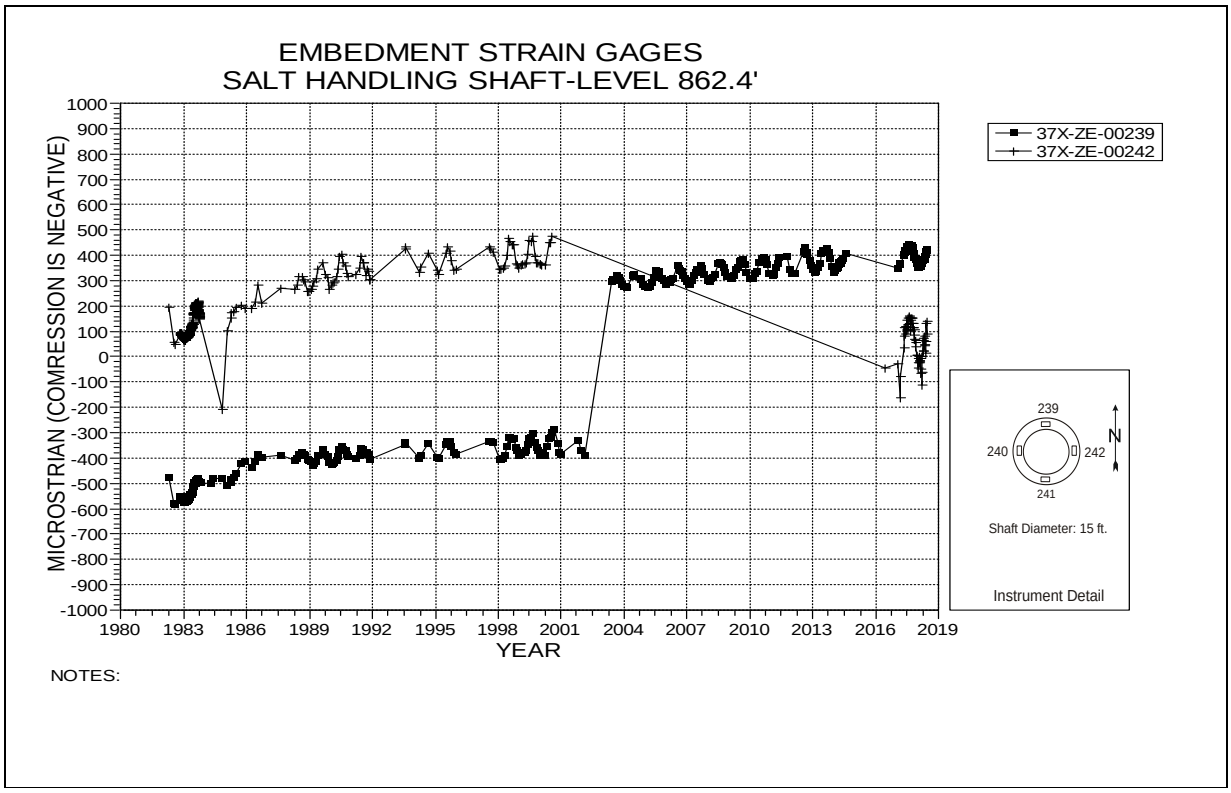

Figure 2-11 Embedment Strain Gauge – Salt Handling Shaft Key – Level 862.4

3.0 INSTRUMENTATION SUMMARY FOR SHAFT STATIONS

The following Instrumentation data analysis is for the Salt Handling Shaft Station, Waste Shaft Station, and the area around the Air Intake Shaft. Table 3-1 presents data analyses for each of the Salt Handling Shaft Station instruments. Figures 3-1 through 3-4 present plots of the instrumentation data for the Salt Handling Shaft Station.

Table 3-2 presents data and analysis for the Waste Shaft Station. Plots from the instrumentation in the Waste Shaft Station are presented as Figure 3-5.

Table 3-3 and Figures 3-6 through 3-14 present the data from borehole extensometers and rock bolt load cells located in the immediate area around the Air Intake Shaft.

Table 3-1
Salt Handling Shaft Station Data Analysis

Convergence Points									
Field Tag	Location	Figure Number	Last Reading 2017-2018		Cumulative Displacement (inches)	Closure Rate 2017 to 2018 (in/year)	Closure Rate 2016 to 2017 (in/year)	Rate Change Percent	Comments
			Date	Inches					
E0-S18-8 A-E	E0-S18	3-1	06/15/18	10.948	32.1	1.8	0.9	100%	
E0-S18-6 B-D	E0-S18	3-2	01/18/18	11.454	34.6	2.0	1.1	82%	
E0-S18-5 H-F	E0-S18	3-2	06/15/18	6.829	21.3	1.1	0.8	38%	
E0-S30-6 A-C	E0-S30	3-3	06/15/18	10.940	33.0	1.8	1.7	6%	
E0-S65-5 A-C	E0-S65	3-4	06/15/18	7.471	22.8	1.2	1.1	9%	

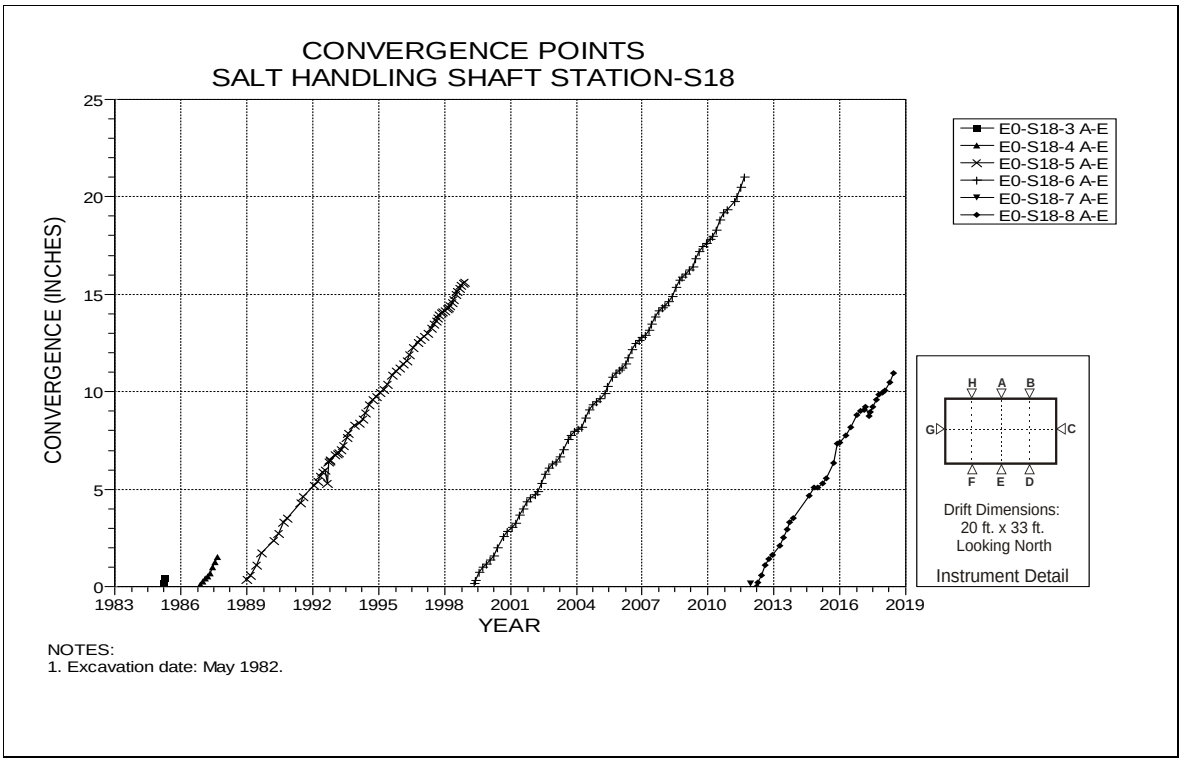

Figure 3-1 Convergence Point Array – Salt Handling Shaft Station at S18 – Centerline – Roof to Floor

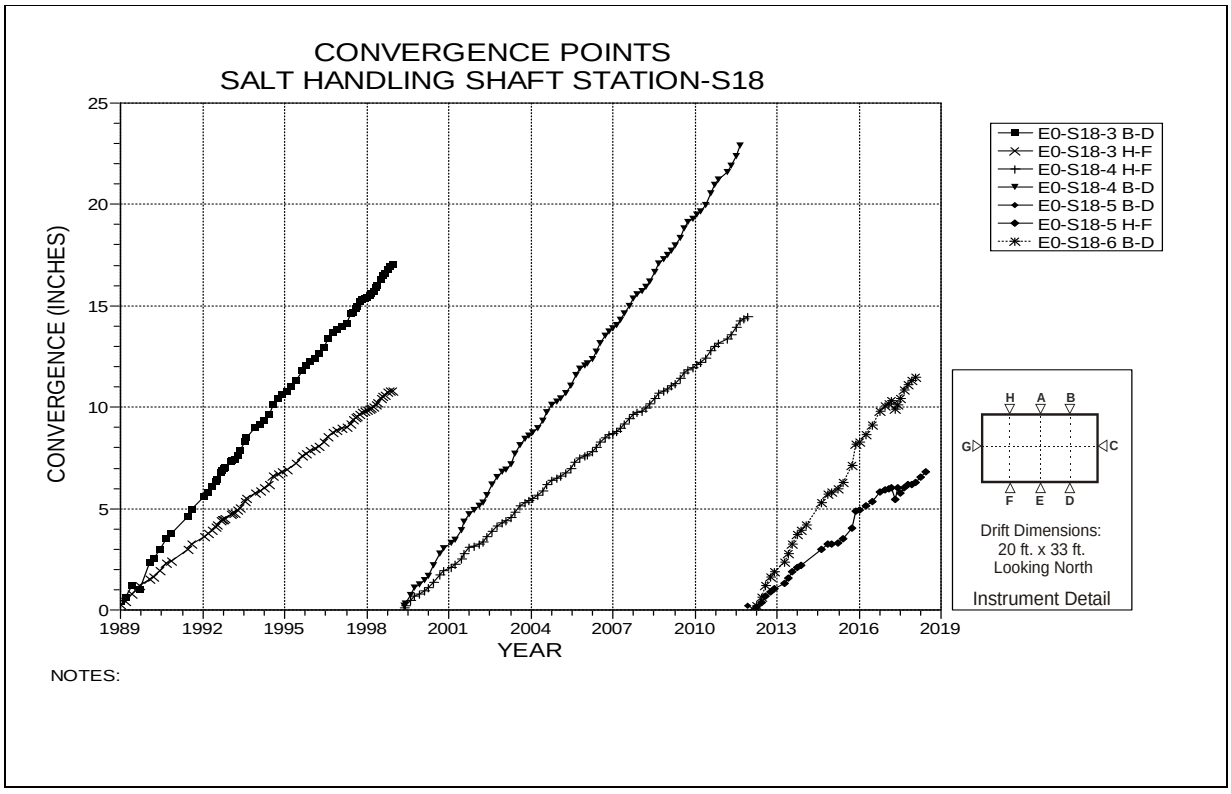

Figure 3-2 Convergence Point Array – Salt Handling Shaft Station at S18 – Quarter Point – Roof to Floor

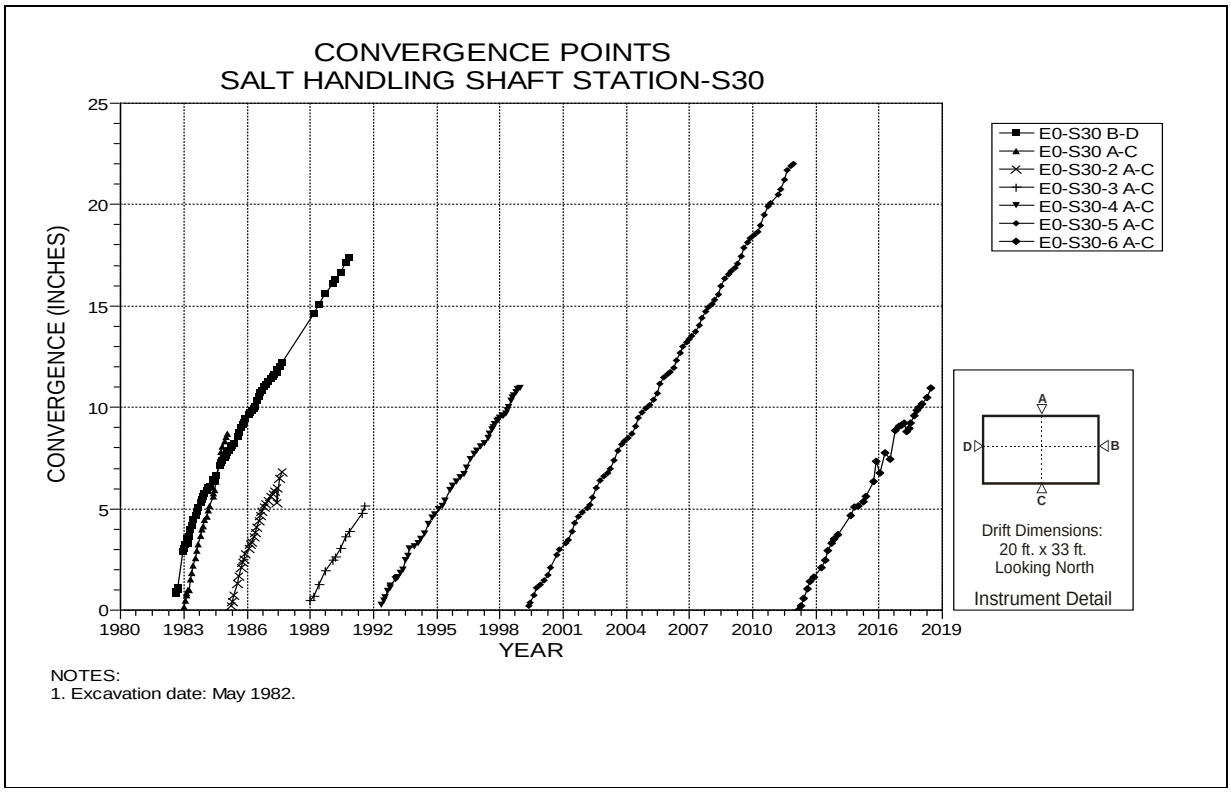

Figure 3-3 Convergence Point Array –
Salt Handling Shaft Station at S30 – Roof to Floor

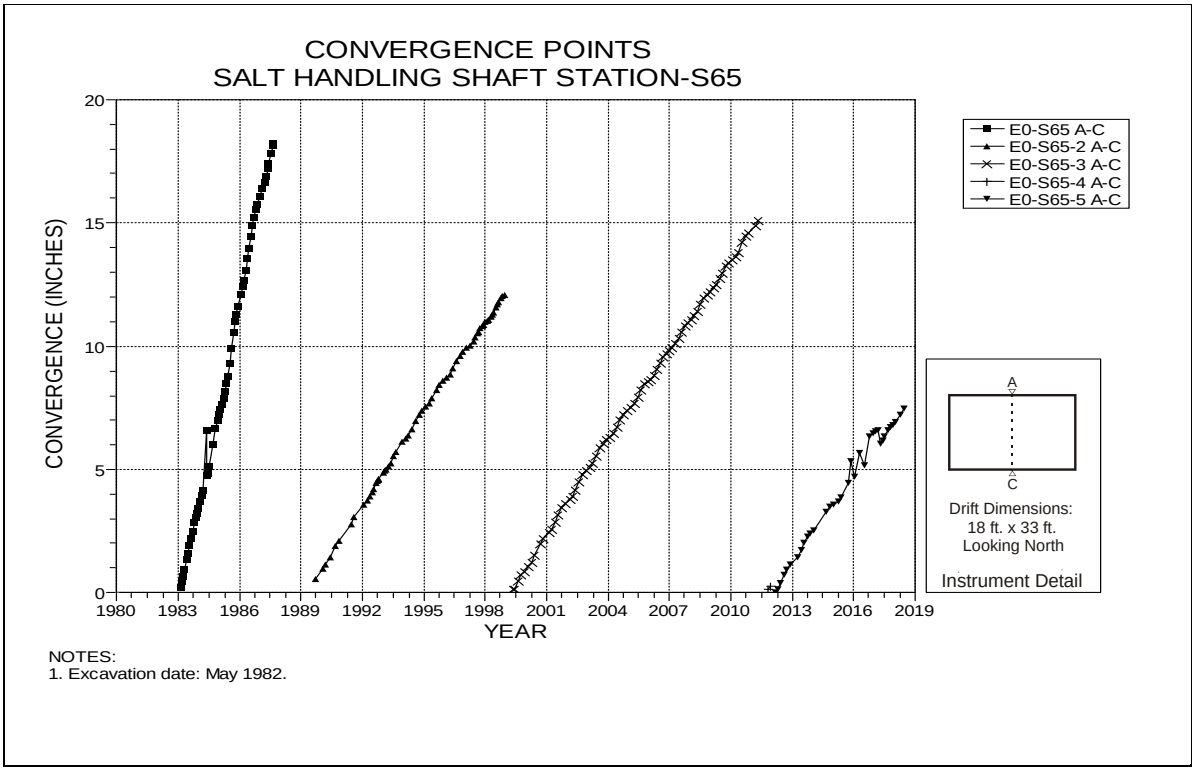

Figure 3-4 Convergence Point Array – Salt Handling Shaft Station at S65 –
Roof to Floor

Table 3-2
Waste Shaft Station Data Analysis

Extensometers								
Field Tag	Location	Figure Number	Date of Last Reading	Collar Displacement Relative to Deepest Anchor (inches)	Displacement Rate 2017 to 2018 (in/year)	Displacement Rate 2016 to 2017 (in/year)	Rate Change Percent	Comments
51X-GE-00404-2	Waste Shaft Station at E35	3-5	02/26/2018	2.354	0.3	N/A	N/A	

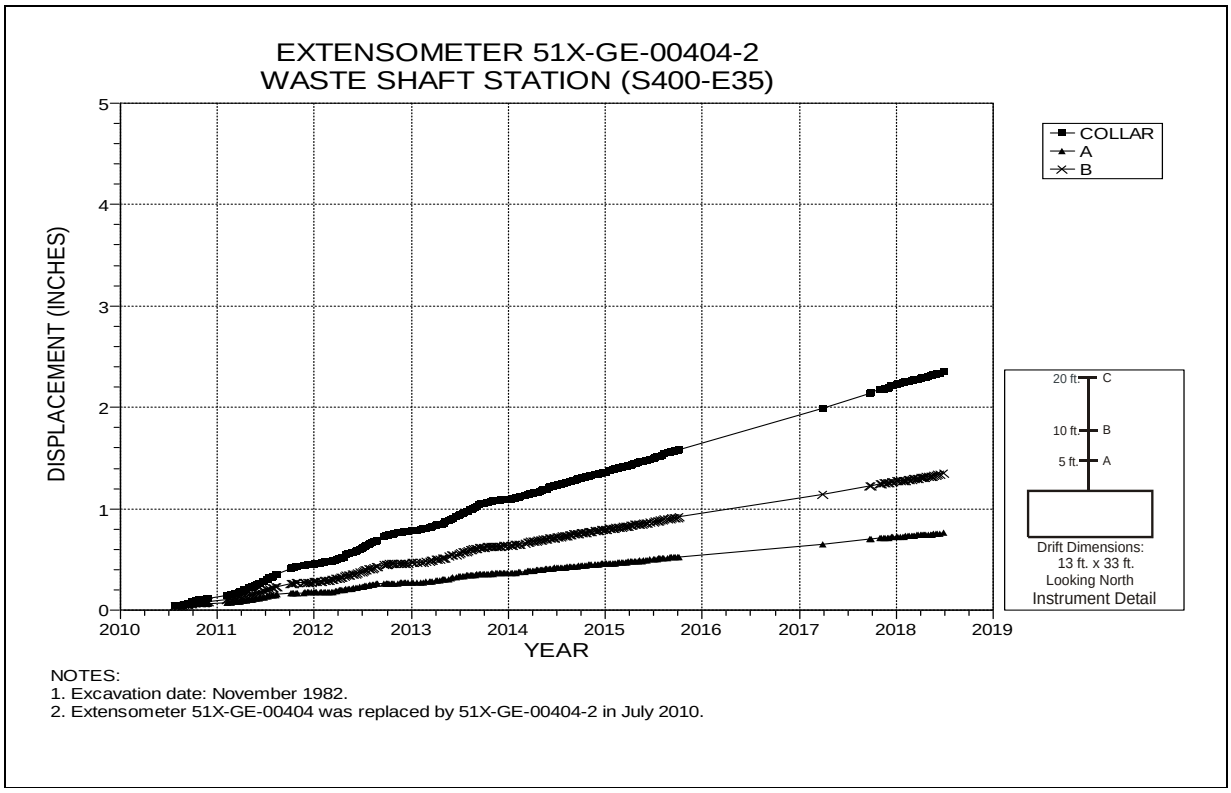

Figure 3-5 Extensometer 51-GE-00404-2 Waste Shaft Station at E35 – Roof

Table 3-3
Air Intake Shaft Station Data Analysis

Extensometers

Field Tag	Location	Figure Number	Date of Last Reading	Collar Displacement Relative to Deepest Anchor (Inches)	Displacement Rate 2017 to 2018 in/year	Displacement Rate 2016 to 2017 in/year	Rate Change Percent	Comments
41X-GE-00122	S65-W620	3-6	06/26/18	4.626	0.3	0.2	50	Calculations performed from anchor B data.
41X-GE-00123	N93-W620	3-7	06/26/18	4.857	0.3	0.3	0	Calculations performed from anchor A data.
51X-GE-00440	AIS North Brow	3-8	04/10/18	0.213	0.2	N/A	N/A	
51X-GE-00441	AIS South Brow	3-9	04/10/18	0.272	0.3	N/A	N/A	
51X-GE-00401	W620-N20	3-10	06/26/18	2.391	0.2	0.2	0	Calculations performed from anchor B data.

Rock Bolt Load Cells

Field Tag	Location	Figure Number	Date of Last Reading	Load (kips)	Comments
51X-WG-00237	AIS Station Brow - South	3-11	06/26/18	1.9	
51X-WG-00238	AIS Station Brow - South	3-11	06/26/18	0.0	
51X-WG-00239	AIS Station Brow - South	3-11	06/26/18	48.3	
51X-WG-00240	AIS Station Brow - South	3-11	06/26/18	1.0	
51X-WG-00242	AIS Station Brow - South	3-12	06/26/18	55.2	
51X-WG-00243	AIS Station Brow - South	3-12	06/26/18	29.5	
51X-WG-00244	AIS Station Brow - South	3-12	06/26/18	26.3	
51X-WG-00246	AIS Station Brow - North	3-13	06/26/18	28.0	
51X-WG-00248	AIS Station Brow - North	3-13	06/26/18	32.6	
51X-WG-00250	AIS Station Brow - North	3-13	06/26/18	11.4	
51X-WG-00251	AIS Station Brow - North	3-14	06/26/18	24.7	
51X-WG-00254	AIS Station Brow - North	3-14	06/26/18	5.5	
51X-WG-00255	AIS Station Brow - North	3-14	06/26/18	15.3	

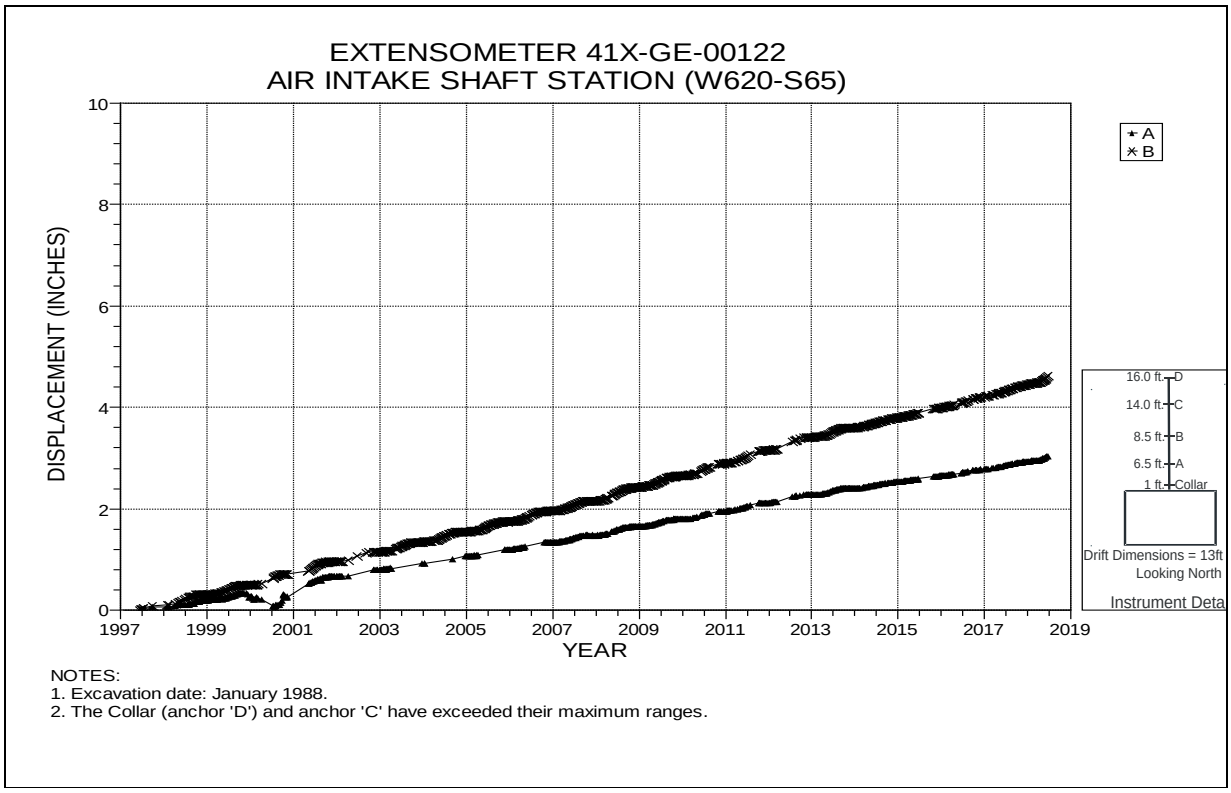

Figure 3-6 Extensometer 41X-GE-00122 – Air Intake Shaft Station at W620 S65 – Roof

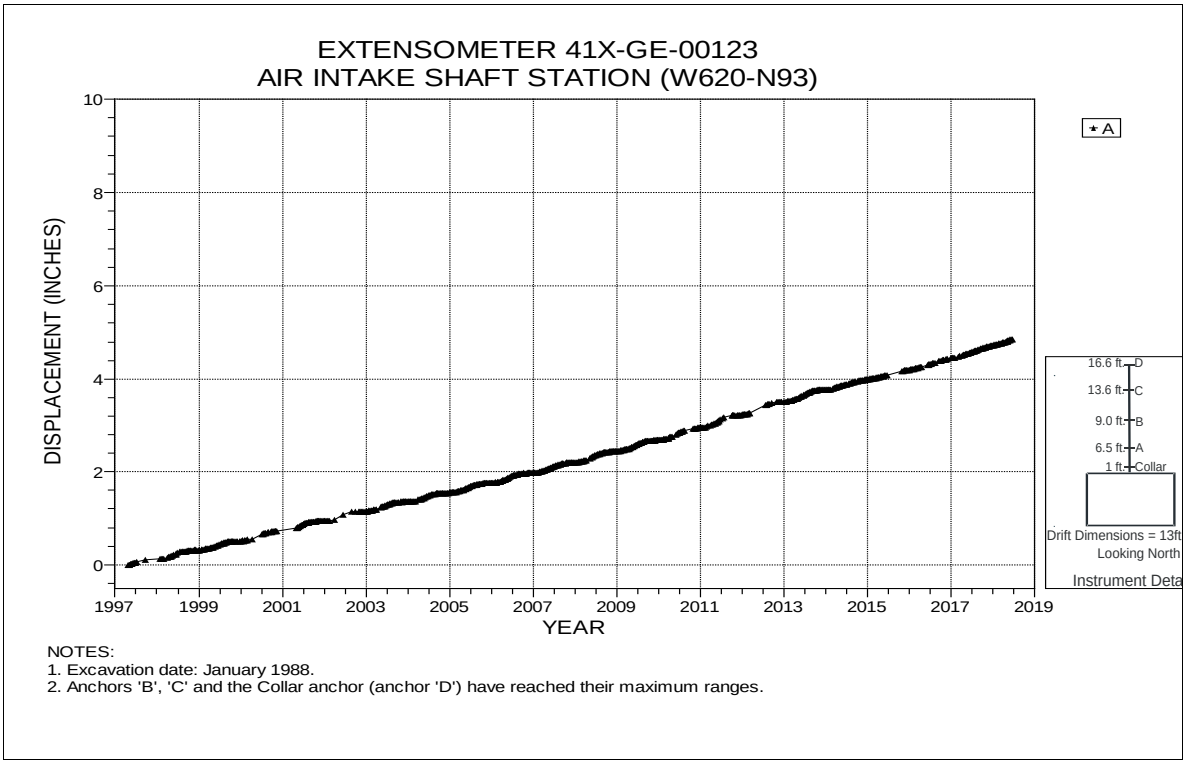

Figure 3-7 Extensometer 41X-GE-00123 – Air Intake Shaft Station at W620 N93 – Roof

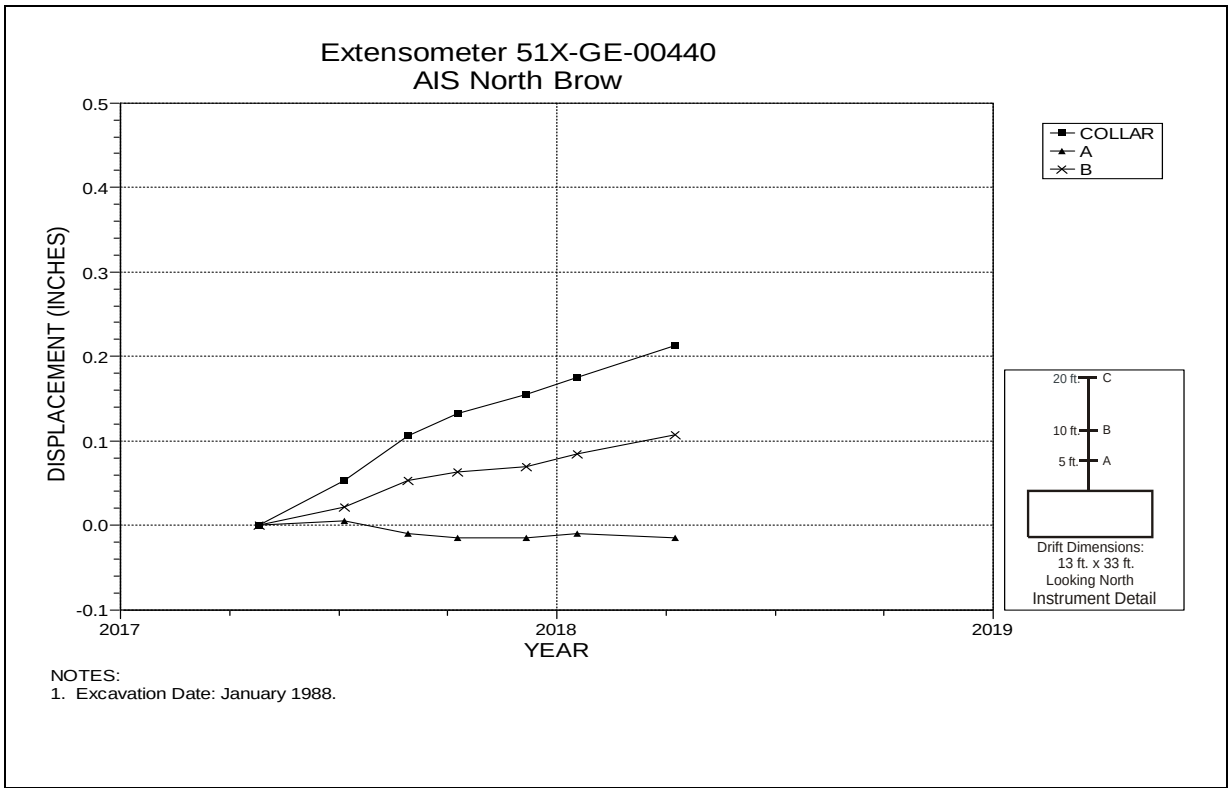

Figure 3-8 Extensometer 51X-GE-00440 Air Intake Shaft at North Brow Station

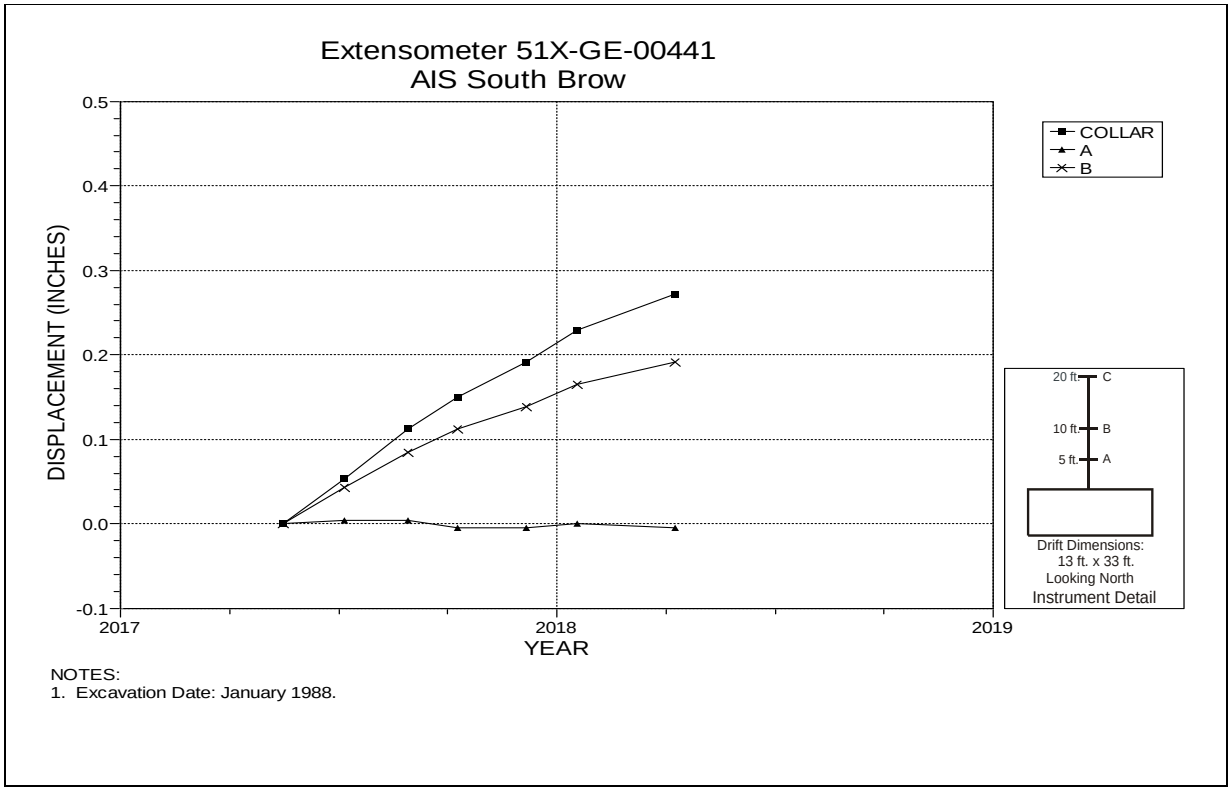

Figure 3-9 Extensometer 51X-GE-00441 Air Intake Shaft South Brow Station

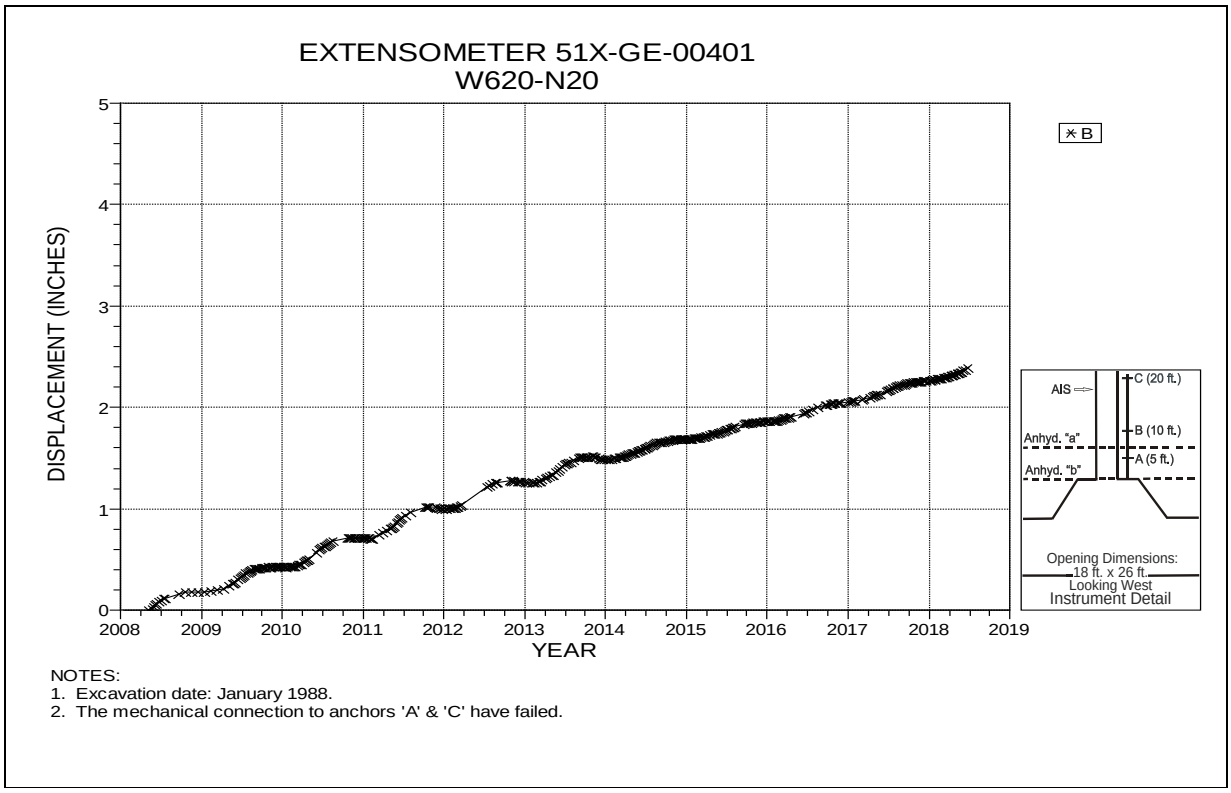

Figure 3-10 Extensometer 51X-GE-00401 Air Intake Shaft Station at W620 N20 – Roof

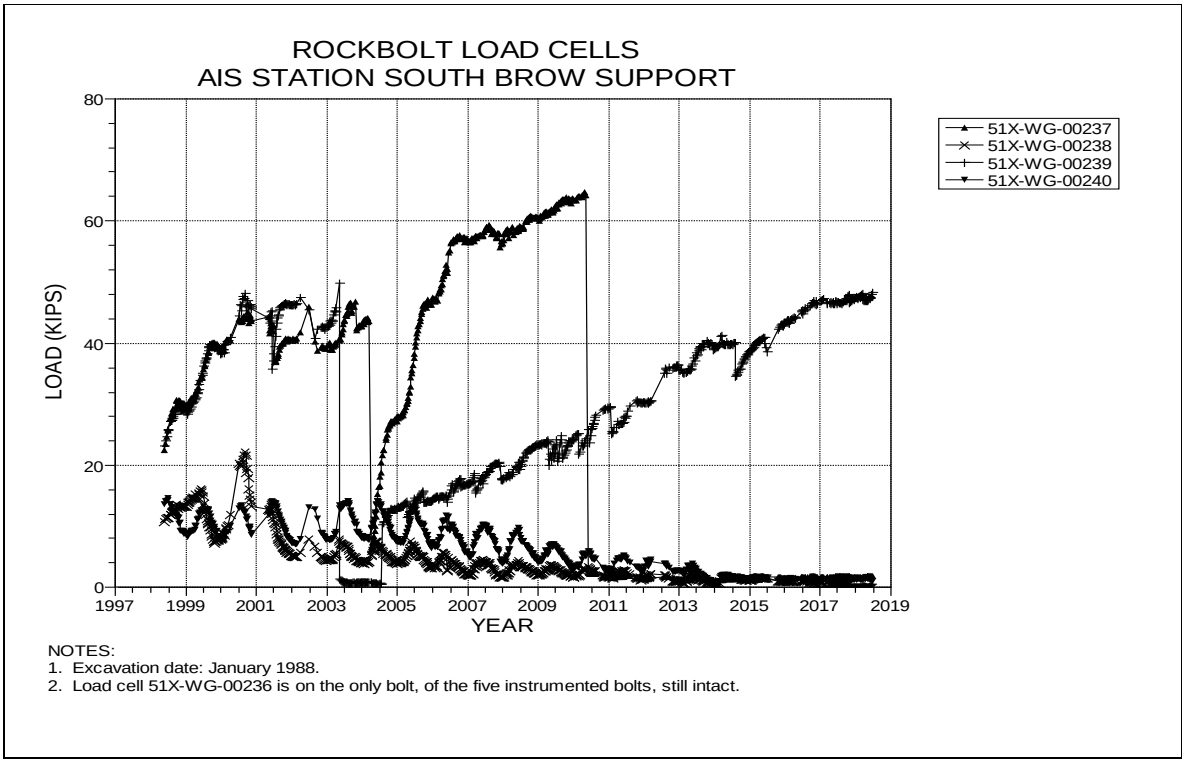

Figure 3-11 Rock Bolt Load Cells – Air Intake Shaft Station – South Brow Support – Bolts (1-5)

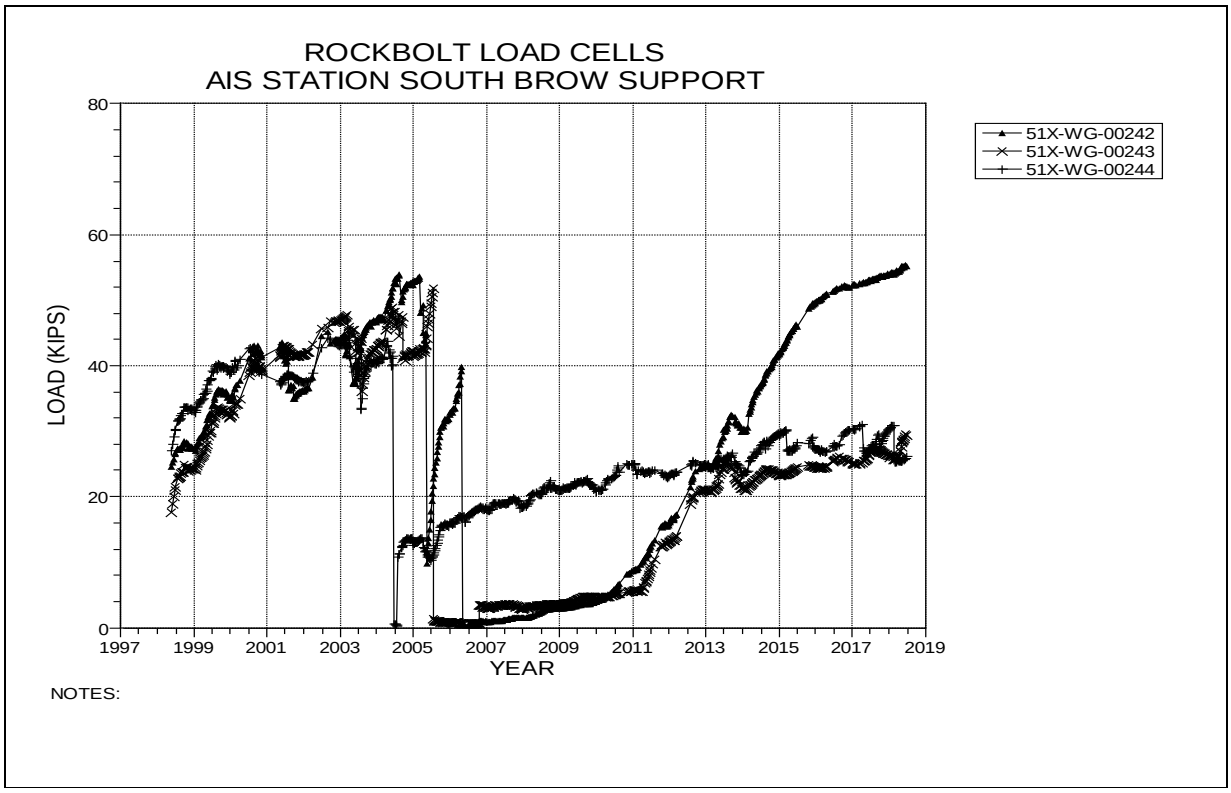

Figure 3-12 Rock Bolt Load Cells –
Air Intake Shaft Station – South Brow Support – Bolts (6-10)

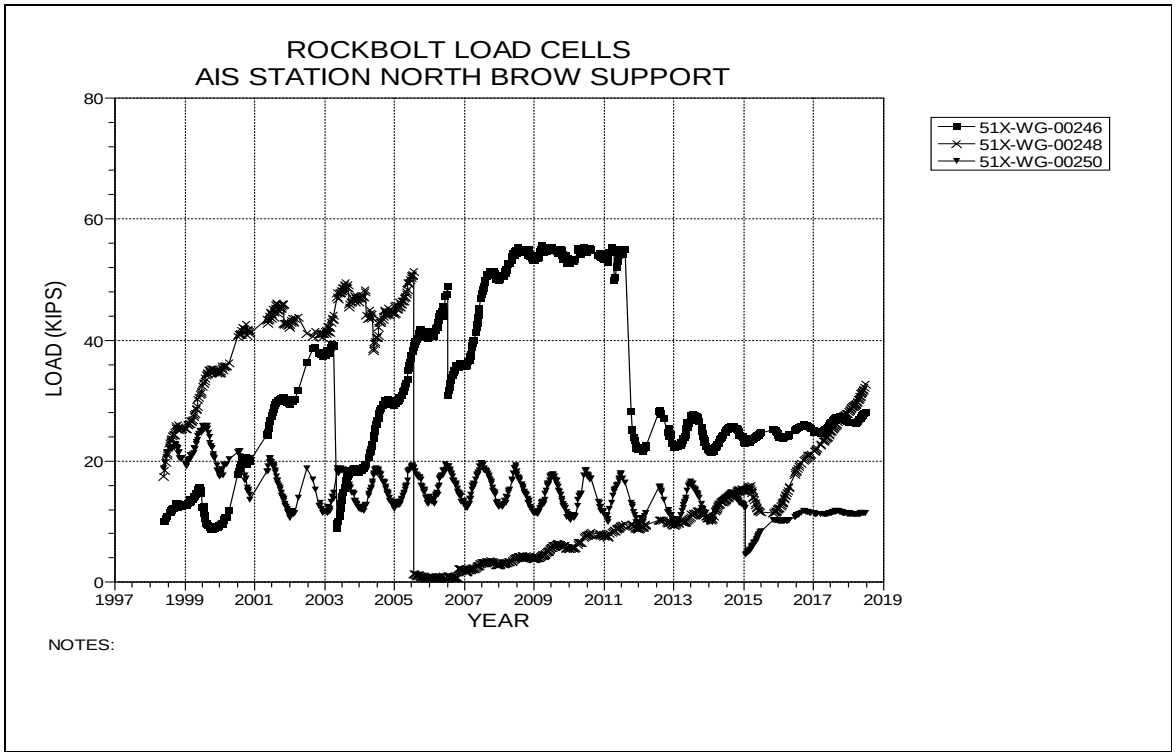

Figure 3-13 Rock Bolt Load Cells –
Air Intake Shaft Station – North Brow Support – Bolts (1-5)

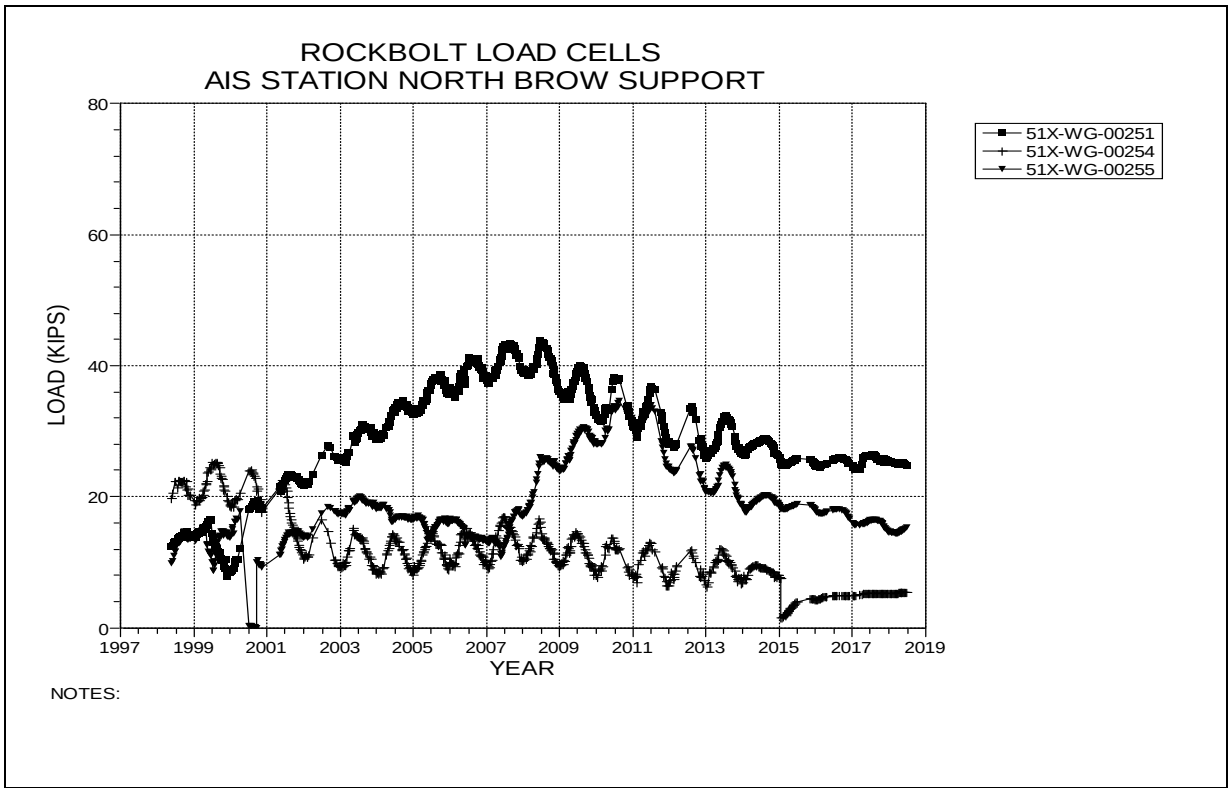

Figure 3-14 Rock Bolt Load Cells –
Air Intake Shaft Station – North Brow Support – Bolts (6-10)

4.0 INSTRUMENTATION SUMMARY FOR THE ACCESS DRIFTS

This chapter presents the instrumentation data and data analyses for the access drifts throughout the WIPP underground. Table 4-1 provides the results of analyses performed on the instrument data including displacement, convergence rates, and rock bolt loading.

Figures 4-1 through 4-4 present data from convergence meters in the access drifts. Figure 4-5 through 4-17 present data from borehole extensometers installed in the access drifts while Figures 4-18 through 4-180 present the convergence point data. Figure 4-181 through 4-184 present data from joint meters installed at the S1950/E300 overcast and the access drifts.

Table 4-1 Access Drifts Data Analysis

Convergence Meters								
Field Tag	Location	Figure Number	Date of Last Reading	Collar Displacement Relative to Deepest Anchor (inches)	Displacement Rate 2017 to 2018 (in/year)	Displacement Rate[1] 2016 to 2017 (in/year)	Rate Change Percent[1]	Comments
51X-CW-01037	E140-S2750	4-1	5/24/2018	4.142	3.5	9.53	-63%	
51X-CW-01039	W170-S2735	4-2	5/18/2018	1.936	2.51	N/A	N/A	
51X-CW-01038	W30-S2750	4-3	5/18/2018	5.932	6.55	N/A	N/A	
51X-GE-00442	E300-S2750	4-4	5/15/2018	0.103	1.45	N/A	N/A	
Extensometers								
Field Tag	Location	Figure Number	Date of Last Reading	Collar Displacement Relative to Deepest Anchor (inches)	Displacement Rate 2017 to 2018 (in/year)	Displacement Rate[1] 2016 to 2017 (in/year)	Rate Change Percent[1]	Comments
51X-GE-00355	E0-N300	4-5	10/10/2017	7.989	2.5	0.5	-150	Maximum range reached 10/17/18.
51X-GE-00353	E0-N626	4-6	6/26/2018	13.367	1.6	1.8	-13	
51X-GE-00352	E0-N940	4-7	6/26/2018	11.990	1.6	0.7	56	
51X-GE-00364	E140-N1266	4-8	6/26/2018	10.747	1.2	0.7	42	Maximum range reached during this reporting period
51X-GE-00428-2	E140-S1150	4-9	3/12/2018	12.809	1.6	1.7	-6	
51X-GE-00429	E140-S1450	4-10	3/12/2018	13.227	1.5	2.1	-40	
51X-GE-00431	E140-S1775	4-11	3/12/2018	13.329	1.6	2.0	-22	
51X-GE-00432	E140-S1850	4-12	3/12/2018	11.922	1.8	1.6	13	
51X-GE-00433-2	E140-S2065	4-13	3/12/2018	12.343	1.2	1.2	2	Maximum range reached during this reporting period
51X-GE-00434	E140-S2265	4-14	3/12/2018	7.849	1.7	1.6	6	
51X-GE-00374	E300-N1186	4-15	6/26/2018	11.814	2.1	1.1	49	
51X-GE-00388	E300-N1266	4-16	6/26/2018	8.795	1.3	0.7	44	
51X-GE-00373	E300-N1341	4-17	6/26/2018	9.576	1.6	0.9	42	

Table 4-1 Access Drifts Data Analysis (continued)

Convergence Points									
			Last Reading 2017-2018						
Field Tag	Location	Figure Number	Date	Inches	Cumulative Displacement (inches)	Closure Rate 2017 to 2018 (in/year)	Closure Rate[1] 2016 to 2017 (in/year)	Rate Change Percent[1]	Comments
CORE-W20 A-C	CORE STORAGE W20	4-18	05/22/18	27.628	27.628	1.1	1.0	10	
CORE-W30 A-C	CORE STORAGE W30	4-18	05/22/18	29.155	29.155	1.1	1.1	0	
CORE-W51 A-C	CORE STORAGE W51	4-18	05/22/18	33.906	33.906	1.3	1.3	0	
E0-N75 A-C	E0-N75	4-19	06/15/18	32.448	32.448	2.7	1.4	93	
E0-N225-2 A-C	E0-N225	4-20	04/03/18	29.035	29.035	1.7	0.8	113	
E0-N300-6 A-C	E0-N300	4-21	04/03/18	13.002	29.339	1.9	2.1	-10	
E0-N460-3 A-C	E0-N460	4-22	06/15/18	37.524	57.613	2.6	2.5	4	
E0-N562 A-C	E0-N562	4-23	04/03/18	29.771	29.771	2.6	2.2	18	
E0-N626-5 A-C	E0-N626	4-24	06/15/18	5.040	76.436	3.3	2.5	32	
E0-N686 A-C	E0-N686	4-25	06/15/18	37.556	37.556	2.8	N/A	N/A	
E0-N780-2 A-C	E0-N780	4-26	06/15/18	31.724	52.146	2.3	2.2	5	
E0-N940-5 A-C	E0-N940	4-27	06/15/18	35.808	83.860	3.8	2.1	81	
E0-N1100-5 A-C	E0-N1100	4-28	06/15/18	22.593	57.017	1.8	2.0	-10	
E0-N1266-4 A-C	E0-N1266	4-29	04/03/18	34.548	71.455	3.0	2.5	20	
EO-N1420-2 A-C	EO-N1420	4-30	06/15/18	17.325	17.325	1.4	1.3	8	
N140-E90-3 A-C	N140-E90	4-31	06/15/18	3.676	22.311	1.0	0.9	11	
E140-N5-7 A-C	E140-N5	4-32	06/15/18	15.425	62.318	3.1	3.2	-3	
E140-N150-6 A-C	E140-N150	4-33	06/15/18	10.064	40.810	2.1	2.1	0	
E140-N220-4 A-C	E140-N220	4-34	04/04/18	14.888	57.045	3.0	3.2	-6	
E140-N355-2 A-C	E140-N355	4-35	06/15/18	27.926	36.470	2.6	3.0	-13	
E140-N460-3 A-C	E140-N460	4-36	06/15/18	36.018	56.849	2.7	2.7	0	
E140-N562-2 A-C	E140-N562	4-37	06/15/18	38.586	38.586	3.3	3.2	3	
E140-N626-3 A-C	E140-N626	4-38	06/15/18	50.578	83.148	4.1	3.7	11	
E140-N686-2 A-C	E140-N686	4-39	06/15/18	38.998	38.998	2.9	2.9	0	
E140-N780-3 A-C	E140-N780	4-40	06/15/18	5.029	73.162	3.0	3.0	0	
E140-N940-2 A-C	E140-N940	4-41	06/15/18	50.836	80.235	4.9	5.2	-6	

Table 4-1 Access Drifts Data Analysis (continued)

Convergence Points (continued)									
Field Tag	Location	Figure Number	Last Reading 2017-2018 Date	Last Reading 2017-2018 Inches	Cumulative Displacement (inches)	Closure Rate 2017 to 2018 (in/year)	Closure Rate[1] 2016 to 2017 (in/year)	Rate Change Percent[1]	Comments
E140-N1100-2 A-C	E140-N1100	4-42	06/15/18	23.912	43.635	2.2	2.3	-4	
E140-N1266-3 A-C	E140-N1266	4-43	06/15/18	37.573	75.328	3.5	3.6	-3	
E140-N1420-2 A-C	E140-N1420	4-44	06/15/18	25.513	41.983	2.3	2.3	0	
E140-S90-4 A-C	E140-S90	4-45	06/15/18	23.445	41.158	2.3	2.6	-12	
E140-S262-5 A-C	E140-S262	4-46	05/16/18	11.619	48.640	2.3	2.3	0	
E140-S460-7 A-C	E140-S460	4-47	05/16/18	3.287	63.561	2.2	2.0	10	
E140-S460-2 B-D	E140-S460	4-47	03/09/18	34.157	40.101	1.3	1.2	8	
E140-S550-6 A-C	E140-S550	4-48	05/16/18	14.196	56.163	1.9	1.8	6	
E140-S700-8 A-D	E140-S700	4-49	05/16/18	17.166	47.206	2.5	2.3	9	
E140-S700-7 B-C	E140-S700	4-50	05/16/18	4.598	49.198	2.0	1.6	25	
E140-S700-7 E-F	E140-S700	4-51	05/16/18	1.669	31.253	1.5	1.5	0	
E140-S850-10 A-C	E140-S850	4-52	05/16/18	13.323	71.059	2.7	2.6	4	
E140-S1000-4 A-C	E140-S1000	4-53	05/16/18	8.814	49.161	1.7	1.5	13	
E140-S1025-6 A-C	E140-S1025	4-54	05/16/18	2.307	37.171	2.0	1.9	5	
E140-S1075-5 A-E	E140-S1075	4-55	05/16/18	15.384	44.186	3.1	2.7	15	
E140-S1075-5 B-D	E140-S1075	4-56	05/16/18	6.823	28.914	1.4	1.1	27	
E140-S1075-6 H-F	E140-S1075	4-57	05/16/18	2.257	10.401	2.3	N/A	N/A	
E140-S1150-6 A-G	E140-S1150	4-58	05/16/18	3.463	61.087	3.0	3.3	-9	
E140-S1150-2 E-I	E140-S1150	4-59	03/09/18	25.616	26.477	1.4	1.2	17	
E140-S1150-7 B-F	E140-S1150	4-60	05/16/18	14.880	47.337	2.1	1.7	24	
E140-S1150-6 L-H	E140-S1150	4-61	05/16/18	9.166	34.964	1.7	1.5	13	
E140-S1225-6 A-E	E140-S1225	4-62	05/16/18	4.120	55.329	3.9	3.1	26	
E140-S1225-6 B-D	E140-S1225	4-63	05/16/18	1.390	45.866	1.6	N/A	N/A	
E140-S1225-4 H-F	E140-S1225	4-63	05/16/18	10.983	36.366	1.9	0.6	217	
E140-S1300-5 A-C	E140-S1300	4-64	05/16/18	8.343	46.286	1.7	1.1	55	
E140-S1378-4 A-E	E140-S1378	4-65	05/16/18	18.157	18.157	3.0	2.9	3	

Table 4-1 Access Drifts Data Analysis (continued)

Convergence Points (continued)									
Field Tag	Location	Figure Number	Last Reading 2017-2018		Cumulative Displacement (inches)	Closure Rate 2017 to 2018 (in/year)	Closure Rate[1] 2016 to 2017 (in/year)	Rate Change [1]	Comments
			Date	Inches					
E140-S1378-6 B-D	E140-S1378	4-66	05/16/18	1.977	9.963	1.8	1.8	0	
E140-S1378-4 H-F	E140-S1378	4-67	05/16/18	20.589	66.451	4.3	2.4	79	
E140-S1450-6 A-G	E140-S1450/1456	4-68	05/16/18	19.598	70.385	3.3	3.5	-6	
E140-S1450-4 B-F	E140-S1450/1456	4-69	05/16/18	9.047	49.380	1.6	-1.2	-233	
E140-S1450-3 I-E	E140-S1450/1456	4-70	03/09/18	11.464	29.556	1.6	1.4	14	
E140-S1450-4 L-H	E140-S1450/1456	4-71	05/16/18	15.807	51.098	2.9	2.8	4	
E140-S1534-4 A-E	E140-S1534	4-72	05/16/18	14.836	68.319	2.8	2.6	8	
E140-S1534-5 B-D	E140-S1534	4-73	05/16/18	12.502	47.049	2.4	0.6	300	
E140-S1534-5 H-F	E140-S1534	4-74	05/16/18	4.262	50.764	2.9	2.6	12	
E140-S1600-7 A-C	E140-S1600	4-75	05/16/18	14.419	56.365	3.6	2.7	33	
E140-S1687-4 B-D	E140-S1687	4-76	05/16/18	13.222	49.964	2.5	2.4	4	
E140-S1687-4 H-F	E140-S1687	4-76	05/16/18	15.869	52.637	2.8	3.0	-7	
E140-S1775-4 A-G	E140-S1775	4-77	05/16/18	20.544	88.730	3.6	3.5	3	
E140-S1775-6 B-F	E140-S1775	4-78	05/16/18	5.836	76.186	3.7	3.6	3	
E140-S1775-4 L-H	E140-S1775	4-78	03/09/18	11.082	43.667	2.3	2.1	10	
E140-S1775-3 I-E	E140-S1775	4-79	03/09/18	20.774	34.995	2.0	1.7	18	
E140-S1862-4 A-E	E140-S1862	4-80	03/09/18	18.103	71.101	3.3	3.1	6	
E140-S1862-4 B-D	E140-S1862	4-81	05/16/18	21.014	69.675	4.2	3.7	14	
E140-S1862-4 H-F	E140-S1862	4-81	05/16/18	10.538	36.891	2.0	1.7	18	
E140-S1950-7 A-C	E140-S1950	4-82	05/16/18	21.231	77.621	3.8	3.6	6	
E140-S2007-8 A-C	E140-S2007	4-83	05/16/18	24.726	69.253	4.3	3.9	10	
E140-S2065-8 A-C	E140-S2065	4-84	05/16/18	4.030	67.780	3.6	3.7	-3	
E140-S2122-8 A-C	E140-S2122	4-85	05/16/18	4.397	64.350	3.9	4.0	-3	
E140-S2275-7 A-C	E140-S2275	4-86	05/16/18	28.206	107.143	5.7	5.2	10	
E140-S2350-7 A-C	E140-S2350	4-87	05/16/18	27.360	110.073	5.5	4.9	12	
E140-S2425-6 A-C	E140-S2425	4-88	05/16/18	23.984	79.490	4.6	4.5	2	
E140-S2520-4 A-C	E140-S2520	4-89	05/16/18	20.371	61.147	3.9	3.6	8	
E140-S2634-2 A-C	E140-S2634	4-90	11/20/17	21.236	78.211	3.8	3.9	-2.6	See Rate Change Calculation (1)

Table 4-1 Access Drifts Data Analysis (continued)

Convergence Points (continued)									
Field Tag	Location	Figure Number	Last Reading 2017-2018 Date	Last Reading 2017-2018 Inches	Cumulative Displacement (inches)	Closure Rate 2017 to 2018 (in/year)	Closure Rate[1] 2016 to 2017 (in/year)	Rate Change Percent[1]	Comments
E300-N45-2 A-E	E300-N45	4-91	06/15/18	9.738	42.619	2.0	2.0	0	
E300-N45-2 H-F	E300-N45	4-91	06/15/18	8.592	38.131	1.8	1.8	0	
E300-N170-3 A-E	E300-N170	4-92	06/15/18	11.229	44.703	2.5	2.4	4	
E300-N170-3 H-F	E300-N170	4-92	06/15/18	9.295	39.590	2.1	2.0	5	
E300-N280 A-C	E300-N280	4-93	06/15/18	1.895	1.895	1.6	1.4	14	
E300-N300 A-C	E300-N300	4-94	06/15/18	1.753	1.753	1.5	1.3	15	
E300-N440 A-C	E300-N440	4-95	06/15/18	1.935	1.935	1.6	1.5	7	
E300-N500 A-C	E300-N500	4-96	06/15/18	1.508	1.508	1.3	1.2	8	
E300-N1100-2 A-C	E300-N1100	4-97	06/15/18	12.199	14.424	2.9	2.7	7	
E300-N1262-4 A-C	E300-N1262	4-98	06/22/18	19.884	24.561	4.1	3.5	17	
E300-N1341-3 A-C	E300-N1341	4-99	06/15/18	18.740	23.195	4.3	3.6	19	
E300-N1420 A-C	E300-N1420	4-100	06/15/18	25.054	25.054	2.5	2.2	14	
E300-S45-3 A-E	E300-S45	4-101	06/15/18	7.948	35.152	1.7	1.6	6	
E300-S45-3 B-D	E300-S45	4-101	06/15/18	8.350	33.541	1.4	1.7	-18	
E300-S45-3 H-F	E300-S45	4-101	06/15/18	6.858	30.107	1.5	1.5	0	
E300-S90-3 A-C	E300-S90	4-102	06/15/18	6.594	26.871	1.5	1.4	7	
E300-S250-2 A-C	E300-S250	4-103	06/15/18	14.248	18.633	1.0	0.7	43	
E300-S250-2 B-D	E300-S250	4-103	01/18/18	14.871	18.917	0.6	0.8	-25	
E300-S700-2 A-C	E300-S700	4-104	11/01/17	10.029	29.759	1.6	1.7	-6	
E300-S2275-2 A-C	E300-S2275	4-105	03/14/18	21.977	35.403	3.4	3.4	-1	
E300-S2350-2 A-C	E300-S2350	4-106	03/14/18	32.972	48.536	5.0	5.2	-4	
E300-S2634-2 A-C	E300-S2634	4-107	03/14/18	16.068	29.453	1.5	2.5	-40	
N215-W500-2 A-C	N215-W500	4-108	06/15/18	19.478	37.807	1.3	1.2	8	
N215-W500-2 B-D	N215-W500	4-108	01/18/18	17.501	24.319	0.6	0.9	-33	
N215-W620-2 A-C	N215-W620	4-109	06/15/18	15.197	31.415	1.1	1.1	0	
N250-E220-3 A-E	N250-E220	4-110	12/05/17	12.793	52.751	3.0	3.0	0	
N250-E220-3 B-D	N250-E220	4-111	06/15/18	8.296	44.436	1.7	1.7	0	

Table 4-1 Access Drifts Data Analysis (continued)

Convergence Points (continued)

Field Tag	Location	Figure Number	Last Reading 2017-2018 Date	Last Reading 2017-2018 Inches	Cumulative Displacement (inches)	Closure Rate 2017 to 2018 (in/year)	Closure Rate[1] 2016 to 2017 (in/year)	Rate Change Percent[1]	Comments
N250-E220-3 H-F	N250-E220	4-112	12/05/17	7.780	36.068	1.9	1.9	0	
N300-W170-2 A-C	N300-W170	4-113	06/15/18	24.113	46.373	1.7	1.7	0	
N300-W170-2 B-D	N300-W170	4-113	01/18/18	23.378	31.573	0.9	1.2	-25	
N460-E70-3 A-C	N460-E70	4-114	06/15/18	25.273	41.719	1.8	1.9	-5	
N460-E310 A-C	N460-E310	4-115	06/15/18	2.431	2.431	2.0	2.0	0	
N780-E70 A-C	N780-E70	4-116	06/15/18	21.411	21.411	1.6	0.7	129	
N1420-E212 A-C	N1420-E212	4-117	06/15/18	1.750	1.750	1.7	1.7	0	
N1420-E79 A-C	N1420-E79	4-118	06/15/18	1.936	1.936	1.9	2.1	-10	
S1000-E120-3 A-C	S1000-E120	4-119	05/16/18	15.097	23.537	1.2	0.9	33	
S1000-E160 -3 A-C	S1000-E160	4-120	05/16/18	9.322	17.532	0.9	0.7	29	
S1000-E58-4 A-C	S1000-E58	4-121	05/16/18	17.260	32.726	1.4	1.2	17	
S1000-E58-2 B-D	S1000-E58	4-121	03/09/18	25.640	27.184	1.3	1.0	30	
S1000-W98-2 A-C	S1000-W98	4-122	05/22/18	27.867	46.615	2.1	2.0	5	
S1300-E120 A-C	S1300-E120	4-123	05/16/18	20.924	20.924	1.0	0.9	11	
S1300-E160 A-C	S1300-E160	4-124	05/16/18	36.518	36.518	2.3	2.0	15	
S1300-E24-2 A-C	S1300-E24	4-125	05/22/18	1.703	27.686	1.5	1.5	0	
S1300-W100-3 A-C	S1300-W100	4-126	05/22/18	28.280	52.283	2.6	1.5	73	
S1600-E110-2 A-C	S1600-E110	4-127	05/16/18	5.573	22.295	1.2	1.0	20	
S1600-E170-2 A-C	S1600-E170	4-128	05/16/18	6.090	24.401	1.2	1.1	9	
S1950-E113-4 A-C	S1950-E113	4-129	05/16/18	17.087	20.963	1.3	1.1	18	
S1950-E160 A-C	S1950-E160	4-130	05/16/18	2.032	2.032	1.8	1.7	6	
S1950-E226 A-C	S1950-E226	4-131	05/16/18	1.979	1.979	1.8	1.8	0	
S1950-W100-2 A-C	S1950-W100	4-132	05/22/18	4.125	5.096	3.6	3.6	0	
S2180-E220 A-C	S2180-E220	4-133	08/14/17	24.759	24.759	1.8	1.9	-5	
S2520-E220 A-C	S2520-E220	4-134	01/09/18	30.711	30.711	2.1	1.9	11	
S2520-W100-2 A-C	S2520-W100	4-135	05/16/18	20.394	40.074	3.4	3.1	10	
S700-E180 A-C	S700-E180	4-136	05/16/18	23.042	23.042	1.7	N/A	N/A	
S700-E205-3 A-C	S700-E205	4-137	05/16/18	23.234	40.663	2.0	N/A	N/A	

Table 4-1 Access Drifts Data Analysis (continued)

Convergence Points (continued)

Field Tag	Location	Figure Number	Last Reading 2017-2018		Cumulative Displacement (inches)	Closure Rate 2017 to 2018 (in/year)	Closure Rate[1] 2016 to 2017 (in/year)	Rate Change Percent[1]	Comments
			Date	Inches					
S700-W98-3 A-C	S700-W98	4-138	05/22/18	13.059	37.400	2.1	1.9	11	
S90-W120 A-C	S90-W120	4-139	05/22/18	11.649	11.649	0.6	0.6	0	
S90-W120 B-D	S90-W120	4-139	05/24/18	12.565	12.565	0.7	0.5	40	
S90-W400-3 A-C	S90-W400	4-140	05/22/18	2.486	21.338	0.6	0.5	20	
S90-W400-3 B-D	S90-W400	4-140	05/22/18	2.568	20.905	0.6	0.5	20	
S90-W590-2 A-C	S90-W590	4-141	05/22/18	7.701	17.030	0.6	0.5	20	
S90-W590-2 B-D	S90-W590	4-141	05/22/18	12.346	16.153	0.5	0.4	25	
S90-W620 A-C	S90-W620	4-142	05/22/18	31.969	31.969	1.0	0.8	25	
W170-N150-3 A-C	W170-N150	4-143	05/22/18	6.348	14.700	0.6	0.5	20	
W170-S5-2 A-C	W170-S5	4-144	05/22/18	2.574	18.770	0.6	0.5	20	
W170-S5-2 B-D	W170-S5	4-144	05/22/18	14.373	22.139	0.8	0.7	14	
W170-S90-3 A-C	W170-S90	4-145	05/22/18	14.399	21.601	0.9	0.7	29	
W170-S232-2 A-C	W170-S232	4-146	05/22/18	10.526	16.115	0.7	0.5	40	
W170-S232-2 B-D	W170-S232	4-146	05/22/18	14.065	16.707	0.7	0.6	17	
W170-S400 A-C	W170-S400	4-147	05/22/18	19.997	19.997	0.8	0.8	0	
W170-S560-4 A-C	W170-S560	4-148	05/22/18	7.565	18.384	0.9	0.7	29	
W170-S560-4 B-D	W170-S560	4-148	01/16/18	1.755	20.207	2.3	0.8	188	
W170-S700-3 A-C	W170-S700	4-149	05/22/18	4.541	29.819	1.1	1.0	10	
W170-S850-8 A-E	W170-S850	4-150	05/22/18	3.372	24.326	0.8	0.7	14	
W170-S850-3 C-G	W170-S850	4-151	05/22/18	18.011	28.824	1.1	0.9	22	
W170-S1000-3 A-C	W170-S1000	4-152	05/22/18	11.346	34.259	1.2	1.1	9	
W170-S1150-5 A-E	W170-S1150	4-153	05/24/18	4.020	29.061	0.8	0.9	-11	
W170-S1150-2 C-G	W170-S1150	4-154	05/22/18	21.055	32.632	1.3	1.2	8	
W170-S1300-4 A-C	W170-S1300	4-155	05/22/18	21.092	42.050	2.4	2.3	4	
W170-S1445-4 A-C	W170-S1445	4-156	05/22/18	18.465	29.757	2.4	2.1	14	
W170-S1600-4 A-C	W170-S1600	4-157	05/22/18	23.973	38.738	3.6	3.3	9	
W170-S1779-3 A-C	W170-S1779	4-158	05/22/18	19.820	34.791	2.7	2.3	17	

Table 4-1 Access Drifts Data Analysis (continued)

Convergence Points (continued)

Field Tag	Location	Figure Number	Last Reading 2017-2018		Cumulative Displacement (inches)	Closure Rate 2017 to 2018 (in/year)	Closure Rate[1] 2016 to 2017 (in/year)	Rate Change Percent[1]	Comments
			Date	Inches					
W170-S1950-3 A-C	W170-S1950	4-159	05/22/18	16.340	29.521	1.9	1.8	6	
W170-S2060-3 A-C	W170-S2060	4-160	05/22/18	10.931	29.175	1.9	1.7	12	
W170-S2180-3 A-C	W170-S2180	4-161	06/13/18	14.007	37.571	2.4	2.2	9	
W170-S2520-2 A-C	W170-S2520	4-162	05/09/18	22.694	43.289	3.4	3.1	10	
W30-S90 A-C	W30-S90	4-163	05/22/18	1.198	1.198	0.9	1.2	-25	
W30-S120-3 A-C	W30-S120	4-164	05/22/18	4.085	31.731	0.9	0.8	13	
W30-S250-5 A-C	W30-S250	4-165	05/22/18	14.272	40.505	1.3	1.0	30	
W30-S400-2 A-C	W30-S400	4-166	05/22/18	11.153	28.981	1.1	0.8	38	
W30-S500-3 A-C	W30-S500	4-167	05/22/18	4.927	35.334	1.2	1.0	20	
W30-S700-5 A-C	W30-S700	4-168	05/22/18	16.734	51.011	2.2	1.8	22	
W30-S850-6 A-E	W30-S850	4-169	05/22/18	8.914	38.931	2.2	2.1	5	
W30-S850-5 B-D	W30-S850	4-170	05/22/18	5.508	25.917	1.3	1.2	4	
W30-S850-4 H-F	W30-S850	4-170	05/22/18	8.915	31.112	2.1	2.0	8	
W30-S1000-5 A-C	W30-S1000	4-171	05/22/18	15.311	53.490	2.0	1.9	5	
W30-S1150-2 A-C	W30-S1150	4-172	05/22/18	32.711	34.212	3.4	3.5	-3	
W30-S1300-2 A-C	W30-S1300	4-173	05/22/18	16.234	37.472	2.3	1.9	21	
W30-S1453-3 A-C	W30-S1453	4-174	05/22/18	4.238	33.466	2.8	2.4	17	
W30-S1600-3 A-C	W30-S1600	4-175	07/27/17	18.568	37.698	N/A	2.9	N/A	
W30-S1775-5 A-C	W30-S1775	4-176	05/22/18	6.570	34.584	4.2	3.9	8	
W30-S1950-3 A-C	W30-S1950	4-177	05/22/18	14.249	43.923	3.3	3.1	6	
W30-S2067-4 A-C	W30-S2067	4-178	09/13/17	13.352	40.292	3.7	3.0	23	
W30-S2520-4 A-C	W30-S2520	4-179	05/16/18	14.767	43.756	3.4	3.1	10	
W30-S2635-3 A-C	W30-S2655	4-180	05/18/18	19.836	38.726	N/A	2.7	N/A	Not enough data for current period

Table 4-1 Access Drifts Data Analysis (continued)

Joint Meters								
Field Tag	Location	Figure Number	Date	Cumulative Displacement (inches)	Closure Rate 2017 to 2018 (in/year)	Closure Rate 2016 to 2017 (in/year)	Rate Change Percent	Comments
51X-CG-02706	S1950-E300-SW	4-181	06/07/2018	3.430	0.2	0.3	-33%	
51X-CG-02883-3	E140-S1529	4-182	06/07/2018	-0.289	0.0	0.0	0%	
51X-CG-02885-2	E140-S1545	4-183	06/07/2018	0.910	0.0	N/A	N/A	
51X-CG-02875-2	E140-S1795	4-184	06/07/2018	0.700	0.0	0.0	0%	

[1] N/A – Insufficient data available to perform the calculation. This is usually due to the inability to read the instruments because of activities such as the removal of an instrument due to floor, rib, or back trimming; locations blocked by equipment or waste disposal; installation timing, access issues, etc.

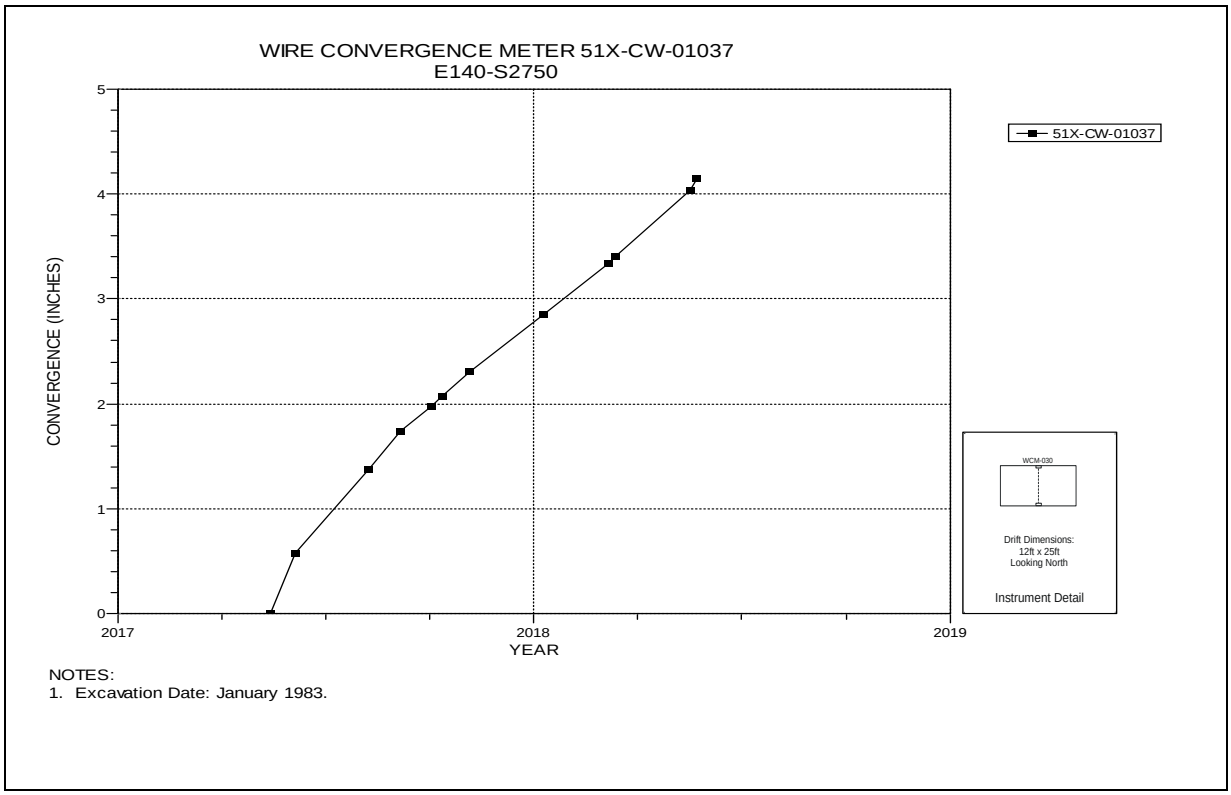

Figure 4-1 Wire Convergence Meter 51X-CW-01037 – E140 S2750 – Roof to Floor

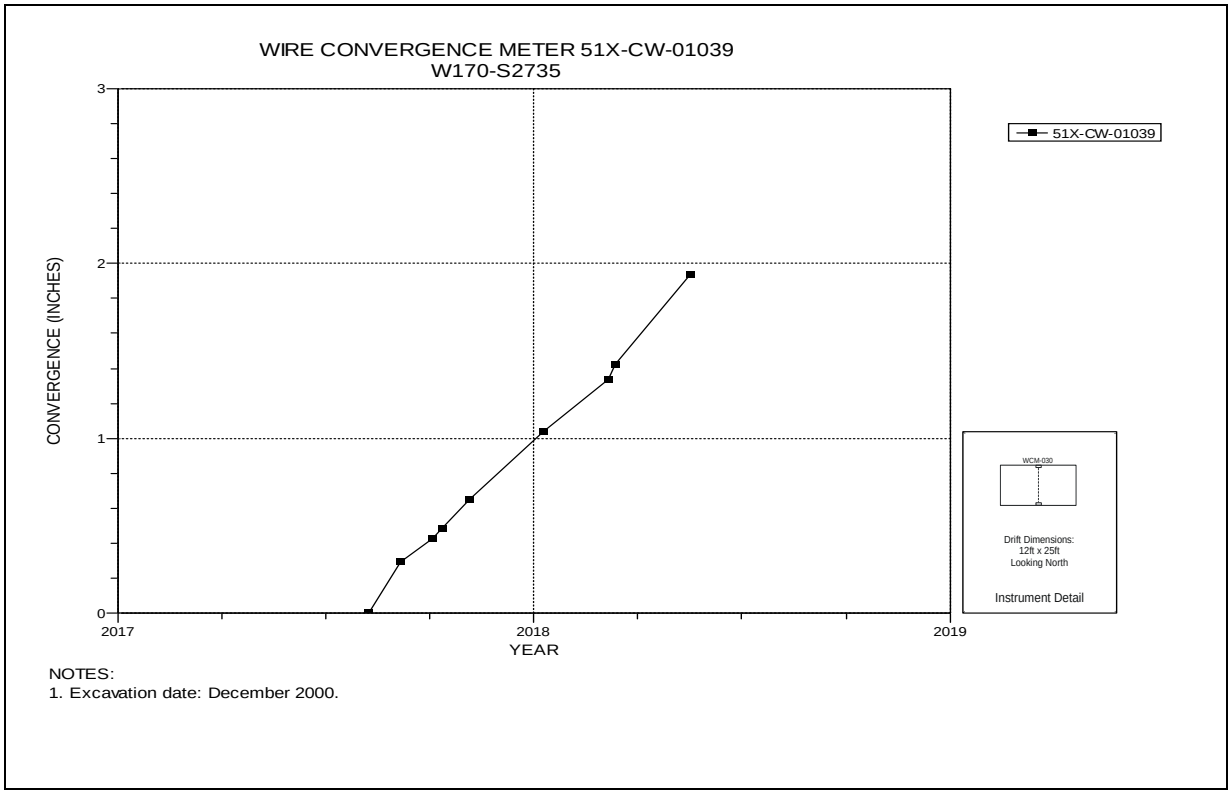

Figure 4-2 Wire Convergence Meter 51X-CW-01039 – W170 S2735 – Roof to Floor

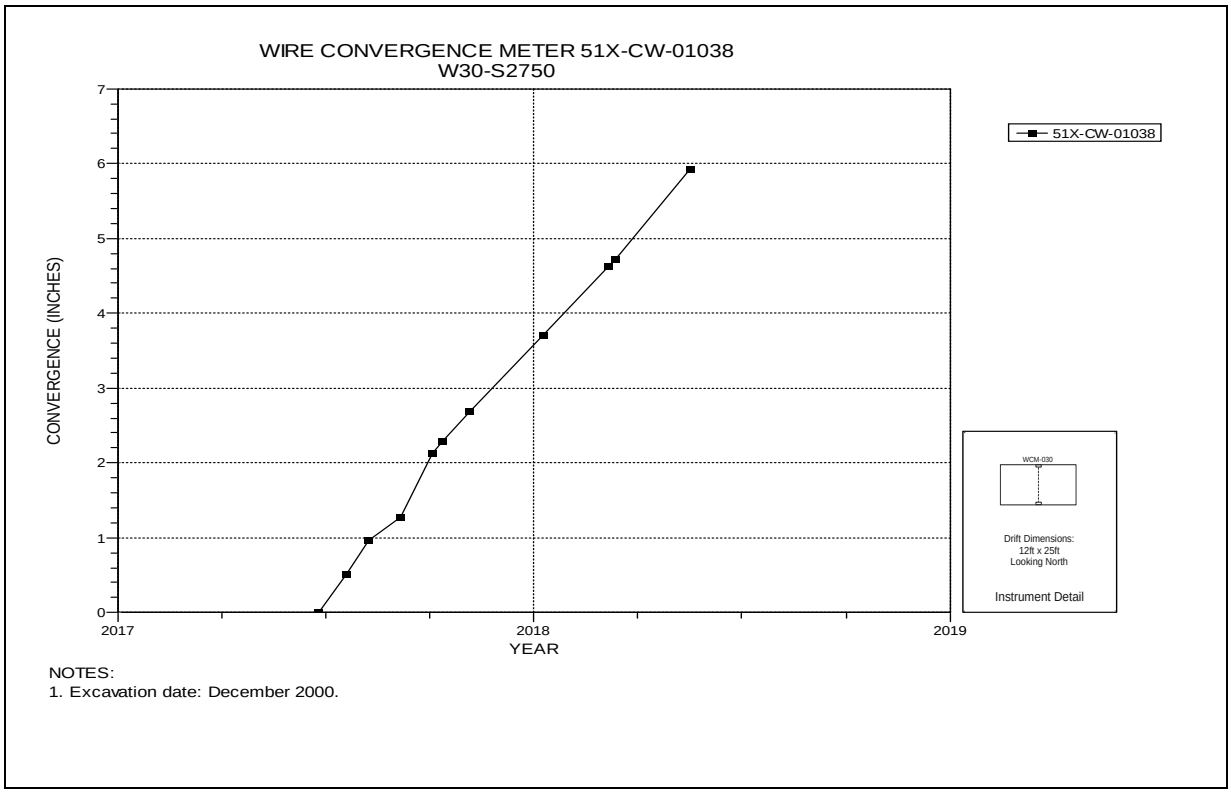

Figure 4-3 Wire Convergence Meter 51X-CW-01038 – W30 S2750 – Roof

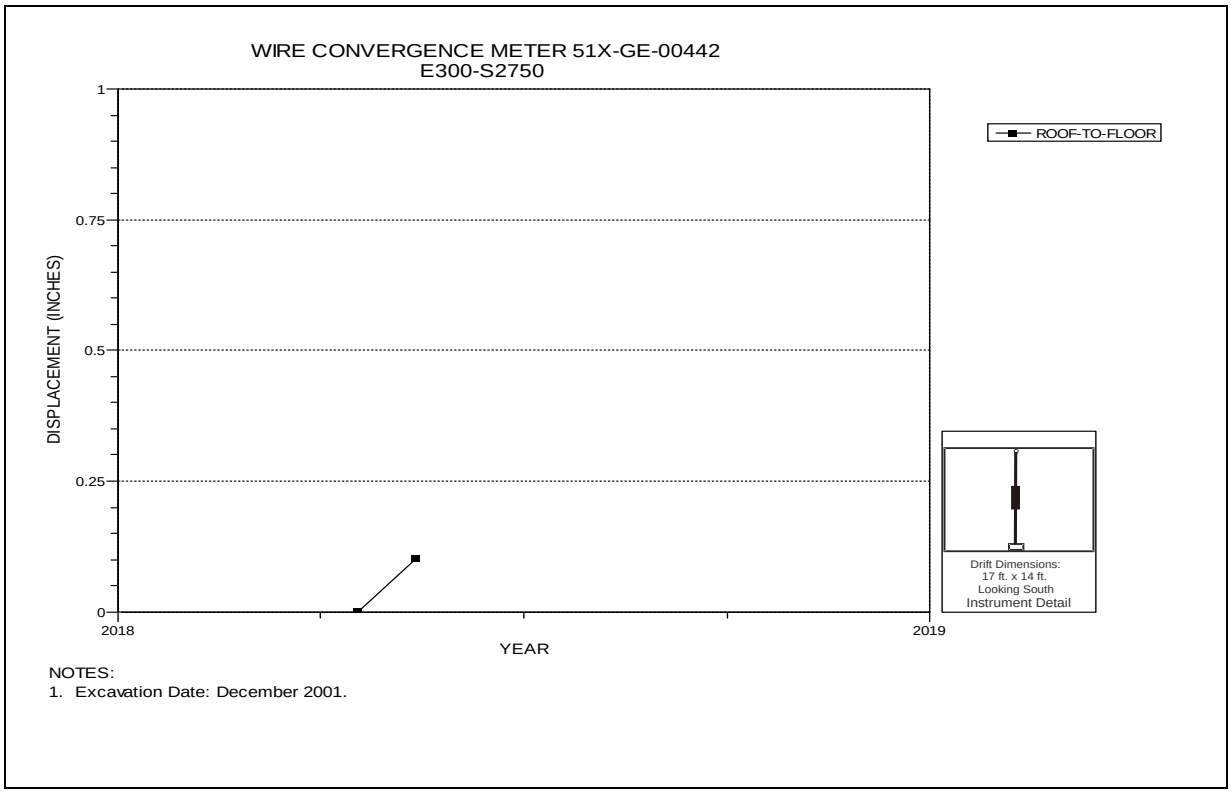

Figure 4-4 Wire Convergence Meter 51X-GE-00442 – E300 S2750 – Roof

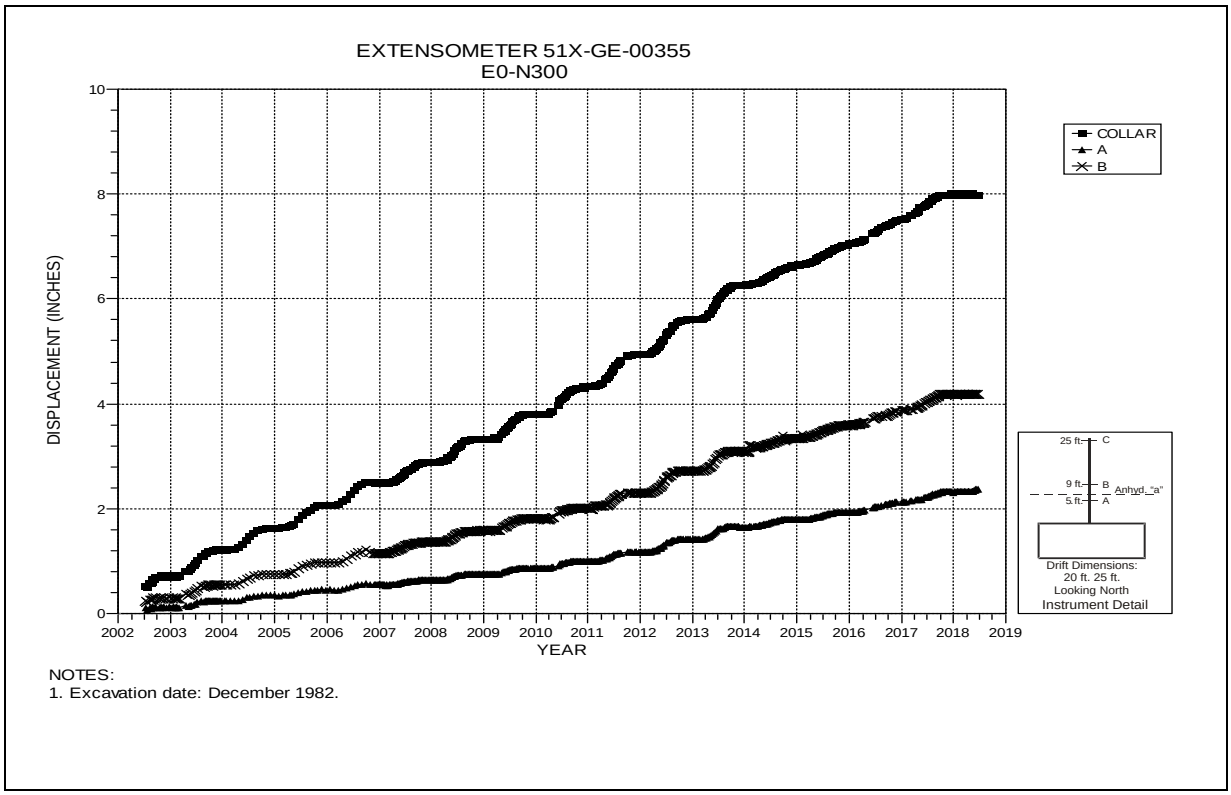

NOTES:
1. Excavation date: December 1982.

Figure 4-5 Extensometer 51X-GE-00355 – E0 N300 – Roof

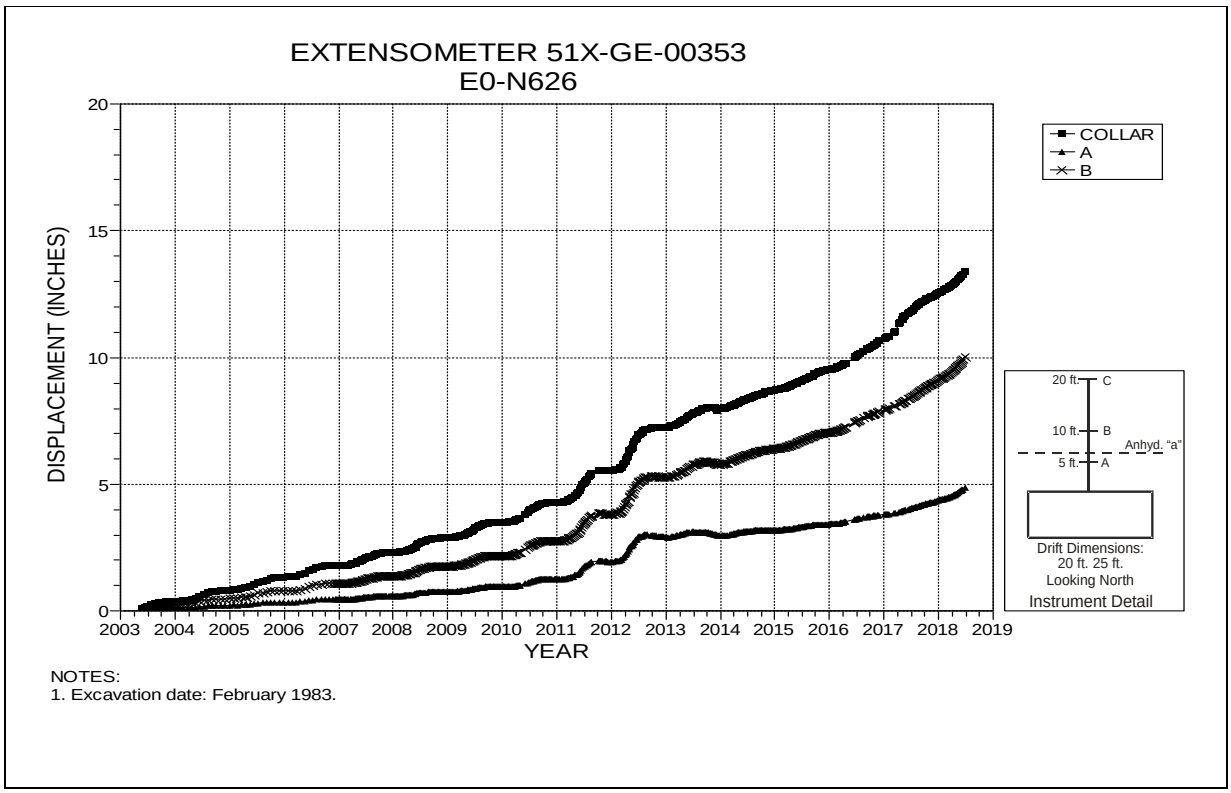

NOTES:
1. Excavation date: February 1983.

Figure 4-6 Extensometer 51X-GE-00353 – E0 N626 – Roof

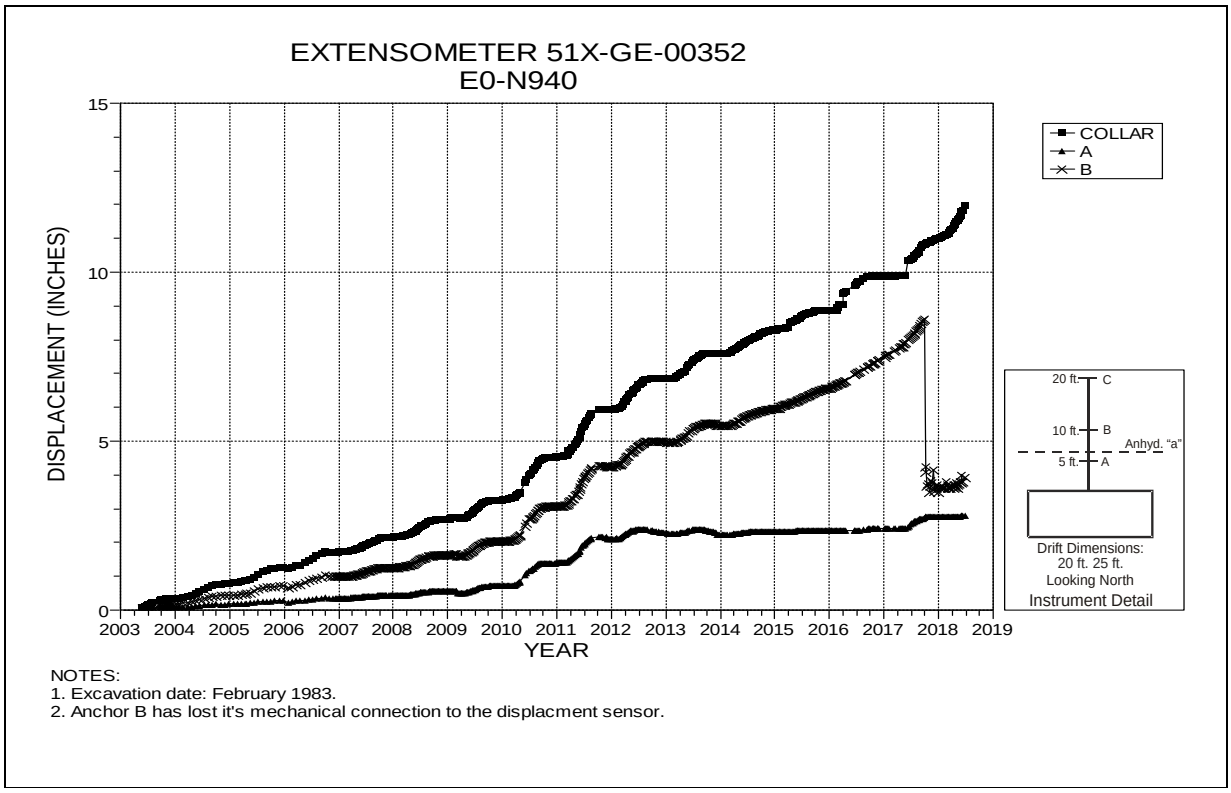

Figure 4-7 Extensometer 51X-GE-00352 – E0 N940 – Roof

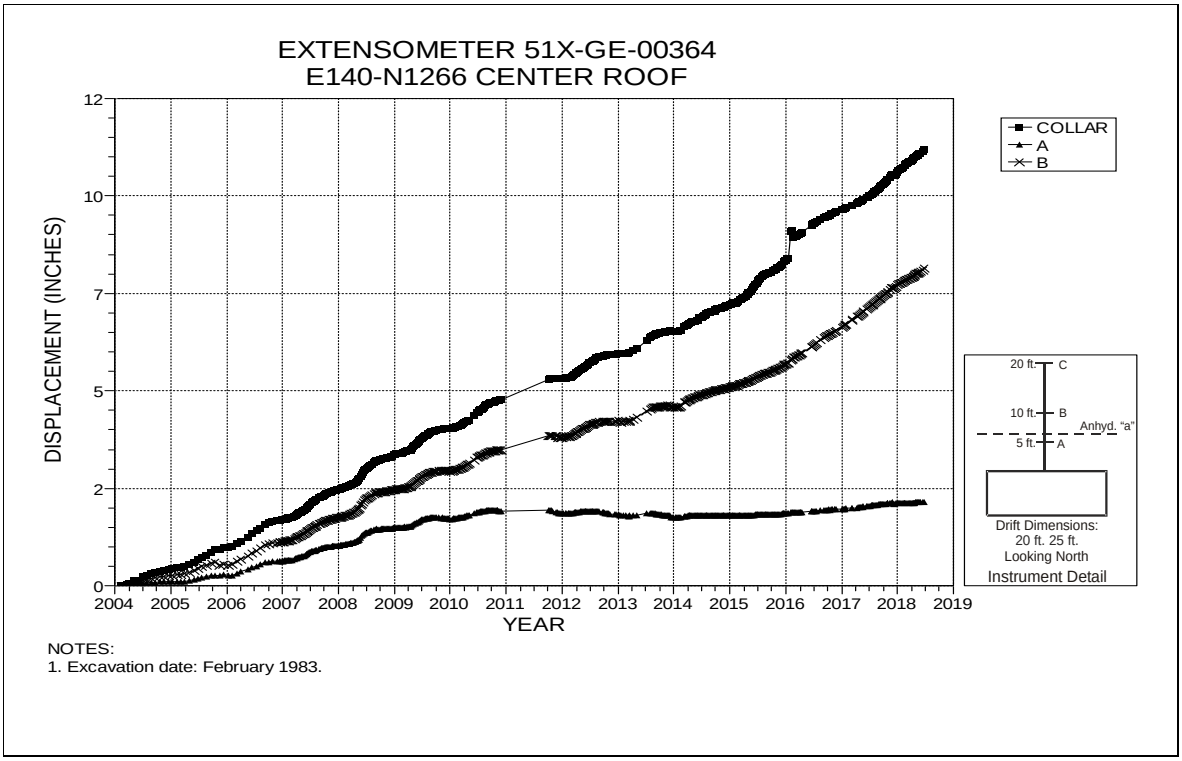

Figure 4-8 Extensometer 51X-GE-00364 – E140 N1266 – Roof

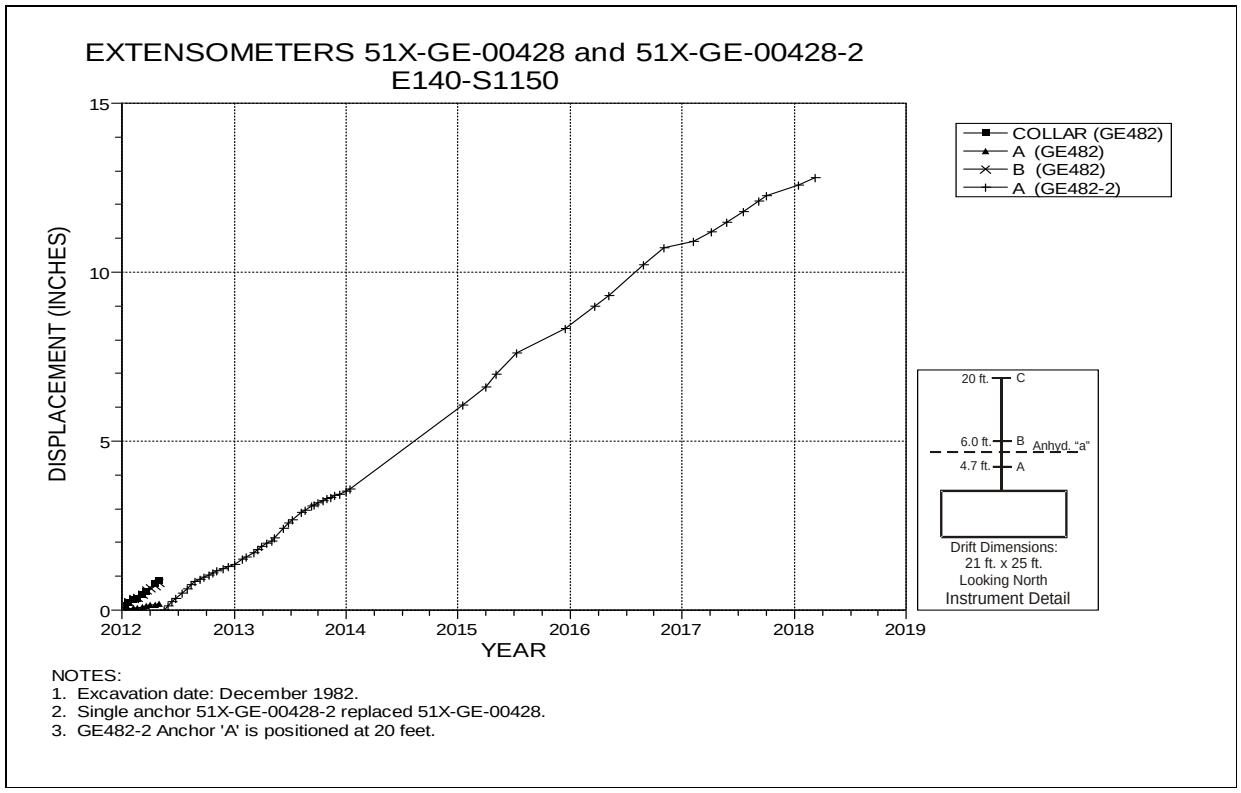

Figure 4-9 Extensometer 51X-GE-00428-2 – E140 S1150 – Roof

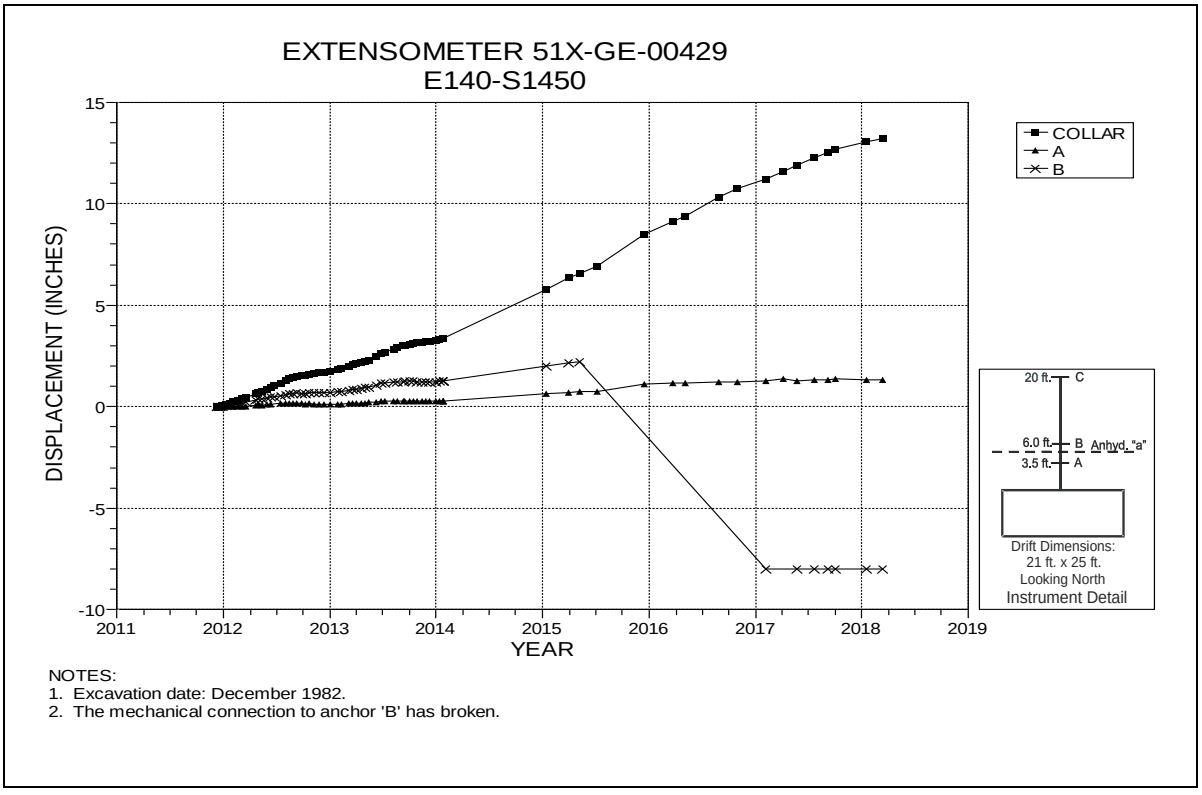

Figure 4-10 Extensometer 51X-GE-00429 – E140 S1450 – Roof

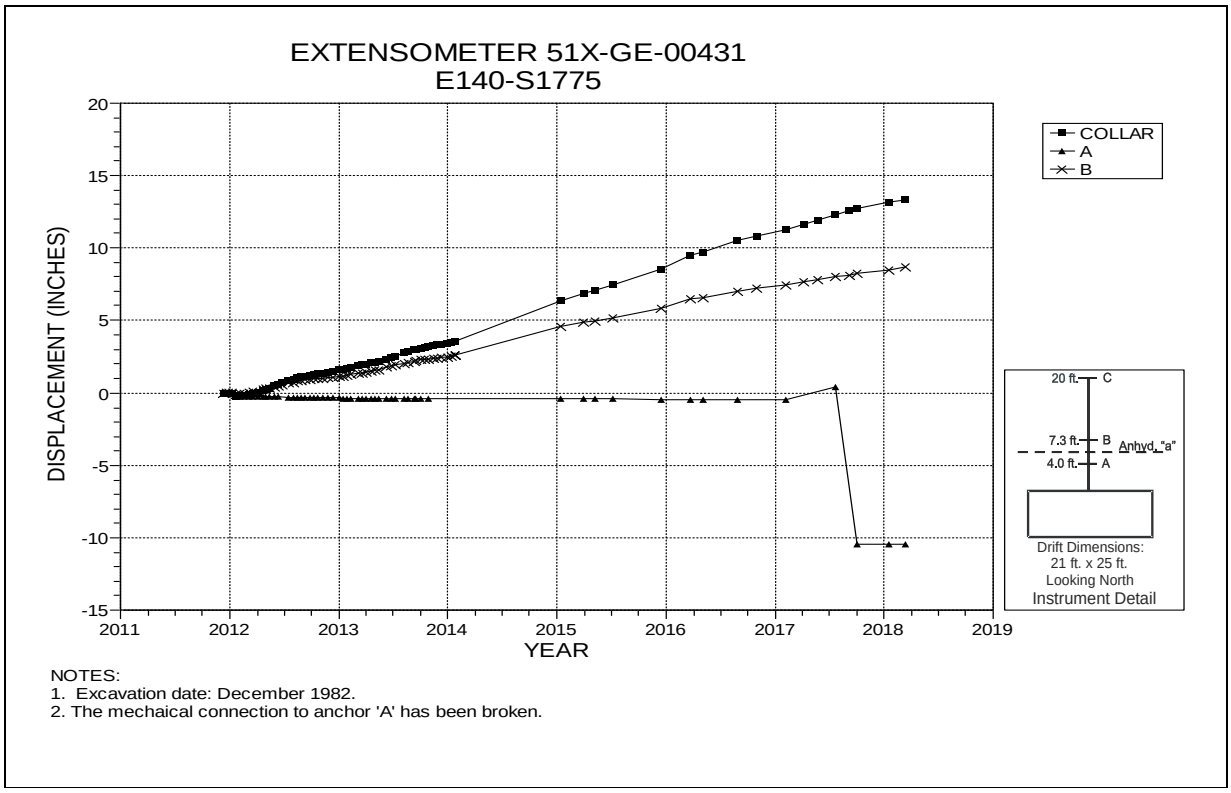

Figure 4-11 Extensometer 51X-GE-00431 – E140 S1775 – Roof

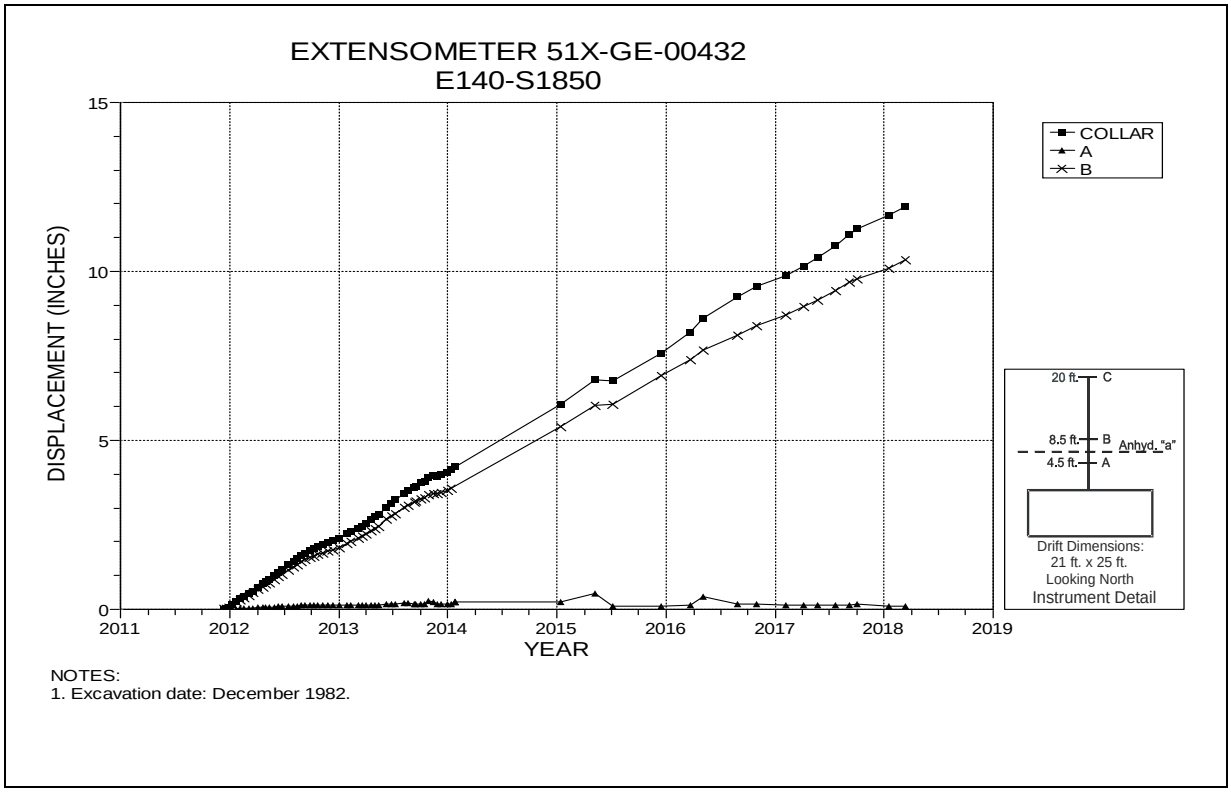

Figure 4-12 Extensometer 51X-GE-00432 – E140 S1850 – Roof

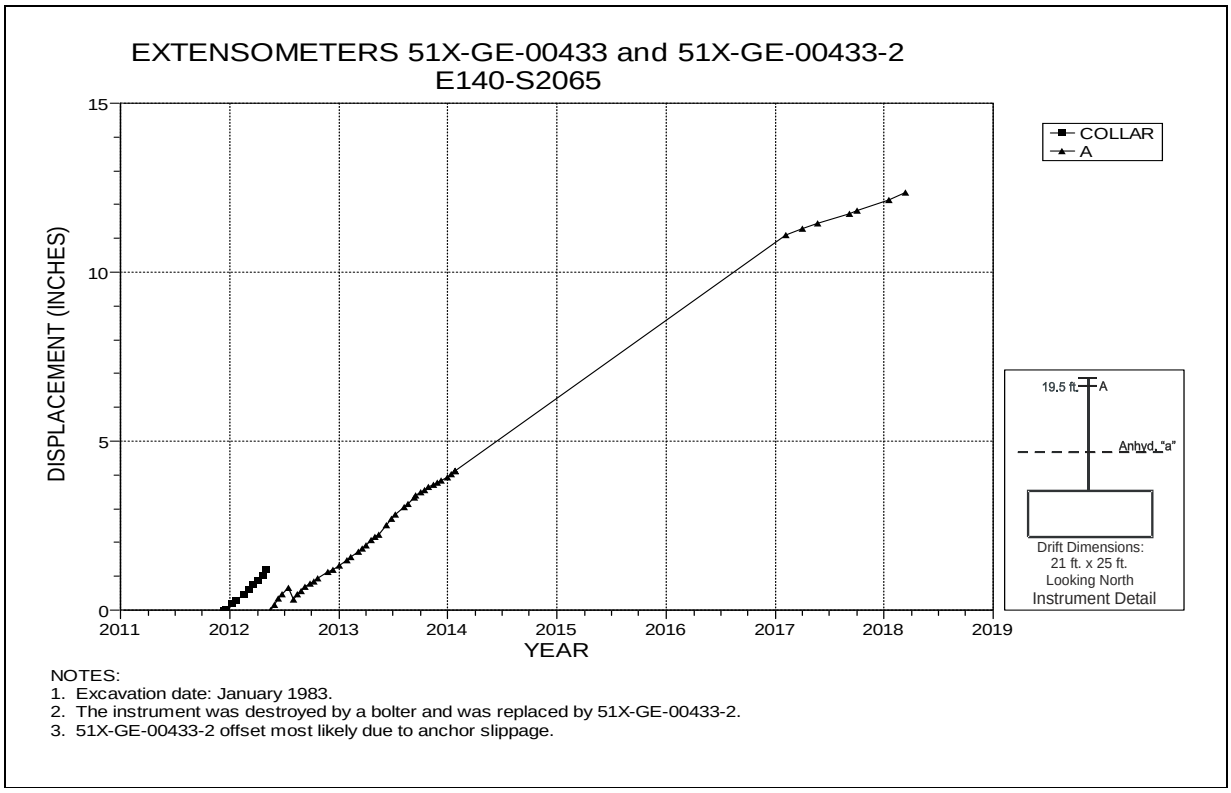

NOTES:
1. Excavation date: January 1983.
2. The instrument was destroyed by a bolter and was replaced by 51X-GE-00433-2.
3. 51X-GE-00433-2 offset most likely due to anchor slippage.

Figure 4-13 Extensometer 51X-GE-00433-2 – E140 S2065 – Roof

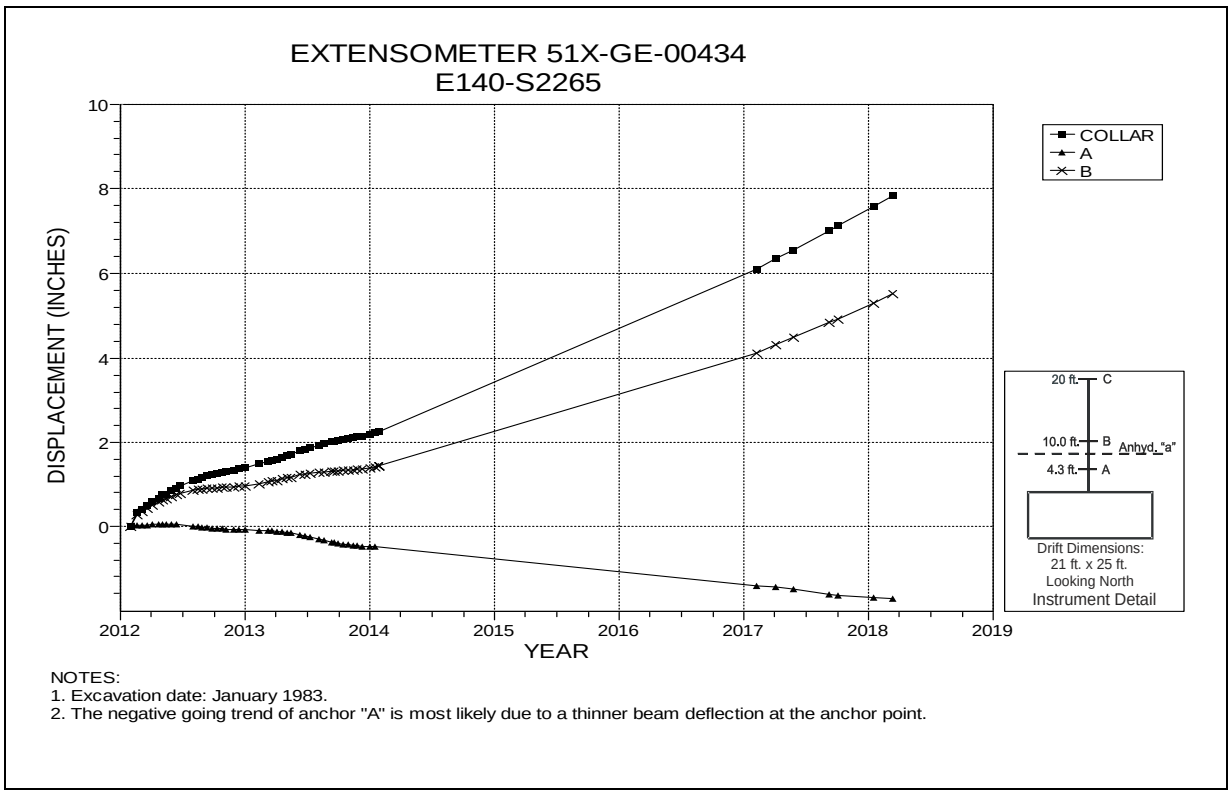

NOTES:
1. Excavation date: January 1983.
2. The negative going trend of anchor "A" is most likely due to a thinner beam deflection at the anchor point.

Figure 4-14 Extensometer 51X-GE-00434 – E140 S2265 – Roof

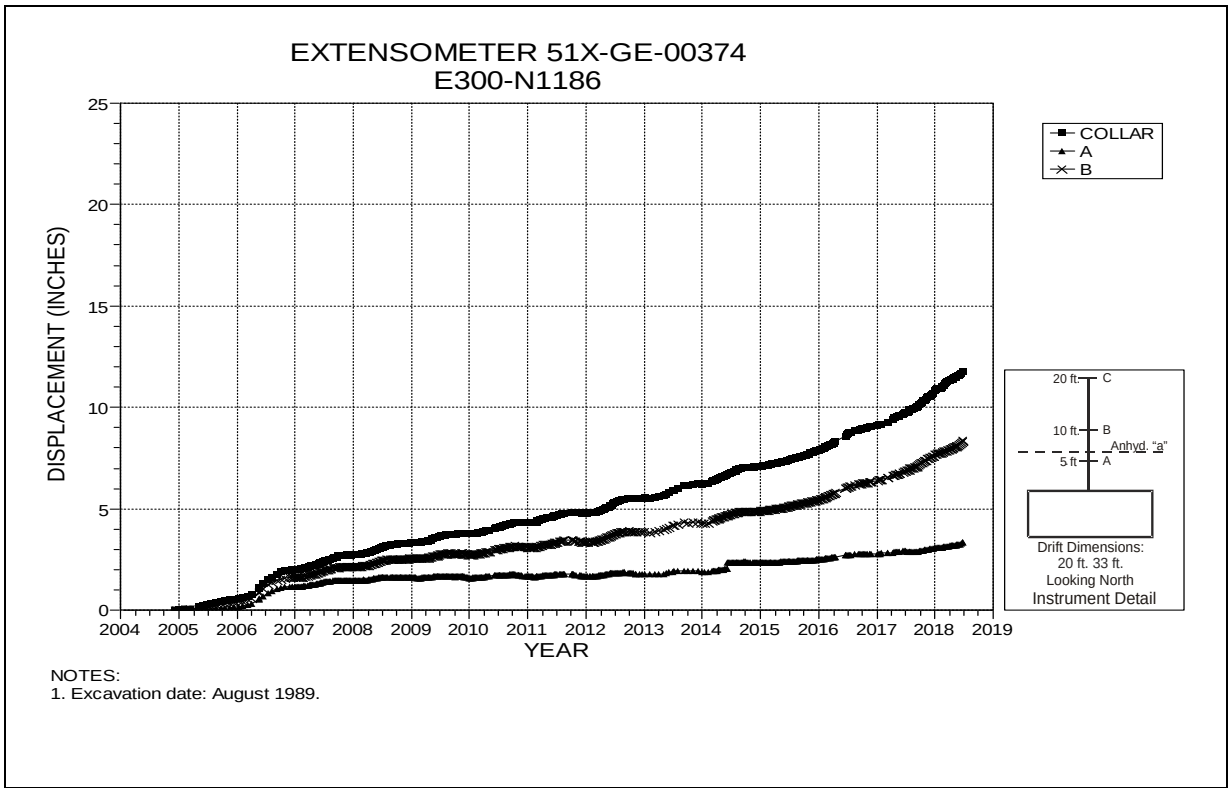

Figure 4-15 Extensometer 51X-GE-00374 – E300 N1186 – Roof

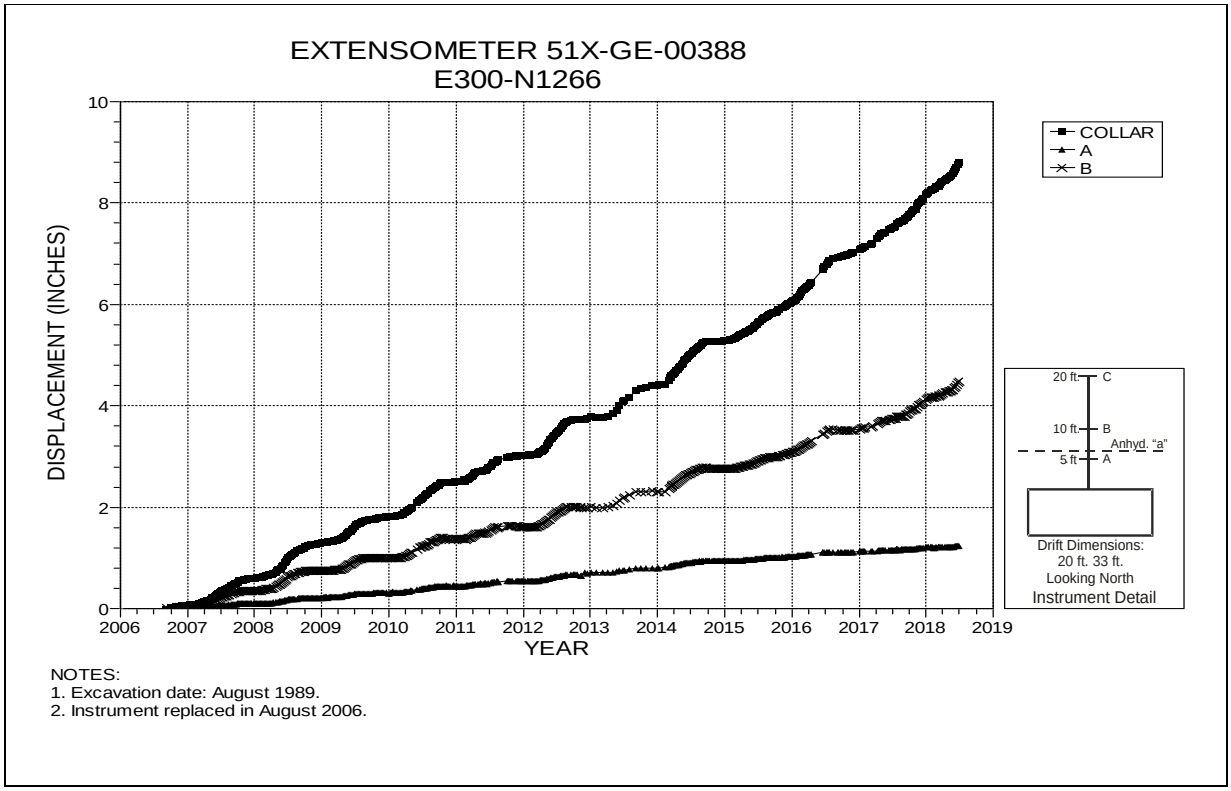

Figure 4-16 Extensometer 51X-GE-00388 – E300 N1266 – Roof

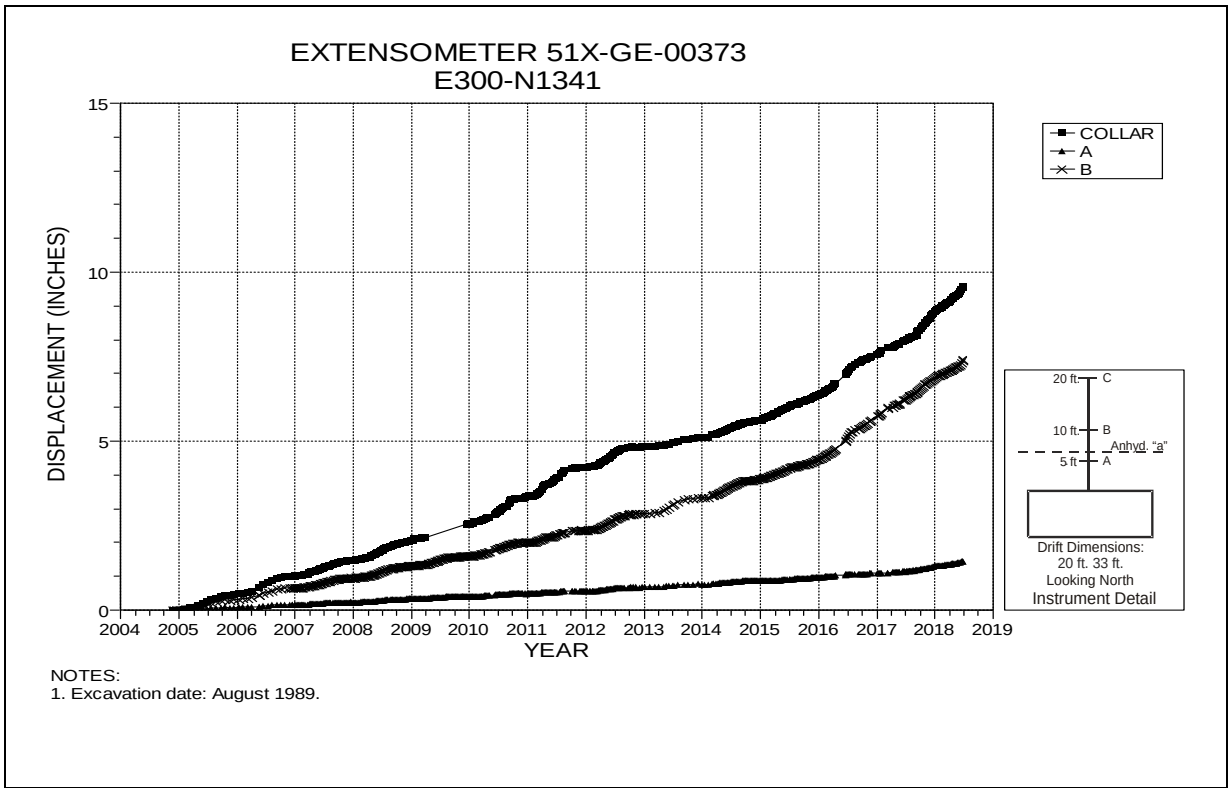

Figure 4-17 Extensometer 51X-GE-00373 – E300 N1341 – Roof

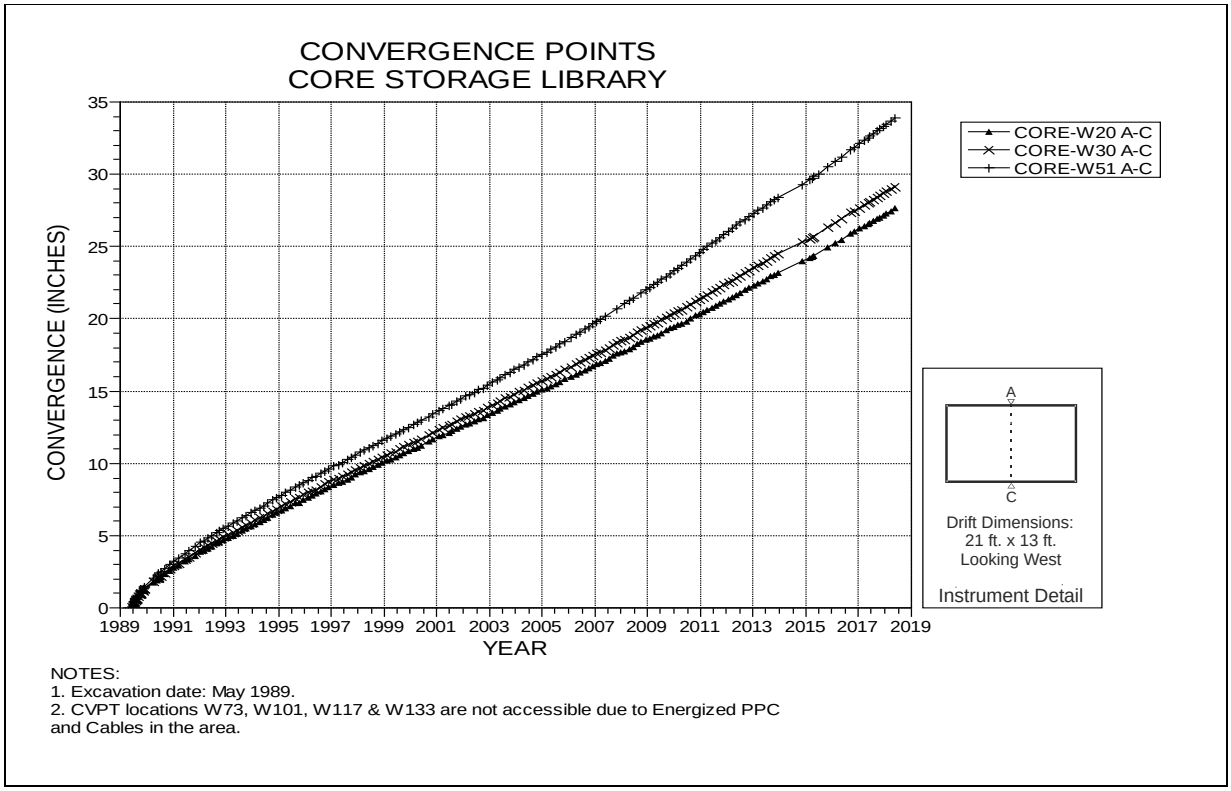

Figure 4-18 Core Storage Library – Roof to Floor – Centerline

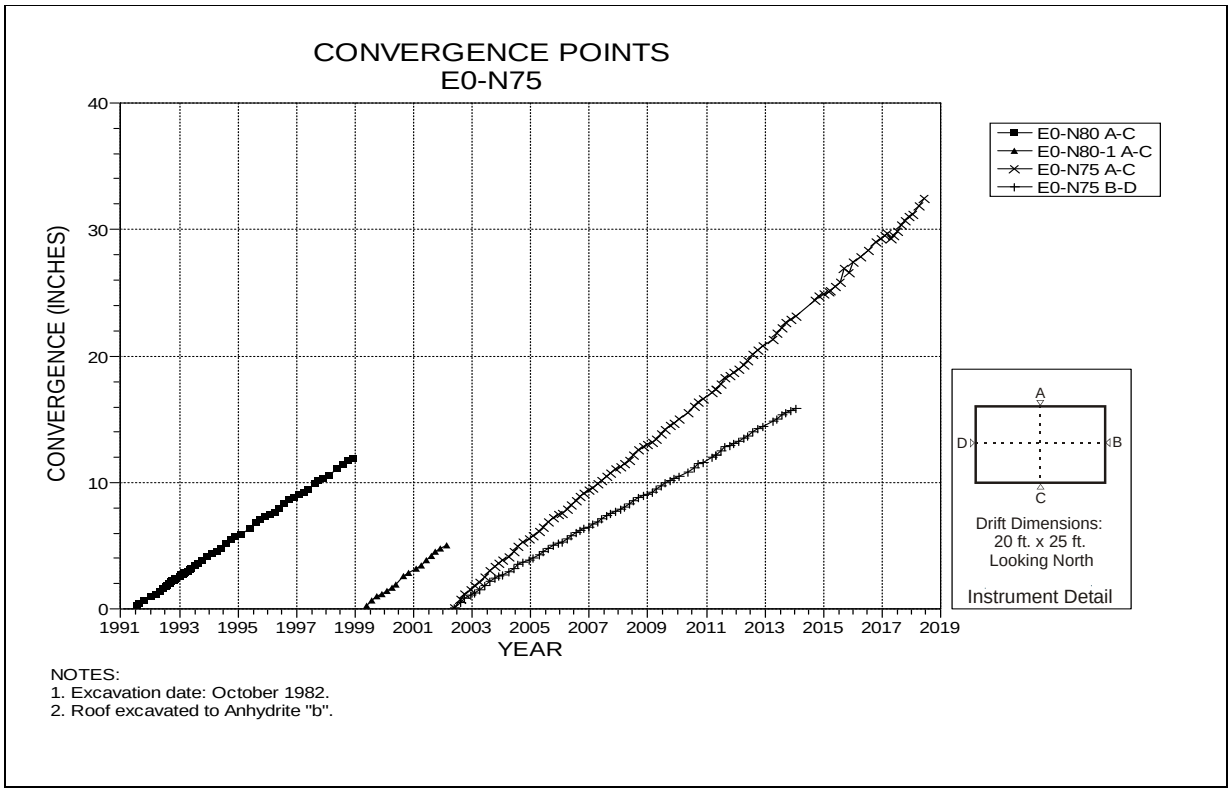

Figure 4-19 Convergence Point Array – E0 N75 – All Chords

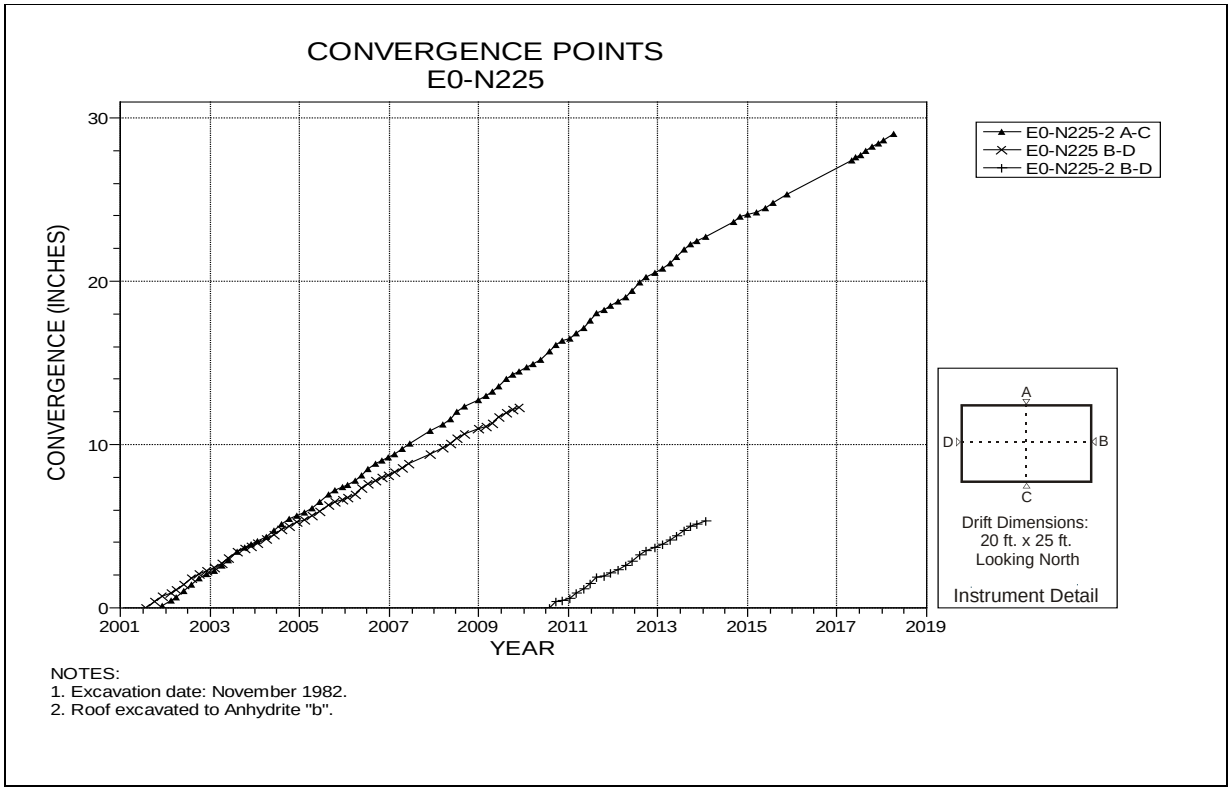

Figure 4-20 Convergence Point Array – E0 N225 – Roof to Floor – Centerline

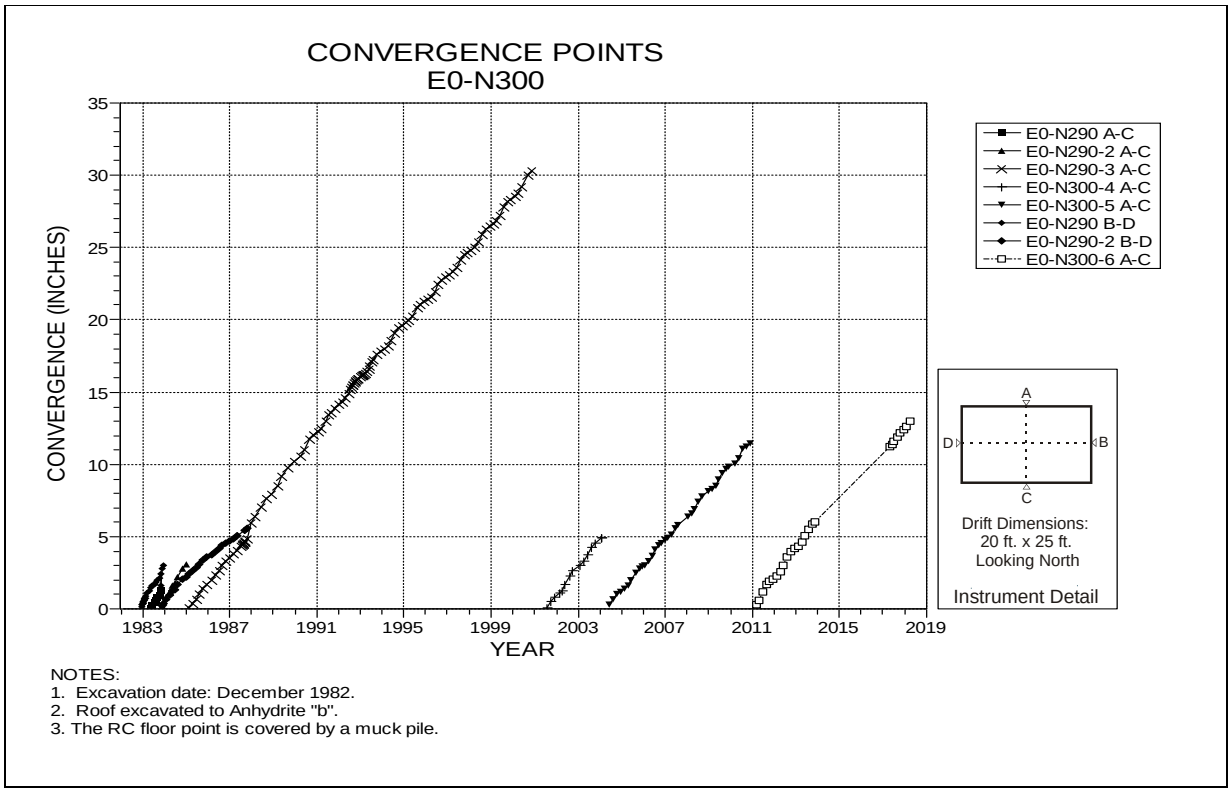

Figure 4-21 Convergence Point Array – E0 N300 – Roof to Floor – Centerline

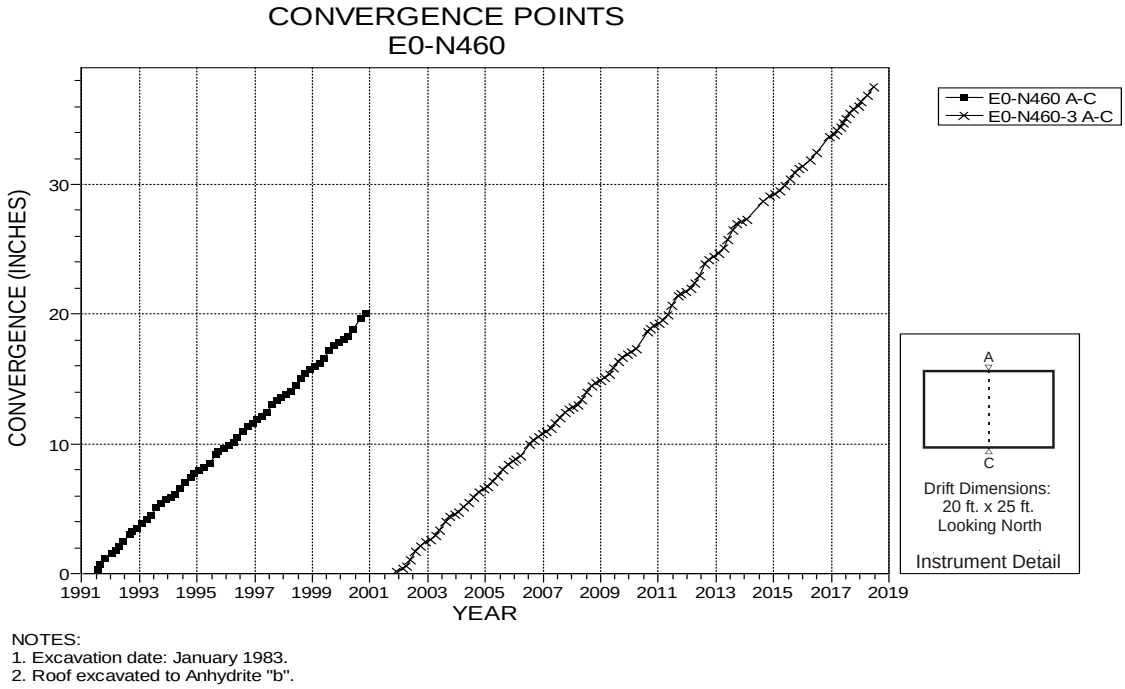

Figure 4-22 Convergence Point Array – E0 N460 – Roof to Floor – Centerline

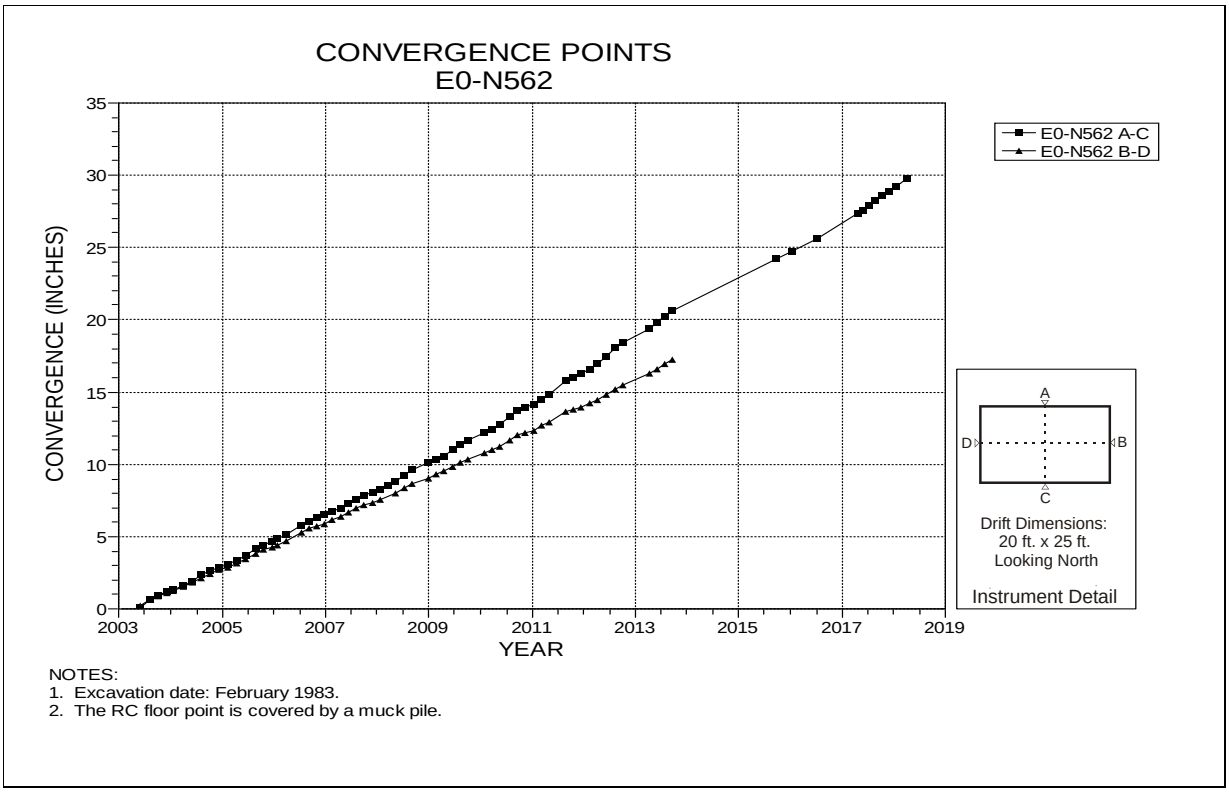

Figure 4-23 Convergence Point Array – E0 N562 – All Chords

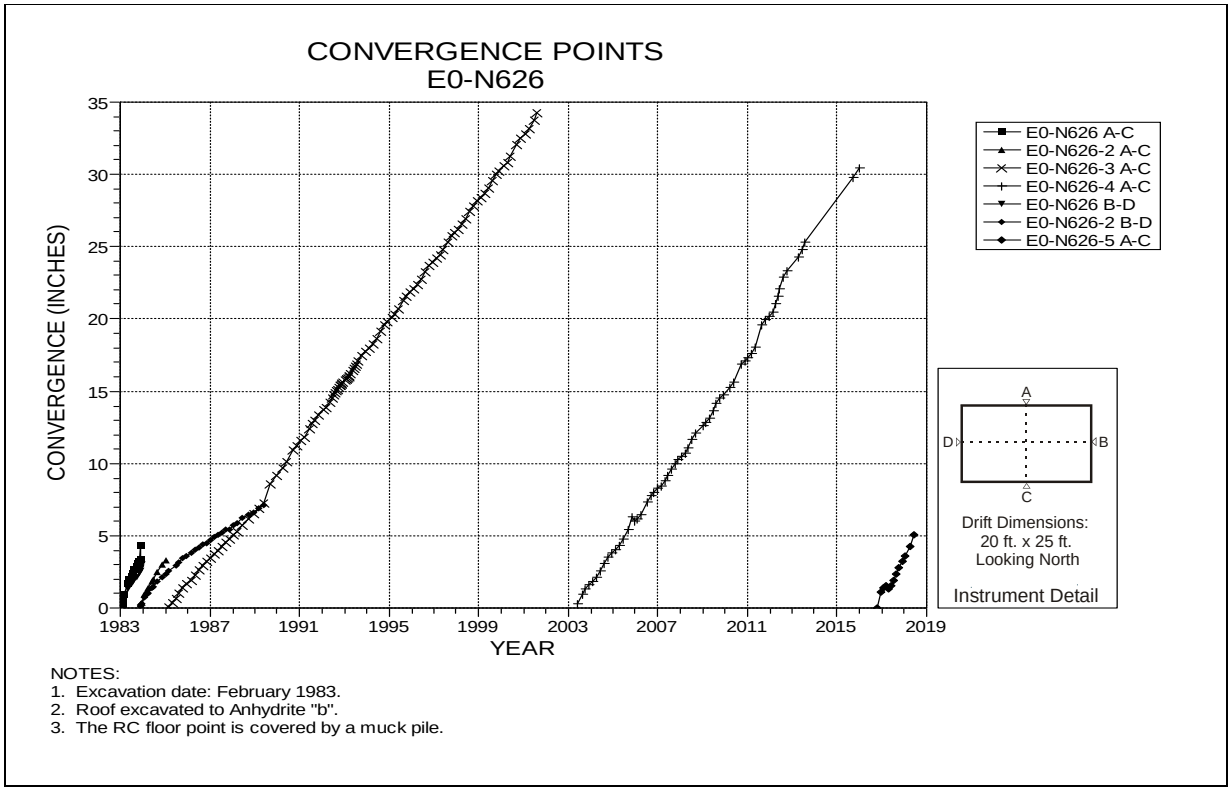

Figure 4-24 Convergence Point Array – E0 N626 – Roof to Floor – Centerline

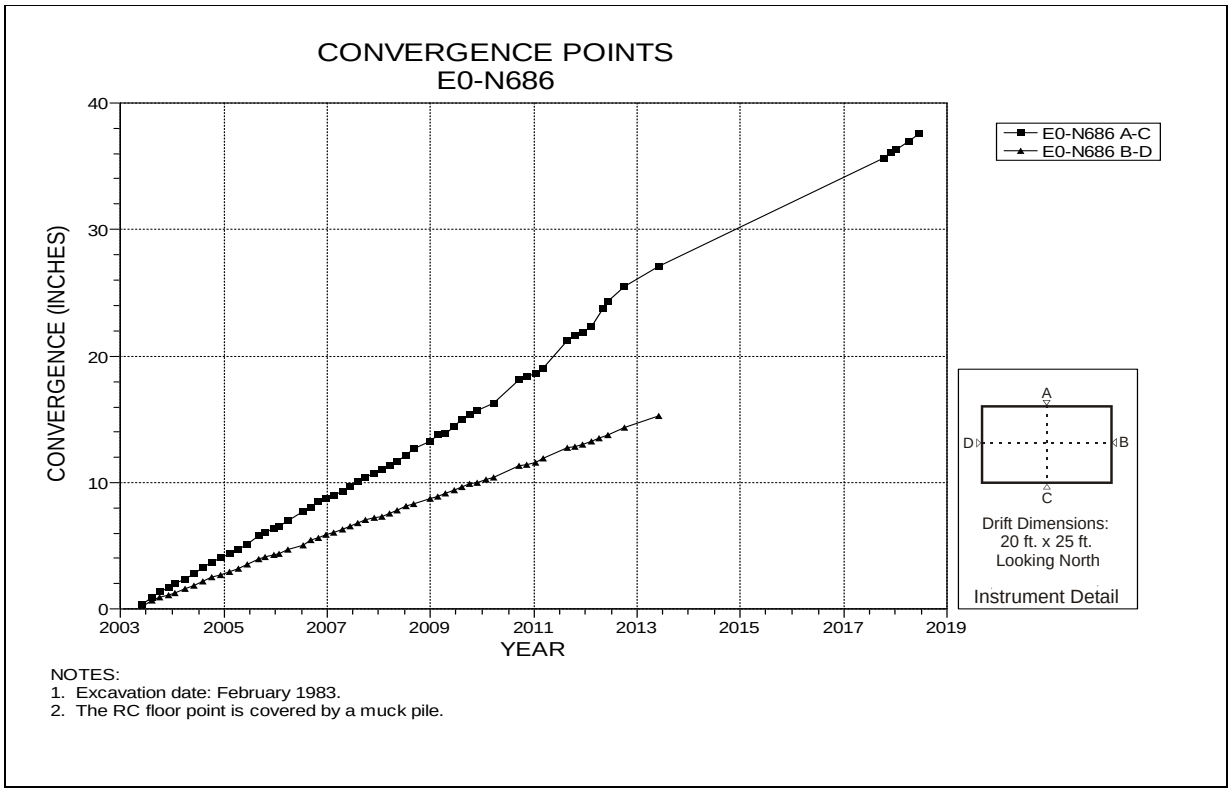

Figure 4-25 Convergence Point Array – E0 N686 – Roof to Floor – Centerline

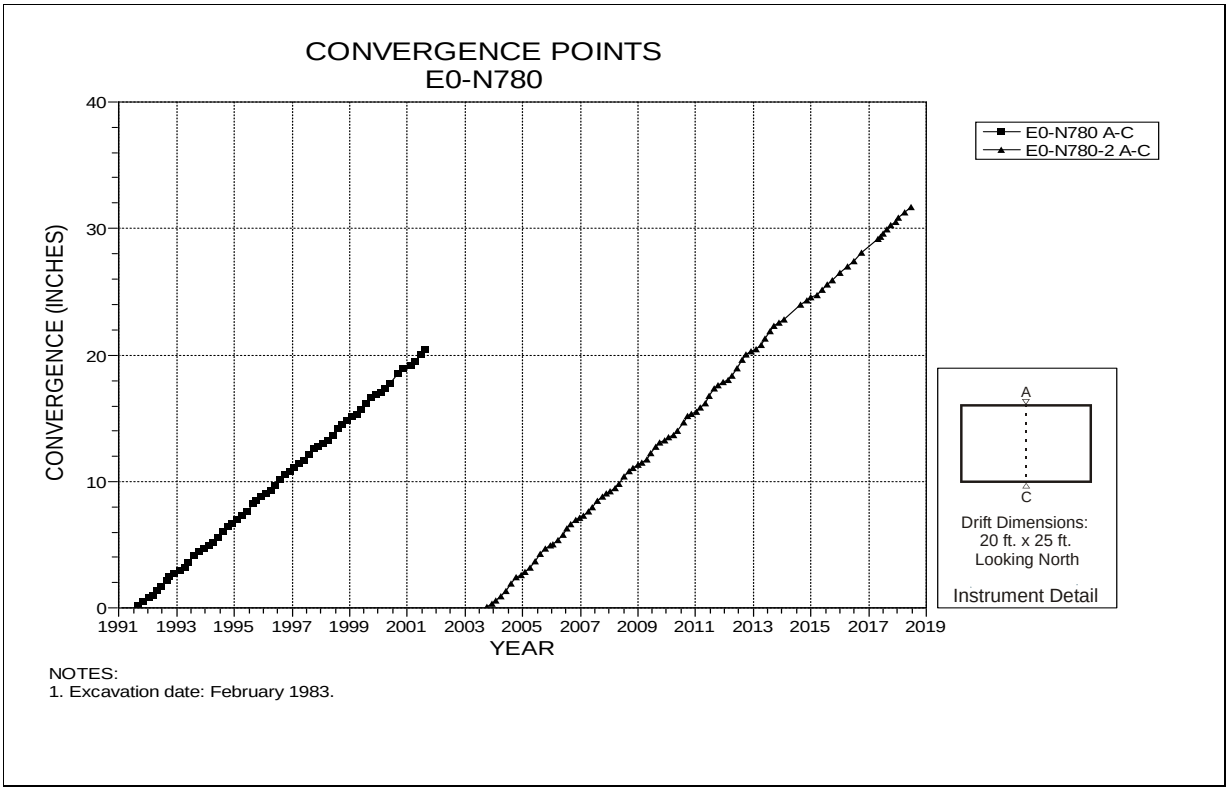

Figure 4-26 Convergence Point Array – E0 N780 – Roof to Floor – Centerline

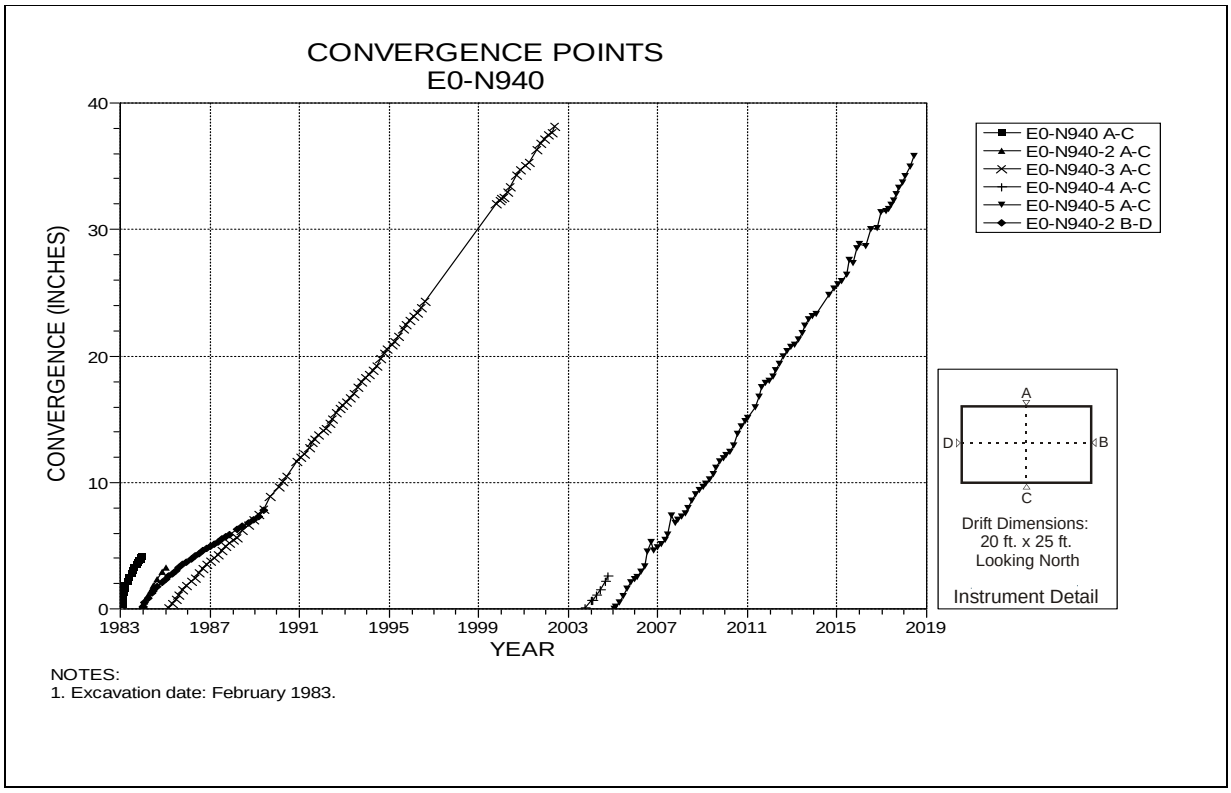

Figure 4-27 Convergence Point Array – E0 N940 – All Chords

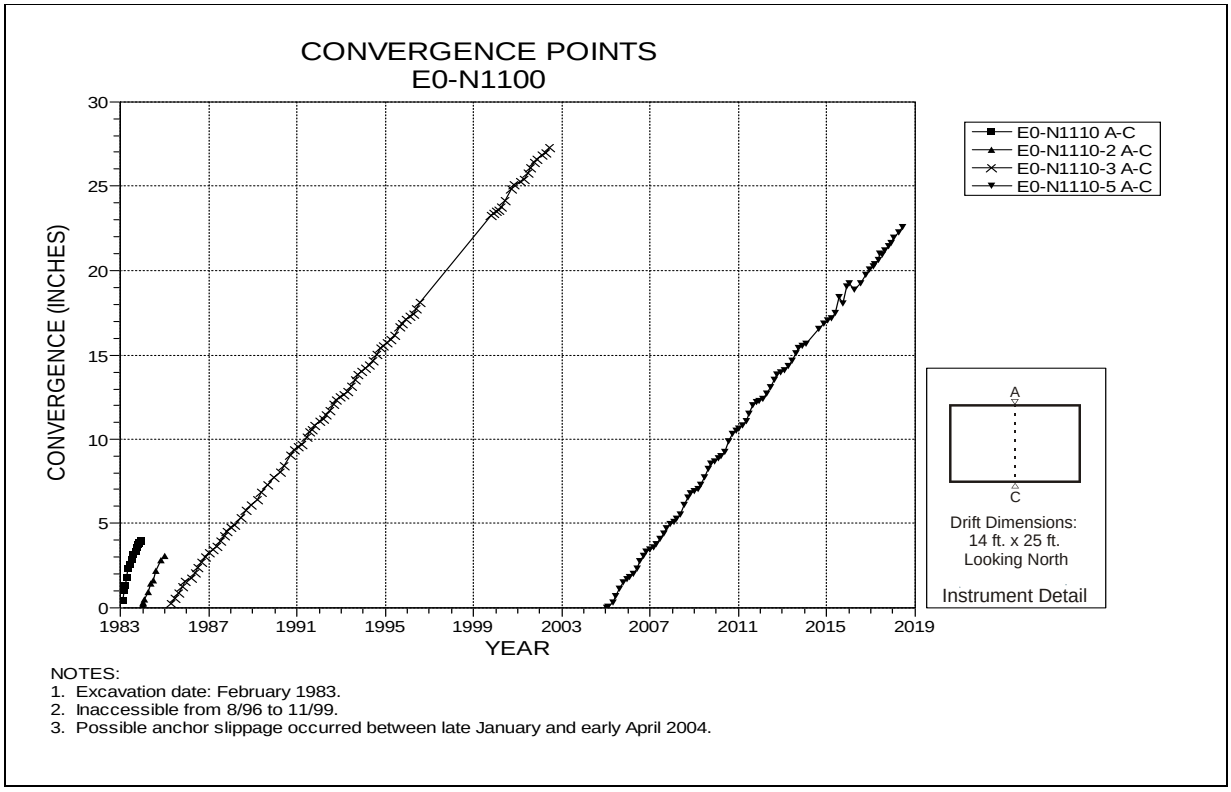

Figure 4-28 Convergence Point Array – E0 N1100 – Roof to Floor – Centerline

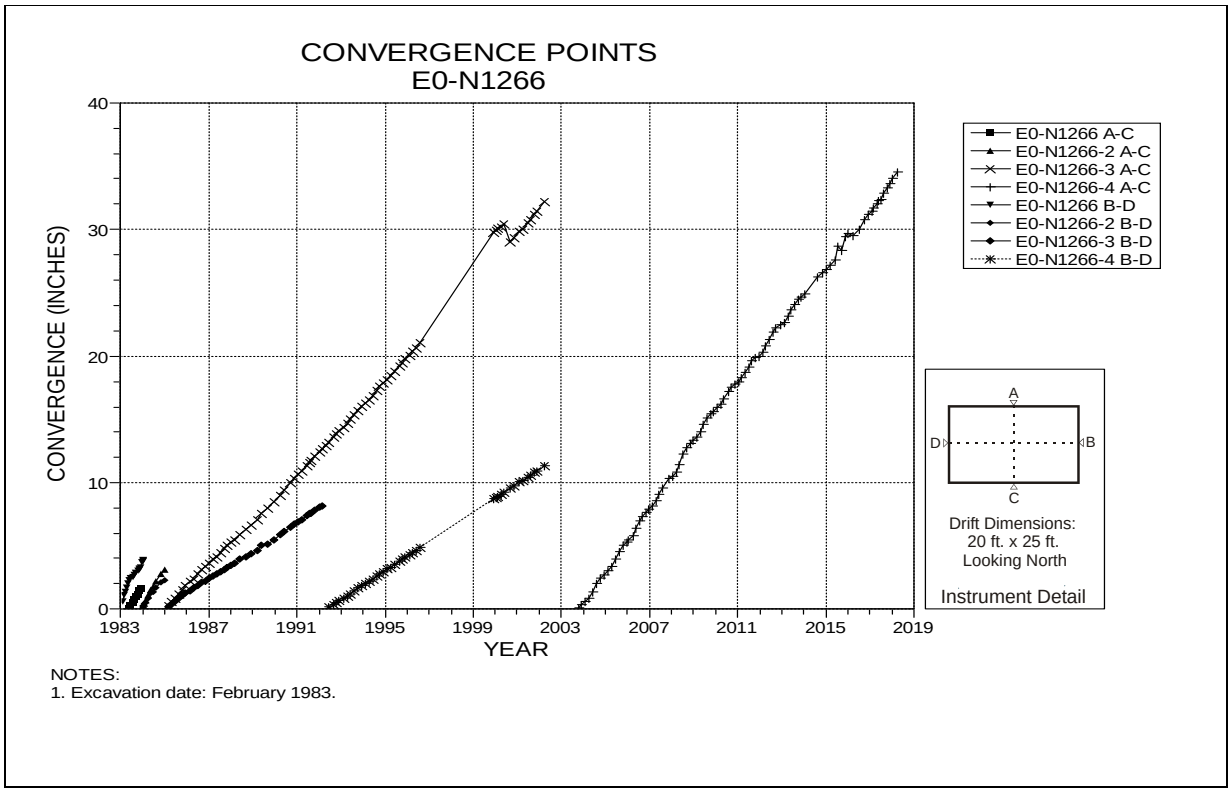

Figure 4-29 Convergence Point Array – E0 N1266 – All Chords

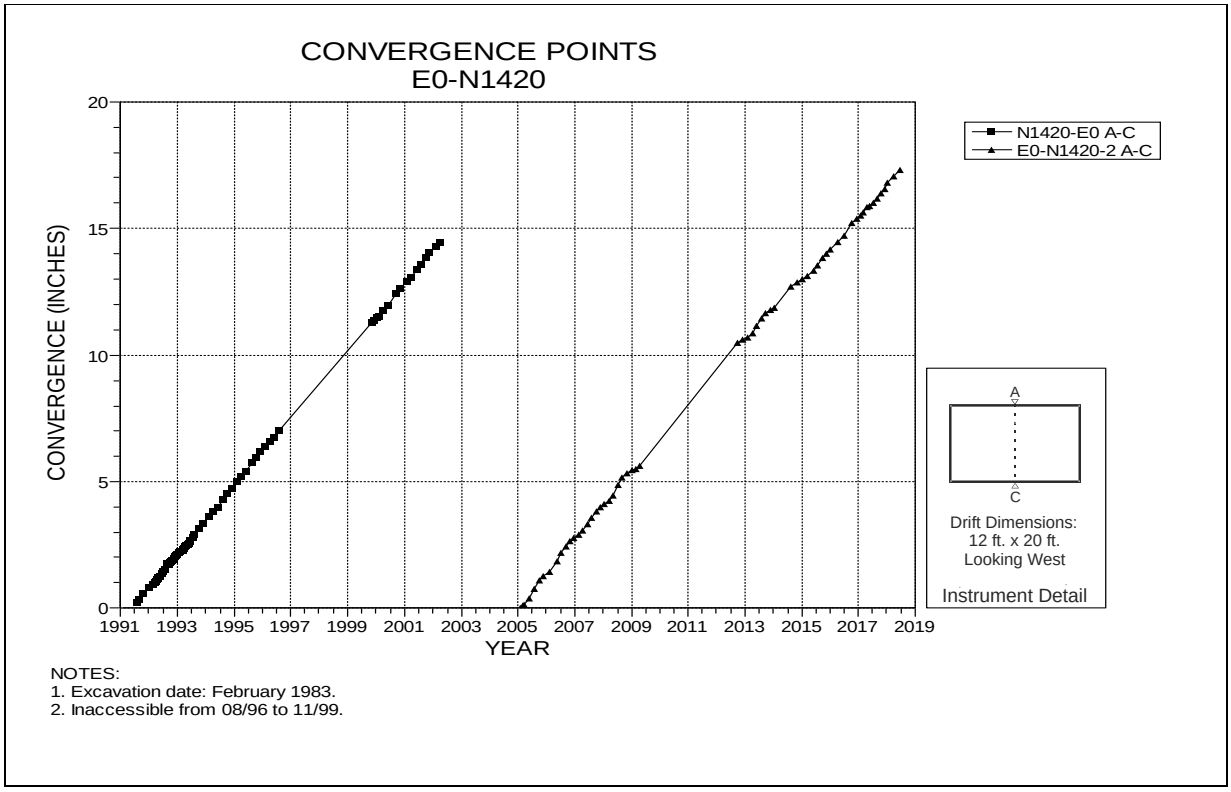

Figure 4-30 Convergence Point Array – E0 N1420 – All Chords

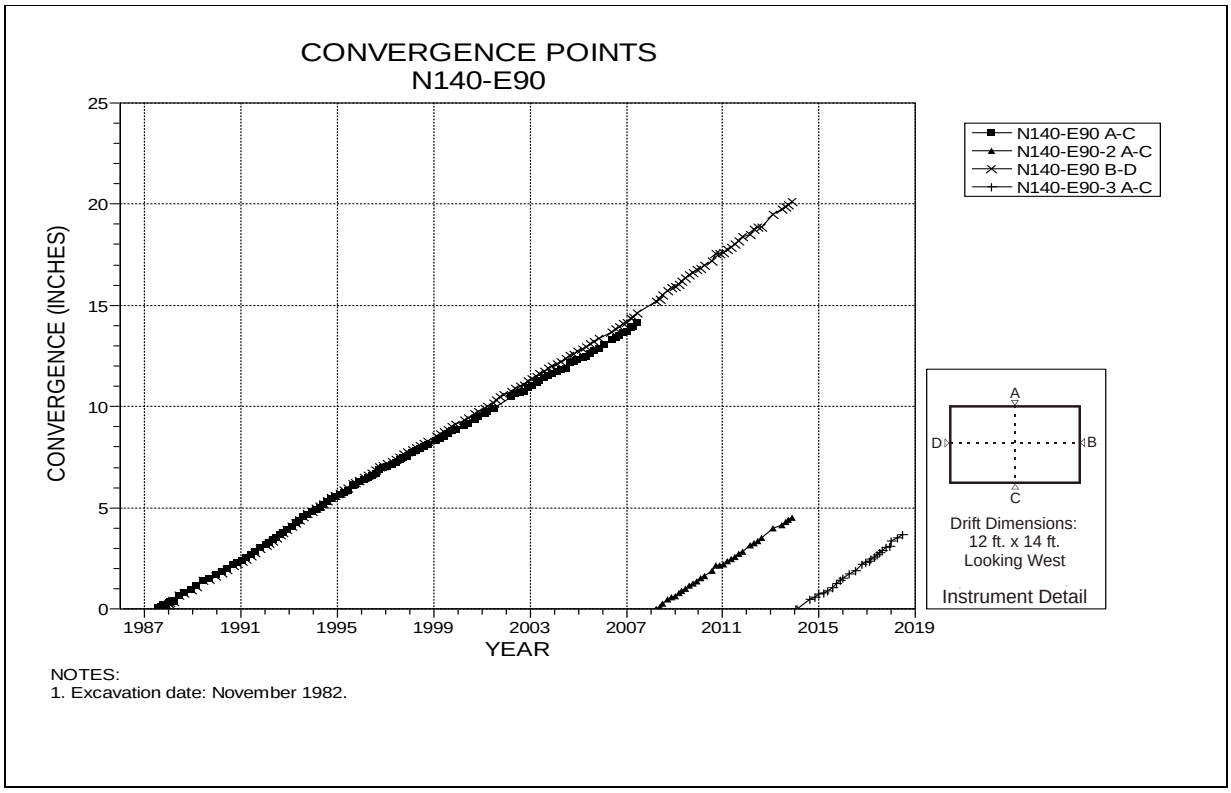

Figure 4-31 Convergence Point Array – N140 E90 – All Chords

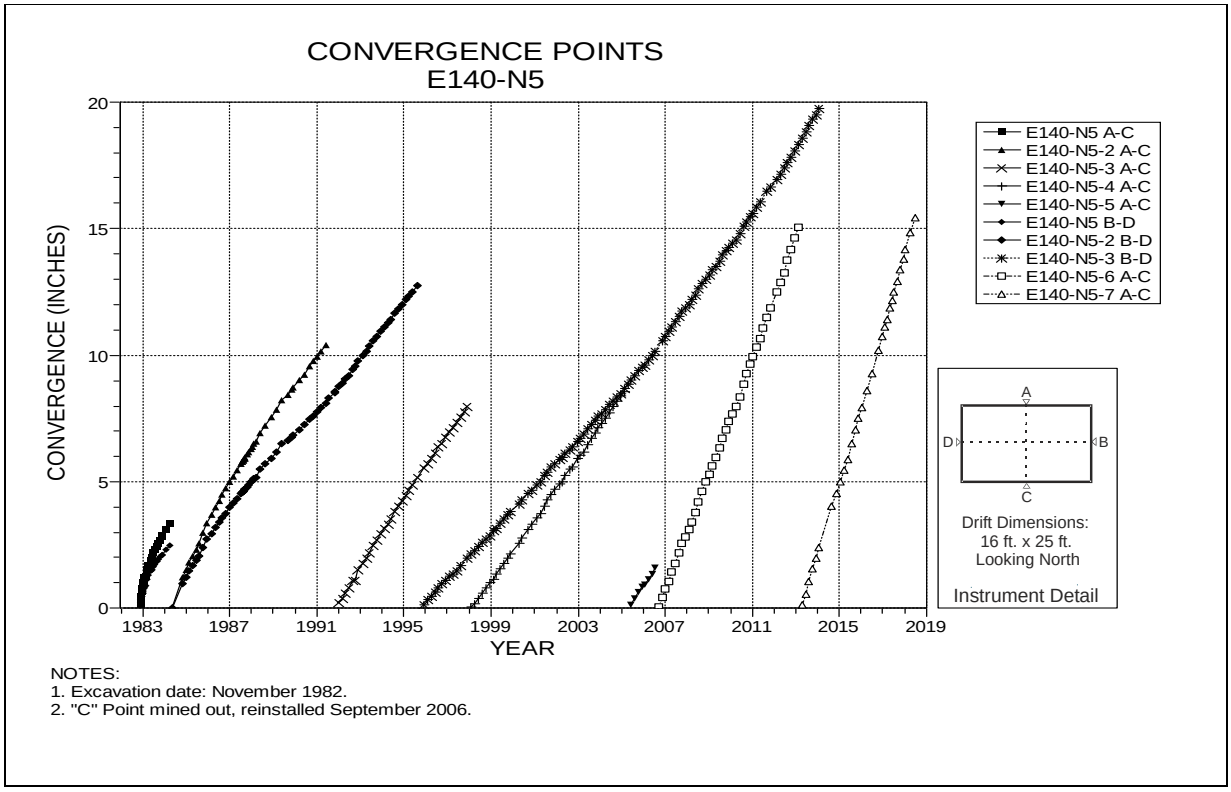

Figure 4-32 Convergence Point Array – E140 N5 – All Chords

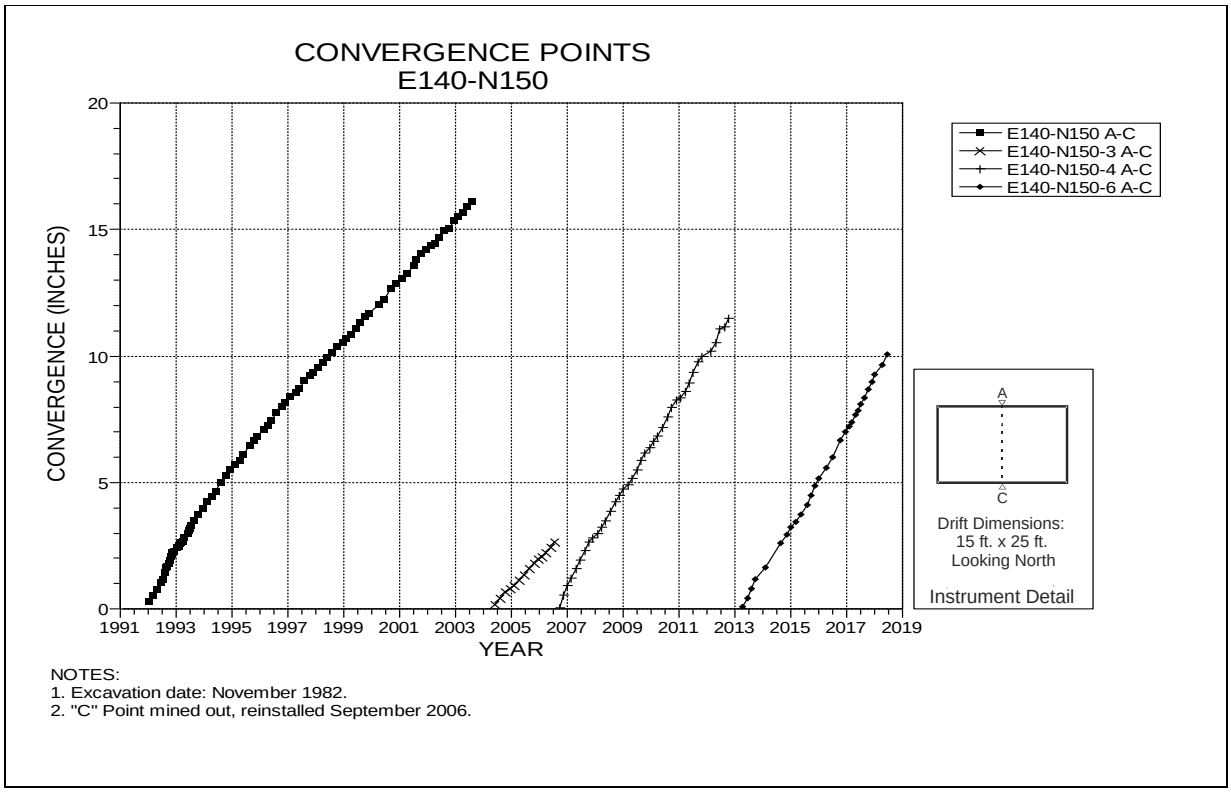

Figure 4-33 Convergence Point Array – E140 N150 – Roof to Floor – Centerline

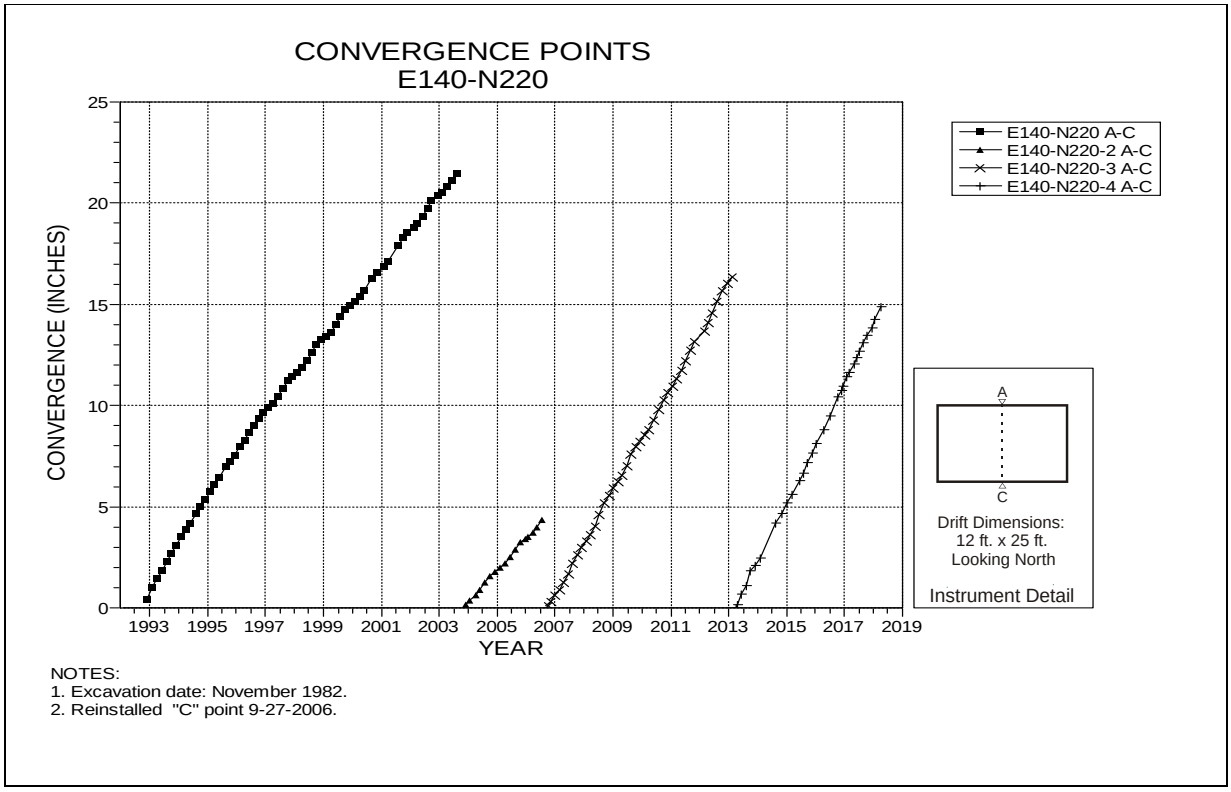

Figure 4-34 Convergence Point Array – E140 N220 – Roof to Floor – Centerline

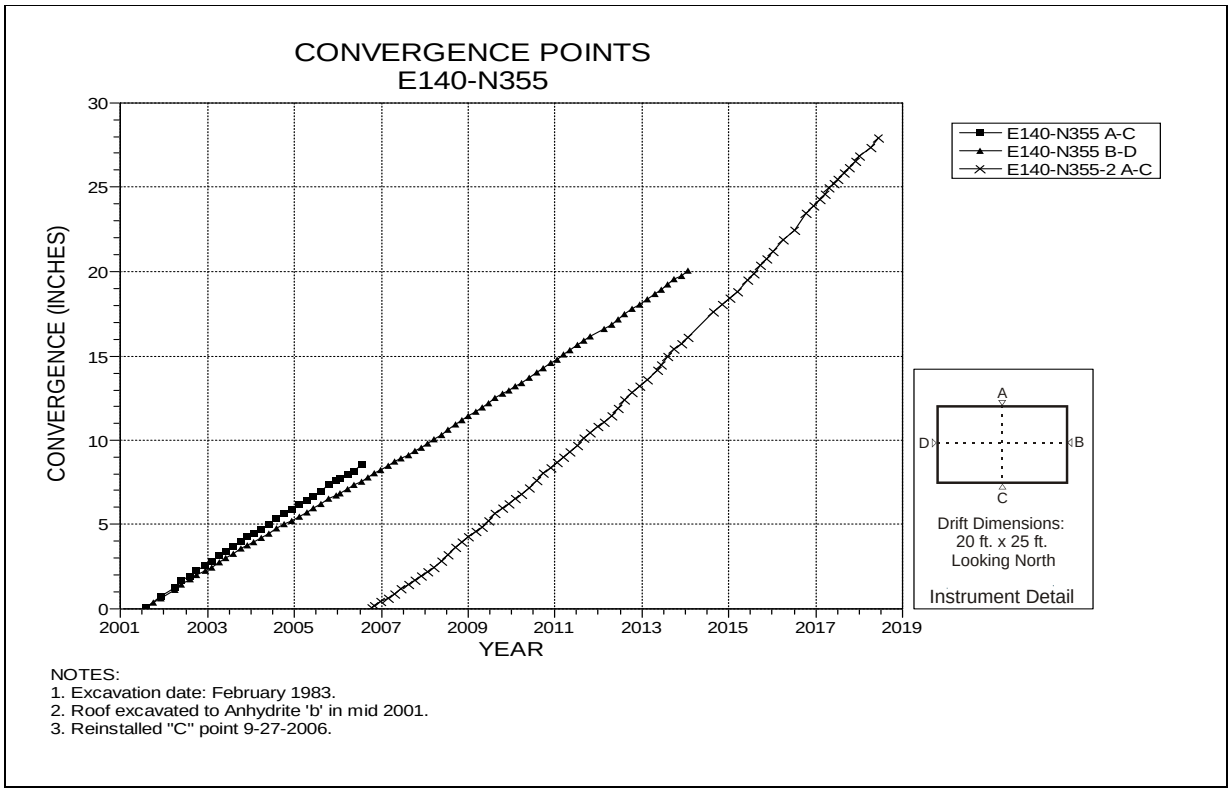

Figure 4-35 Convergence Point Array – E140 N355 – All Chords

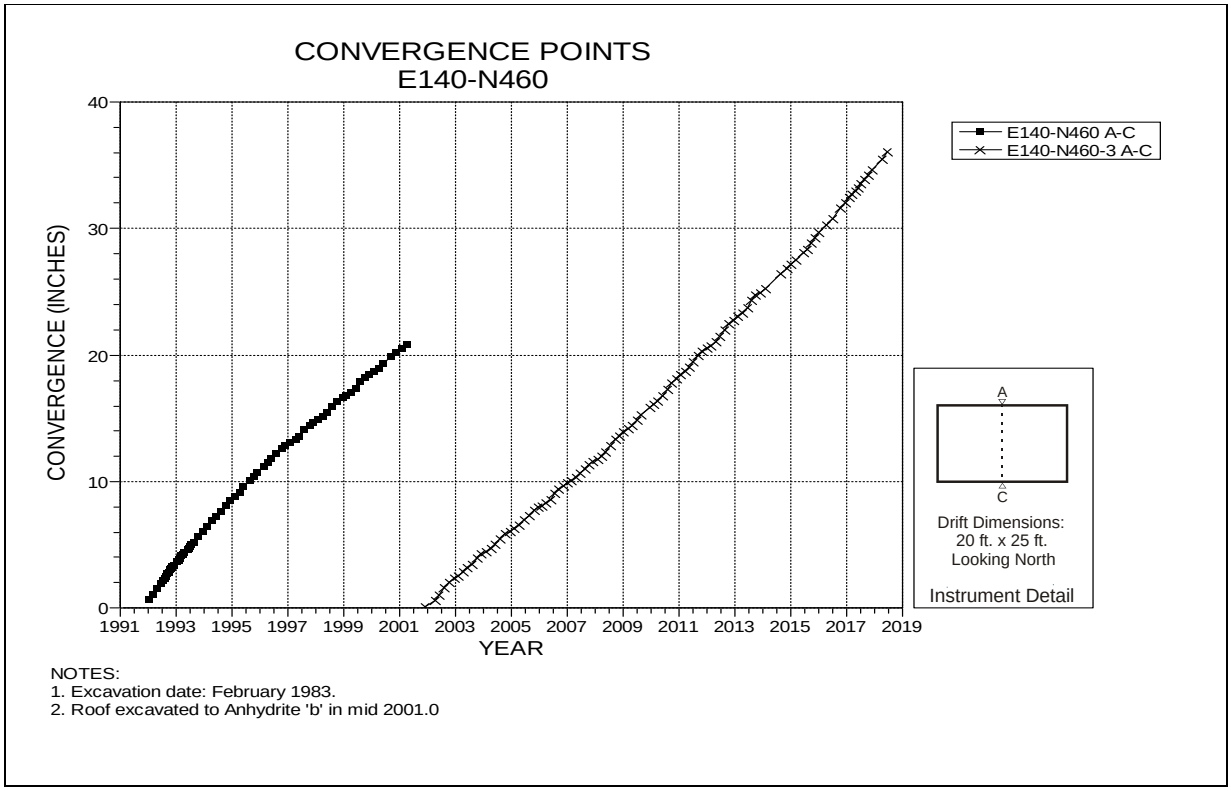

Figure 4-36 Convergence Point Array – E140 N460 – Roof to Floor – Centerline

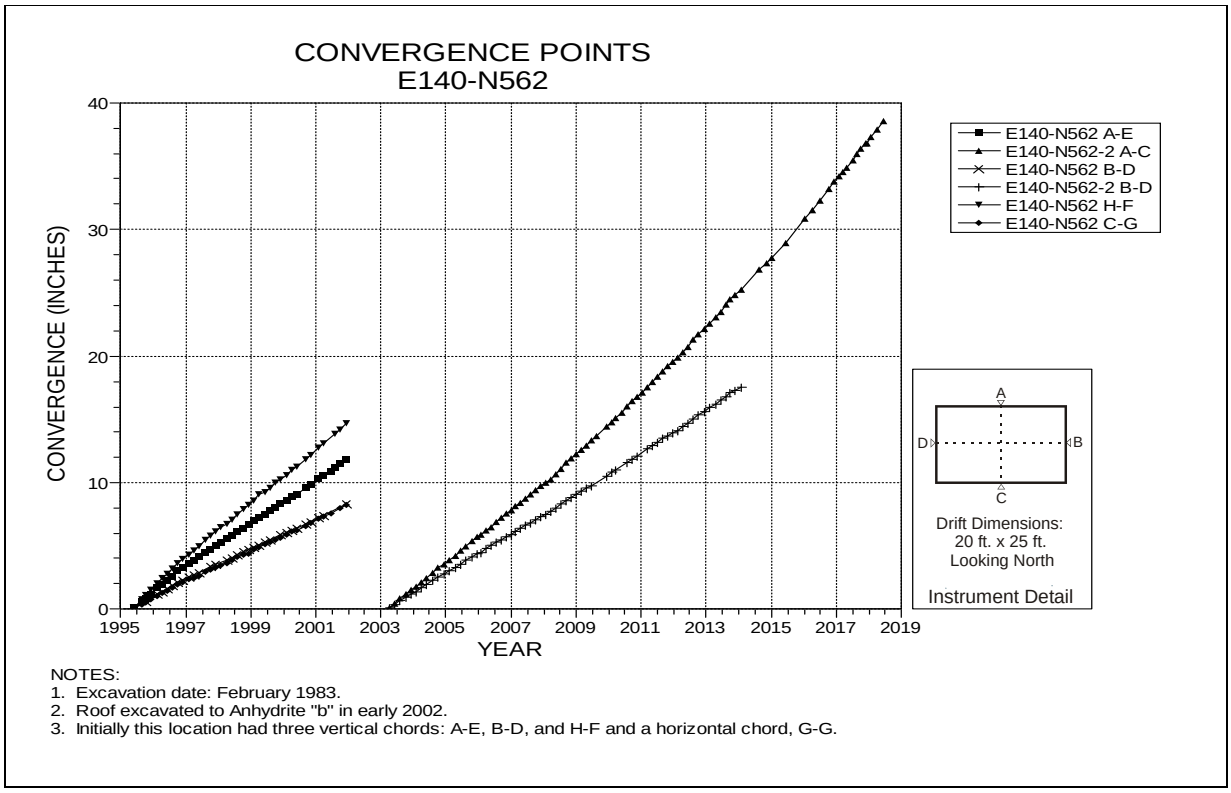

NOTES:
1. Excavation date: February 1983.
2. Roof excavated to Anhydrite "b" in early 2002.
3. Initially this location had three vertical chords: A-E, B-D, and H-F and a horizontal chord, G-G.

Figure 4-37 Convergence Point Array – E140 N562 – All Chords

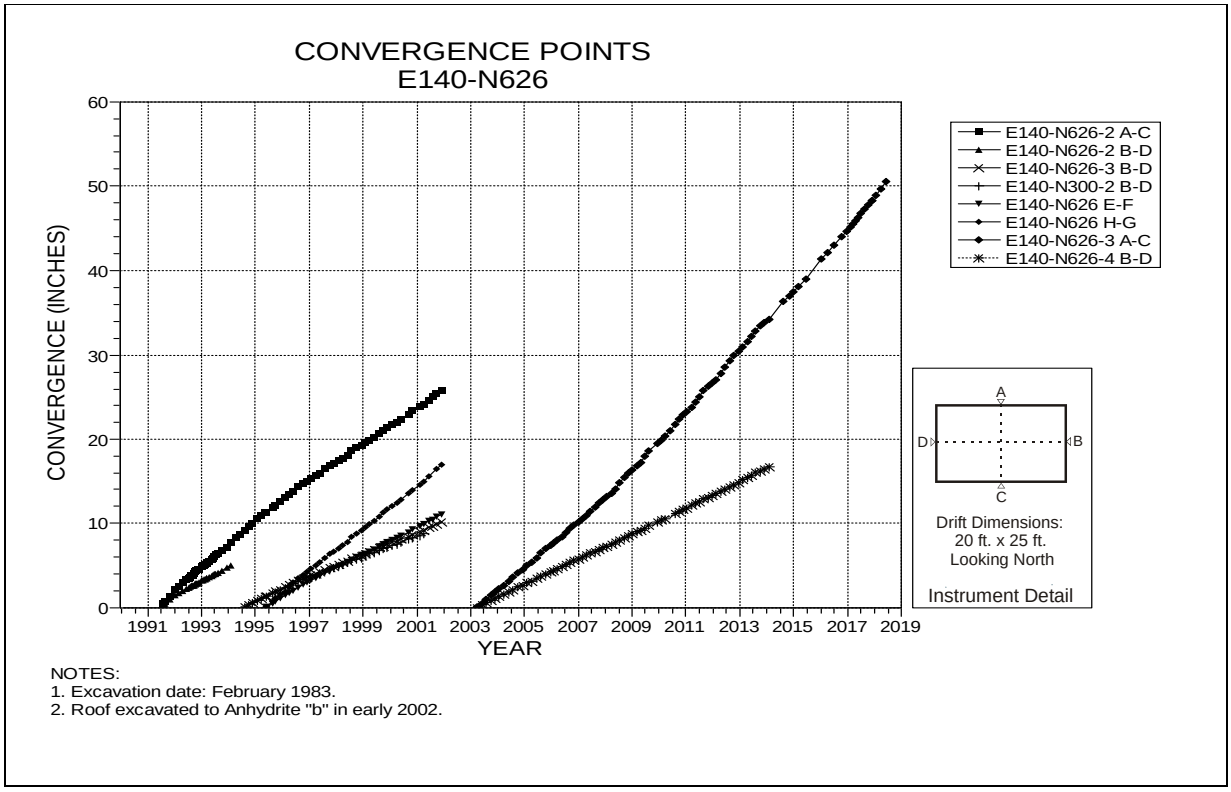

NOTES:
1. Excavation date: February 1983.
2. Roof excavated to Anhydrite "b" in early 2002.

Figure 4-38 Convergence Point Array – E140 N626 – All Chords

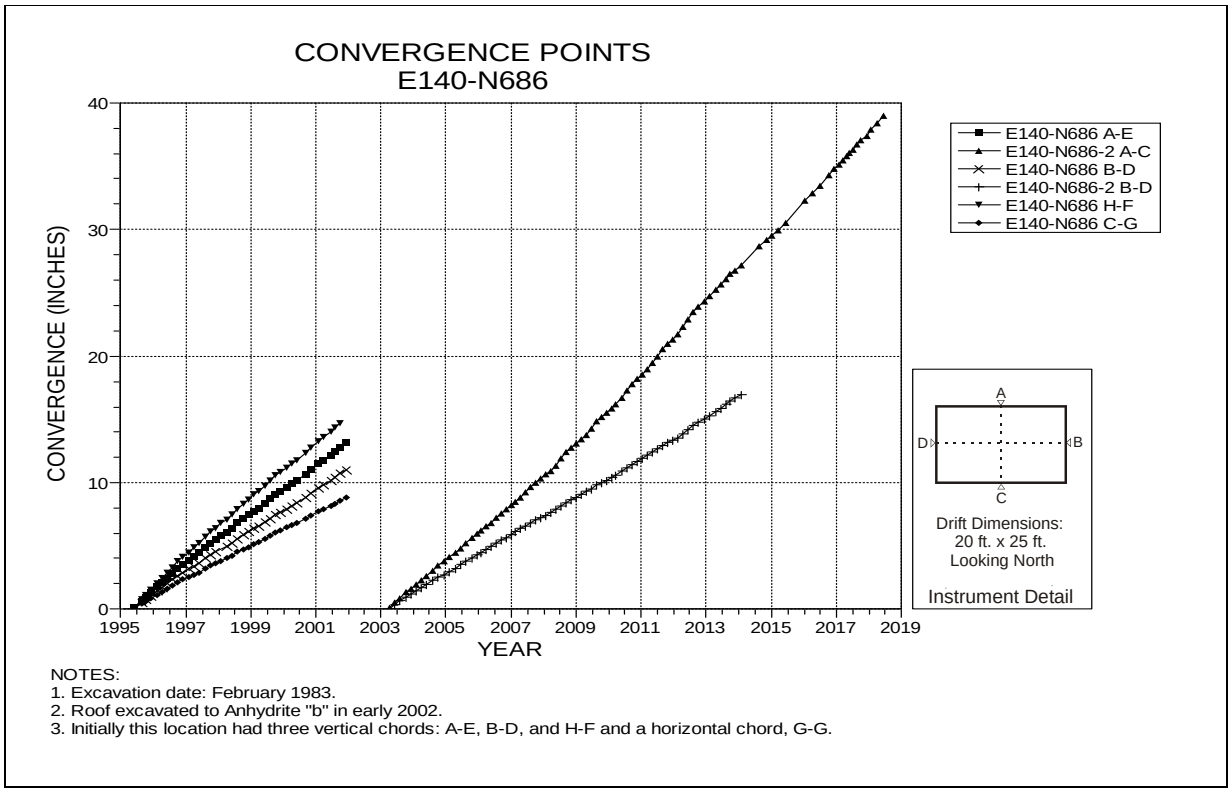

Figure 4-39 Convergence Point Array – E140 N686 – All Chords

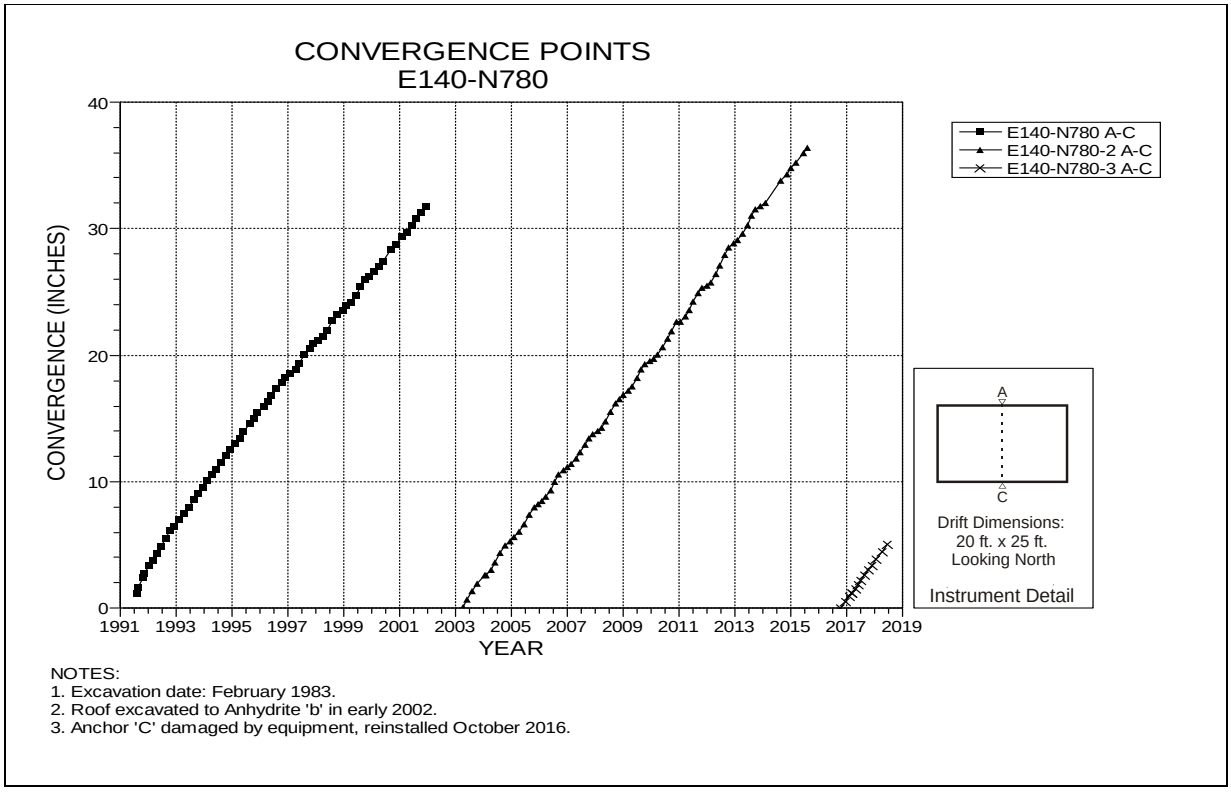

Figure 4-40 Convergence Point Array – E140 N780 – Roof to Floor – Centerline

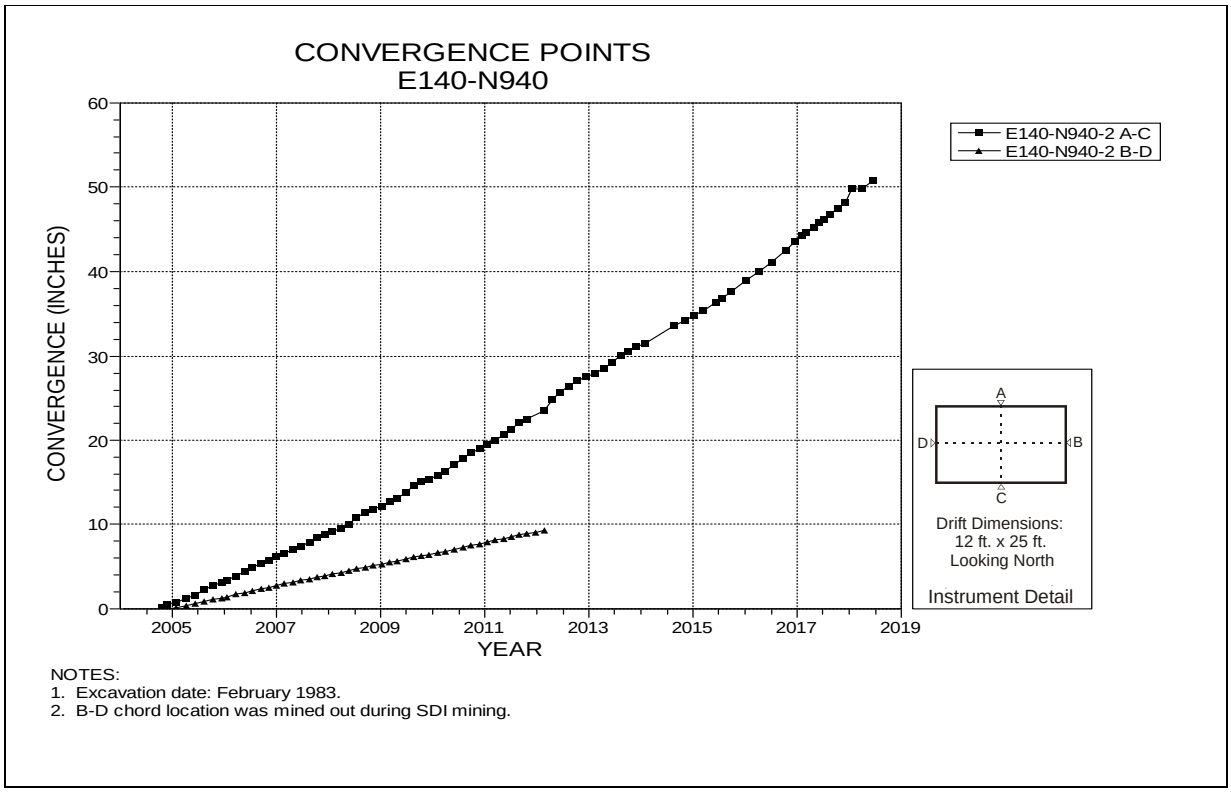

Figure 4-41 Convergence Point Array – E140 N940 – All Chords

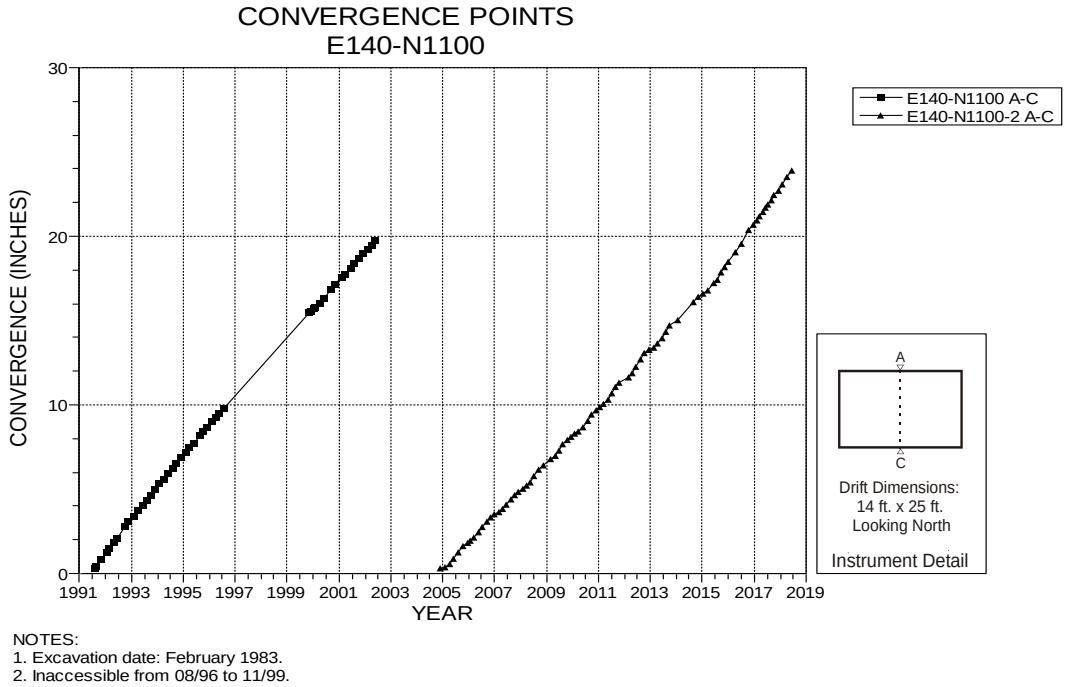

Figure 4-42 Convergence Point Array – E140 N1100 – Roof to Floor – Centerline

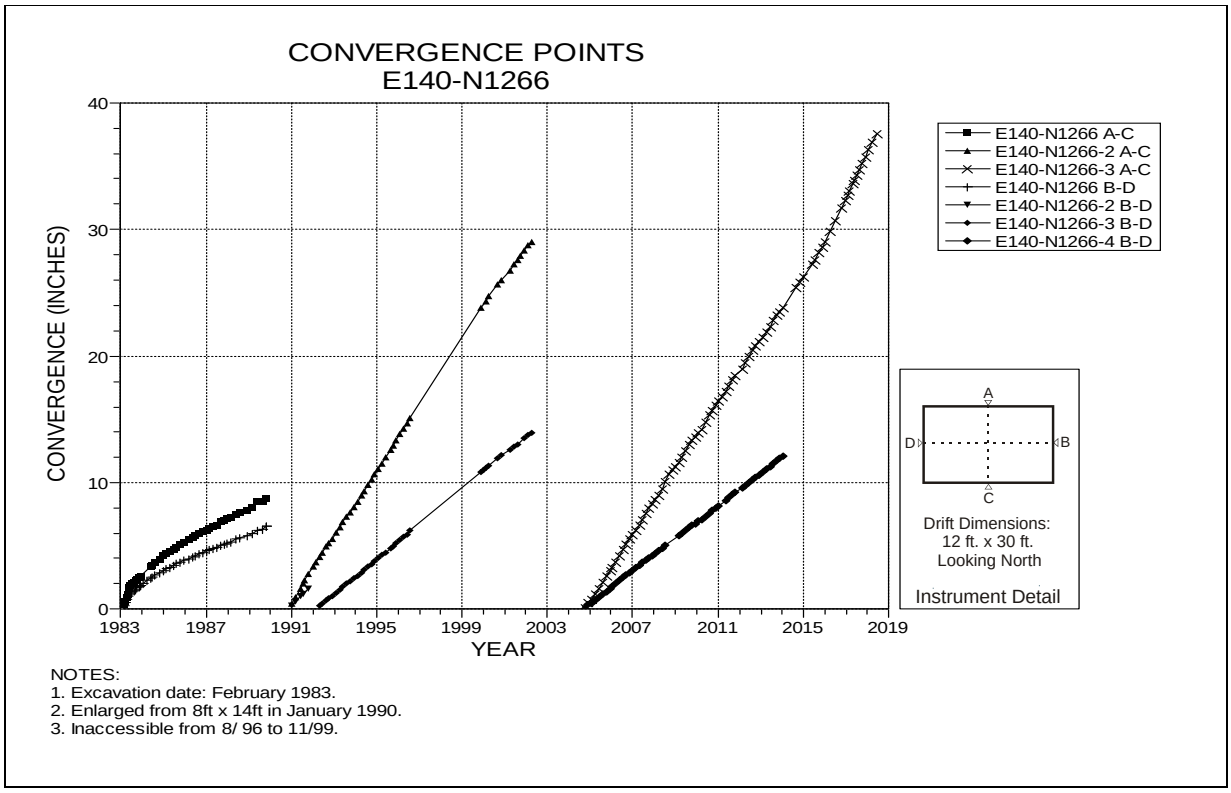

Figure 4-43 Convergence Point Array – E140 N1266 – Roof to Floor – Centerline

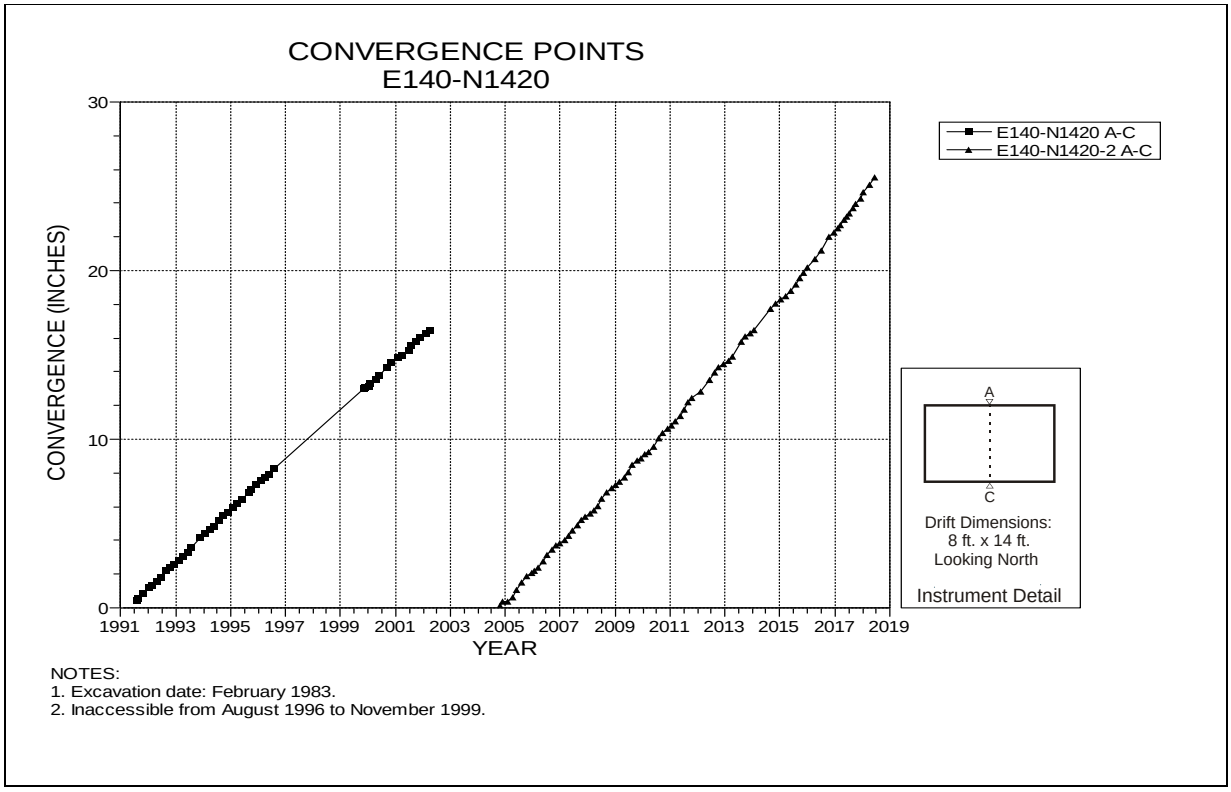

Figure 4-44 Convergence Point Array – E140 N1420 – Roof to Floor – Centerline

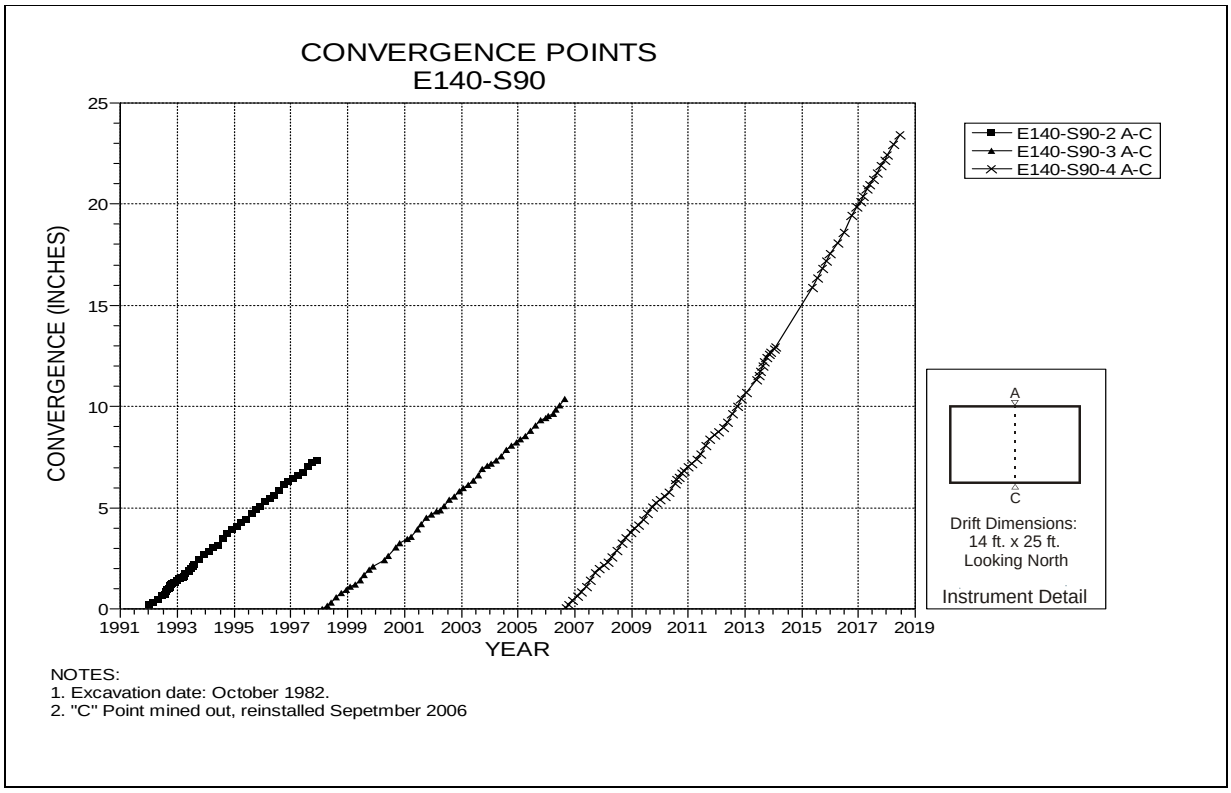

Figure 4-45 Convergence Point Array – E140 S90 – Roof to Floor – Centerline

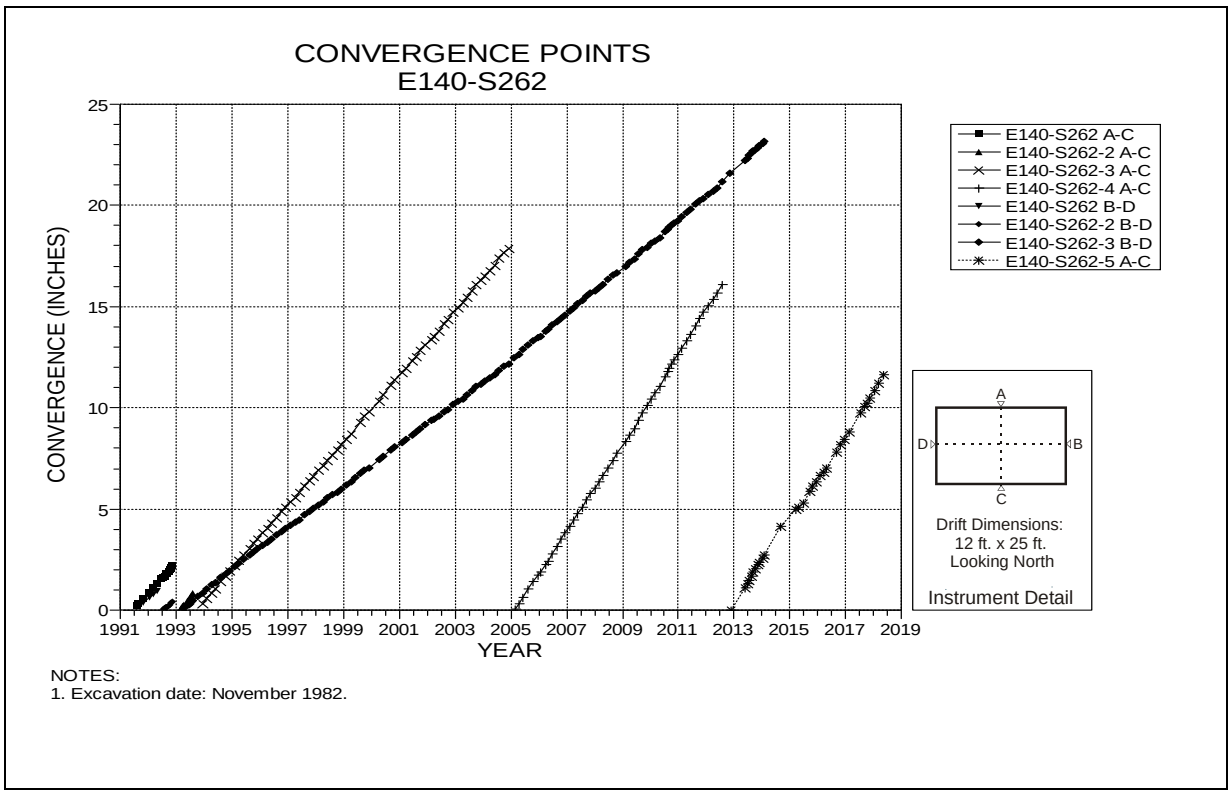

Figure 4-46 Convergence Point Array – E140 S262 – All Chords

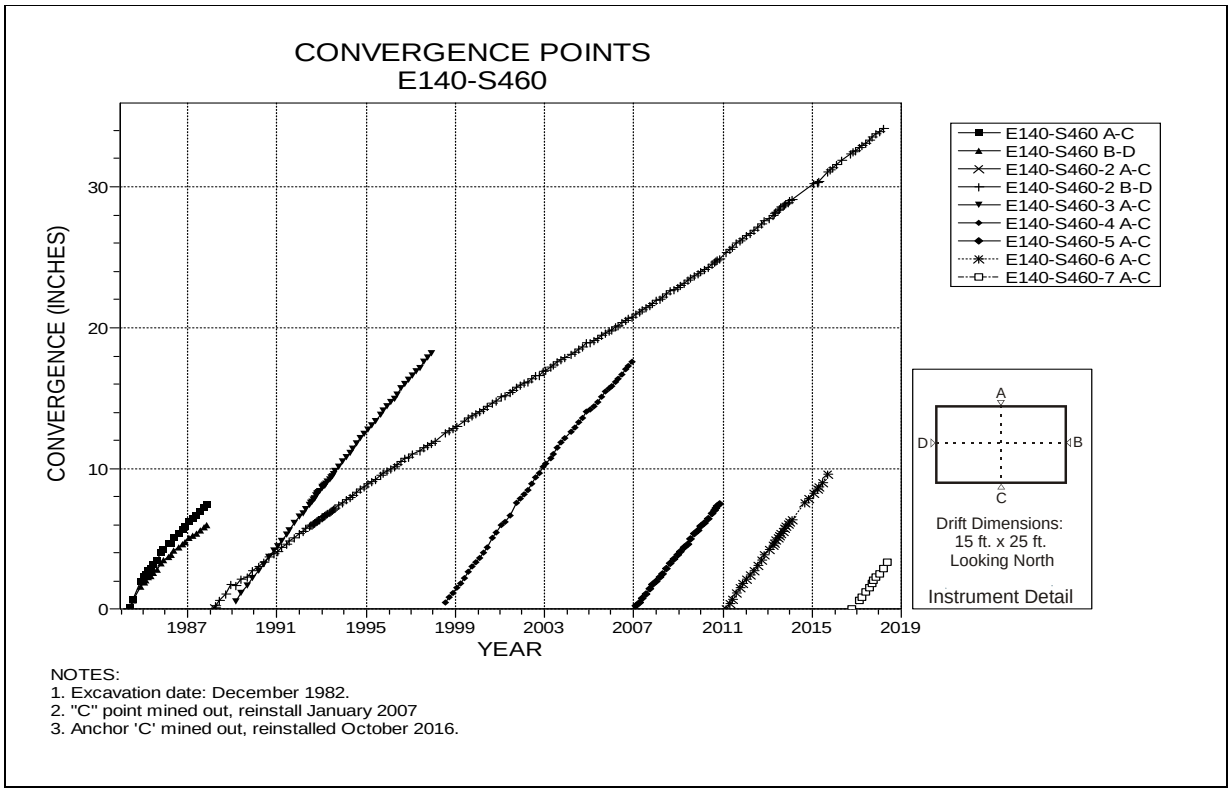

Figure 4-47 Convergence Point Array – E140 S460 – All Chords

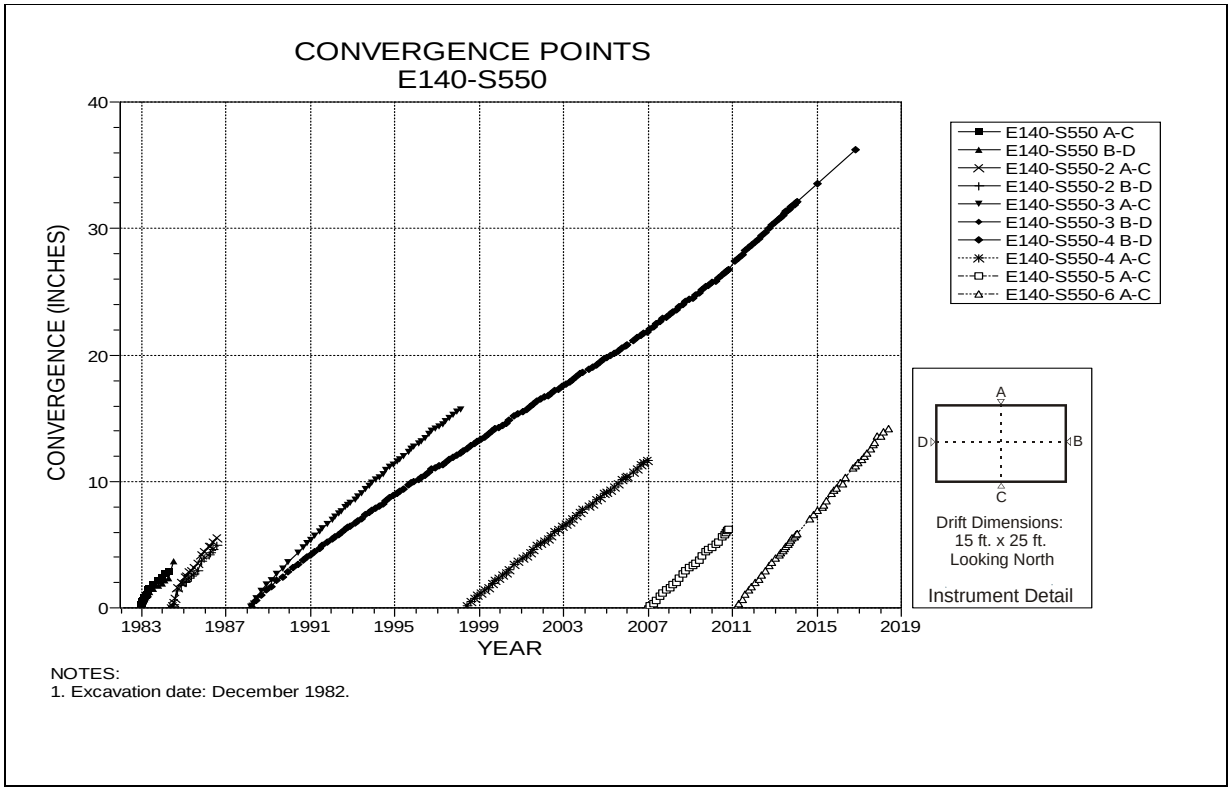

Figure 4-48 Convergence Point Array – E140 S550 – All Chords

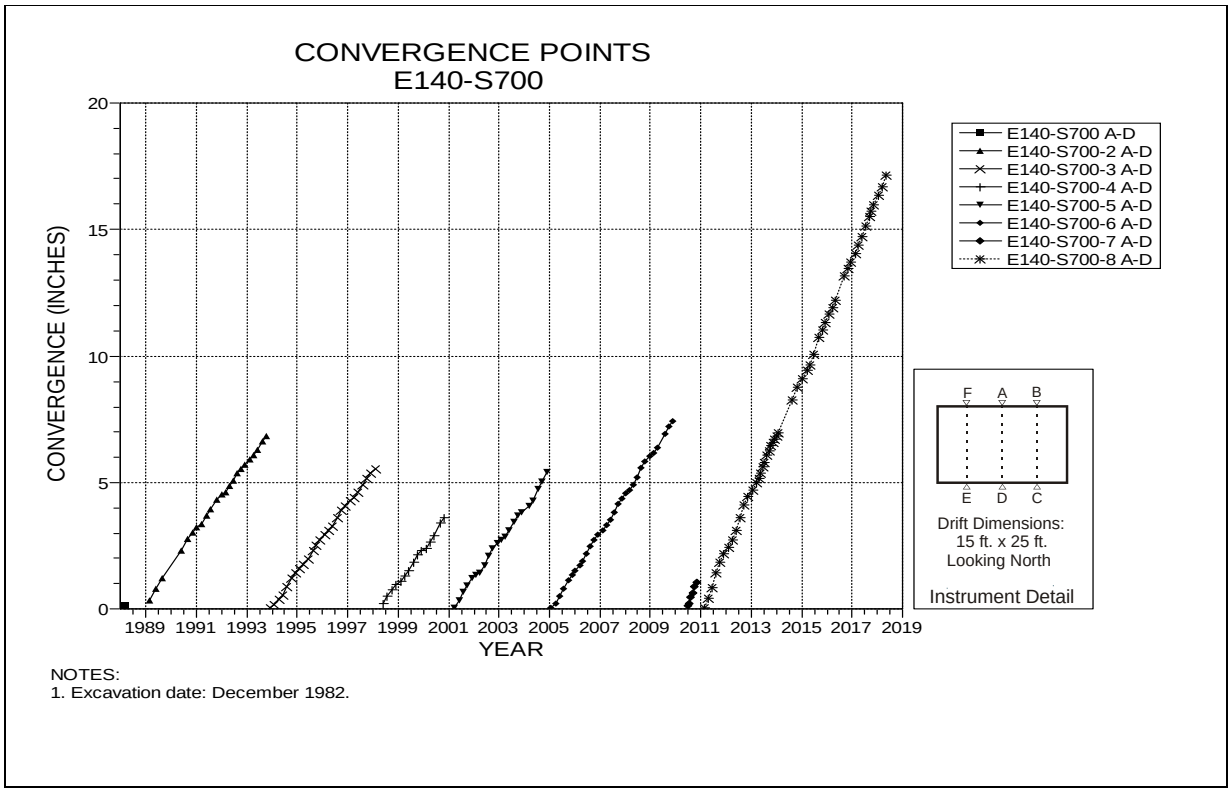

Figure 4-49 Convergence Point Array – E140 S700 – Roof to Floor – Centerline

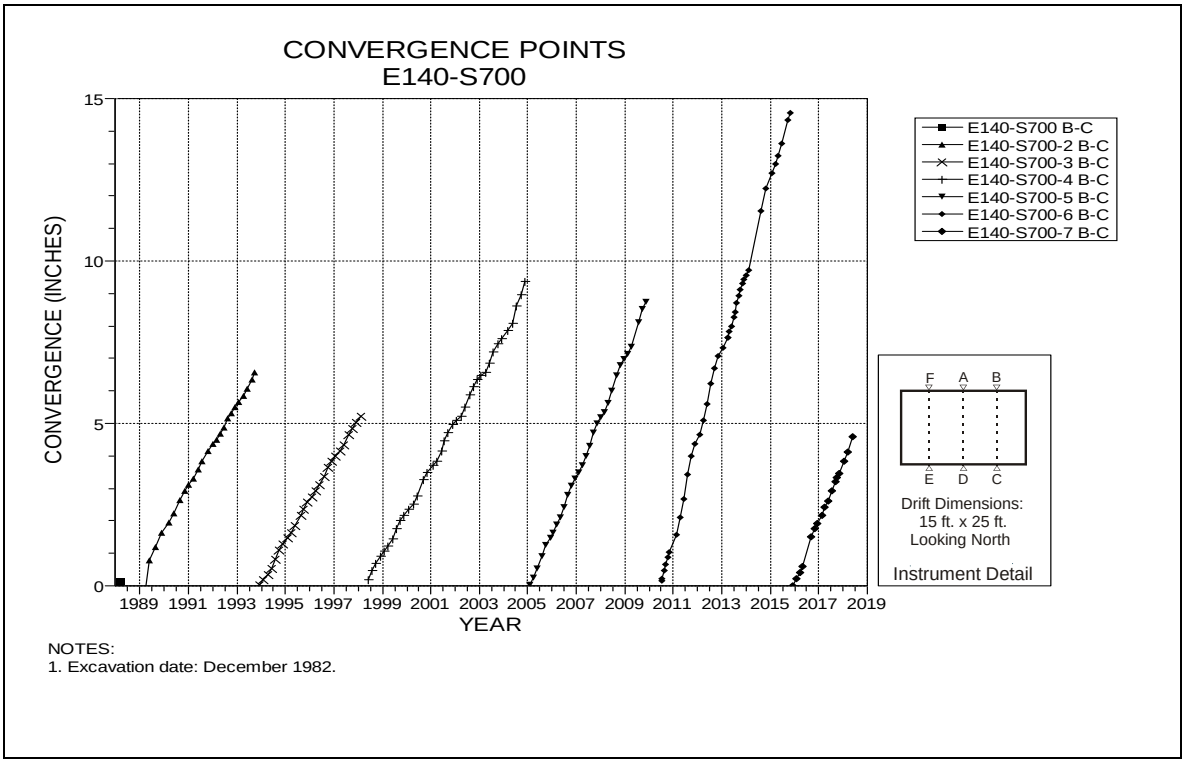

Figure 4-50 Convergence Point Array – E140 S700 –
Roof to Floor – East Quarter Point

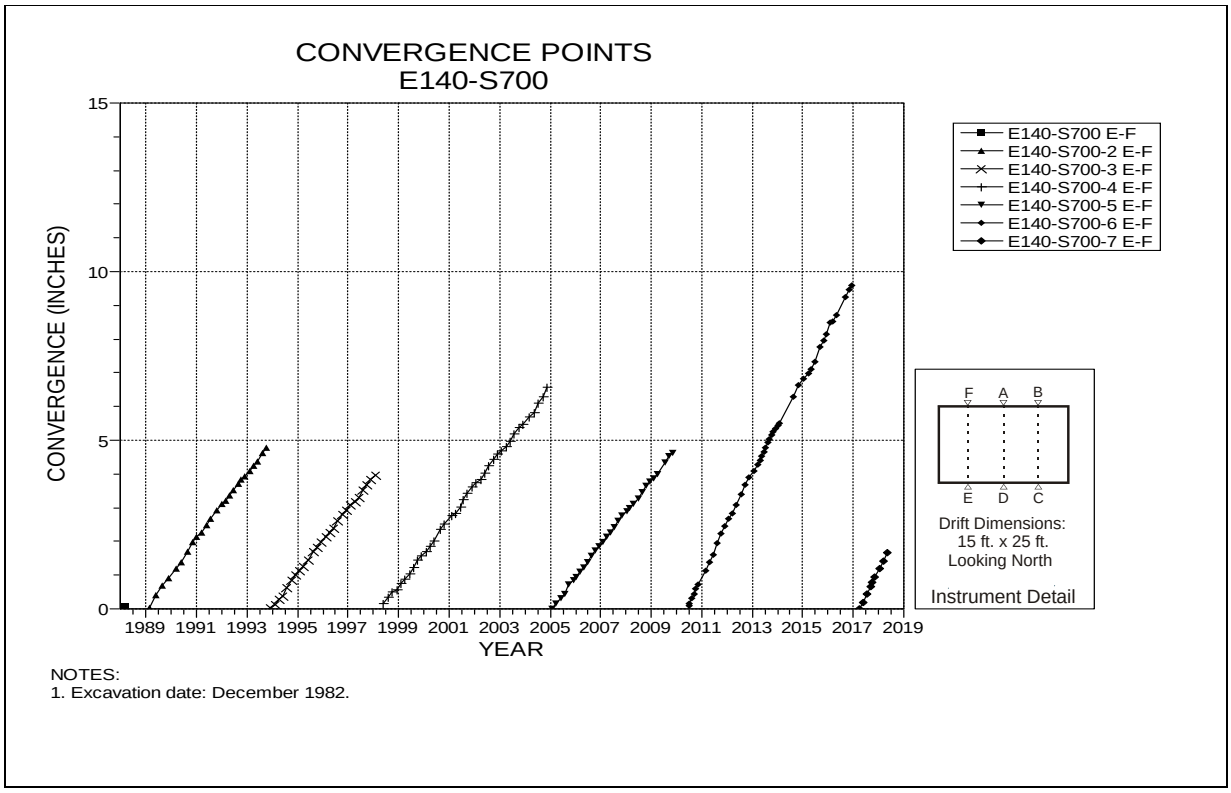

Figure 4-51 Convergence Point Array – E140 S700 – Roof to Floor – West Quarter Point

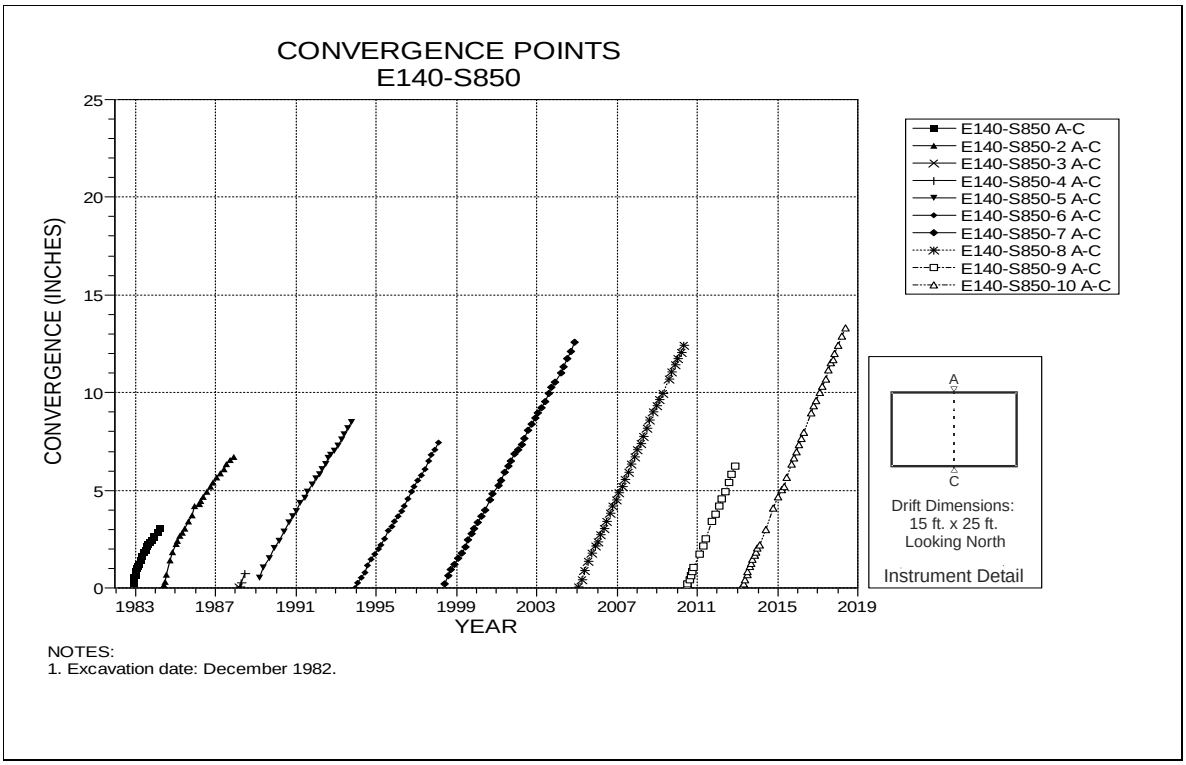

Figure 4-52 Convergence Point Array – E140 S850 – Roof to Floor – Centerline

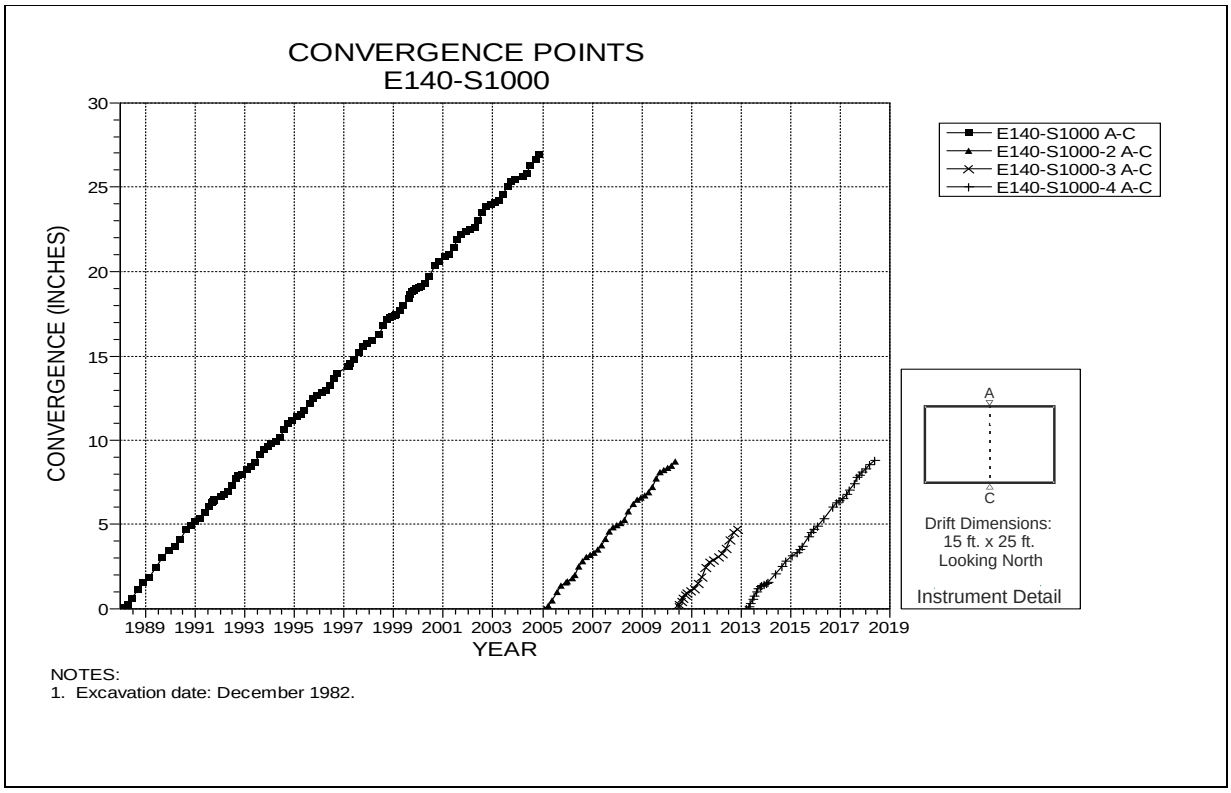

Figure 4-53 Convergence Point Array – E140 S1000 – Roof to Floor – Centerline

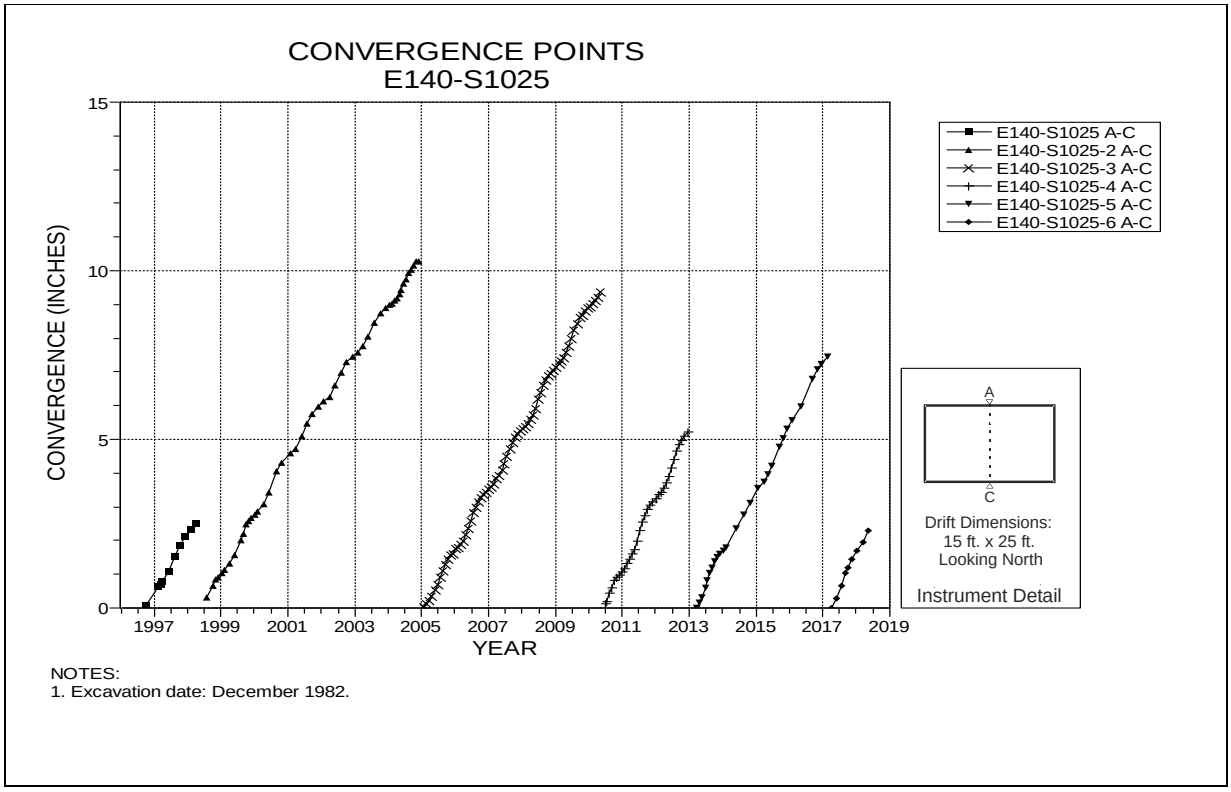

Figure 4-54 Convergence Point Array – E140 S1025 – Roof to Floor – Centerline

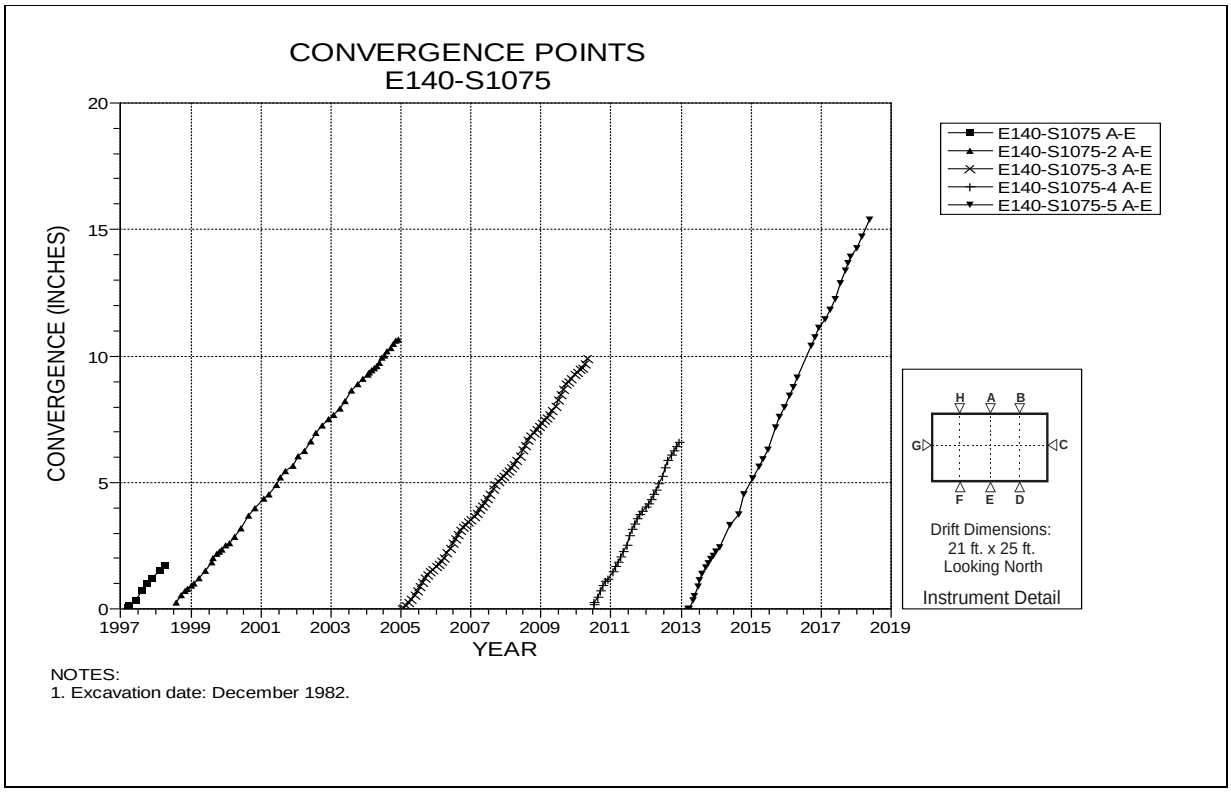

Figure 4-55 Convergence Point Array – E140 S1075 – Roof to Floor – Centerline

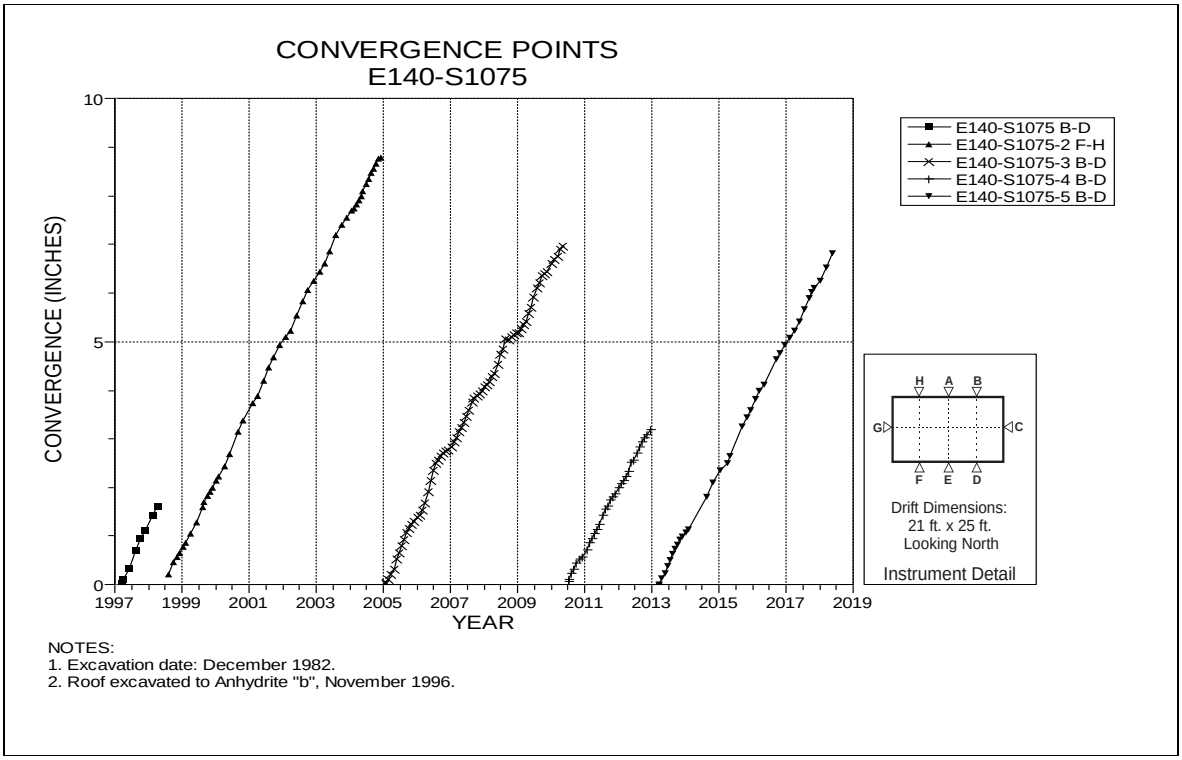

Figure 4-56 Convergence Point Array –
E140 S1075 – Roof to Floor – East Quarter Point

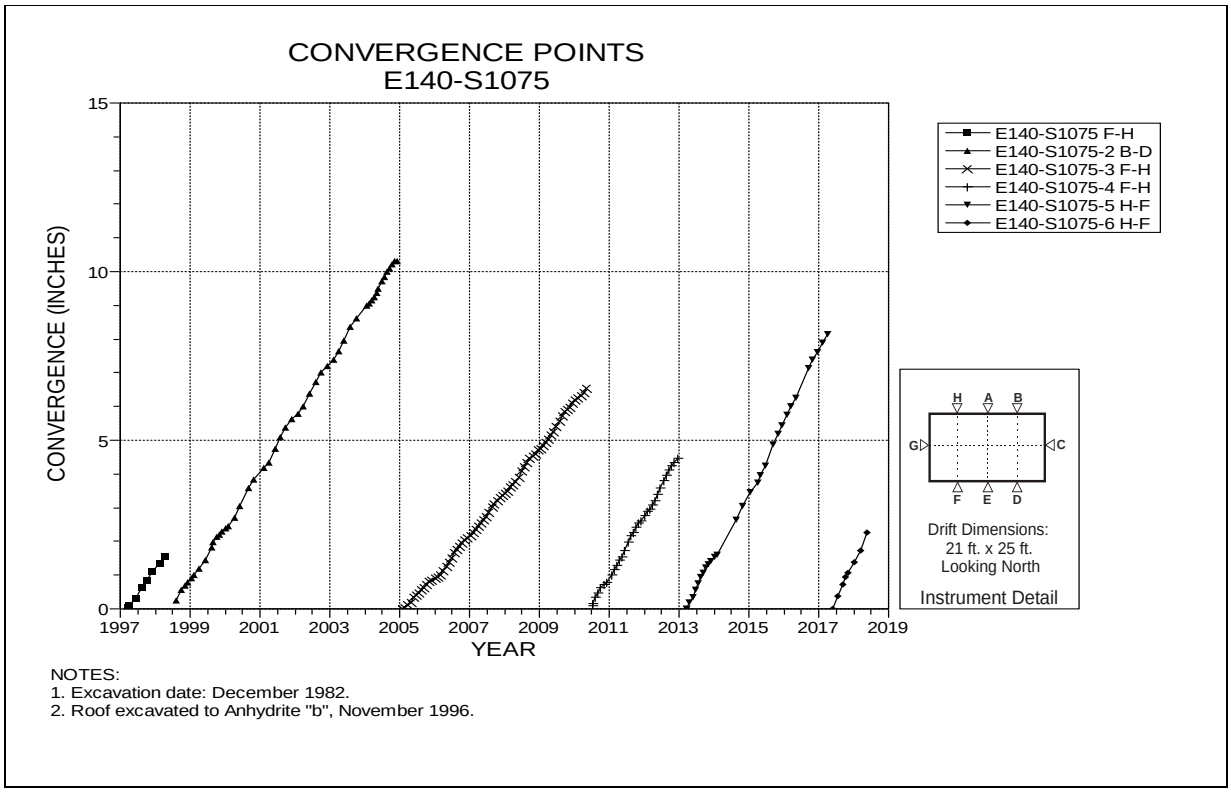

Figure 4-57 Convergence Point Array – E140 S1075 – Roof to Floor – West Quarter Point

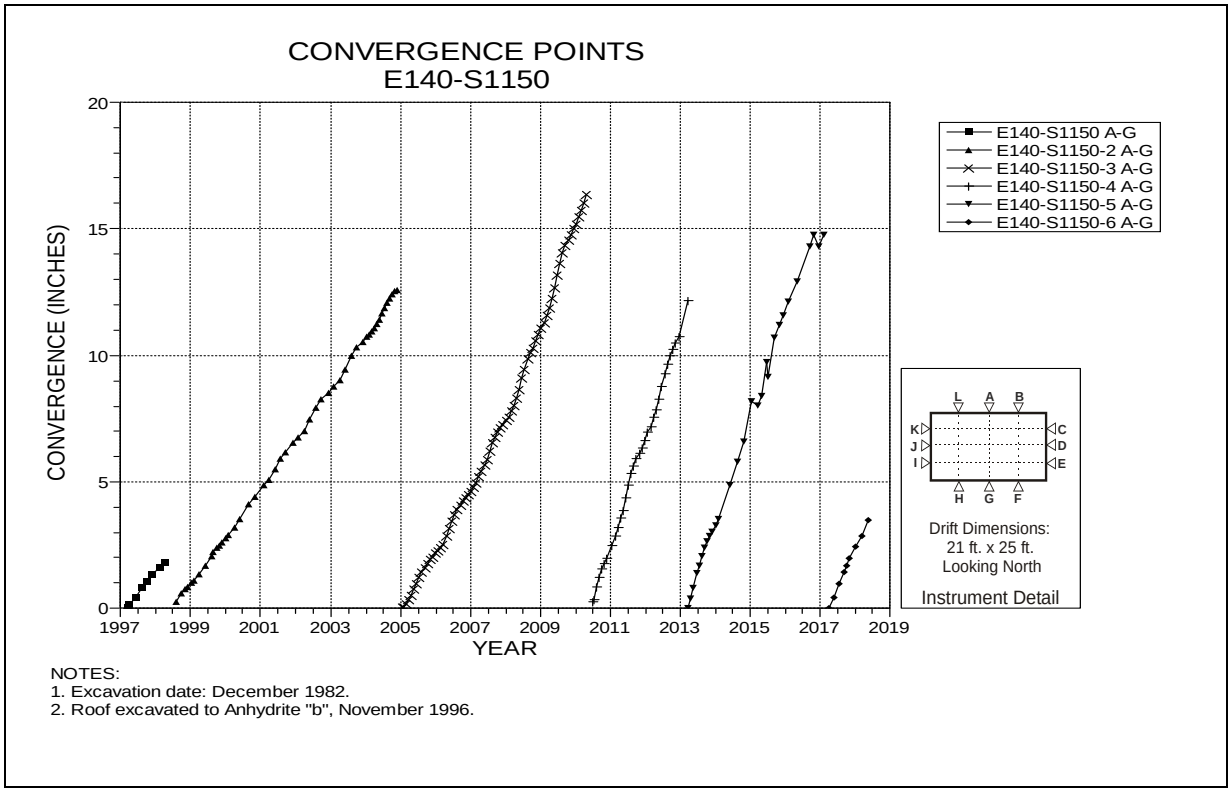

Figure 4-58 Convergence Point Array – E140 S1150 – Roof to Floor – Centerline

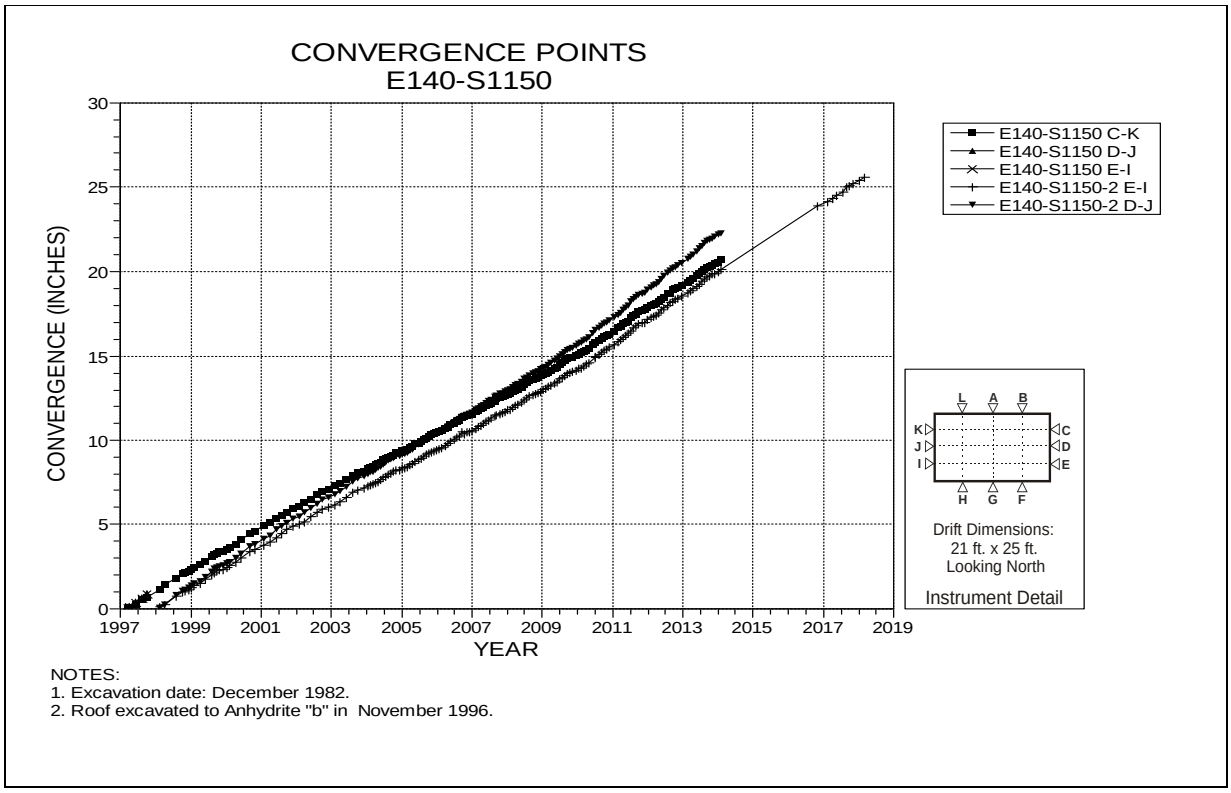

Figure 4-59 Convergence Point Array –
E140 S1150 – Roof to Floor – East Quarter Point

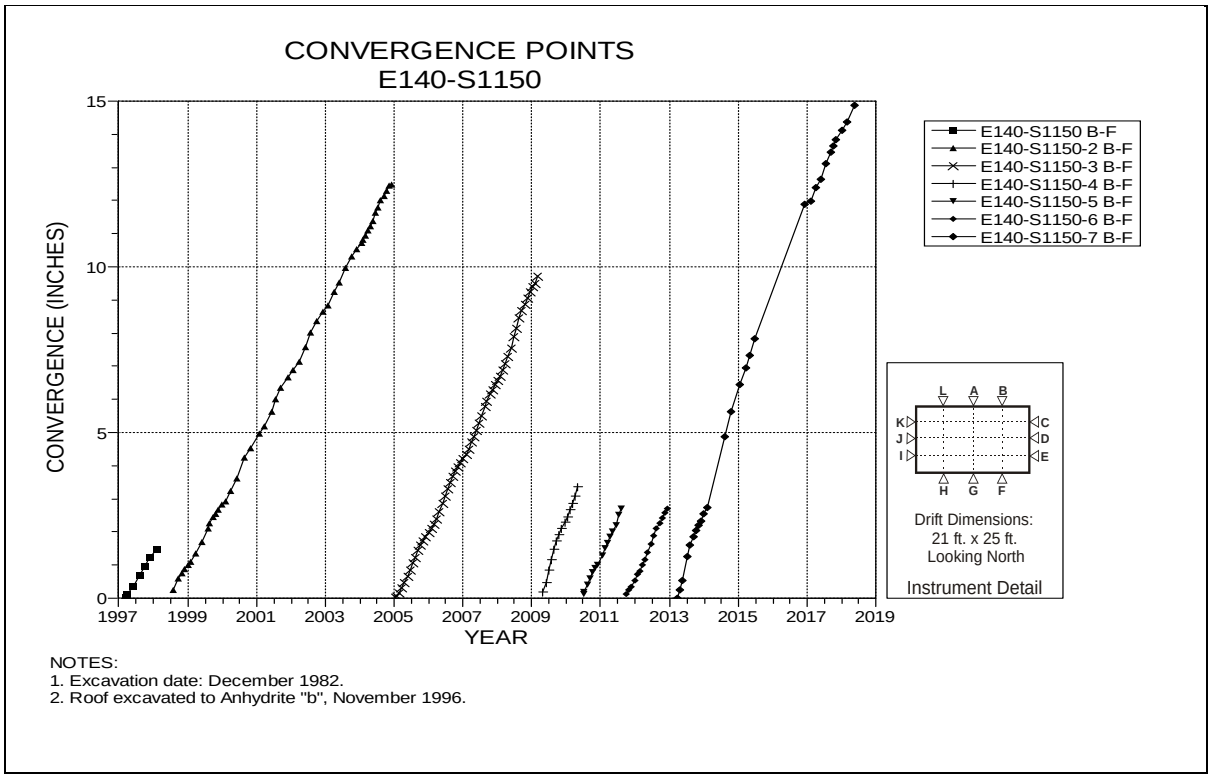

Figure 4-60 Convergence Point Array – E140 S1150 – Rib to Rib

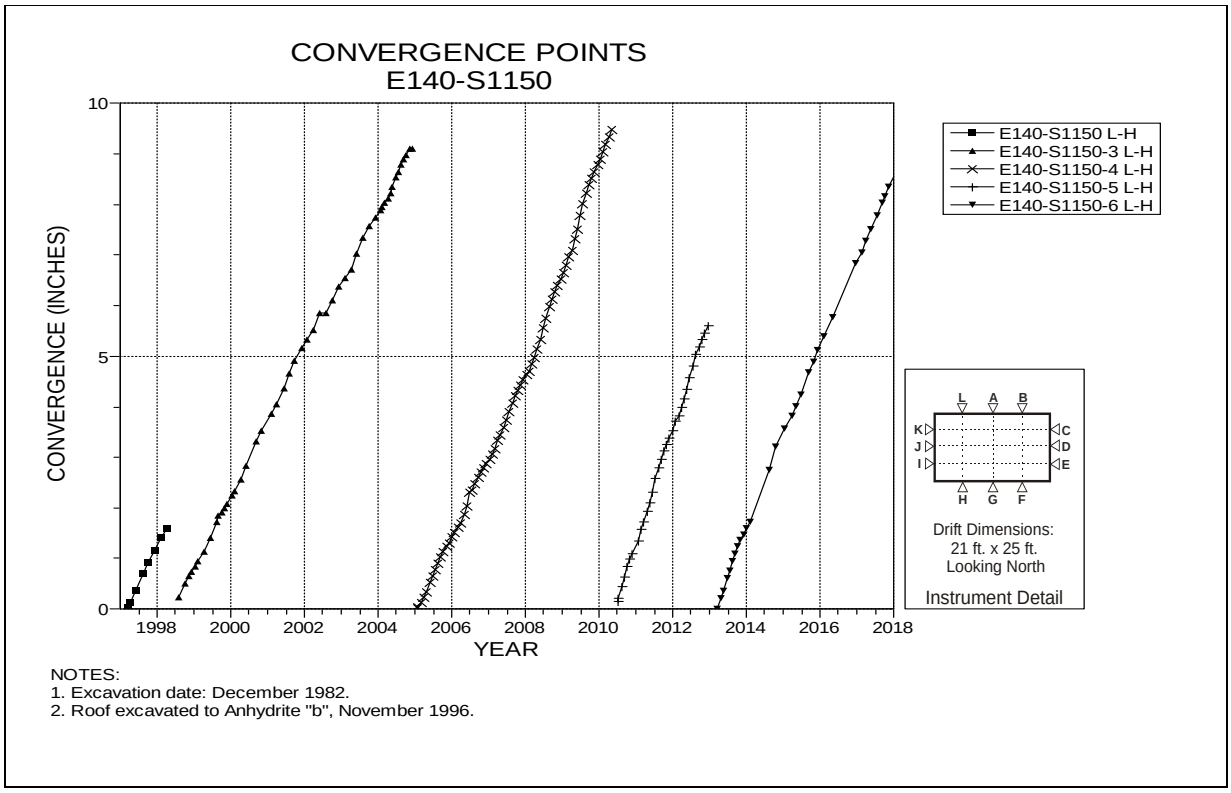

Figure 4-61 Convergence Point Array –
E140 S1150 – Roof to Floor – West Quarter Point

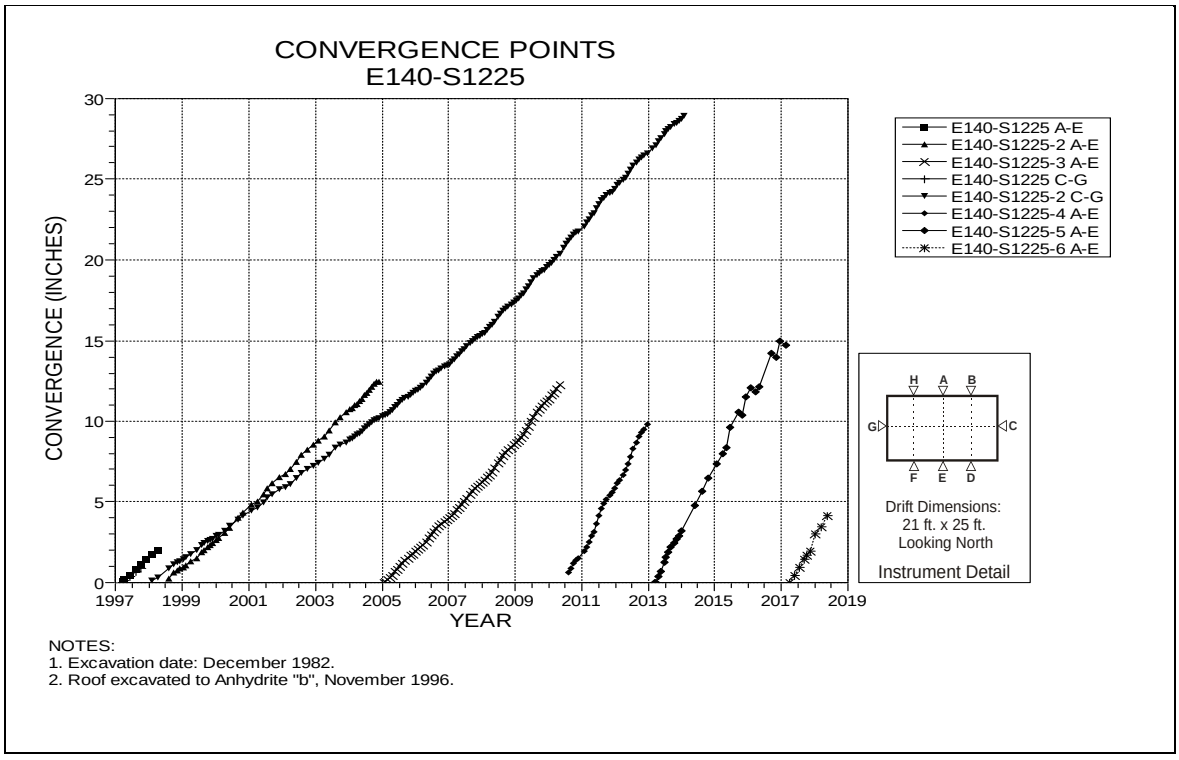

Figure 4-62 Convergence Point Array – E140 S1225 – Roof to Floor – Centerline

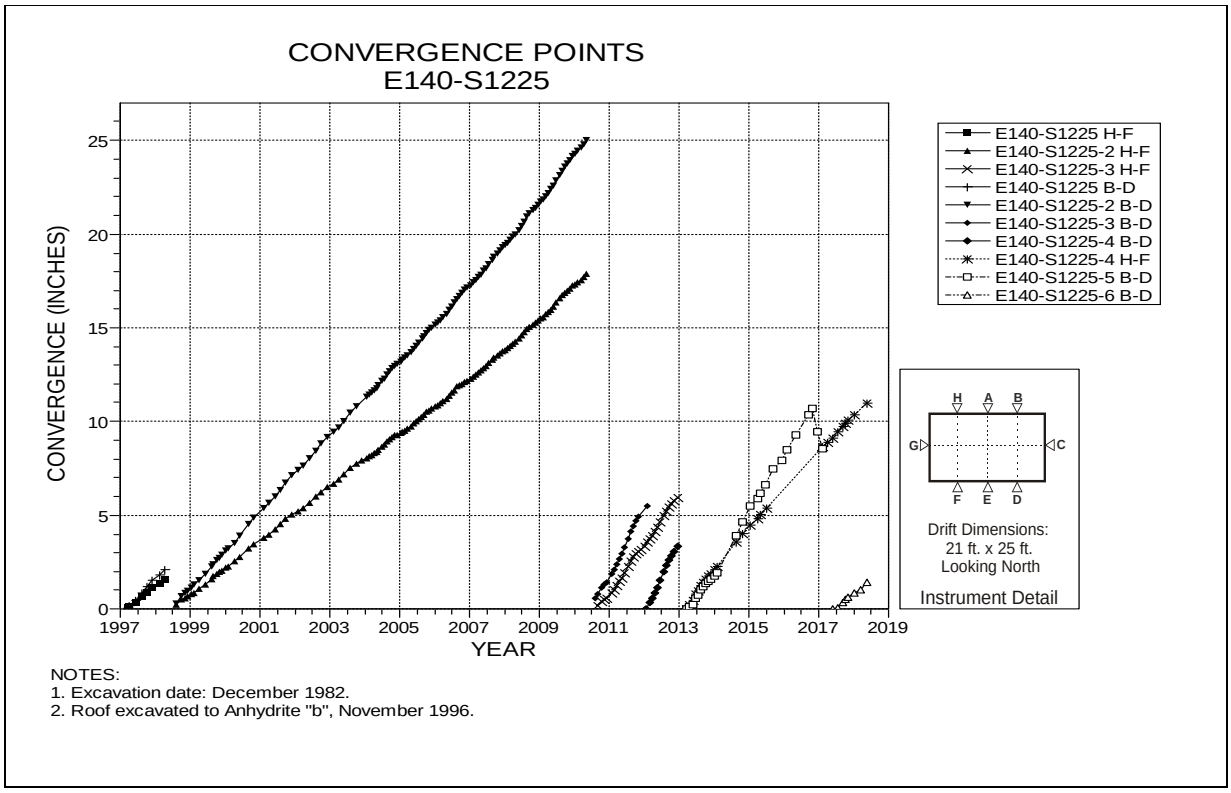

Figure 4-63 Convergence Point Array –
E140 S1225 – Roof to Floor – Quarter Points

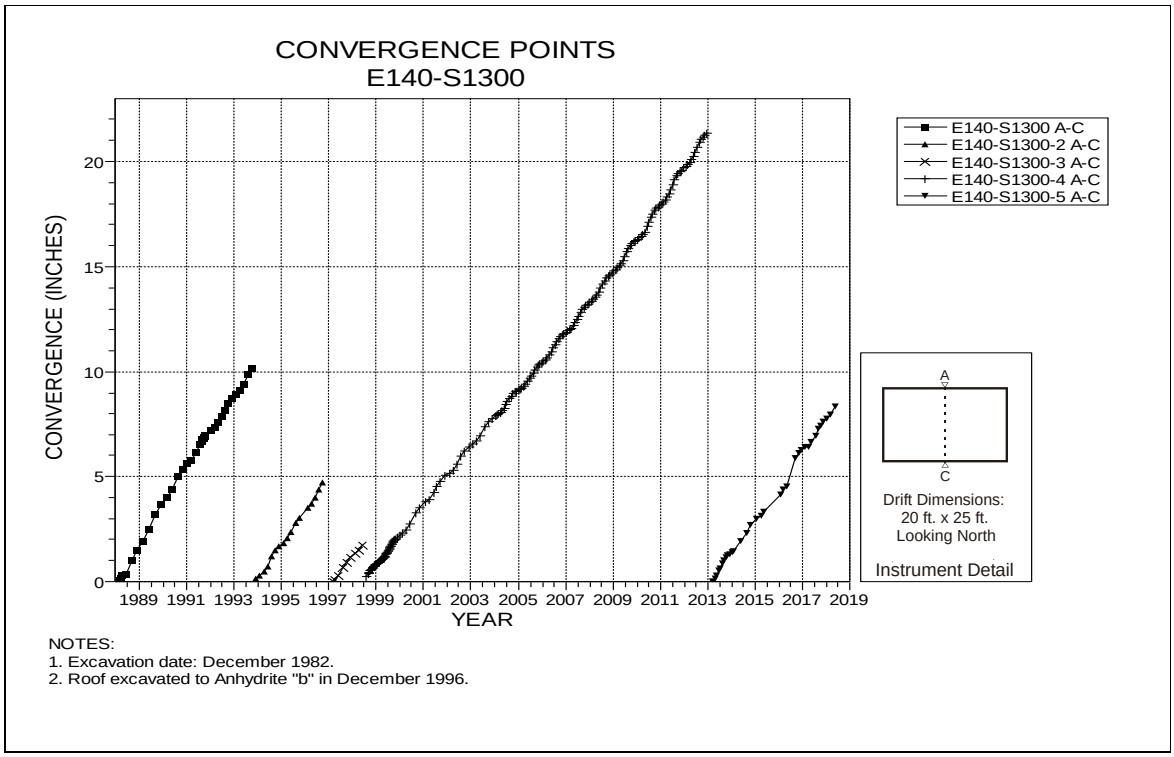

Figure 4-64 Convergence Point Array – E140 S1300 – Roof to Floor – Centerline

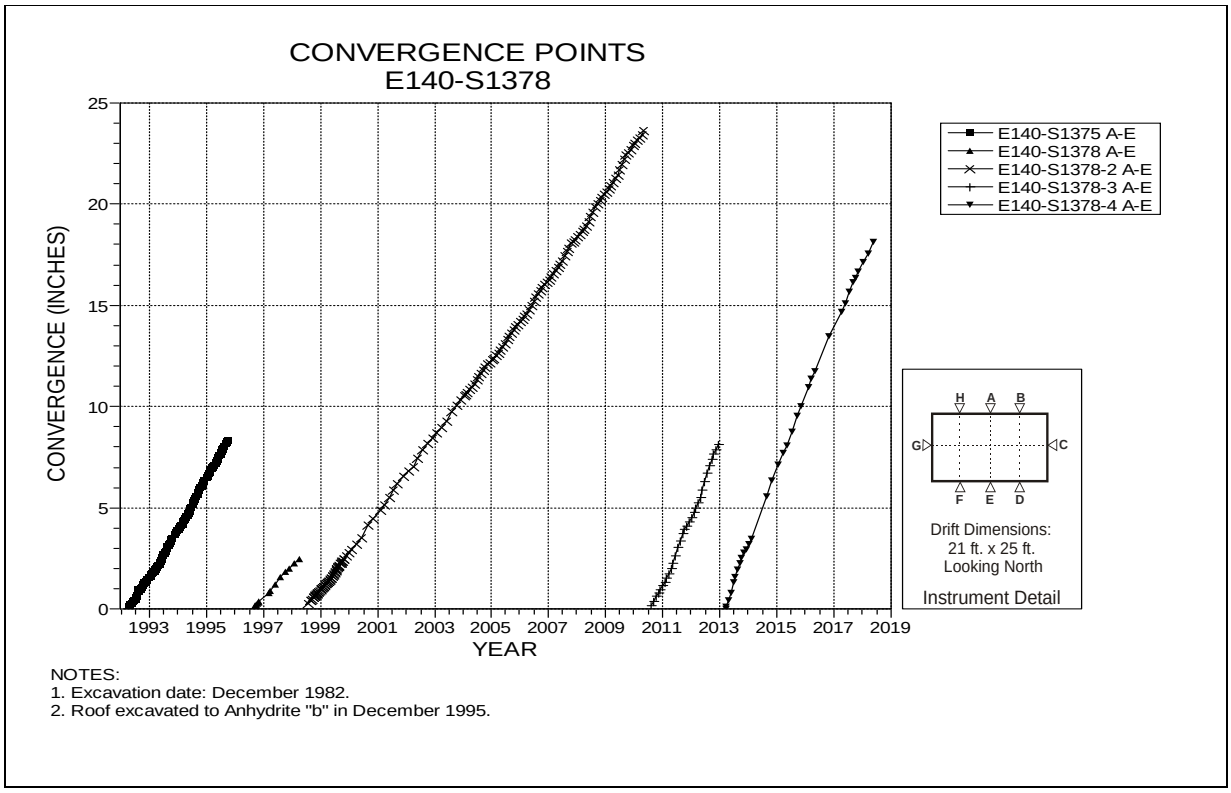

Figure 4-65 Convergence Point Array – E140 S1378 – Roof to Floor – Centerline

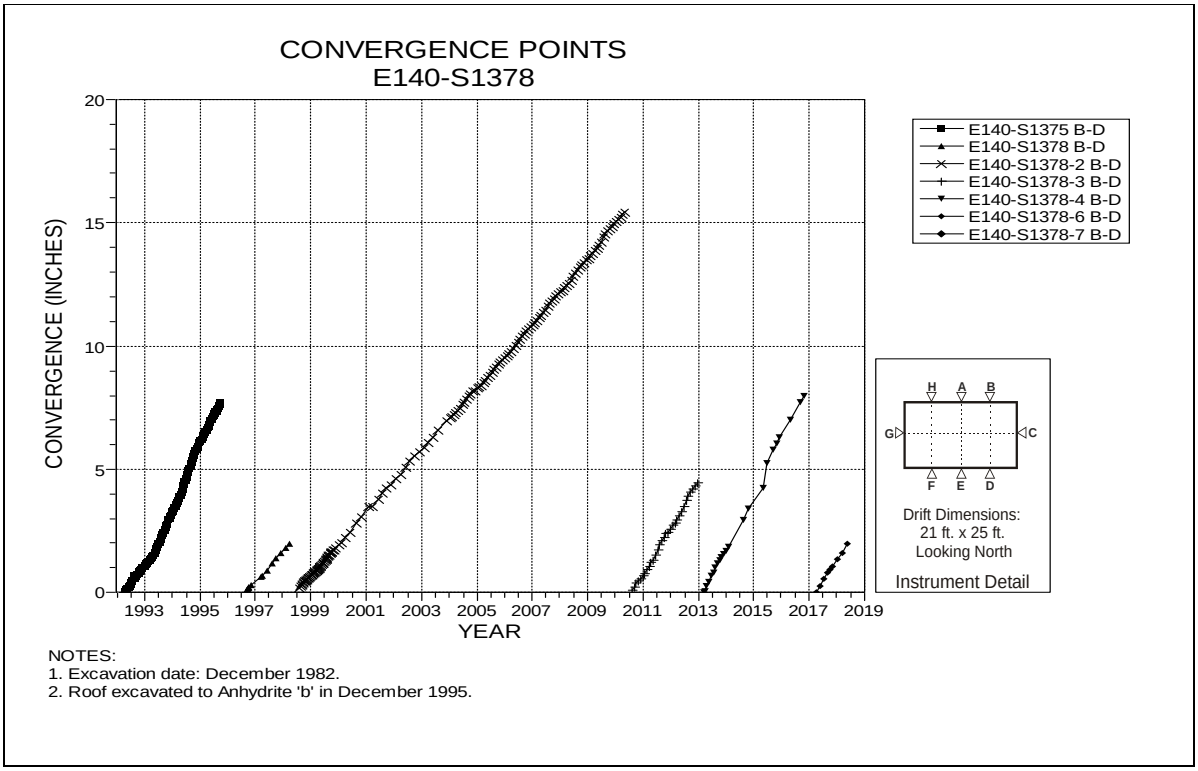

Figure 4-66 Convergence Point Array –
E140 S1378 – Roof to Floor – East Quarter Point

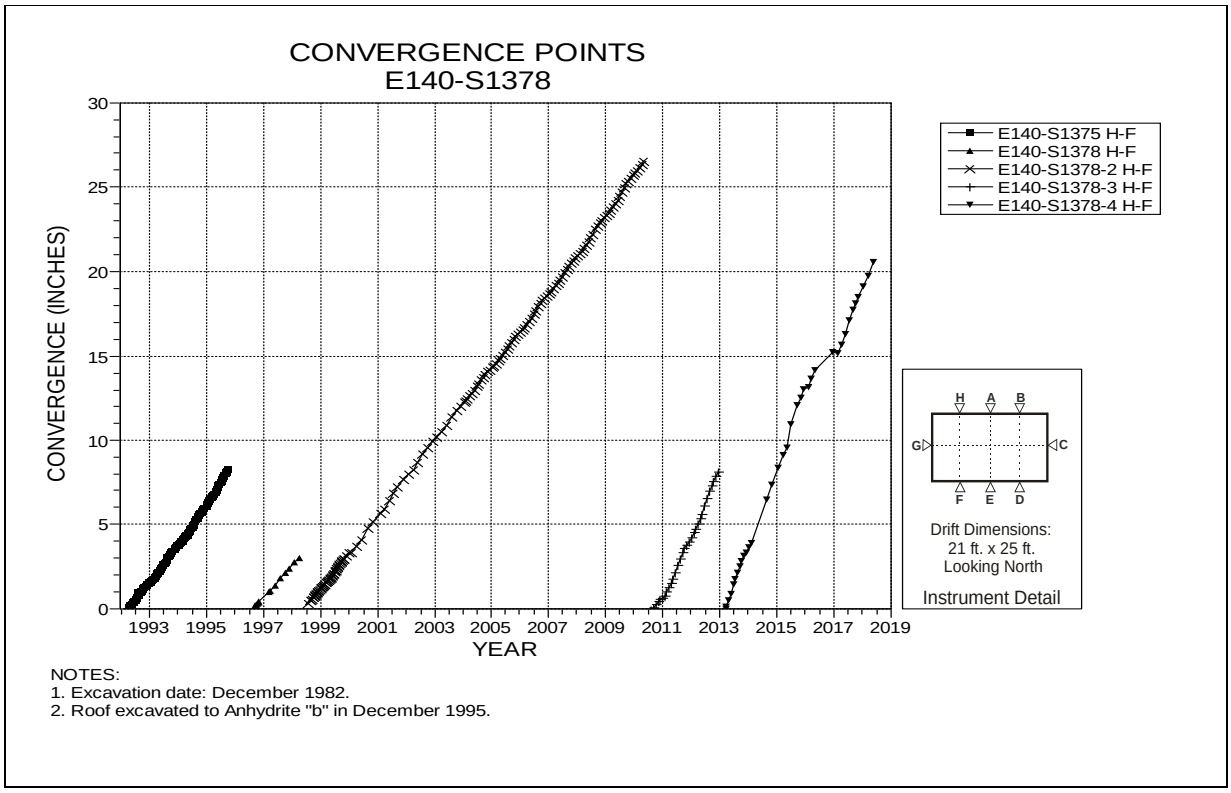

Figure 4-67 Convergence Point Array –
E140 S1378 – Roof to Floor – West Quarter Point

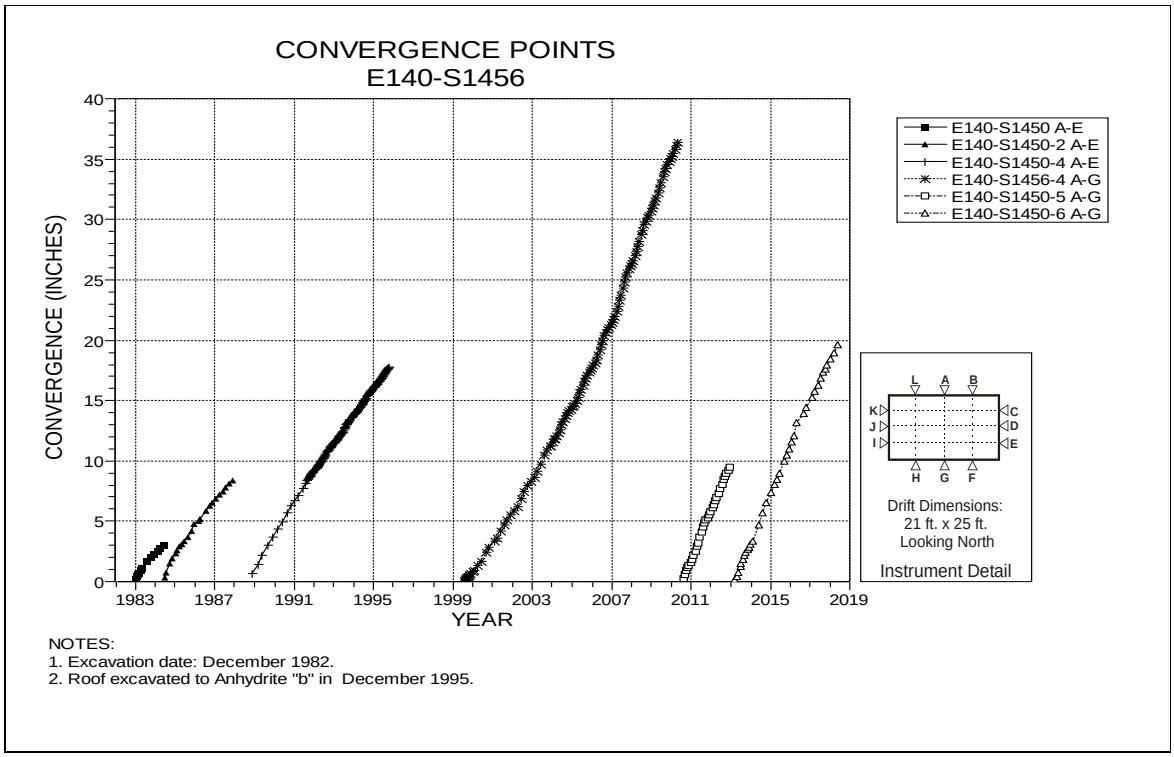

Figure 4-68 Convergence Point Array – E140 S1450 – Roof to Floor – Centerline

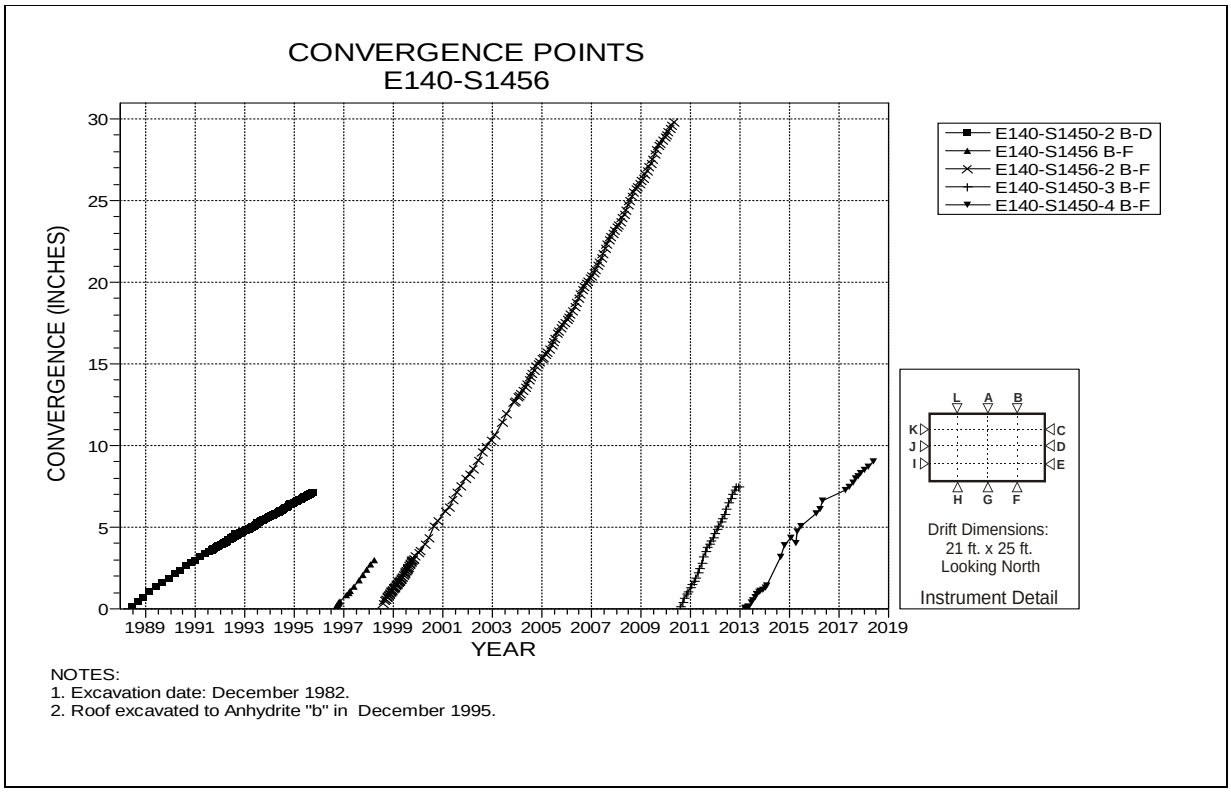

Figure 4-69 Convergence Point Array –
E140 S1450 – Roof to Floor – East Quarter Point

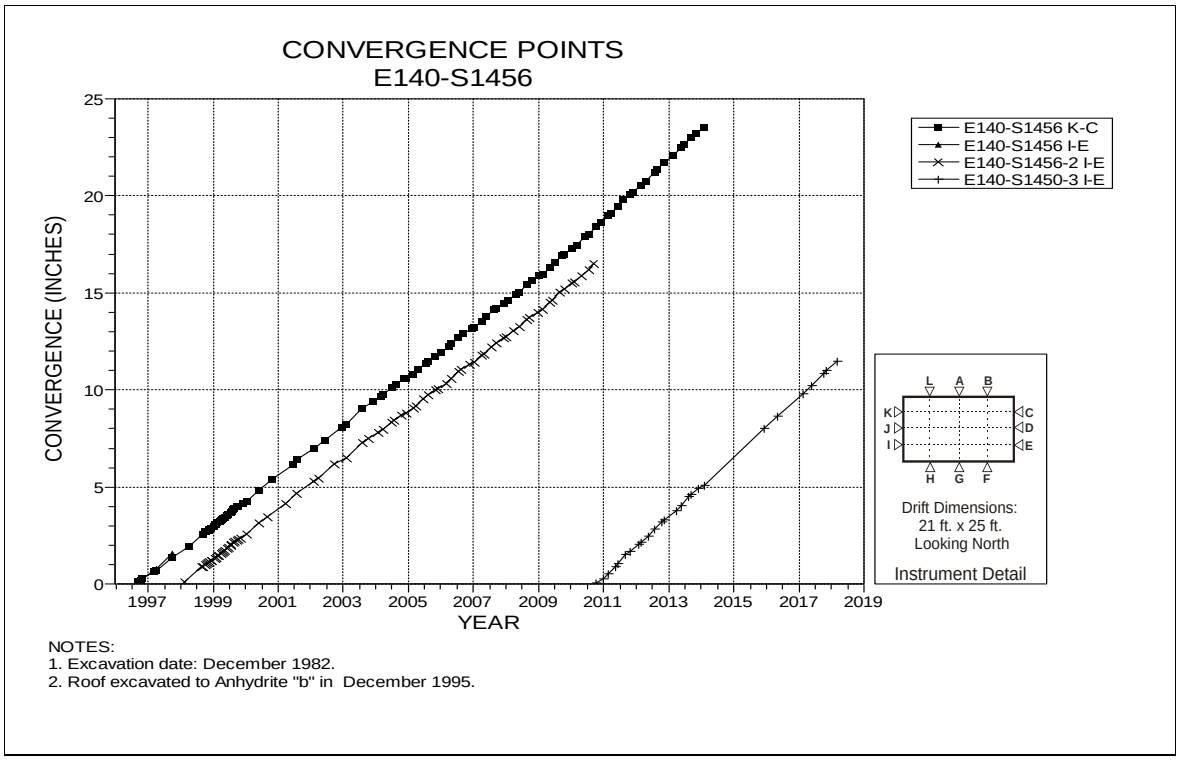

Figure 4-70 Convergence Point Array – E140 S1450 – Rib to Rib

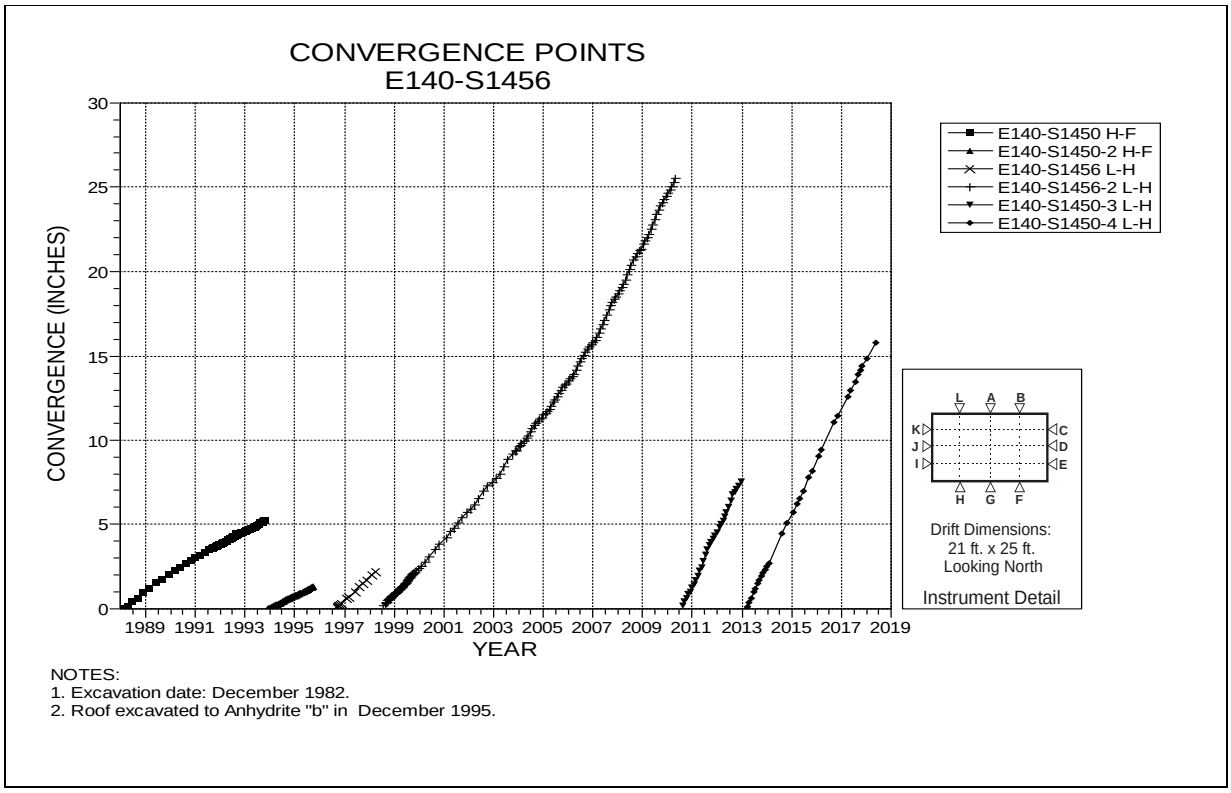

Figure 4-71 Convergence Point Array –
E140 S1450 – Roof to Floor – West Quarter Point

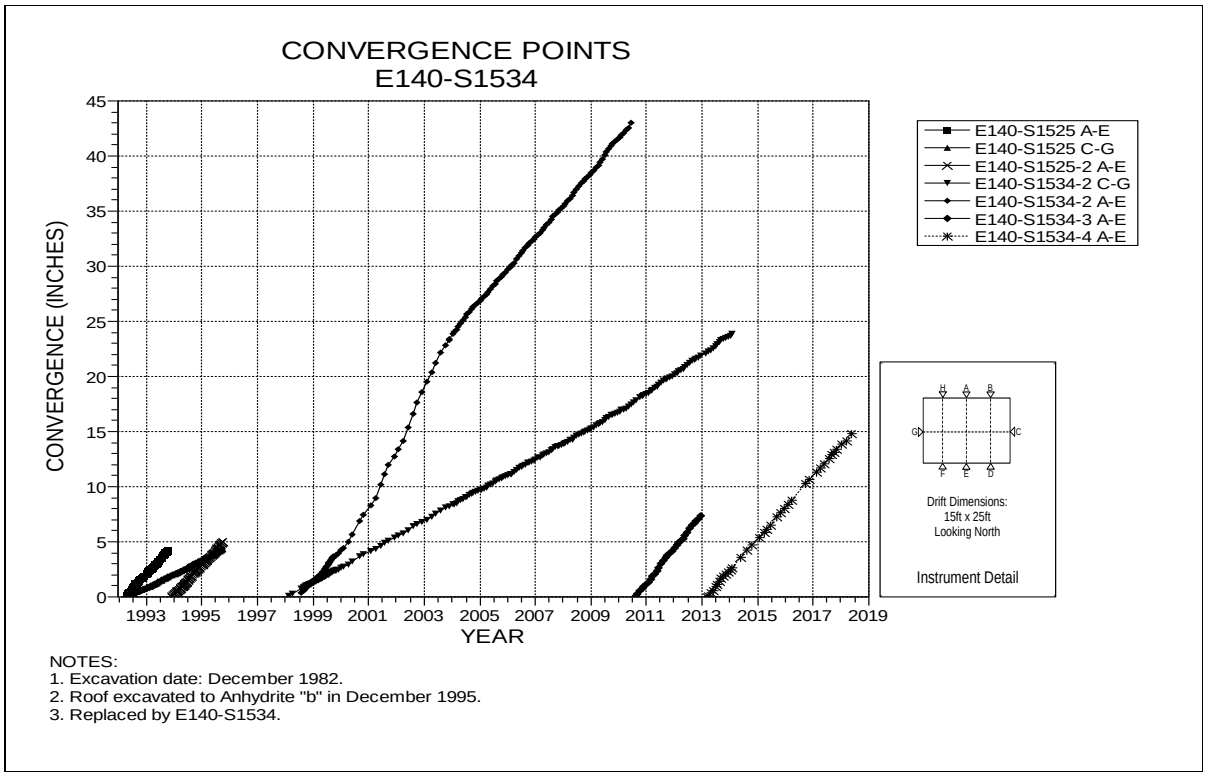

Figure 4-72 Convergence Point Array – E140 S1534 – All Chords

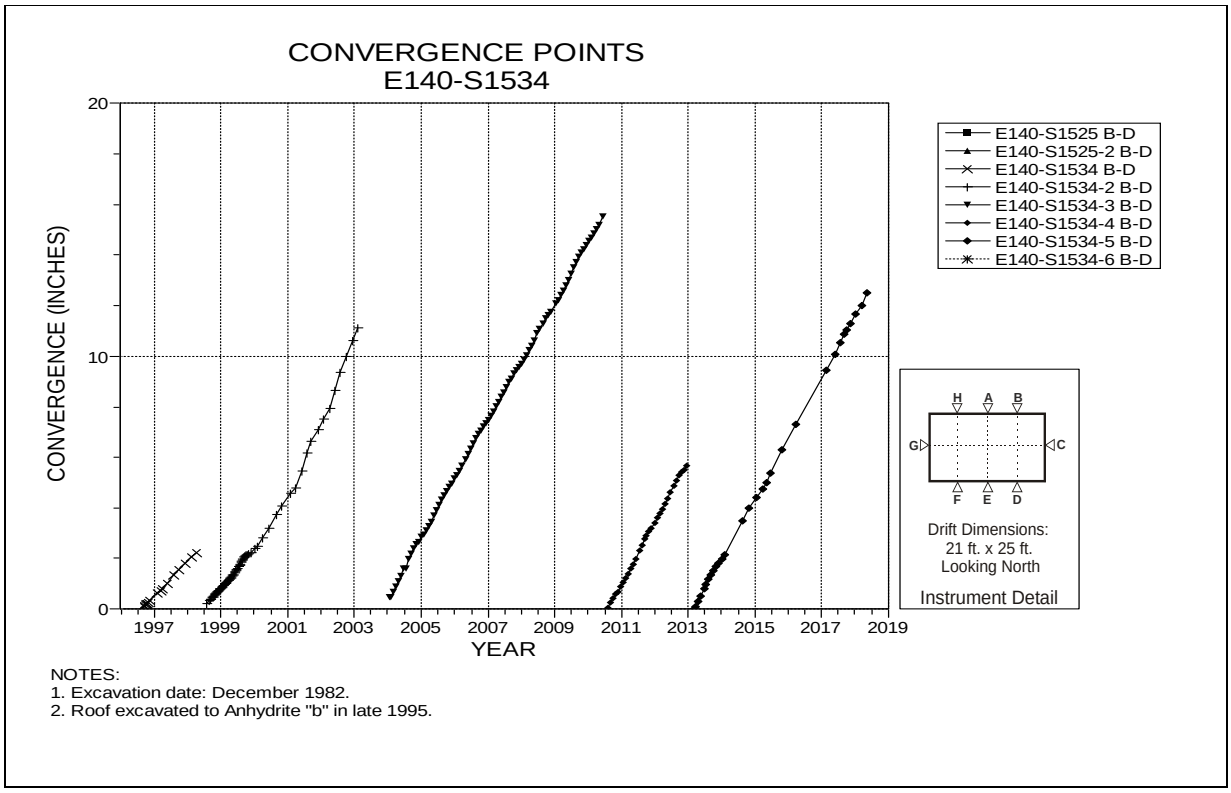

Figure 4-73 Convergence Point Array –
E140 S1534 – Roof to Floor – East Quarter Point

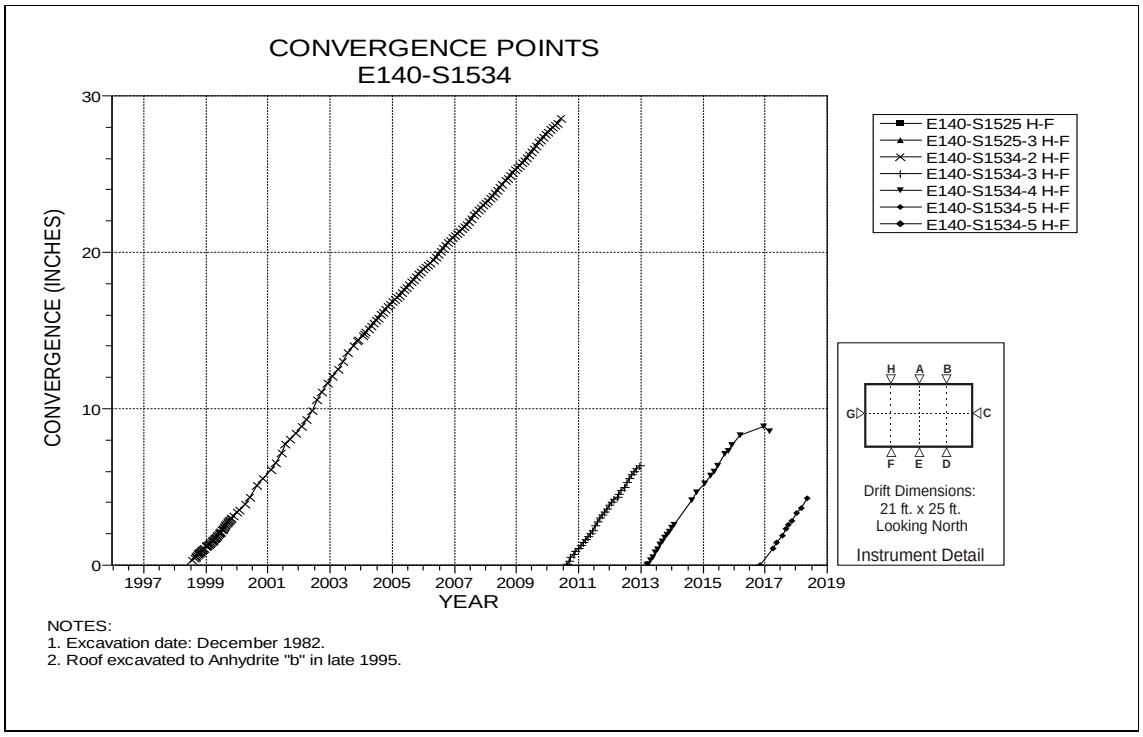

Figure 4-74 Convergence Point Array –
E140 S1534 – Roof to Floor – West Quarter Point

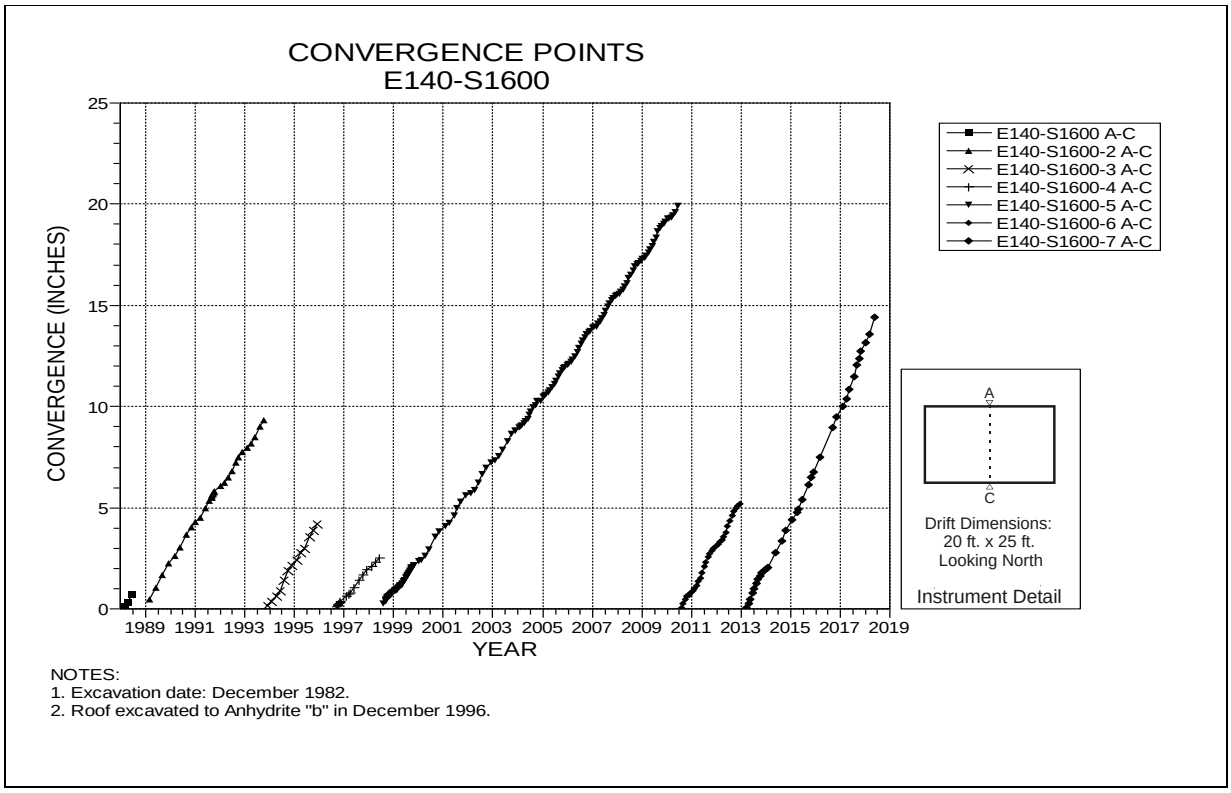

Figure 4-75 Convergence Point Array – E140 S1600 – Roof to Floor – Centerline

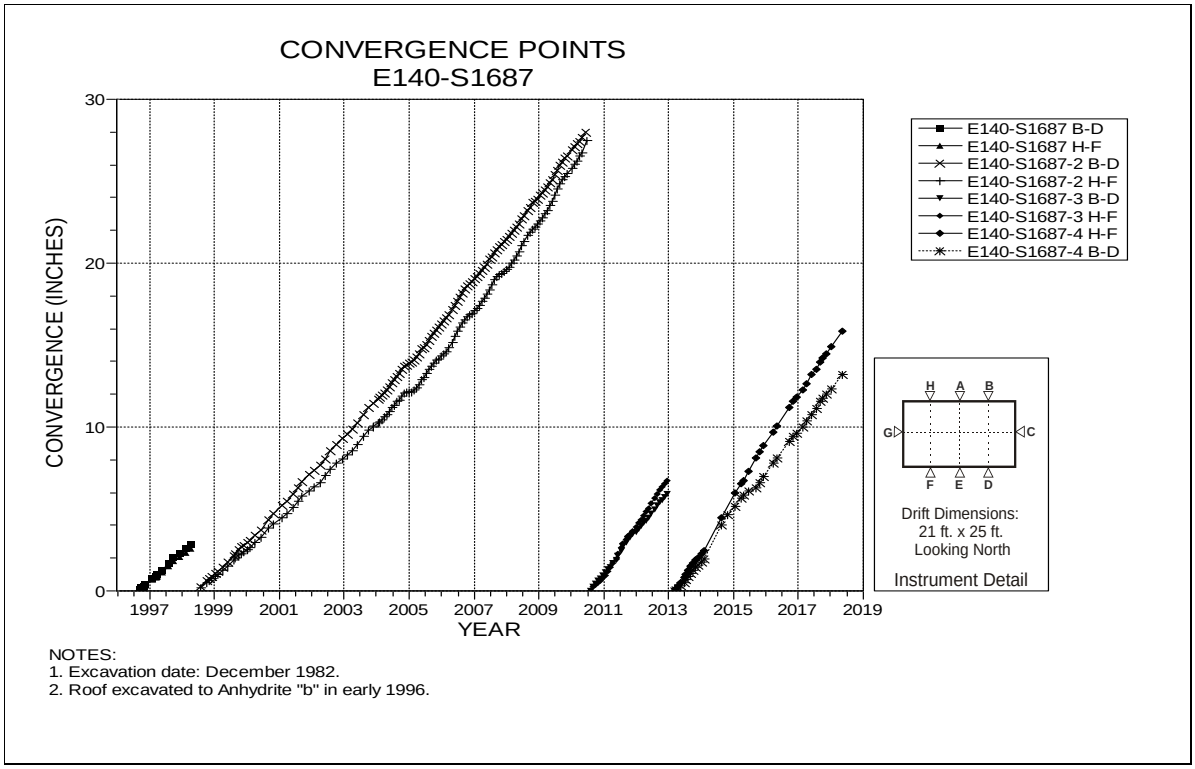

Figure 4-76 Convergence Point Array –
E140 S1687 – Roof to Floor – Quarter Point

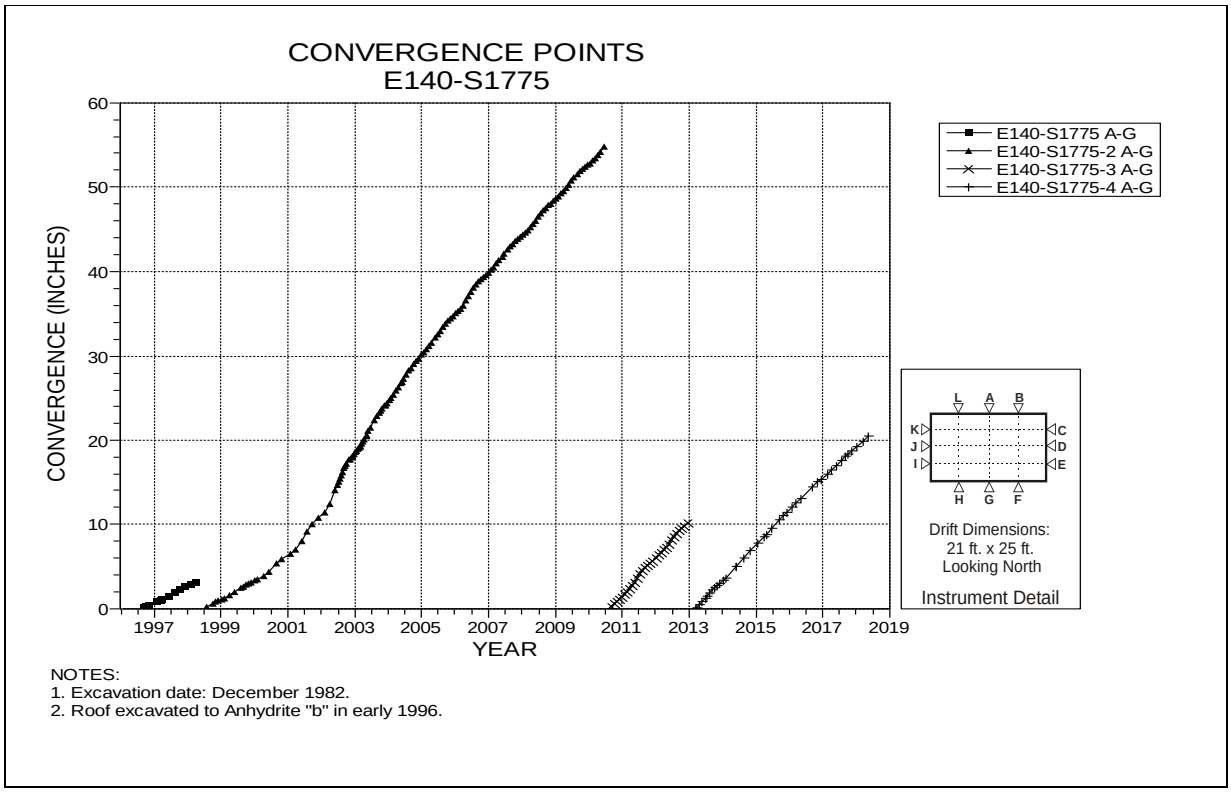

Figure 4-77 Convergence Point Array – E140 S1775 – Roof to Floor – Centerline

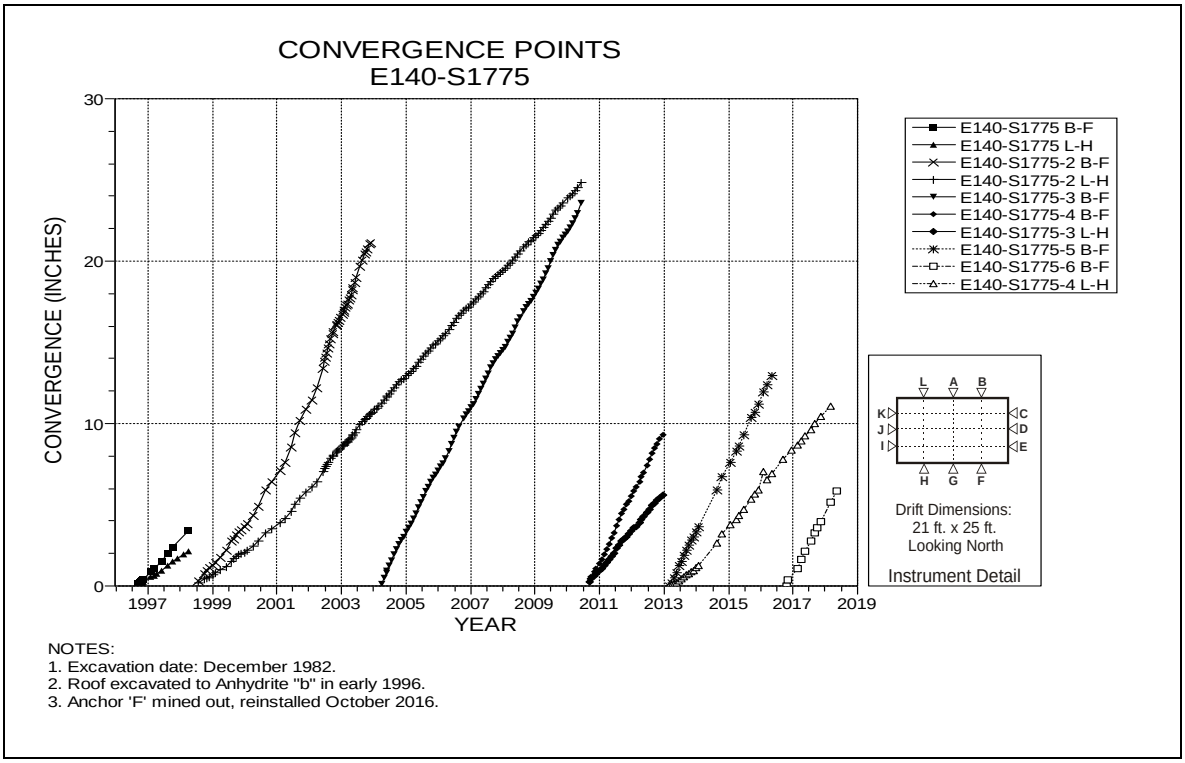

Figure 4-78 Convergence Point Array –
E140 S1775 – Roof to Floor – East and West Quarter Points

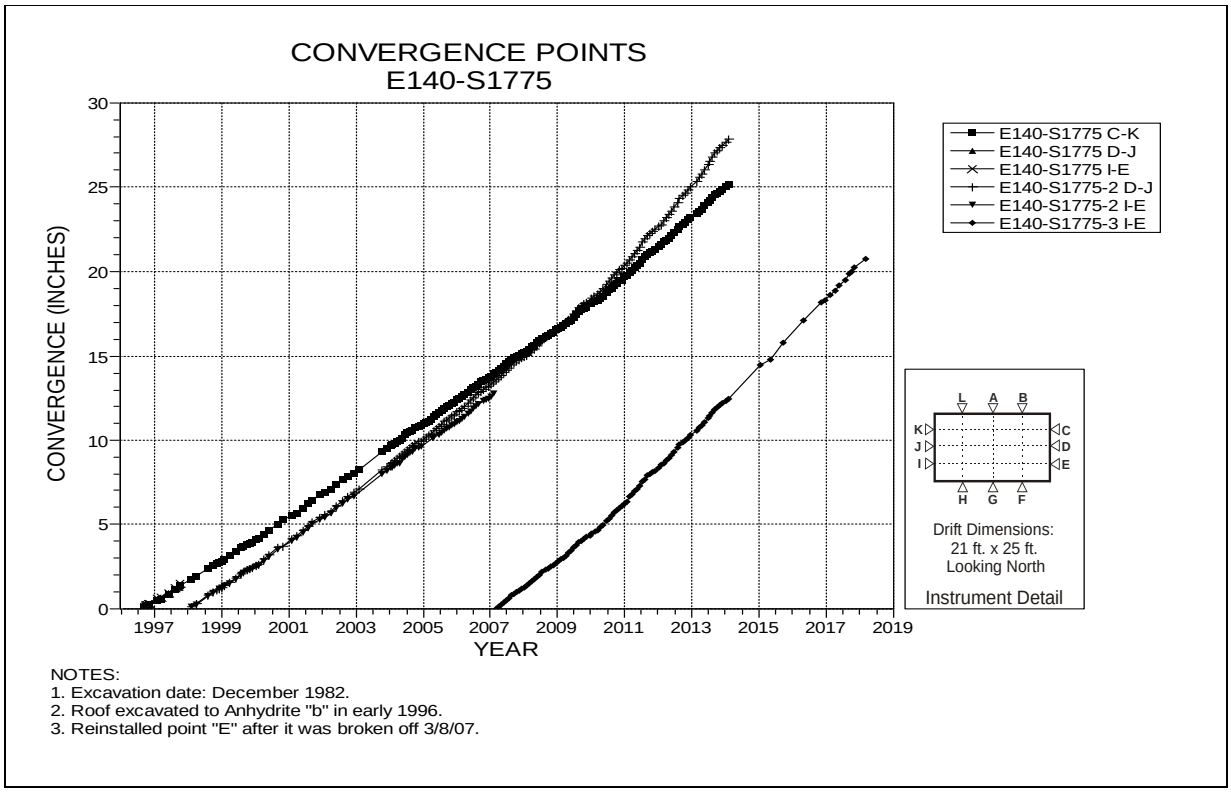

Figure 4-79 Convergence Point Array – E140 S1775 – Rib to Rib

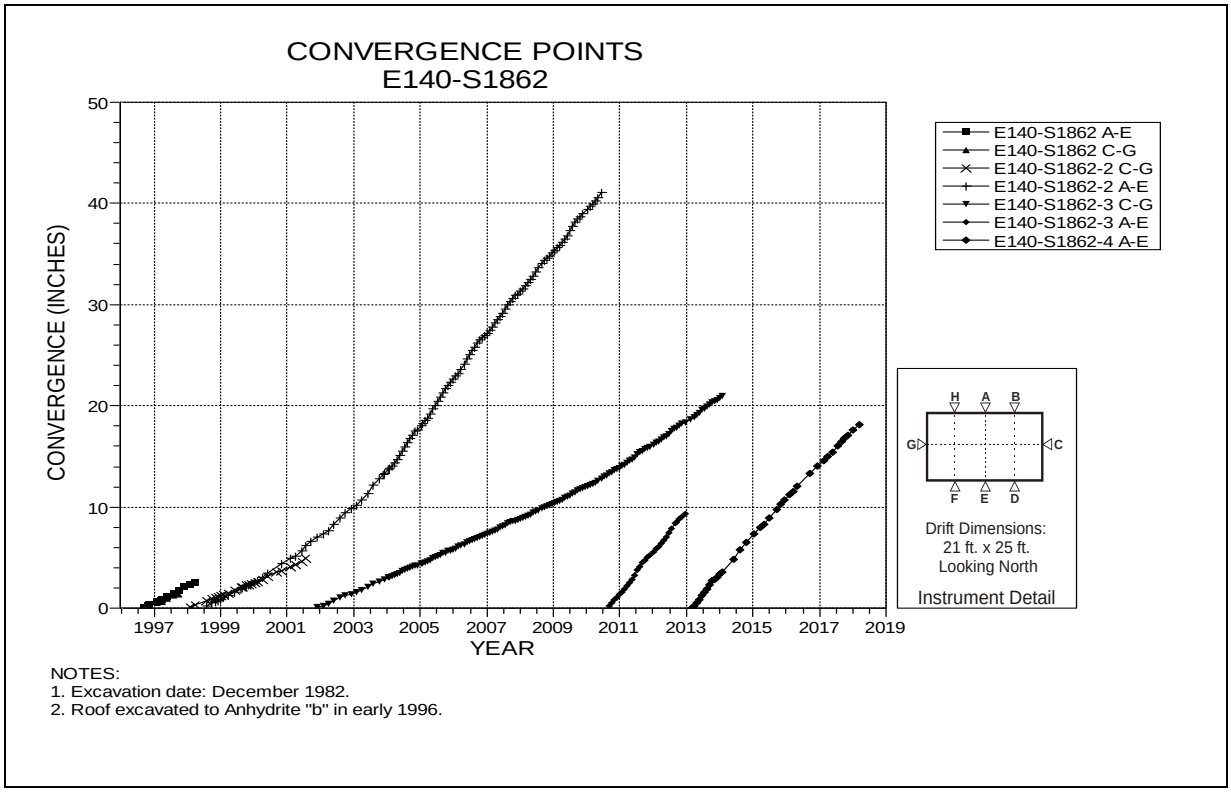

Figure 4-80 Convergence Point Array – E140 S1862 – Roof to Floor – Centerline

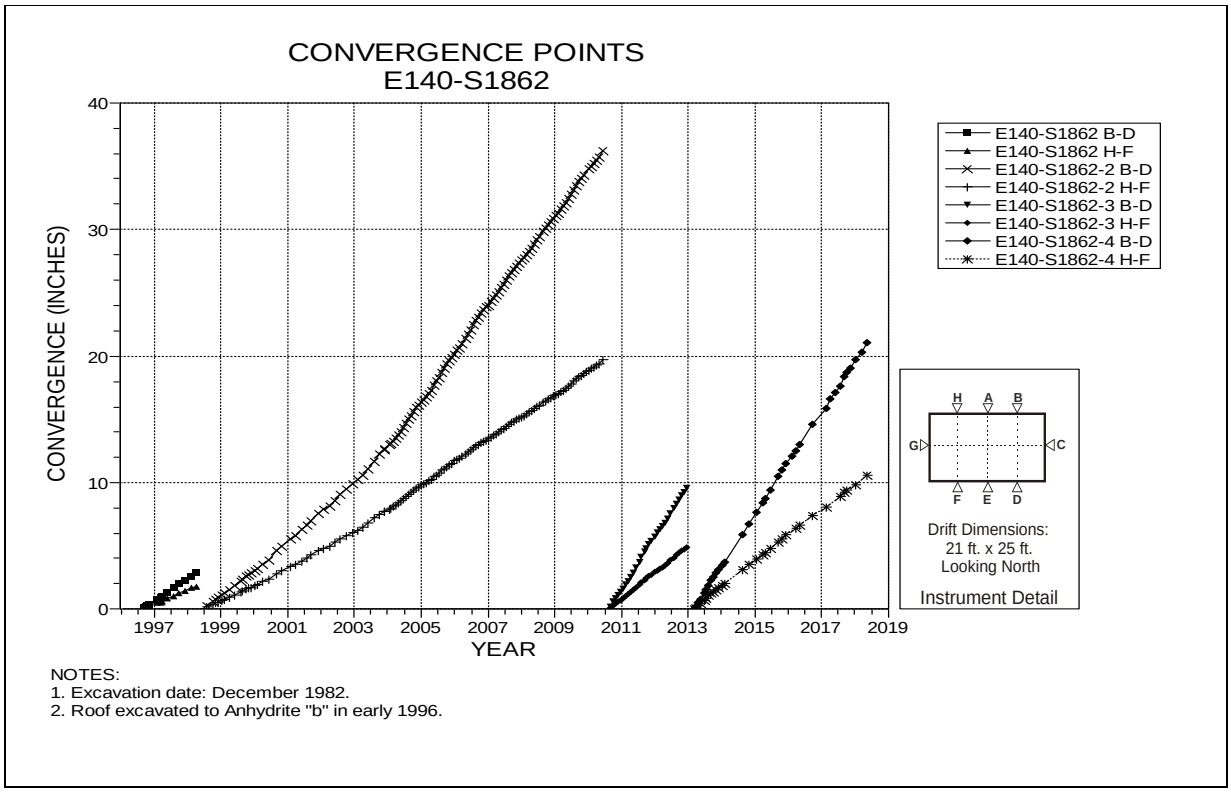

Figure 4-81 Convergence Point Array –
E140 S1862 – Roof to Floor – East and West Quarter Points

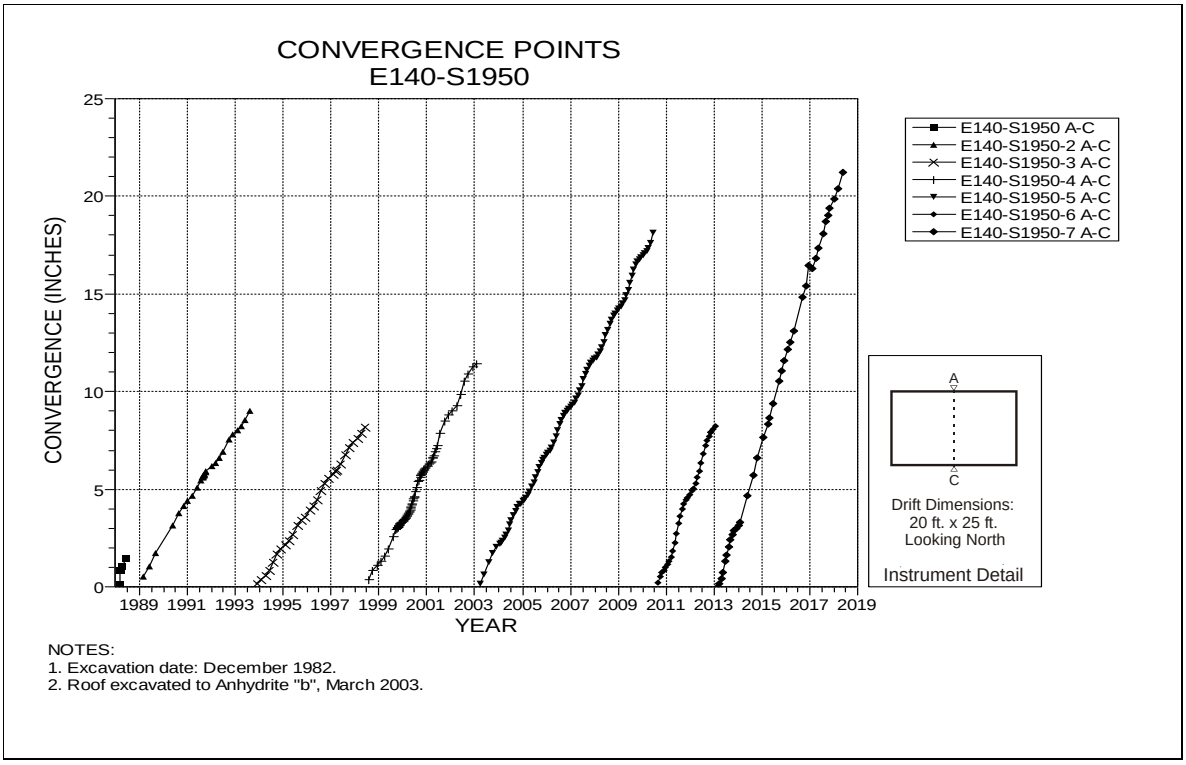

Figure 4-82 Convergence Point Array – E140 S1950 – Roof to Floor – Centerline

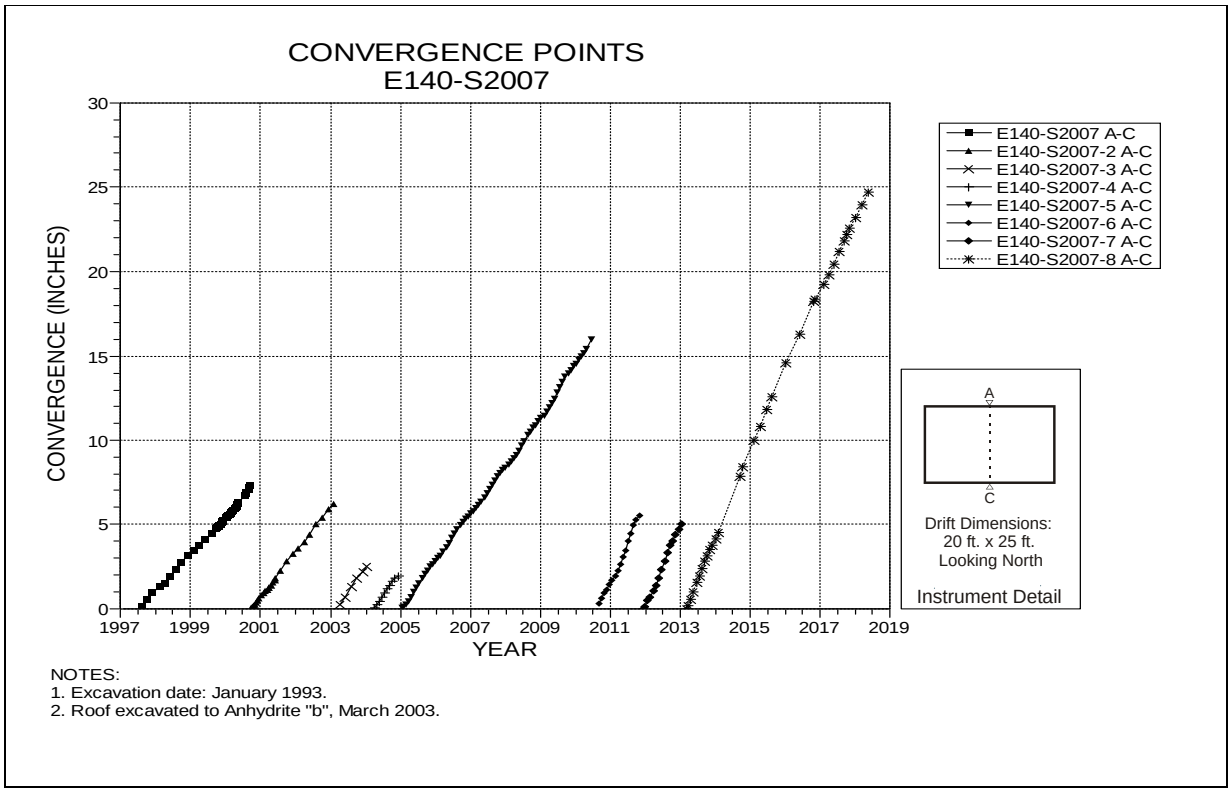

Figure 4-83 Convergence Point Array – E140 S2007 – Roof to Floor – Centerline

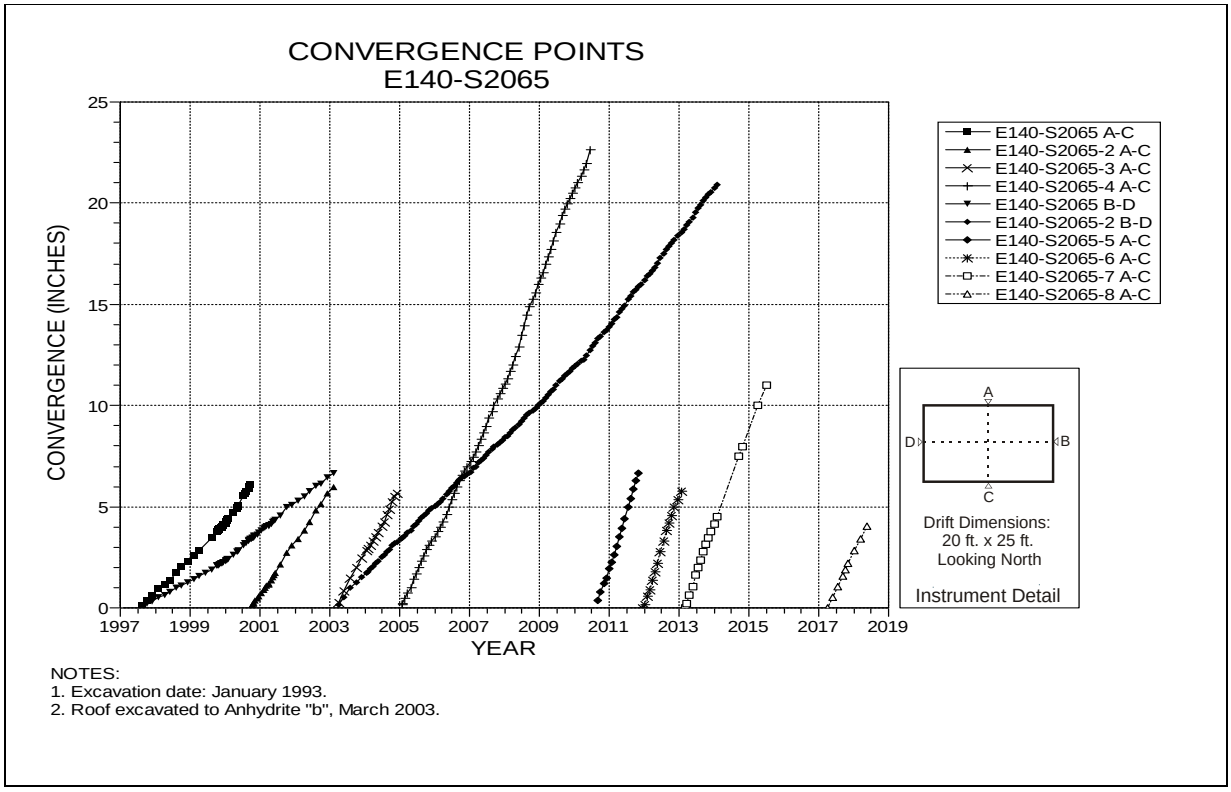

Figure 4-84 Convergence Point Array – E140 S2065 – Roof to Floor – Centerline

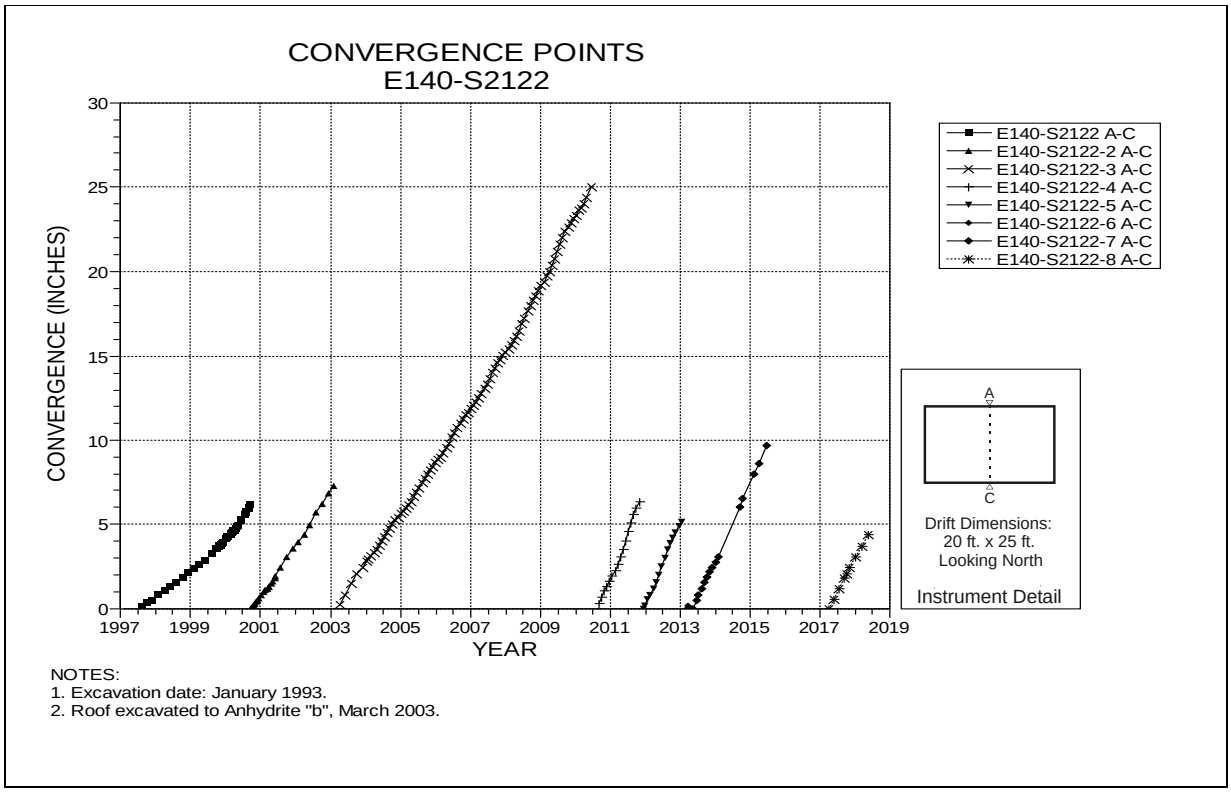

Figure 4-85 Convergence Point Array – E140 S2122 – Roof to Floor – Centerline

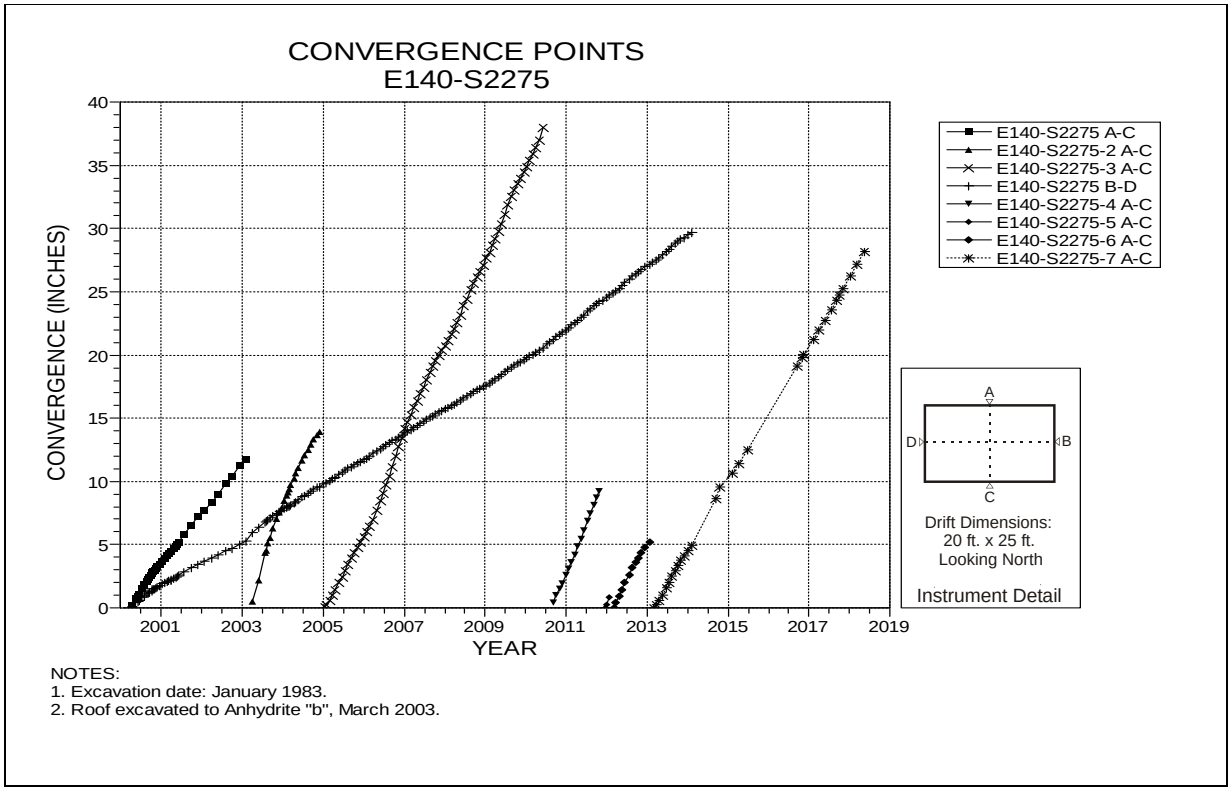

Figure 4-86 Convergence Point Array – E140 S2275 – Roof to Floor – Centerline

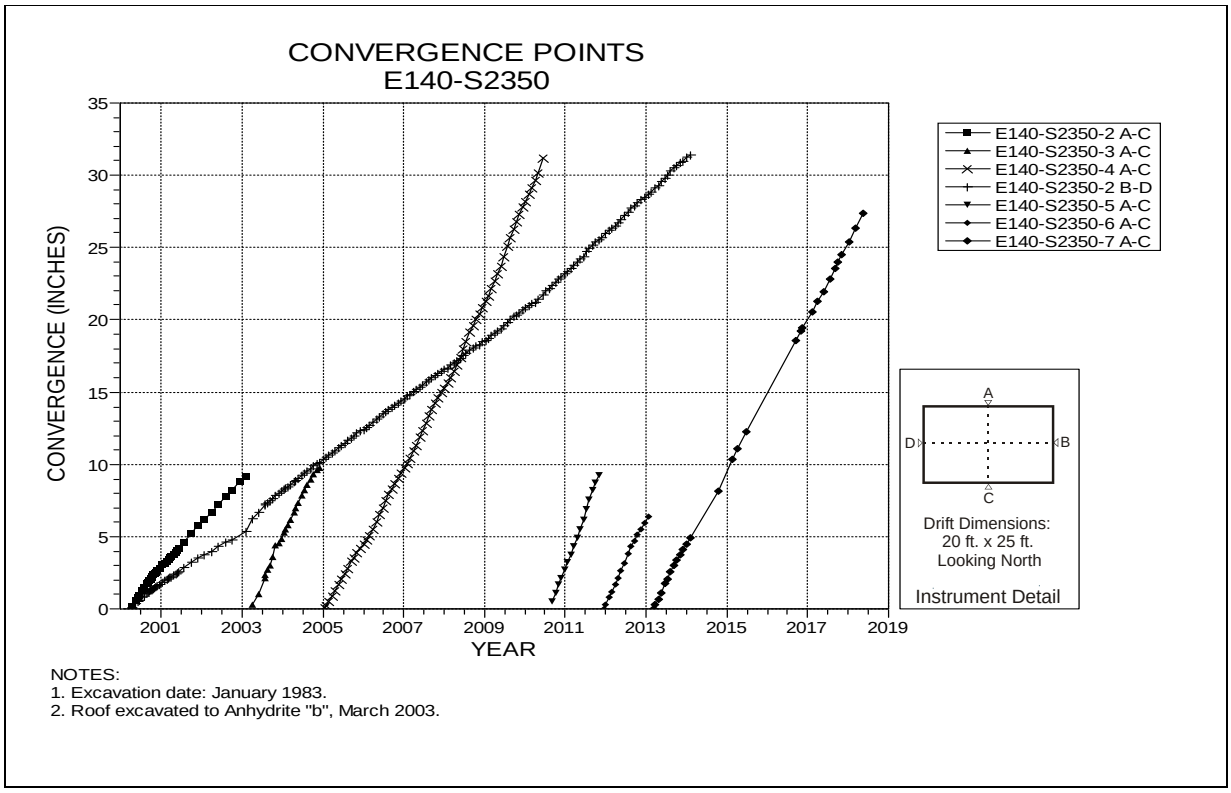

Figure 4-87 Convergence Point Array – E140 S2350 – Roof to Floor – Centerline

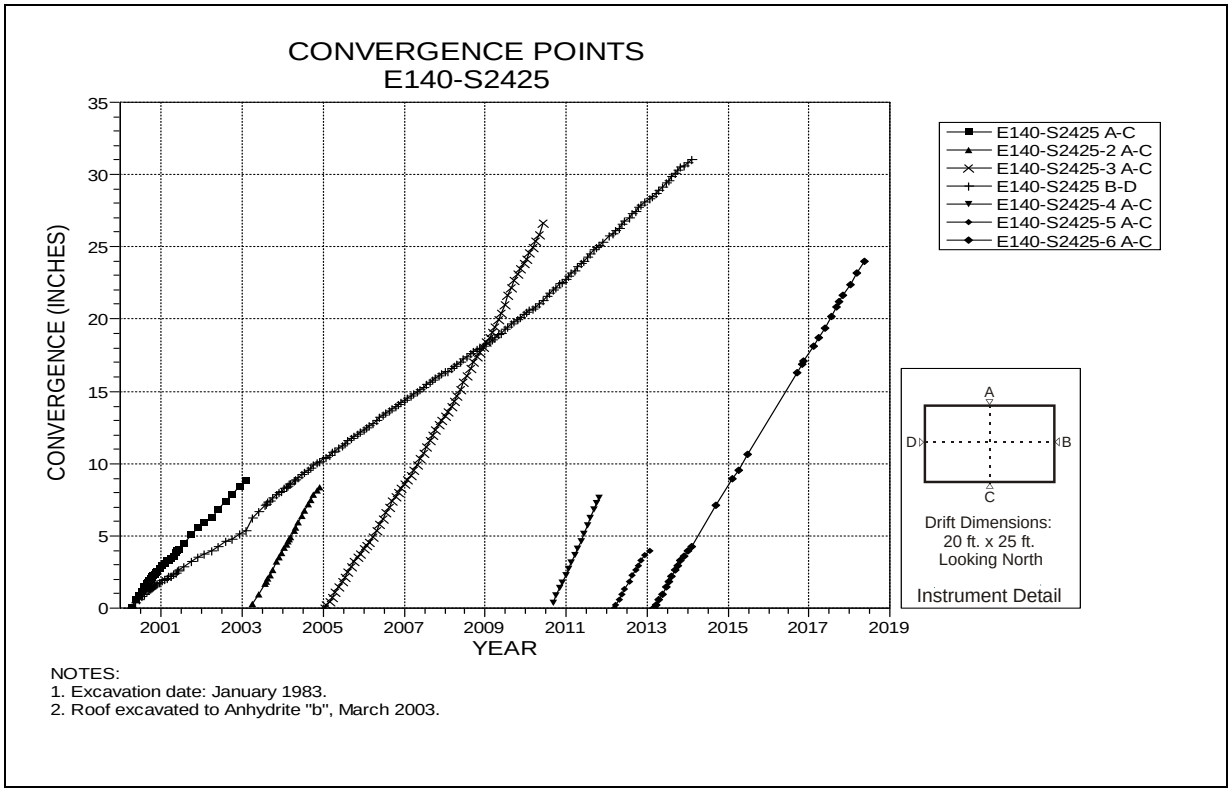

Figure 4-88 Convergence Point Array – E140 S2425 – All Chords

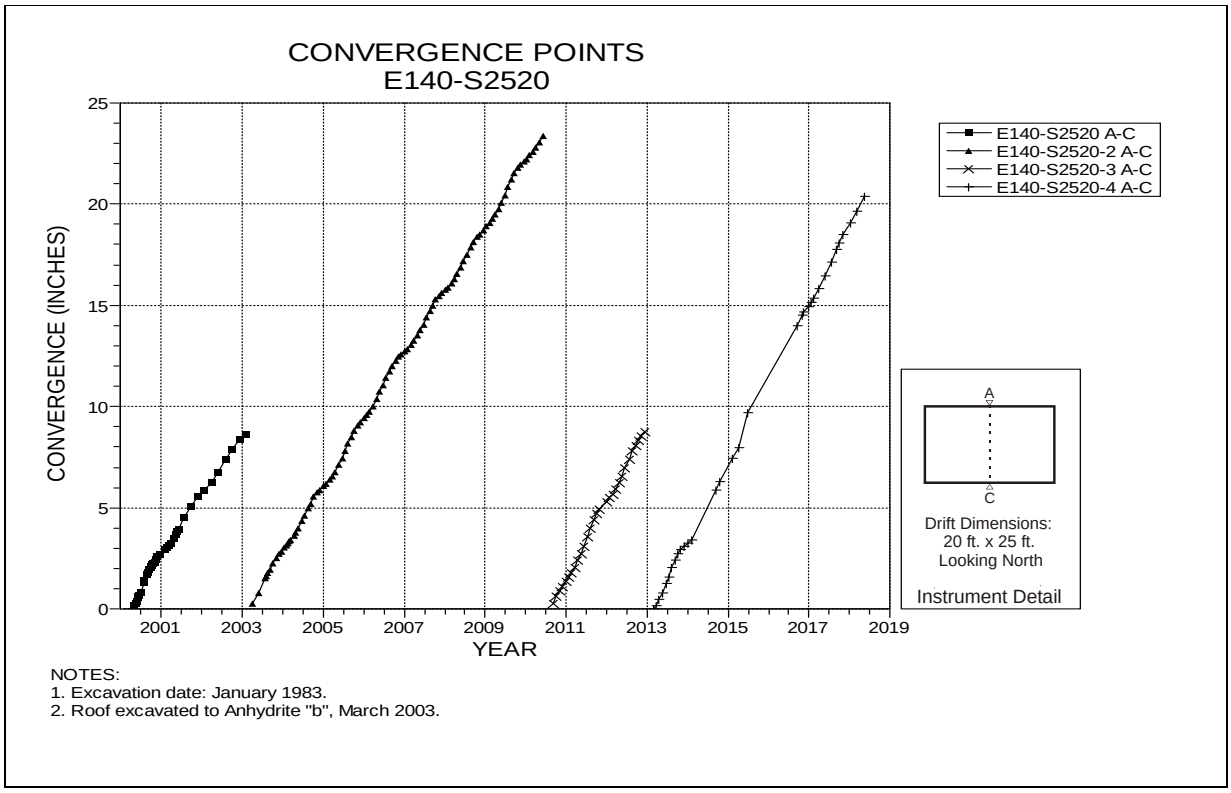

Figure 4-89 Convergence Point Array – E140 S2520 – Roof to Floor – Centerline

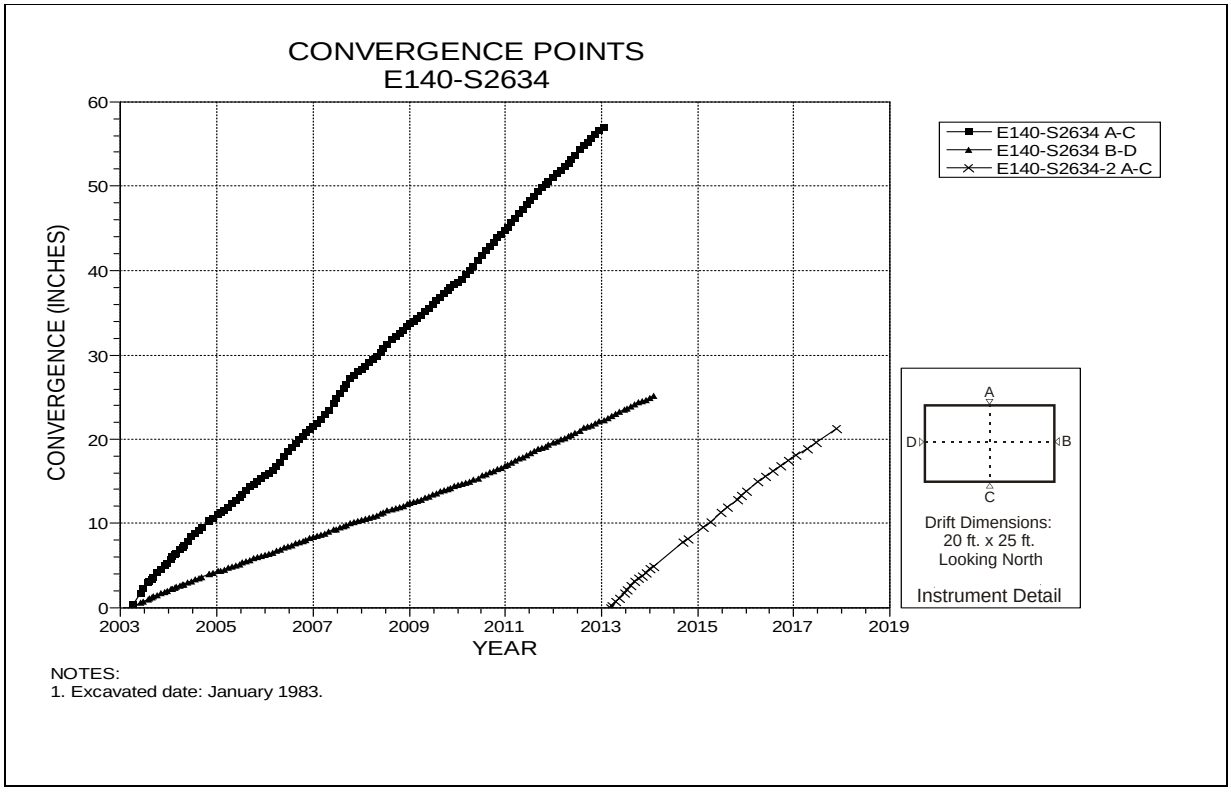

Figure 4-90 Convergence Point Array – E140 S2634 – All Chords

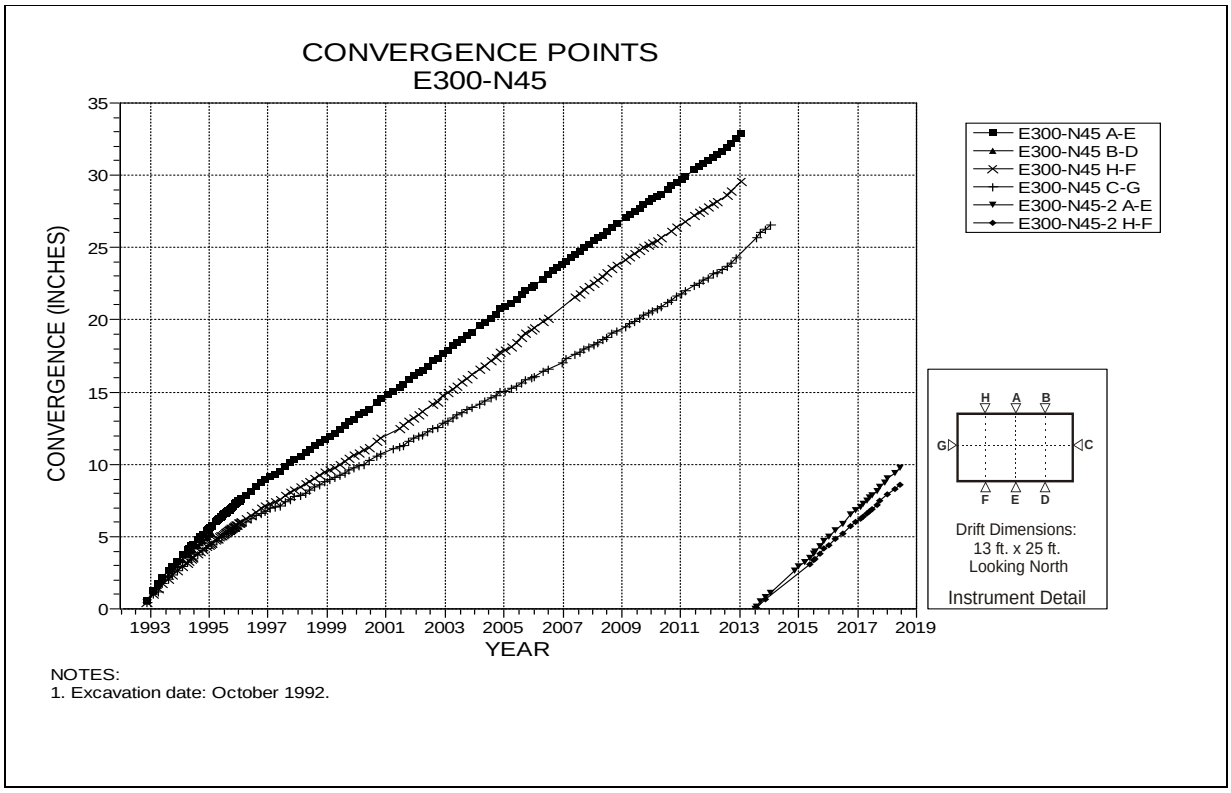

Figure 4-91 Convergence Point Array –
E300 N45 – Roof to Floor – Centerline and West Quarter Points

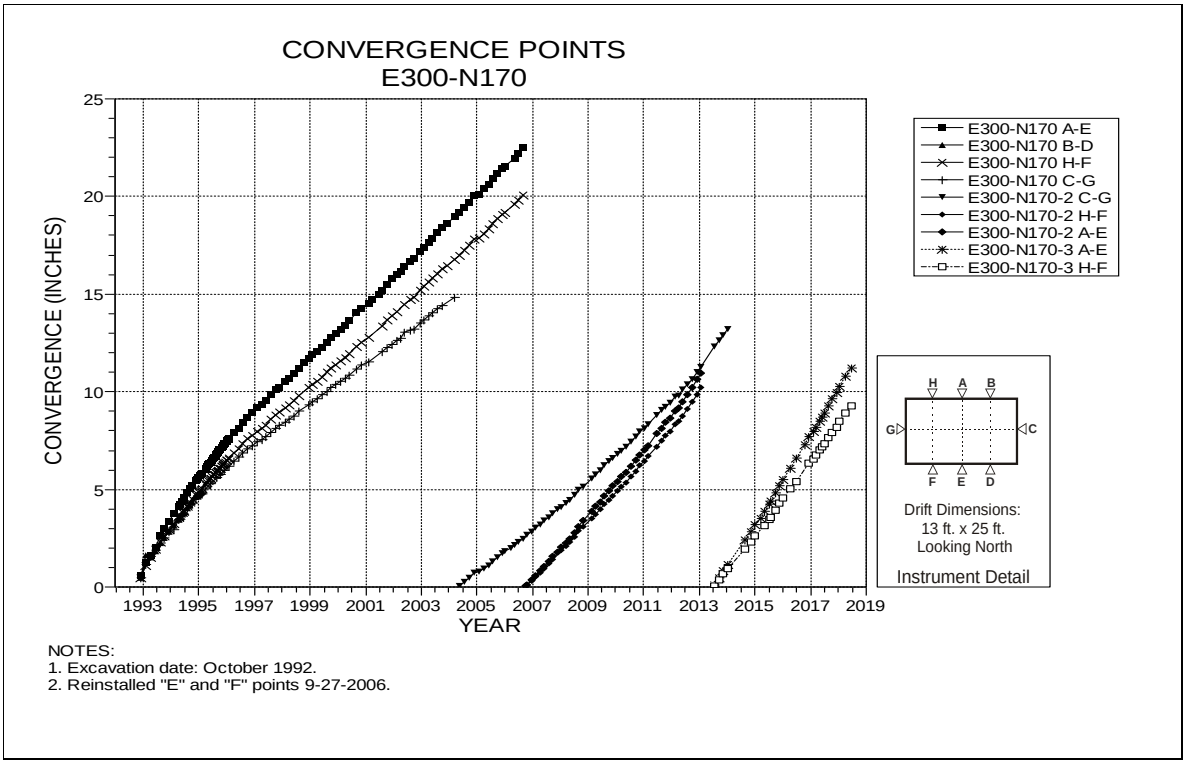

Figure 4-92 Convergence Point Array –
E300 N170 – Roof to Floor – Centerline and West Quarter Points

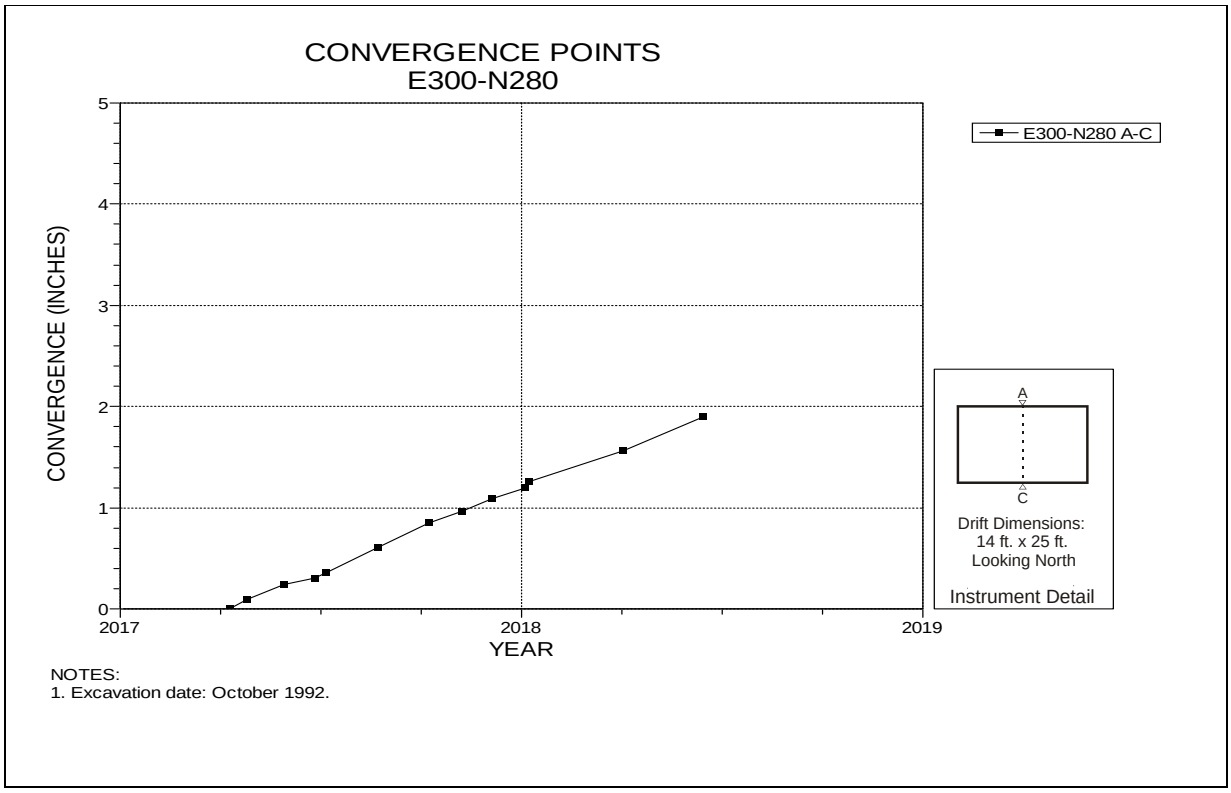

Figure 4-93 Convergence Point Array – E300 N280 – Roof to Floor – Centerline

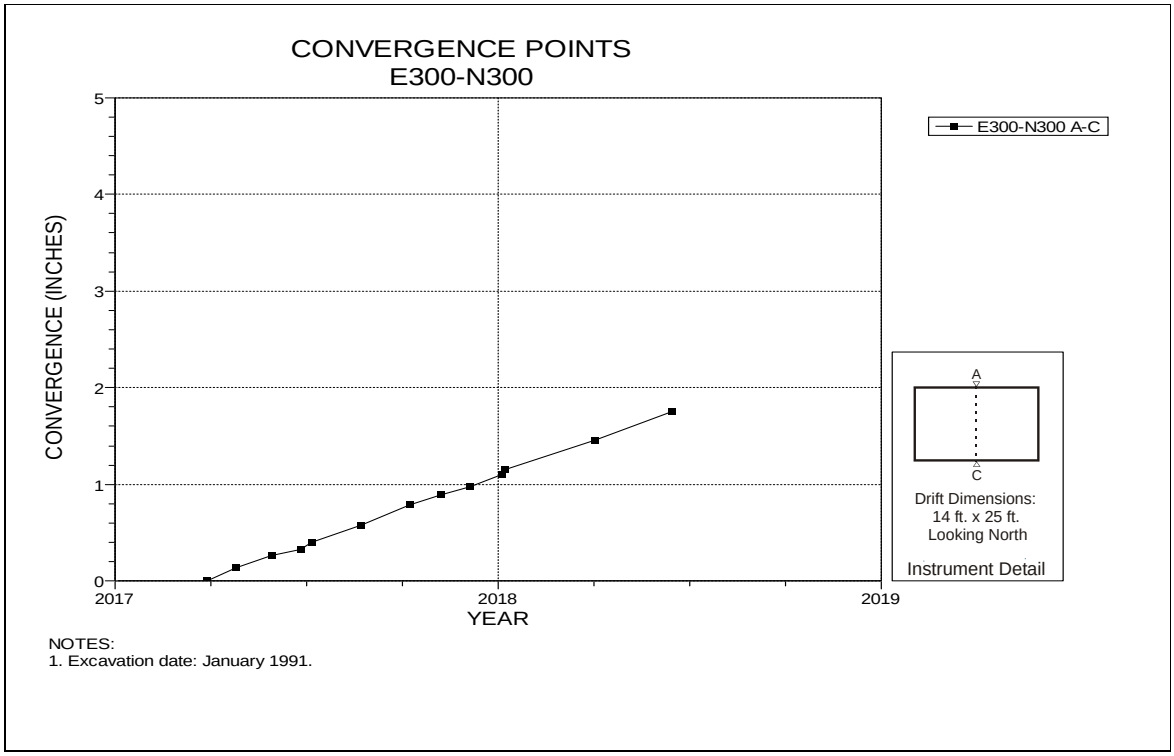

Figure 4-94 Convergence Point Array – E300 N300 – Roof to Floor – Centerline

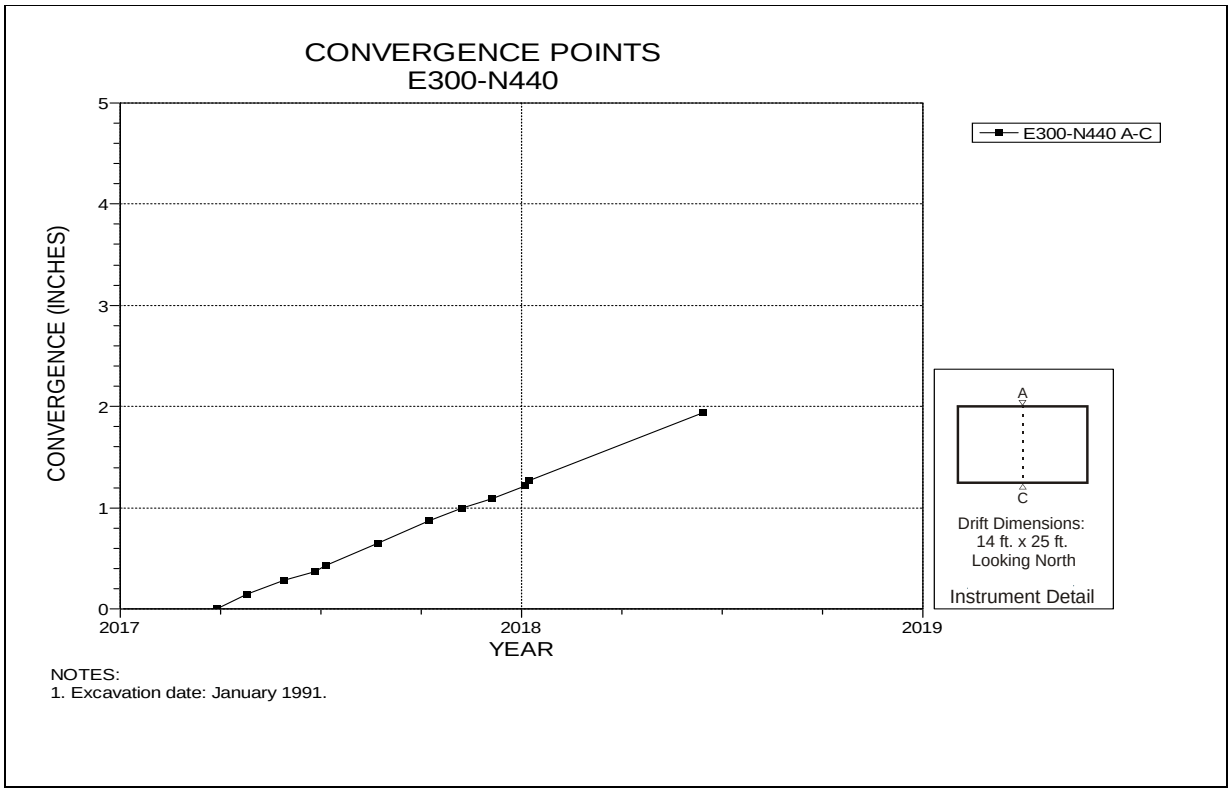

Figure 4-95 Convergence Point Array – E300 N440 – Roof to Floor – Centerline

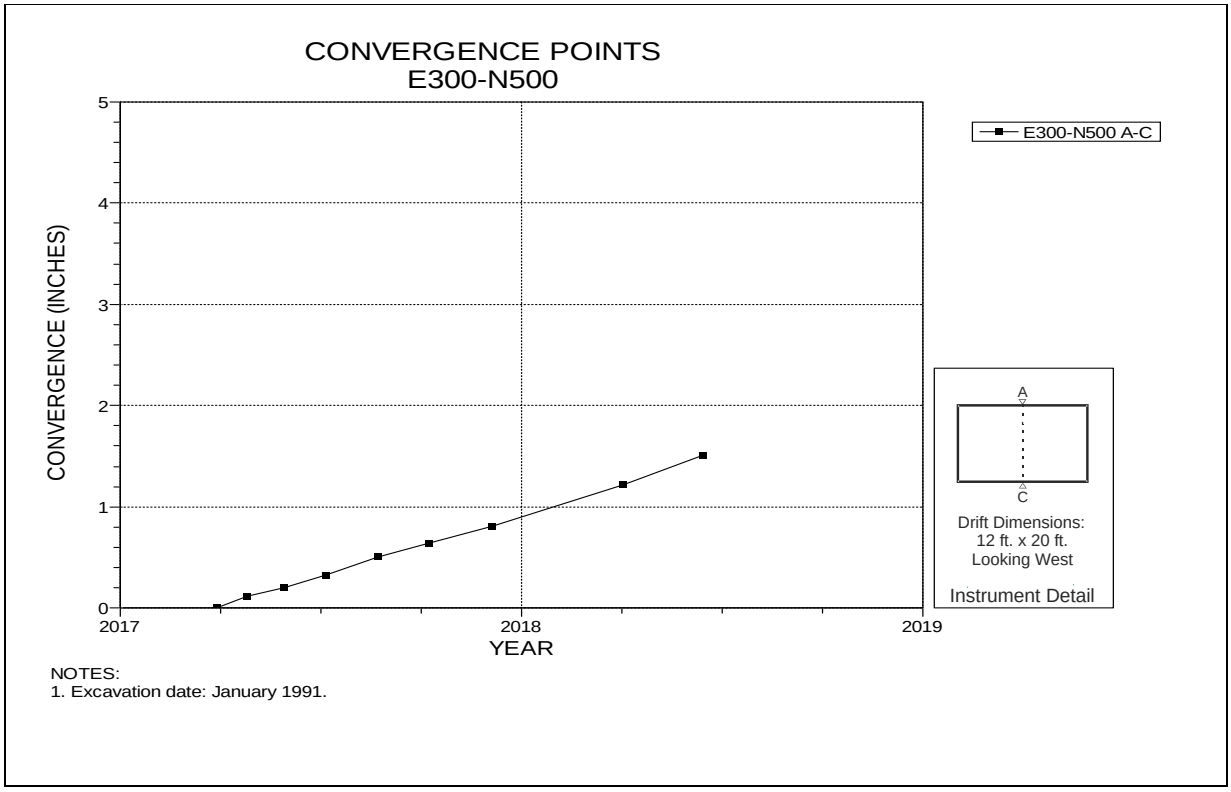

Figure 4-96 Convergence Point Array – E300 N500 – Roof to Floor – Centerline

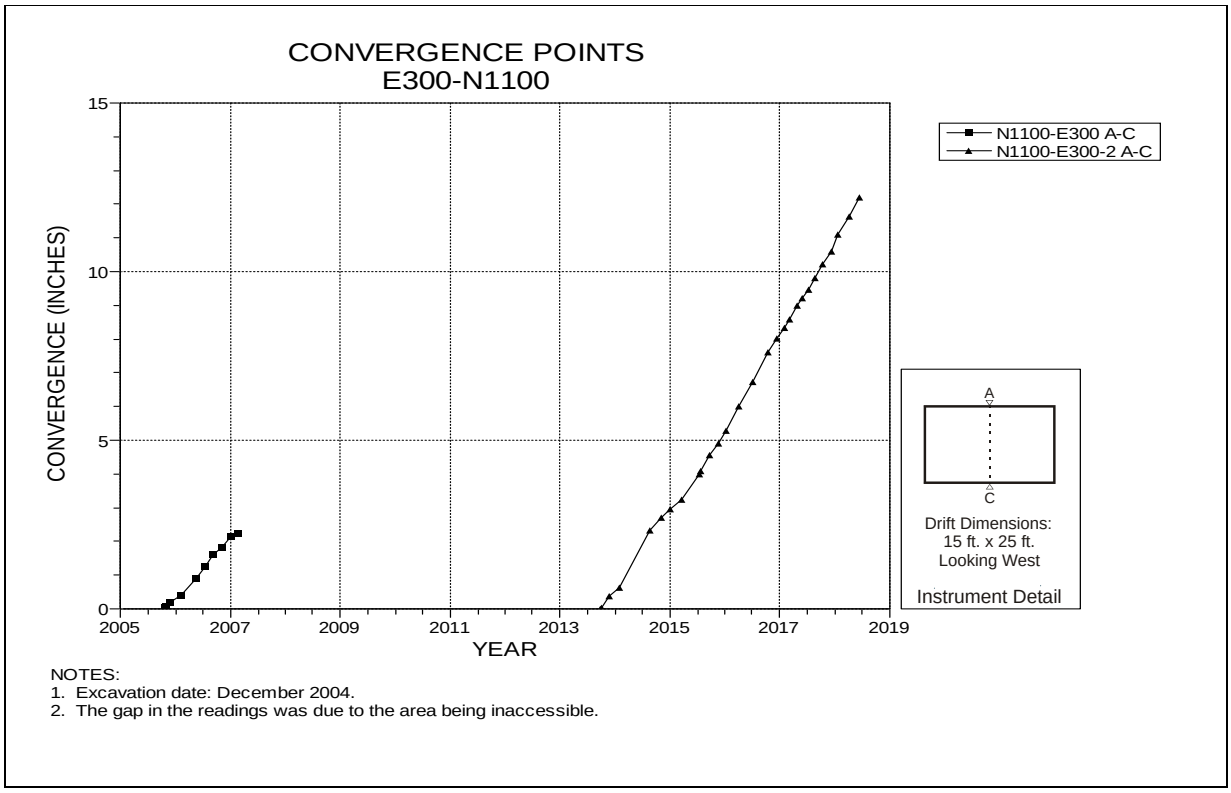

Figure 4-97 Convergence Point Array – E300 N1100 – Roof to Floor – Centerline

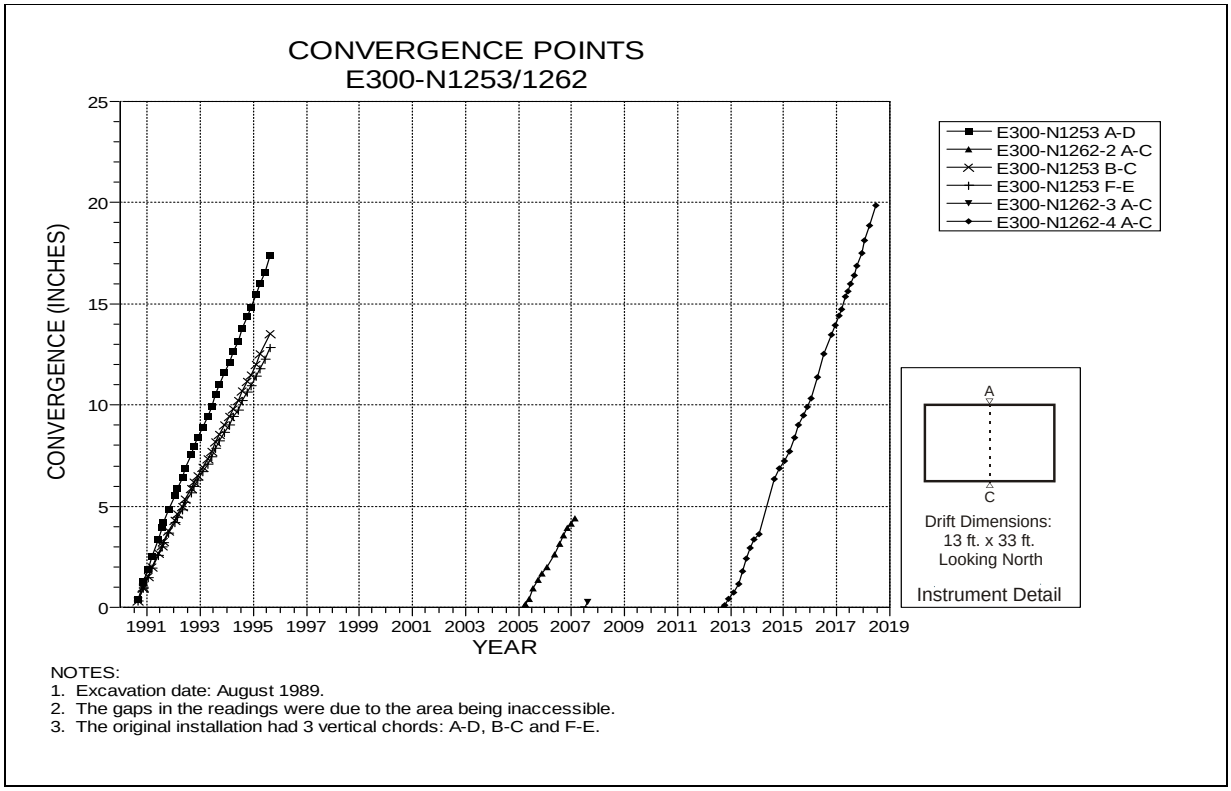

Figure 4-98 Convergence Point Array – E300 N1262 – All Chords

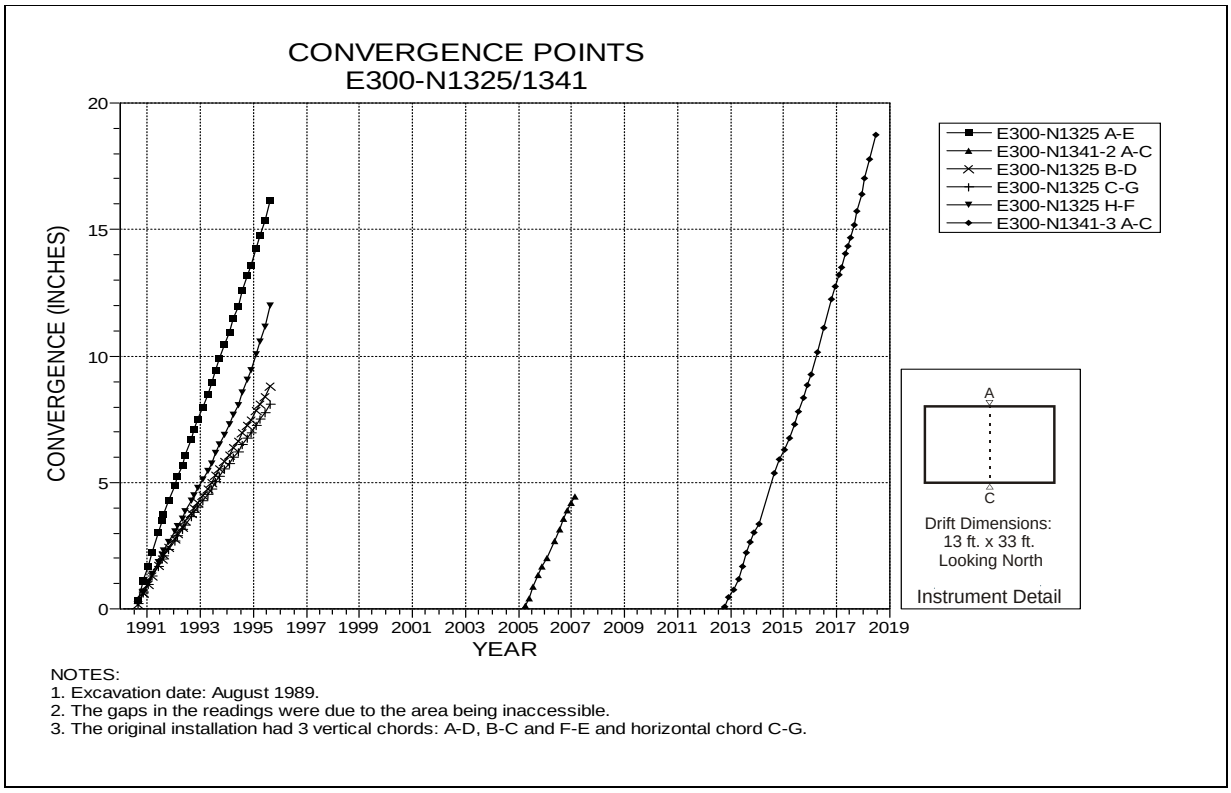

Figure 4-99 Convergence Point Array – E300 N1341 – All Chords

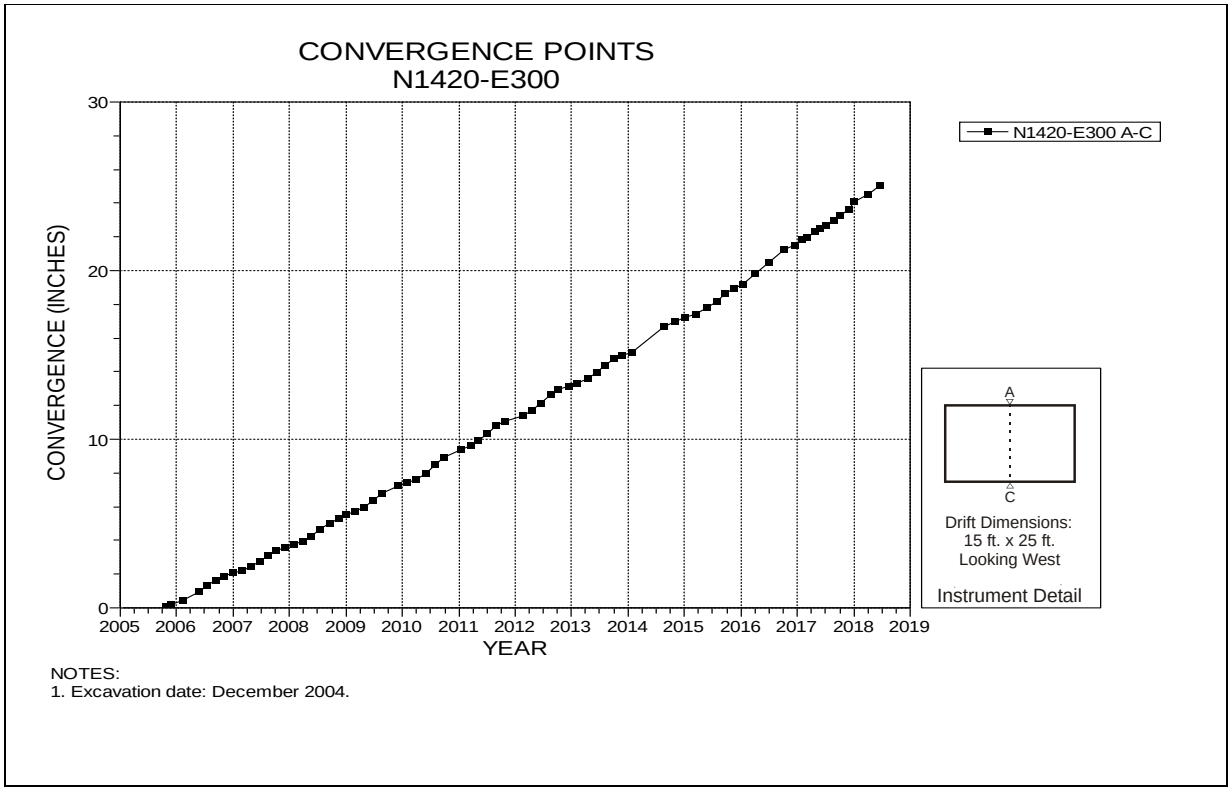

Figure 4-100 Convergence Point Array – E300 N1420 – Roof to Floor – Centerline

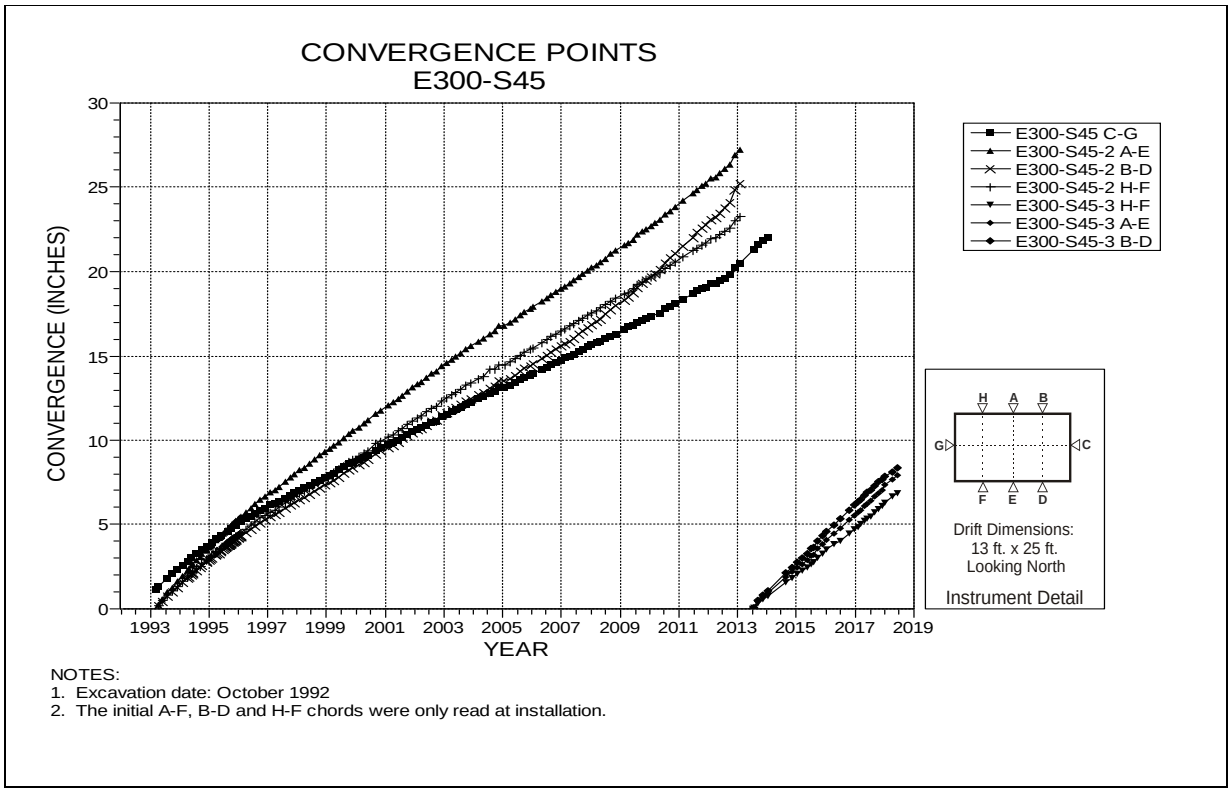

NOTES:
1. Excavation date: October 1992
2. The initial A-F, B-D and H-F chords were only read at installation.

Figure 4-101 Convergence Point Array – E300 S45 – Roof to Floor – All Chords

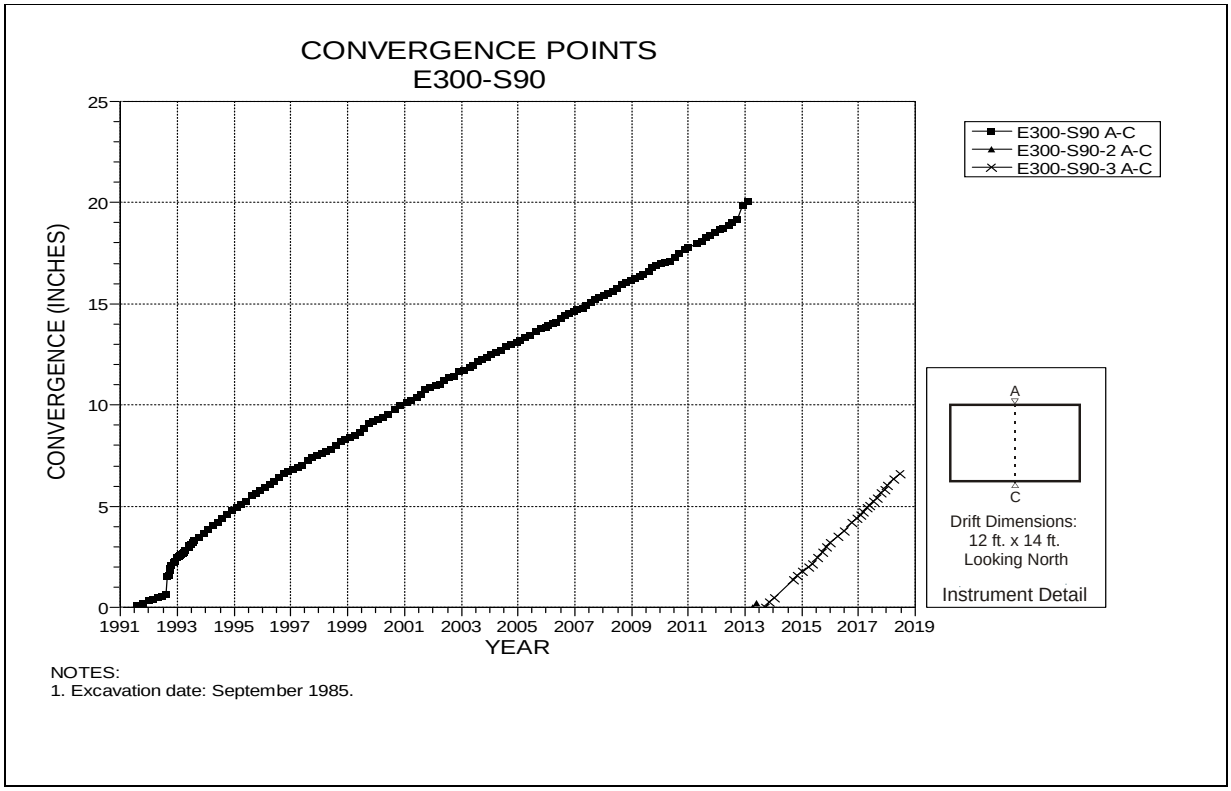

NOTES:
1. Excavation date: September 1985.

Figure 4-102 Convergence Point Array – E300 S90 – Roof to Floor – Centerline

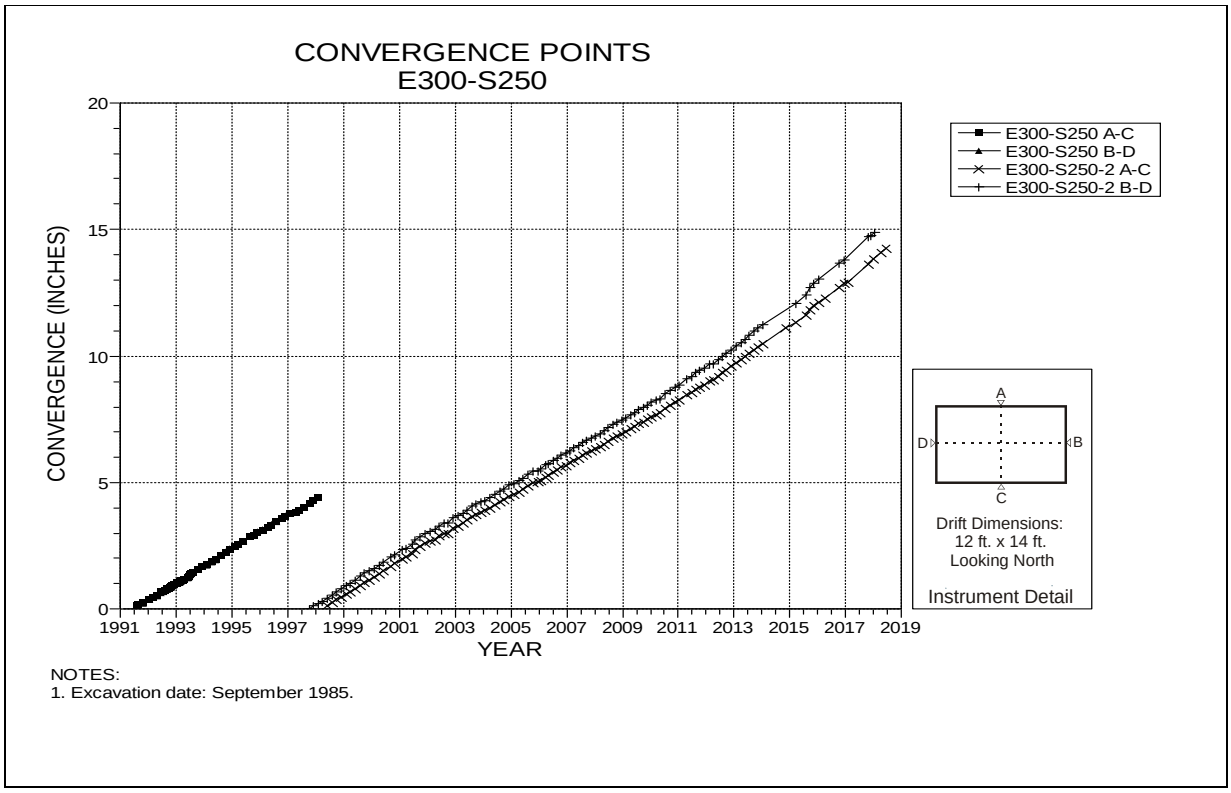

Figure 4-103 Convergence Point Array – E300 S250 – All Chords

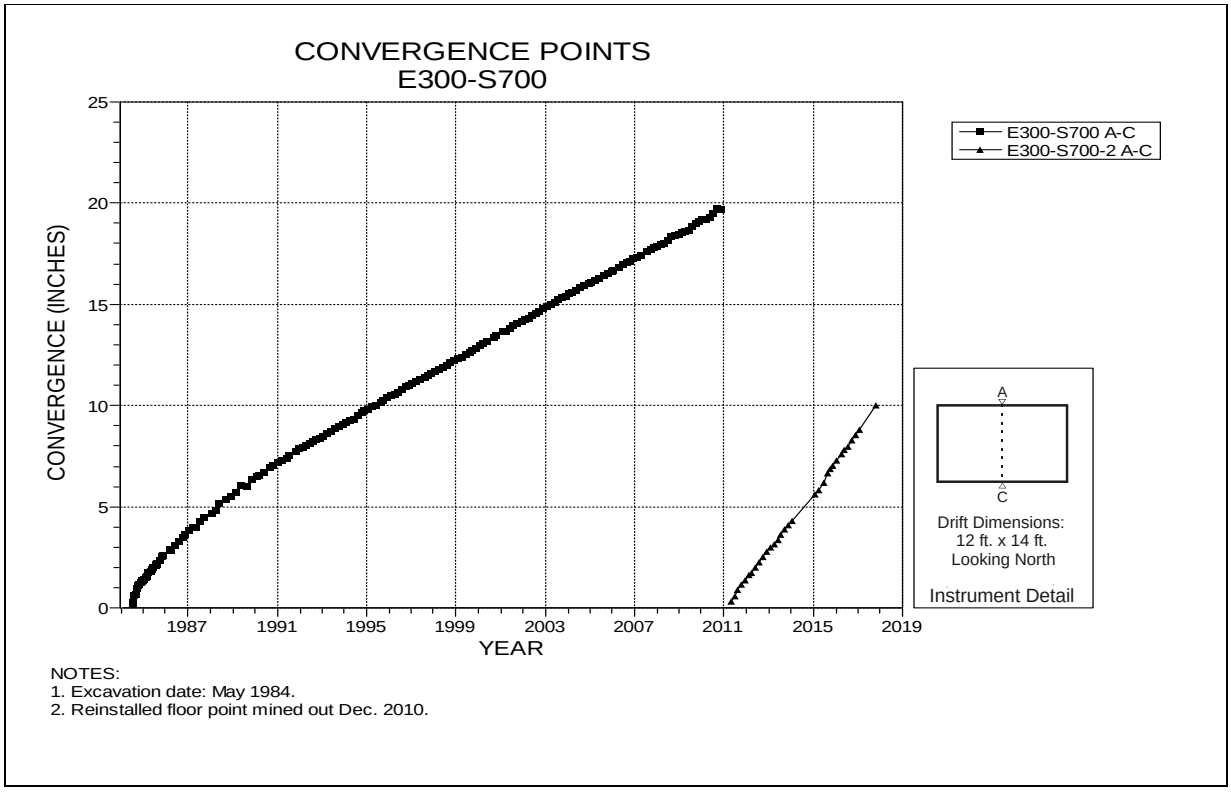

Figure 4-104 Convergence Point Array – E300 S700 – Roof to Floor – Centerline

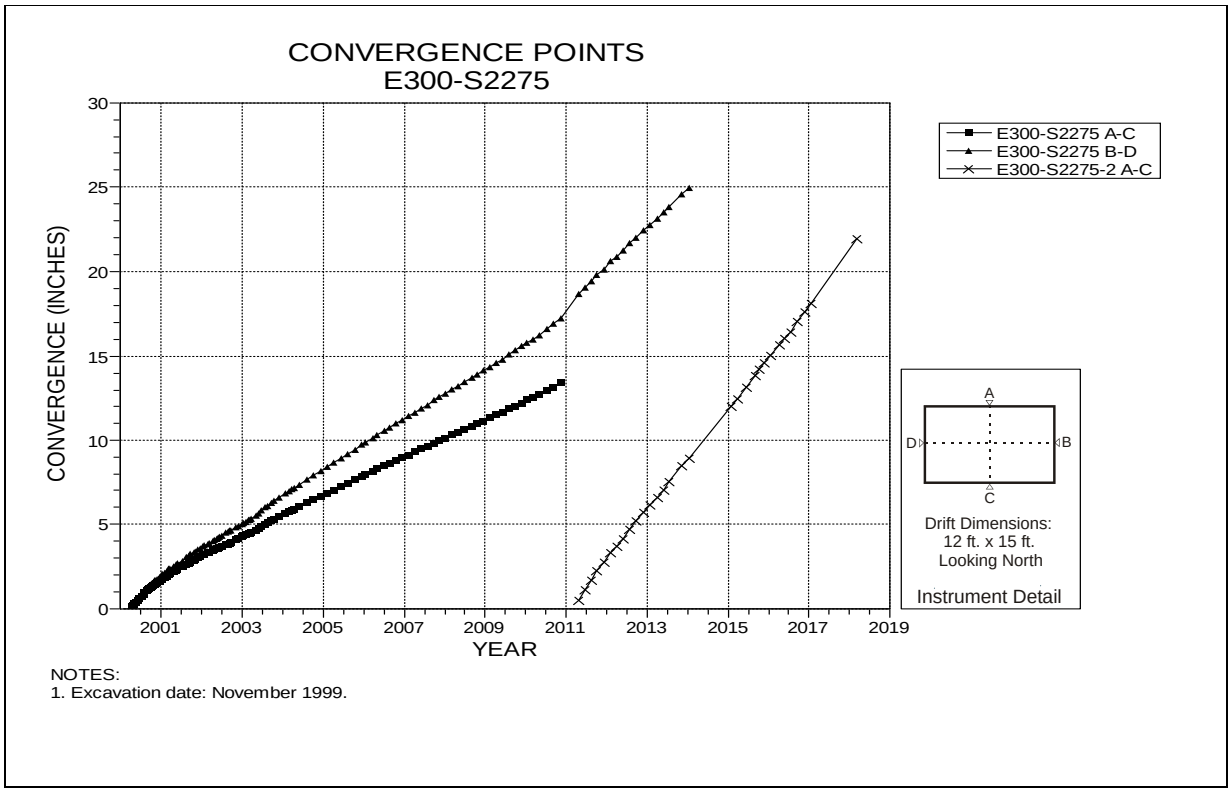

Figure 4-105 Convergence Point Array – E300 S2275 – Roof to Floor – Centerline

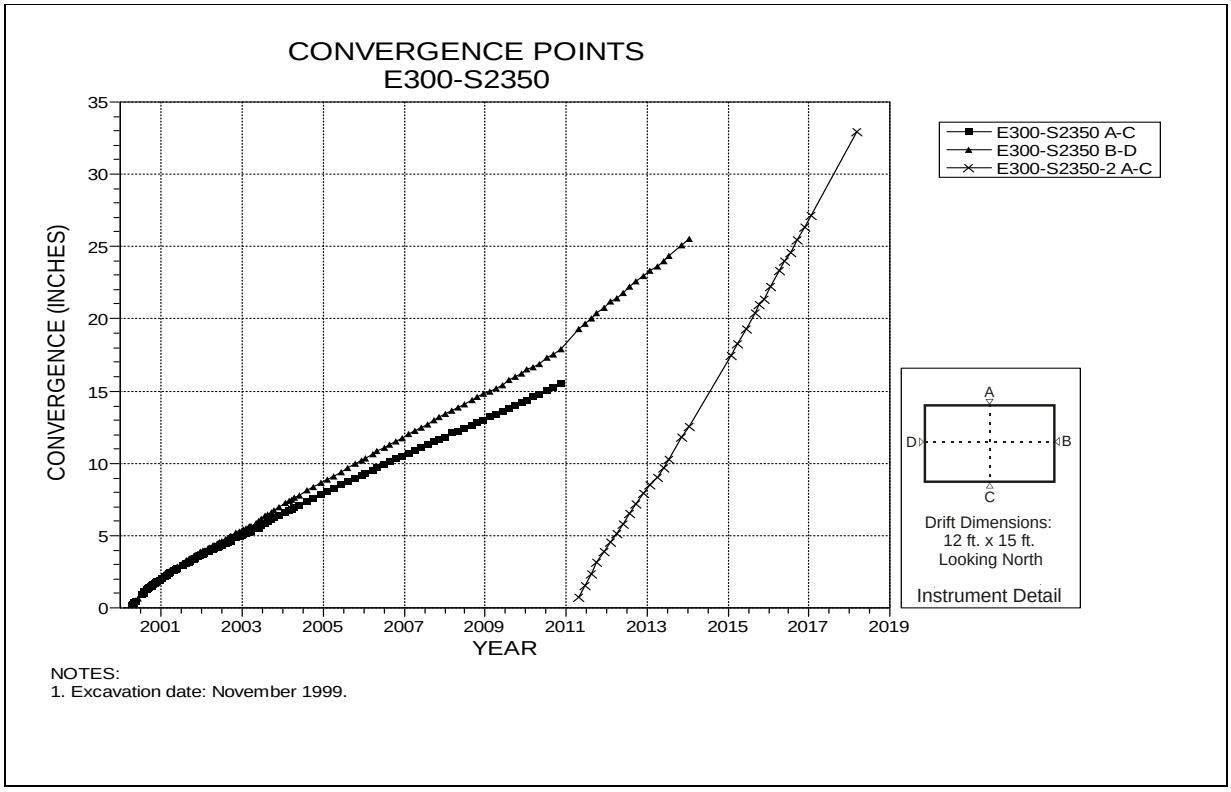

Figure 4-106 Convergence Point Array – E300 S2350 – Roof to Floor – Centerline

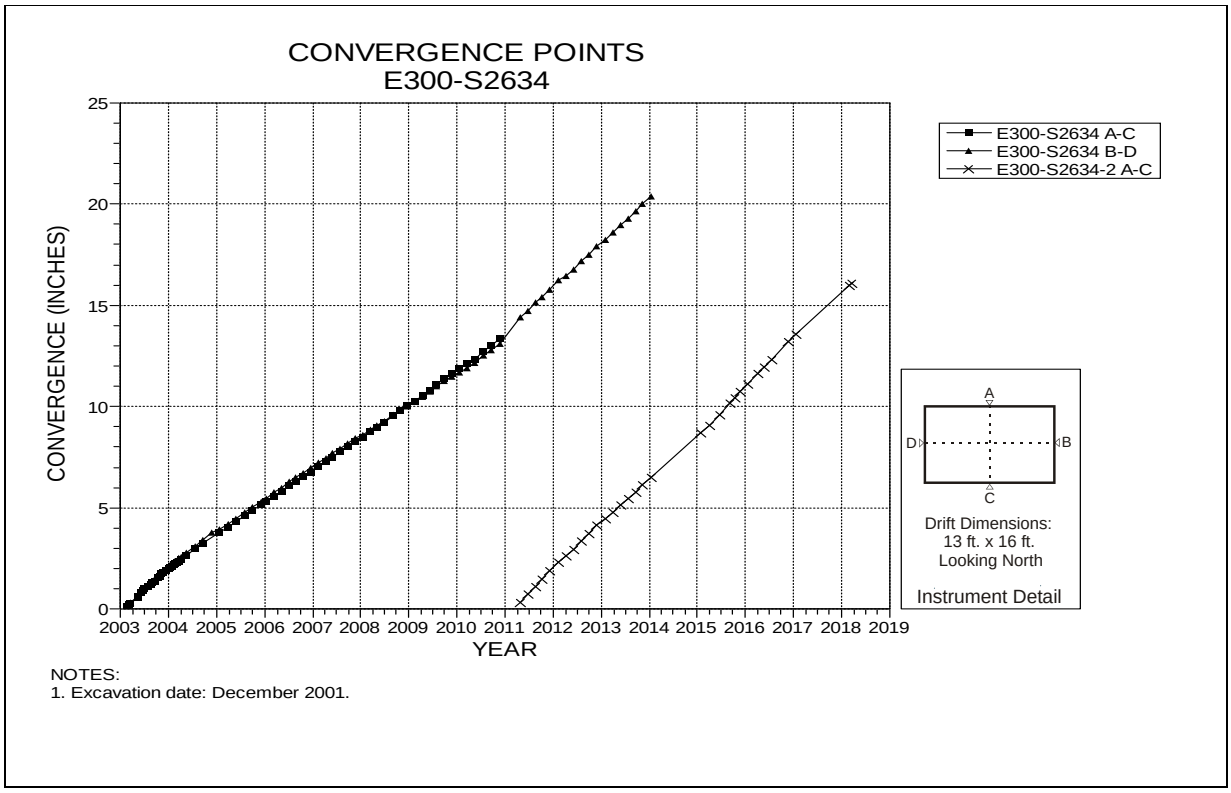

NOTES:
1. Excavation date: December 2001.

Figure 4-107 Convergence Point Array – E300 S2634 – All Chords

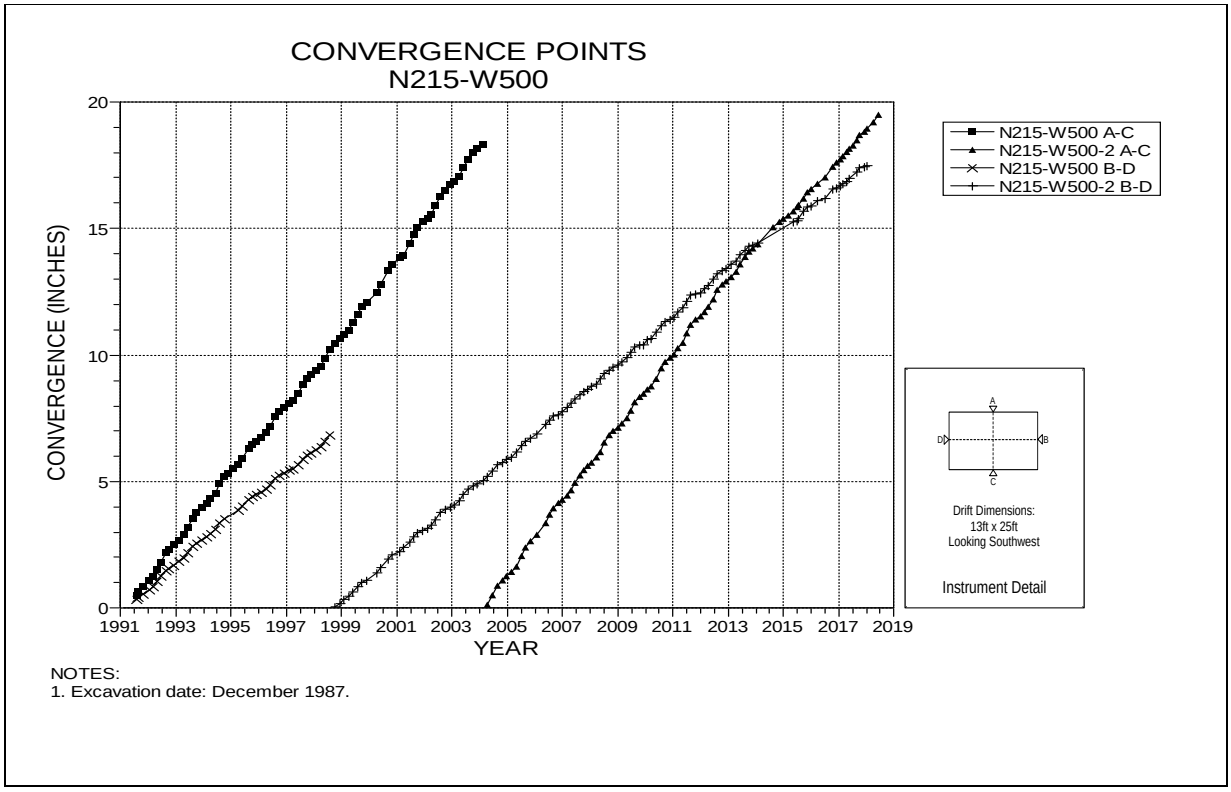

NOTES:
1. Excavation date: December 1987.

Figure 4-108 Convergence Point Array – N215 W500 – All Chords

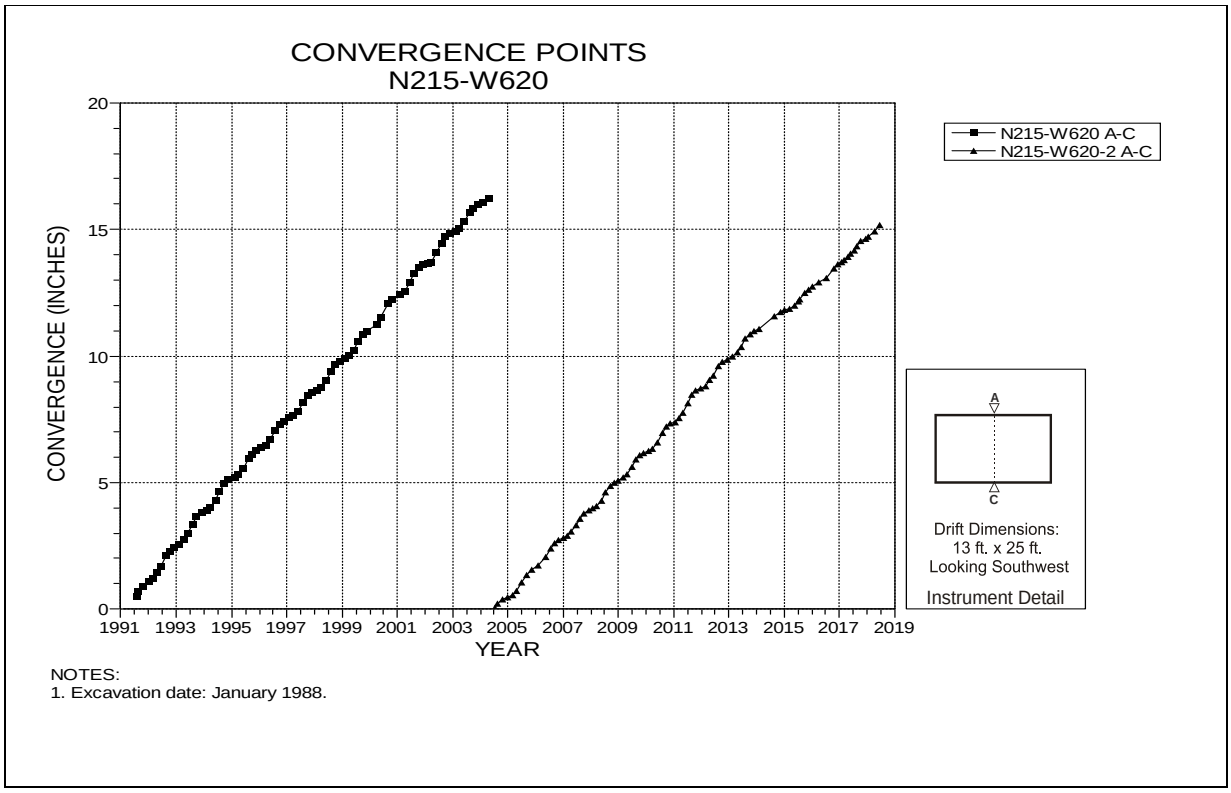

Figure 4-109 Convergence Point Array – N215 W620 – Roof to Floor – Centerline

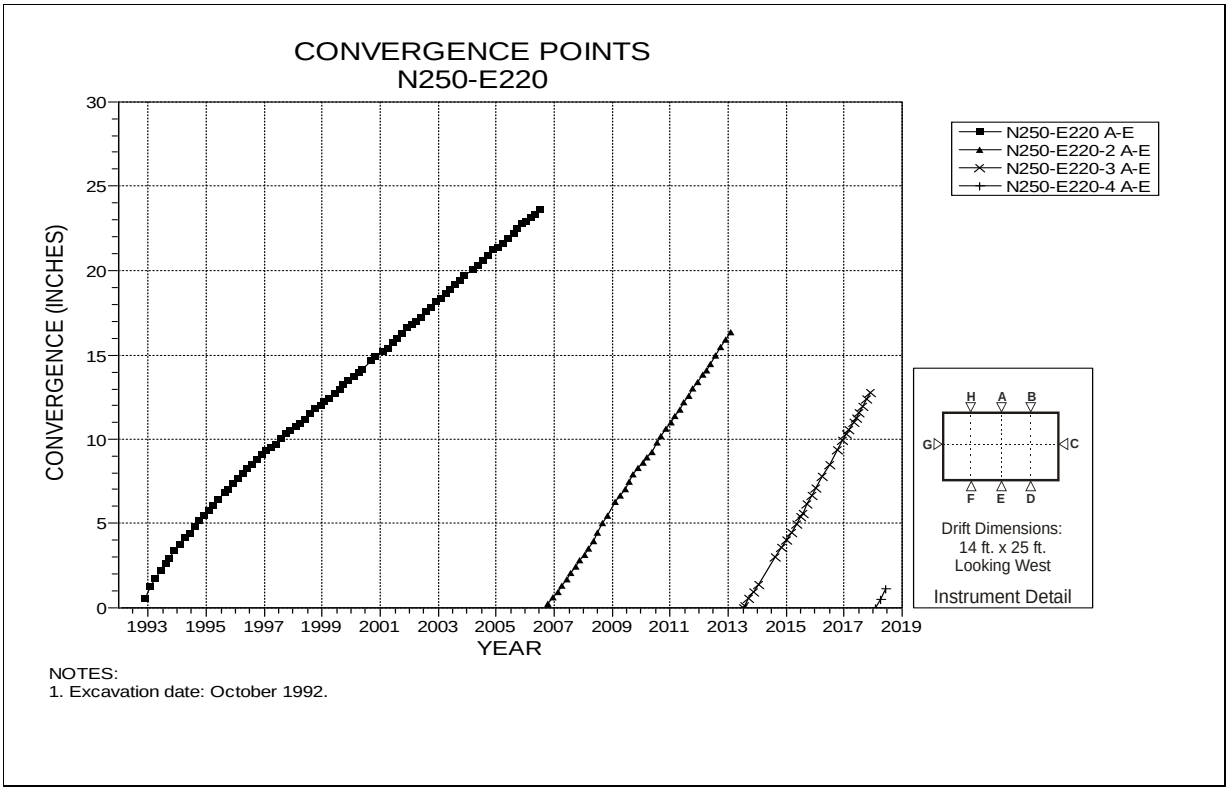

Figure 4-110 Convergence Point Array – N250 E220 – Roof to Floor – Centerline

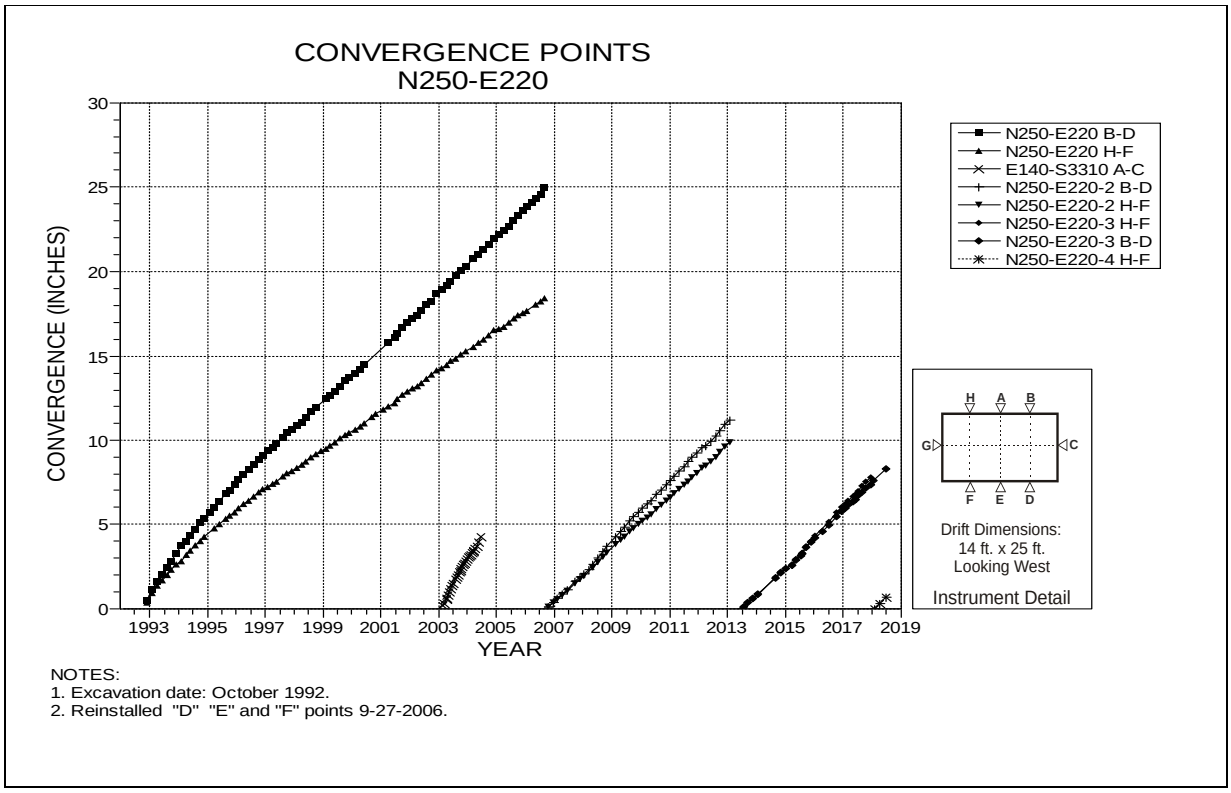

Figure 4-111 Convergence Point Array – N250 E220 – Roof to Floor – Quarter Points

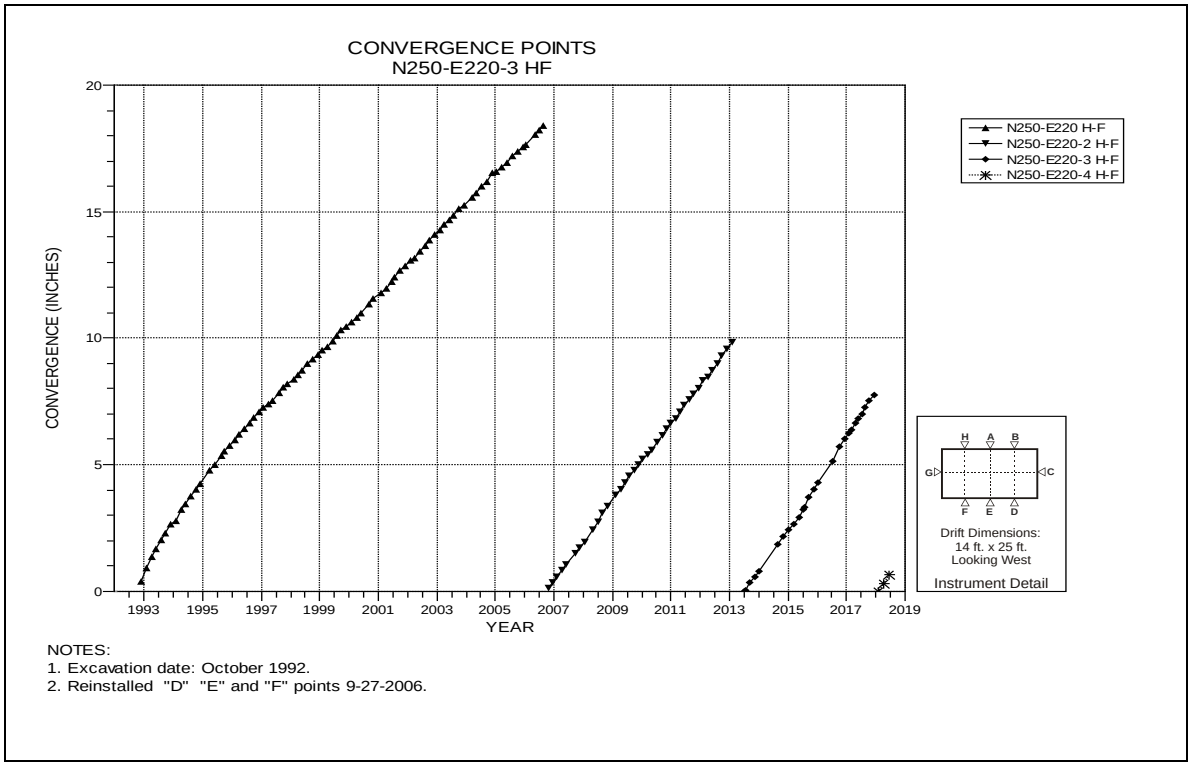

Figure 4-112 Convergence Point Array –
N250 E220 – Roof to Floor – West Quarter Point

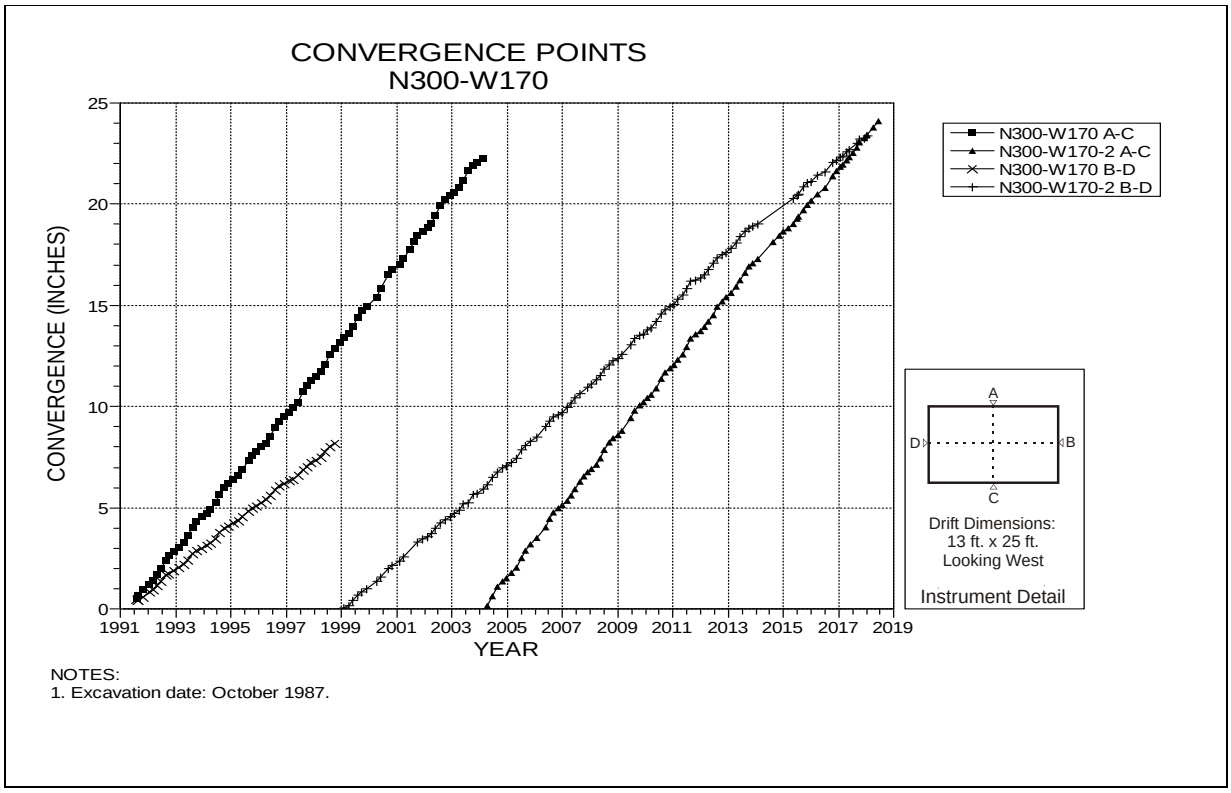

Figure 4-113 Convergence Point Array – E300 N170 – Roof to Floor – Centerline

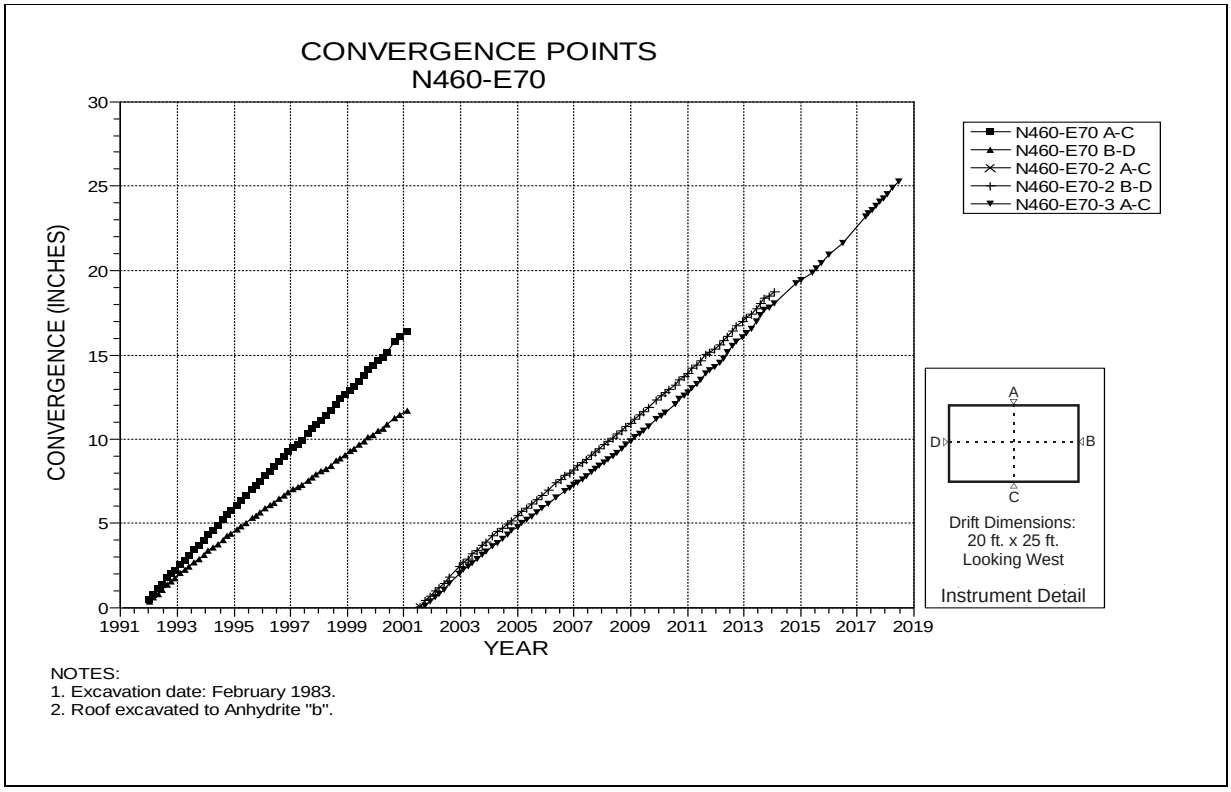

Figure 4-114 Convergence Point Array – E300 N170 – Roof to Floor - Centerline

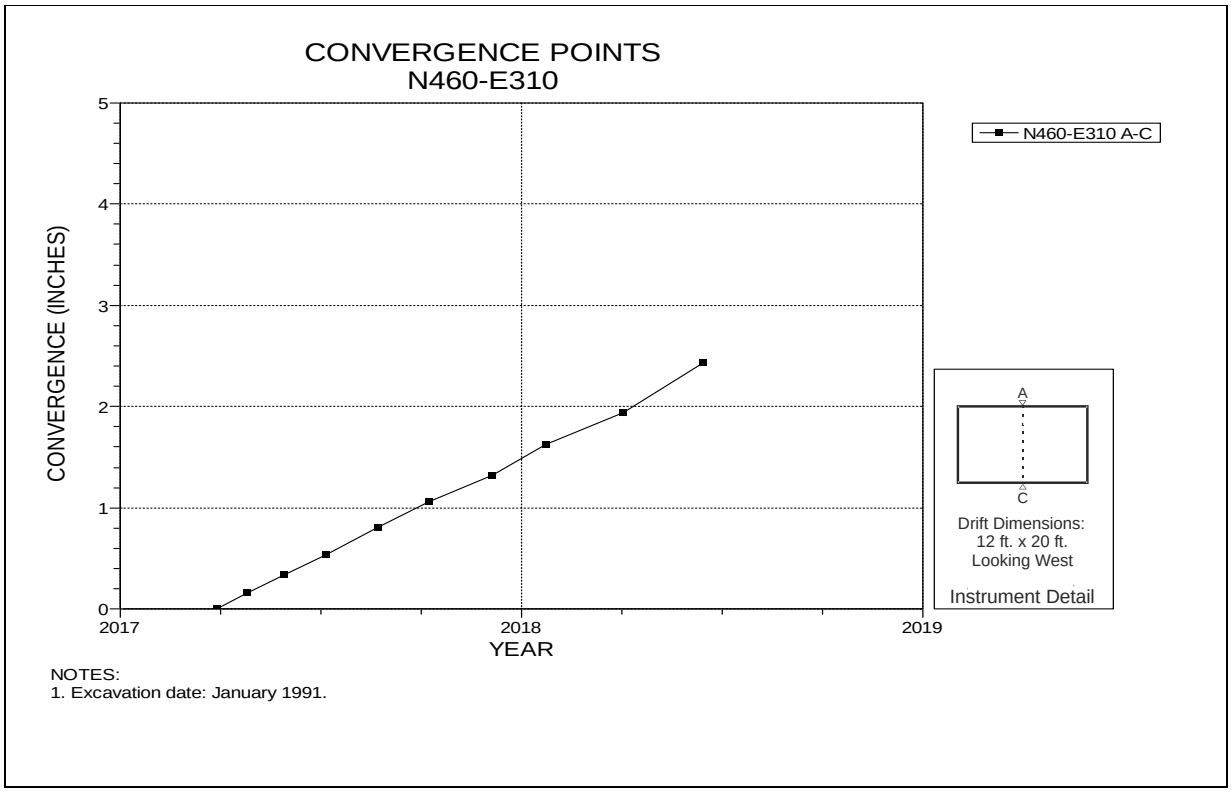

Figure 4-115 Convergence Point Array –N460 E70 – All Chords

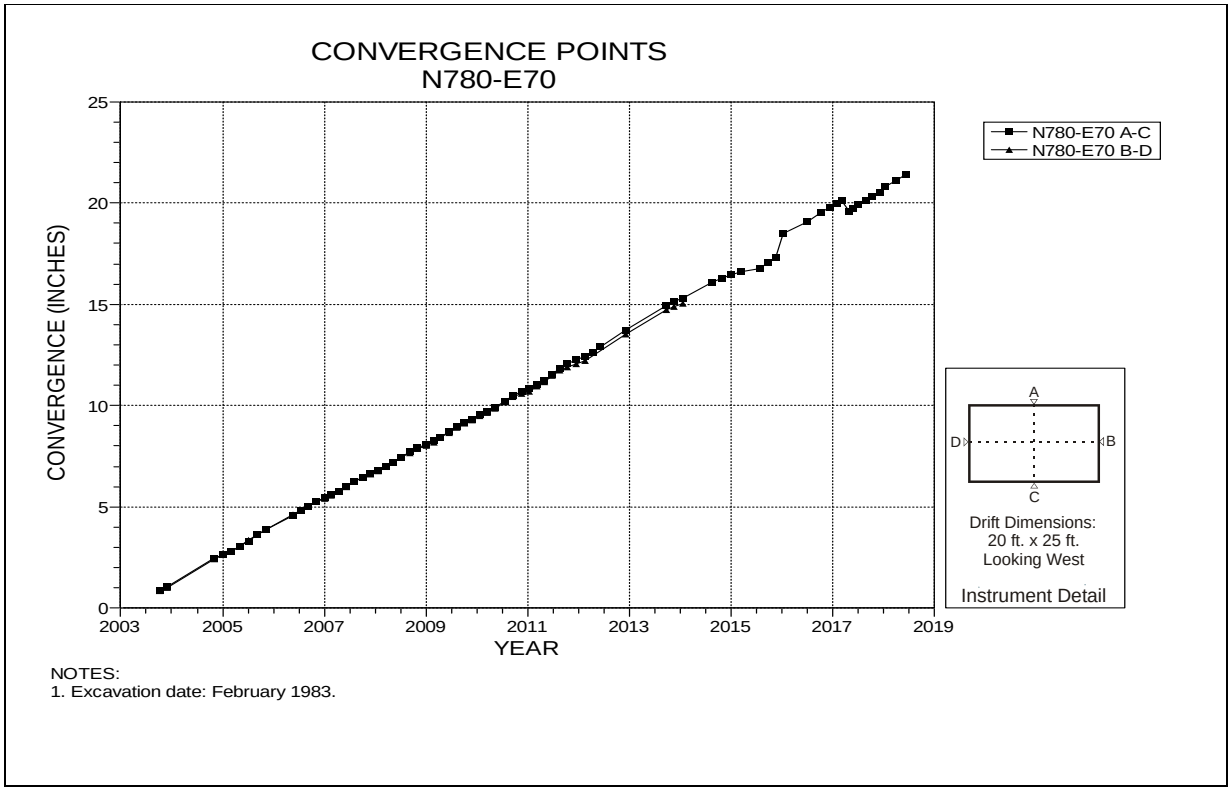

Figure 4-116 Convergence Point Array – N780 E70 – Roof to Floor – Centerline

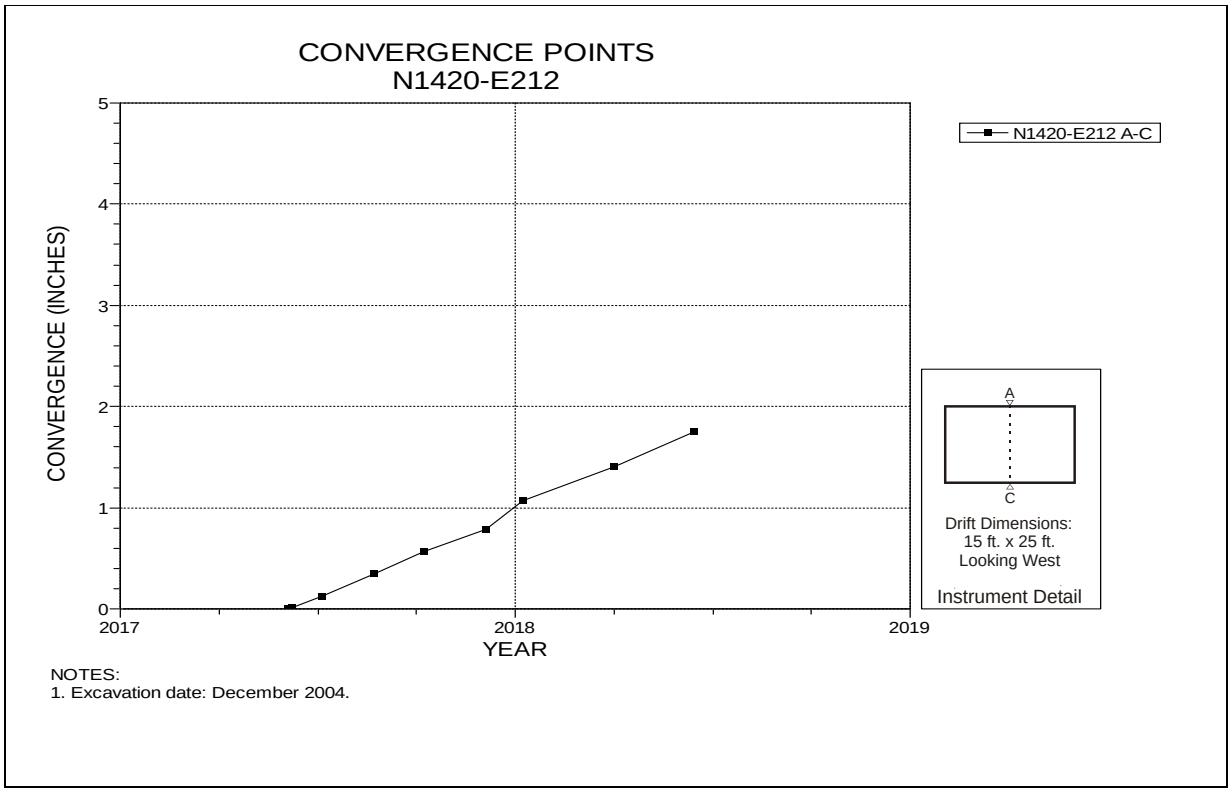

Figure 4-117 Convergence Point Array – N1420 E212 – All Chords

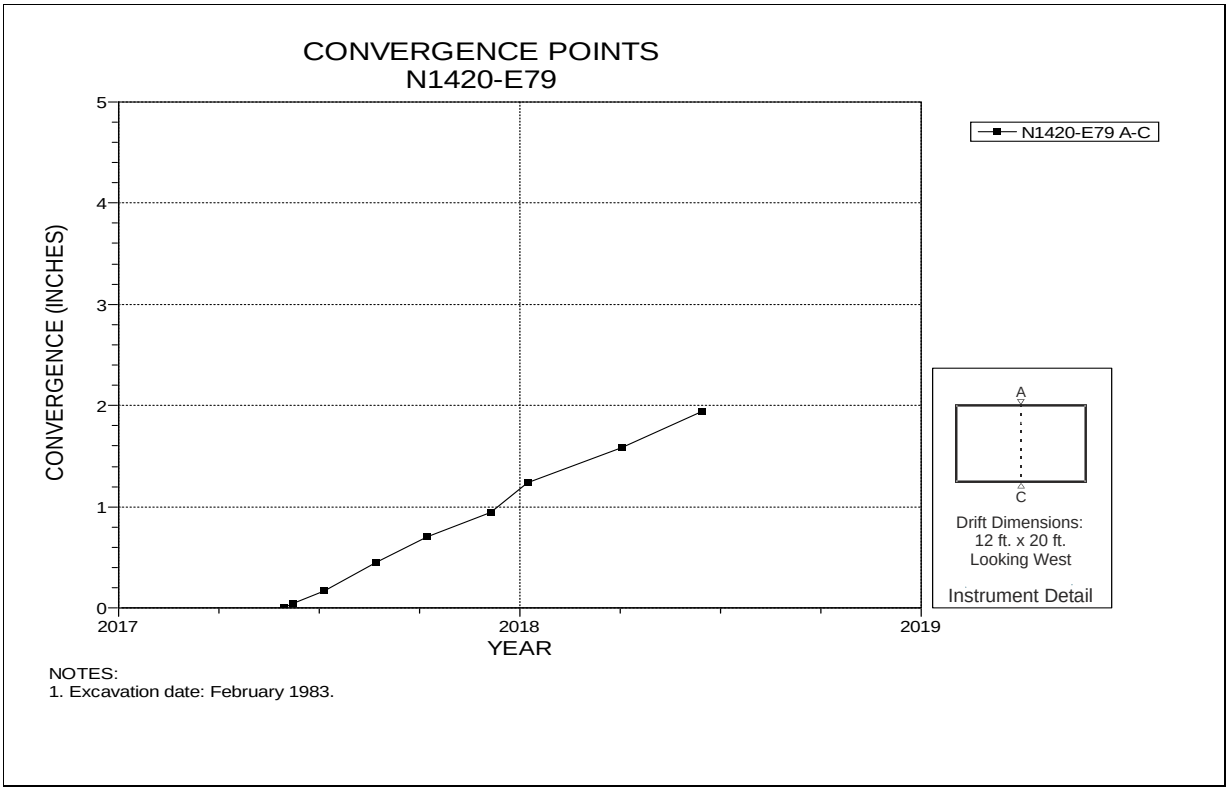

Figure 4-118 Convergence Point Array – N1420 E79 – Roof to Floor – Centerline

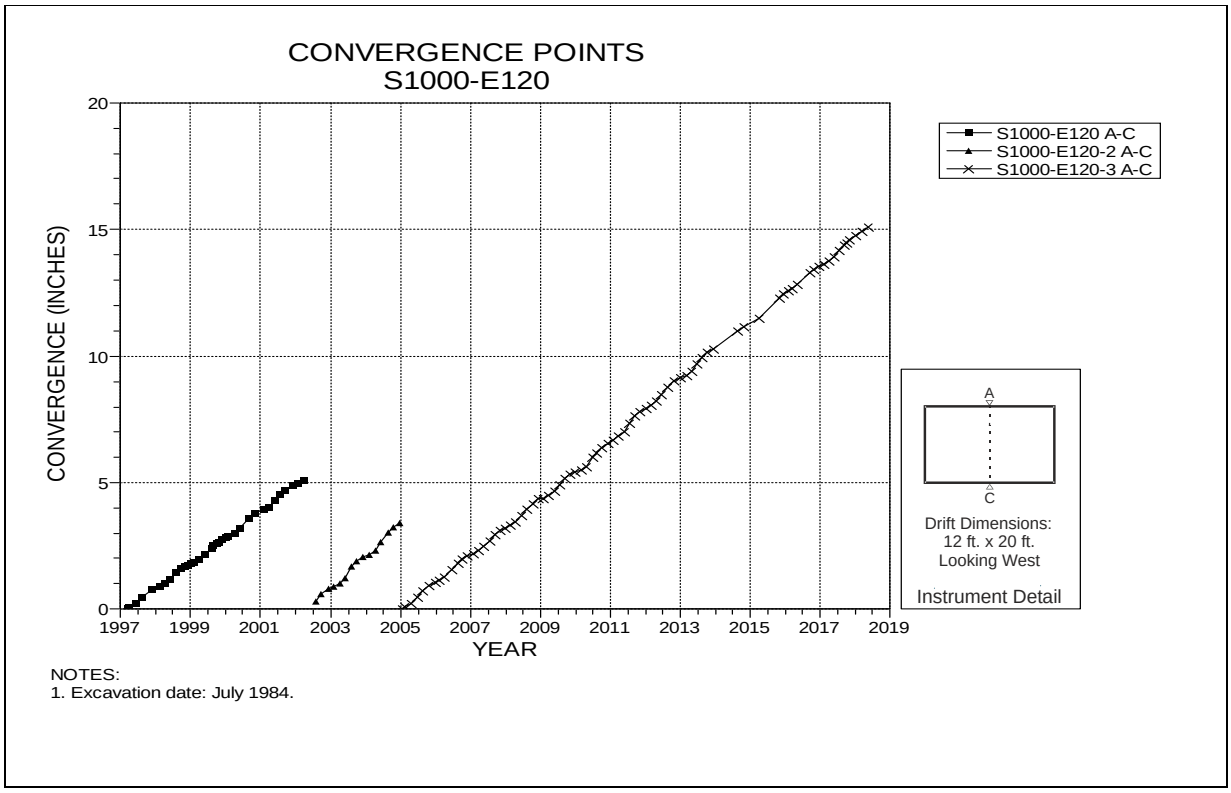

Figure 4-119 Convergence Point Array – S1000 E120 – Roof to Floor – Centerline

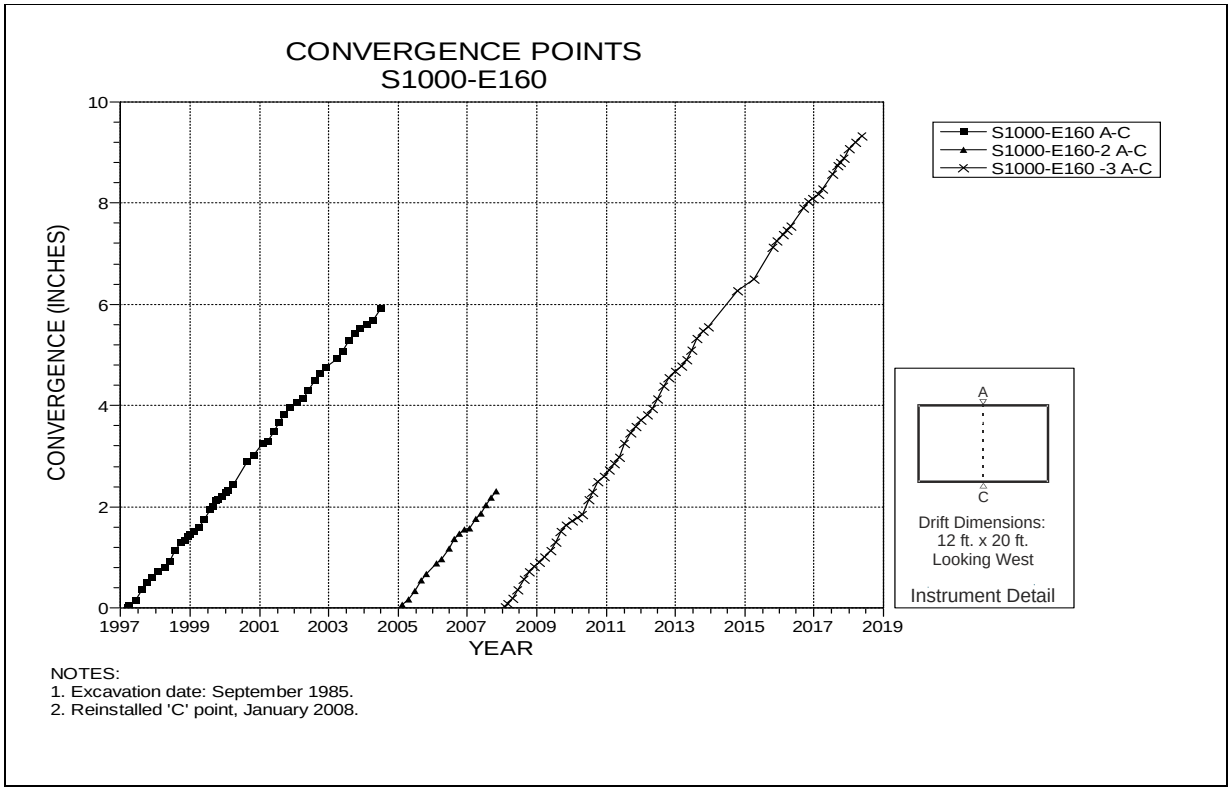

Figure 4-120 Convergence Point Array – S1000 E160 – Roof to Floor – Centerline

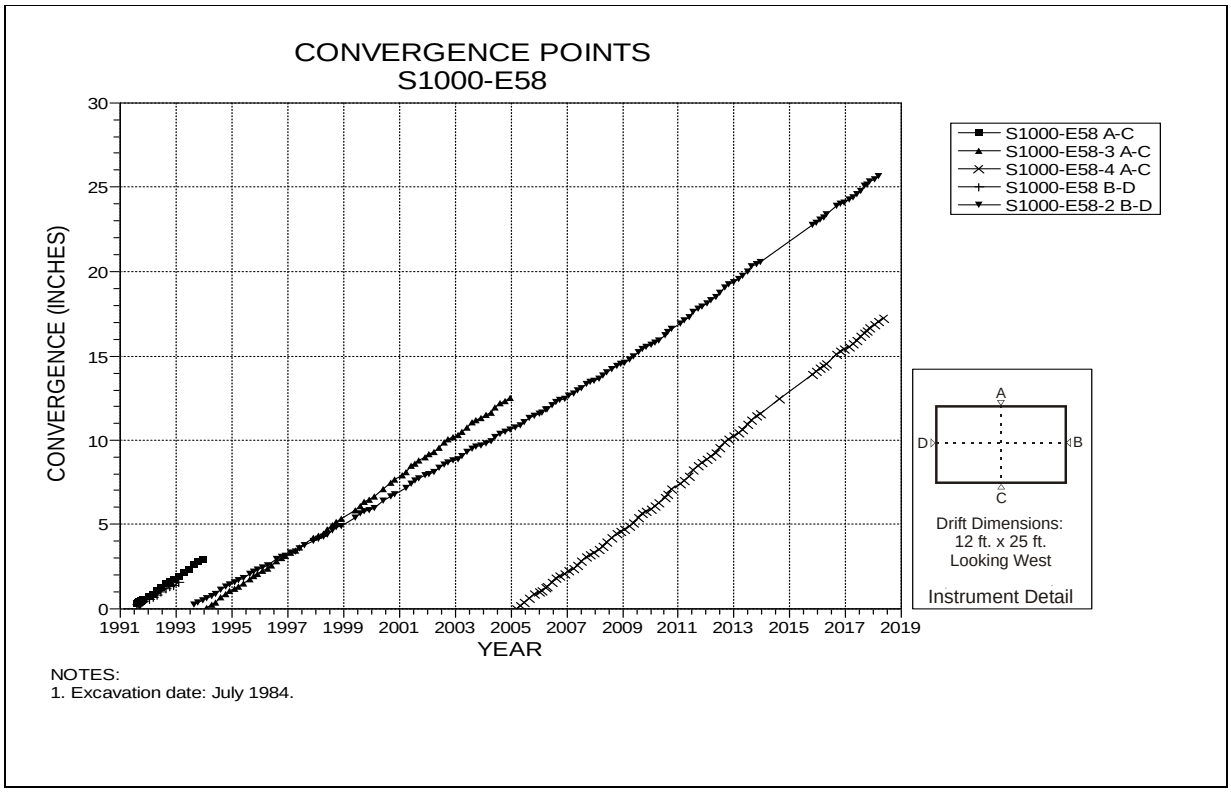

Figure 4-121 Convergence Point Array – S1000 E58 – All Chords

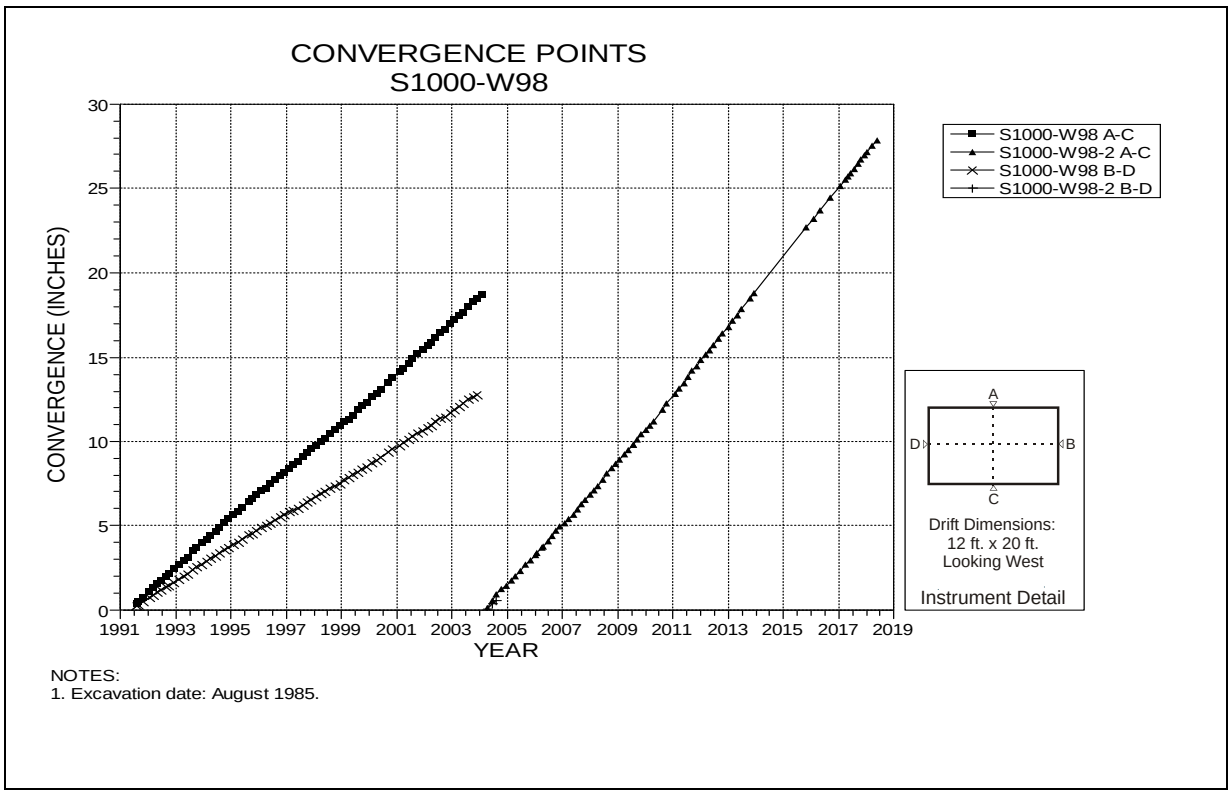

Figure 4-122 Convergence Point Array – S1000 W98 – All Chords

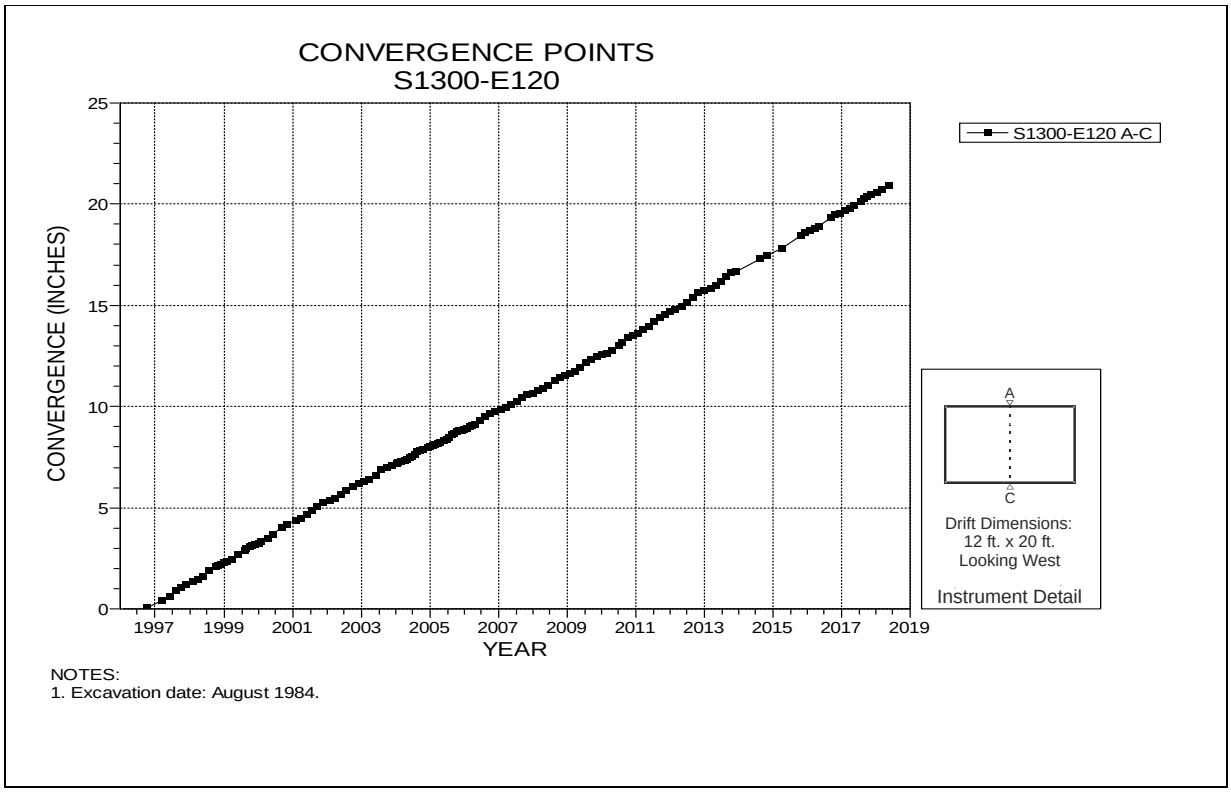

Figure 4-123 Convergence Point Array – S1300 E120 – Roof to Floor – Centerline

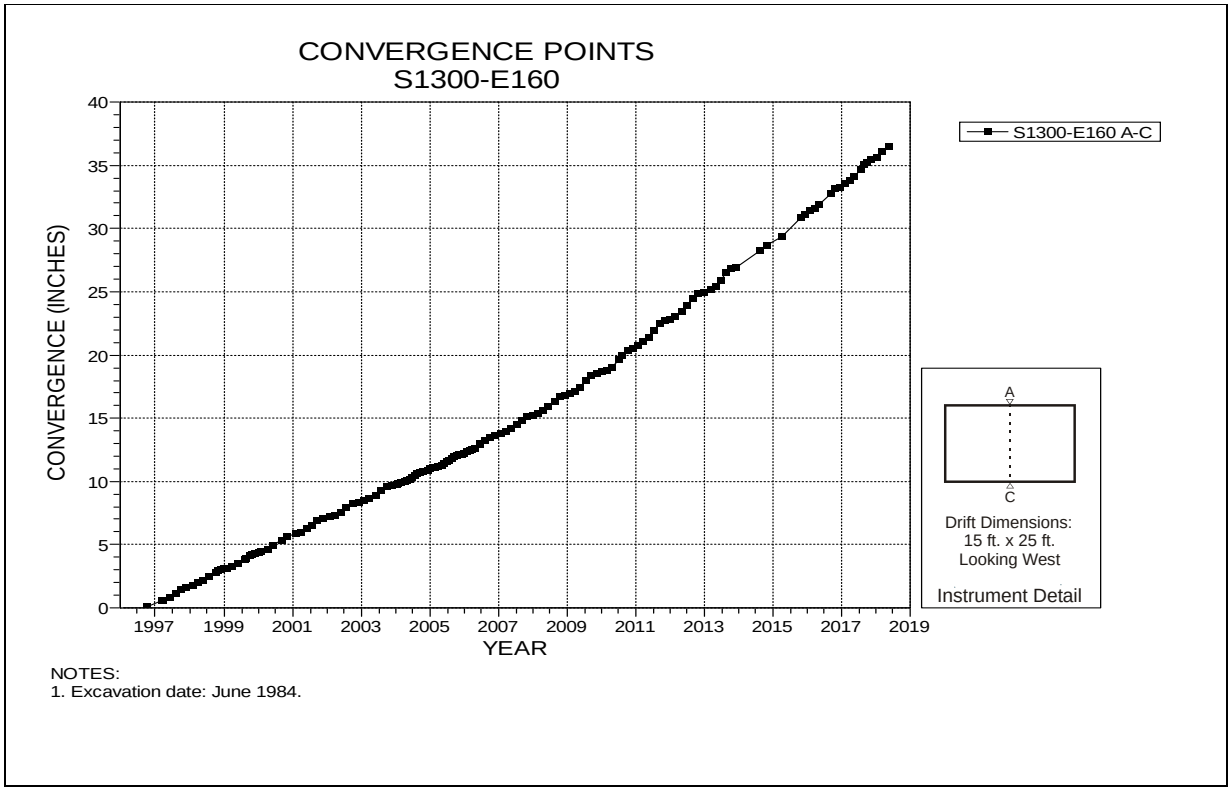

Figure 4-124 Convergence Point Array – S1300 E160 – Roof to Floor – Centerline

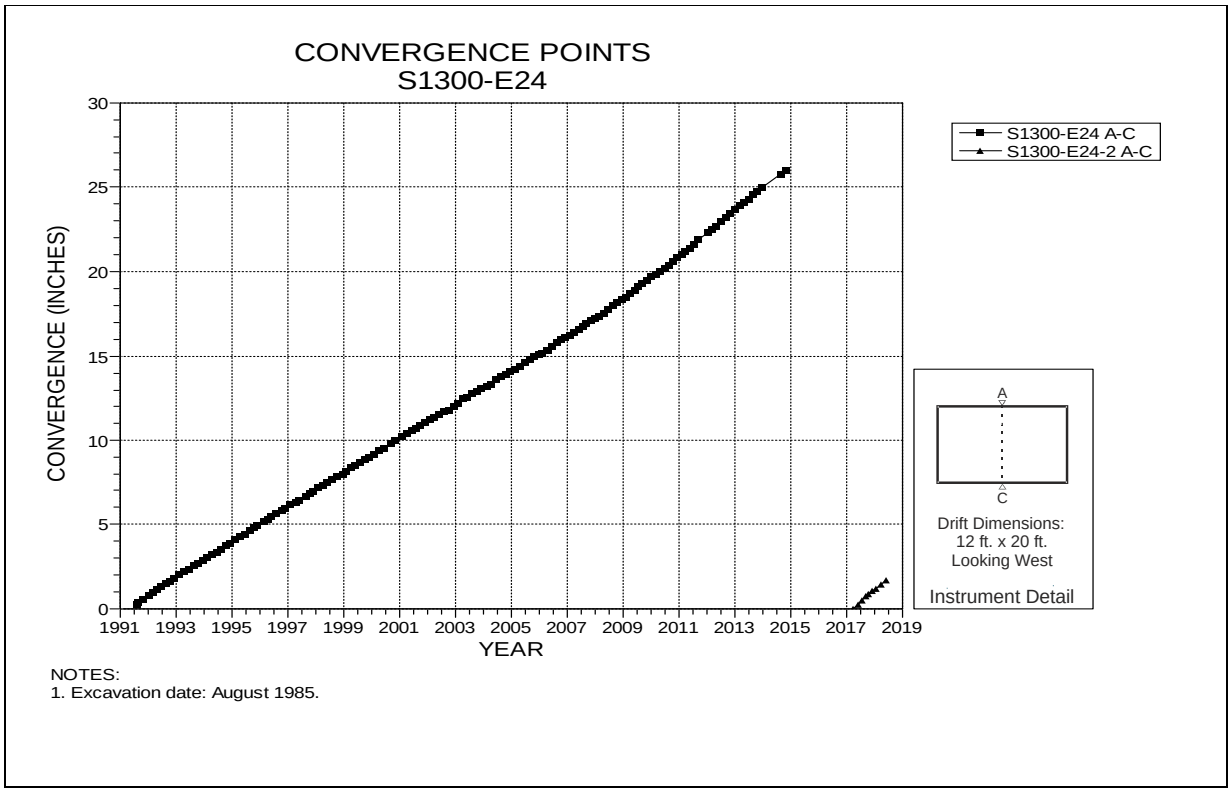

Figure 4-125 Convergence Point Array – S1300 E24 – Roof to Floor – Centerline

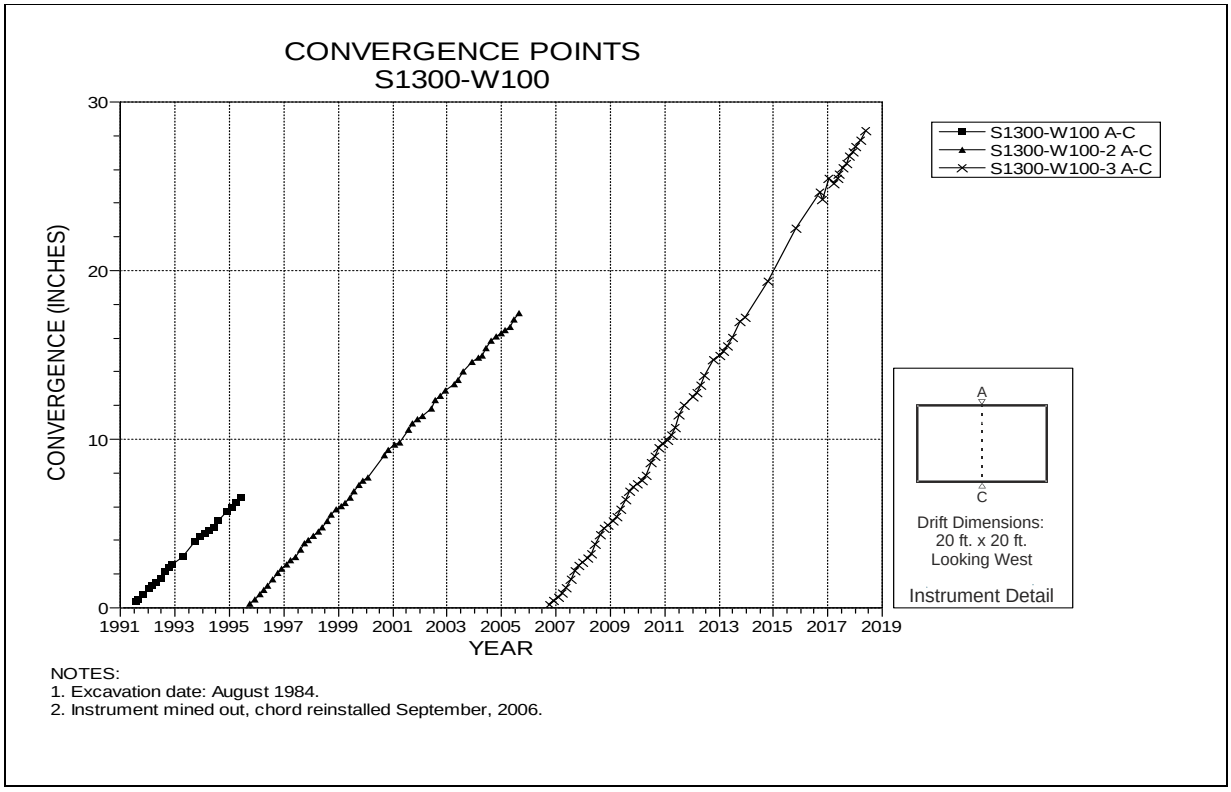

Figure 4-126 Convergence Point Array – S1300 W100 – Roof to Floor – Centerline

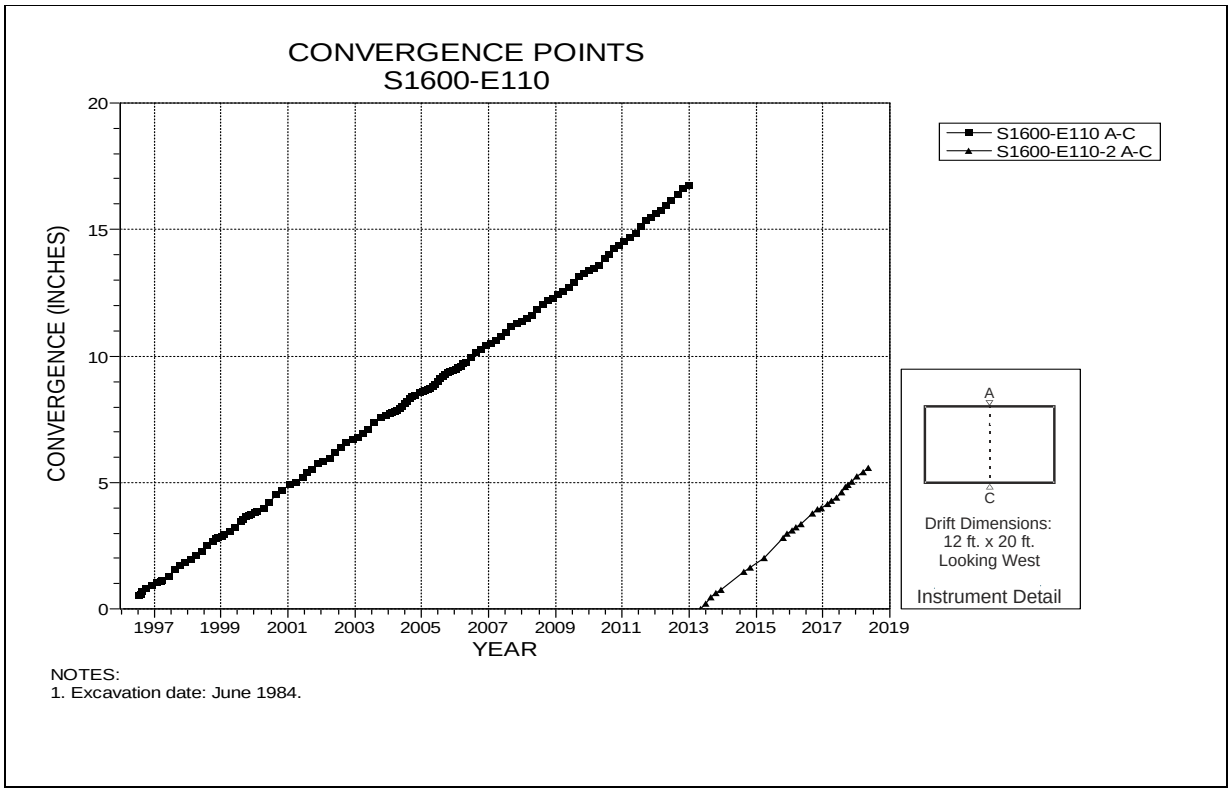

Figure 4-127 Convergence Point Array – S1600 E110 – Roof to Floor – Centerline

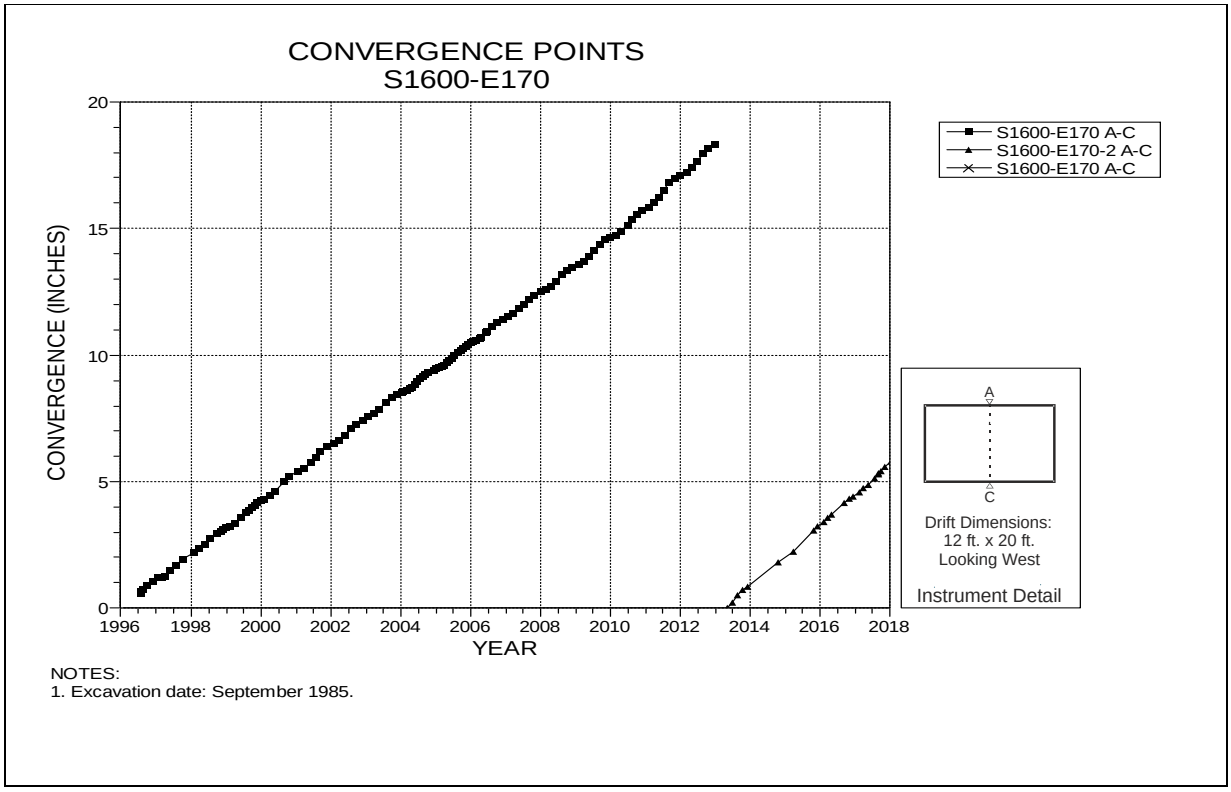

Figure 4-128 Convergence Point Array – S1600 E170 – Roof to Floor – Centerline

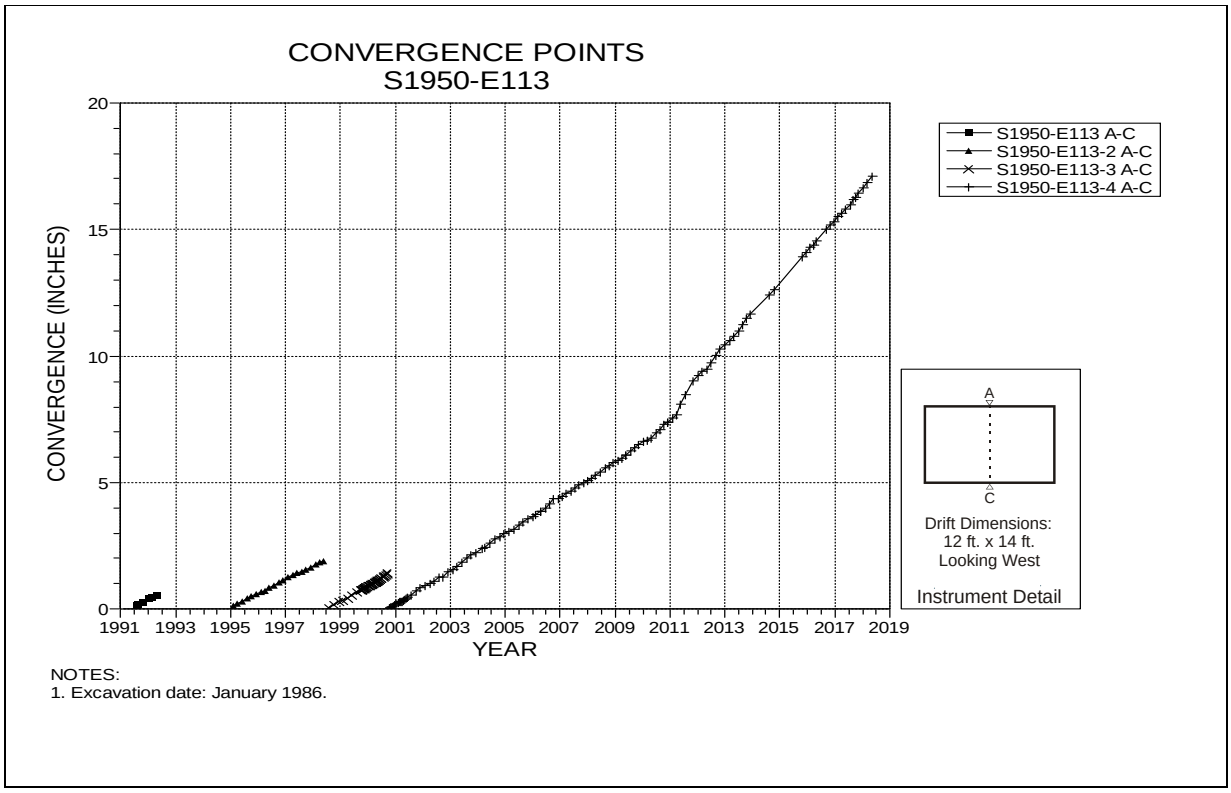

Figure 4-129 Convergence Point Array – S1950 E113 – Roof to Floor – Centerline

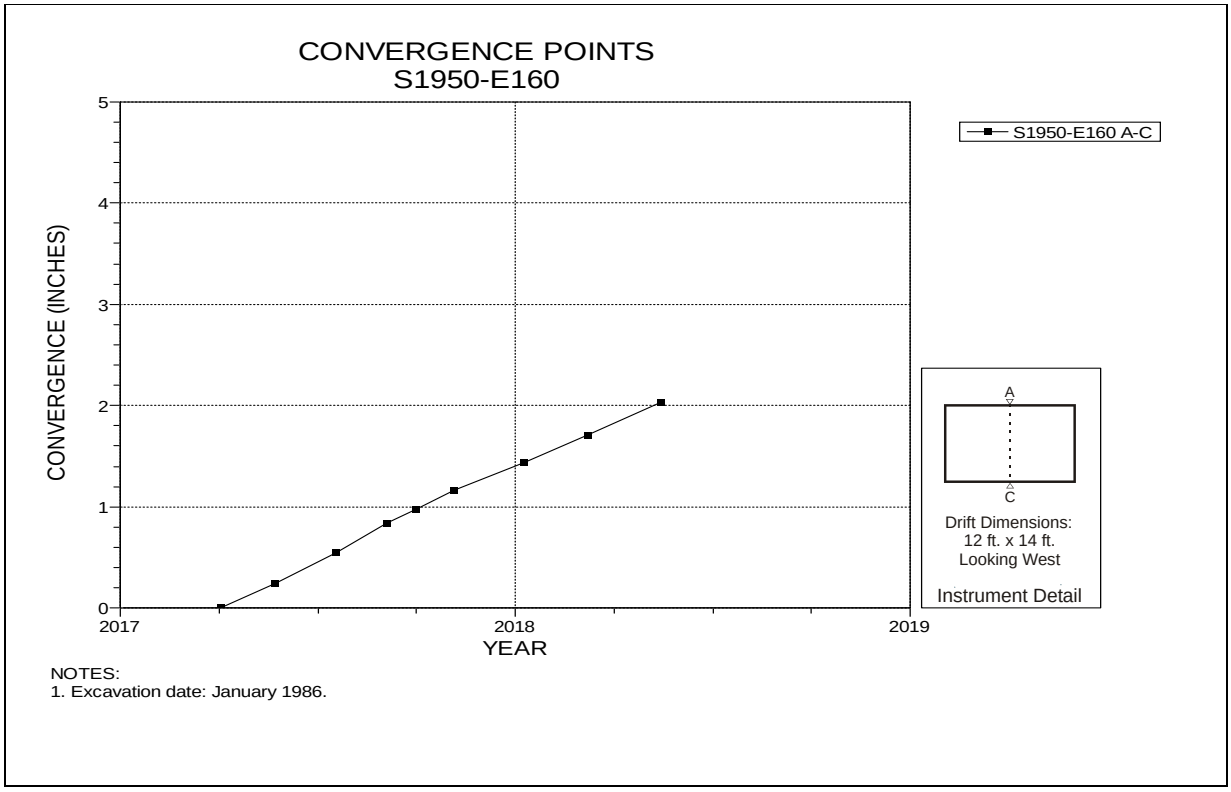

Figure 4-130 Convergence Point Array – S1950 E160 – Roof to Floor – Centerline

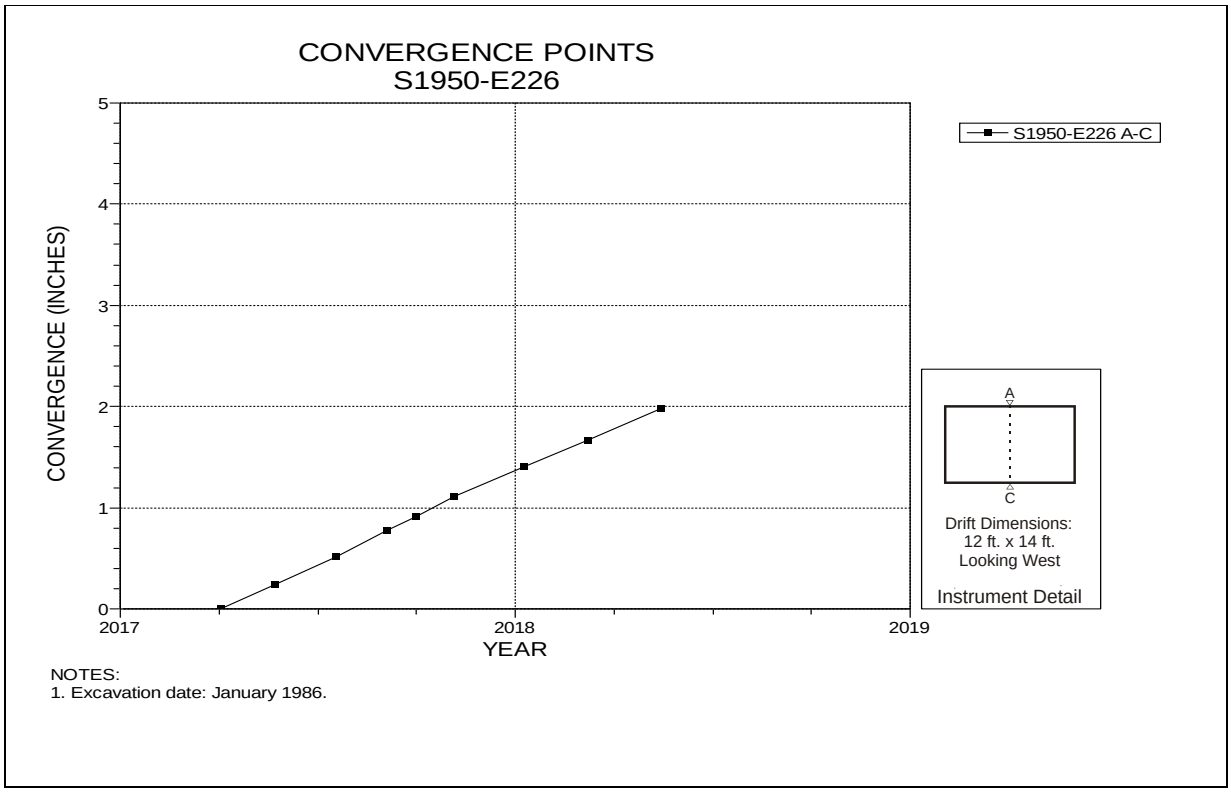

Figure 4-131 Convergence Point Array – S1950 E226 – Roof to Floor – Centerline

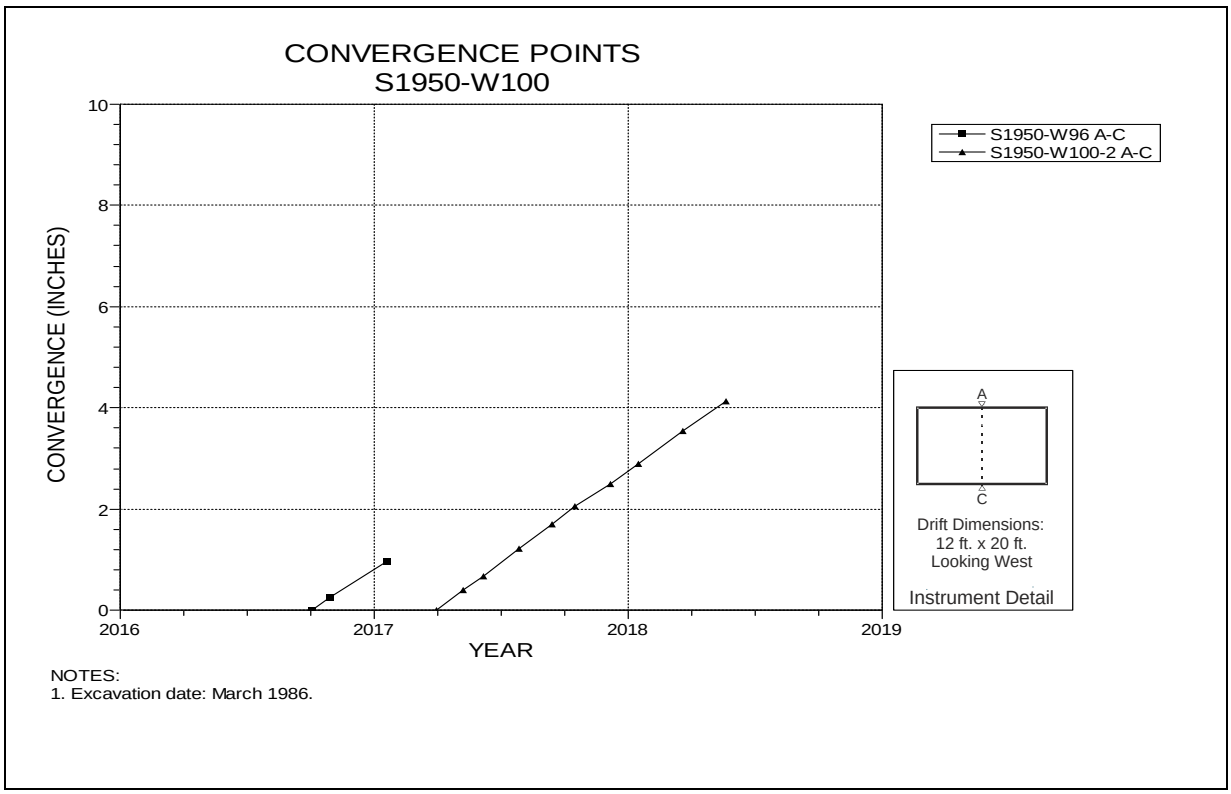

Figure 4-132 Convergence Point Array – S1950 W100 – Roof to Floor – Centerline

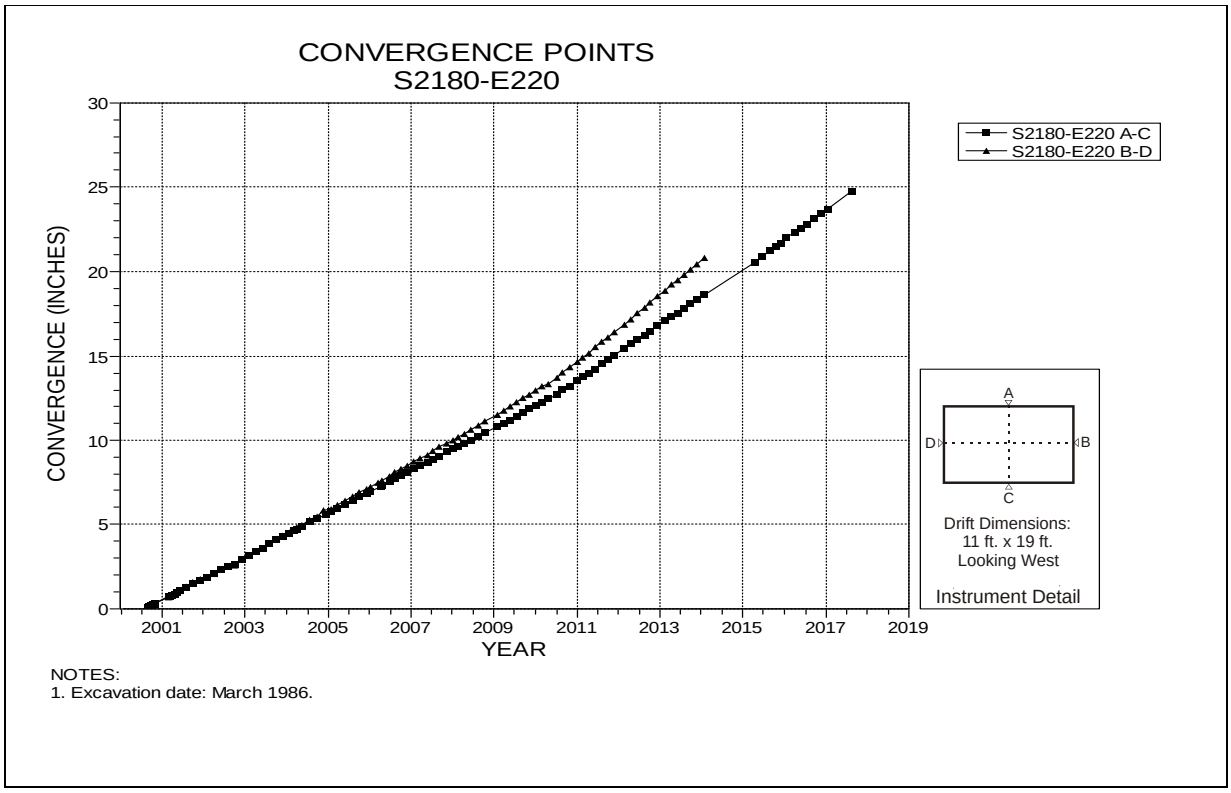

Figure 4-133 Convergence Point Array – S2180 E220 – All Chords

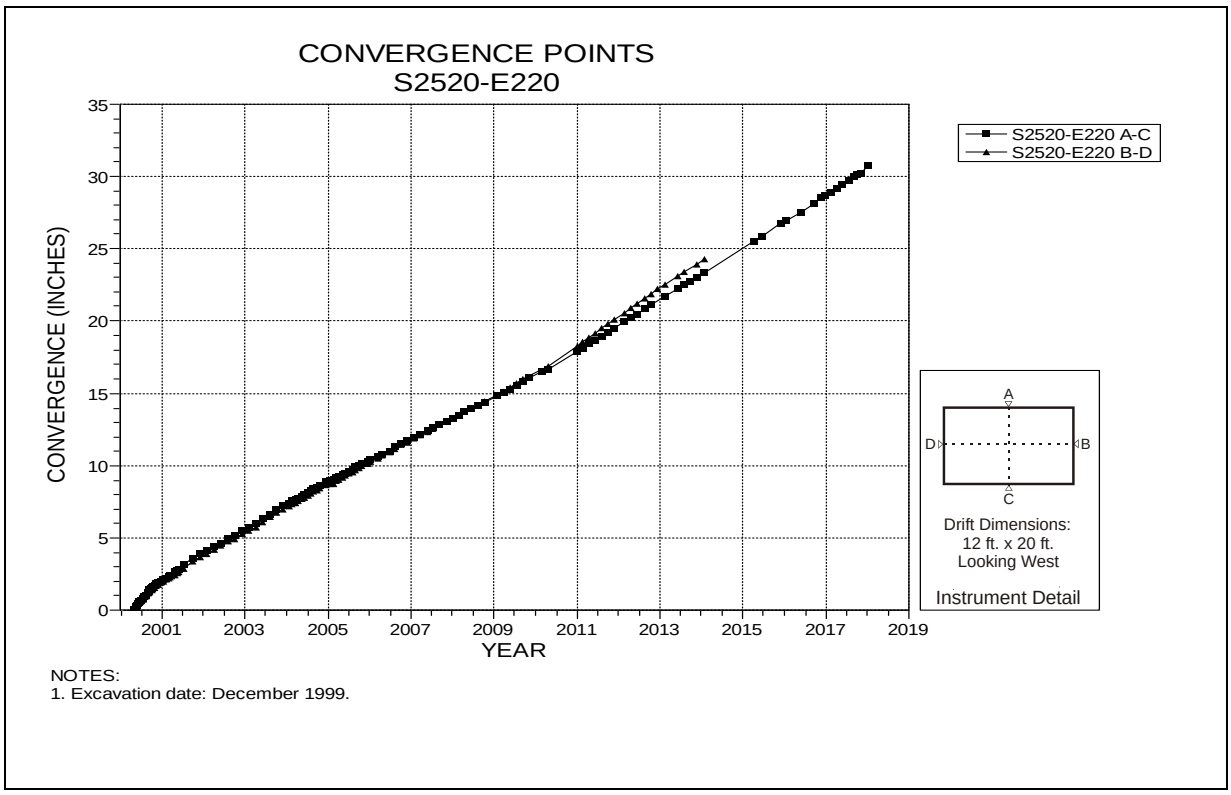

Figure 4-134 Convergence Point Array – S2520 E220 – All Chords

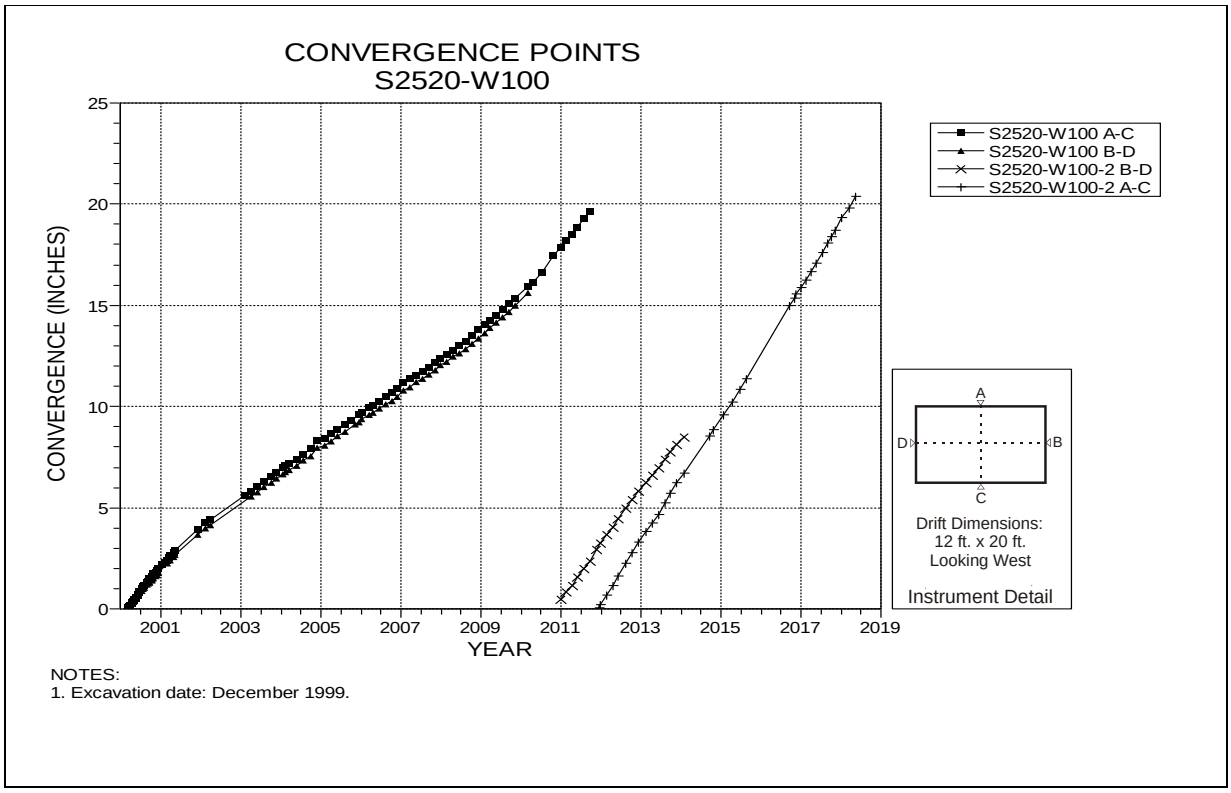

Figure 4-135 Convergence Point Array – S2520 W100 – All Chords

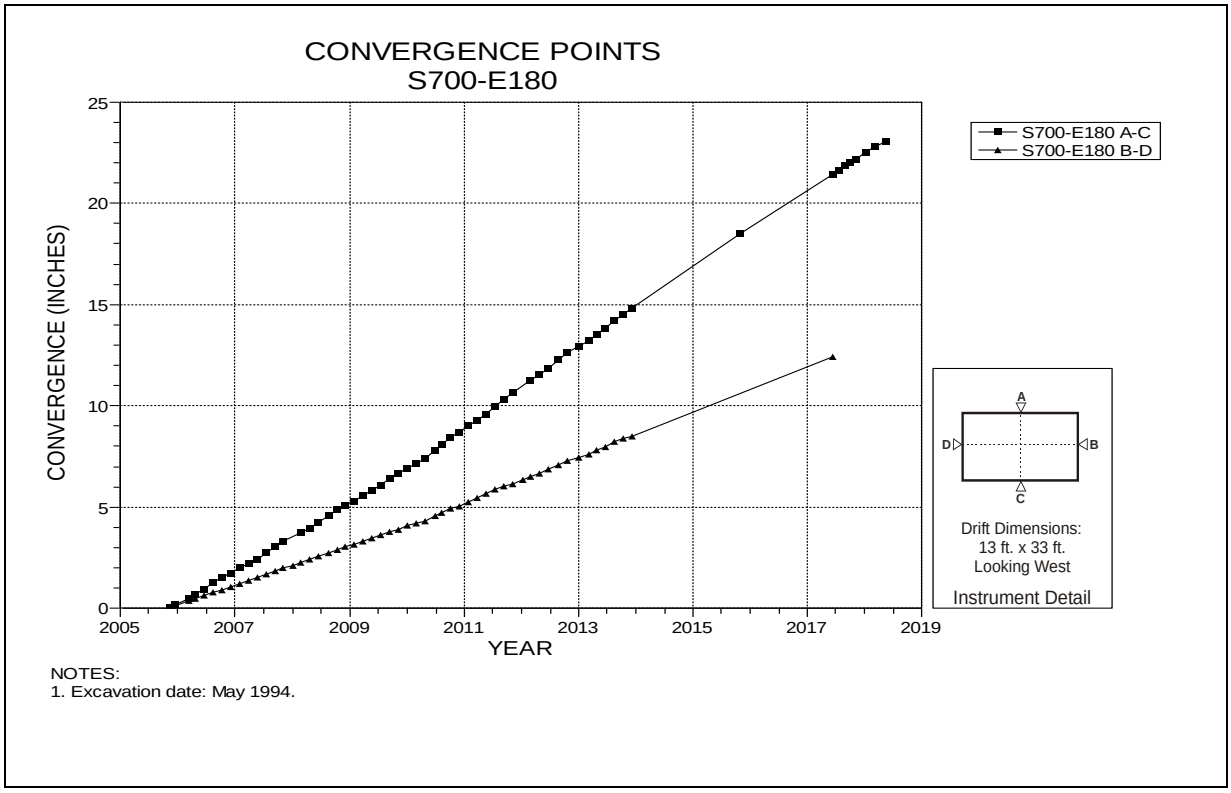

Figure 4-136 Convergence Point Array – S700 E180 – All Chords

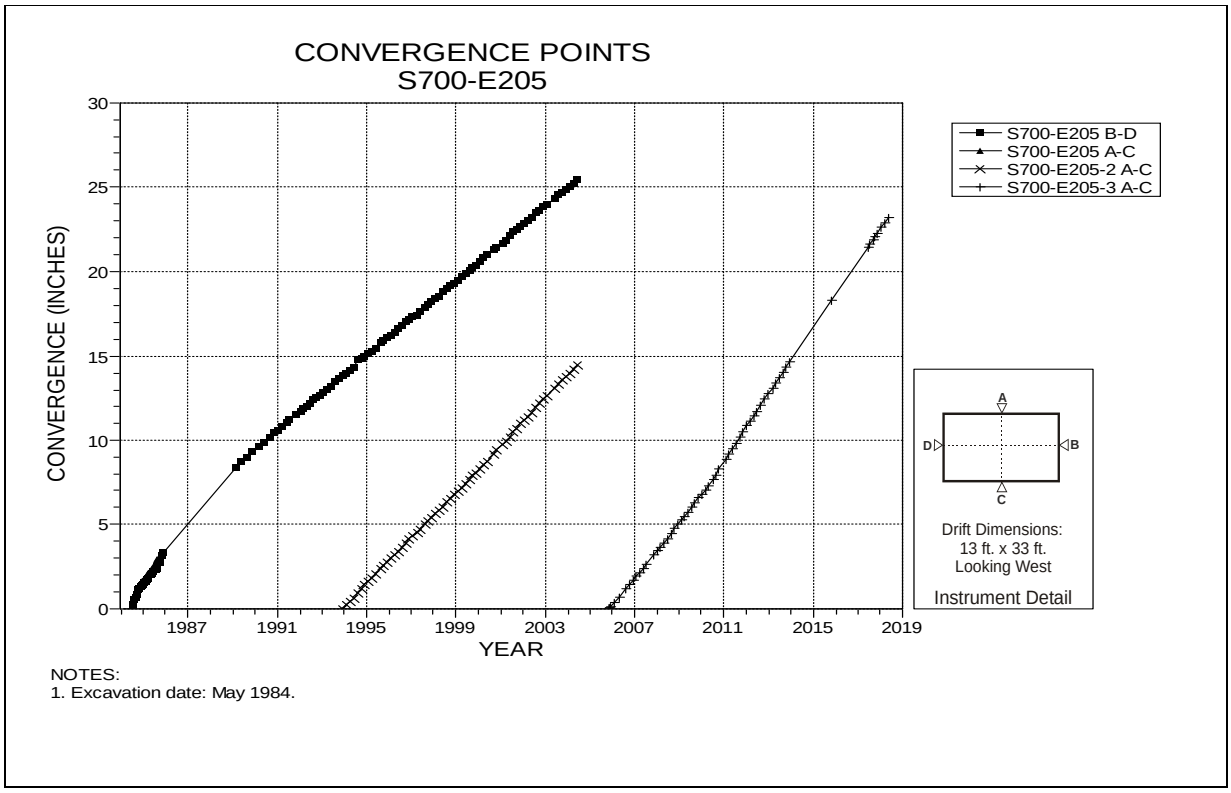

Figure 4-137 Convergence Point Array – S700 E205 – All Chords

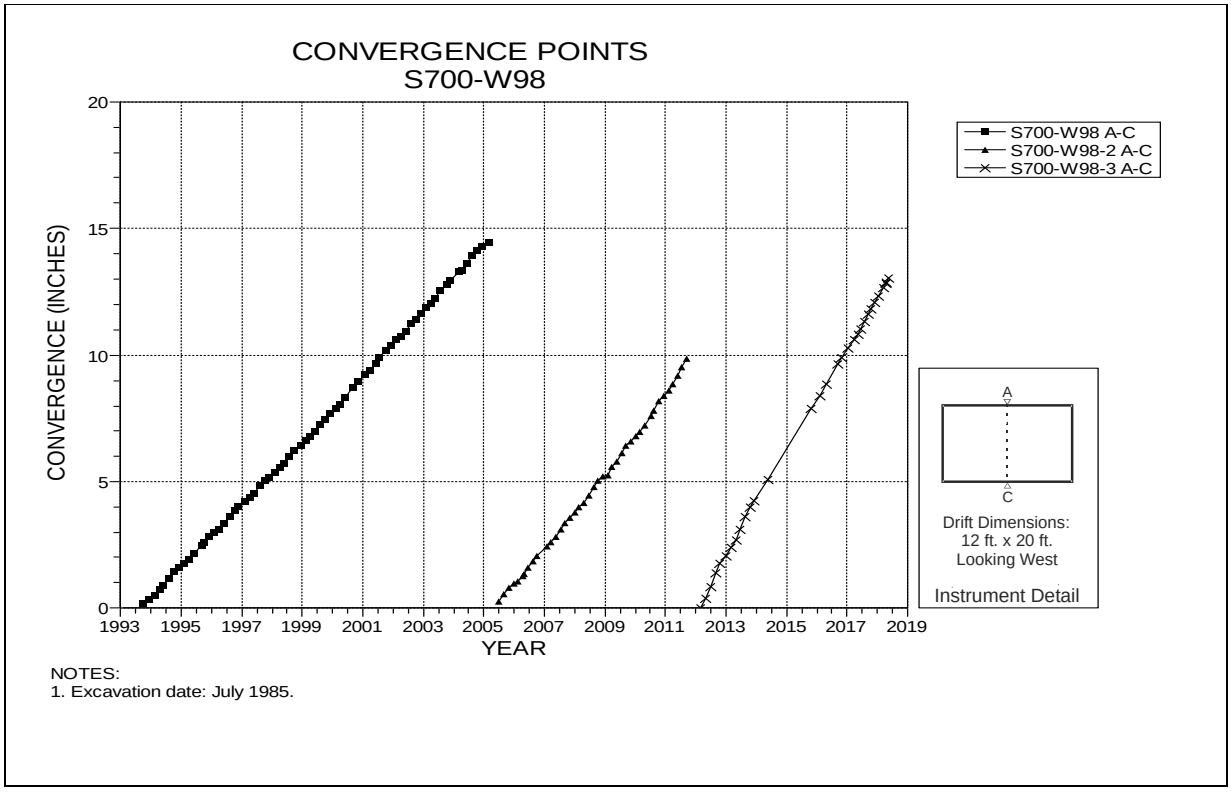

Figure 4-138 Convergence Point Array – S700 W98 – Roof to Floor – Centerline

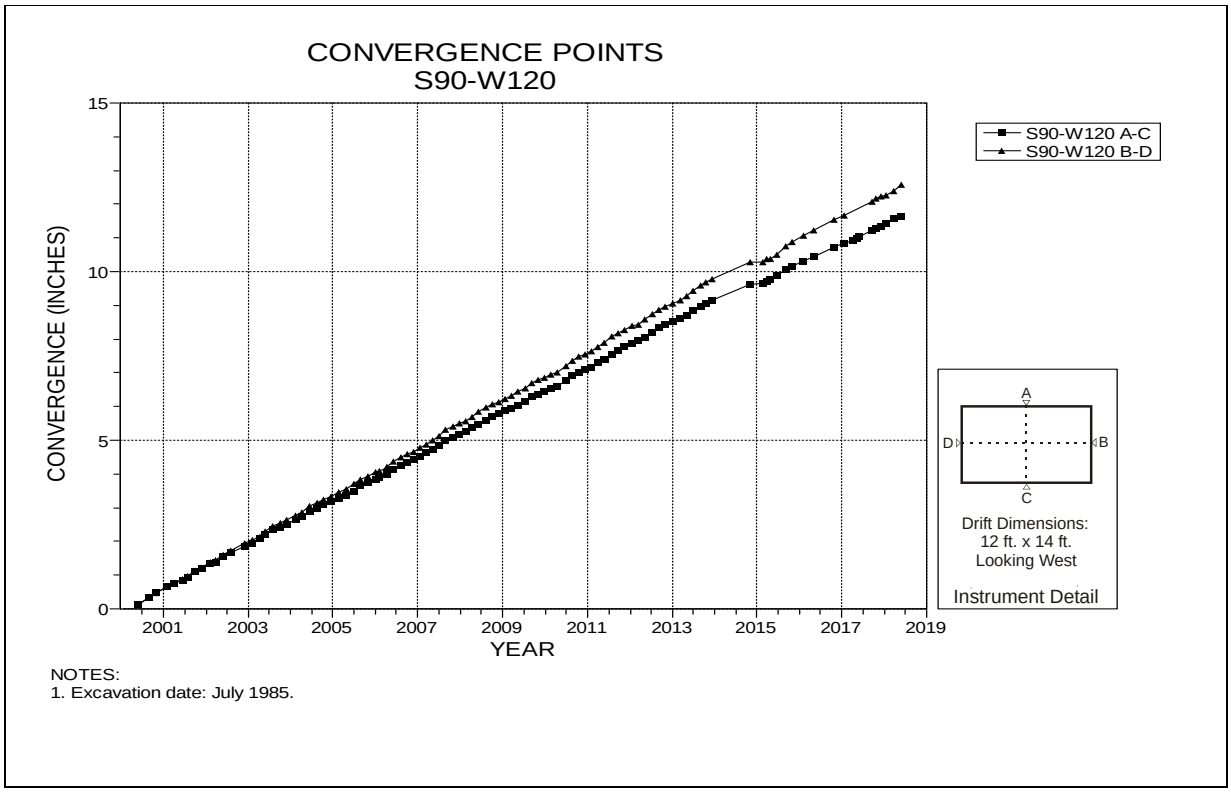

Figure 4-139 Convergence Point Array – S90 W120 – All Chords

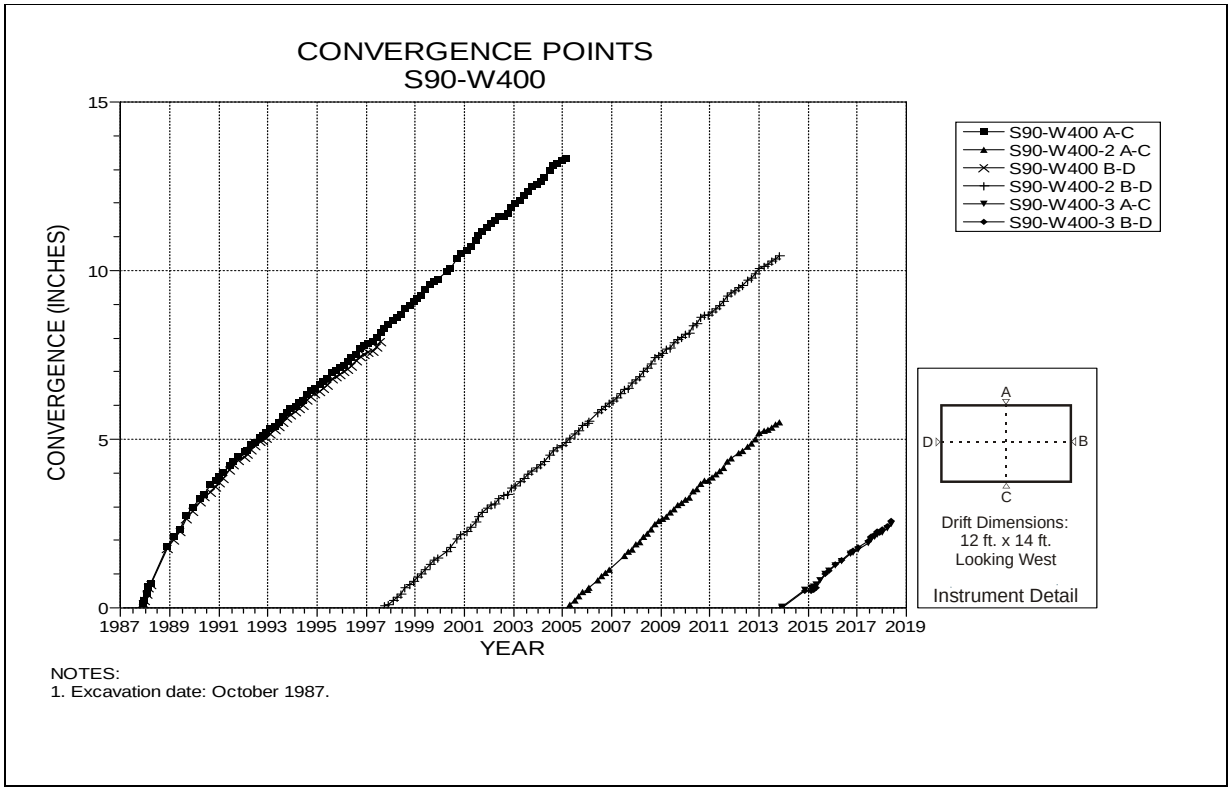

Figure 4-140 Convergence Point Array – S90 W400 – All Chords

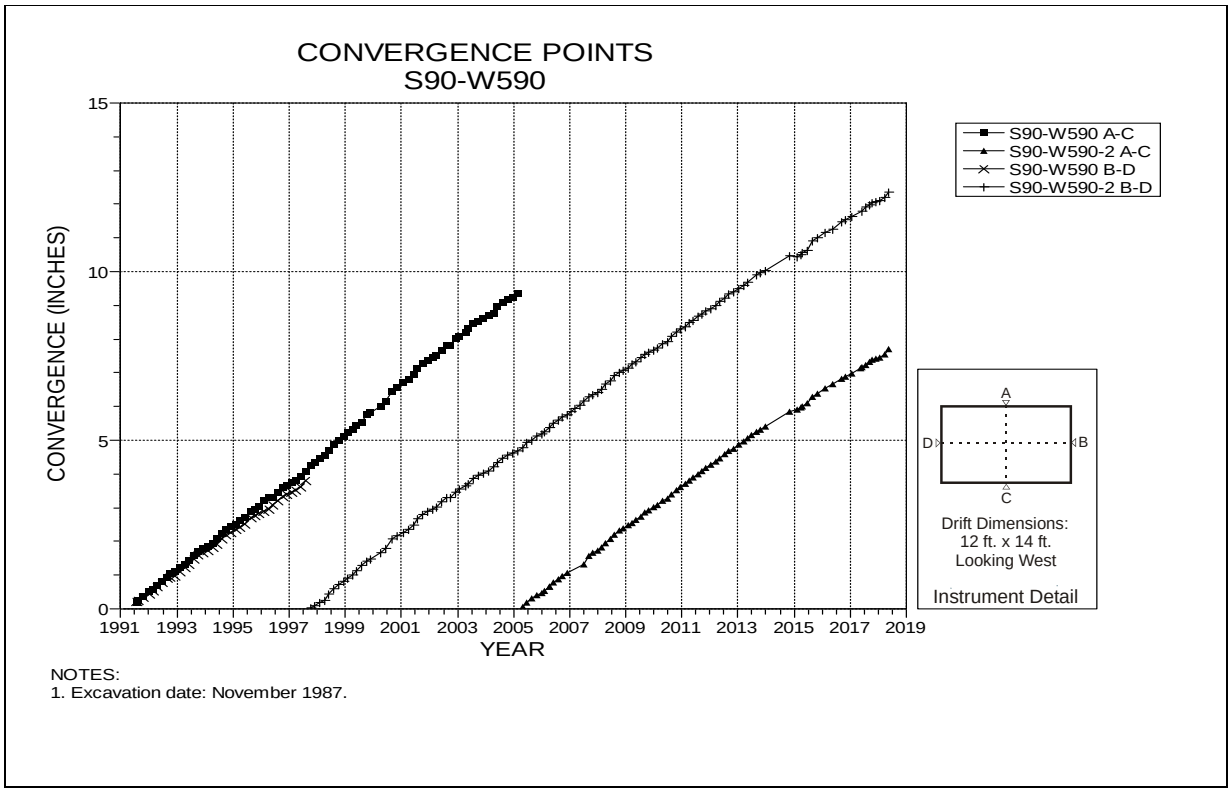

Figure 4-141 Convergence Point Array – S90 W590 – All Chords

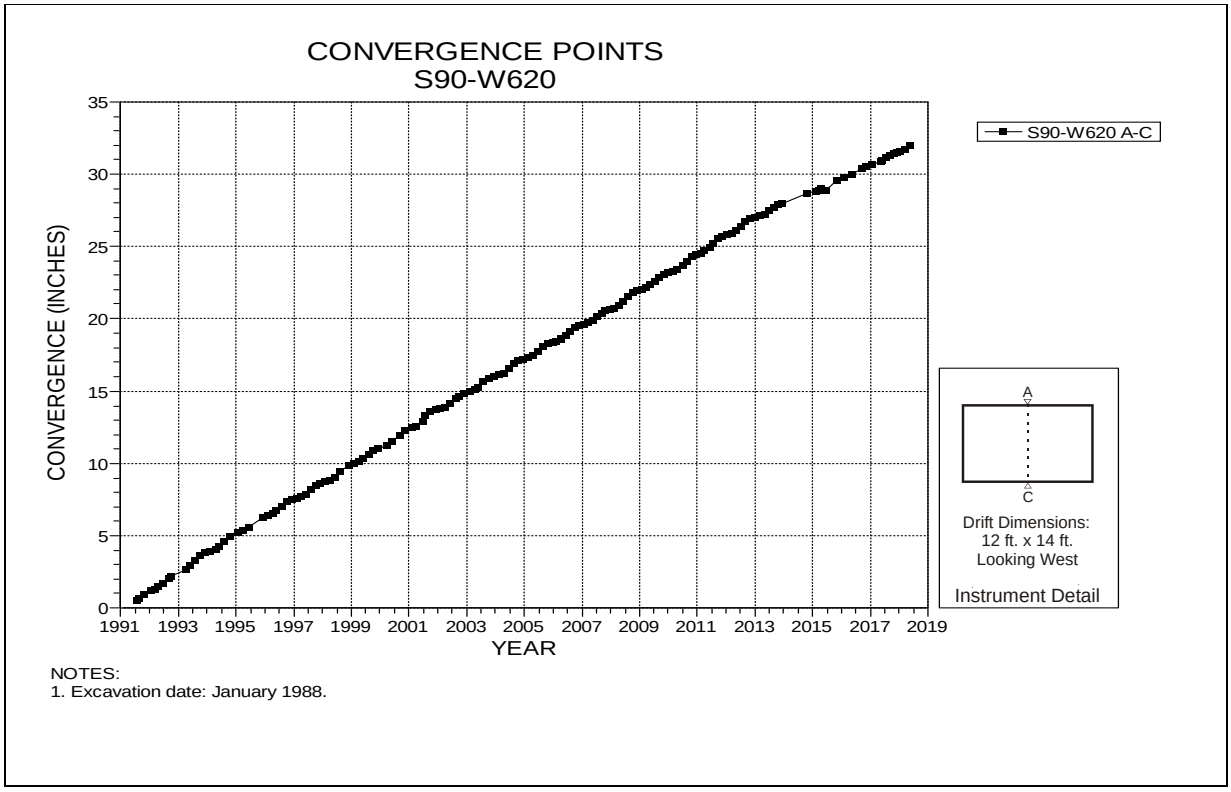

Figure 4-142 Convergence Point Array – S90 W620 – Roof to Floor – Centerline

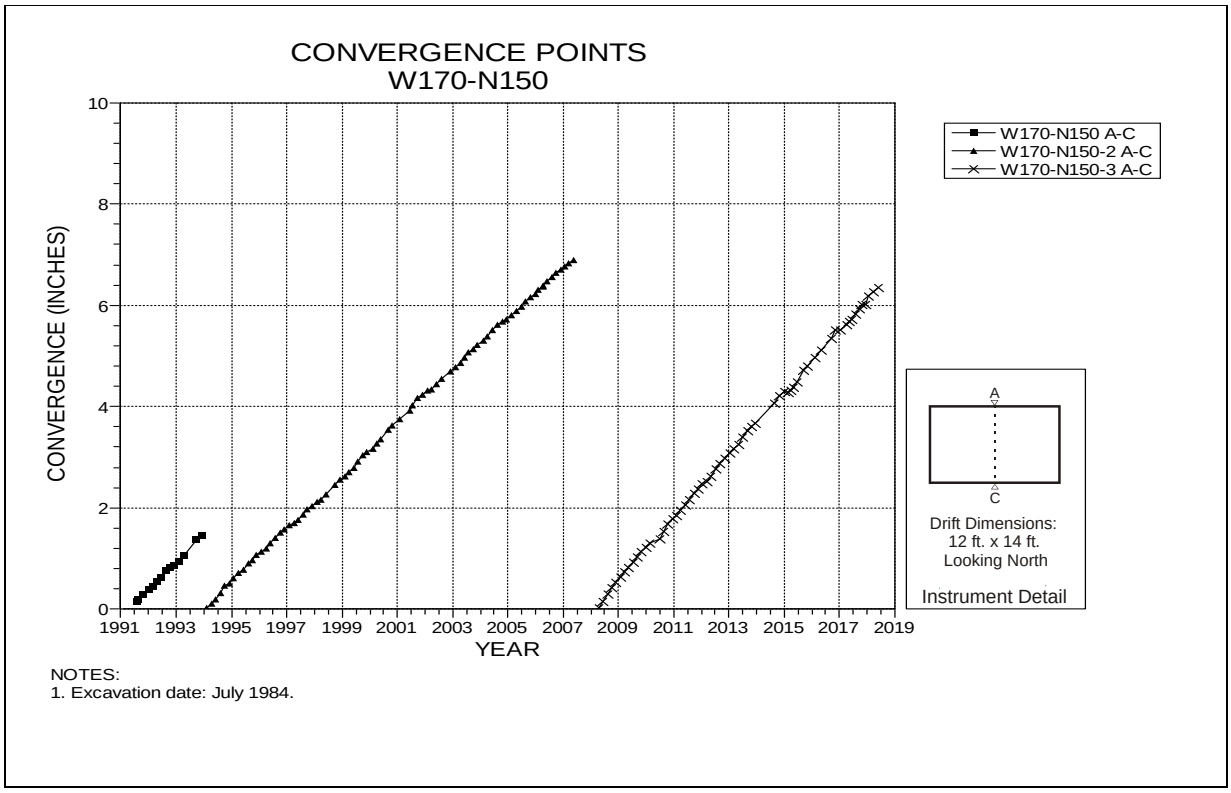

Figure 4-143 Convergence Point Array – W170 N150 – Roof to Floor – Centerline

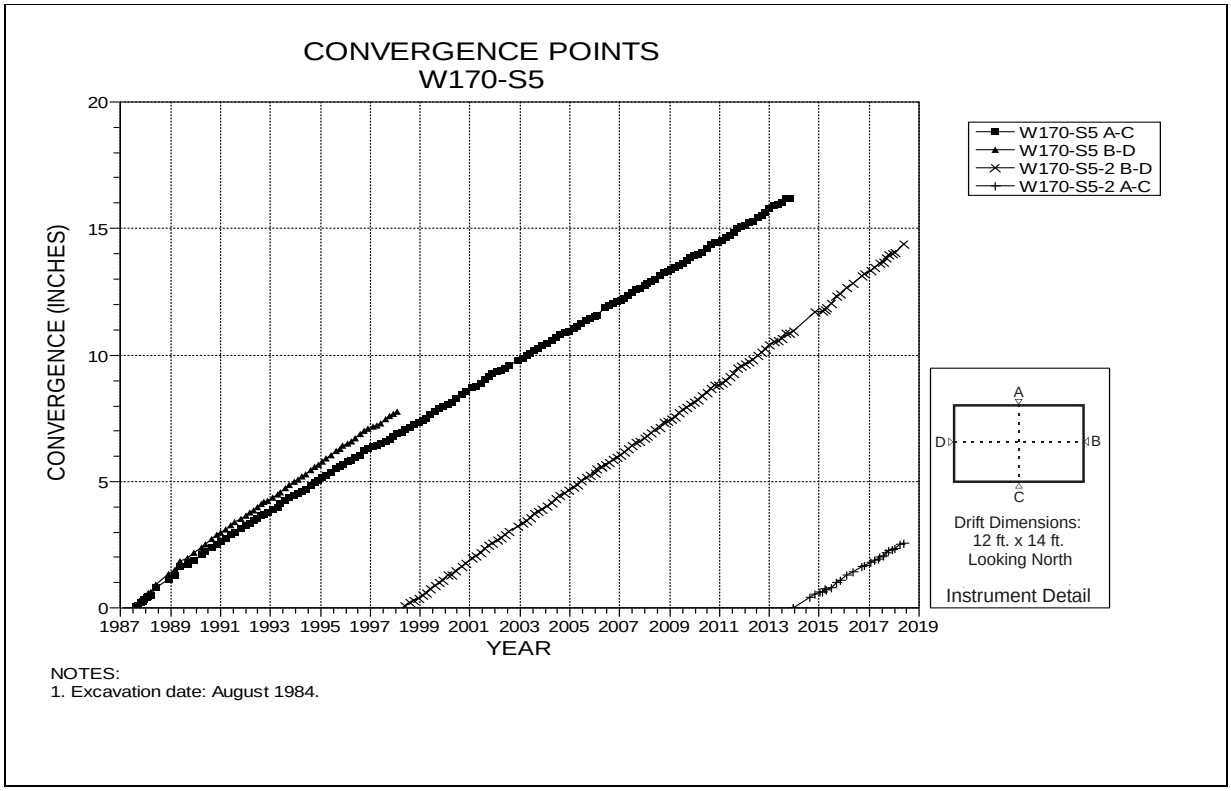

Figure 4-144 Convergence Point Array – W170 S5 – All Chords

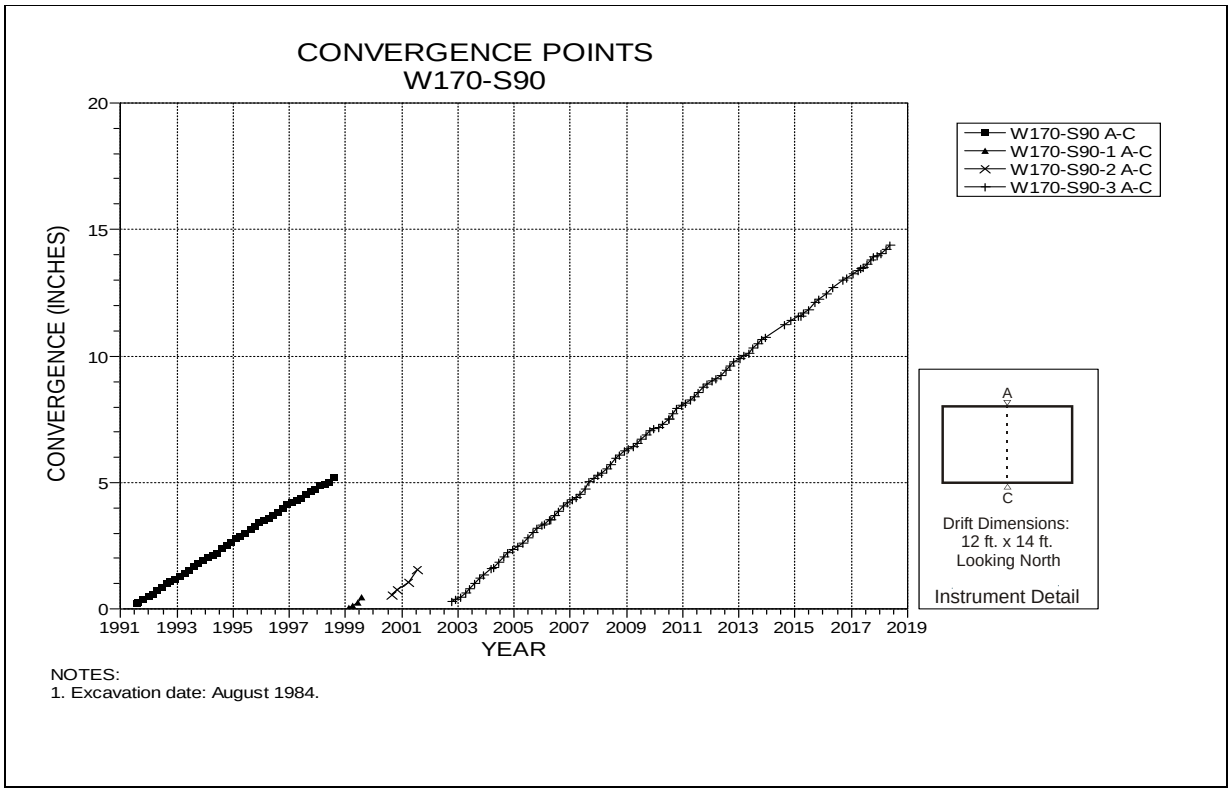

Figure 4-145 Convergence Point Array – W170 S90 – Roof to Floor – Centerline

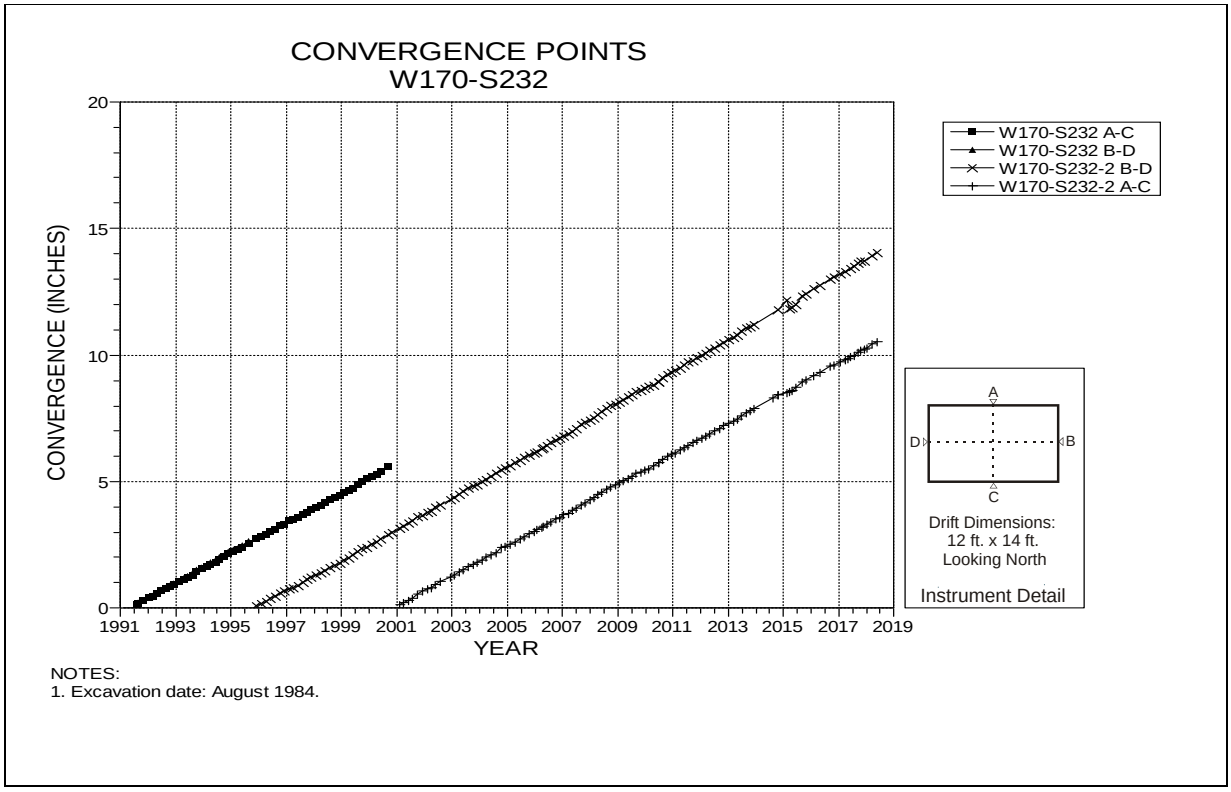

Figure 4-146 Convergence Point Array – W170 S232 – All Chords

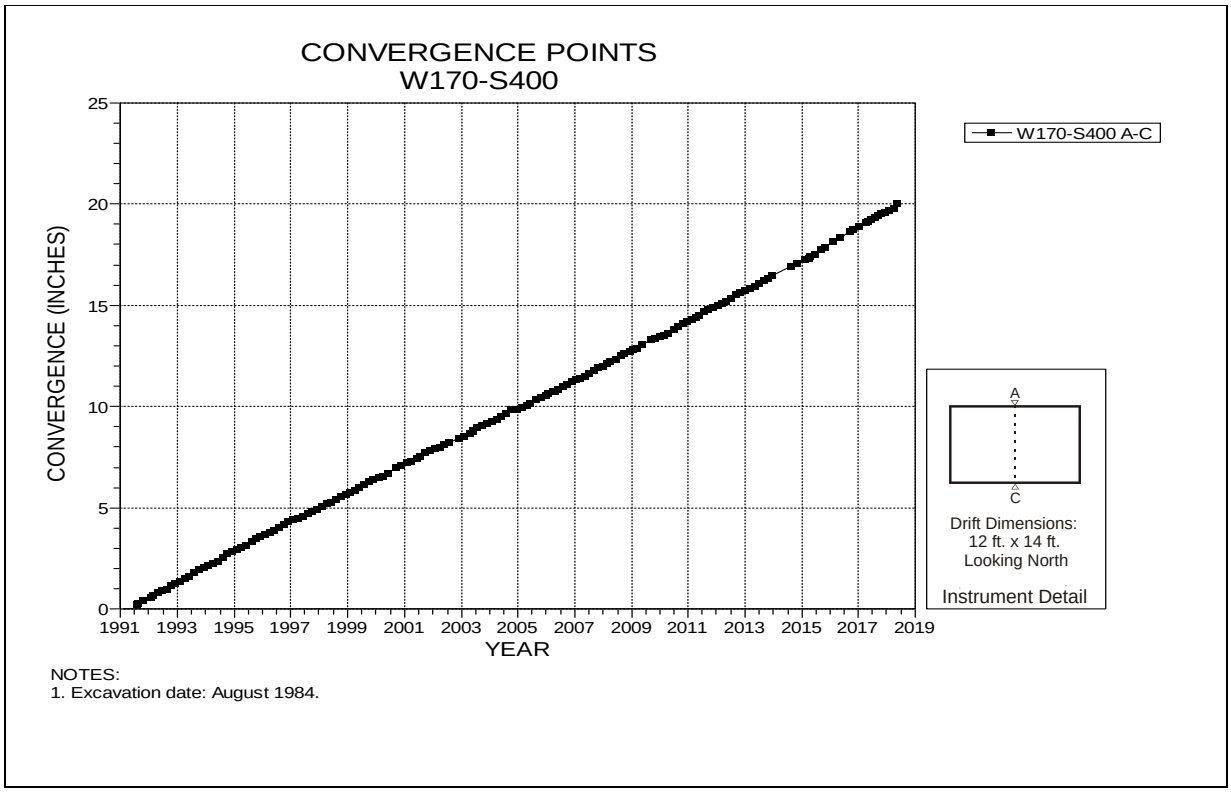

Figure 4-147 Convergence Point Array – W170 S400 – Roof to Floor – Centerline

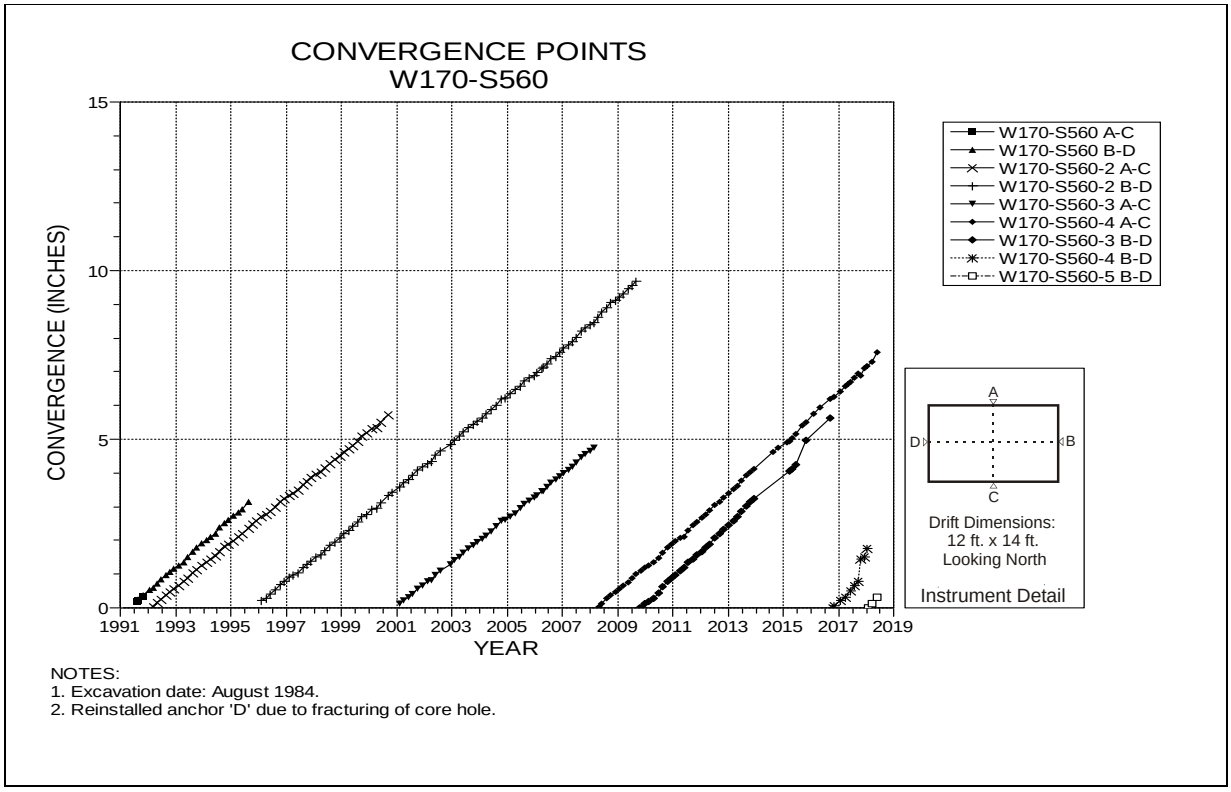

Figure 4-148 Convergence Point Array – W170 S560 – All Chords

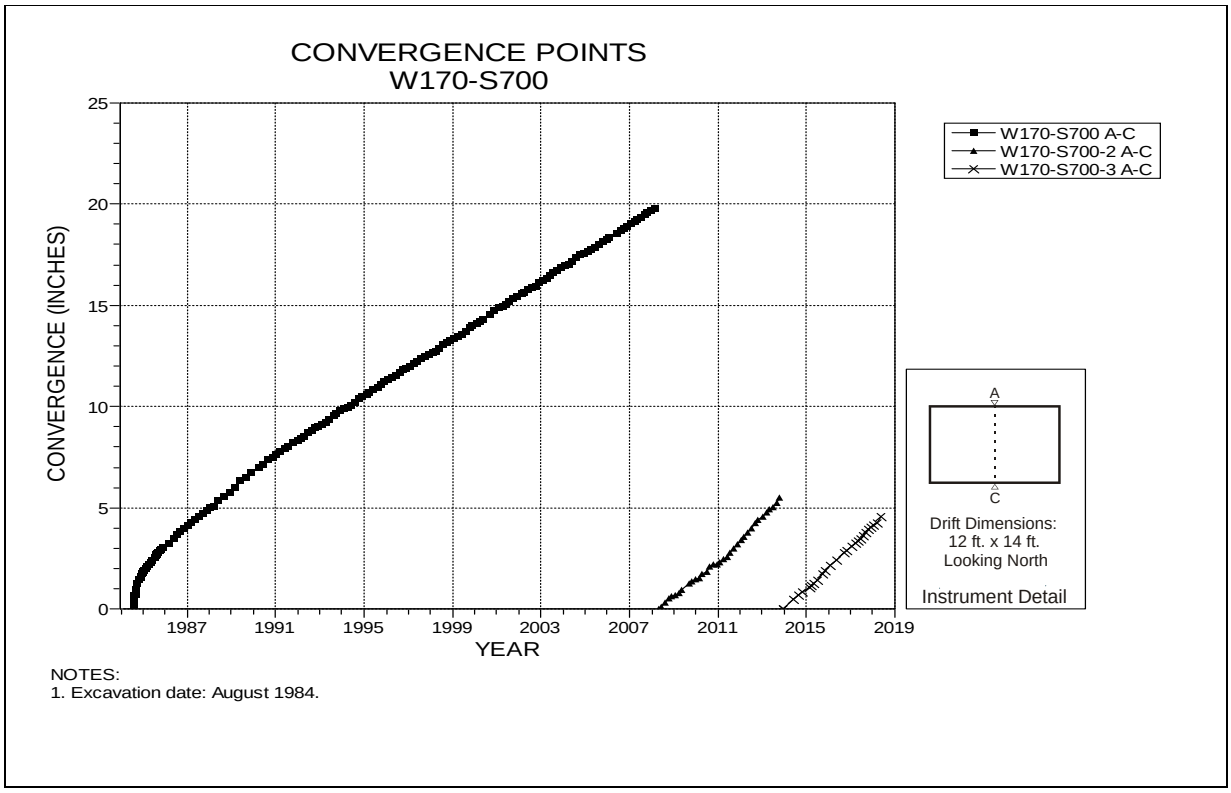

Figure 4-149 Convergence Point Array – W170 S700 – Roof to Floor – Centerline

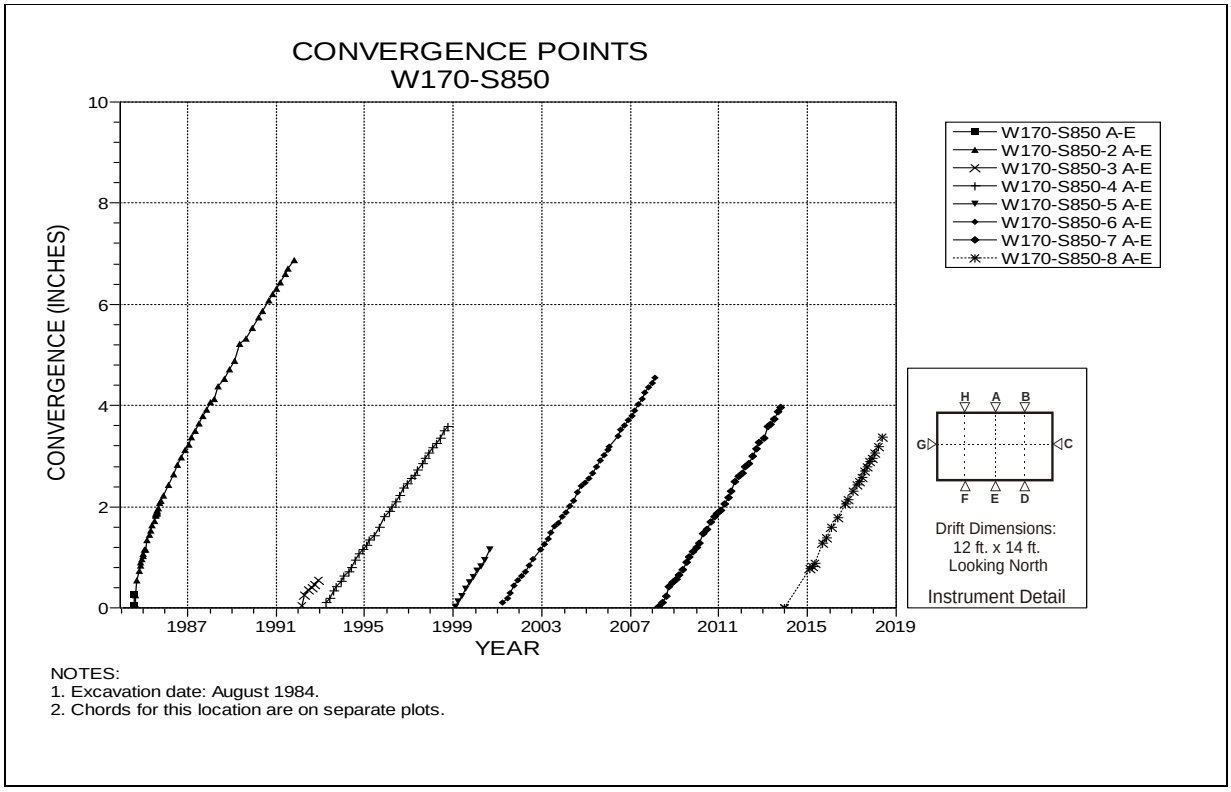

Figure 4-150 Convergence Point Array – W170 S850 – Roof to Floor – Centerline

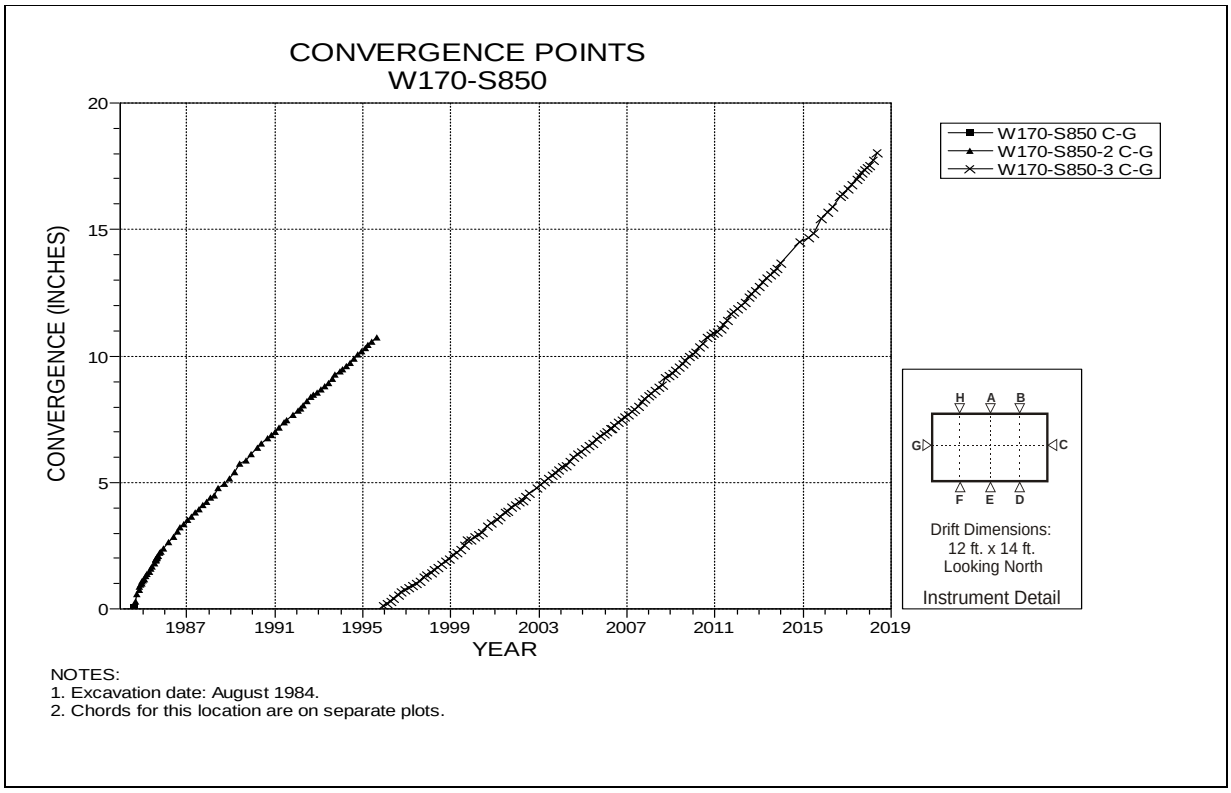

Figure 4-151 Convergence Point Array – W170 S850 – Rib to Rib

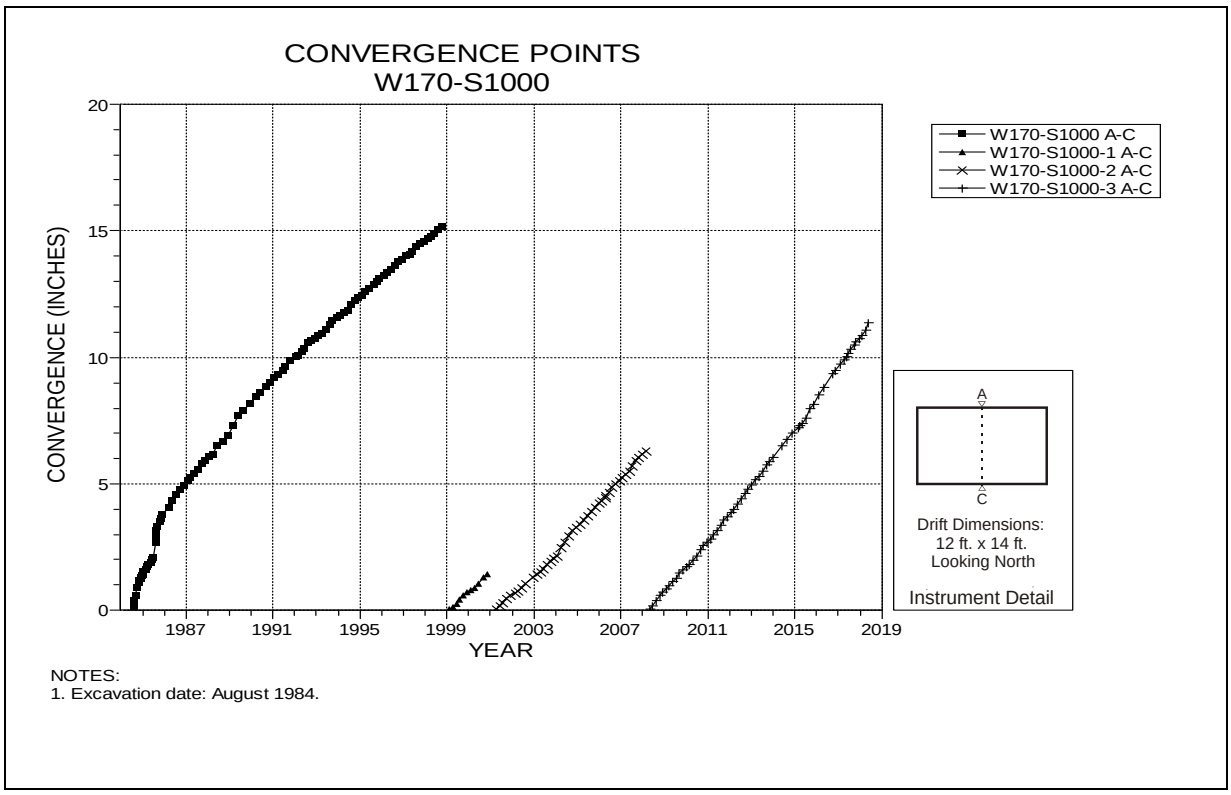

Figure 4-152 Convergence Point Array – W170 S1000 – Roof to Floor – Centerline

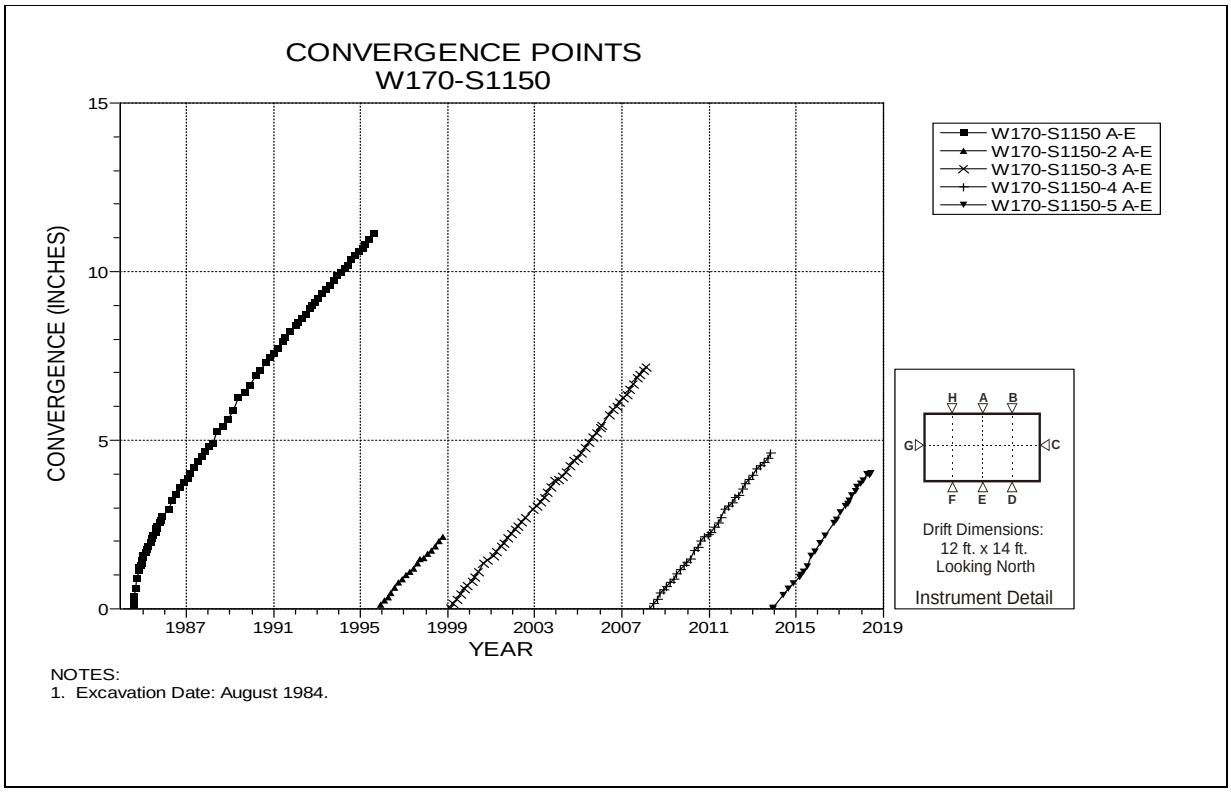

Figure 4-153 Convergence Point Array – W170 S1150 – Roof to Floor – Centerline

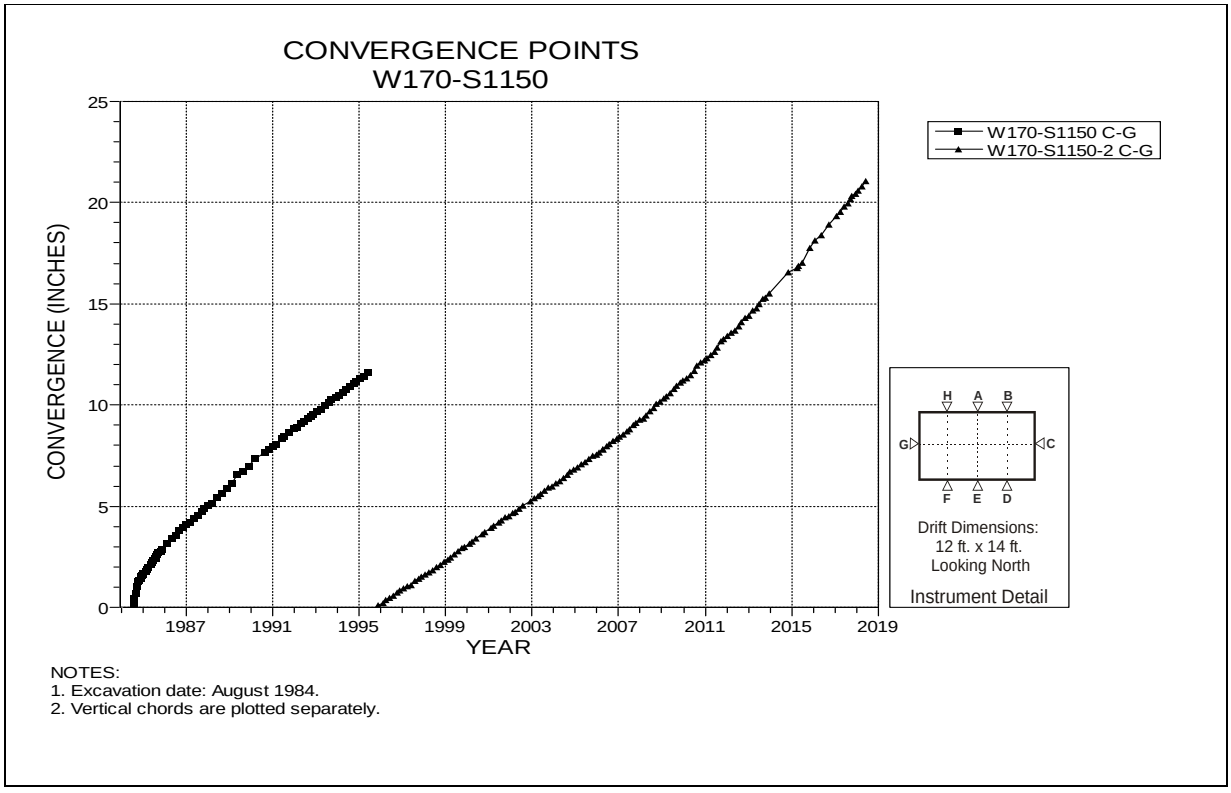

Figure 4-154 Convergence Point Array – W170 S1150 – Rib to Rib

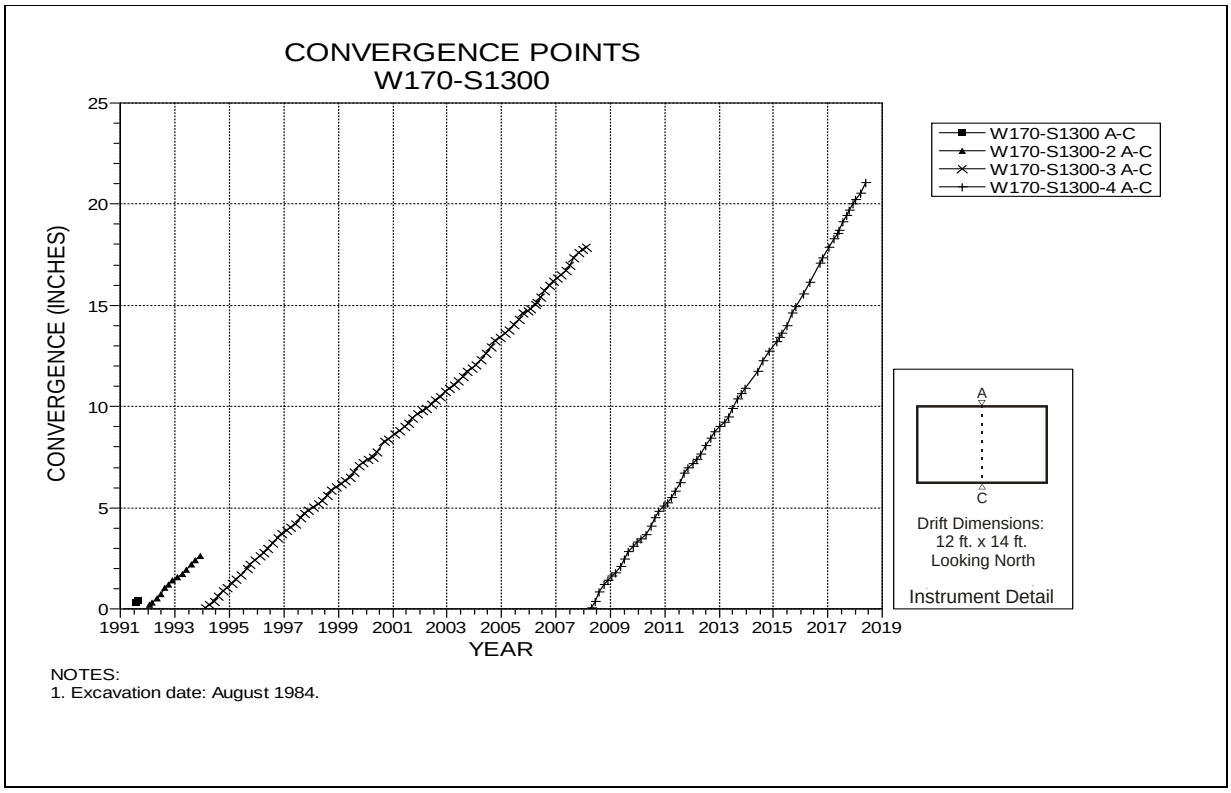

Figure 4-155 Convergence Point Array –W170 S1300 – Roof to Floor – Centerline

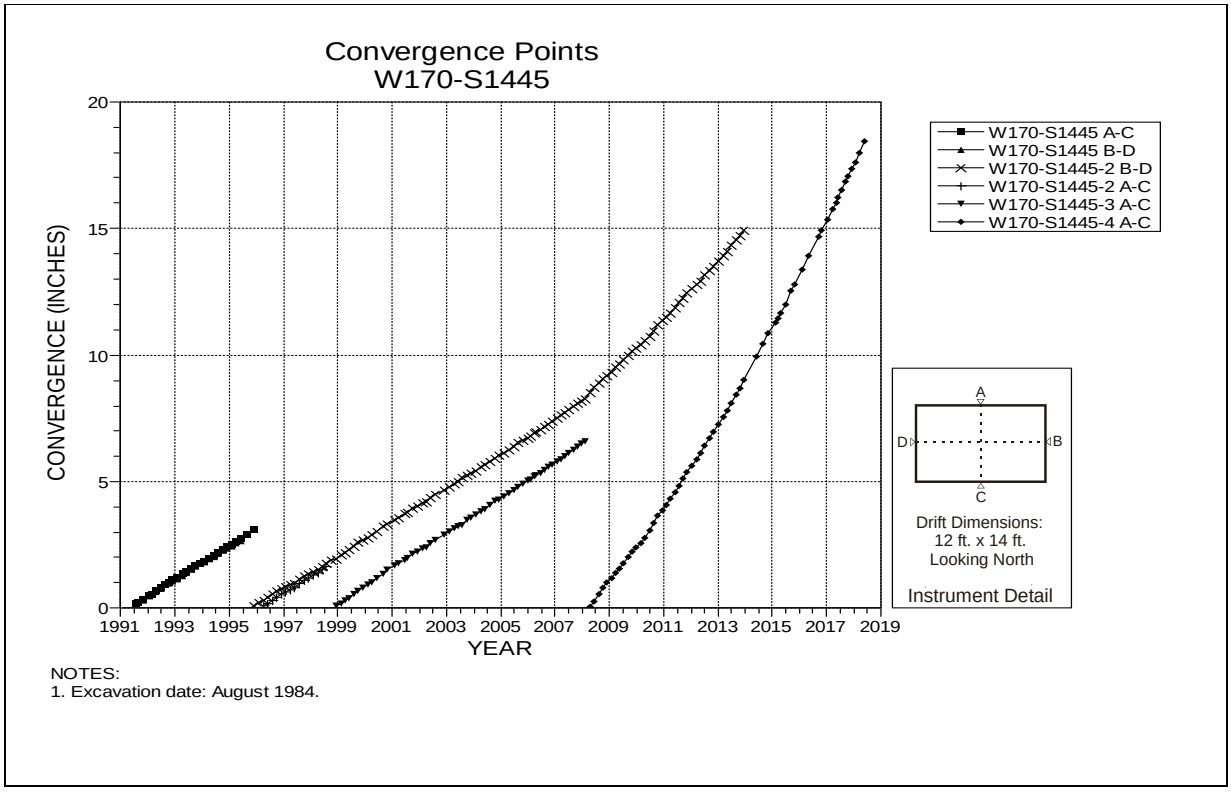

Figure 4-156 Convergence Point Array – W170 S1445 – All Chords

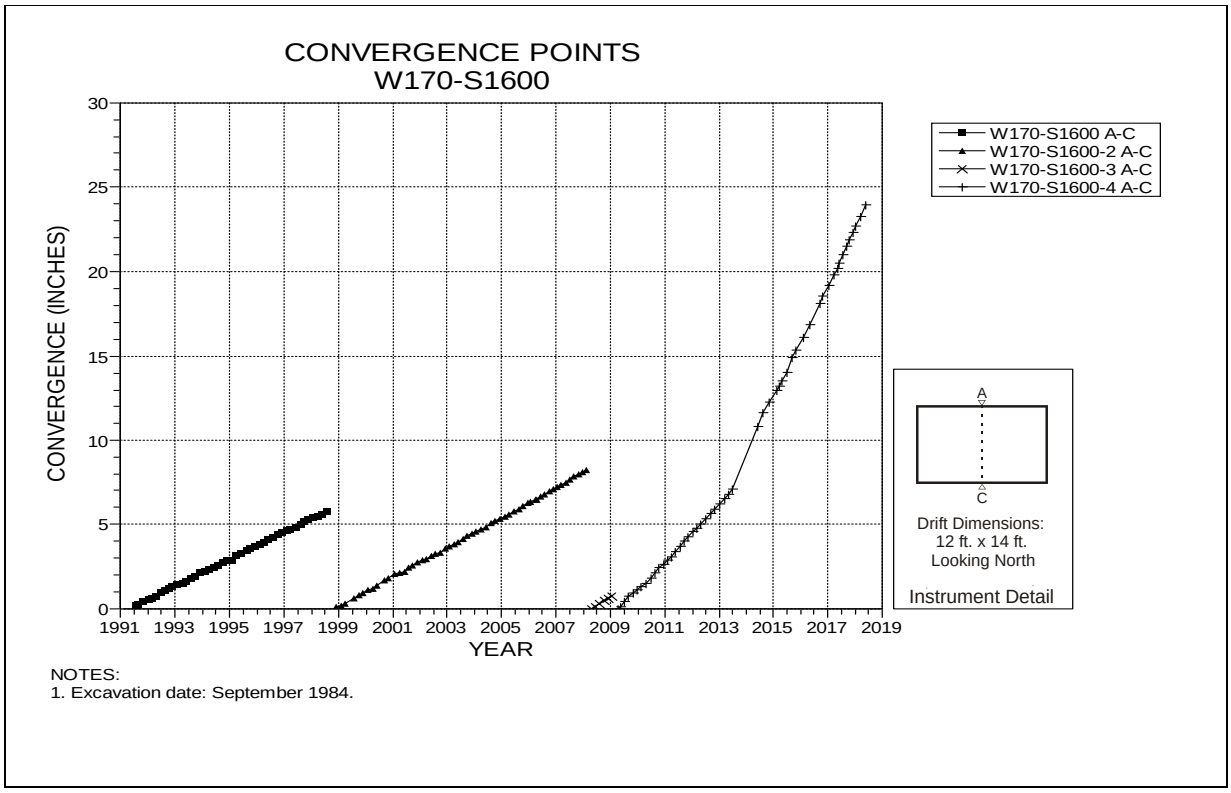

Figure 4-157 Convergence Point Array – W170 S1600 – Roof to Floor – Centerline

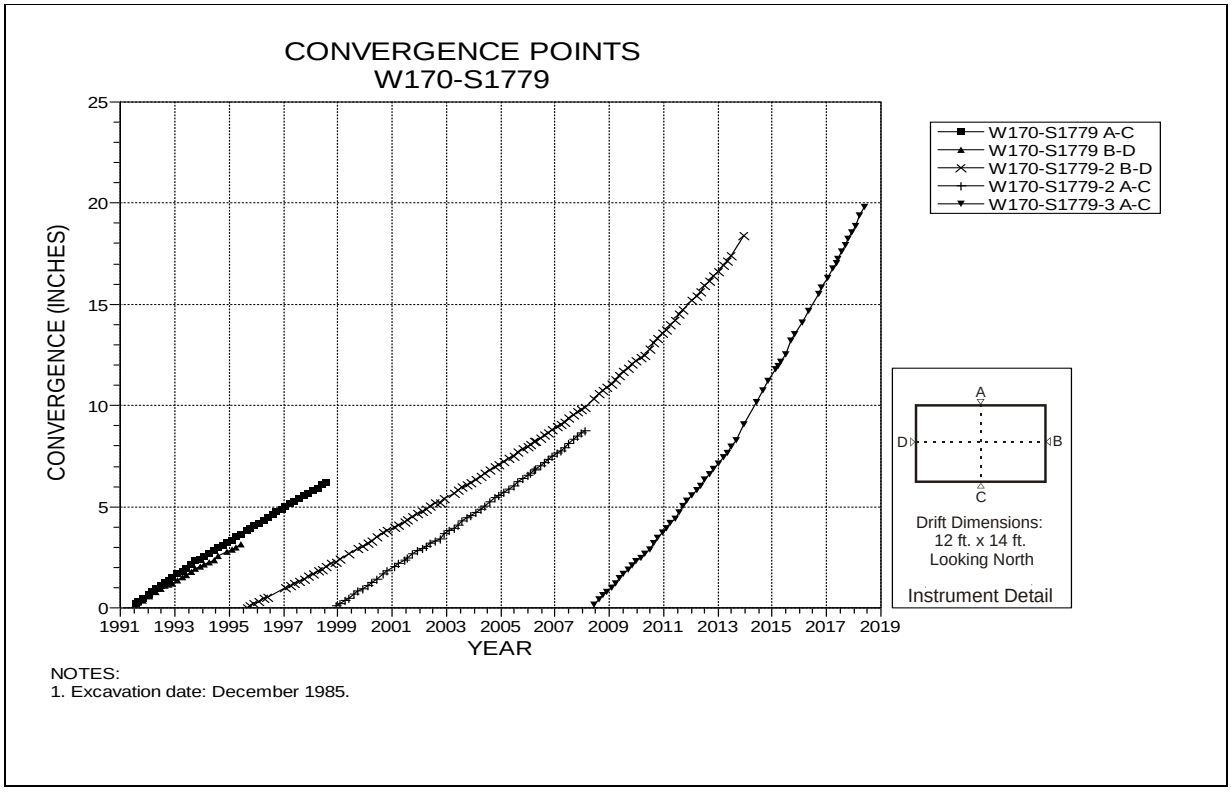

Figure 4-158 Convergence Point Array – W170 S1779 – All Chords

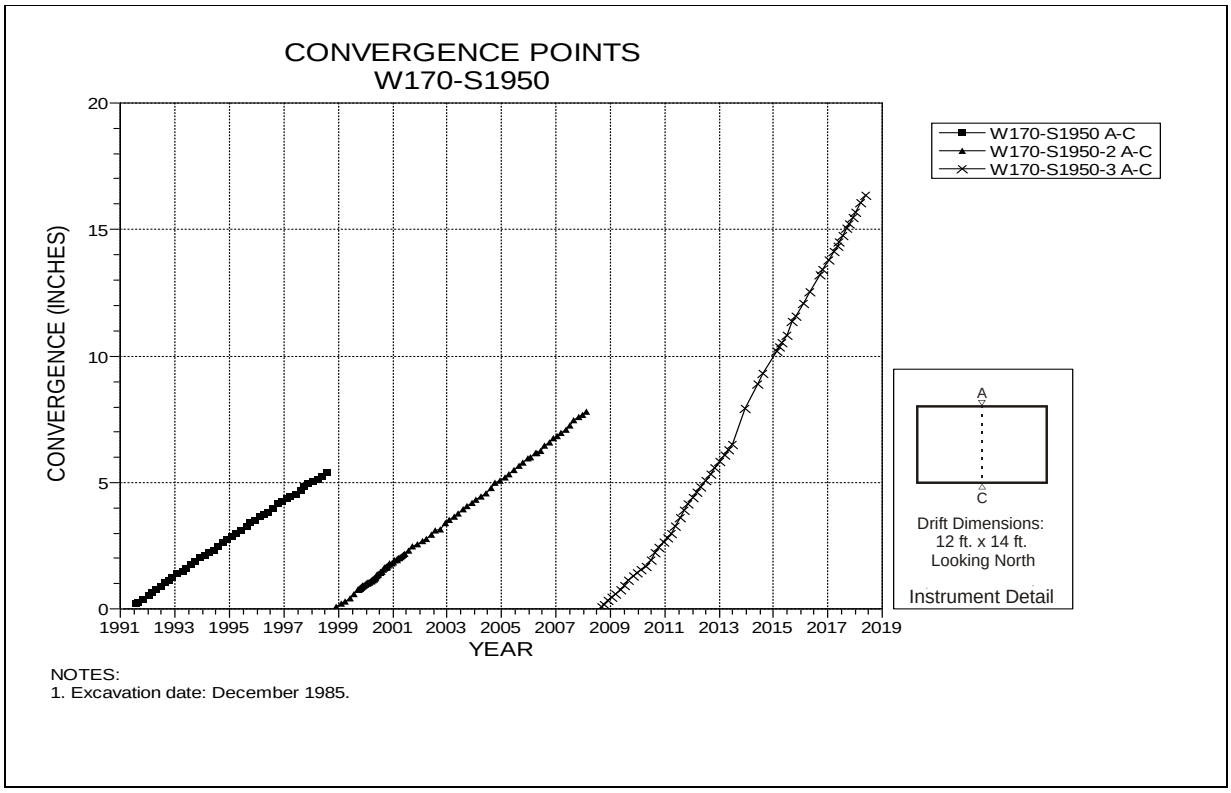

Figure 4-159 Convergence Point Array – W170 S1950 – Roof to Floor – Centerline

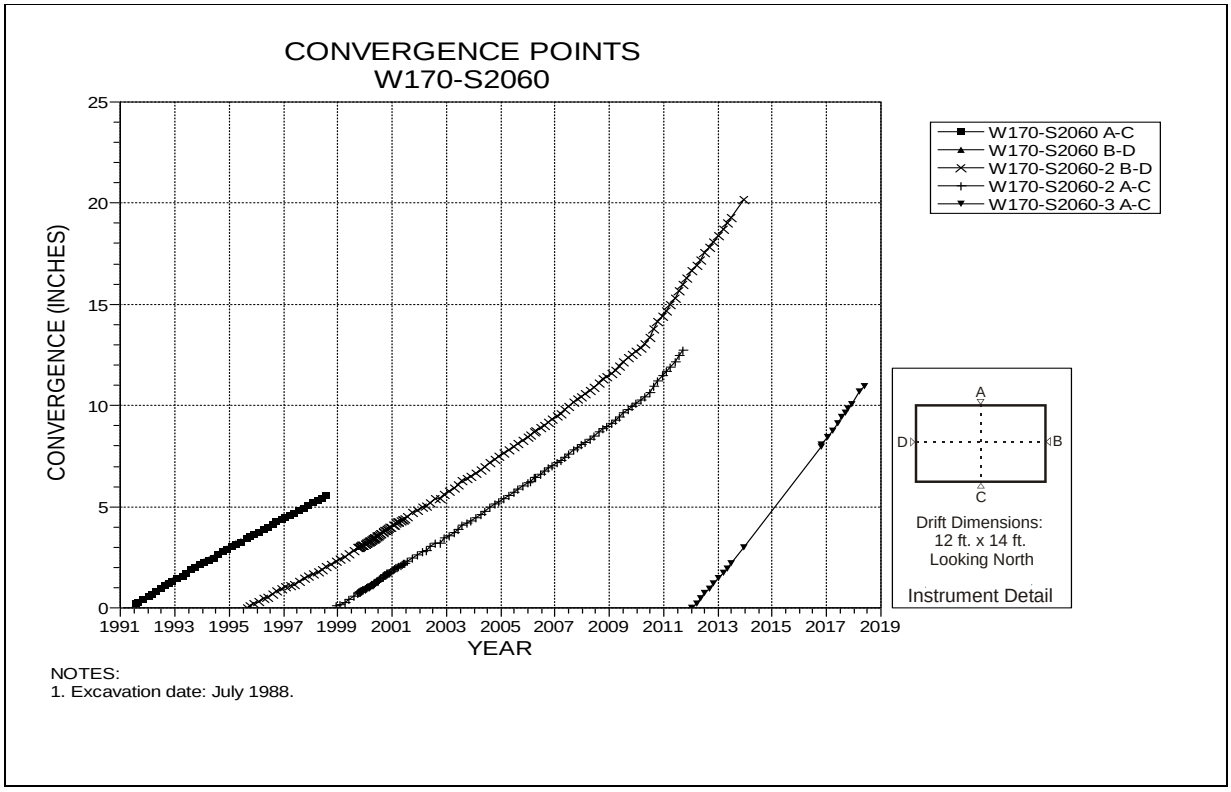

Figure 4-160 Convergence Point Array – W170 S2060 – Roof to Floor – Centerline

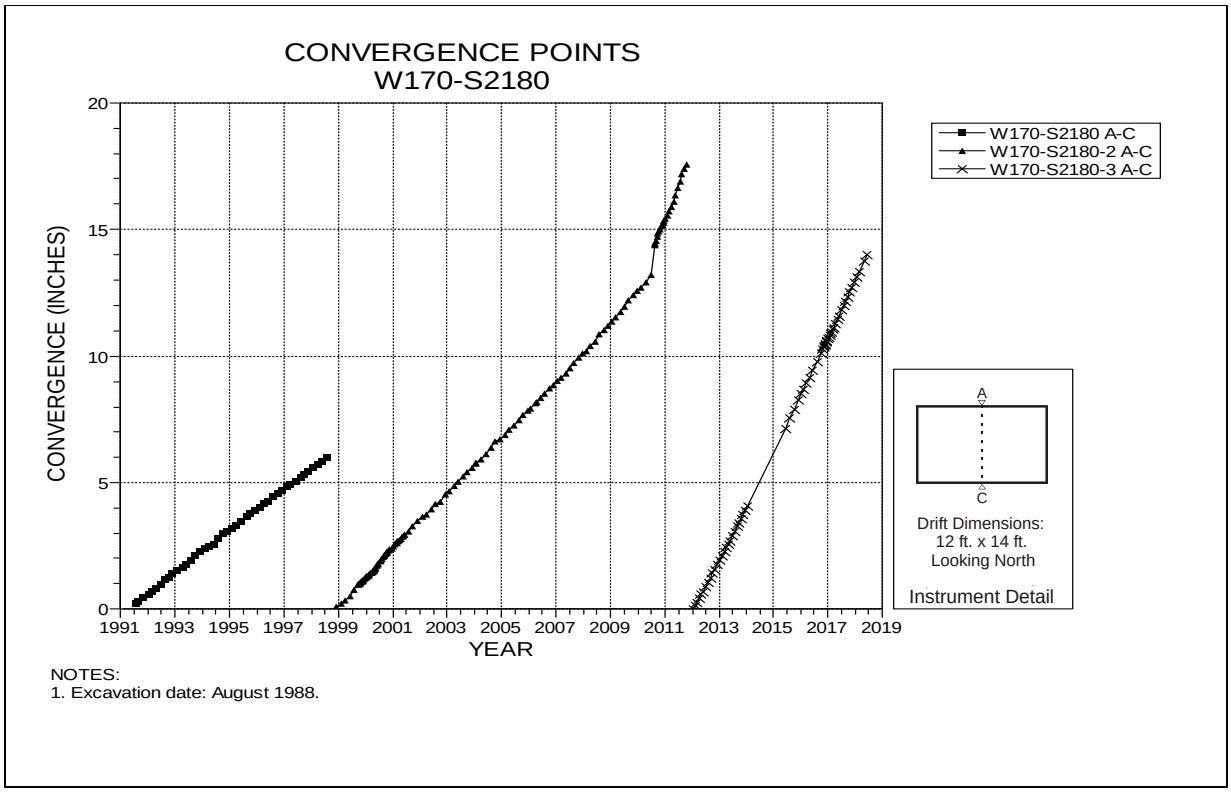

Figure 4-161 Convergence Point Array – W170 S2180 – Roof to Floor – Centerline

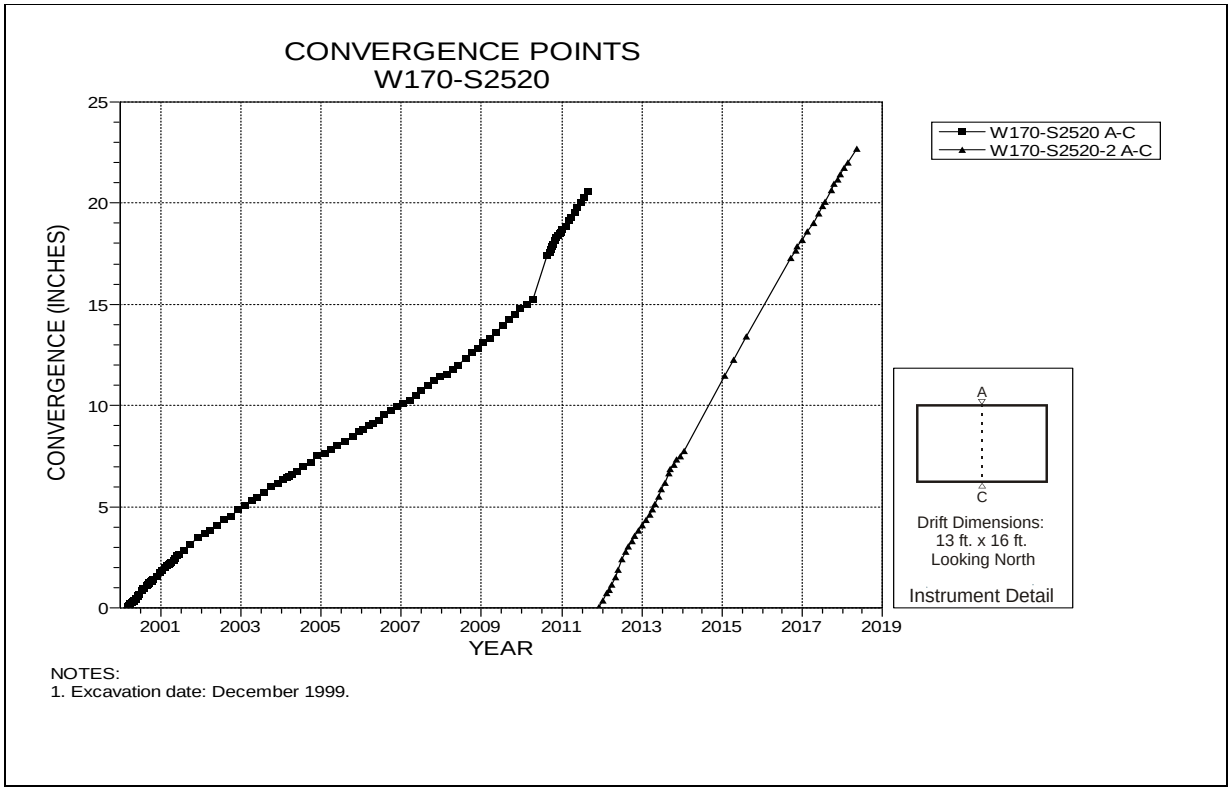

Figure 4-162 Convergence Point Array – W170 S2520 – Roof to Floor – Centerline

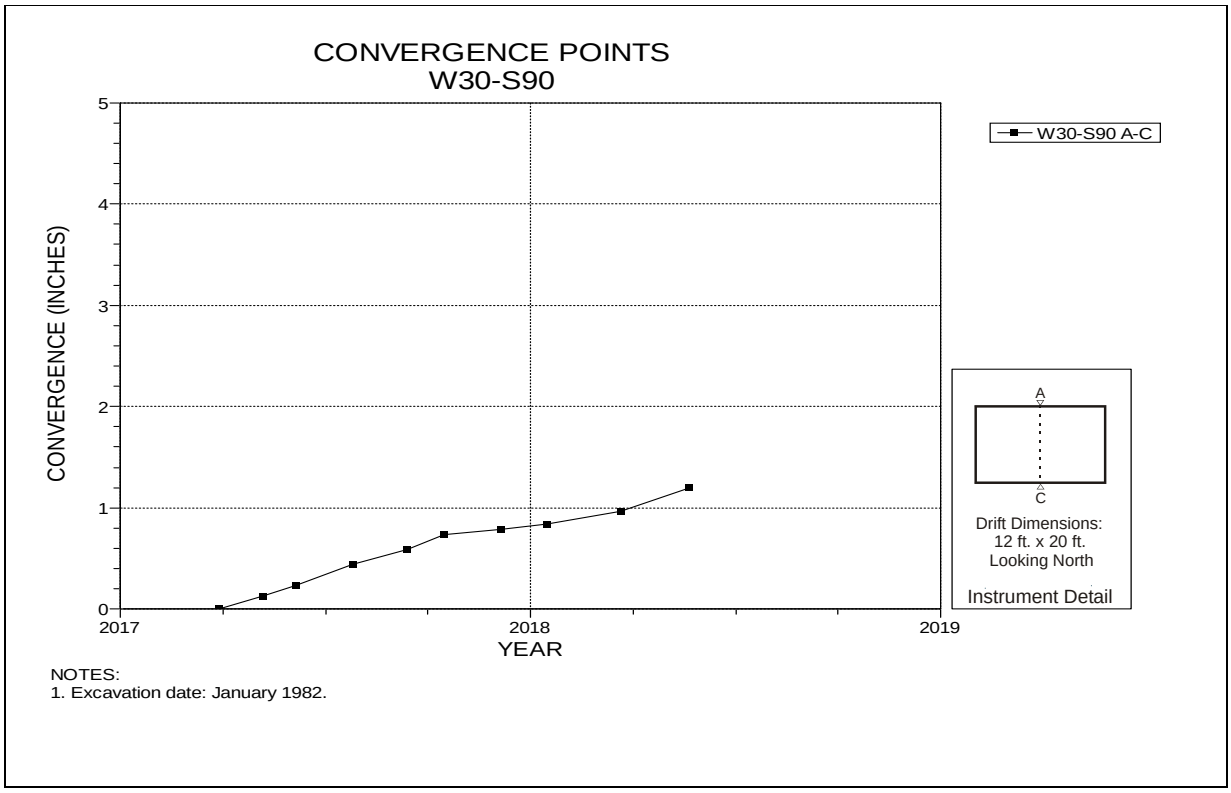

Figure 4-163 Convergence Point Array – W30 S90 – Roof to Floor – Centerline

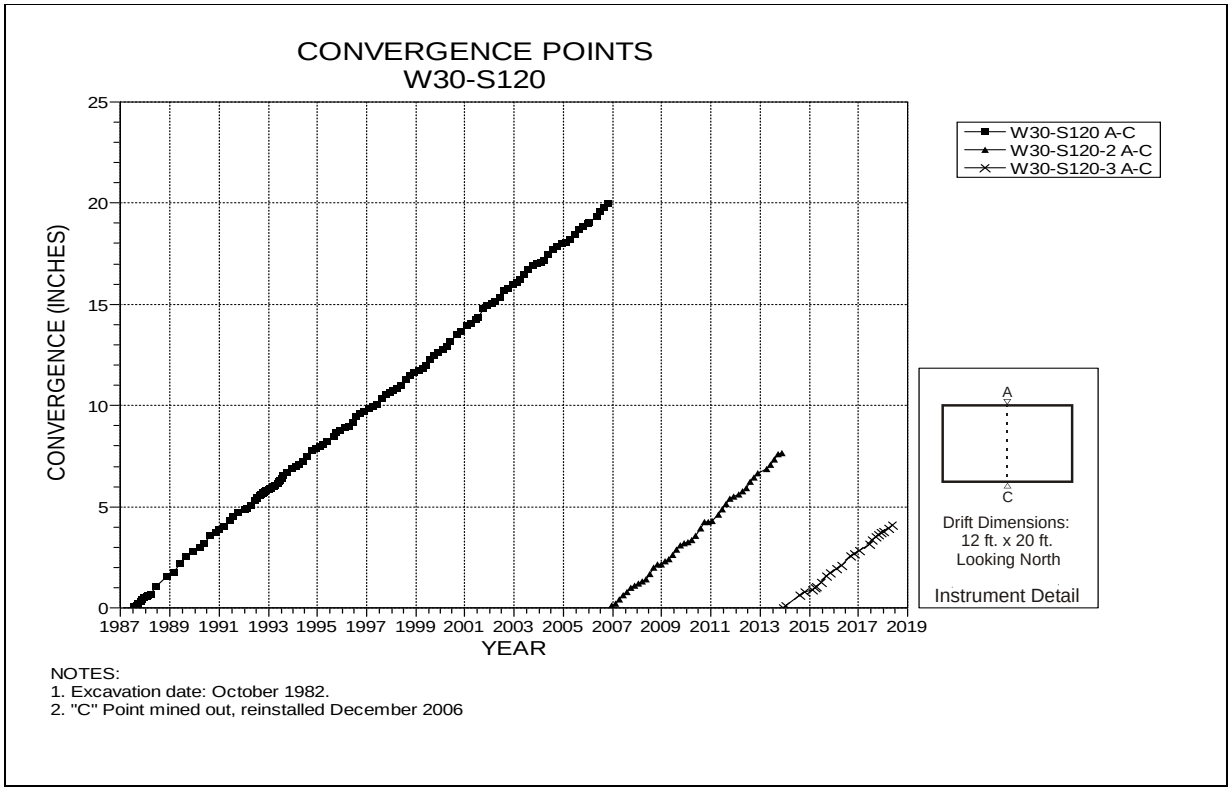

Figure 4-164 Convergence Point Array – W30 S120 – Roof to Floor – Centerline

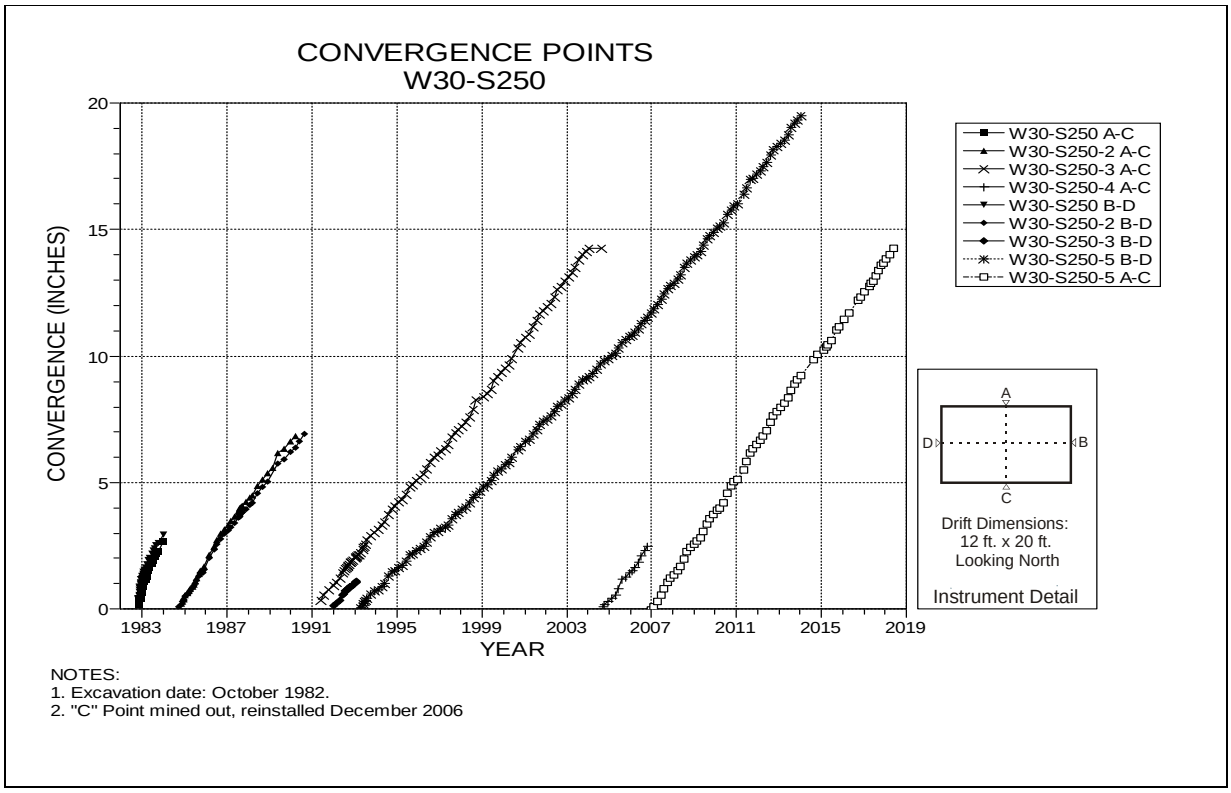

Figure 4-165 Convergence Point Array – W30 S250 – All Chords

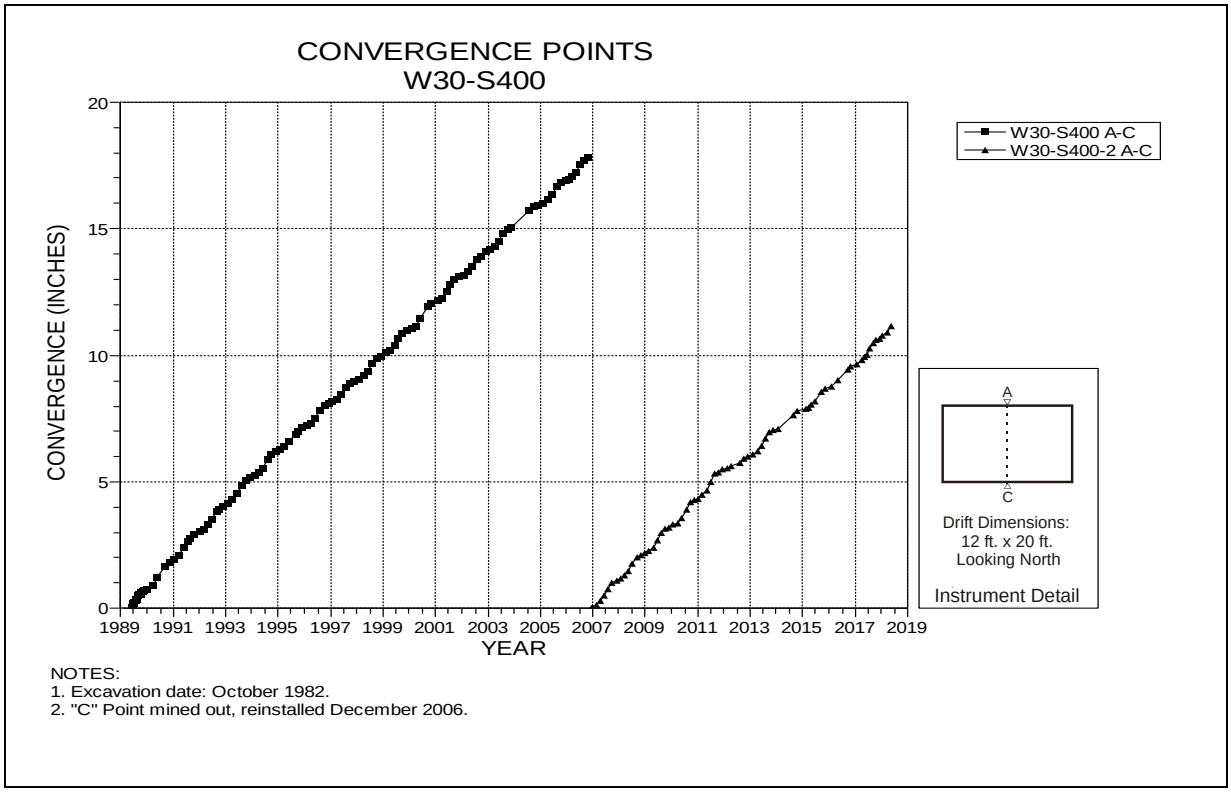

Figure 4-166 Convergence Point Array – W30 S400 – Roof to Floor – Centerline

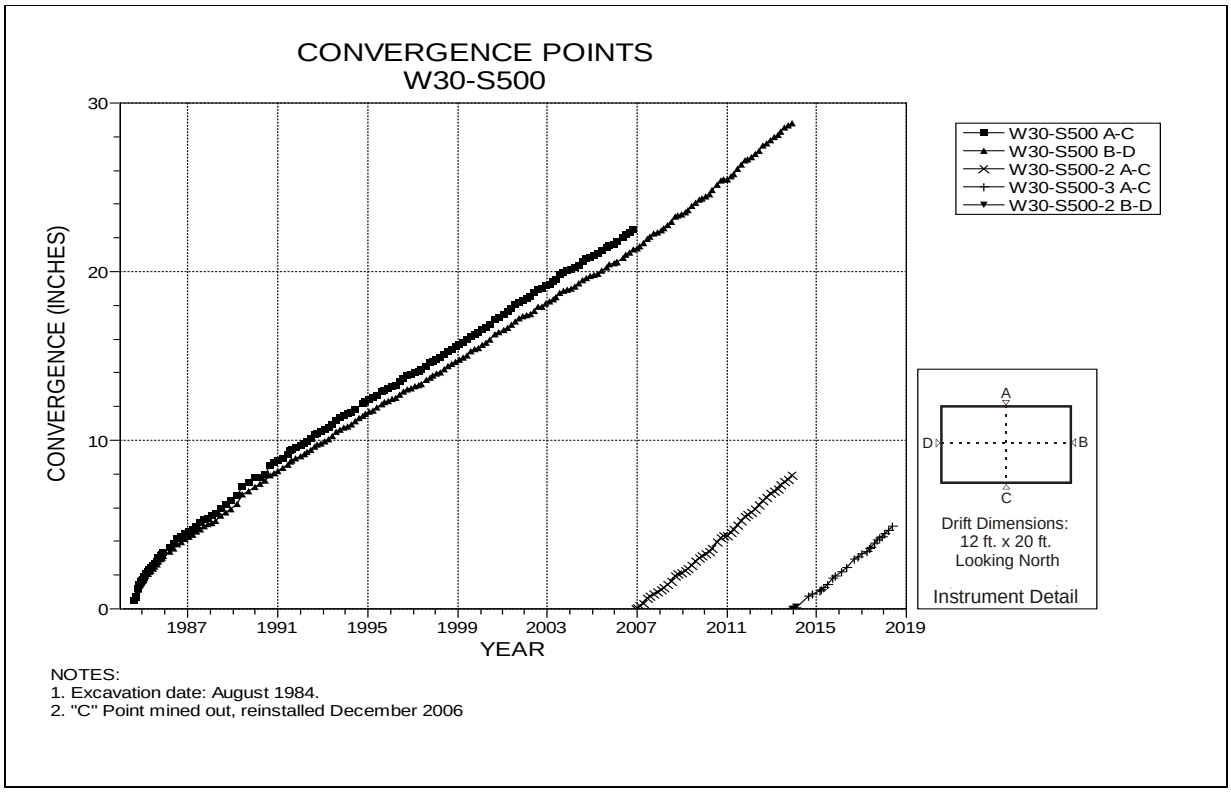

Figure 4-167 Convergence Point Array – W30 S500 – All Chords

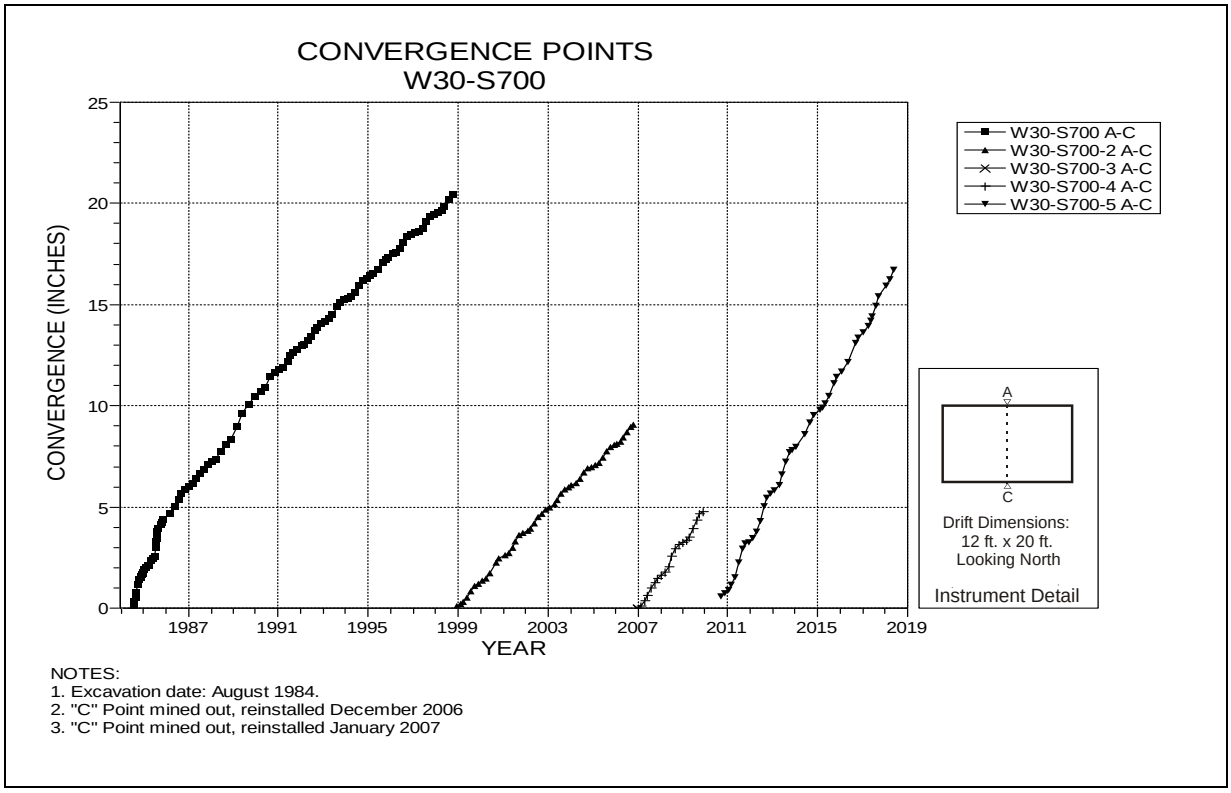

Figure 4-168 Convergence Point Array – W30 S700 – Roof to Floor – Centerline

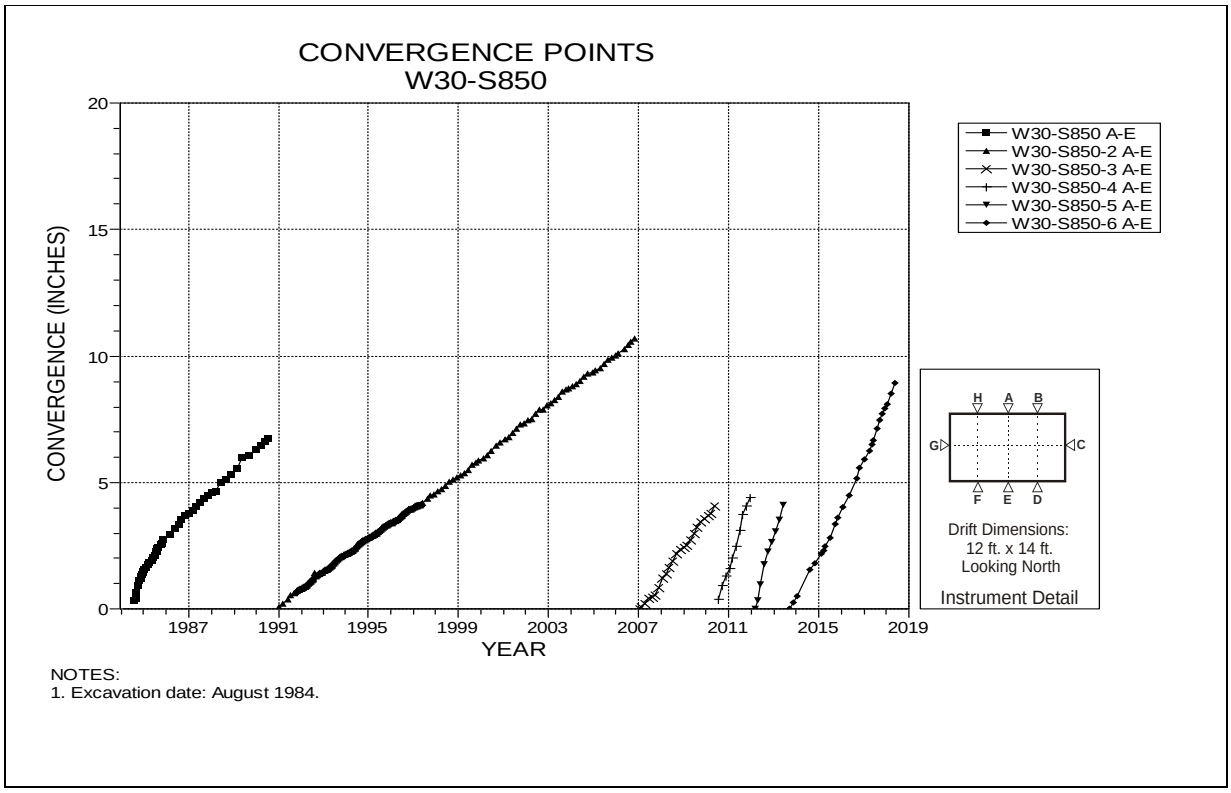

Figure 4-169 Convergence Point Array – W30 S850 – Roof to Floor – Centerline

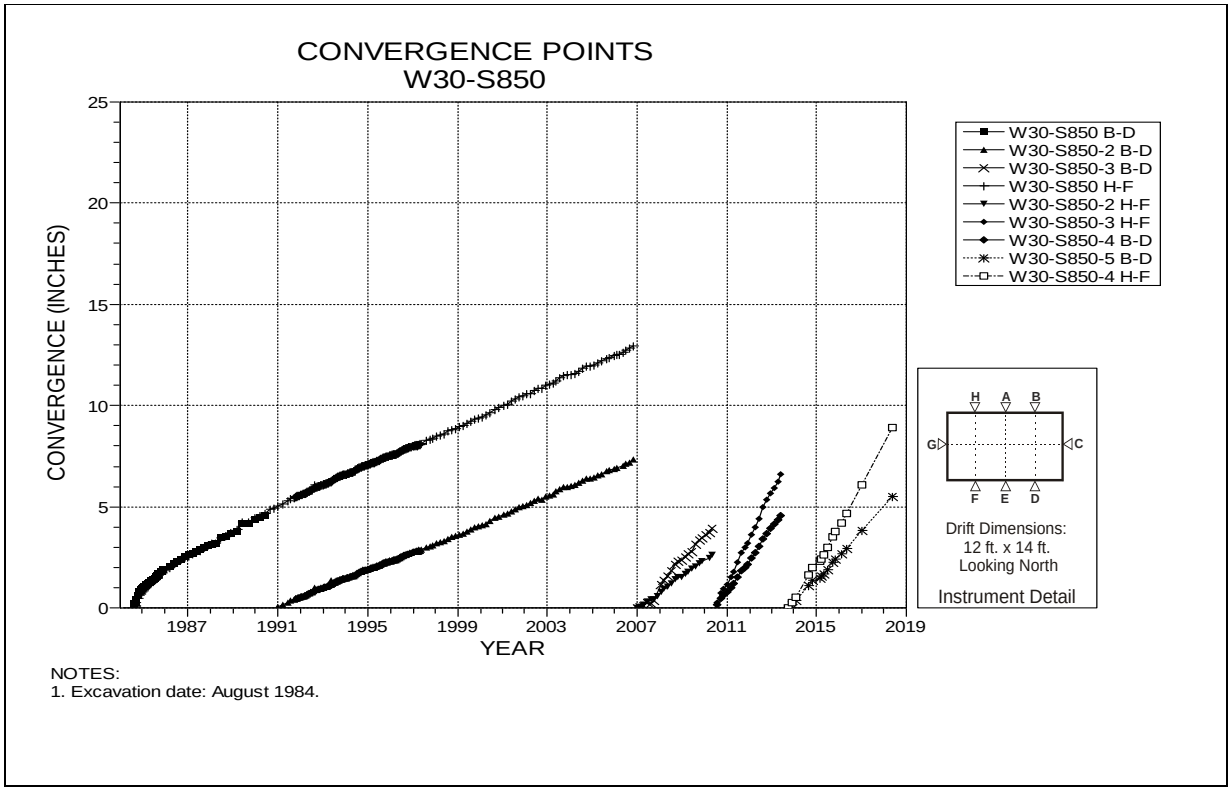

Figure 4-170 Convergence Point Array – W30 S850 – Quarter Points

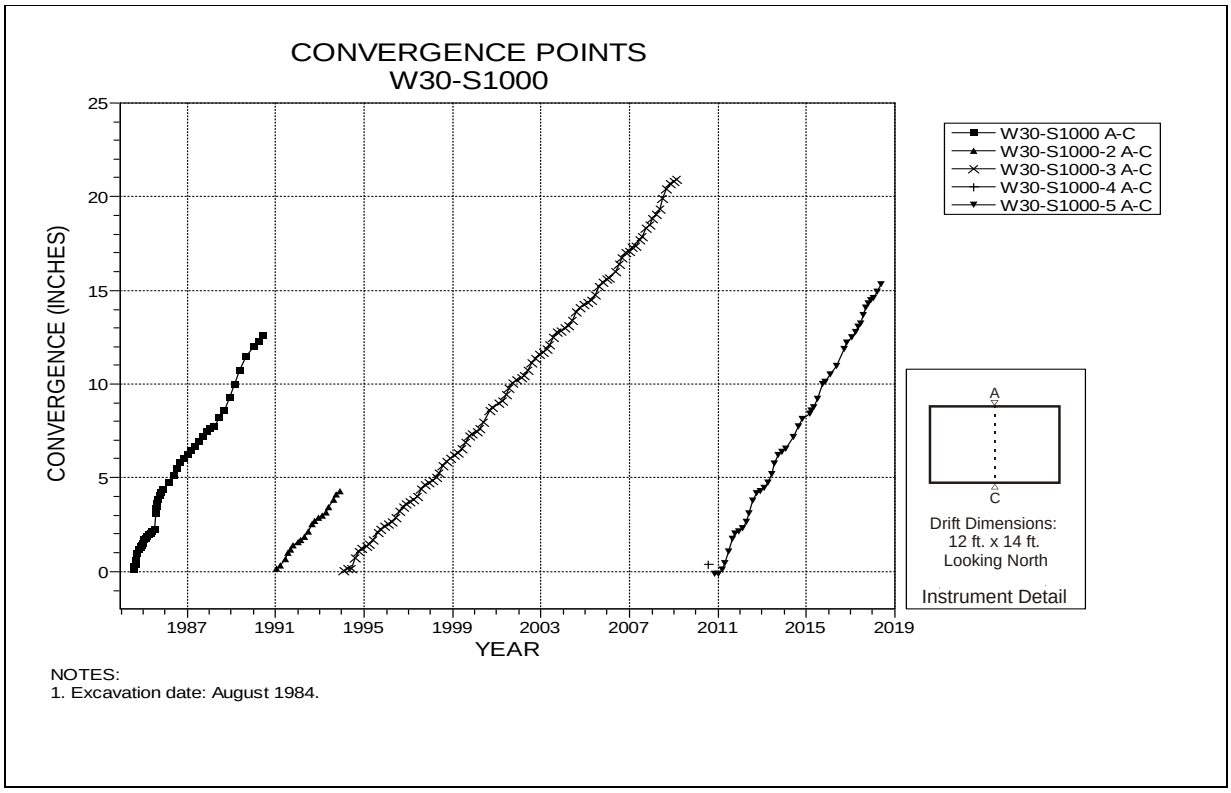

Figure 4-171 Convergence Point Array – W30 S1000 – Roof to Floor – Centerline

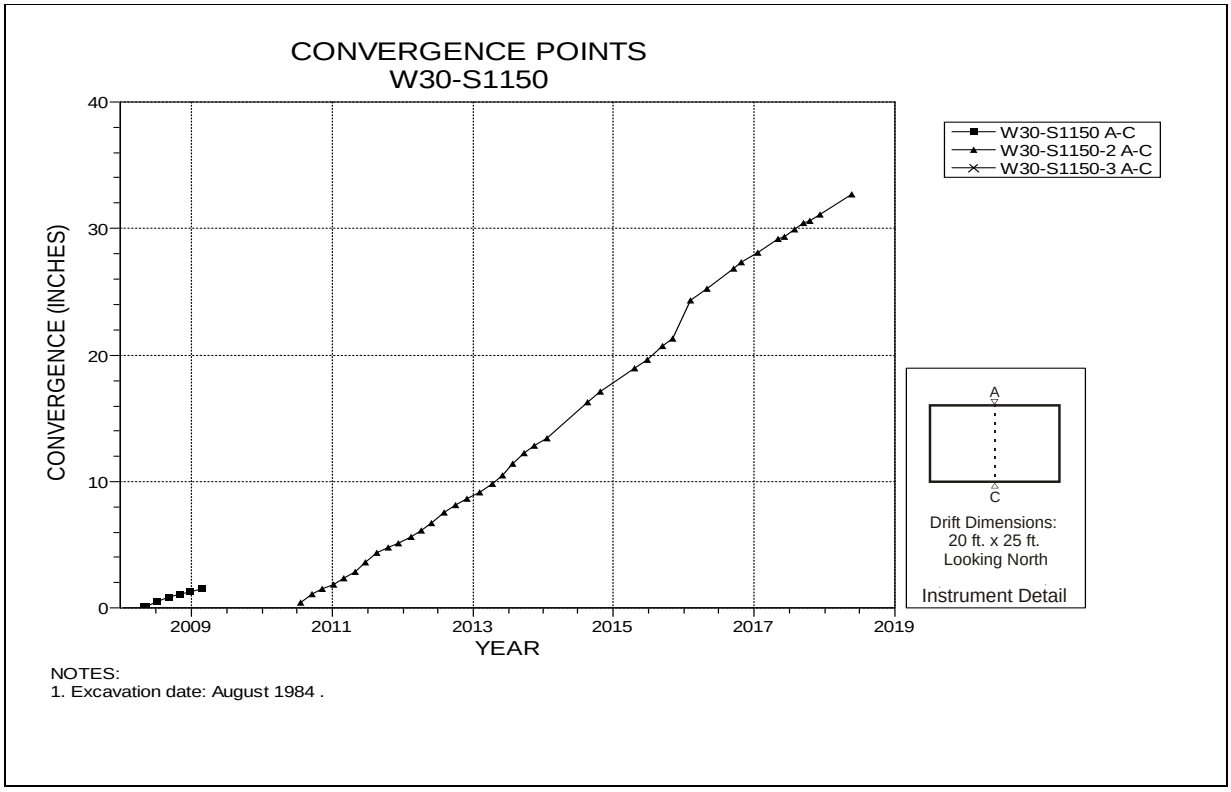

Figure 4-172 Convergence Point Array – W30 S1150 – Roof to Floor – Centerline

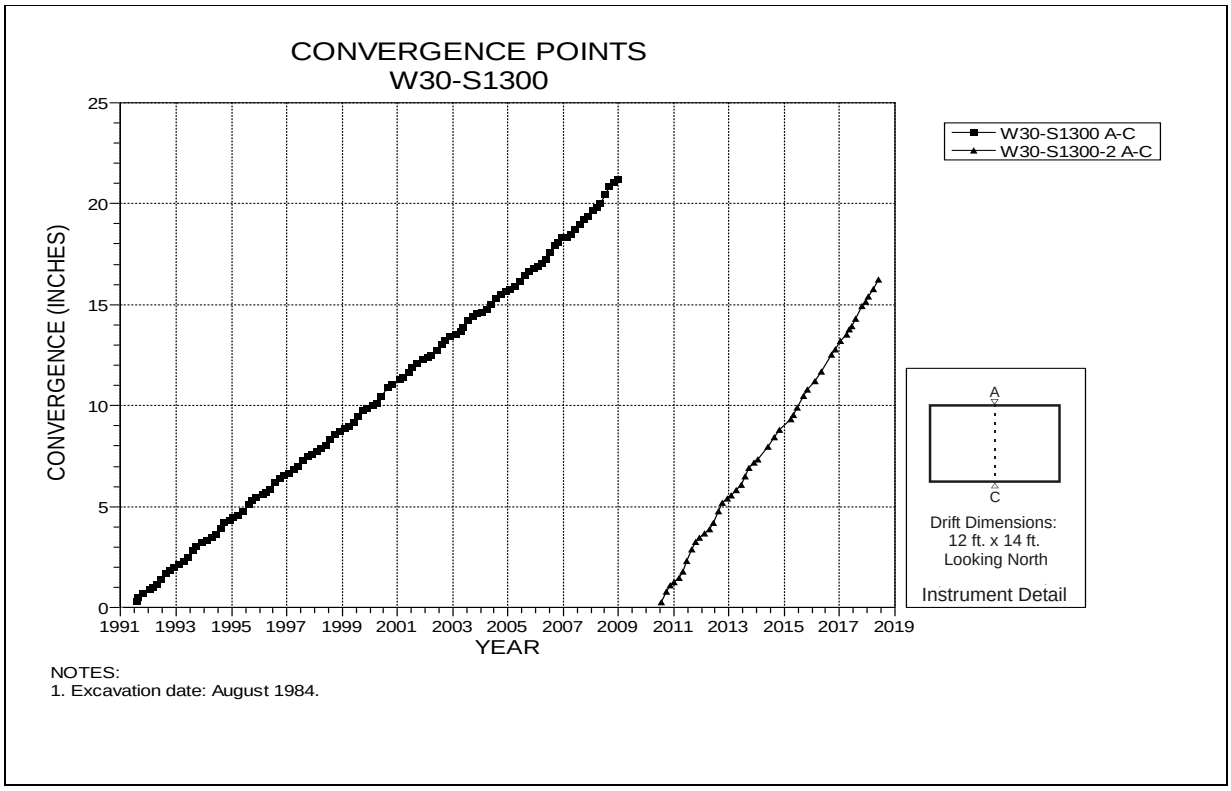

Figure 4-173 Convergence Point Array – W30 S1300 – Roof to Floor – Centerline

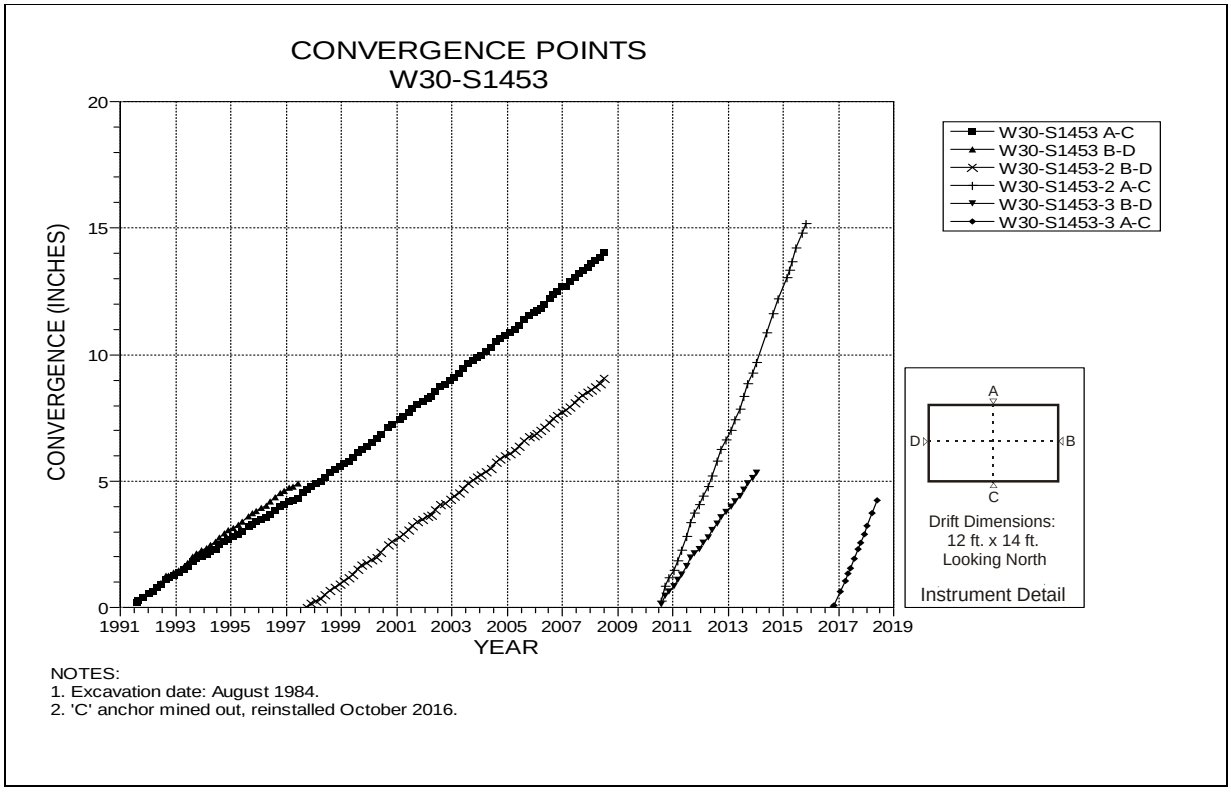

Figure 4-174 Convergence Point Array – W30 S1453 – All Chords

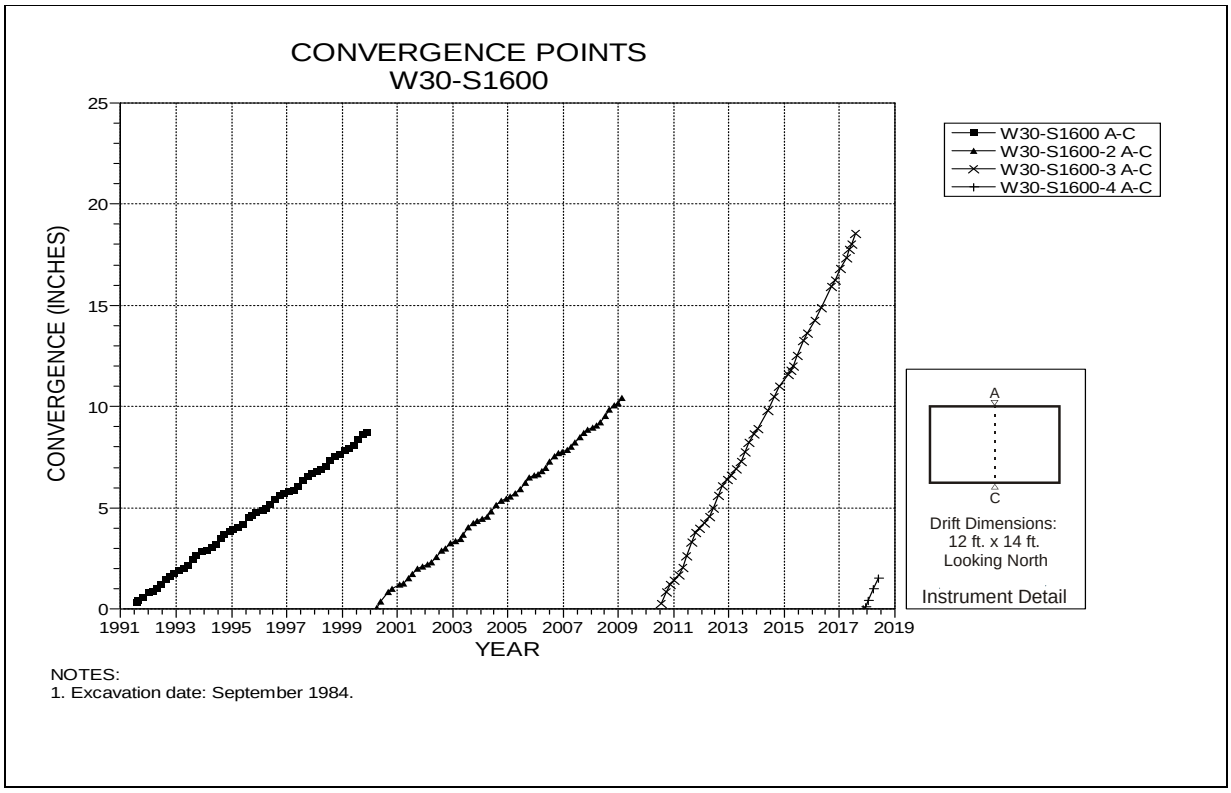

Figure 4-175 Convergence Point Array – W30 S1600 – Roof to Floor – Centerline

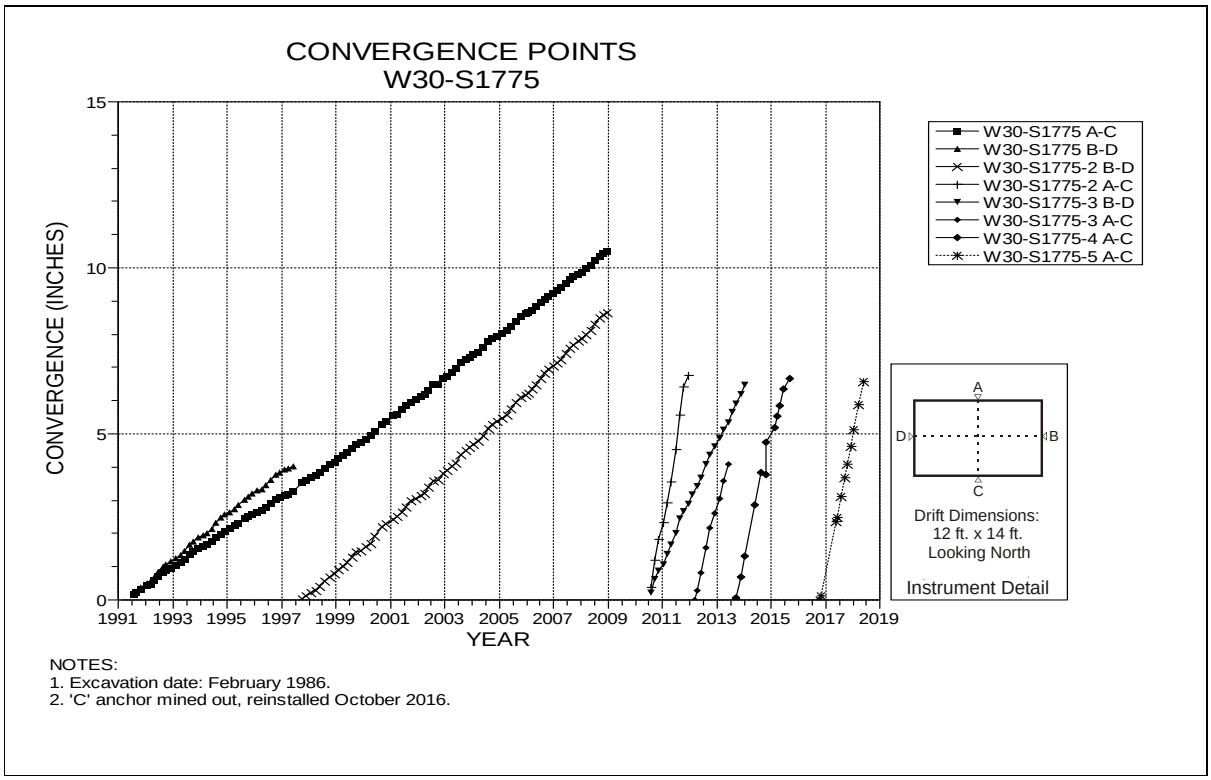

Figure 4-176 Convergence Point Array – W30 S1775 – All Chords

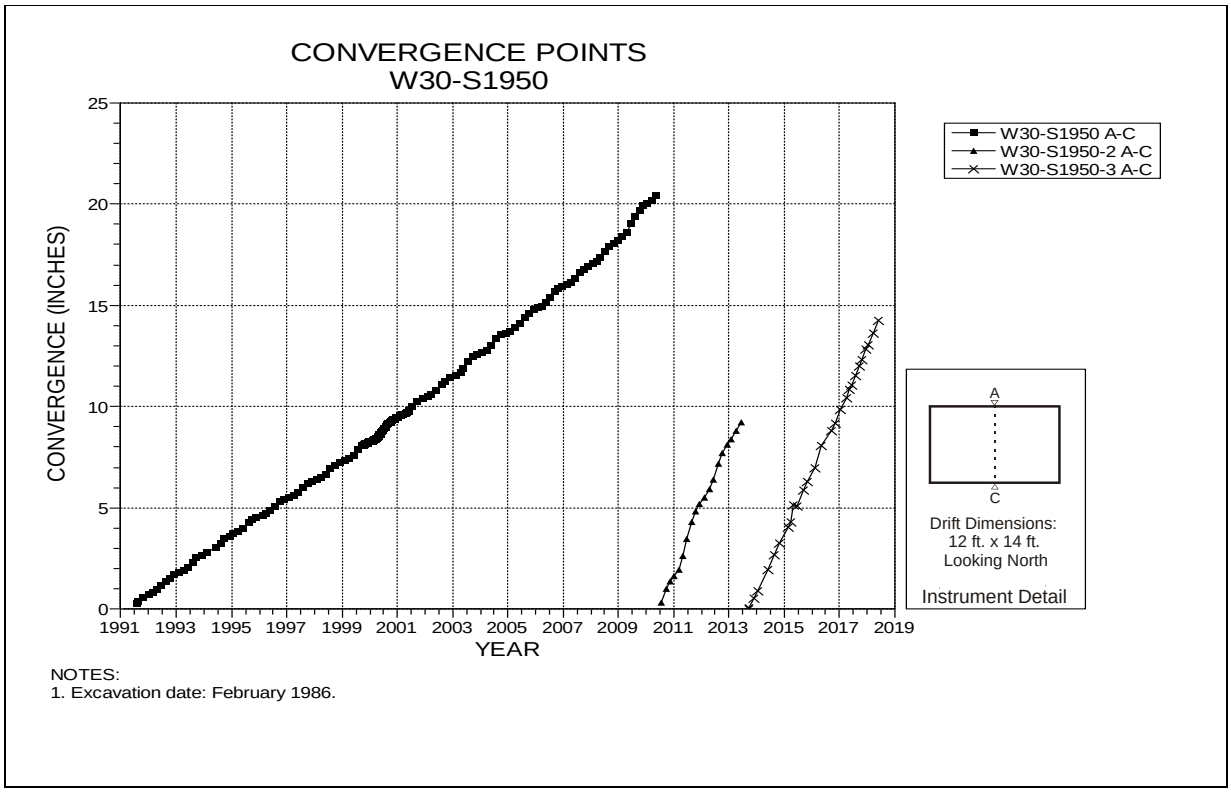

Figure 4-177 Convergence Point Array – W30 S1950 – Roof to Floor – Centerline

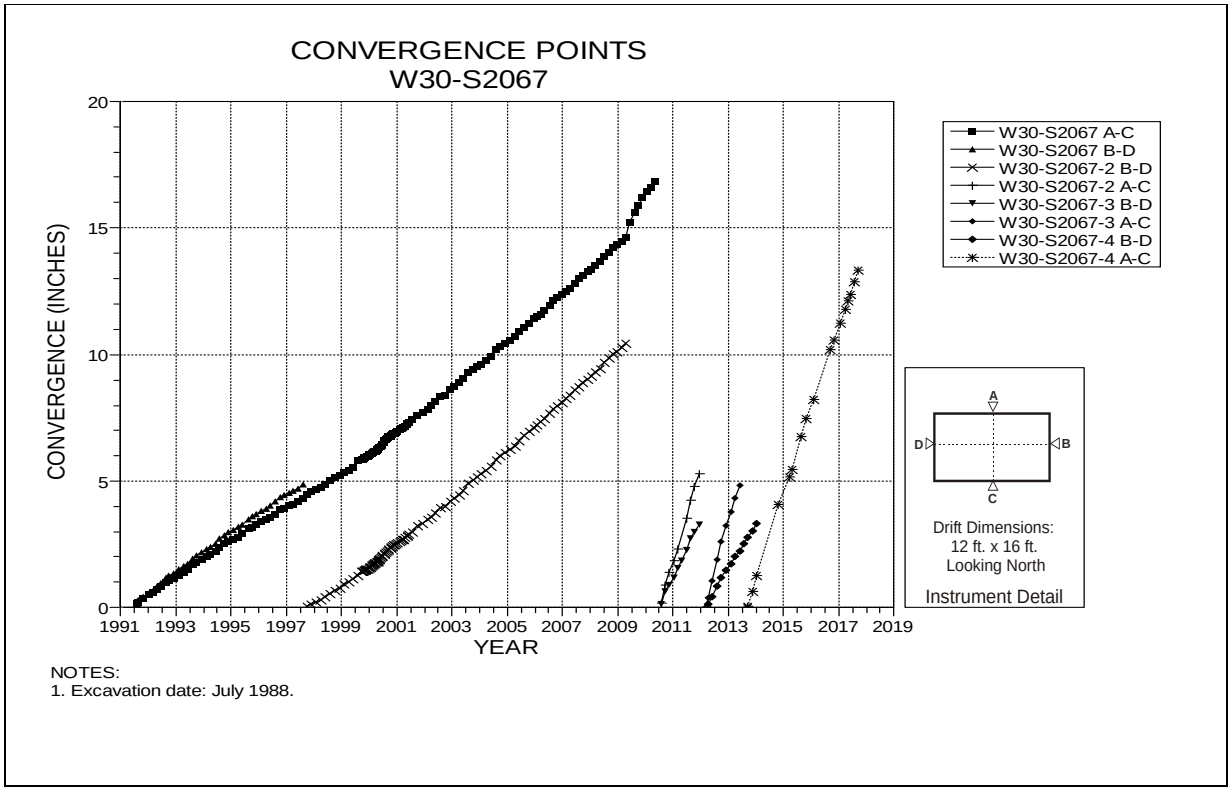

Figure 4-178 Convergence Point Array – W30 S2067 – All Chords

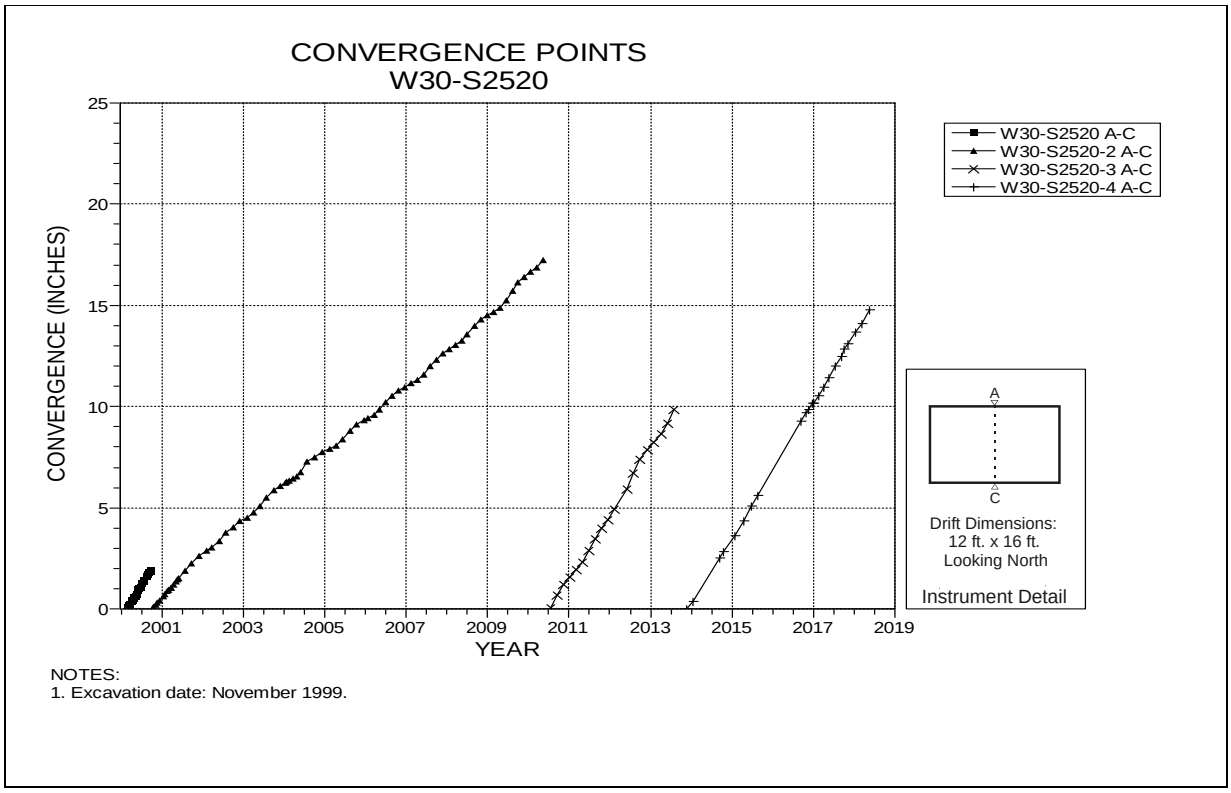

Figure 4-179 Convergence Point Array – W30 S2520 – Roof to Floor – Centerline

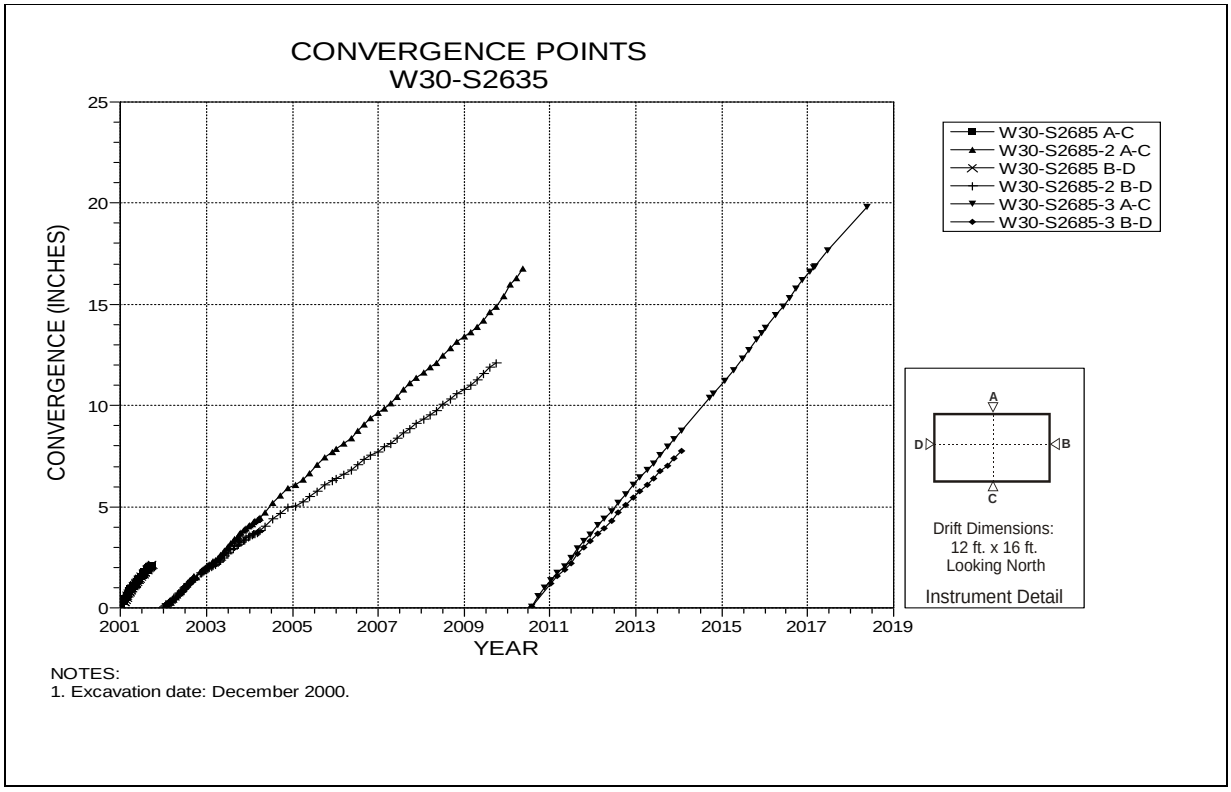

Figure 4-180 Convergence Point Array – W30 S2635 – All Chords

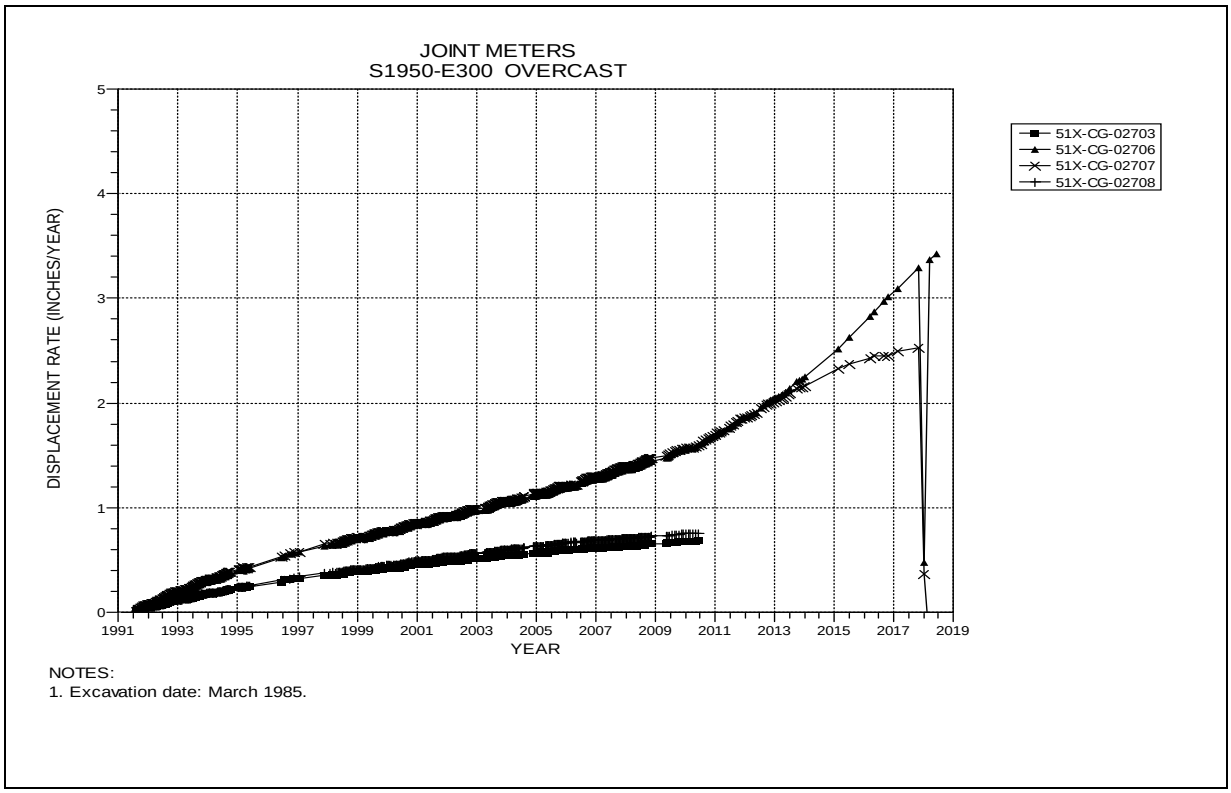

Figure 4-181 Joint Meter – S1950 E300 Overcast

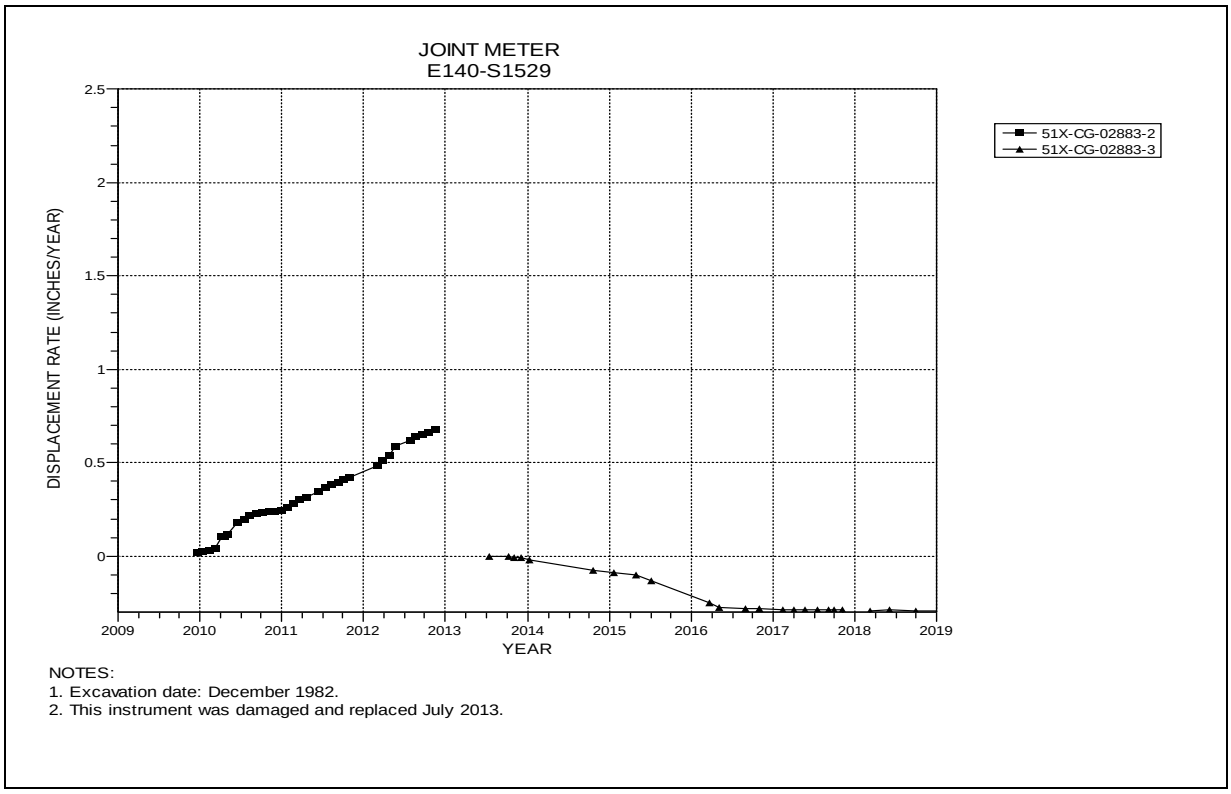

Figure 4-182 Joint Meter – E140 S1529

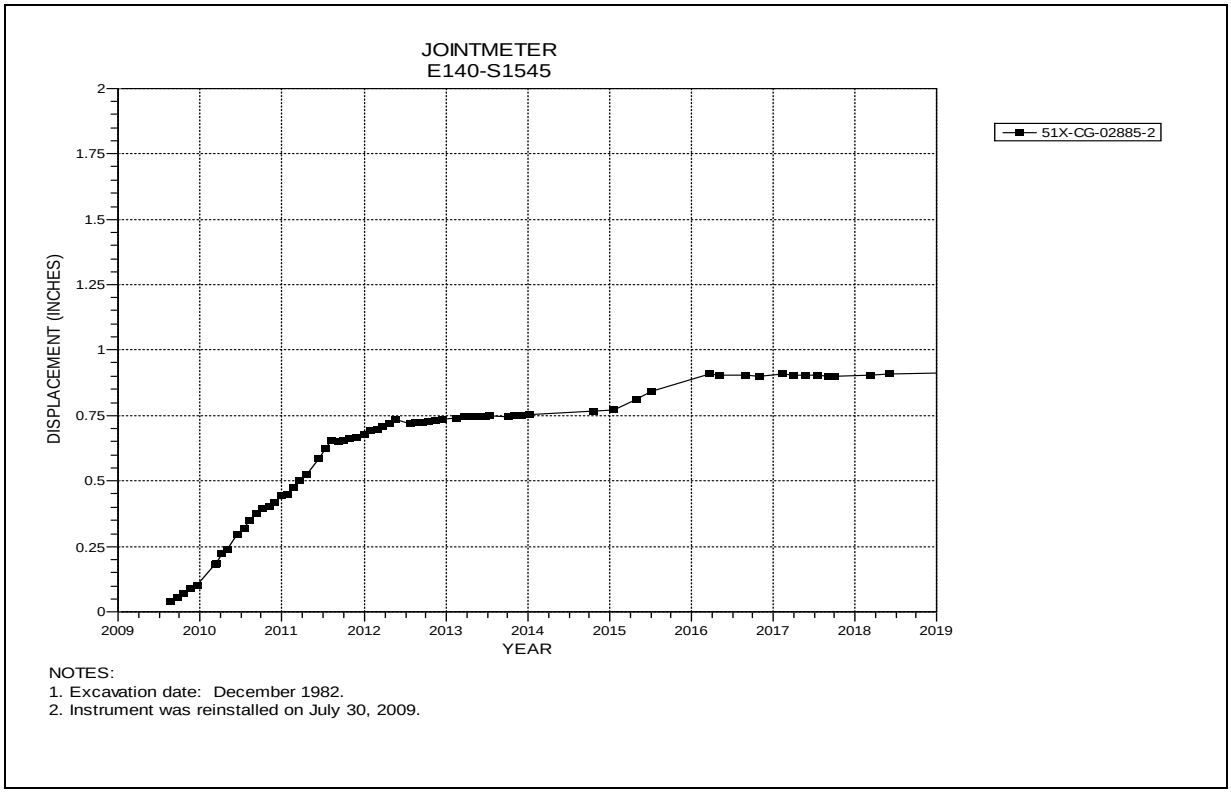

Figure 4-183 Joint Meter – E140 S1545

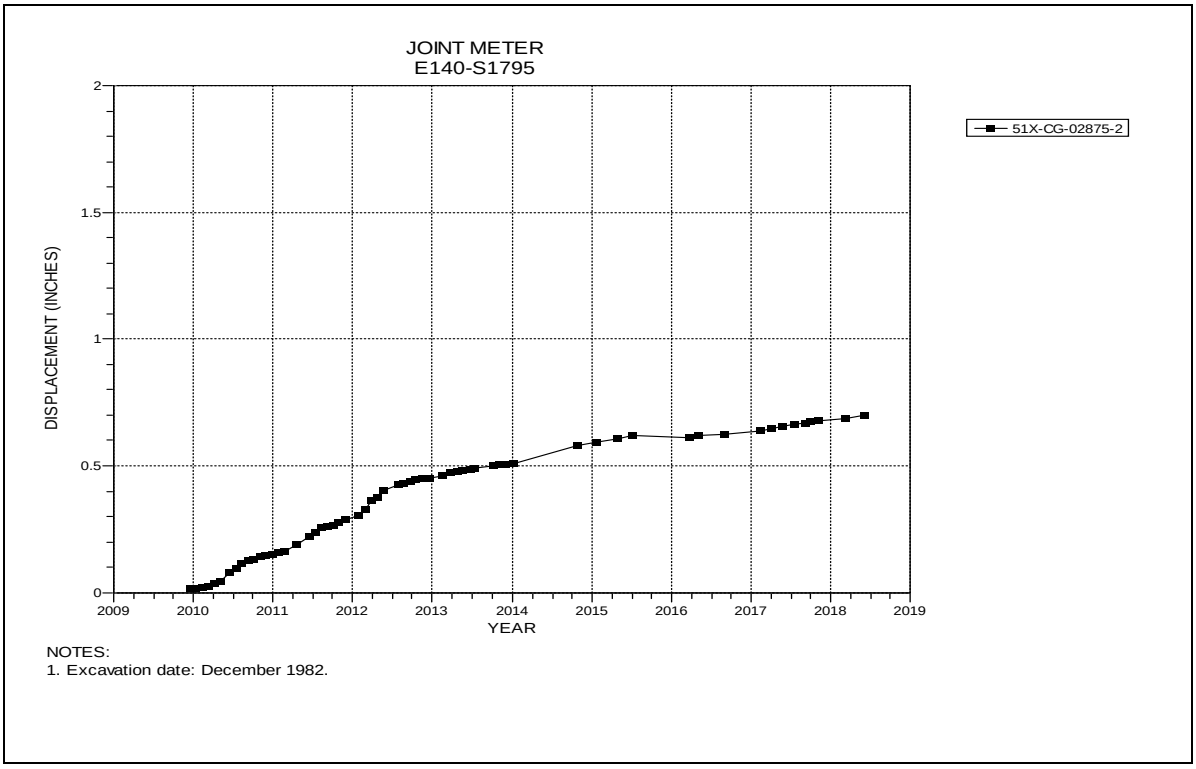

Figure 4-184 Joint Meter – E140 S1795

5.0 INSTRUMENTATION SUMMARY FOR THE WASTE DISPOSAL AREA

This chapter presents a summary of the data collected from instruments located in the Waste Disposal Area at the WIPP. Table 5-1 presents data and analysis of the access drifts associated with Panel 7. Plots of the instrument data are presented as Figures 5-1 through 5-29.

Table 5-1
Panel 7 Access Drifts Data Analysis

Convergence Points

Field Tag	Location	Figure Number	Last Reading 2017 to 2018		Cumulative Displacement (inches)	Closure Rate[4] 2017 to 2018 (in/year)	Closure Rate[4] 2016 to 2017 (in/year)	Rate Change Percent[4]	Comments
			Date	Inches					
S2180-W285-2 A-C	S2180-W285	5-1	6/13/2018	11.367	11.813	1.6	1.4	14	
S2180-W585-4 A-C	S2180-W585	5-2	6/13/2018	27.826	37.803	5.2	3.3	58	
S2180-W660-4 A-C	S2180-W660	5-3	6/13/2018	25.264	34.673	3.5	4.9	-29	
S2180-W790-3 A-C	S2180-W790	5-4	11/20/2017	24.091	34.663	2.8	5.3	-47	
S2180-W855-3 A-C	S2180-W855	5-5	12/18/2017	21.300	31.674	3.0	2.7	11	
S2180-W920-3 A-C	S2180-W920	5-6	2/22/2018	21.477	31.358	3.0	4.1	-27	
S2180-W985-4 A-C	S2180-W985	5-7	8/3/2017	20.952	36.998	3.0	5.2	-42	
S2180-W1050-2 A-C	S2180-W1050	5-8	8/3/2017	17.491	26.064	3.7	4.4	-16	
W390-S2275-3 A-C	W390-S2275	5-9	6/13/2018	29.056	36.990	4.9	5.0	-2	
W390-S2350-3 A-C	W390-S2350	5-10	6/13/2018	21.980	28.544	4.0	3.9	3	
W390-S2425-4 A-C	W390-S2425	5-11	5/9/2018	5.295	28.351	3.3	3.8	-13	
W520-S2275-3 A-C	W520-S2275	5-12	6/13/2018	32.867	41.319	4.7	6.3	-25	
W520-S2350-3 A-C	W520-S2350	5-13	6/13/2018	21.913	34.782	3.6	-0.5	-820	Floor point displaced by equipment
W520-S2425-4 A-C	W520-S2425	5-14	6/13/2018	4.872	35.738	3.6	2.2	64	
W660-S2275-3 A-C	W660-S2275	5-15	8/3/2017	21.440	30.456	4.3	4.3	0	
W660-S2350-3 A-C	W660-S2350	5-16	6/13/2018	24.859	41.588	3.5	3.1	13	
W660-S2425-3 A-C	W660-S2425	5-17	8/3/2017	21.798	34.352	5.6	3.2	75	
W920-S2350-4 A-C	W920-S2350	5-18	1/22/2018	2.178	26.644	1.7	2.5	-32	
W920-S2425-4 A-C	W920-S2425	5-19	1/22/2018	2.940	25.937	2.0	3.6	-44	
S2520-W285-5 A-C	S2520-W285	5-20	6/13/2018	6.782	29.771	4.6	4.2	10	
S2520-W390-4 A-C	S2520-W390	5-21	6/13/2018	5.588	28.192	3.7	3.5	6	
S2520-W455-3 A-C	S2520-W455	5-22	6/13/2018	23.618	31.308	3.6	3.7	-3	
S2520-W520-3 A-C	S2520-W520	5-23	6/13/2018	25.491	38.269	3.9	4.6	-15	
S2520-W585-5 A-C	S2520-W585	5-24	6/13/2018	5.215	27.391	3.6	3.8	-5	
S2520-W660-3 A-C	S2520-W660	5-25	6/13/2018	26.648	40.082	5.1	5.6	-9	
S2520-W725-5 A-C	S2520-W725	5-26	6/13/2018	23.877	32.828	3.3	3.8	-13	
S2520-W790-5 A-C	S2520-W790	5-27	6/13/2018	4.927	30.142	3.4	3.4	0	
S2520-W855-3 A-C	S2520-W855	5-28	6/13/2018	24.045	37.978	3.5	3.1	13	
S2520-W920-5 A-C	S2520-W920	5-29	6/13/2018	3.668	26.939	2.8	1.6	75	

[4] N/A – Insufficient data available to perform the calculation. This is usually due to the inability to read the instruments because of activities such as the removal of an instrument due to floor, rib or back trimming; locations blocked by equipment or waste disposal; installation timing, access issues, etc.

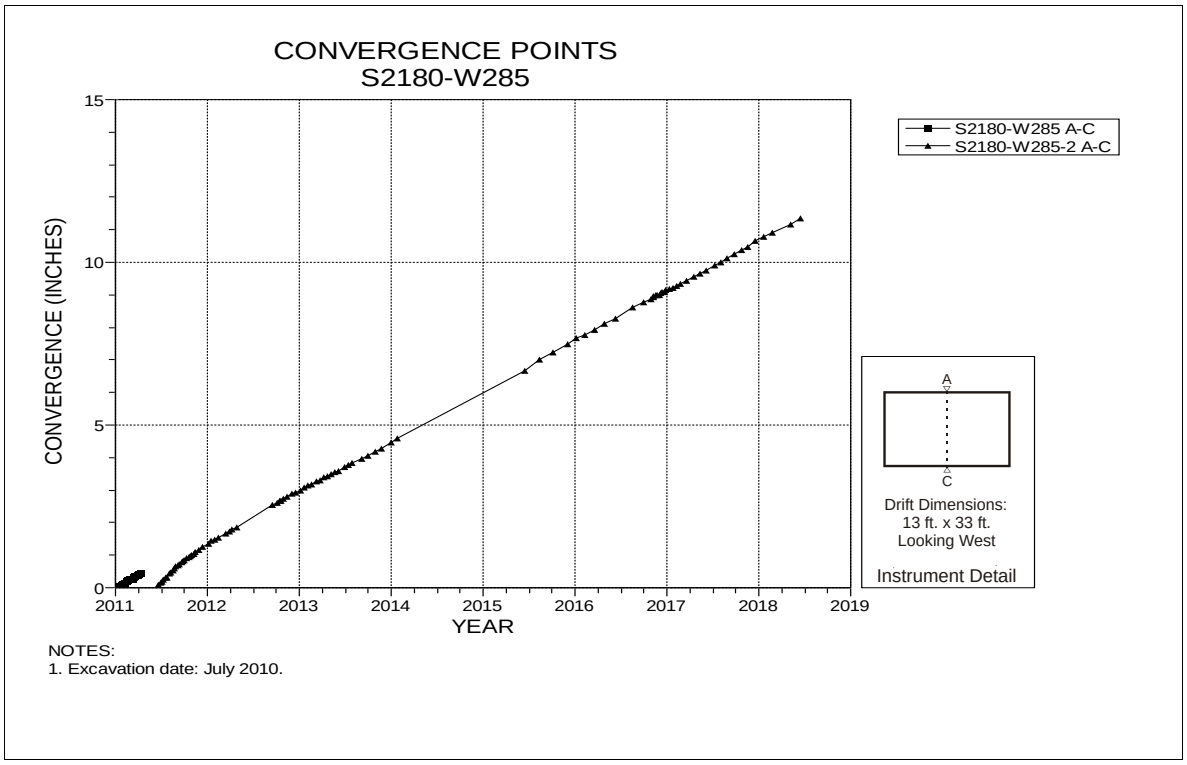

Figure 5-1 Convergence Point Array – S2180 W285 – Roof to Floor

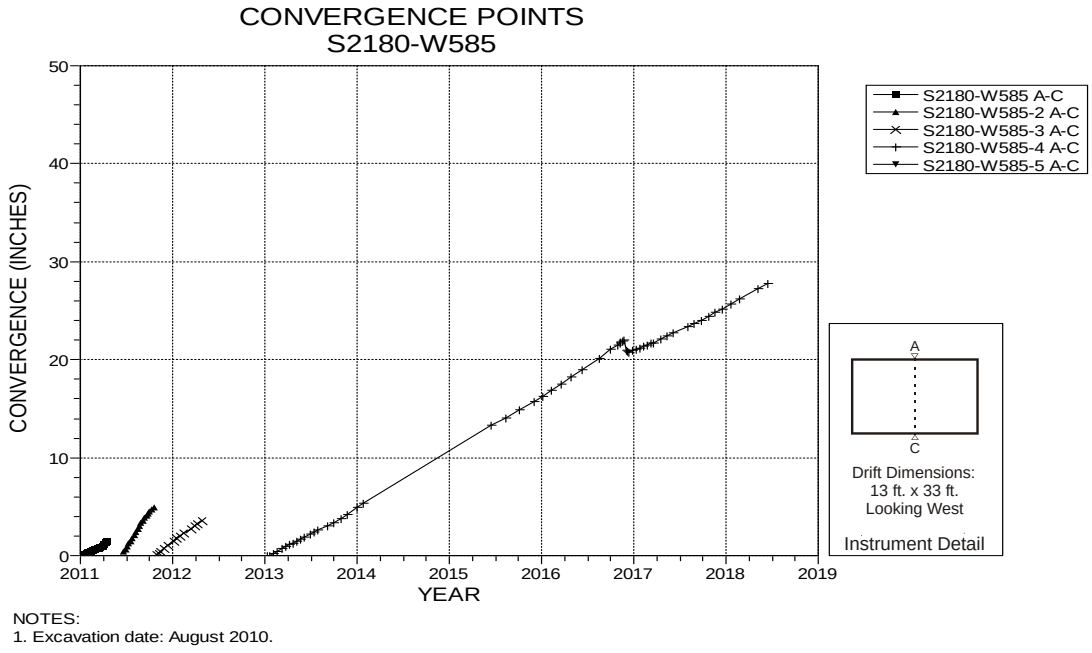

Figure 5-2 Convergence Point Array – S2180 W585 – Roof to Floor

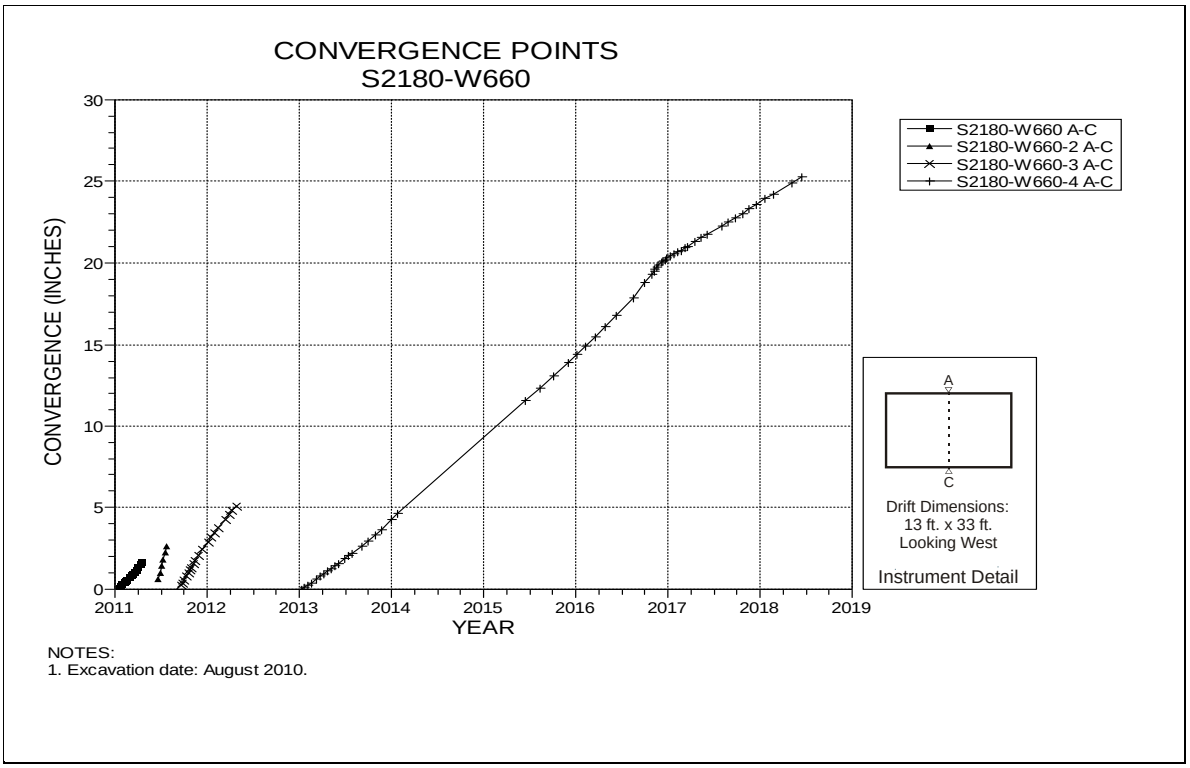

Figure 5-3 Convergence Point Array – S2180 W660 – Roof to Floor

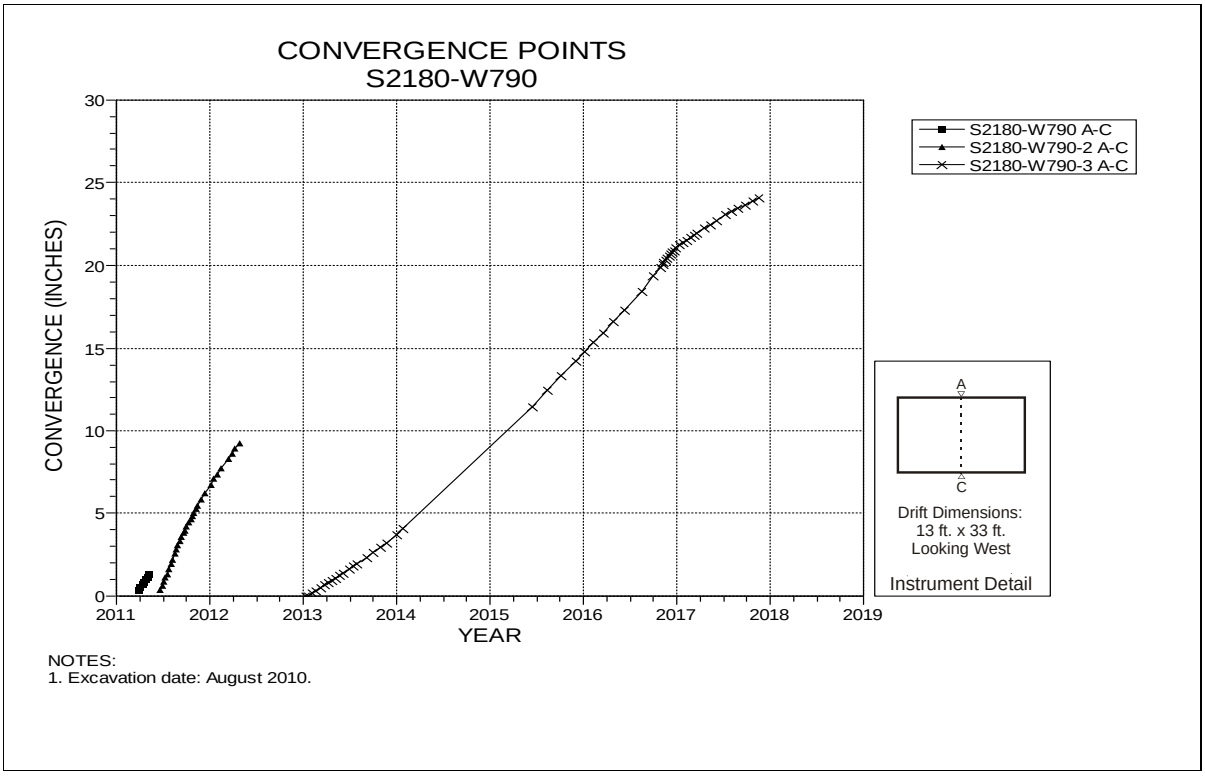

Figure 5-4 Convergence Point Array – S2180 W790 – Roof to Floor

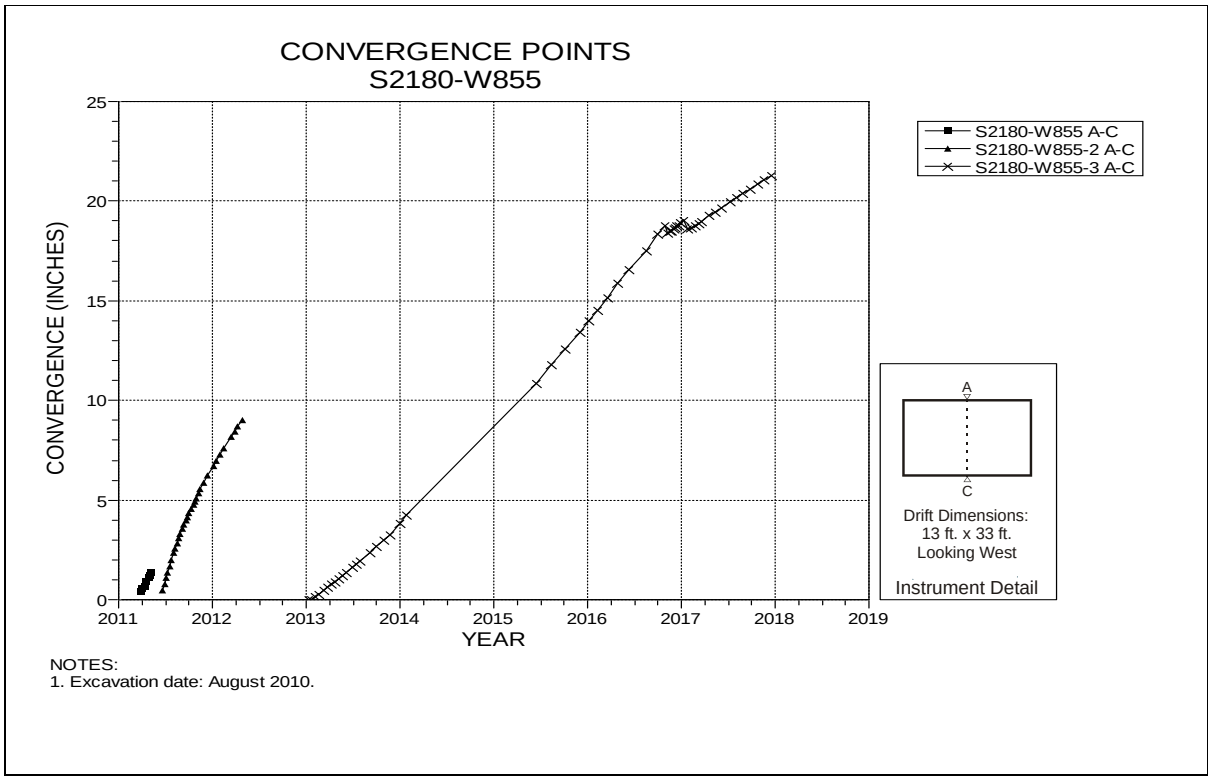

Figure 5-5 Convergence Point Array – S2180 W855 – Roof to Floor

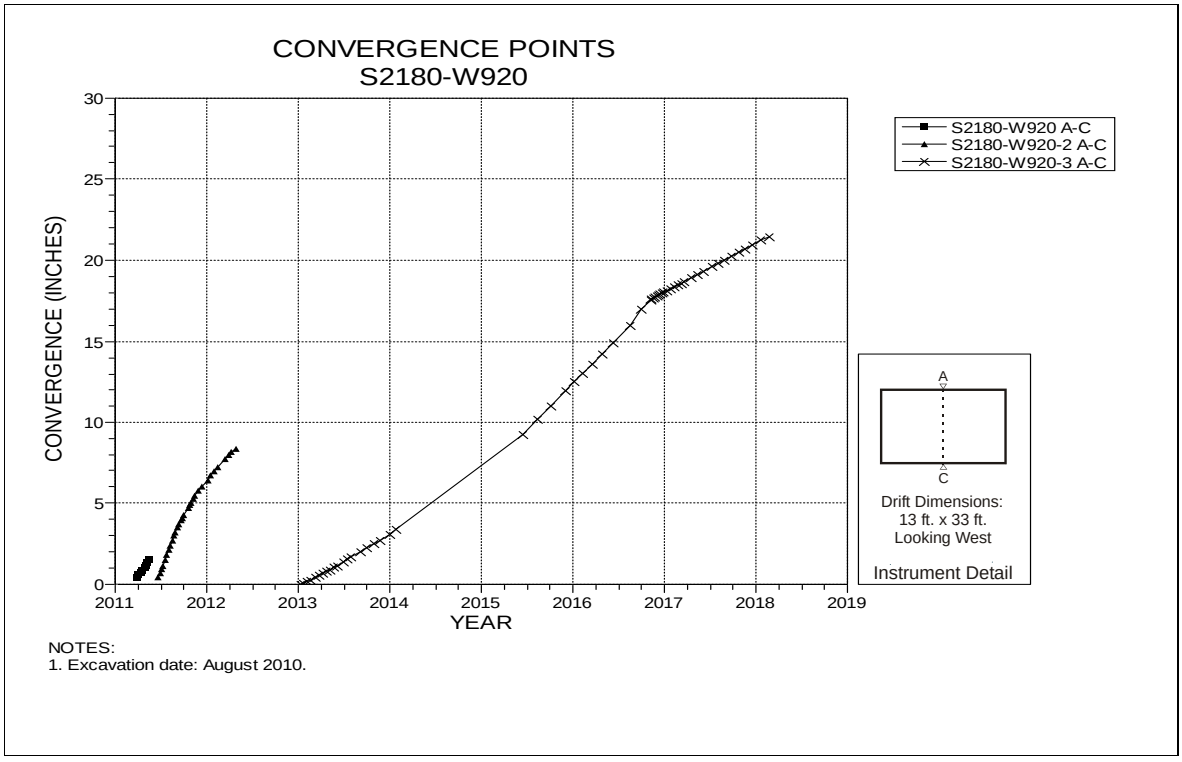

Figure 5-6 Convergence Point Array – S2180 W920 – Roof to Floor

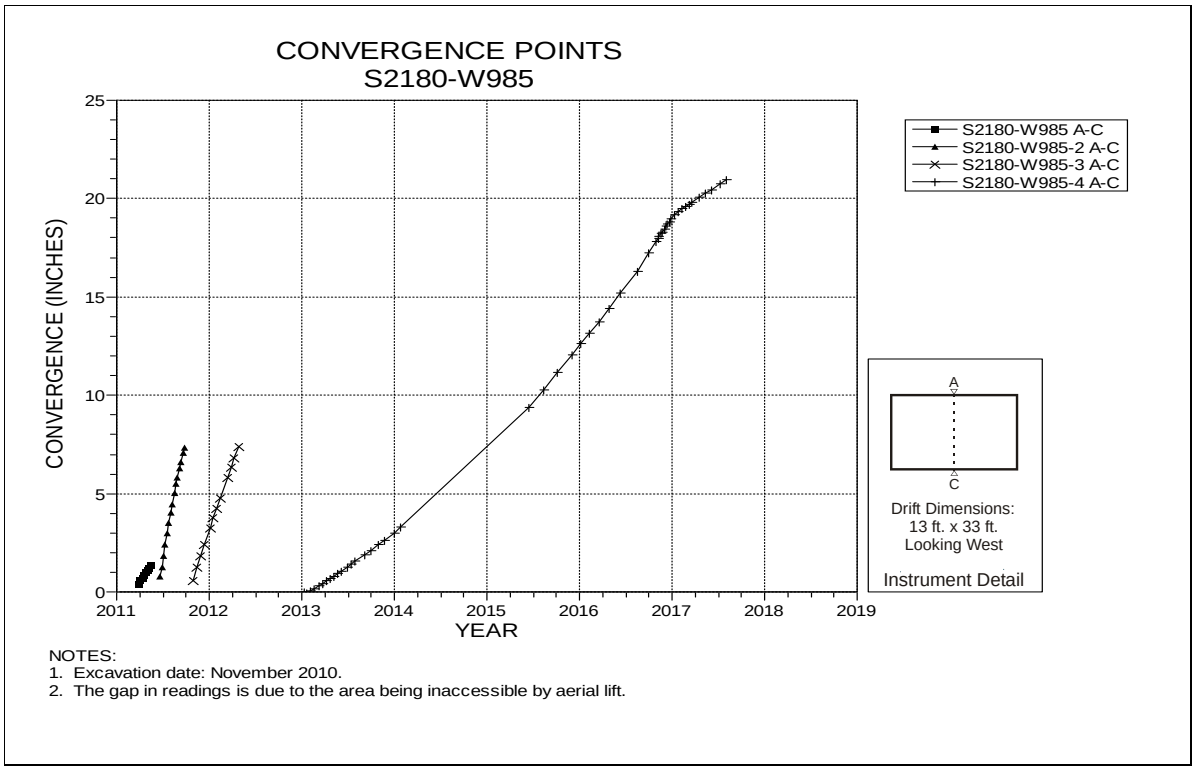

Figure 5-7 Convergence Point Array – S2180 W985 – Roof to Floor

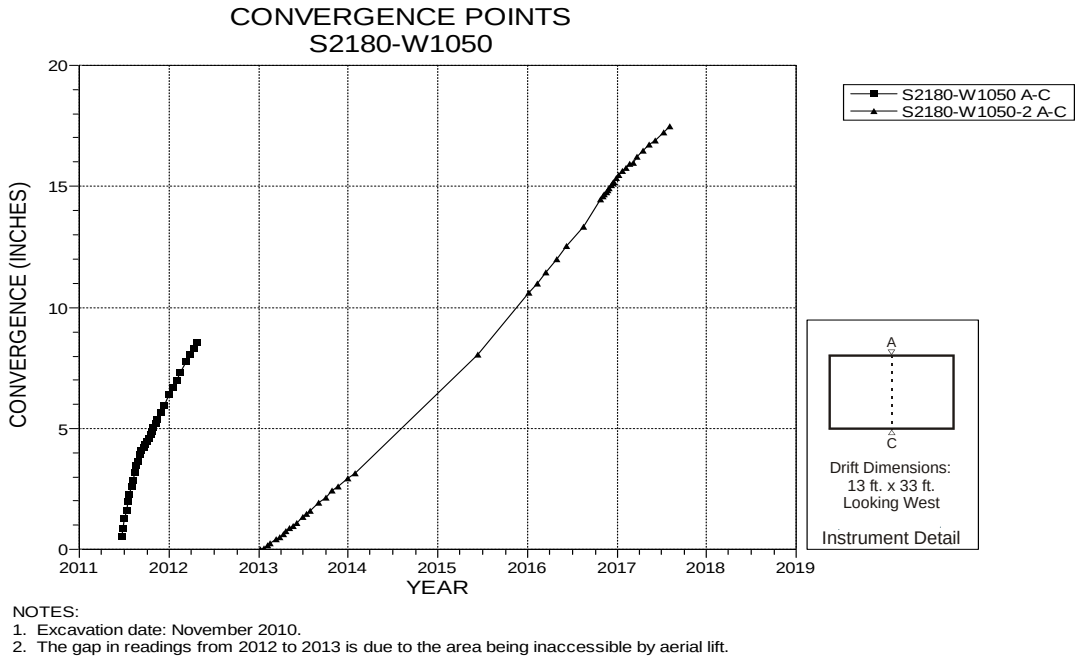

Figure 5-8 Convergence Point Array – S2180 W1050 – Roof to Floor

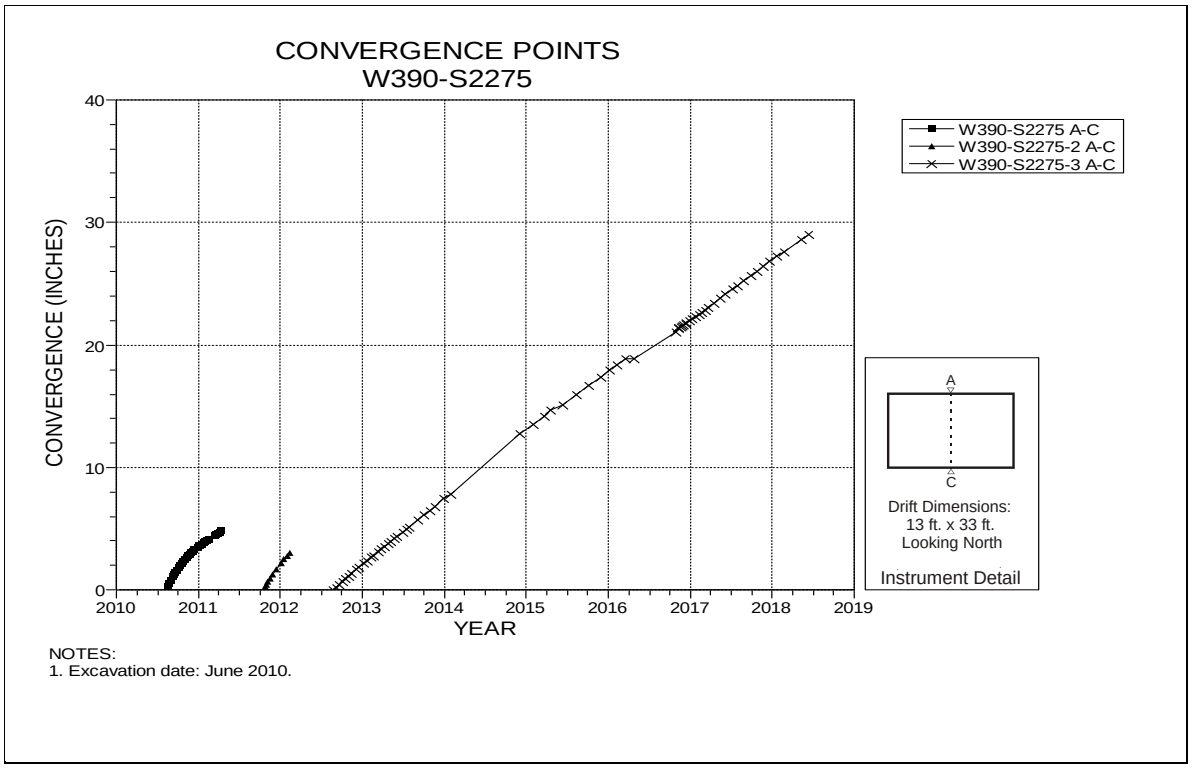

Figure 5-9 Convergence Point Array – W390 S2275 – Roof to Floor

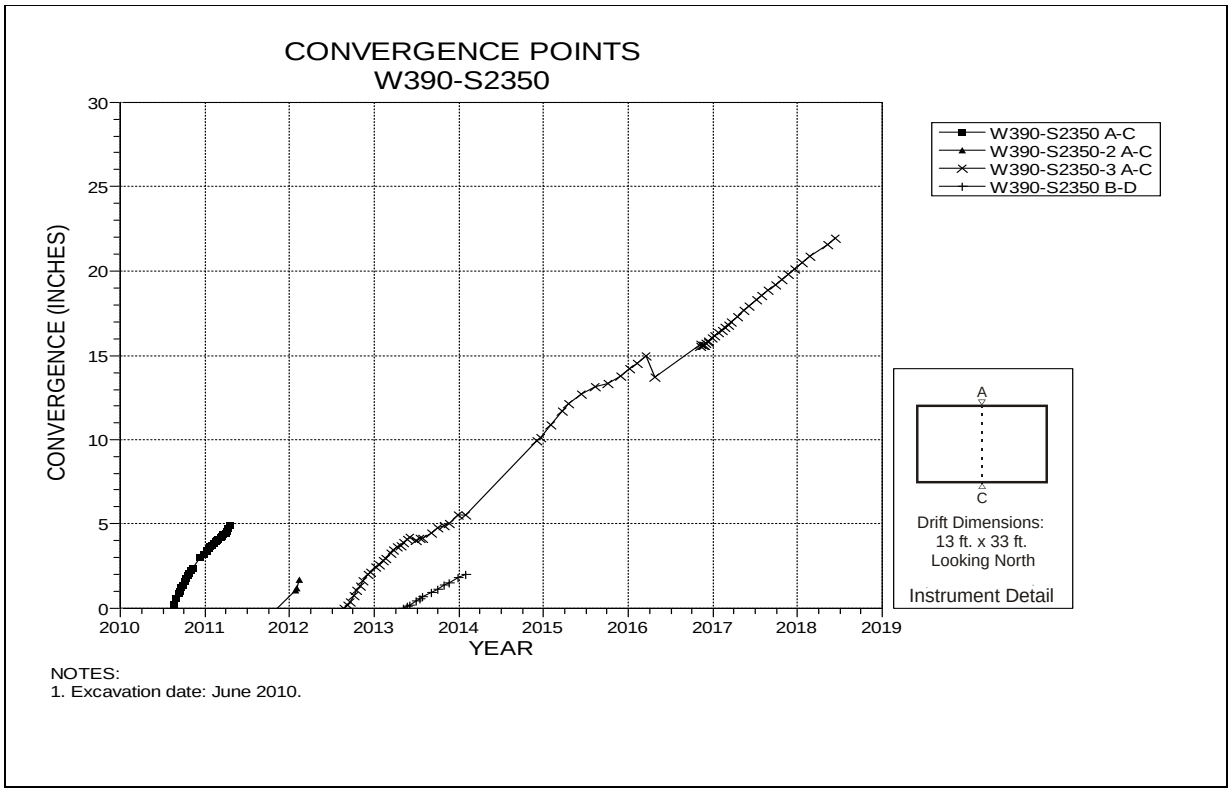

Figure 5-10 Convergence Point Array – W390 S2350 – Roof to Floor

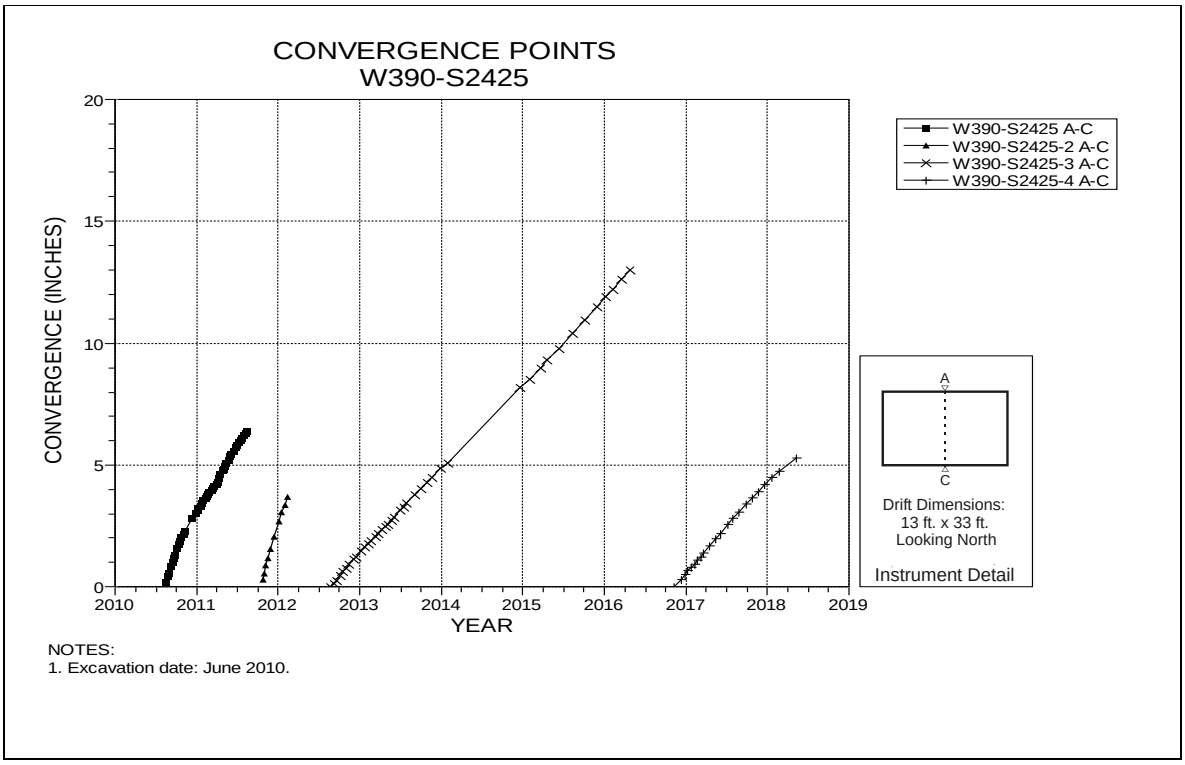

Figure 5-11 Convergence Point Array – W390 S2425 – Roof to Floor

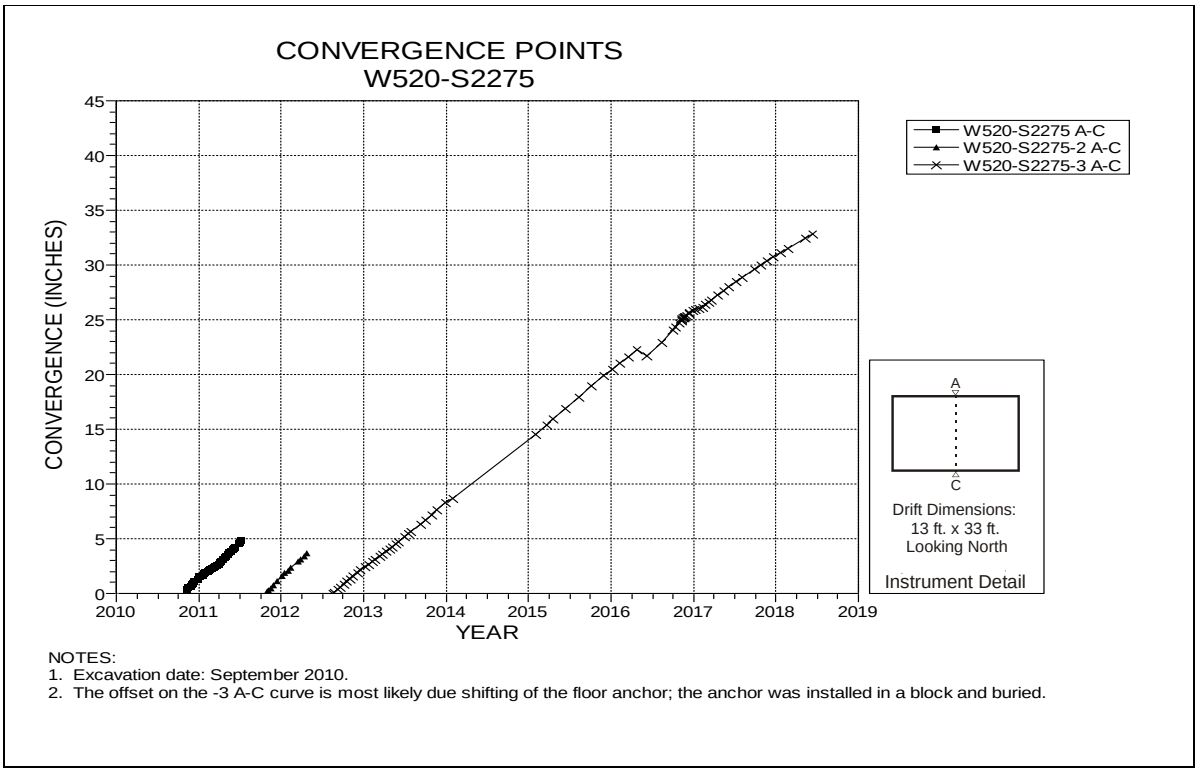

Figure 5-12 Convergence Point Array – W520 S2275 – Roof to Floor

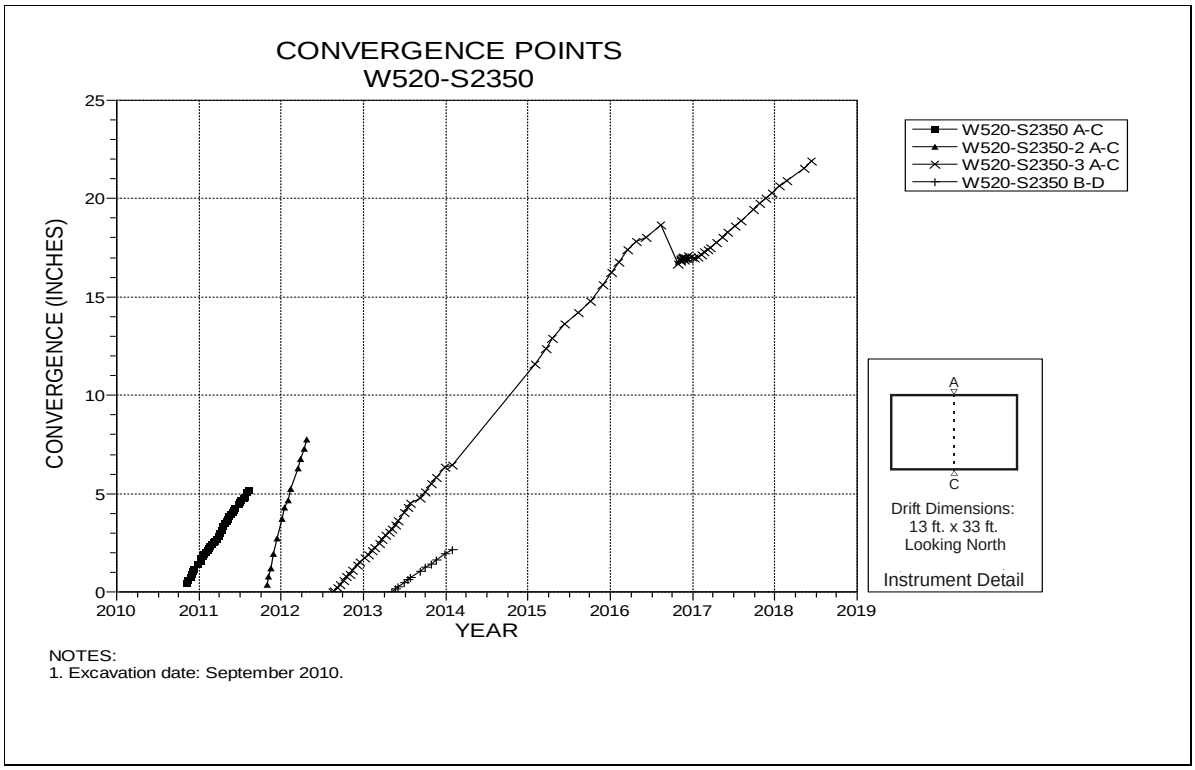

Figure 5-13 Convergence Point Array – W520 S2350 – Roof to Floor

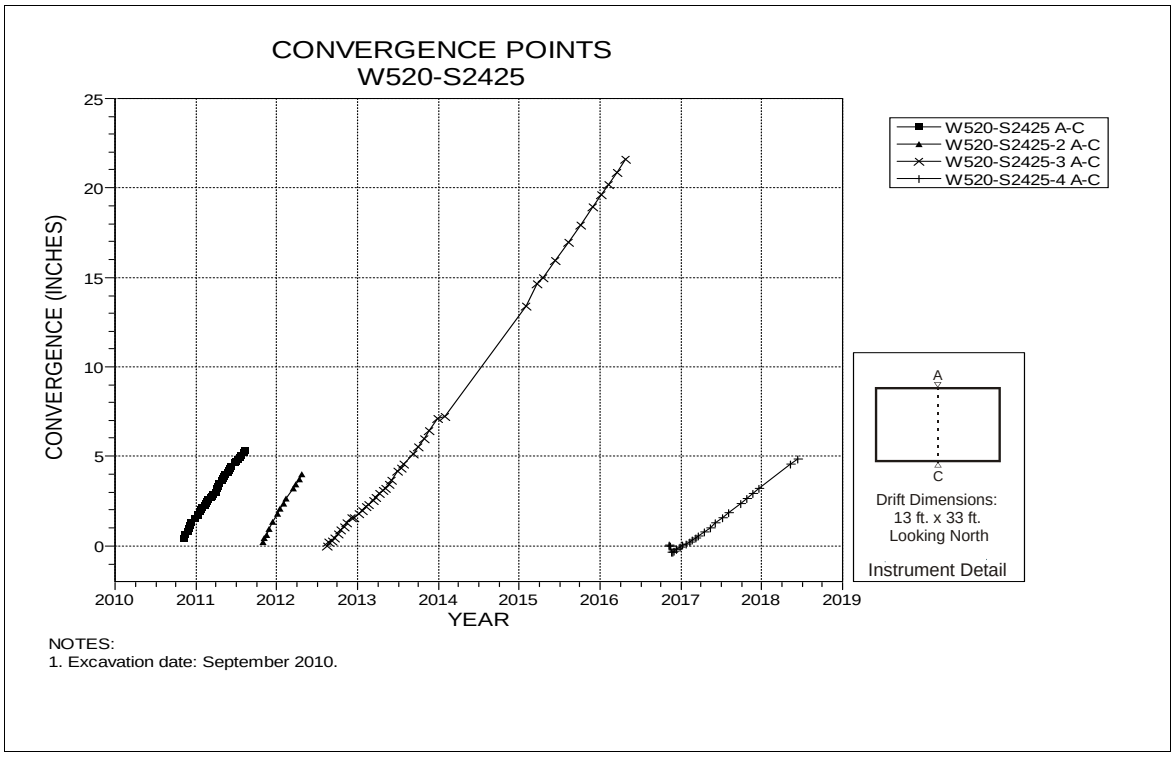

Figure 5-14 Convergence Point Array – W520 S2425 – Roof to Floor

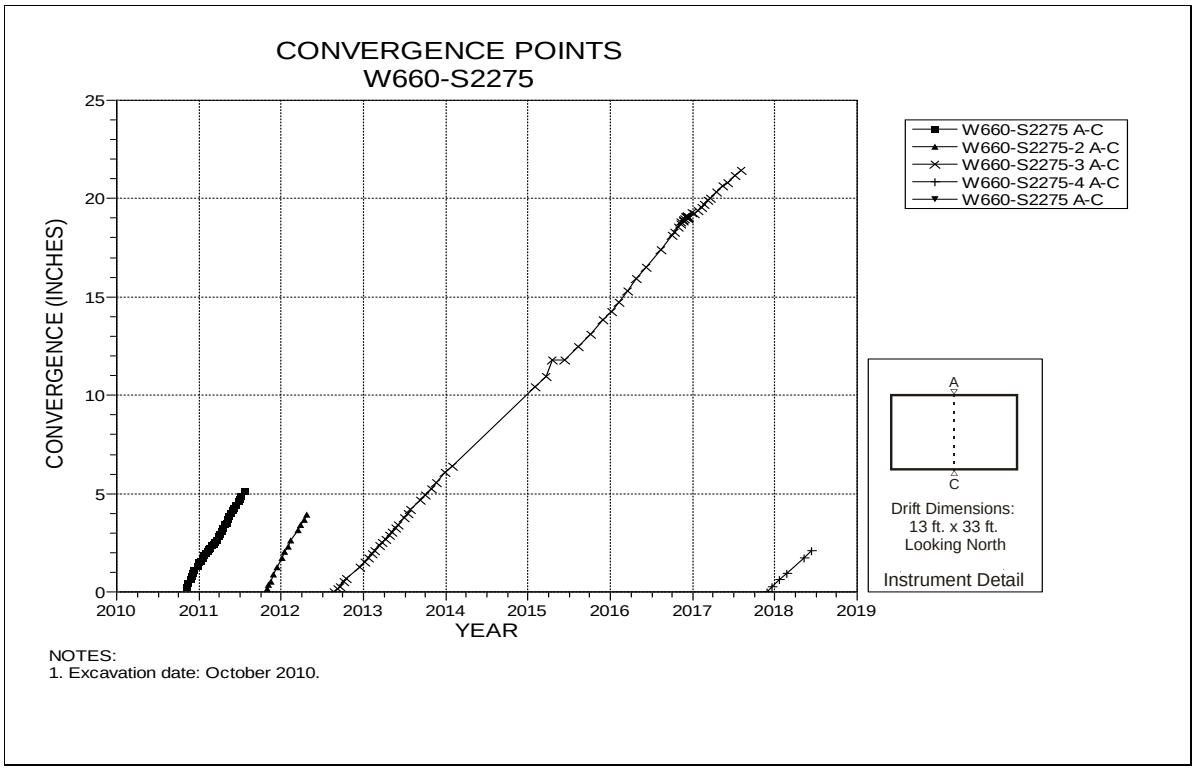

Figure 5-15 Convergence Point Array – W660 S2275 – Roof to Floor

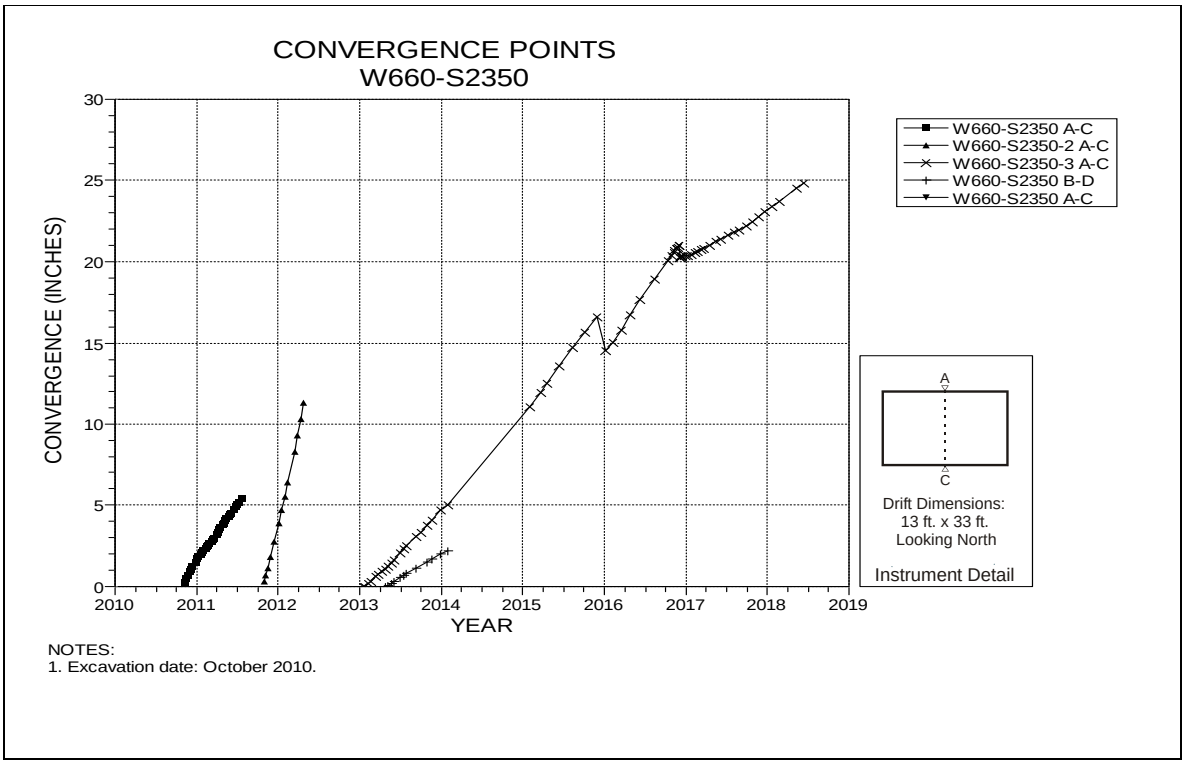

Figure 5-16 Convergence Point Array – W660 S2350 – Roof to Floor

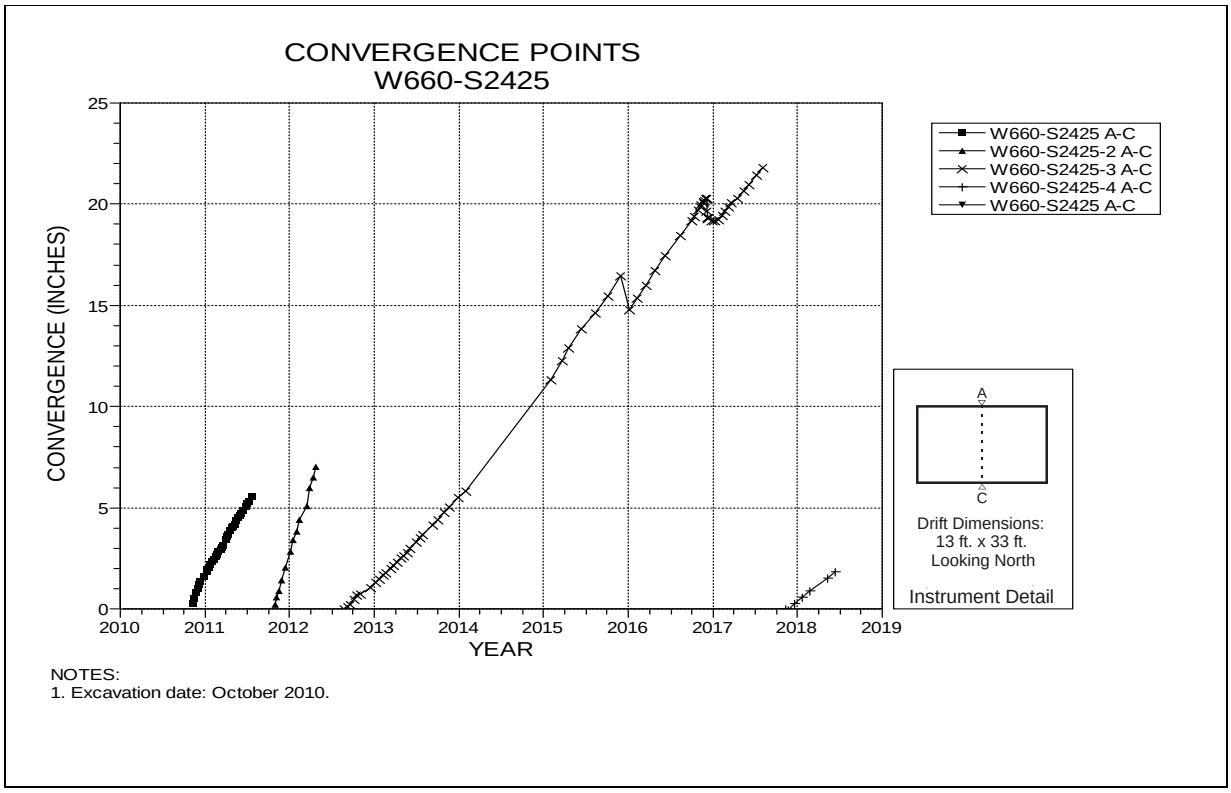

Figure 5-17 Convergence Point Array – W660 S2425 – Roof to Floor

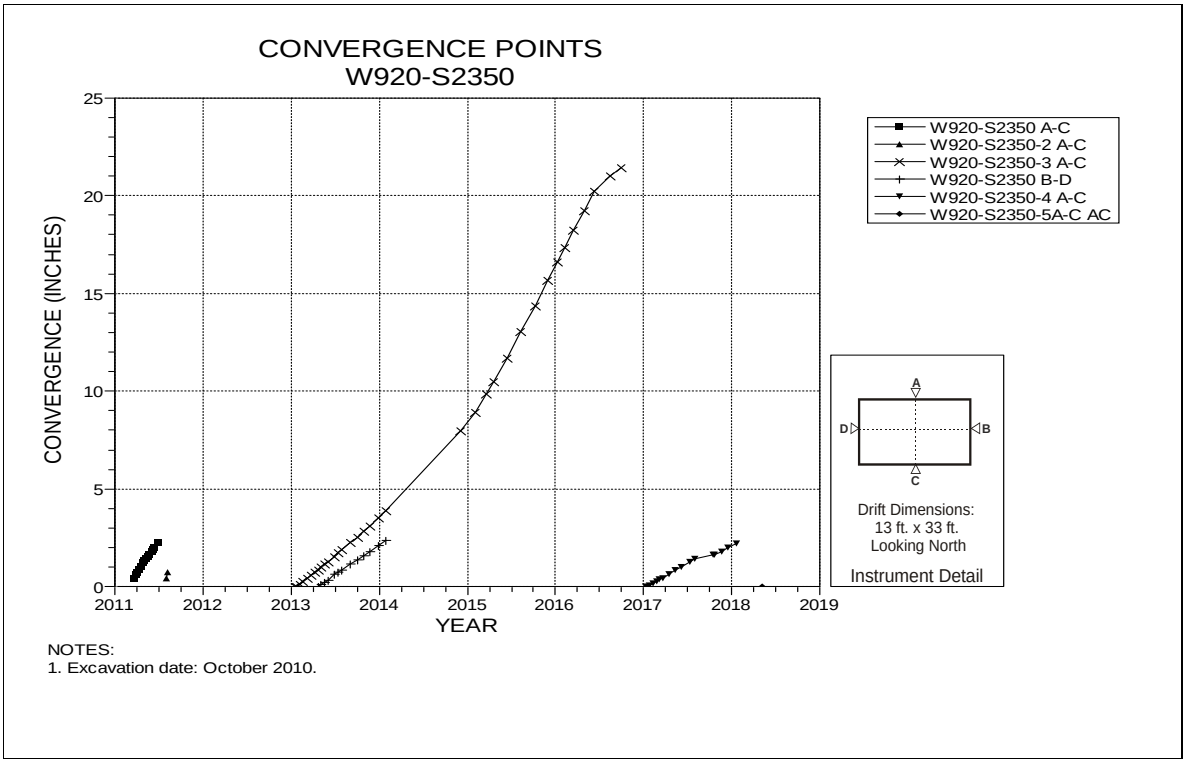

Figure 5-18 Convergence Point Array – W920 S2350 – Roof to Floor

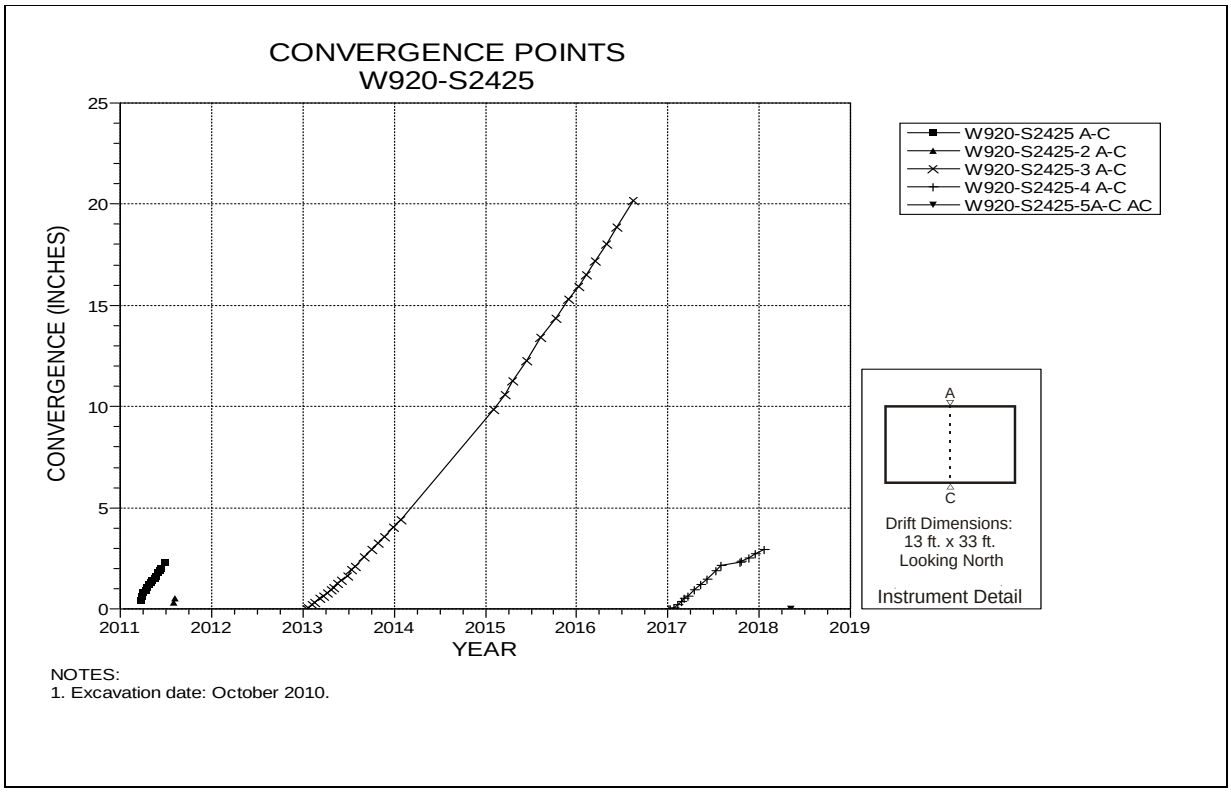

Figure 5-19 Convergence Point Array – W920 S2425 – Roof to Floor

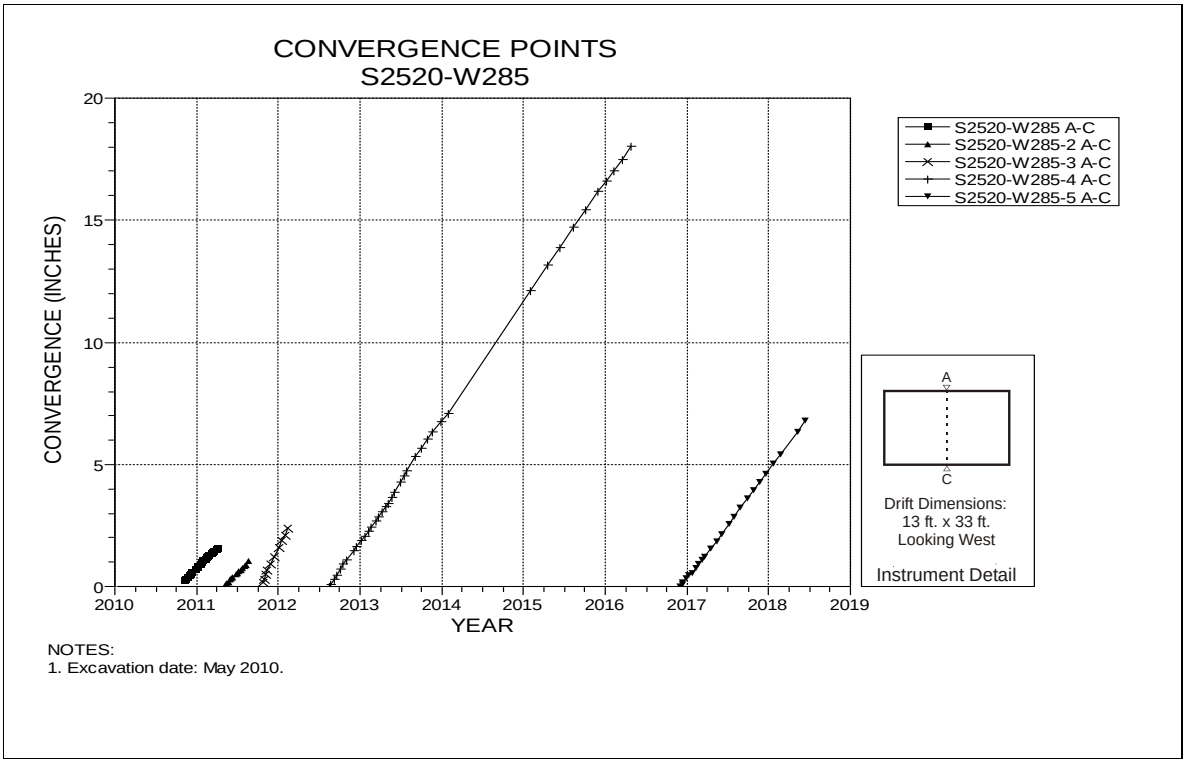

Figure 5-20 Convergence Point Array – S2520 W285 – Roof to Floor

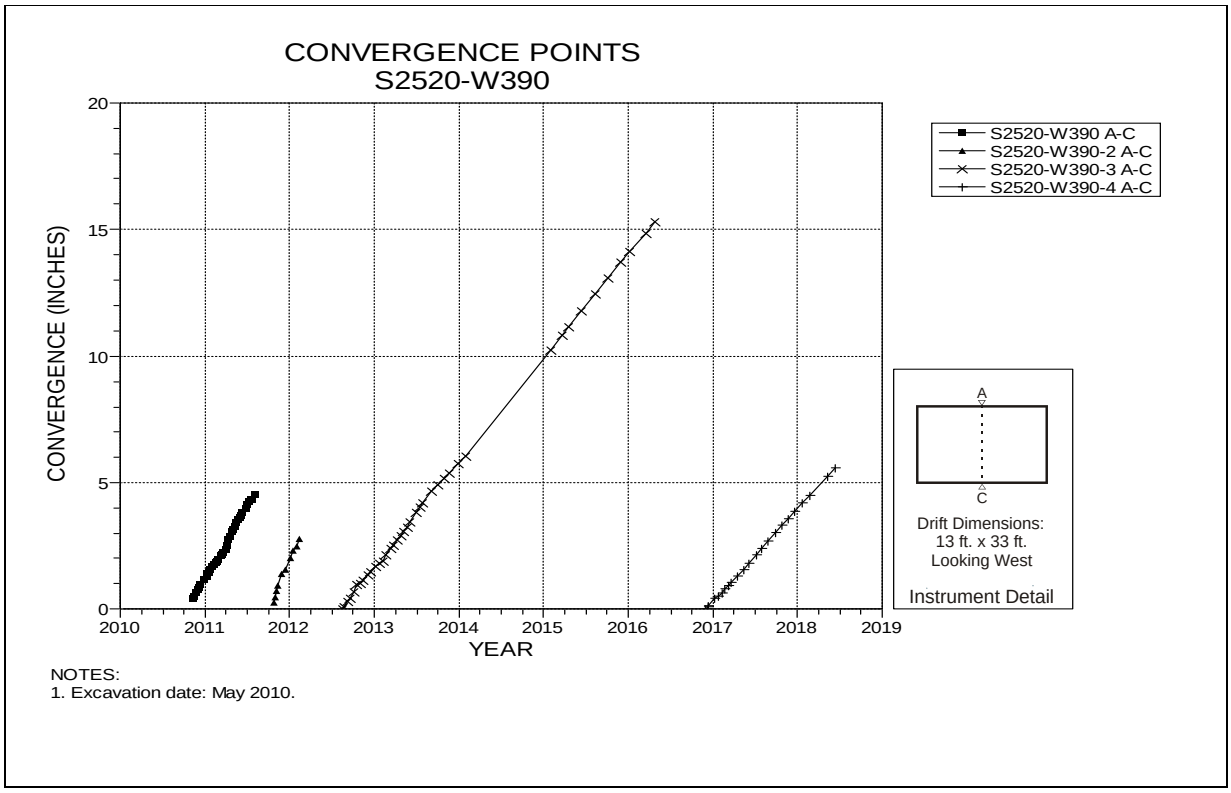

Figure 5-21 Convergence Point Array – S2520 W390 – Roof to Floor

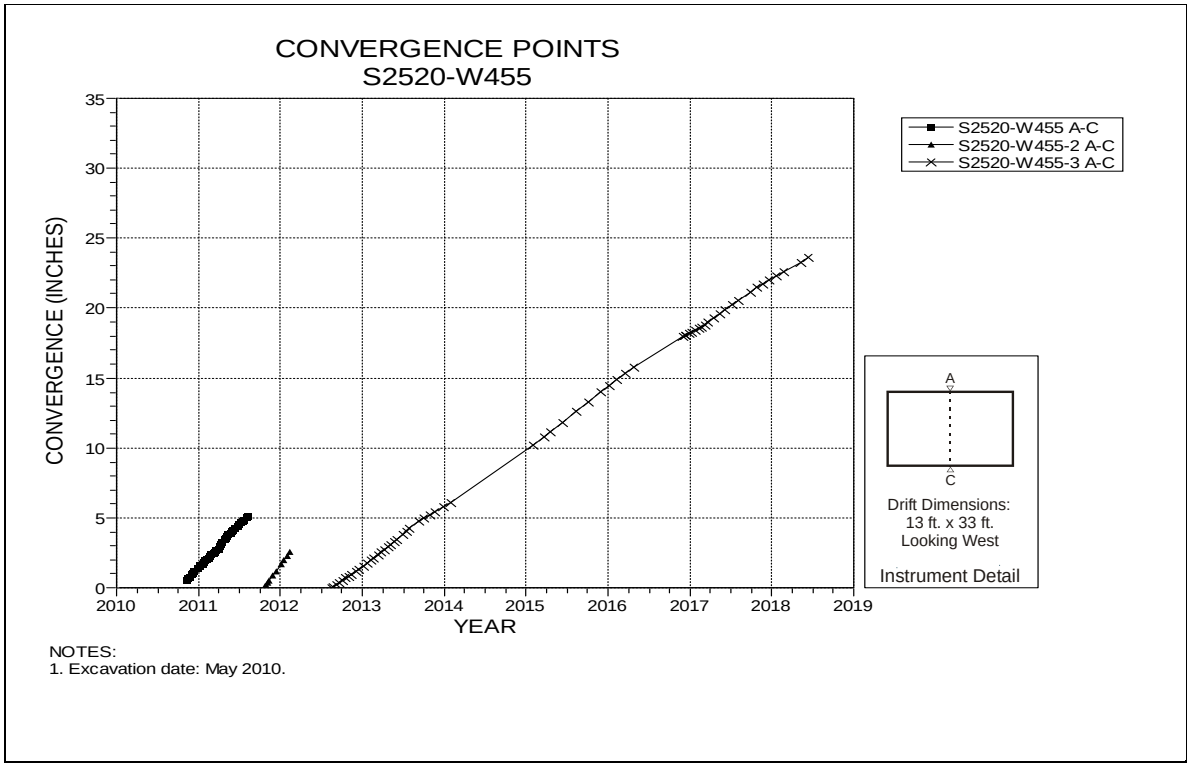

Figure 5-22 Convergence Point Array – S2520 W455 – Roof to Floor

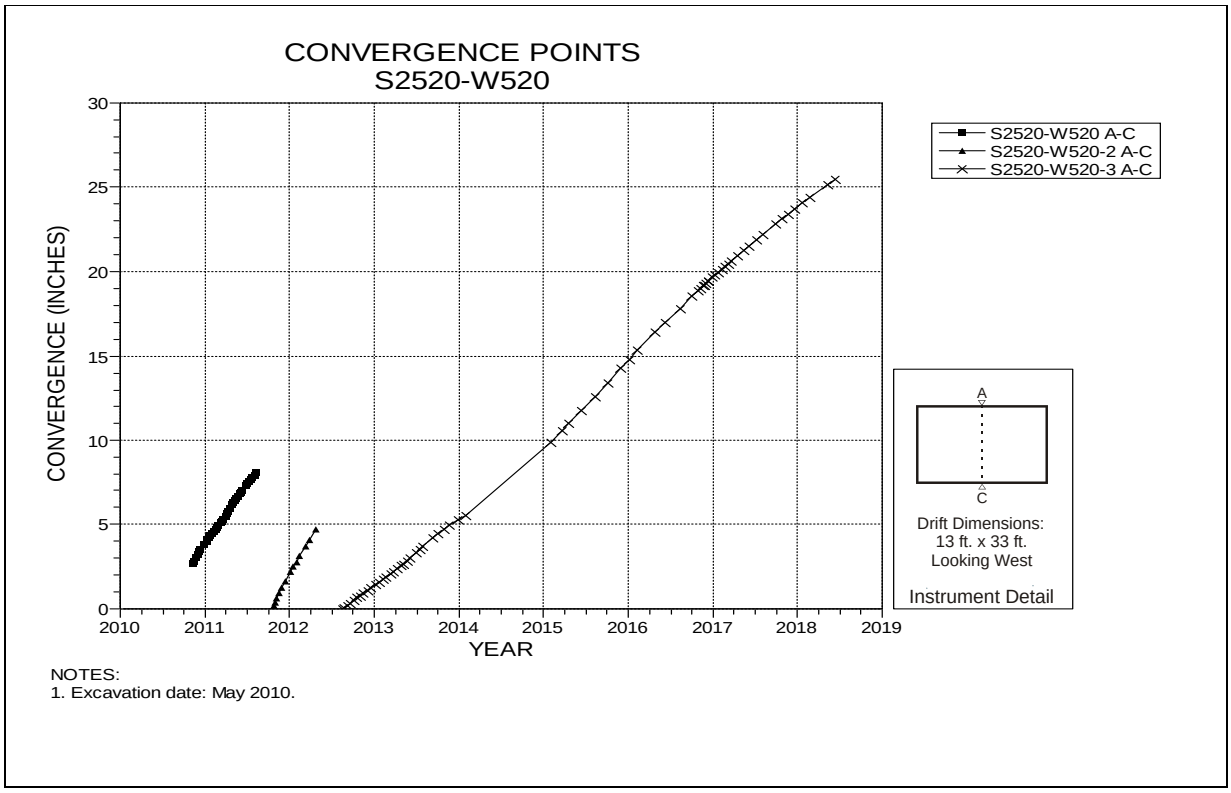

Figure 5-23 Convergence Point Array – S2520 W520 – Roof to Floor

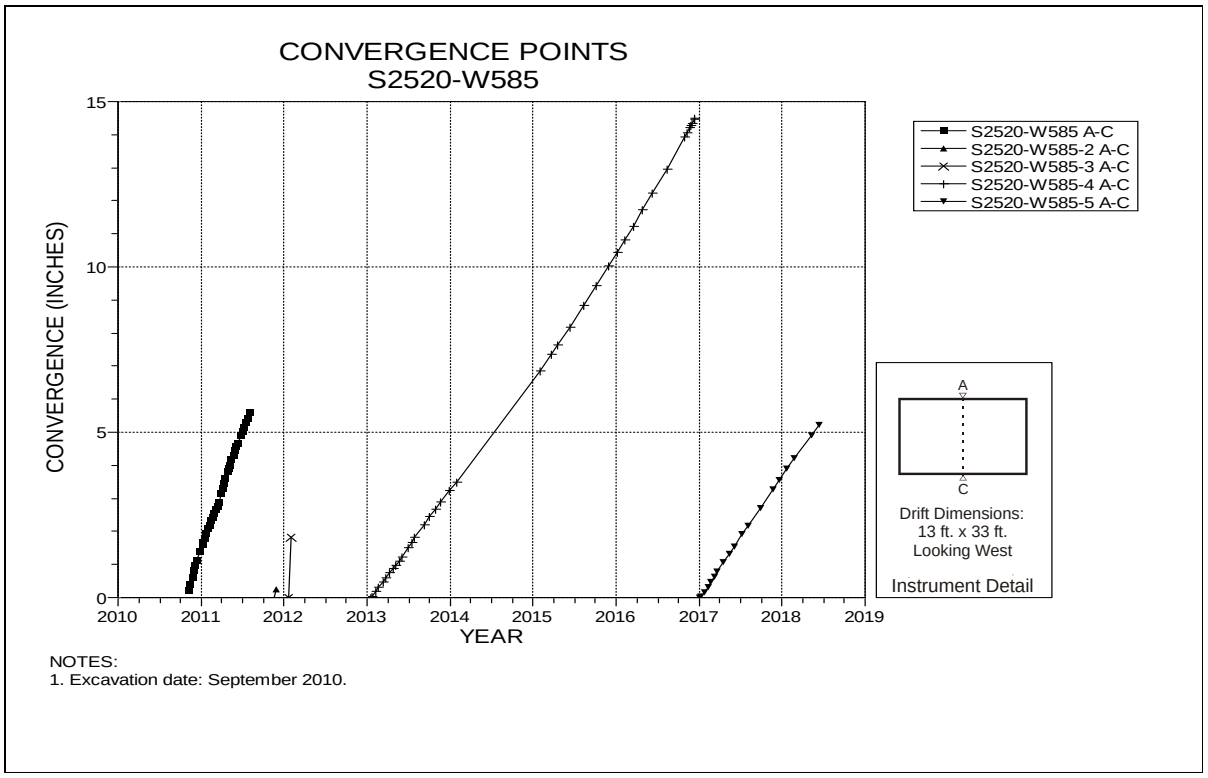

Figure 5-24 Convergence Point Array – S2520 W585 – Roof to Floor

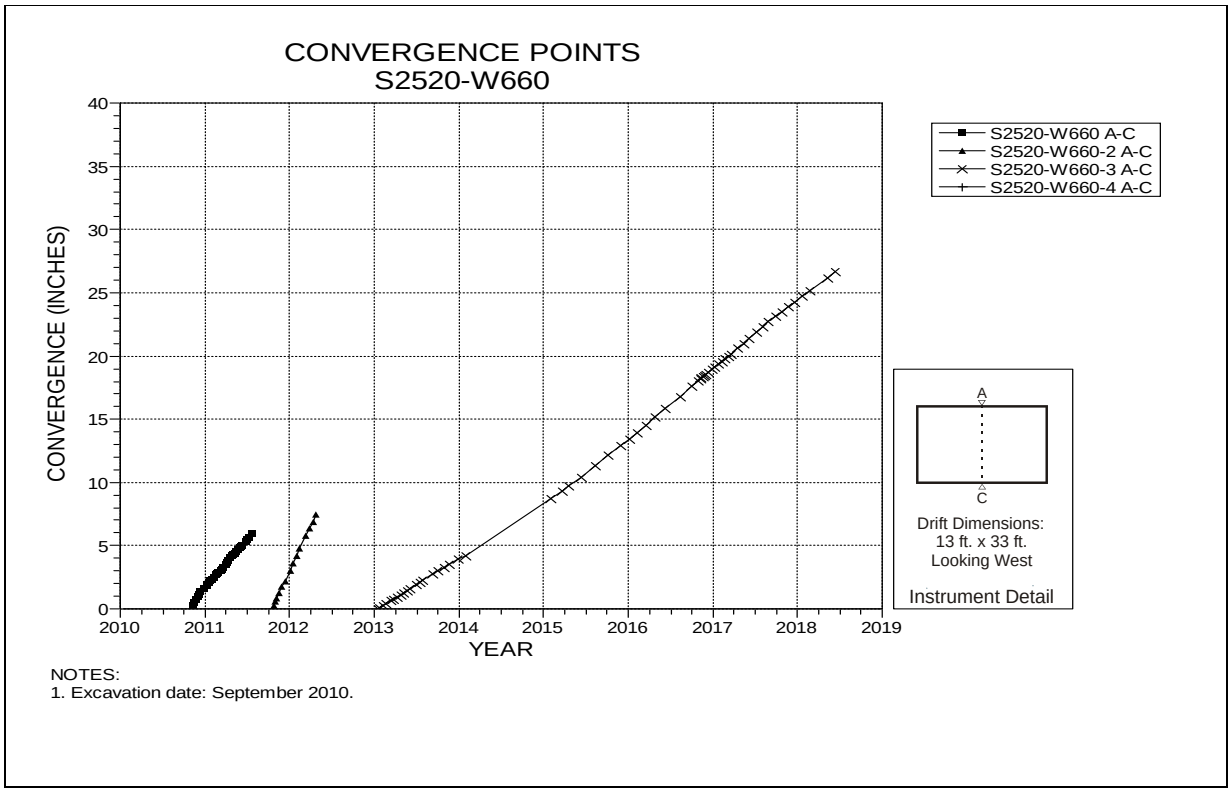

Figure 5-25 Convergence Point Array – S2520 W660 – Roof to Floor

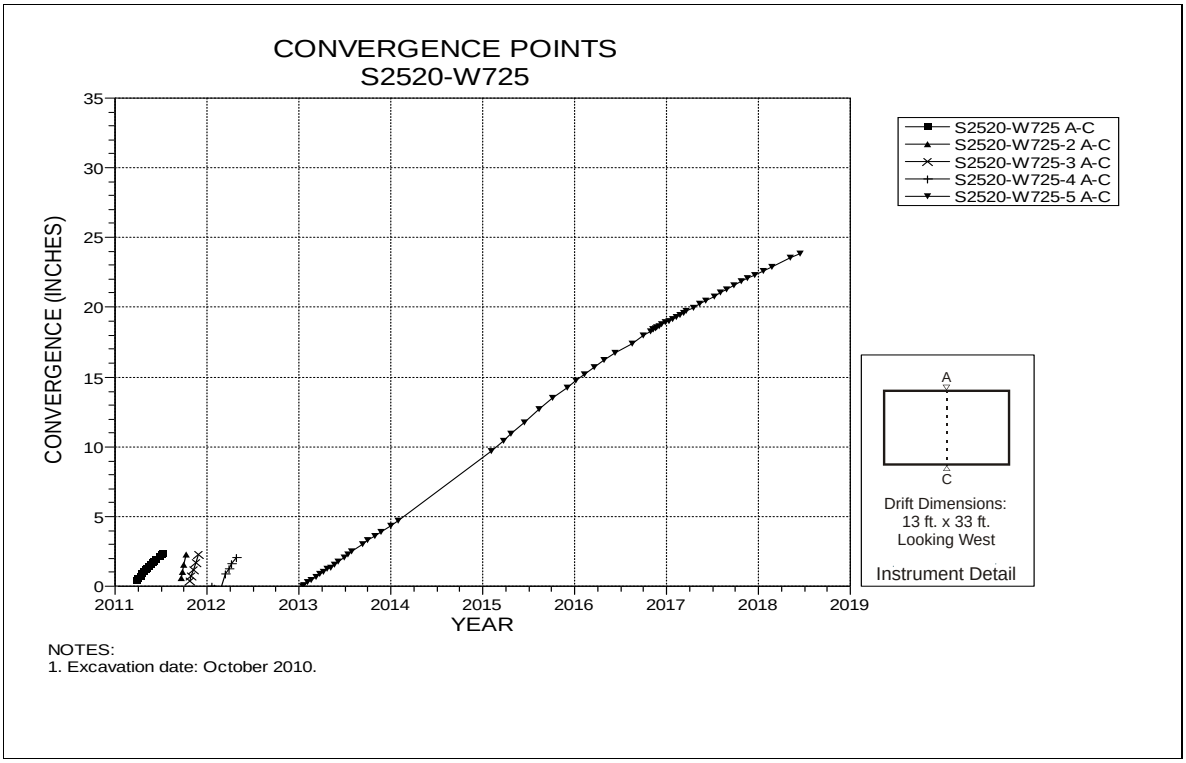

Figure 5-26 Convergence Point Array – S2520 W725 – Roof to Floor

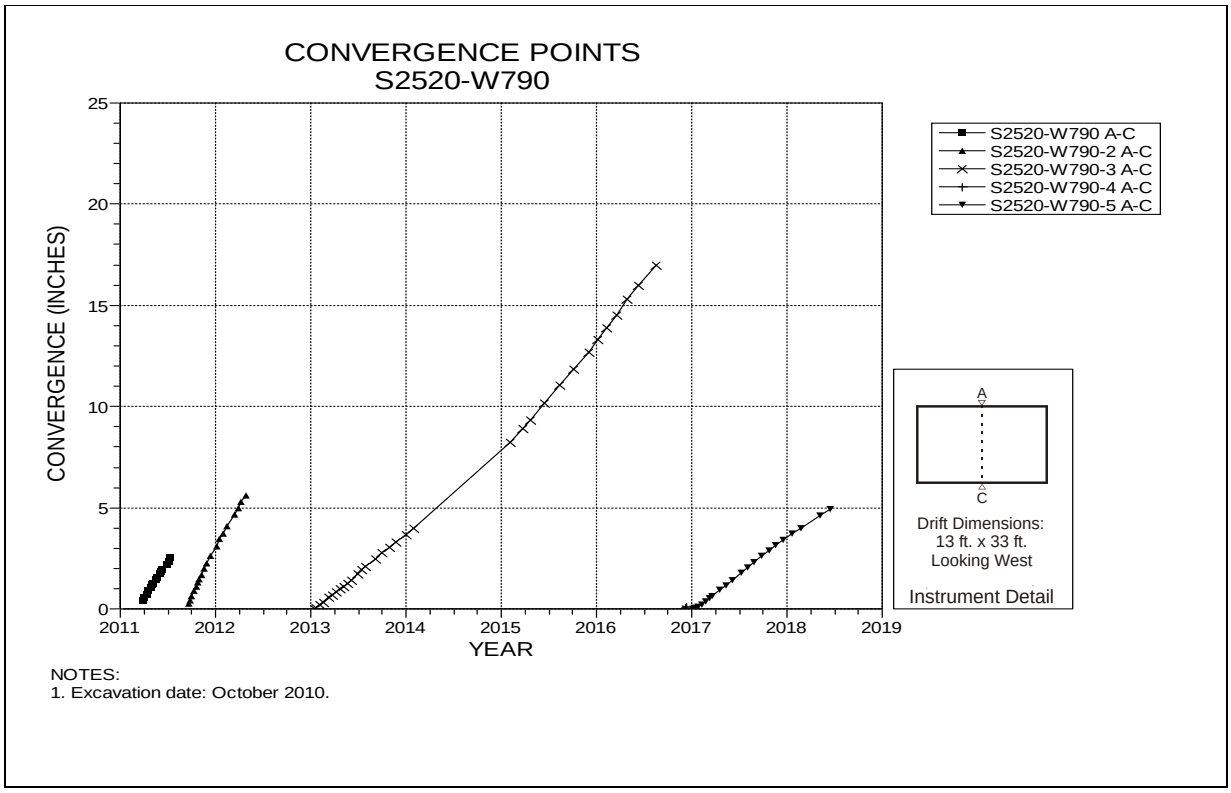

Figure 5-27 Convergence Point Array – S2520 W790 – Roof to Floor

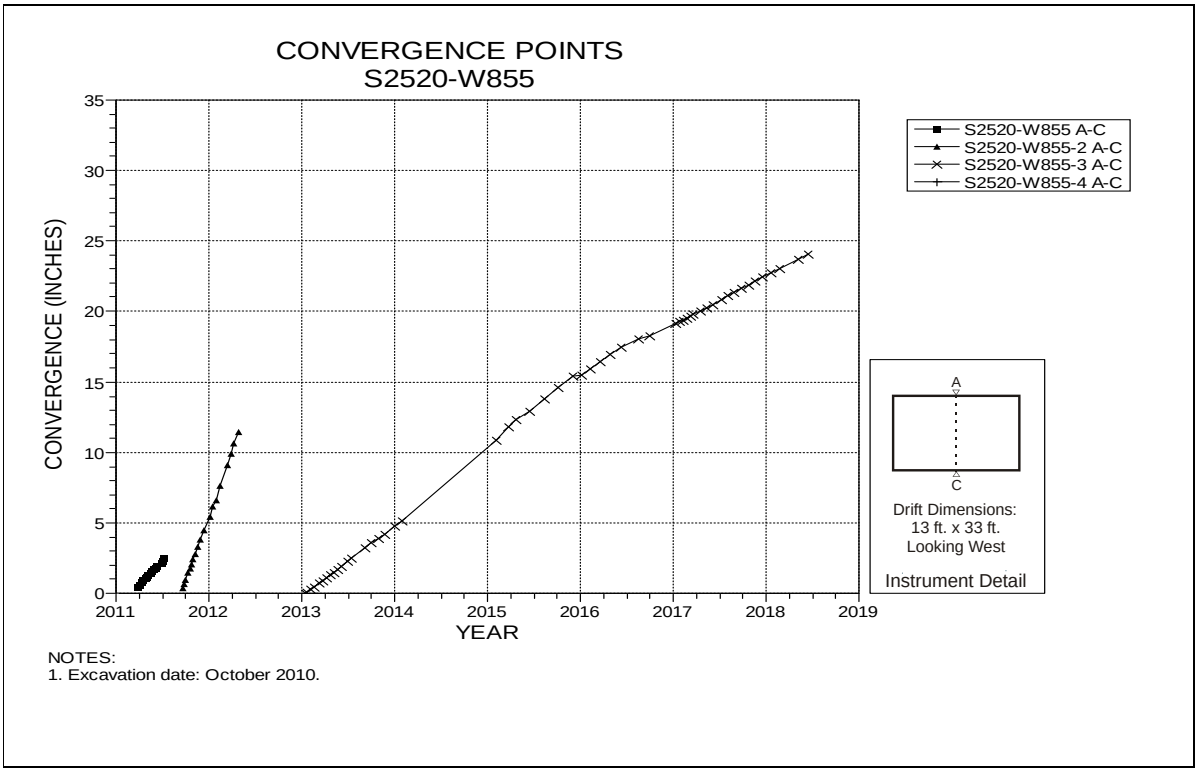

Figure 5-28 Convergence Point Array – S2520 W855 – Roof to Floor

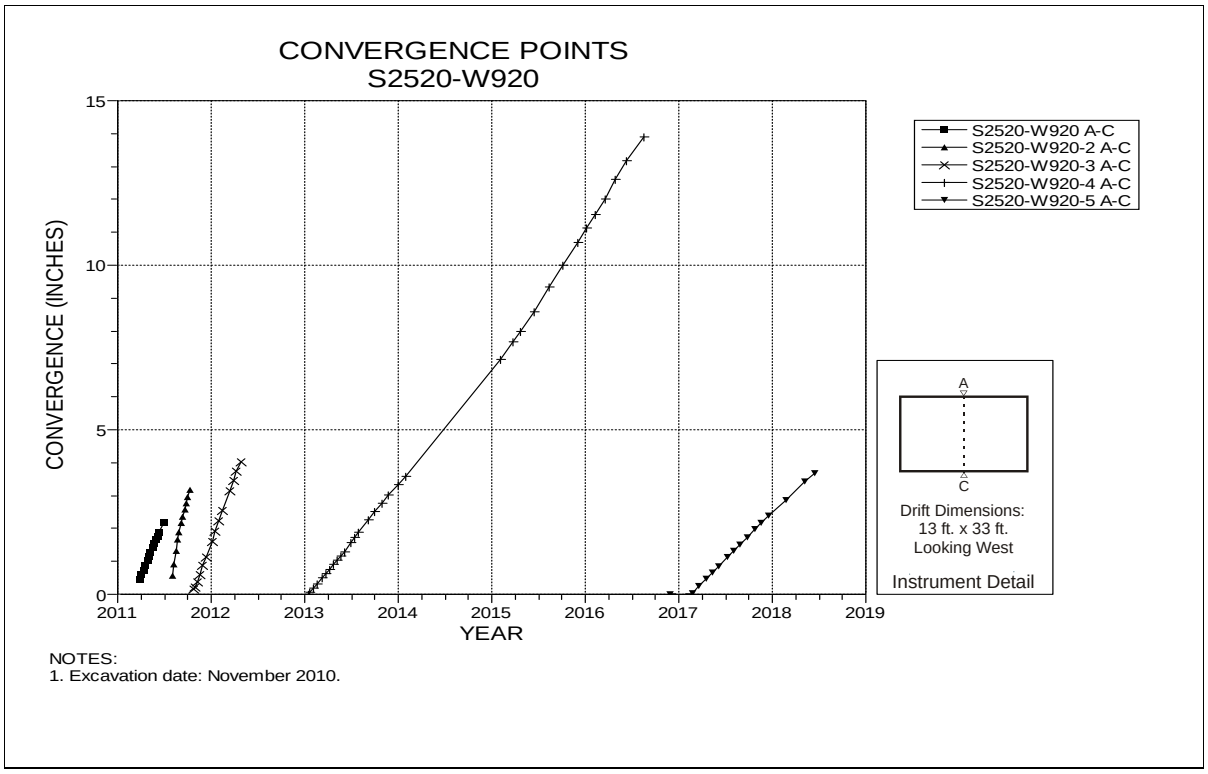

Figure 5-29 Convergence Point Array – S2520 W920 – Roof to Floor

6.0 INSTRUMENTATION SUMMARY FOR THE SDI AREA

Historically, this chapter presented a summary of the data collected from radial convergence points located in the SDI area at the WIPP. However, access to the SDI area was prohibited during this reporting period due to lack of ventilation resources which led to inadequate ground maintenance (Figure 6-1). Consequently, no new data was acquired for analysis and presentation during this reporting period.

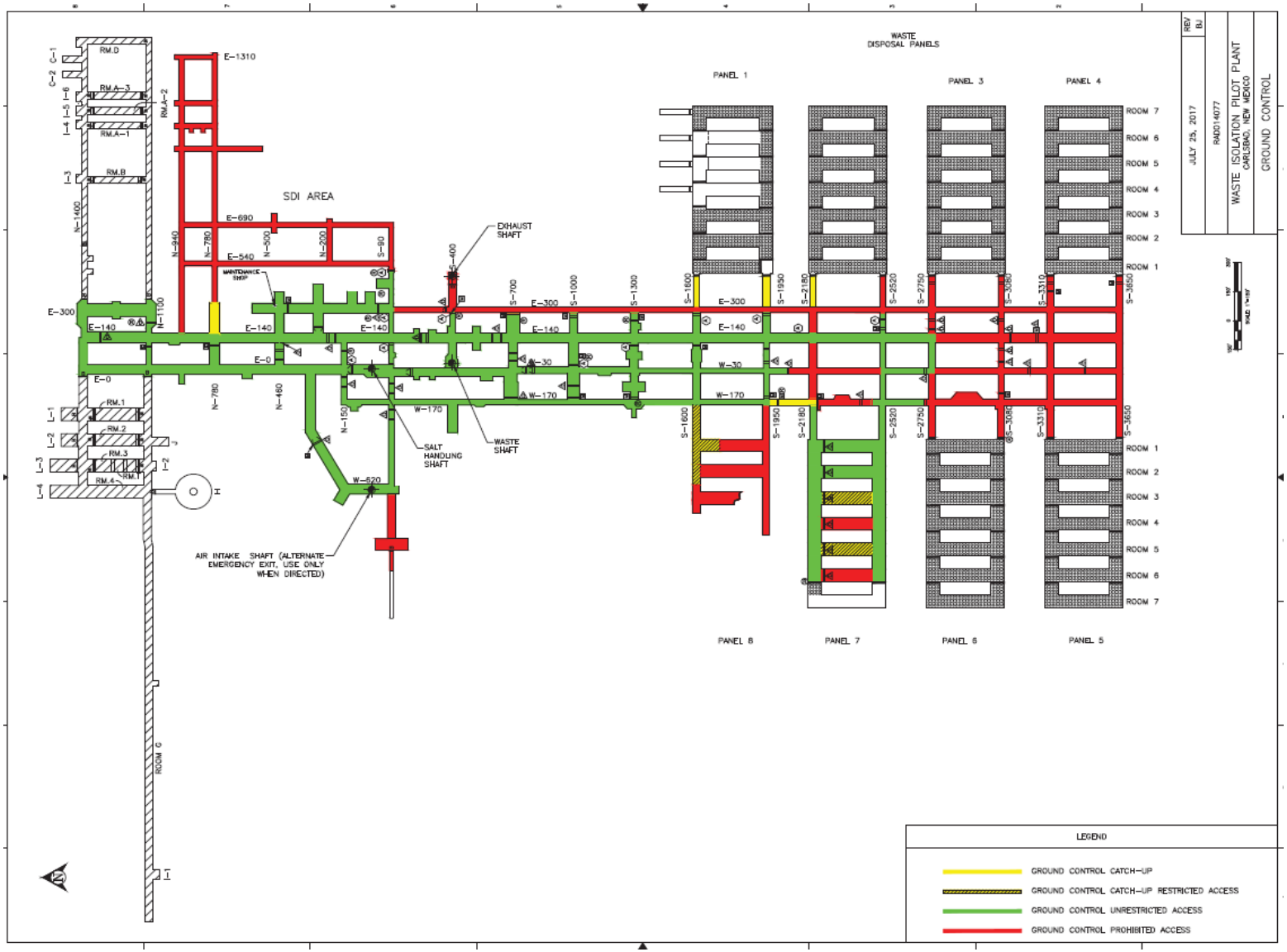

Figure 6-1 Ground Control Map - July 2017

7.0 GEOSCIENCE SUMMARY FOR THE WASTE DISPOSAL AREA

Chapter 7 historically presented data acquired to support the WIPP Geoscience Program. This included fracture maps of excavation surfaces, stratigraphic mapping, and drilling vertical observation holes to monitor clay seam displacements and other significant geological features. The significant reduction in ventilation following the radiological release event has curtailed the frequent use of man-lifting vehicles to conduct fracture and stratigraphic mapping in the underground. Consequently, there is no data to report. These functions are performed intermittently, through visual ground control inspections to determine corrective measures to be taken.